Tomohiro Kuwae · Masakazu Hori

Editors

Blue Carbon in Shallow Coastal Ecosystems

Carbon Dynamics, Policy, and Implementation

Springer

Blue Carbon in Shallow Coastal Ecosystems

Tomohiro Kuwae • Masakazu Hori
Editors

Blue Carbon in Shallow Coastal Ecosystems

Carbon Dynamics, Policy,
and Implementation

Springer

Editors
Tomohiro Kuwae
Coastal and Estuarine Environment
Research Group
Port and Airport Research Institute
Yokosuka, Japan

Masakazu Hori
National Research Institute of Fisheries
and Environment of Inland Sea
Japan Fisheries Research and Education
Agency
Hatsukaichi, Hiroshima, Japan

Foreword

Tomohiro Kuwae and Masakazu Hori's *Blue Carbon in Shallow Coastal Ecosystems: Carbon Dynamics, Policy, and Implementation* is a major contribution to blue carbon science, providing a solid reference source to those starting to consider this important aspect of environmental sciences. Most importantly, this book provides a unique effort to broaden the scope of blue carbon by also addressing nonconventional blue carbon ecosystems, such as macroalgal stands and corals, with a rich suite of examples from a range of coastal ecosystems in Japan. As a unique contribution, the contributing authors integrate the fluxes of CO_2 that these coastal habitats support at the global scale for the first time, a prerequisite to evaluate the efficiency of various policy actions to strengthen the role of blue carbon ecosystems in climate change mitigation. I strongly recommend this book to students and scholars interested in climate change and the role that conservation and restoration of coastal ecosystems may play in mitigating climate change.

Professor of Marine Science, Red Sea Research Center   Carlos M. Duarte
King Abdullah University of Science and Technology,
Thuwal, Saudi Arabia

Preface

The term "blue carbon" was coined by the United Nations Environment Programme in 2009 and is still rather new. However, this concept and the role of blue carbon stored in shallow coastal ecosystems (SCEs) as a climate mitigation measure have attracted the interest of many people worldwide. Some such typical ecosystems (e.g., mangroves, tidal marshes, and seagrass meadows) are now being called "blue carbon ecosystems." The number of publications dealing with blue carbon has been increasing exponentially since the genesis of the term, and the science of blue carbon and its role within the context of the mitigation of global warming seem to be rapidly maturing. However, there are very few comprehensive books about blue carbon and the role of carbon storage and CO_2 uptake in SCEs.

The suppression of CO_2 emissions to the atmosphere by blue carbon storage is a process that reduces atmospheric CO_2 concentrations and mitigates climate change indirectly. The net uptake of atmospheric CO_2 through the exchange of CO_2 at the air–ecosystem interface accomplishes the same goal directly. The role of both blue carbon storage and CO_2 gas uptake should therefore be considered when SCEs are targeted for climate change mitigation. However, we feel that there is a disciplinary division between these two blue carbon-related sciences: ecologists seem to focus on biological processes, biogeochemists consider carbon cycling, and meteorologists study greenhouse gas fluxes and physicochemical processes.

In addition to the classical blue carbon SCEs, other SCEs, including macroalgal beds, tidal flats, coral reefs, and embayments, are drawing attention as sites that could potentially contribute to climate change mitigation. However, there is very little published scientific information on these new potential climate change mitigation areas.

From the standpoint of policy and implementation, about 20% of the countries that approved the Paris Agreement have pledged in their Nationally Determined Contributions (NDCs) to use SCEs as a climate change mitigation option and are moving toward measuring blue carbon inventories. About 40% of those same countries have pledged to use SCEs to adapt to climate change. Australia has begun including blue carbon as a national carbon offset scheme, and as discussed in this book, Yokohama City, Japan, has also started using SCEs for carbon credit trading.

Blue Carbon in Shallow Coastal Ecosystems: Carbon Dynamics, Policy, and Implementation

Chapter 1. Introduction

Carbon Stock and Flow at Ecosystem Scales

Carbon Storage

Chapter 2. Background, Theory, Sediments

Chapter 3. Mangroves

Chapter 4. Seagrasses and Macroalgae

Chapter 5. Tidal Flat Ecosystems

Gas Exchange

Chapter 6. Background, Theory, Methods, Shallow Coastal Ecosystems

Chapter 7. Mangroves

Chapter 8. Tidal Flat and Marsh Ecosystems

Carbon Stock and Flow at Estuarine and Coastal Scales

Chapter 9. Seagrass Carbon Transport

Chapter 10. Carbon Dynamics in Coral Reefs

Chapter 11. Carbon Dynamics in Human-dominated Waters

Policy and Implementation

Chapter 12. Carbon Offset Project Utilizing Coastal Waters

Chapter 13. Future of Blue Carbon

Fig. 1 Overview of this book

An overview and the highlights of this book are shown in Fig. 1 and Table 1, respectively. In consideration of the background described above, we chose the subject, purpose, and features of this book as follows:

1. Compilation of very recent studies and quantitative assessment of relevant processes and mechanism to demonstrate how much SCEs can take up CO_2 and store carbon and how they can contribute to climate change mitigation

Table 1 Chapter highlights

Chapter 1	Introduction of blue carbon and carbon cycling (carbon storage and CO_2 gas flux) in shallow coastal ecosystems
Chapter 2	Distribution pattern and chemical and genetic characteristics of sedimentary organic carbon on a timescale of several thousand years and factors controlling rates of burial in marine and seagrass sediments
Chapter 3	Global distribution of mangrove biomass, carbon stocks, and carbon burial rates in mangroves
Chapter 4	Japan nationwide estimate of carbon sequestration potential (annual plant tissue production) in seagrass and macroalgal beds
Chapter 5	Carbon stocks and flows in tidal flat ecosystems, especially for rates of microalgal production and bivalve-related organic and inorganic carbon, with special emphasis on Japanese sites
Chapter 6	Theory, methods (bulk formula, chamber, eddy-covariance), and empirical studies of air-water CO_2 fluxes in shallow coastal waters, which are sinks for atmospheric CO_2.
Chapter 7	Three types of CO_2 fluxes (atmosphere-ecosystem, air-soil, air-water) in mangrove ecosystems, with special emphasis on the Sundarban, the world's largest mangrove forest
Chapter 8	Three types of CO_2 fluxes (atmosphere-ecosystem, air-sediment, air-water) in tidal flat and marsh ecosystems, with special emphasis on Japanese sites
Chapter 9	Numerical model to estimate transport of the sequestered carbon from eelgrass beds through shallow coastal waters to the deep sea, and the process of carbon storage both within eelgrass beds and off sites
Chapter 10	Carbon cycle (CO_2 sink/source, carbon storage, and export) in coral reefs and interrelationships between coral reefs and other ecosystems such as seagrass meadows and mangroves
Chapter 11	Blue carbon ecosystems, estuaries, and embayments as sinks for atmospheric CO_2 under some biogeochemical and socio-economic conditions, e.g., appropriate management of wastewater treatment
Chapter 12	A social experiment conducted by Yokohama City, Japan, that served to counter climate change and included a novel carbon offset campaign utilizing coastal waters
Chapter 13	Summary of carbon flows and stocks in various shallow coastal ecosystems reported in previous chapters, current status of blue carbon discussions at the international level, and future needs for policy making and social implementation

2. Inclusion of not only classical blue carbon ecosystems (i.e., mangroves, seagrass meadows, and salt marshes) but also macroalgal beds, tidal flats, coral reefs, and shallow waters near urban areas to show the potential of these ecosystems to serve as new carbon sinks

3. A thorough review of the literature, including many Japanese case studies, on blue carbon studies of not only topics that are currently research foci (i.e., sedimentary carbon stocks and accumulation rates [indirect processes for reducing atmospheric CO_2]) but also exchanges of CO_2 gas between the atmosphere and SCEs (direct processes for reducing atmospheric CO_2), carbon storage in the water column as refractory organic carbon, and off-site carbon storage (e.g., the deep sea)

4. Compilation of international policies and frameworks related to blue carbon and a case study of the application and implementation thereof (carbon offset credit) in Japan

We hope that this book will provide readers with a comprehensive and up-to-date understanding of the state-of-the-art science, technology, and policies related to blue carbon. We believe that publication of this book is timely because the Paris Agreement calls for initiation of climate change measures in 2020 and many countries have pledged in their NDCs to utilize SCEs as described above.

We anticipate that the audience of this book will be broad and will include professionals (e.g., managers and policymakers in local and national governments, conservationists, engineers involved with dredging companies, costal environmental consultancies, NPOs, and NGOs), academics (coastal ecologists, biogeochemists, fisheries scientists, civil engineers, and climate scientists), and all levels of students and educators from undergraduates to university faculty.

Acknowledgments

Yokosuka, Japan   Tomohiro Kuwae
Hiroshima, Japan   Masakazu Hori

Contents

Chapter 1
Blue Carbon: Characteristics of the Ocean's Sequestration and Storage Ability of Carbon Dioxide

Masakazu Hori, Christopher J. Bayne, and Tomohiro Kuwae

Abstract The first life on Earth evolved in the ocean about 3.5 billion years ago. Photosynthetic organisms, which first appeared in the ocean, eventually changed the oxygen and carbon dioxide concentrations in the atmosphere to the current concentrations. This gaseous exchange was the first and can be considered as the most important ecosystem service provided by marine ecosystems. That service has been on-going from the first primitive photosynthetic organism to the present and reflects the ability of the oceans to absorb carbon dioxide. Nevertheless, recent discussions of sequestration of CO_2 have mainly promoted the concept of land-based green carbon sequestered by terrestrial ecosystems.

The Blue Carbon Report, which was released in 2009, has shown that more than 50% of the carbon dioxide absorbed by the plants on Earth is actually cycled into the ocean; the remainder of the carbon dioxide absorbed by plants is stored in terrestrial ecosystems. More than half of the carbon stored in the ocean has been sequestered by shallow coastal ecosystems, which account for only 0.5% or less of the total ocean area. In addition, there is good evidence that shallow coastal ecosystems have been greatly affected by human activities and continue to be seriously denuded. However, the importance of shallow coastal ecosystems has not yet emerged as common knowledge within society in general, and full comprehension of the role of shallow coastal ecosystems has not yet been applied to climate change mitigation and adaptation strategies. For example, shallow coastal ecosystems are not considered in the inventory of absorbed carbon dioxide. One reason is that the sequestration and storage processes of blue carbon are complex, and it is still difficult to determine what criteria are essential for calculating the relative efficacy of carbon sequestration in shallow coastal ecosystems versus terrestrial ecosystems. In this chapter, which introduces this book, we give an overview of the key points of

M. Hori (✉) · C. J. Bayne
National Research Institute of Fisheries and Environment of Inland Sea, Japan Fisheries Research and Education Agency, Hatsukaichi, Hiroshima, Japan
e-mail: mhori@affrc.go.jp

T. Kuwae
Coastal and Estuarine Environment Research Group, Port and Airport Research Institute, Yokosuka, Japan

1

the Blue Carbon Report. We then try to provide a better understanding of the blue carbon concept by explaining the important characteristics of blue carbon ecosystems. We use the carbon absorption process in seagrass meadows as an example to illustrate important concepts.

1.1 Introduction

The first life on Earth evolved in the ocean. Living organisms first appeared in the ocean about 3.5 billion years ago, and their metabolic activities eventually contributed to the exchange between oxygen and carbon dioxide concentrations in the atmosphere. The metabolic functions of photosynthesis established an environment where organisms could, through evolution, adapt to life on land. This gas exchange was the first and can be considered as the most important ecosystem service provided by the ocean. Eventually, during the process of biological evolution over billions of years, the ecosystem diversified and its services multiplied. These changes were accompanied by the emergence and extinction of numerous species. One marine ecosystem service has been on-going from the first primitive life to the present: the absorption and sequestration of carbon dioxide in the ocean.

When people think of organisms that absorb carbon dioxide, many think of large trees and the rich forests where these trees are found. Stark green blankets composed of terrestrial plants and extensive forests such as rainforests and boreal forests come to mind. There is no doubt that these land plants assimilate carbon dioxide and contribute to the mitigation of greenhouse gases.

A report that significantly modified this perception, however, was jointly published in 2009 by the United Nations Environment Program Planning Unit (UNEP), the United Nations Food and Agriculture Organization (FAO), and the United Nations Educational Science and Culture Organization (UNESCO) (Nellemann et al. 2009; hereinafter this report is referred to as the UNEP report, using the acronym of the first organization). In the report, "Blue Carbon" is described as carbon dioxide absorbed by living marine organisms. Actually, a little less than half of the carbon dioxide biologically captured in the world is absorbed by terrestrial ecosystems, and marine ecosystems account for a majority of the carbon dioxide that is absorbed. Furthermore, more than half of the carbon stored in the ocean is initially absorbed in shallow coastal waters. The words "blue carbon", which were used for the first time in this report, characterize the carbon taken up by the ocean because of the action of marine organisms.

Experts, especially in oceanography and biogeochemistry, initially recognized the fact that marine organisms absorb an amount of carbon dioxide equivalent to that absorbed by land plants. However, this fact has been hardly recognized by the public. In addition, the UNEP report's conclusion that most of the carbon dioxide absorbed by the ocean is accumulated in shallow coastal areas was surprising, even to research scientists. The UNEP report stimulated the initiation of blue carbon

studies, and research directed at determining to what extent blue carbon is seques-tered in shallow coastal areas has become popular recently.

We therefore begin this chapter with a discussion of the UNEP report. We then explain recent trends in studies of blue carbon formation, sequestration, and storage in shallow coastal areas, and outline the processes associated with carbon sequestra-tion and storage in carbon-storage ecosystems known as carbon sinks. This book includes extensive reviews of research and practices related to the use of various shallow coastal ecosystems such as tidal flats, saltmarshes, coral reefs, mangrove forests, and seagrass meadows. In this chapter, we also discuss biological aspects of the sequestration and storage of blue carbon by focusing on the key role played by eelgrass beds. The following sections describe various CO_2 absorption mechanisms and carbon sequestration and storage processes. This information is essential to understanding the biological characteristics of eelgrass beds, including their biodi-versity and ecosystem services. Finally, we explain why an understanding of biodi-versity and the functionality of the whole ecosystem are essential for maintaining and nurturing the carbon sequestration and storage services provided by shallow coastal ecosystems.

1.2   Blue Carbon Advocacy

On the one hand, it is common to see headlines such as "Deforestation, acceleration of global warming", "Conservation of forests prevents global warming", or similar words in the social mass media such as television programs and newspapers. In contrast, it is uncommon to find headings such as "Decreases of underwater forests and seaweed beds cause acceleration of global warming". This difference in public awareness is a major reason why the UNEP report was published. The report was intended to enhance public awareness of the differences in climate change counter-measures between the land and ocean.

Many people understand that terrestrial forest ecosystems are under threat owing to a variety of factors, including deforestation, desertification, forest fires, and the effects of climate change. These perturbations have been major factors causing the increase of atmospheric carbon dioxide concentrations. However, marine ecosys-tems, especially the ocean floor in shallow coastal areas where phytoplankton and marine macrophytes such as seaweeds and seagrasses grow abundantly, play an important role in absorbing carbon dioxide. This ecosystem service and the area of the seafloor where macrophytes are found have decreased greatly in recent years. Macrophyte-dominated marine ecosystems, like terrestrial forests, are now on the verge of a crisis. Although marine organisms and shallow coastal waters are some-times considered important from the standpoint of biodiversity and seafood produc-tion, few people associate marine organisms with absorption of carbon dioxide. The major concerns for the ocean with respect to climate change seem to relate to loss of biodiversity. Coral reefs, for example, are threatened with decline because of ocean acidification and increasing water temperatures. Here we consider the
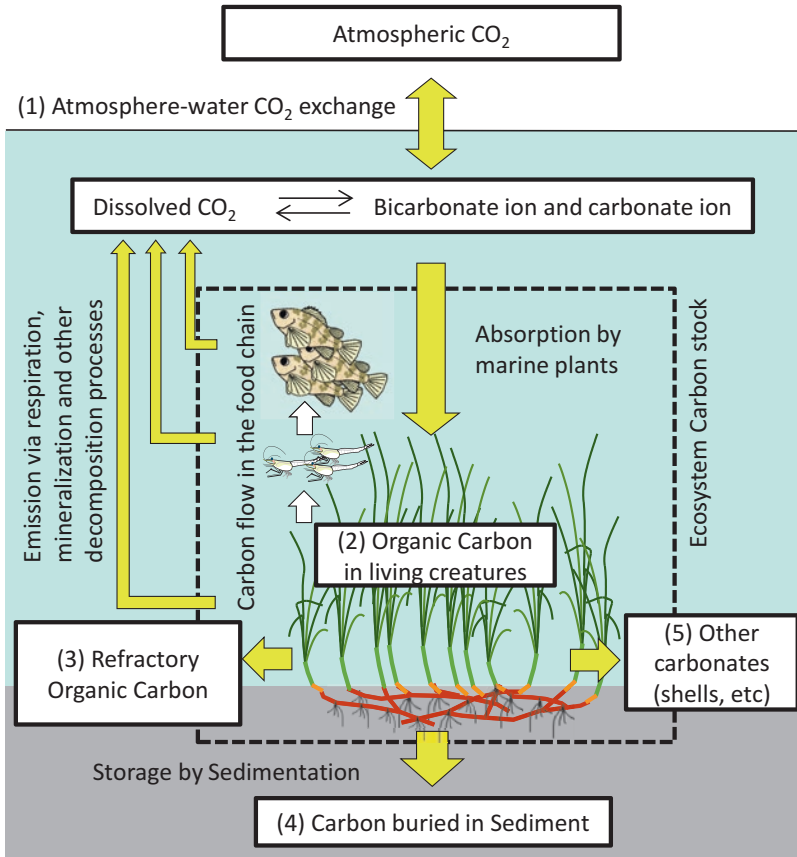
Fig. 1.1 Schematic diagram of major carbon cycle and carbon sequestration/storage in shallow coastal ecosystems

message of the UNEP report—that shallow coastal ecosystems contribute greatly to mitigating global warming. This message has not been adequately communicated to the public.

1.2.1   What Is Blue Carbon?

In order to understand the contents of the UNEP report, it is necessary to define some technical terms about the processes involved in the transfer of carbon dioxide (hereinafter referred to as CO_2) from the atmosphere to the ocean, where it may become blue carbon, and the storage of this blue carbon in the sediments of shallow coastal areas or the deep ocean floor (Fig. 1.1). In the UNEP report, blue carbon is defined as green carbon in the sea, and green carbon is defined as carbon that plants

have assimilated via photosynthesis and incorporated into organic matter. In a terrestrial ecosystem, green carbon is taken up directly as CO_2 from the atmosphere into a plant to make organic carbon. Hence the amount of organic carbon in the terrestrial realm can be equated to the amount of green carbon itself.

However, unlike terrestrial plants, generally marine plants cannot fix CO_2 until CO_2 from the atmosphere has become dissolved in seawater. The process of dissolution is complex. In a nutshell, physicochemical processes control the rates of CO_2 absorption from the atmosphere by seawater and its release from seawater to the atmosphere. The factors that control CO_2 absorption and release by seawater are the difference between the partial pressure of atmospheric CO_2 and the partial pressure of CO_2 dissolved in the seawater. When the partial pressure in the atmosphere is greater than (less than) the partial pressure in the seawater, there is a net influx (efflux) of CO_2 from the atmosphere (ocean) to the ocean (atmosphere). Chapter 6 provides details (Tokoro et al. 2018).

Photosynthesis by marine plants lowers the dissolved CO_2 concentration in the ocean. In addition, increases (decreases) in the water temperature cause the CO_2 solubility to decrease (increase). Upwelling and vertical mixing can cause large amounts of dissolved CO_2 from lower depths to be introduced into the surface mixed layer and thereby affect the vertical distribution of CO_2. The wind speed at the sea surface also influences the exchange of CO_2 with the atmosphere. Most of the CO_2 dissolved in seawater dissociates into bicarbonate and carbonate ions. At the pH of typical seawater, the bicarbonate ion concentration greatly exceeds the carbonate ion concentration at equilibrium. As dissolved CO_2 in seawater increases, the amount of dissolved inorganic carbon (DIC) that occurs in the form of bicarbonate ions increases, and hydrogen ions are released. These hydrogen ions are the cause of ocean acidification; they lower the pH of the seawater. Marine plants grow by taking up some of the DIC in seawater and converting it into organic matter via photosynthesis. At the present time, the CO_2 partial pressure is lower in the sea than in the atmosphere. Hence, there is a net influx of CO_2 from the atmosphere into the ocean (see Chaps. 6 and 11; Tokoro et al. 2018, Kuwae et al. 2018). The net influx of CO_2 into the ocean is therefore not always equal to the rate of CO_2 sequestration by marine plants. Seagrass species are well known to take up dissolved CO_2 in preference to bicarbonate ions (Larkum et al. 2006).

CO_2 taken up by marine plants is converted to organic carbon and becomes part of the plant biomass. Chapter 4 provides details (Yoshida et al. 2018). Afterward, depending on the rates of photosynthesis, respiration, growth, and mortality, some of the organic carbon is converted back into inorganic carbon and returned to the sea. Chapter 9 provides details (Abo et al. 2018). Alternatively, the plants may be consumed by herbivores, in which case the organic carbon becomes part of the biomass of the herbivores. The animals convert some of the organic carbon to DIC via respiration, but the carbon that is not respired remains in the form of organic matter. As predators consume prey in the food chain, some organic carbon consumed by predators is converted to DIC via respiration, but the rest is retained as organic carbon. The overall process by which CO_2 from the atmosphere enters the ocean and is

incorporated as organic carbon in the organisms that make up the marine food chain is called "sequestration".

There is another important process in addition to sequestration. Some of the organic carbon sequestered in the sea is refractory. This refractory organic carbon is difficult for organisms to respire because of its chemical nature, and even the organic carbon that can be easily decomposed is often stored because it is incorporated into sediments, where low oxygen concentrations slow rates of decomposition. Some organic carbon may also be transported to the deep sea, where it is isolated from the CO_2 flux between atmosphere and ocean. Such organic matter may be preserved in the sediment or in the deep ocean on a time scale of decades, centuries, or even millennia (Chap. 2; Miyajima and Hamaguchi 2018, Chap. 9; Abo et al. 2018, and Chap. 11; Kuwae et al. 2018). The processes by which organic carbon is isolated from the carbon cycle between the ocean and atmosphere and converted to a state where it is stored for a long time is called "storage" in this book.

There are six major carbon pools in marine ecosystems: (1) sedimentary organic carbon (SOC), (2) particulate inorganic carbon in sediment (carbonates), (3) organic carbon in living marine organisms, (4) shell and skeletal inorganic carbon, (5) dissolved organic carbon in seawater, and (6) DIC in seawater. All of these six pools contribute to the sequestration and storage of atmospheric CO_2, but the residence time of carbon in these pools (the time during which the carbon is stored in the ocean before it is returned to the atmospheric as CO_2) varies.

It should be noted that an increase of a carbon pool does not necessarily lead to a reduction of atmospheric CO_2 concentrations. For example, when inorganic carbonates are produced (e.g., calcification associated with the growth of shellfish and corals), CO_2 is also formed as a byproduct of the chemical reaction (see Chaps. 6 and 10) (Tokoro et al. 2018; Watanabe and Nakamura 2018). Therefore, as carbonates are formed, the partial pressure of dissolved CO_2 increases, and this increase may lead to an efflux of CO_2 into the atmosphere.

The carbon residence time is long in both SOC (because of the slow decomposition of organic matter) and RDOC in seawater (see Chaps. 2 and 11) (Miyajima and Hamaguchi 2018; Kuwae et al. 2018). Although the DIC in seawater is the largest among the six pools, the residence time of CO_2 in the DIC is short because the bicarbonate ion in the DIC is readily converted into CO_2 as a result of carbonate chemistry equilibrium (pH decrease). Moreover, the organic carbon in living organisms also undergoes large spatiotemporal fluctuations and is rather unstable compared to SOC and RDOC.

In the UNEP report, blue carbon is described as the CO_2 absorbed by living marine organisms. However, blue carbon is more accurately characterized as "carbon that is sequestered or stored in the ocean by marine organisms". An ecosystem refers to an interactive complex of biological communities and the abiotic environment affecting them within a particular place. The physicochemical factors are more complex in the water column of the ocean than in terrestrial ecosystems. To evaluate the role of blue carbon in mitigating effects of climate change, it is therefore important to understand not only the amount of organic carbon sequestered and stored by marine organisms but also the carbon cycle in the ecosystem.
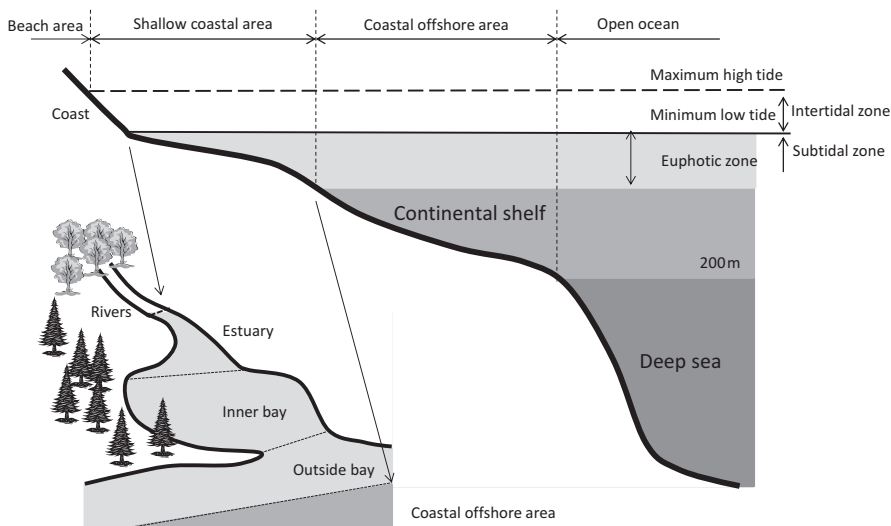
Fig. 1.2 Oceanographic topography and structure as defined in this book. This classification differs somewhat from the classification generally used in oceanography and divides the coastal area into a shallow and offshore region. The estuary, the inland bay, and the area outside of the bay are included in the shallow coastal area

The terminology used in this book to characterize oceanographic topography should also be defined. Shallow coastal areas, for example, are important for sequestering and storing blue carbon, but how are these areas defined? In the field of oceanography, the coastal area corresponding to the continental shelf with depths shallower than 200 m is normally defined as the coastal area, and the area of the ocean extending from the continental slope to the deep sea is defined as the offshore area (Fig. 1.2). However, photosynthesis is impossible without light, and because light sufficient for photosynthesis does not penetrate to ocean depths greater than about 200 m, marine plants are not found on the seabed at depths greater than 200 m. The euphotic zone is the part of the water column where there is adequate light for photosynthesis. The depth of the euphotic zone depends on the transparency of the water and varies from place to place; the euphotic zone may be as shallow as several tens of meters and up to 80 m deep in coastal areas that are hardly affected by human activities. In this book, the coastal zone from the coastline to the depth of the euphotic zone is referred to as the shallow coastal area, and the sea above the continental shelf from the depth of the euphotic zone to 200 m is defined as the coastal offshore area. Areas deeper than 200 m are defined as the open ocean.

1.2.2 *Blue Carbon Report*

The goal of the UNEP report was not only to present the scientific evidence that the ocean absorbs more CO_2 than land, but also to point out that the shallow coastal areas are extremely important sites of carbon sequestration and storage. At the beginning the UNEP report states, "The purpose of the report highlights the clear role played by oceans and marine ecosystems in climate control, to help marine policy planning for climate change" and to develop countermeasures for climate change using blue carbon. The first chapter of the UNEP report discusses the carbon cycle on a global scale and explains the effects of the large contribution of the ocean to the carbon cycle. The second chapter describes the anthropogenic emissions of greenhouse gases (CO_2, methane, etc.) and compares those emissions with the rate of CO_2 taken up by terrestrial organisms. The third chapter explains the processes that make up the carbon cycle and the role of the ocean in mitigating global warming. The fourth chapter discusses the sequestration and storage of blue carbon in shallow coastal areas and the associated mechanisms. The fifth chapter concerns the degradation and loss of shallow coastal areas. The importance of these areas for blue carbon sequestration and storage accounts for much of the concern over their degradation and loss.

In addition to the biogeochemical aspects of blue carbon, the UNEP report addresses social issues in chapters six to eight and stresses that, "The objective is to help policy planning". The sixth chapter explains that the sequestration and storage of blue carbon in healthy ecosystems is closely related to human well-being. The seventh chapter presents examples to illustrate the ecological-based adaptation and mitigation measures necessary to maintain a healthy coastal ecosystem despite future climate changes. The eighth and concluding chapter discusses five key policy options. The following is an outline of the UNEP report.

1. Of the carbon isolated by biological processes on Earth, marine organisms sequester 55%. Green carbon is a collective term that includes all carbon incorporated into organic matter through the photosynthetic activity of plants (the term 'blue carbon' is defined later in the UNEP report; only carbon incorporated into terrestrial organisms and marine organisms is currently called 'green carbon', and 'blue carbon', respectively). Forms of carbon that human beings have used (greenhouse gases such as CO_2), such as particulate matters and smoke from the combustion of fossil fuel, timber or vegetation, are called black carbon and brown carbon, respectively. Concentrations of black and brown carbon have been increasing steadily with global economic development, and their influence on climate, food production, and human beings is increasing. Natural ecosystems that absorb CO_2 are reducing the concentrations of black and brown carbon and mitigating their adverse impacts. However, the rate of decline of the capacity of natural ecosystems to absorb CO_2 is one to two times faster than the rate of reduction of black and brown carbon released annually by global transportation. In other words, the amount of CO_2 that remains in the atmosphere without being

absorbed exceeds the reduction of CO_2 emissions associated with efforts to regulate emissions at present.

2. Maintaining and improving the CO_2 sequestration and storage functions in terrestrial and marine ecosystems is extremely important for mitigating climate change effects. The contribution of forests to these functions is evaluated through mechanisms such as the market economy. Because the contribution of the ocean remains underestimated, the purpose of this report is to highlight the contribution of the oceans to the reduction of atmospheric CO_2 concentrations and the important role the oceans, and especially shallow coastal areas, play in stopping further degradation. An option for achieving that goal might be introduction of a market economy mechanism to evaluate the contribution of CO_2 sequestration by the ocean. Exploring the effectiveness of a CO_2 reduction plan with the ocean is also aimed as the main focus.

3. The ocean plays a major role in the global carbon cycle of Earth. The ocean is the largest sink for long-term sequestration of carbon. In fact, a little over 90% of the CO_2 on the planet (40 teratons: tera means 10 raised to the power 12, i.e., 10^{12}) is found in the ocean.

4. Coastal ecosystems with plant foundation species such as mangrove forests, saltmarshes, and seagrass beds account for less than 0.5% of the ocean area, but these act as the largest sink of blue carbon. They account for 50–71% of the total carbon stock preserved in marine sediments. Although the plant biomass in these three ecosystems is only 0.05% that of terrestrial plants, annual carbon storage in these ecosystems is roughly equivalent to the amount of carbon stored by all terrestrial plants on Earth. In other words, these three ecosystems are the most effective global carbon sink. Hereinafter, the mangrove forest, saltmarsh, and seagrass ecosystems are collectively referred to as the blue carbon ecosystem).

5. The blue carbon ecosystem is the most efficient ecosystem for storing carbon, but it is also the most rapidly disappearing ecosystem on Earth. Its rate of disappearance is more than 4 times that of tropical rainforests. Recently, the average rate of decrease of the blue carbon ecosystem has been preliminarily estimated to be 2–7% per year. This rate of decrease is seven times the rate half a century ago. If measures for protecting it are not implemented, most coastal vegetation may be lost within the next 20 years. If further degradation of coastal vegetation is prevented and logging of tropical rainforests is greatly reduced, there is a possibility that recent CO_2 emissions can be reduced by as much as 25%.

6. Maintaining the blue carbon ecosystem will also have positive economic effects; it will improve food safety and living standards and increase the ability of people living in coastal areas to adapt to the effects of climate change. Although the coastal area is only 7% of the total ocean area, the blue carbon and coral reef ecosystems are among the most important fishing grounds all over the world; they provide about 50% of the worldwide fisheries resources. Approximately 3 billion people are provided with nutrition essential for life activities from coastal areas. Also, coastal areas provide about 50% of animal protein and minerals consumed by 4 billion people living in developing countries.

7. The blue carbon ecosystem provides a wide range of benefits to human society besides fishery resources. Water purification, reduced coastal pollution, increased nutrient supplies, increased soil stability, decreased coastal erosion, reduction of effects of extreme weather events, and protection of the coastline are examples of other benefits derived from the blue carbon ecosystem. The value of these ecosystem services has been estimated to be equivalent to at least 25 trillion dollars per year. Therefore, the blue carbon ecosystem is one of the highest valued ecosystems. Degradation of the blue carbon ecosystem is caused not only by overuse of natural resources beyond their sustainable level but also by inadequate watershed management and inappropriate coastal development. The conservation and restoration of shallow coastal areas, by enhancing the health of local residents, employment opportunities, and food safety, enhance human well being. These services are among the benefits derived from integrated coastal management, which takes into consideration important characteristics of the target community.

8. Loss of the blue carbon ecosystem is an immediate threat to the global environment and human society. Consideration of the blue carbon ecosystem is the largest missing item in the recent climate change mitigation strategy. Considering the integrated management of the shallow coastal areas and oceans and including conservation and restoration of the blue carbon ecosystem area would be the most effective win–win scenario (i.e. killing two birds with one stone) for mitigation of climate change impacts to date. However, this strategy is still not recognized by international protocols and market economic systems. The following objectives illustrate the steps needed to conserve, restore, and manage the blue carbon ecosystem.

(1) Establish a global blue carbon fund to protect and manage shallow coastal areas and other marine ecosystems as carbon sinks.

Add a mechanism to approve the use of carbon credits through carbon sequestration and storage in marine ecosystems within the international policy agreements on climate change. Because blue carbon can be treated in the same way as green carbon in tropical rainforests, it can be included in the protocol on CO_2 emission control and climate change mitigation.

Establish standards and measurement methods for carbon sequestration appropriate for the global environment in the future.

Strengthen collaborations and consider the framework of financial resources.

Prioritize integrated coastal planning and management at the sustainable ecosystem level in order to strengthen the resilience of coastal vegetation and to maintain the safety of food and livelihood, especially around the hotspots of the blue carbon ecosystem.

(2) Protect 80% of existing seagrass beds, saltmarshes, and mangrove forests by promptly conducting effective management.

(3) Reduce or eliminate the threats confronting blue carbon ecosystems and manage these ecosystems with new perspectives that facilitate robust recoveries.

(4) Maintain food and livelihood safety of the marine ecosystem by conducting comprehensive and integrated ecosystem management to improve resilience to environmental change by both human societies and nature.
(5) Implement the following mitigation measures to create a win–win situation with respect to ocean resources;

Improve the efficiency of energy used in marine transportation, fisheries, and aquaculture, and in marine leisure and tourism.

Encourage sustainable and environmentally friendly harvesting of marine food resources, such as seaweed farming.

Lessen activities that negatively impact the carbon absorption capacity of the ocean.

When promoting business, contracting, or coastal development, prioritize the restoration and protection of coastal macrophytes, which provides not only seafood and income, but also carbon sequestration and storage.

Manage coastal ecosystems to increase and expand the distribution of seagrass beds, mangrove forests, and saltmarshes. Transform coastal development so as to rehabilitate coastal macrophytes as natural capital.

1.2.3   Present Status of Blue Carbon Ecosystems

In the UNEP report, mangrove forests, saltmarshes, and seagrass beds are all called blue carbon sinks, and they are most important in the sequestering and storing of ocean CO_2. These carbon sinks not only make a large contribution to the sequestration and storage of CO_2, but they also provide a variety of important ecological services, such as food and livelihood safety to human beings. From this standpoint, the blue carbon ecosystem is comparable to a rainforest in the terrestrial realm. In this section, we describe the characteristics of a blue carbon ecosystem, and we explain how and why it sequesters and effectively stores carbon.

In accord with the logic of the UNEP report, the morphological and structural arrangement of vegetation can be mentioned as a feature common to mangrove forests, saltmarshes, and seagrass beds. Saltmarshes and seagrass beds are formed by herbaceous plants, which are known to have a high shoot density and high growth rate (Pennings and Bertness 2001, Williams and Heck 2001). First, this dense vegetation creates a three-dimensional structure in the sea, provides a habitat for various marine organisms, and restricts the flow of seawater. Second, the vegetation grows in soft sediments, which are essential for carbon storage. In all mangrove forests, saltmarshes, and seagrass beds, dense vegetation restricts the flow of seawater and traps organic carbon drifting in the water column. The trapped organic carbon then accumulates in the sediment, where it is stored on site on time scales of centuries or more. There is a misconception that organic carbon is consumed and rapidly decomposed in extremely shallow coastal areas because of the high rates of biological processes, but the amount of organic carbon stored in these systems is

equivalent to the amount stored in terrestrial forests and the deep ocean on the same timeframe. The mechanism responsible for the high carbon sequestration and storage of blue carbon ecosystems accounts for this equivalence.

A characteristic that is not common to the three ecosystems is the habitat where the vegetation is formed. Saltmarshes and mangrove forests are formed in intertidal zones that undergo repeated submergence and emergence because of the tides. In extremely shallow waters, stems and leaves may emerge above the water but never dry out. These conditions are found especially at the mouths of brackish water estuaries, where freshwater and seawater mix with each other. Carbon dioxide from the atmosphere is then directly fixed via photosynthesis when the leaves are exposed to the atmosphere. For that reason, although these two ecosystems are clearly defined as blue carbon in the UNEP report, some researchers may regard saltmarshes and mangrove forests as being intermediate between green carbon and blue carbon systems. In other words, of the three ecosystems called blue carbon ecosystems, only seagrass beds consist of plants that are strictly marine and can sequester and store carbon in the subtidal zone. However, it has become clear that CO_2 in the atmosphere can also be directly absorbed by eelgrass. Chapter 6 provides details (Tokoro et al. 2018). The depths at which seagrass beds are found depend on which seagrass species forms the bed and can be as great as about 60 m (Coles et al. 2009). Seagrass beds are found over a wide range of salinities (Lirman and Cropper 2003, Koch et al. 2007). These characteristics of seagrasses suggest that they can be much more widely distributed than saltmarshes and mangrove forests, the habitats of which are restricted to intertidal areas along the coast. In the future, it will be very desirable to find a way to expand the areal distribution of seagrass beds (See Chaps. 12 and 13 for details; Nobutoki et al. 2018, Kuwae and Hori 2018) to achieve the coastal management goal of maintaining and improving the role of shallow coastal ecosystems in sequestering and storing blue carbon. Achieving that goal is one of the main reasons that seagrass beds are frequently cited as representative examples of blue carbon ecosystem in this chapter.

Table 1.1 compares some of the characteristics of seagrass beds, mangrove forests, and saltmarshes and the amounts of blue carbon they store versus the whole ocean. The values for seagrass beds, however, are derived from data for the genus *Posidonia* in the Mediterranean Sea and coastal waters of Australia as well as for some other fast-growing tropical seagrass species. It is therefore possible that the rates for seagrass beds are overestimates. The authors of the UNEP report have pointed out this potential bias, and caution is therefore necessary when citing this value. In particular, it is believed that belowground production tends to be larger for the genus *Posidonia* than for other seagrass genera, and thus the amount of organic carbon stored in the sediment tends to be greater in seagrass beds dominated by *Posidonia*. For example, in Japan the rate of organic carbon storage by eelgrass (*Zostera marina*) is almost equal to the rate of storage by the genus *Posidonia* in Australia, but it is only about one-fifth the rate of storage by the genus *Posidonia* in the Mediterranean (see Chap. 2 for details; Miyajima and Hamaguchi 2018).

Among the coastal macrophyte communities, mangrove forests and saltmarshes have the same storage rate per unit area, and those rates are slightly higher than the

Table 1.1 The areal distribution and carbon storage rates of shallow coastal ecosystems, modified from the UNEP report (Nellemann et al. 2009)

	Area ($\times 10^6$ km^2)	Storage rate per area (Average value and range) (Carbon t/ha/year)	Annual carbon storage amount (Range) (Carbon Tg/year)
Seagrass beds	0.33 (0.6)	0.83, 0.56–1.82 (1.37)	27.4–44 (82)
Mangrove forests	0.17 (0.3)	1.39, 0.20–6.54 (1.89)	17–23.6 (57)
Saltmarshes	0.4 (0.8)	1.51, 0.18–17.3 (2.37)	60.4–70 (190)
Three ecosystem totals	0.9 (1.7)	1.23, 0.18–17.3 (1.93)	114–131 (329)
Estuary/inner bay/outside bay (not included in above)	1.8	0.5	81.0
Continental shelf area	26.6	0.2	45.2
Above two total			126.2
Coastal area total			237.6 (454)
Percentage of blue carbon ecosystem relative to coastal area			46.89 (0.72)
Deep sea	330.0	0.00018	6.0
Total ocean			243.62 (460)
Percentage of blue carbon ecosystem relative to total ocean			45.73 (0.71)

The storage rate was calculated from the amount of organic carbon deposited in the sediment per unit area per unit time. The values in parentheses indicate the maximum value of the 95% confidence interval of the data

rates for seagrass beds. However, because seagrass beds have a more extensive distribution than mangrove forests, calculations of the rate of carbon storage for the whole earth have made more use of the value for seagrass beds than of that for mangrove forests. In the most recent calculations since the UNEP report, some revisions have been made to the value of each blue carbon ecosystem. The carbon storage rate of saltmarshes is the lowest, whereas the rates for mangrove forests and seagrass beds are similar (Table 1.2, Bridgham 2014). However, saltmarshes, mangrove forests, and seagrass beds all have a higher carbon storage rate than other coastal areas such as estuaries, continental shelves, and the deep sea. According to the IPCC Fifth Report (2013), since the Industrial Revolution, the total amount of black and brown carbon released by industrial activities has been about 555 billion tons, of which 160 billion tons are sequestered and stored as green carbon and 155 billion tons are sequestered and stored as blue carbon. The remaining 240 billion tons are in the atmosphere. In recent years, it is estimated that the annual rates of absorption by terrestrial vegetation and the ocean have been 2.3 billion tons C per year and 2.4 billion tons C per year, respectively. Recent emissions from human activities have averaged 9.4 billion tons C per year, and the residual amount in the atmosphere has been 4.7 billion tons C per year (Chap. 11; Kuwae et al. 2018). The total carbon sequestration rate on Earth has therefore been about 4.7 billion tons C per year. The areal carbon storage rate of blue carbon ecosystems is estimated to be 20–30 times that of terrestrial vegetation such as tropical rainforests (Table 1.2). Therefore, despite the fact that the total area of blue carbon ecosystems is less than

Table 1.2 Comparison of amounts and rates of carbon storage between blue carbon ecosystems and major ecosystems

	Global area (×10³ km²)	Carbon storage amount per area (Carbon Mg /ha)	Carbon storage rate per area (Carbon g/m²/year)	Annual carbon storage amount (Range) (Carbon Tg/year)
Seagrass beds	177	140	101	18
Mangrove forests	138	864	163	23
Saltmarshes	51	162	151	7.7
Peatlands	3341	1497	11	36
Tropical forests	19,623	238	4.0	79
Temperate forests	10,400	196	5.1	53
Boreal forests	13,700	117	4.6	49
Tropical savannah/ grasslands	15,000	187		
Temperate grasslands	9000	159	2.2	20
Shrublands	8500	122		
Deserts	18,000	91	0.8	14
Tundra	8000	166	1.2	10
Cropland	14,000	150		
Extreme	24,000	1		
Dessert/rock/ice				

Modified from Bridgham (2014)

2% that of tropical rainforests, the carbon storage rates of blue carbon ecosystems and tropical rainforests are similar.

It is therefore apparent that the area of coastal macrophytes makes a large contribution to the reduction of greenhouse gases, like terrestrial forests. However, the UNEP report also shows that coastal macrophytes are disappearing faster than tropical rainforests. The areas lost since the 1940s corresponds to about 35%, 35%, and 25% of the areas previously occupied by mangrove forests, seagrass beds, and saltmarshes, respectively. The decline of coastal macrophyte communities has continued. The recent estimated rate of decrease have been about 1.5 percent per year for these coastal vegetation, meaning that 0.15–1.02 billion tons of carbon dioxide are being released annually (Pendleton et al. 2012).

The areal extent of the blue carbon ecosystem along the Japanese coast has not been an exception to this pattern; a significant decrease has occurred. In particular, the areas occupied by saltmarshes and seagrass beds have decreased as a result of coastal developments throughout Japan for the past 100 years. The only exceptions to this pattern have been the mangrove forests in the Nansei Islands. The area of freshwater and saltwater marshes was about 2100 km² (of which Hokkaido accounted for 84%) in the 1910's and 1920's. That area had declined to only 820 km² (of which Hokkaido still accounted for 86%) in 1999 (Geospatial Information

Authority of Japan 2016). In addition, according to published data on seagrass beds in Japan, 2000 ha of eelgrass beds disappeared in only 13 years from 1978 to 1991. Moreover, in the Seto Inland Sea, where the area of eelgrass beds is large, about 16,000 ha of eelgrass beds disappeared between 1960 and 1991 because of coastal development and deterioration of water quality (Port and Airport Department, Chugoku Regional Bureau, 2016). Recently, however, seagrass beds have started to increase in Japan because of water quality improvements that have resulted from legal restrictions on nutrient inputs from the watersheds in some areas (Hori et al. 2018). This example illustrates the possibilities for restoring coastal macrophyte communities through water quality control and natural ecosystem resilience.

1.2.4 Other Ecosystems as Carbon Sinks

The UNEP report emphasizes the importance of the blue carbon ecosystem, where macrophytes sequester organic carbon and store it in the sediment. However, the blue carbon ecosystem is not the only sink of blue carbon in the ocean. Of the blue carbon storage capacity of the ocean, 30–50% is found outside the blue carbon ecosystem, and there are also shallow coastal water blue carbon sinks that have not yet been evaluated. Macroalgae are the most abundant vegetation in addition to the vascular plants found in blue carbon ecosystems.

   In recent years, scientific evidence has shown that macroalgae that grow on rocks in the absence of sediment also contribute to carbon storage after sequestering atmospheric CO_2 (Krause-Jensen and Duarte 2016). The carbon may be stored somewhere different from the place where the CO_2 is sequestered by the macroalgae, such as in tidal flats or the deep sea. If the connection between the discrete sources and sinks of blue carbon can be explained, it will be possible to assess the contribution of macroalgal vegetation to the blue carbon sink. Discussions about macroalgal vegetation as a blue carbon sink are incomplete in the UNEP report because there was inadequate understanding of the source–sink relationship at the time the report was written. Although there are no sufficiently accurate published summaries of the distribution of macroalgae at the global level, the UNEP report mentions that the evaluation of macroalgae with the largest distribution area and the largest amount of production on Earth is the next task. In this book, an example of macroalgal sequestration of CO_2 from the atmosphere is described in Chap. 6 (Tokoro et al. 2018), and Chap. 4 describes an example of a calculation of the amount of organic carbon sequestered by macroalgae along the coast of Japan (Yoshida et al. 2018). Chapter 2, which concerns organic carbon storage within seagrass beds, includes a discussion of carbon sources derived from macroalgae and phytoplankton that have drifted in and accumulated in the seagrass meadows (Miyajima and Hamaguchi 2018). There are estimated values of eelgrass (but not seaweed) exhibiting the same transportation process from shallow coastal areas to the deep sea as Chap. 9 (Abo et al. 2018). There is also much carbon storage derived from green carbon by a similar process in coastal marine ecosystems such as tidal

flats and estuaries, which are ecotones between the land and ocean. Chapter 11 (Kuwae et al. 2018) also discusses the fact that phytoplankton in estuaries and within bays can contributes to carbon storage.

1.3 Characteristics of Sequestration and Storage in Blue Carbon Ecosystems

In this section, the mechanism by which blue carbon ecosystems sequester and store blue carbon is discussed. To understand how blue carbon ecosystems sequester and store blue carbon, it is essential to understand the function of each ecosystem and its biological characteristics. We first describe the general biological characteristics of blue carbon ecosystems and also biogeographic features. The species that support the base of the ecosystem and that determine the biological and physicochemical characteristics of the ecosystem have been termed foundation species (Ellison et al. 2005). Blue carbon ecosystems have characteristic foundation species. They therefore provide characteristic ecosystem services, not just blue carbon sequestration and storage.

1.3.1 Saltmarshes on Tidal Flats

Saltmarshes form in the upper coastal intertidal zone, which is regularly flooded by seawater during high tides. The vegetation consists of dense stands of salt-tolerant plants including herbs, grasses, and short shrubs (Adams 1990, Woodroffe 2002). The dense vegetation exhibits extremely high primary production and also provides coastal protection by trapping and binding sediments (Woodroffe 2002, Chap. 8). Saltmarshes, along with seagrass ecosystems and mangrove forests, are sites of effective organic carbon sequestration and storage. These three ecosystems have recently been called blue carbon ecosystems, but they were originally recognized as ecosystems supporting diverse communities that include terrestrial organisms such as angiosperms, insects, birds, and mammals as well as marine organisms such as algae, molluscs, crustaceans, and fish (Pennings and Bertness 2001).

Saltmarshes are commonly found on shorelines that consist of muddy or sandy tidal flats with sluggish tidal movement and low wave action at almost all latitudes, but they are largely replaced by mangrove forests in the subtropics and tropics. (Pennings and Bertness 2001). Saltmarshes are therefore located primarily in temperate and higher latitudes (Fig. 1.3a). On the latest global map of saltmarshes by Mcowen et al. (2017), the global coverage of saltmarshes is estimated to be about 5.5×10^6 ha.

Fig. 1.3a Global map of saltmarsh distribution (bold-lined areas). Created with reference to UNEP-WCMC (2017a)

Species diversity in saltmarshes is not very high because the flora must be tolerant of harsh environments such as extremes in salinity, submersion, and anoxic sediment conditions. Marsh plant communities are well known for zonation based on the tidal level. The dominant species, which include glassworts and cordgrass (Pennings and Bertness 2001) or reeds (Chap. 8; Otani and Endo 2018), are determined by biogeographical constraints and the characteristics of the abiotic environment such as salinity and tidal levels.

1.3.2 Mangrove Forests on Tidal Flats in Subtropical and Tropical Regions

Mangrove forests also form unique coastal plant communities. They are found at the interface of land and sea, a habitat that encompasses elements of both terrestrial and marine environments. Mangrove forests are therefore sometimes characterized as terrestrial forests, despite the fact that mangrove trees grow in saline or brackish water in tropical and subtropical regions. Mangrove forests and saltmarshes become established under similar environmental conditions, but the former are found at subtropical and tropical latitudes and the latter in temperate and subarctic latitudes (Fig. 1.3b). The areal extent of mangrove forests has been thoroughly studied and is estimated to be about 1.52×10^7 ha globally (Chap. 3; Inoue 2018).

Mangrove forests consist of salt-tolerant mangrove trees that have complex salt-filtration systems as well as complex root systems to survive saltwater immersion and the anoxic conditions of the sediments. Red mangroves (*Rhizophora* spp.) can

b

Fig. 1.3b Global map of mangrove distribution (bold-lined areas). Created with reference to UNEP-WCMC (2017b)

exclude salt because their roots function as ultra-filtration systems to exclude sodium salts (Chap. 3; Inoue 2018). In addition, red mangroves have prop roots that extend into the water from higher up on the stem of the plant and can absorb air through pores in their bark. Black mangroves produce many pneumatophores that protrude from the soil like snorkels and allow them to breathe even in anoxic sediments rich in organic carbon.

The dense roots of mangroves form complex structures in the water that slow the flow of water and enhance sediment deposition as efficiently as other blue carbon ecosystems. The vegetative structures also protect coastal areas from erosion, storm surge, and tsunamis (Mazda et al. 2005, Danielsen et al. 2005), a service recognized as one form of Ecosystem-based Disaster Risk Reduction (Eco-DRR). The foundation species in coastal blue carbon ecosystems therefore provide a variety of ecosystem services shown as Chap. 13 (Kuwae and Hori 2018). The implication is that conservation and enhancement of blue carbon sequestration and storage will produce co-benefits for human beings.

1.3.3 Submerged Marine Plants and Differences in the Characteristics of Seagrasses and Other Species

There are two major groups of marine plants associated with blue carbon. One group is the phytoplankton, which are more-or-less neutrally buoyant in the water column. The other is a group of benthic plants. The latter is further broadly classified into two types: seaweeds and seagrasses. Both groups of marine plants are very

much involved in the sequestration and storage of blue carbon, but their contributions to blue carbon sequestration and storage differ between the two types of plants.

Phytoplankton is a designation that encompasses all floating photosynthetic organisms and therefore includes a wide variety of species. Although the functions of individual species and taxonomic groups vary, the function of sequestering CO_2 through photosynthesis is common. Benthic plants are secured to and live on the bottom of the ocean. Depending on the taxonomic group, the size and morphological characteristics of benthic plants ranges from a few micrometers to over 10 m. Benthic algae avoid drifting away from the ocean floor by attaching to hard, rocky substrates. Seaweeds are an especially large group of algae with a high ability to sequester blue carbon. The main groups of seaweeds are the relatives of kelp (family Succarinae, Eckloniae, etc.) and members of the *Sargassum* genus. Chapter 4 (Yoshida et al. 2018) provides details.

Neither neutrally buoyant phytoplankton nor macroalgae attached to rocks can directly bury blue carbon in the sediment. However, because both phytoplankton and macroalgae have high growth rates, their CO_2 uptake rates are very high (Chap. 4; Yoshida et al. 2018, Chap. 11; Kuwae et al. 2018). Because both phytoplankton and attached macroalgae take up inorganic carbon in large quantities from the surrounding seawater, the CO_2 partial pressure of the seawater surrounding them becomes lower than the CO_2 partial pressure in the atmosphere; hence, there is an influx of CO_2 from the atmosphere (Chap. 6; Tokoro et al. 2018). The carbon sequestered by phytoplankton and macroalgae can contribute to blue carbon storage if it is transported ex situ to shallow coastal areas or to the deep sea and subsequently buried in the sediments (Krause-Jensen and Duarte 2016).

Seagrasses are taxonomically different from macroalgae. The seagrass species are angiosperms that returned from the land to the ocean. Therefore, species of seagrass are classified differently from marine algae. Macroalgae are thought to have first appeared about 3 billion years ago, whereas seagrasses are believed to have evolved from terrestrial plants about 100 million years ago (Kato et al. 2003). Whereas algae include about 10,000 species (Murphy et al. 2015), seagrasses are divided into three families (four families if Posidoniaceae, the oldest lineage, is considered) with about 60 species (Short et al. 2007). Seagrasses may seem like rare plants because there are only 60 species of seagrasses on Earth, but in fact they are distributed over most of the Earth, from the tropics to the subarctic regions. They are absent only in polar regions (Fig. 1.3c). Among the 60 seagrass species, those distributed in the tropics and subtropics have lower shoot heights than those found in temperate latitudes (Hemminga and Duarte 2000). The canopy heights of tropical seagrasses are generally on the order of 10 cm, whereas those of temperate species such as *Zostera* sp. are more than 1 m and sometimes more than 2 m when environmental conditions are favorable for their growth.

The largest difference between seagrasses and other marine plants is that seagrasses are flowering plants that bloom in the sea and produce seeds. They therefore possess roots, stems and leaves; in addition, they inhabit areas with sandy or muddy sediment, and their roots and rhizomes penetrate into the sediment. Bamboos are analogous plants on land. Seagrasses extend their rhizomes in networks within the
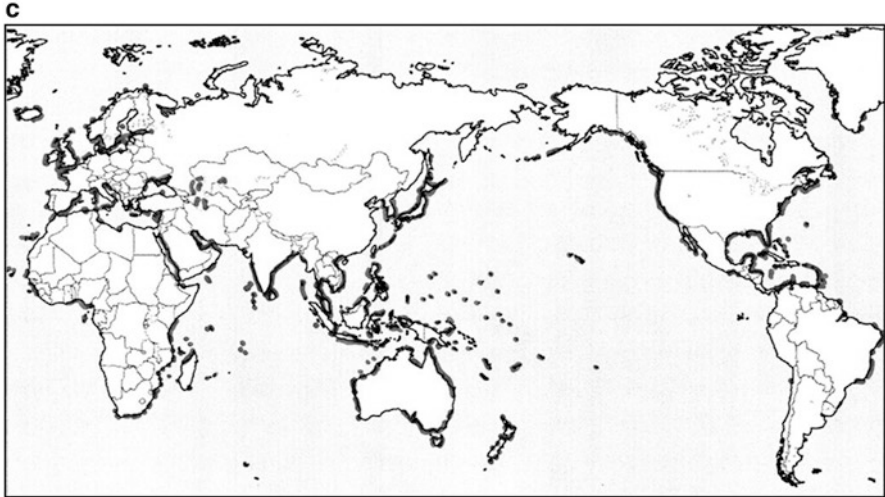
Fig. 1.3c Global map of seagrass distribution (bold-lined areas). Created with reference to UNEP-WCMC (2017c)

sediments, and new shoots can emerge above the sediment from that network. By increasing the number of their shoots in this way, it is possible for seagrasses to increase the coverage density of beds quickly. This method of propagation is called vegetative propagation. At the same time, it is also possible for seagrasses to multiply by producing seeds and allowing currents to disperse them. New shoots grow from the seeds if the seeds settle in a favorable location. This method of propagation is called seed propagation, or sexual propagation. The combination of these two reproductive modes makes it possible for a single seagrass species to cover an extensive area.

The rates of primary production in seagrass beds are the highest of any plant community on Earth (Duarte et al. 2010). Seagrass leaves have sheaths that extend from the sediment into the water column; the leaves grow rapidly and have the ability to sequester blue carbon as rapidly as any other marine plant. The three-dimensional structure slows the flow of seawater and promotes the accumulation of organic matter suspended in the water. Seagrasses thereby facilitate the storage of blue carbon. In addition, seagrass rhizomes extend into the sediment like a mesh that stabilizes bottom sediment. The stabilized sediment resists resuspension of deposited organic matter and enhances the storage of blue carbon by promoting sedimentation (Hendriks et al. 2008). In addition, the anoxic environment of the sediment suppresses decomposition of organic matter and thereby minimizes emission of blue carbon (Kristensen and Holmer 2001). The rhizomes also play a role as an organ for storing carbohydrates.

However, the ecological characteristics of roots, rhizomes, sheaths, and leaves differ among seagrass species. In general, leaves and sheaths exposed to seawater above the sediment are referred to as the aboveground parts of the seagrasses; the

rhizomes and roots in the sediment are collectively referred to as the belowground part. Differences in the biomasses of the aboveground and belowground parts as well as differences in reproductive and vegetative growth strategies of course influence the amount of blue carbon that is sequestered and stored. The aforementioned *Posidonia* is a typical example. *Posidonia* species such as *Posidonia oceanica* produce more belowground biomass than other seagrass species, and because accumulation of the belowground biomass forms a stratified structure, the storage of carbon is considerably greater for *Posidonia oceanica* than for other seagrass species. Also, even within the same species, the amount of production in the aboveground and belowground parts varies with local environmental factors. It is therefore difficult to say how much sequestration and storage of blue carbon takes place in a certain location if the data were collected in other locations or for other species. At the time the UNEP report was published, there were no data about eelgrass and no information about its role in sequestering and storing blue carbon. The absence of such information was one of the incentives for the publication of this book. In the next section, we explain the ecological characteristics of eelgrass to provide a better understanding of how eelgrass beds sequester and store blue carbon, as explained in Chap. 2 and later chapters.

1.3.4   Eelgrass: Characteristics of Zostera marina

Among the Japanese blue carbon ecosystems, we focus in this section on eelgrass. Eelgrass, *Zostera marina*, is said to be the most widely distributed marine plant on Earth and spreads uniformly from the temperate zone of the northern hemisphere to the subarctic zone (Orth et al. 2006). Fig. 1.3c shows the approximate global distribution of seagrass species. About 100 million years ago, *Zostera* species evolved in the temperate waters of Asia. After that time the habitat of *Zostera* sp. expanded as continental drift changed ocean basins and currents (Orth et al. 2006). At that time, the Indian continent and the African continent were not connected to the Eurasian continent. The Tethys Sea separated Asia from the Mediterranean Sea/European continent and extended through the present location of the Atlantic Ocean to the North American continent. Eelgrass is thought to have passed through this ocean corridor, circled the earth, and reached the Pacific coast of North America. This Tethys Sea corridor is believed to be the reason why eelgrass was able to spread throughout the northern hemisphere.

In addition, although eelgrass plants have an average lifespan of about 60 years (Hemminga and Duarte 2000), in a suitable habitat a single genet can live for more than 1000 years (Reusch et al. 1999). This long lifetime makes it possible for an eelgrass bed to store carbon in the sediments for a long period of time, similarly to the way terrestrial forests store carbon in soil. Studying eelgrass therefore helps to elucidate carbon sequestration and storage mechanisms in coastal macrophyte communities found throughout both hemispheres. The broad geographical distribution of eelgrass is extremely important from the standpoint of identifying countermea-

Table 1.3 Seagrass species and the ranges of their distributions along the coast of Japan

Name	General distribution	Code[a]
ZOSTERACEAE		
Phyllospadix iwatensis	Northeastern Japan	1
Phyllospadix japonicus	Northeastern Japan	2
Zostera asiatica	Pacific coast of Northern Honsyu, Hokkaido	3
Zostera caespitosa	Northern Honsyu, Hokkaido, Japan Sea	4
Zostera caulescens	Eastern Honsyu, Japan Sea	5
Zostera japonica	From Hokkaido to Southwestern Islands	6
Zostera marina	From Hokkaido to southern Kyushu	7
CYMODOCEACEAE		
Cymodocea rotundata	Southwestern Islands	8
Cymodocea serrulata	Southwestern Islands	9
Halodule piniforlia	Southwestern Islands	10
Halodule uninervis	Southwestern Islands	11
Syringodium isoetifolium	Southwestern Islands	12
HYDROCHARITACE		
Enhalus acoroides	Yaeyama Islands	13
Thalassia hemprichii	Southwestern Islands	14
Halophila decipiens	Southwestern Islands	15
Halophila ovalis	From northern Honsyu to Southwestern Islands	16

[a]Note: The general distribution of each species is shown with its number code in Supplemental Fig. 1.1

sures against global warming. This consideration is also one of the main reasons why several chapters in this book focus on eelgrass.

Among the 60 seagrass species, three families comprising 15 marine species have been identified along the coast of Japan. The coast of Japan is therefore a seagrass hotspot (Table 1.3). In particular, there are endemic species of the genus *Zostera*, which are found along the Japanese archipelago. The area of seagrass beds along the coast of Japan is about 6×10^4 ha (Chap. 4; Yoshida et al. 2018). Among these seagrasses, the Zosteraceae family dominates in the main islands of Japan, from the northern border to Kagoshima Bay (on the south coast of Kyushu), which forms the southern limit of the distribution of *Zostera marina* (Fig. 1.4). In the Ryukyu Islands, which constitute the southern part of the Japanese archipelago, *Zostera japonica* and species of the families Cymodoceaceae and Hydrocharitaceae are found. Eelgrass has two modes of reproduction (vegetative propagation and seed propagation) as described above, and as a result it has two life cycles (Fig. 1.5). The life cycle based on seed propagation lasts only 1 year. Germination from seeds occurs from autumn to winter, and the plant continues to grow as a flower-only stock, characterized as flowering shoots. Flowering and fruiting occurs from spring to early summer, and the plants die after seeding. They remain as seeds in the summer and germinate in autumn and winter. The cycle is then repeated. In this life
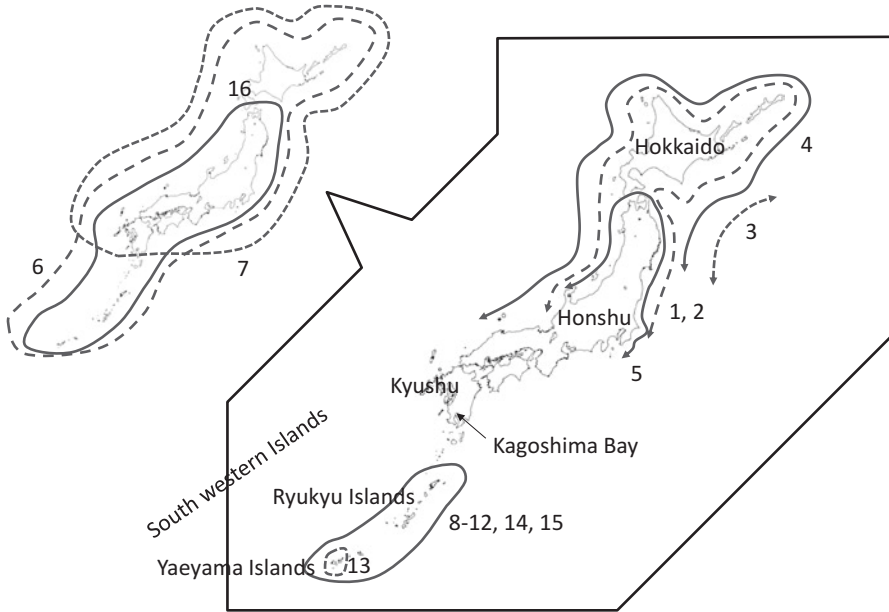
Fig. 1.4 General distribution of each seagrass species in Japan. See Table 1.3 for meaning of number codes
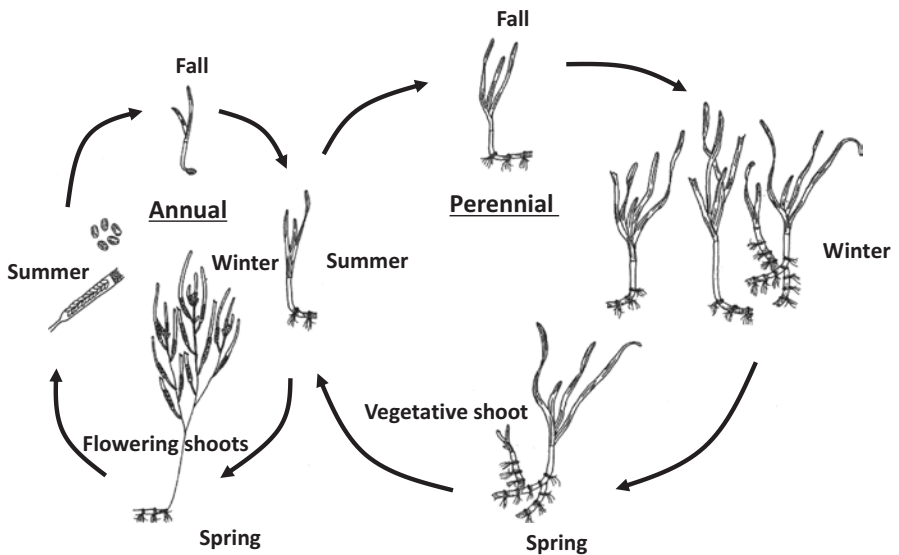

Fig. 1.5 Life cycle of eelgrass (*Zostera marina*). The left side shows the annual life cycle of flowering shoots, and the right side illustrates the perennial life cycle of vegetative shoots

cycle, a rhizome is not created, and the aboveground part of the plant withers after 1 year. The eelgrass enters a non-vegetative state once each year.

The other life cycle is a perennial life cycle that uses both reproductive modes to propagate. First it germinates from a seed and resembles an annual shoot, but later it grows rhizomes and leaves as vegetative shoots. In the summer, when the seawater temperature rises, some leaves die, but many aboveground and belowground parts survive. From autumn to winter, the rhizome expands again, new vegetative shoots sprout from the expanded rhizomes, and vegetative growth continues. Depending on the nutritional status of the plants, seed propagation similar to the annual cycle may also occur.

It is unclear how the eelgrass switches between the life cycles for different purposes and how environmental conditions determine which life cycle will be used. In general, it is thought that perennial life cycles predominate when the habitat is suitable for eelgrass, and an annual life cycle is more common in harsh environments (Hemminga and Duarte 2000). For example, at the southern limit in Kagoshima Bay, the life cycle of eelgrass is annual. This life cycle enables the eelgrass to survive over the summer as seeds when the high temperatures would otherwise be lethal (Japan Fisheries Agency 2007, Shimabukuro et al. 2012). Of these two life cycles, the perennial cycle is associated with the highest rate of storage of blue carbon. In the case of the annual cycle, even if blue carbon is stored in the sediment via sedimentation facilitated by the aboveground parts, it is often resuspended during the summer season when the vegetative structure completely disappears. Therefore, even though the annual cycle can sequester carbon, the annual cycle of eelgrass, like that of macroalgae, is considered to store relatively little blue carbon compared to the perennial cycle.

1.4 Toward Maintenance, Improvement, and Management of Blue Carbon Sinks with Co–benefits

To explain the choice of topics discussed in detail in this book, we have summarized the UNEP report on blue carbon, the current status of blue carbon sinks, and the importance of seagrasses as blue carbon sinks. In this section, we explain the knowledge needed from a management standpoint to maintain and improve the blue carbon sink as an ecosystem service of the seagrass ecosystem along with other ecosystem services. Knowledge of the biological community and the interactions therein, the trophic level structure, and the physical environment suitable for growth are required to conserve and restore perennial eelgrass communities. Such conservation and restoration are important for the sequestration and storage of blue carbon. We therefore first introduce the characteristics of eelgrass plants as an ecosystem and then discuss ecosystem management based on that knowledge.
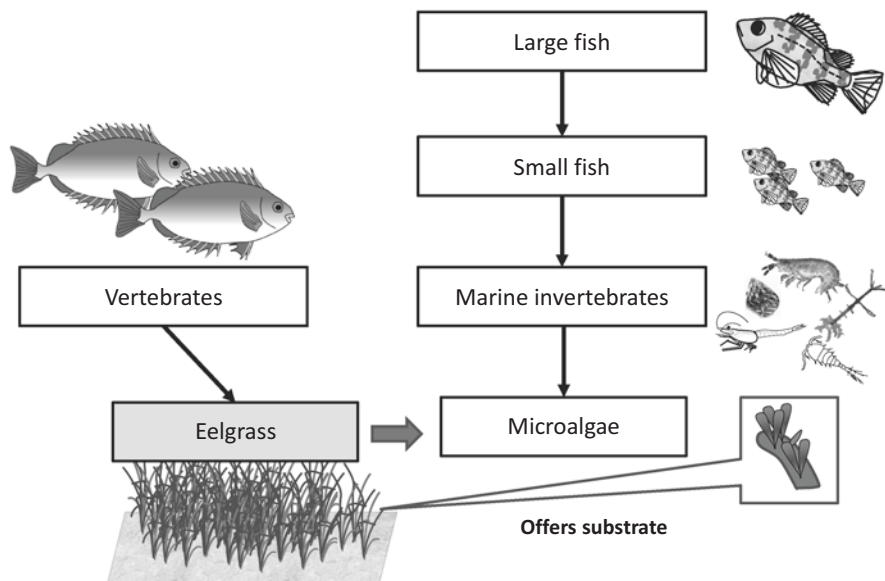
Fig. 1.6   General trophic structure of eelgrass beds

1.4.1   Biodiversity and Community Structure of Eelgrass Beds

Figure 1.6 shows the basic trophic level structure of the biological community associated with seagrass beds. Few marine animals feed directly on seagrasses. Among invertebrates, it is known that some gammaridean amphipods or sea urchins can directly graze seagrass vegetation. More vertebrates than invertebrates can feed directly on seagrasses (Valentine and Duffy 2007). Those vertebrates include dugongs and manatees, sea turtles, and some waterfowl and fish species. Eelgrass beds form habitat for large numbers of various small marine invertebrates, including grazers such as gammaridean amphipods, caprellids, mysid shrimps, and snails, which are generally less than a few centimeters in size. These grazers feed predominantly on microalgae (such as epiphytic diatoms) that grow on eelgrass leaves. Small fish feed on these grazers, and larger fish, which feed on small fish, are the top predators. If we compare this trophic structure of the seagrass-associated community with those of terrestrial ecosystems, grazers are equivalent to insects; small fish are equivalent to large insects that eat other insects, spiders and frogs; and large fish correspond to birds. In particular, the three-dimensional structure created by eelgrass beds becomes a shelter that protects small fishes from predators and waves. The abundant grazers function as food for small fish. Eelgrass beds are thus known as nurseries for marine organisms.

Organisms that feed directly on eelgrass will thus affect the sequestration and storage of blue carbon. Among the animal communities in eelgrass beds, grazers

that consume epiphytes on the seagrass leaves play an especially important role in the sequestration and storage of blue carbon. The epiphytes growing on the leaves are an important source of primary production that support the associated animal community. However, if the epiphyte biomass becomes excessive, the epiphytes will smother the leaves, hinder photosynthesis by the eelgrass itself, and may cause the eelgrass to die. Small grazers therefore play an important role in removing microalgae, preventing epiphytic biomass from becoming excessive, and thereby improving the growth of the eelgrass shoots.

The importance of this function has been demonstrated in field experiments throughout the entire area of eelgrass distribution in the northern hemisphere (Duffy et al. 2015). In those studies, 15 experimental sites were established in all areas where eelgrass is found in the northern hemisphere, and growth of eelgrass was used as a short-term index of ecosystem functionality at each site. The diversity and abundance of small invertebrates were artificially manipulated simultaneously at all experimental sites for this large-scale comparison. The results showed that as the diversity and abundance of invertebrate grazers increased, the amount of eelgrass growth increased significantly (Hori 2015). This result suggests that the growth of eelgrass and the associated rate of carbon sequestration are affected by invertebrate grazers. If the grazers disappear, the growth of eelgrass will be reduced by the epiphytes. The reduction of growth would cause a partial collapse of the three-dimensional structure and distribution of the eelgrass beds. Such an impact would lower the tendency of the eelgrass beds to effect sedimentation (Chap. 2; Miyajima and Hamaguchi 2018) and further reduce their storage of blue carbon.

The grazers, of course, affect more than the relationship between eelgrass and the associated epiphytes and grazers. Predatory pressures of small fish on grazers can change the diversity and abundance of grazers, and large fish can change the predation pressure on grazers from small fish. In this way, the mechanism associated with sequestering and storing blue carbon in eelgrass beds includes not only the biological characteristics of the above-mentioned eelgrass itself but also the inter-relationships of the many creatures inhabiting the eelgrass beds. In other words, the diversity of the whole biological community is involved. Also, the structure of the eelgrass beds and the associated biological community are closely related to the supply of nutrients, the cycling of materials, and the physicochemical environment included in the ecosystem. Taking into consideration the entire ecosystem is important for its management of for maintaining and improving the role of eelgrass beds in sequestering and storing blue carbon.

1.4.2   Ecosystem Management of Eelgrass

The UNEP report also emphasized the importance of implementing management policies that target not only coastal vegetation but also the whole ecosystem, i.e. ecosystem management. According to the literature (Iwasa et al. 2003), ecosystem management is defined as managing not only for target species but also for multiple

species and ecosystems as a strategy for management of biological resources. Here, biological resource management means maintaining biological resources useful for humans in a sustainable and efficient manner. This management strategy not only targets effective and appropriate resource use but also the maintenance of habitats that enable successful reproduction of the target species and prey and predator interactions throughout the entire ecosystem.

Ecosystem management was originally assumed to focus on resources used by humans, but in recent years the viewpoint that consideration should be given to ecosystems for their own sake has become stronger. Biological resources used by humans are now considered as ecosystem services. This concept includes the idea that biological resources consist of natural capital (stock) and surplus capital (flow). The latter originates from the natural capital, and the surplus is used by human beings as ecosystem services (Ministry of the Japanese Environment 2014). Although human life is supported by "ecosystem services, which bring various blessings from nature" such as food, water, climate mitigation, etc., there is no universally accepted method to evaluate such ecosystem services. The fact that the value of the natural environment is not being determined appropriately and that the natural environment is used excessively as a resource for business activities of companies freely or at low cost is viewed as a large problem in the world.

The idea of regarding the natural environment as "natural capital" and appropriately evaluating and managing it as capital that supports business activities was first proposed in the final report led by the UNEP and the government of Germany, "The Economics of Ecosystem and Biodiversity", in the 2010 Convention of Biological Diversity (COP10). At the 2012 UN-sponsored "United Nations Conference on Sustainable Development" (Rio + 20), "The Declaration of Natural Capital" was proposed as a way to communicate this idea of "natural capital" to society, so that financial institutions around the world could incorporate the idea that natural capital should be recognized in the context of financial products and services. This concept was adopted by the "Intergovernmental Science-Policy Platform on Biodiversity and Ecosystem Services" (IPBES), which is described in Chap. 13. Fundamentally, the idea suggests that appropriately determining the value of natural capital and managing it accordingly will stabilize the lives of citizens and increase the sustainability of corporate operations. If management is based on this idea, then the goal of management will be effective and appropriate use of natural capital. With respect to blue carbon, coastal flowering plants are natural capital, and thus the sequestration and storage of CO_2 is an ecosystem service provided by that natural capital.

In addition to sequestering and storing blue carbon, seagrass beds provide various ecosystem services to human beings. As noted in the UNEP Report, seagrass beds are an important habitat of biological production that supports coastal seafood production. The sedimentation function of seagrass beds not only facilitates sequestration and storage of CO_2 but also helps to buffer coastlines from sea level rise and increased storm damage associated with climate change. For the purpose of effectively and appropriately using these ecosystem services, it is important to consider ecosystem management of natural capital. An example pointed out in the previous

section was the role of biodiversity in eelgrass growth. Maintaining and improving the sequestration and storage function of blue carbon thus requires management of the entire ecosystem. The other ecosystem services cited here will also be greatly influenced by the productivity of the eelgrass and the scale of the vegetative structure. Proper management of seagrass vegetation as a natural capital will provide ecosystem services that support human societies in coastal regions. Management that maintains and improves the sequestration and storage function of blue carbon must be one of the cornerstones of any approach to balance the conservation and restoration of natural ecosystems with the economic activities of human beings. Specific examples and the recent efforts of the international community are introduced in Chaps. 12 and 13 (Nobutoki et al. 2018; Kuwae and Hori 2018).

1.4.3   Conclusion: The Prospects for Blue Carbon Research

In this chapter, through an interpretation of the Blue Carbon Report, we have pointed out the ecological issues that underlie the sequestration and storage of blue carbon in shallow coastal areas. If the interaction between the global scientific aspects of CO_2 sequestration and the biological driving forces behind them have been clarified, the aim of this chapter will have been achieved. Before the word "blue carbon" was envisaged, studies directly related to blue carbon, such as the calculation of primary production and amount of organic carbon deposited in the sediment, were actively conducted in saltmarshes, mangrove forests, and seagrass beds. However, these studies were aimed at elucidating local ecological processes, such as the ecosystem function of the target ecosystem and the mechanism by which biodiversity is created and maintained.

The authors themselves are interested in the organic carbon contained in the sediments of eelgrass beds in the context of food web theory. That organic carbon, the leftover organic matter in the sediment, contributes to the food web structure of both the grazing and detritus food chains. As we encountered the word blue carbon, the current data took on another importance in the context of climate change. We hope that those who have read the UNEP report or those who have read this book will have the same impression. The scientific data relevant to blue carbon is very scarce. More and better information is needed to guide policy making and other governance processes in relation to climate change mitigation and adaptation strategies using blue carbon. The ongoing global warming has a fatal influence on coastal vegetation. Rocky-shore denudation, referred to as "sea desertification" or "sea fire", where macroalgal vegetation is suddenly replaced by coralline algae, giving the appearance of rock bleaching, is becoming more typical.

In addition, those who are interested in coastal areas—including administrative officials, companies, and non-profit organizations— realize the increasing global scale of environmental changes. Those organizations and people should aim for a possible sustainable model of blue carbon for society. We wonder if they recognize the importance of coastal management that takes into consideration blue carbon. Is

green carbon considered in the context of forest management in terrestrial areas? There is no doubt that coastal vegetation such as seagrass beds help to sustain our food supply and protect our coastlines. In recent years, concern has emerged regarding changes in the distribution of commercial fish species and the decline of the catch due to global warming. Some of these changes have been due to loss of fish habitat, that is, loss of vegetated coastal areas due to global warming. In contrast, coastal vegetation itself functions to mitigate global warming. Protecting coastal vegetation should therefore be considered a fundamental component of a solution to many concerns about global warming. We sincerely hope that this book can assist in solving this problem.

References

Abo K, Sugimatsu K, Hori M, Yoshida G, Shimabukuro H, Yagi H, Nakayama A, Tarutani K (2018) Quantifying the fate of captured carbon: from seagrass meadow to deep sea. In: Kuwae T, Hori M (eds) Blue carbon in shallow coastal ecosystems: carbon dynamics, policy, and implementation. Springer, Singapore, pp 251–271

Adam P (1990) Saltmarsh ecology. Cambridge University Press, New York

Bridgham SD (2014) Carbon dynamics and ecosystem processes. In: Batzer DP, Sharitz RR (eds) Ecology of freshwater and estuarine wetlands. University of California Press, Berkeley, pp 277–309

Coles R, Mckenzie L, De'ath G, Roelofs A, Long WL (2009) Spatial distribution of deep-water seagrass in the inter-reef lagoon of the Great Barrier Reef World Heritage Area. Mar Ecol Prog Ser 392:57–68

Danielsen F, Sorensen MK, Olwig MF, Selvam V, Parish F, Burgess ND, Hiraishi T, Karunagaran VM, Rasmussen MS, Hansen LB, Quarto A, Suryadiputra N (2005) The Asian tsunami: a protective role for coastal vegetation. Science 310:643

Duarte CM, Marba N, Gacia E, Fourqurean JW, Beggins J, Barron C, Apostolaki ET (2010) Seagrass community metabolism: assessing the carbon sink capacity of seagrass meadows. Glob Biogeochem Cycles 24. https://doi.org/10.1029/2010GB003793

Duffy JE, Reynolds PL, Bostrom C, Coyer JA, Cusson M, Donadi S, Douglass JG, Eklof JS, Engelen AH, Eriksson BK, Fredriksen S, Gamfeldt L, Gustafsson C, Hoarau G, Hori M, Hovel K, Iken K, Lefcheck JS, Moksnes P, Nakaoka M, O'Connor M, Olsen JL, Richadson JP, Ruesink JL, Sotka EE, Thormar J, Whalen MA, Stachowicz JJ (2015) Biodiversity mediates top-down control in eelgrass ecosystems: a global comparative-experimental approach. Ecol Lett 18:696–705

Ellison AM, Bank MS, Clinton BD, Colburn EA, Elliottk A, Ford CR, Foster DR, Kloeppel BD, Knoepp JD (2005) Loss of foundation species: consequences for the structure and dynamics of forested ecosystems. Front Ecol Environ 3:479–486

Geospatial Information Authority of Japan (2016) The survey report of the change in wetland areas of Japan. http://www.gsi.go.jp/kankyochiri/shicchimenseki2.html

Hemminga MA, Duarte CM (2000) Seagrass ecology. Cambridge University Press, Cambridge, p 298

Hendriks LE, Sintes T, Bouma TJ, Duarte CM (2008) Experimental assessment and modeling evaluation of the effects of the seagrass Posidonia oceanica on flow and particle trapping. Mar Ecol Prog Ser 356:163–173

Hori M (2015) The conservation of seagrass meadows: epifaunal biodiversity will support the ecosystem functionings of seagrass meadows. Yutakana Umi 37:3–6 (in Japanese)

Hori M, Hamaoka H, Hirota M, Lagarde F, Vaz S, Hamaguchi M, Hori J, Makino M (2018) Application of the coastal ecosystem complex concept toward integrated management for sustainable coastal fisheries under oligotrophication. Fish Sci 84:283–292

Inoue T (2018) Carbon sequestration in mangroves. In: Kuwae T, Hori M (eds) Blue carbon in shallow coastal ecosystems: carbon dynamics, policy, and implementation. Springer, Singapore, pp 73–99

IPCC (2013) The fifth assessment report by WG1: the physical science basis and summary for policymakers. (Opened in the Ministry of the Environment, Japan; http://www.env.go.jp/earth/ipcc/5th/)

Iwasa Y, Matsumoto T, Kikuzawa K, The Ecological Society of Japan (2003) The dictionary of ecology. Kyouritsu-syuppan publishing, Tokyo, p 682 (in Japanese)

Japan Fisheries Agency (2007) The guideline for seagrass restoration. pp 128

Kato Y, Aioi K, Omori Y, Takahata N, Satta Y (2003) Phylogenetic analyses of Zostera species based on rbcL and matK nucleotide sequences: implications for the origin and diversification of seagrasses in Japanese waters. Genes Genet Sys 78:329–342

Koch MS, Schopmeyer SA, Kyhn-Hansen C, Madden CJ, Peters JS (2007) Tropical seagrass species tolerance to hypersalinity stress. Aquat Bot 86:14–24

Krause-Jensen D, Duarte CM (2016) Substantial role of macroalgae in marine carbon sequestration. Nat Geosci 9:737–742

Kristensen E, Holmer M (2001) Decomposition of plant materials in marine sediment exposed to different electron acceptors (O_2, NO_3^-, and SO_4^{2-}), with emphasis on substrate origin, degradation kinetics, and the role of bioturbation. Geochim Cosmochim Acta 65:419–433

Kuwae T, Hori M (2018) The future of blue carbon: addressing global environmental issues. In: Kuwae T, Hori M (eds) Blue carbon in shallow coastal ecosystems: carbon dynamics, policy, and implementation. Springer, Singapore, pp 347–373

Kuwae T, Kanda J, Kubo A, Nakajima F, Ogawa H, Sohma A, Suzumura M (2018) CO_2 uptake in the shallow coastal ecosystems affected by anthropogenic impacts. In: Kuwae T, Hori M (eds) Blue carbon in shallow coastal ecosystems: carbon dynamics, policy, and implementation. Springer, Singapore, pp 295–319

Larkum AWD, Drew EA, Ralph PJ (2006) Photosynthesis and metabolism in seagrasses at the cellular level. In: Larkum AWD, Orth RJ, Duarte CM (eds) Seagrasses: biology, ecology and conservation. Springer, Dordrecht, pp 323–345

Lirman D, Cropper WP Jr (2003) The influence of salinity on seagrass growth, survivorship, and distribution within Biscayne Bay, Florida: field experimental, and modeling studies. Estuaries 26:131–141

Mazda Y, Kobashi D, Okada S (2005) Tidal-scale hydrodynamics within mangrove swamps. Wetl Ecol Manag 13:647–655

Mcowen CJ, Weatherdon LV, Bochove JWV, Sulliva E, Blyth S, Zockler C, Stanwell-Smith D, Kingston N, Martin CS, Spalding M, Fletcher S (2017) A global map of saltmarshes. Biod Dat J 5:e11764

Ministry of the Environment (2014) The 2014 report of the Environmental white paper http://www.env.go.jp/policy/hakusyo/past_index.html (in Japanese)

Miyajima T, Hamaguchi M (2018) Carbon sequestration in sediment as an ecosystem function of seagrass meadows. In: Kuwae T, Hori M (eds) Blue carbon in shallow coastal ecosystems: carbon dynamics, policy, and implementation. Springer, Singapore, pp 33–71

Murphy JD, Drosg B, Allen E, Jerney J, Xia A, Herrman C (2015) A perspective on algal biogas. IEA bioenergy, eBook electronic edition, pp 39

Nellemann C, Corcoran E, Duarte CM, et al (2009) Blue carbon: a rapid response assessment. United Nations Environmental Programme, GRID-Arendal, Birkeland Trykkeri AS, Birkeland

Nobutoki M, Yoshihara T, Kuwae T (2018) Carbon offset utilizing coastal waters: Yokohama blue carbon project. In: Kuwae T, Hori M (eds) Blue carbon in shallow coastal ecosystems: carbon dynamics, policy, and implementation. Springer, Singapore, pp 321–346

Orth RJ, Carruthers TJB, Dennison WC, Duarte CM, Fourqurean JW, Heck KL Jr, Hughes AR, Kendrick GA, Kenworthy WJ, Olyarnik S, Short FT, Waycott M, Williams SL (2006) A global crisis for seagrass ecosystems. BioScience 56:987–996

Otani S, Endo T (2018) CO_2 flux in tidal flats and salt marshes. In: Kuwae T, Hori M (eds) Blue carbon in shallow coastal ecosystems: carbon dynamics, policy, and implementation. Springer, Singapore, pp 223–250

Pendleton C, Donato DC, Murray BC, Crooks S, Jenkins WA, Sifleet S, Craft C, Fourqurean JW, Kauffman JB, Marba N, Megonigal P, Pidgeon E, Herr D, Gordon D, Baldera A (2012) Estimating global "blue carbon" emissions from conversion and degradation of vegetated coastal ecosystems. PLoS One 7:e43542. https://doi.org/10.1371/journal.pone.0043542

Pennings SC, Bertness MD (2001) Salt marsh communities. In: Bertness MD, Gaines SD, Hay ME (eds) Marine community ecology. Sinauer Associates, Sunderland, pp 289–316

Port and Airport Department, Chugoku Regional Bureau (2016) The database of the water environments in Seto Inland Sea: change in the area of tidal flats and seagrass and macroalgal beds, the Ministry of Land, Infrastructure, Transport and Tourism. http://www.pa.cgr.mlit.go.jp/chiki/suishitu/seto/env/env_001.html) (in Japanese)

Reusch TB, Bostrom C, Stam WT, Olsen JL (1999) An ancient eelgrass clone in the Baltic. Mar Ecol Prog Ser 183:301–304

Shimabukuro H, Hori M, Yoshimitsu S, Tokunaga N, Igari T, Sasaki K, Nakaoka M, Kawane M, Yoshida G, Hamaguchi M (2012) Genetic differentiation of annual *Zostra marina* growing in Kagoshima Bay, Kagoshima, Japan based on an analysis using microsatellite markers. Nippon Suisan Gakkaishi 78:204–211

Short F, Carruthers T, Dennison W, Waycott M (2007) Global seagrass distribution and diversity: a bioregional model. J Exp Mar Biol Ecol 350:3–20

Tokoro T, Watanabe K, Tada K, Kuwae T (2018) Air–water CO_2 flux in shallow coastal waters: theoretical background, measurement methods, and mechanisms. In: Kuwae T, Hori M (eds) Blue carbon in shallow coastal ecosystems: carbon dynamics, policy, and implementation. Springer, Singapore, pp 153–184

UNEP-WCMC (2017a) Global distribution of Saltmarshes. http://data.unep-wcmc.org/datasets/43

UNEP-WCMC (2017b) Global Distribution of Mangroves. http://data.unep-wcmc.org/datasets/5

UNEP-WCMC (2017c) Global Distribution of Seagrasses. http://data.unep-wcmc.org/datasets/7

Valentine JF, Duffy JE (2007) The central role of grazing in seagrass ecology. In: Larkum AWD, Orth RJ, Duarte CM (eds) Seagrasses: biology, ecology and conservation. Springer, Dordrecht, pp 463–501

Watanabe A, Nakamura T (2018) Carbon dynamics in coral reefs. In: Kuwae T, Hori M (eds) Blue carbon in shallow coastal ecosystems: carbon dynamics, policy, and implementation. Springer, Singapore, pp 273–293

Williams S, Heck KL Jr (2001) Seagrass communities. In: Bertness MD, Gaines SD, Hay ME (eds) Marine community ecology. Sinauer Associates, Sunderland, pp 317–337

Woodroffe CD (2002) Coasts: form, process an evolution. Cambridge University Press, New York

Yoshida G, Hori M, Shimabukuro H, Hamaoka H, Onitsuka T, Hasegawa N, Muraoka D, Yatsuya K, Watanabe K, Nakaoka M (2018) Carbon sequestration by seagrass and macroalgae in Japan: estimates and future needs. In: Kuwae T, Hori M (eds) Blue carbon in shallow coastal ecosystems: carbon dynamics, policy, and implementation. Springer, Singapore, pp 101–127

Chapter 2
Carbon Sequestration in Sediment as an Ecosystem Function of Seagrass Meadows

Toshihiro Miyajima and Masami Hamaguchi

Abstract Seagrass meadows have the potential to sequester large amounts of organic carbon (OC) in underlying sediments as detrital OC. This ecosystem function of seagrass meadows depends not only on the high primary productivity of seagrasses and associated algae, but also on the physical and hydrological properties of seagrass meadows that accumulate fine-grained mineral sediment and allochthonous organic matter and stabilize the sediment. The burial efficiency of OC in marine sediment is constrained principally by (i) structural recalcitrance of accumulated organic matter, (ii) enhancement of OC preservation through organic–mineral interactions, and (iii) the length of the oxygen exposure time in the reactive layer of sediment. We discuss how these mechanisms contribute to and constrain OC sequestration in seagrass sediments. From the sediment source–sink perspective, long-term carbon sequestration capacity can be viewed as an emergent property of coastal vegetated ecosystems such as seagrass meadows. Sequestration of OC also depends on the nature of the OC supplied, which is largely determined by the origin of the OC. The major sources of OC to seagrass meadow sediments are reviewed and classified in terms of their mode of transport and degradability in the early diagenetic process. The available methods of evaluating various OC sources, including recently developed environmental DNA techniques, are also critically reviewed. Finally, available data are compiled on the concentration and burial rate of OC in seagrass meadow sediments and a tentative global estimate of the long-term (~1000 years) OC sequestration rate in seagrass meadows as 1.6–9.4 Tg C year^{-1} is provided. This is lower than previous estimates of the global OC burial rate in seagrass meadows.

T. Miyajima (✉)
Atmosphere and Ocean Research Institute, The University of Tokyo, Kashiwa, Chiba, Japan
e-mail: miyajima@aori.u-tokyo.ac.jp

M. Hamaguchi
National Research Institute of Fisheries and Environment of Inland Sea, Japan Fisheries Research and Education Agency, Hatsukaichi, Hiroshima, Japan

2.1   Introduction

"Blue carbon" is conventionally defined as the organic carbon (OC) produced and stored by "coastal vegetated ecosystems", such as mangroves, seagrass meadows, and tidal salt marshes (Siikamäki et al. 2012). These ecosystems have developed as a result of the adaptation and colonization of certain terrestrial vascular plants to coastal marine environments (e.g., Les et al. 1997). The distribution of coastal vegetated ecosystems is generally confined to well-illuminated land–sea interface zones where clastic (alumino-)silicate and/or biogenic carbonate sediment accumulates. According to recent estimates compiled by Siikamäki et al. (2012), there are ~140,000 km^2 of mangroves, ~320,000 km^2 of seagrass meadows, and ~51,000 km^2 of salt marshes worldwide, although the estimates of seagrass and tidal marsh areas are uncertain. Approximately 95% of mangroves and 70% of seagrass meadows are believed to be in tropical and subtropical regions, whereas salt marsh is typically found in temperate and boreal regions.

Geochemical and biogeochemical processes that transform an element from highly mobile and/or reactive forms into inert, spatially confined reservoirs with much longer residence times are collectively referred to as "sequestration" (Gorham et al. 1979; Klee and Graedel 2004). Carbon biosequestration is a series of ecosystem processes through which atmospheric carbon dioxide (CO_2) is captured first by plants and incorporated into their biomass and then converted through multiple reaction steps into refractory detrital OC, which is stored in soil and sediment reservoirs for a long time. Coastal vegetated ecosystems are characterized by high rates of carbon capture (primary productivity) by dominant vascular plants and associated algae (Hori and Kuwae (2018) in this volume). An even more important characteristic of these ecosystems is the disproportionally large belowground stock of detrital OC compared with living biomass (Table 2.1). In fact, the quantity of OC stored as detrital OC in soils and sediments is, on average, more than double (mangroves; see Inoue (2018) in this volume) or one to two orders of magnitude greater (seagrass meadows and salt marsh) than that of OC stored in living biomass (Donato et al. 2011; Alongi 2012; Fourqurean et al. 2012; Siikamäki et al. 2012; Alongi et al. 2016). For these reasons, these ecosystems have been regarded as the most efficient natural systems for long-term carbon sequestration.

On average, at least half of the detrital OC stored in the soils and sediments of these ecosystems is considered of autochthonous origin, derived mainly from the belowground biomass of vegetation (Middelburg et al. 1997; Bouillon et al. 2008; Kennedy et al. 2010; Miyajima et al. 2015). However, the correlation between the standing stock of biomass OC and the detrital OC pool in soils and sediments is generally weak or absent in mangroves and seagrass meadows (Kennedy et al. 2010; Donato et al. 2011; Fourqurean et al. 2012; Alongi et al. 2016), indicating that the size of the soil and sediment OC pool in these two ecosystem types is not determined simply by the primary production of the vegetation but is also constrained significantly by some other biological or geophysical factors. Identifying these factors and understanding their roles are essential to evaluating the global carbon sequestration capacity of coastal vegetated ecosystems and predicting its future

Table 2.1 Standing stocks of biomass and soil organic carbon (SOC) in different biomes

Biome	Area (10^{12} km^2)	Biomass C (kg C m^{-2}) Aboveground	Belowground	Total	SOC (top 1 m; kg C m^{-2})	SOC/Biomass C	References
Forest							
Boreal forest	12	3.63	1.16	4.79	9.3	1.9	Jackson et al. (1996), Jobbàgy and Jackson (2000)
Temperate deciduous forest	7	7.30	1.68	8.98	17.4	1.9	
Temperate evergreen forest	5	9.78	1.76	11.54	14.5	1.3	
Tropical deciduous forest	7.5	4.82	1.64	6.46	15.8	2.4	
Tropical evergreen forest	17	10.32	1.96	12.28	18.6	1.5	
Grassland							
Tundra	8	0.07	0.48	0.55	14.2	25.7	Jackson et al. (1996), Jobbàgy and Jackson (2000)
Sclerophyllous shrubs	8.5	1.60	1.92	3.52	8.9	2.5	
Temperate grassland	9	0.15	0.56	0.71	11.7	16.4	
Tropical grassland and savanna	15	0.80	0.56	1.36	13.2	9.7	
Coastal wetland							
Mangrove	0.14	–	–	14.75	32.0	2.2	Siikamäki et al. (2012)
Salt marsh	0.051	–	–	0.33	39.3	119.2	
Seagrass meadows	0.32	–	–	0.18	7.0	38.9	
Indonesian mangroves	–	19.10	2.10	21.20	76.1	3.6	Alongi et al. (2016)
Indonesian seagrass meadows	–	0.03	0.12	0.16	13.0	83.9	

trends. In this chapter, we review the distribution pattern and chemical characteristics of sedimentary OC and the major factors that control OC accumulation and burial rates in marine sediments, with a particular emphasis on seagrass meadows.

2.2   Sedimentary Environment of Seagrass Meadows

Seagrass meadows are undersea grassland ecosystems that consist of submerged, salt-tolerant monocotyledonous plants called seagrasses (Fig. 2.1; see also Yoshida et al. (2018) in this volume). The canopy height of seagrass meadows is usually on the order of 10–100 cm, although meadows can be several meters tall (e.g., Fig. 2.1b). Many temperate seagrass meadows are monospecific (Fig. 2.1a, b), while tropical meadows are often multispecific (Fig. 2.1d, e). Epiphytic and/or epibenthic macroalgae often coexist abundantly in seagrass meadows (Fig. 2.1a, d). In contrast to mangroves and tidal marsh plants, which are confined to intertidal zones and take up CO_2 from the atmosphere, seagrasses are adapted to a fully submerged life in
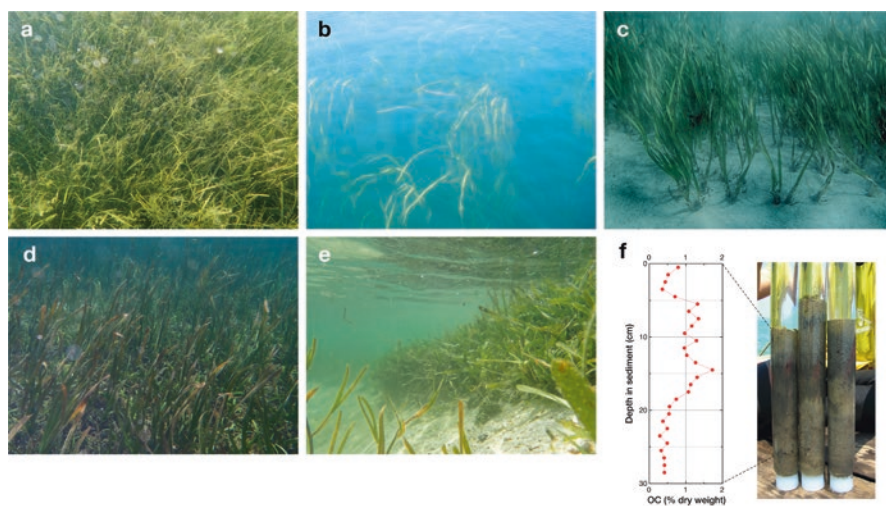
Fig. 2.1 Seagrass meadows and sediments. (**a**) Dense *Zostera marina* meadow associated with the macroalgal epiphytes *Gracilaria* sp. (Thau Lagoon, southern France; *cf.* Hori et al. (2018)); (**b**) the exceptionally tall (up to 7 m) species *Zostera caulescens* (Otsuchi Bay, northeastern Japan; photo taken before the 2011 Great East Japan Earthquake; *cf.* Nakaoka and Aioi (2001)); (**c**) monospecific subtropical meadow of *Enhalus acoroides* on carbonate sediment (Ishigaki Island, southwestern Japan; *cf.* Tanaka and Kayanne (2007)); (**d**) mixed-species tropical meadow dominated by *E. acoroides*, with dense undergrowth of the calcareous alga *Halimeda* spp. (Babeldaob Island, Palau); (**e**) edge of a mound-like structure of *Thalassia hemprichii*-dominated mixed-species subtropical meadow in a back-reef lagoon (Ishigaki Island, southwestern Japan); (**f**) typical vertical profile of OC in seagrass sediment, collected from a mixed meadow of *T. hemprichii* and *E. acoroides* on clastic sediment (Kuraburi, southern Thailand; *cf.* Nakaoka et al. (2004))

seawater and are able to acquire carbon for photosynthesis from dissolved CO_2 and bicarbonate (HCO_3^-) in seawater (Beer et al. 2014). This characteristic of seagrasses gives seagrass meadows a unique role in carbonate chemistry: mitigation of ocean acidification by lowering the ambient partial pressure of CO_2 (pCO_2; Manzello et al. 2012; Unsworth et al. 2012).

Seagrasses typically occur on well-illuminated sandy or muddy bottoms where wave energy is relatively low and the sedimentary environment stable. Excessive sedimentation or erosion prohibits development of meadows (Cabaço et al. 2008). Although some seagrass species occur as deep as 90 m (Duarte 1991), the seagrass meadows that can contribute significantly to carbon capture and sequestration are mostly confined to depths of 20 m or less, even under very transparent waters (e.g., Tanaka and Nakaoka 2007). Sediment materials that support seagrass meadows are categorized into two groups: clastic and biogenic sediments. Clastic sediment materials are silicate and aluminosilicate minerals originally generated on land through weathering of rocks and transported to coastal areas by rivers. Clastic sediment can be classified according to particle size as gravels (>2 mm), sand (0.063–2 mm), silt (0.004–0.063 mm), or clay (<0.004 mm). The particle size distribution of clastic sediment is determined principally by geographic and oceanographic factors, such as the distance from river mouths, water depth, and the hydrodynamic regime. Seagrass meadows usually occur on sediments in which fine sand and/or silt fractions are dominant (Koch 2001). On the other hand, biogenic sediment includes diatomaceous deposits made up of dead planktonic diatom frustules and biogenic carbonate sands originally produced by carbonate-bearing organisms such as reef corals, foraminifera, and calcareous algae. In tropical coastal regions, seagrass meadows are often found on shallow carbonate sand in the back-reef lagoon of coral reefs. As discussed below, the ecosystem function of seagrass meadows in terms of the carbon cycle differs significantly between clastic and carbonate sediments. Moreover, the mode and efficiency of OC sequestration in sediment are strongly constrained by the particle size distribution of the sediment.

It should be emphasized that seagrass meadows and sediments interact closely with each other, as the occurrence and dynamics of seagrass meadows are constrained by sedimentological conditions, while seagrass meadows also influence the accretion and stability of sediment. Several factors are responsible for this function of seagrass meadows. Firstly, seagrass meadows reduce water currents via friction between leaf blades and seawater (Fonseca et al. 1982), accelerating the deposition of fine-grained particles that would be flushed away in the absence of vegetation (Fonseca and Fisher 1986; Gacia et al. 1999). At the same time, sediment resuspension is suppressed, and accumulation of organic detritus is facilitated (Ward et al. 1984). As a result of these effects, the sediment of dense and extensive seagrass meadows is generally richer in fine particles such as silt and clay compared with that of bare areas or sparse seagrass patches adjacent to meadows (Tanaka and Kayanne 2007). As discussed below, fine clastic sediment particles have a greater capacity to hold OC per unit weight than do coarser particles. Thus, the capacity of seagrass meadows to accumulate fine sediment is essential to their carbon sequestration role.

Secondly, seagrass meadows have a filtering effect through which suspended organic particles conveyed by the water current are trapped in the bundle of leaf blades and accumulate in the sediment (Hendriks et al. 2008). This factor greatly increases the supply rate of allochthonous OC per area of sediment.

Thirdly, seagrasses extend horizontal rhizomes outward, forming a network of rhizomes and fine roots that stabilizes the sediment surface under the meadow (Fonseca 1989; Gacia and Duarte 2001). Sediment stabilization by the belowground structure is one of the most notable characteristics shared by all coastal vegetated ecosystems, although the strength of this effect differs largely among species. The most extreme known example may be the dense fine-root structure of the peat-forming mangrove *Rhizophora* spp. (Fujimoto et al. 1999; Ono et al. 2015). No seagrass species produces such a dense root/rhizome system that genuine peat is generated in the underlying sediment. However, a few species, such as Mediterranean *Posidonia oceanica* and subtropical *Thalassia* spp., can accumulate and stabilize fine sediment so effectively using their robust root systems that mound-like microtopography is often generated under their dense meadows (Wanless 1981; Lo Iacono et al. 2008).

2.3 Global Pattern of Sediment Organic Carbon Accumulation

Before proceeding to the specific characteristics and functions of seagrass meadow sediments, we briefly review carbon sequestration in marine sediments from a global perspective in the following sections.

Most of the carbon on the Earth's surface exists in the geosphere as crustal carbonates and sedimentary OC, with only a small fraction (<1%) circulating in the biosphere (Table 2.2). The surface "reactive layer" of marine sediment represents the boundary or interface zone connecting the carbon reservoirs in the biosphere (biogeochemical carbon cycle) to those in the geosphere (geological carbon cycle). Conversely, carbon may be returned from the geosphere to the biosphere, mainly through volcanic eruption, tectonism, and fossil fuel mining. Due to the increasing use of fossil fuels, the flux of carbon from the geosphere to the biosphere, particularly to the atmosphere (>8 Pg year^{-1}), overwhelms the return flux of permanent sequestration in marine sediment at present (~0.2 Pg year^{-1}; Ciais et al. 2013). It has been estimated that the annual atmospheric loading of CO_2 due to fossil fuel burning already exceeds the permanent burial of OC in marine sediment in the second half of the nineteenth century (Boden et al. 2011). However, in the global estimates of carbon budgets discussed above, OC sequestration as a function of coastal vegetated ecosystems is often overlooked.

Globally, the distribution of OC in surface marine sediments is not homogeneous. In several narrow regions, such as upwelling areas and anoxic basins, the concentration of OC in sediments is exceptionally high. Excluding these areas, the OC concentration in surface sediment rarely exceeds 2% of dry weight (Premuzic

Table 2.2 Major reservoirs of carbon in Earth crust, as recompiled after Sundquist and Visser Ackerman (2014) and Houghton (2014)

Reservoirs			Inventory (Pg C)	Percentage
Biosphere	Atmosphere	CO_2	830	0.0008
	Land	Living biomass	550	0.0006
		Soil organic carbon	1500	0.0019
	Ocean	Biomass and particulate organic carbon	3	0.0000
		Dissolved organic carbon	1000	0.0009
		Dissolved inorganic carbon	37,000	0.0048
Boundary zone	Reactive sediment[a]	Organic carbon	650	0.0008
		Inorganic carbon (carbonates)	2500	0.0032
Geosphere		Organic carbon in sediments and sedimentary rocks		
			Total	12,500,000	16.1
			Fossil fuels	5000	0.0064
		Inorganic carbon (carbonates)	65,300,000	83.9

[a]Reactive marine sediment is conventionally defined as the top 50-cm layer of continental shelf sediment and top 30-cm layer of other sediment (Sundquist 1985)

et al. 1982; Romankevich et al. 2009). The global pattern of sediment delivery to the ocean floor is even more heterogeneous and is concentrated mainly in continental shelf zones, especially in areas near large river mouths called depocenters (Gibbs 1981; Berner 1982). The geographic pattern of the OC accumulation rate in sediment can be evaluated as the sediment delivered multiplied by the OC concentration. According to the estimation of Berner (1982) modified by Hedges and Keil (1995), approximately 90% of global OC burial on the ocean floor occurs in large river deltas, continental shelves, and their marginal areas. The detailed site-specific characteristics of the roles of representative continental margin systems in sediment OC burial were discussed in a recent comprehensive review by Bianchi et al. (2018). However, this estimate of global OC burial does not explicitly account for OC burial in coastal vegetated ecosystems. Duarte et al. (2005) estimated the OC burial rates in mangroves, salt marshes, and seagrass meadows based on compilation of the available data on sediment accumulation in these habitats. According to that study, OC burial in these habitats as a whole is roughly comparable with that in the remainder of the world's ocean (Table 2.3). As discussed below, these estimates may not be evaluated using the same time scale, and therefore, direct comparison of estimates is difficult. Further investigation of OC burial rates with more rigorous and consistent treatment of time scales is definitely required for quantitative analysis of global OC sequestration. Nevertheless, the estimates of Duarte et al. (2005) underscore the disproportionately high contribution of coastal vegetated ecosystems to OC sequestration, considering the small areal coverage of these ecosystems (<0.5%) among the world's oceans.

Table 2.3 Estimation of burial rate of organic carbon to marine sediment based on Hedges and Keil (1995) and Schlünz and Schneider (2000)

Sediment type	Hedges and Keil (1995) (Tg C year⁻¹)	Contribution (%)	Schlünz and Schneider (2000) (Tg C year⁻¹)	Contribution (%)	Duarte et al. (2005) (Tg C year⁻¹)	Contribution (%)
Continental shelf and upper slope sediment (total)					98.9	46
Deltaic sediment	70	44	43.4	31	–	–
High-productivity zones	7	4	Not estimated separately		–	–
Other areas	68	42	55.2	40	–	–
Shallow-water carbonate sediment	6	4	Not estimated separately		–	–
Coastal vegetated habitats	Not included in the estimation		Not included in the estimation			
Mangroves	–	–	–	–	23.6	11
Salt marsh	–	–	–	–	60.4	28
Seagrass meadows	–	–	–	–	27.4	13
Pelagic sediment (total)			8.8	6	6.0	3
High-productivity zones	3	2	–	–	–	–
Other areas	5	3	–	–	–	–
Anoxic basins (e.g., Black Sea)	1	1	Not estimated separately		Not estimated separately	
Aeolian dust input	Not included in the estimation		32.0	23	Not included in the estimation	
Total	160	100	139.4	100	216.3	100

Estimates for coastal vegetated habitats by Duarte et al. (2005) are also shown for comparison

2.4 Factors Controlling the Stability of Organic Carbon in Sediments: Degradability of Organic Matter

2.4.1 Concept of Burial Efficiency

Most of the OC deposited in marine sediment is eventually remineralized into CO_2 by the heterotrophic activities of benthic animals and microorganisms at the sediment–water interface and in the surface reactive layer (Emerson et al. 1985). Only a small fraction of OC withstands decomposition during early diagenesis and is buried in deep sediment layers. This fraction is commonly referred to as the OC burial rate or OC burial efficiency. There is some ambiguity in the definition of the burial efficiency, i.e., how deep OC must be buried or how long OC must withstand decomposition to be regarded as "buried". In ideal pelagic sediment cores, the concentration of OC in the top layer (C_0) decreases exponentially down toward deeper layers, approaching a constant concentration (C_∞). C_∞ is theoretically considered to represent permanently buried OC. The OC concentration (C; µmol C (g dry weight)$^{-1}$) at any depth (d; cm) can be approximated as follows:

$$C = (C_0 - C_\infty)\exp(-kd) + C_\infty \quad (k : \text{constant}). \tag{2.1}$$

Then, the burial efficiency B can be defined as

$$B = C_\infty / C_0. \tag{2.2}$$

In the conventional definition of "reactive marine sediment" (Sundquist 1985), early diagenesis is considered to occur primarily in the top 50-cm layer of coastal sediment and the top 30-cm layer of deep pelagic sediment. These values may be used as a practical definition of burial efficiency, such that burial efficiency is defined as the ratio of the OC concentration at the top (C_0) to that at the bottom (C_b) of the reactive layer (Fig. 2.2):

$$B = C_b / C_0. \tag{2.3}$$

However, it is sometimes problematic to apply this definition to seagrass meadow sediments, because the production of belowground tissues by seagrasses disturbs the typical exponential vertical profile of OC represented by Eq. (2.1). The OC concentration often exhibits a maximum in the subsurface layer where the rhizomes and roots of seagrasses are abundant, while OC in the top layer is relatively depleted (e.g., Fig. 2.1f). The typical exponential profile is recognizable in only one (Fig. 2.3a) of the seven examples shown in Fig. 2.3. Multiple mid-layer peaks of OC are sometimes observed (e.g., Fig. 2.3b, d, g), which presumably reflects changing supply rates of both OC and mineral sediment. As a practical solution, seagrass researchers often assume that OC equivalent to the average concentration in the top 20–30 cm of sediment represents the long-term stock of OC, without explicit
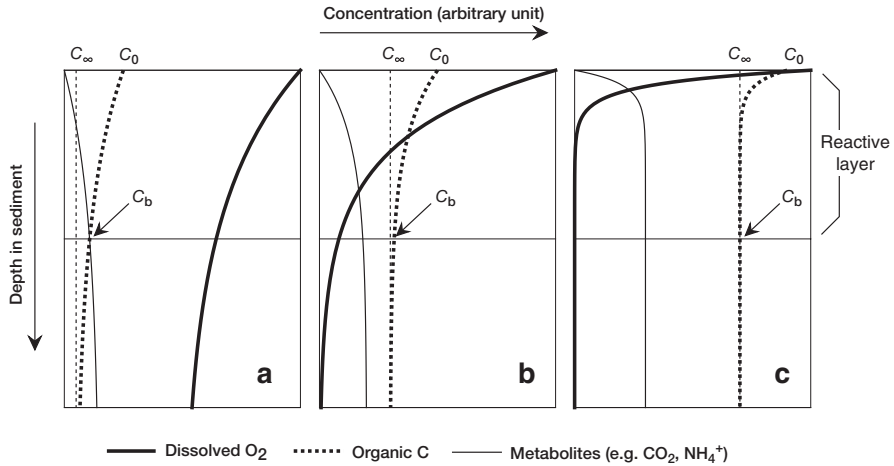
Fig. 2.2 Generalized vertical distributions of the concentrations of dissolved oxygen (O_2), organic carbon (OC), and inorganic metabolites in the surface layer of sediment in oligotrophic (**a**), mesotrophic (**b**), and eutrophic (**c**) environments. C_0 and C_b represent the OC concentrations at the top and bottom of the reactive layer, respectively (see text)

treatment of the burial efficiency in individual sediment cores (Fourqurean et al. 2012; Miyajima et al. 2015; Röhr et al. 2016).

Even when not easily defined and assessed, the concept of burial efficiency and the mechanisms that constrain it are still essential for evaluating and comparing the carbon sequestration potential of various environments. The burial efficiency of organic matter is principally controlled by two factors: the degradability of organic matter in terms of enzymatic degradation, and the availability of metabolic electron acceptors, particularly molecular oxygen (O_2), in the reactive layer of sediment. The former depends on both the inherent structural recalcitrance of organic molecules and physical protection of organic matter against degradation by the sediment mineral matrix, as explained below.

2.4.2 Organic–Mineral Interactions

Organic matter supplied to marine sediment is composed of a broad range of compounds in terms of degradability. Most natural organic matter, such as carbohydrates, proteins, and lipids, are generally decomposable by bacteria. However, some compounds, such as lignin derived from vascular plants and plastics discarded by humans, are highly resistant to microbial decomposition and thus persist for a long time, especially in anoxic sediments. Marine vascular plants such as mangroves and seagrasses also produce lignin. Degradable organic matter such as carbohydrates, proteins, lipids, and nucleic acids usually dominates the OC flux to sediment and is presumed to be mostly decomposed during diagenetic processes. During the course
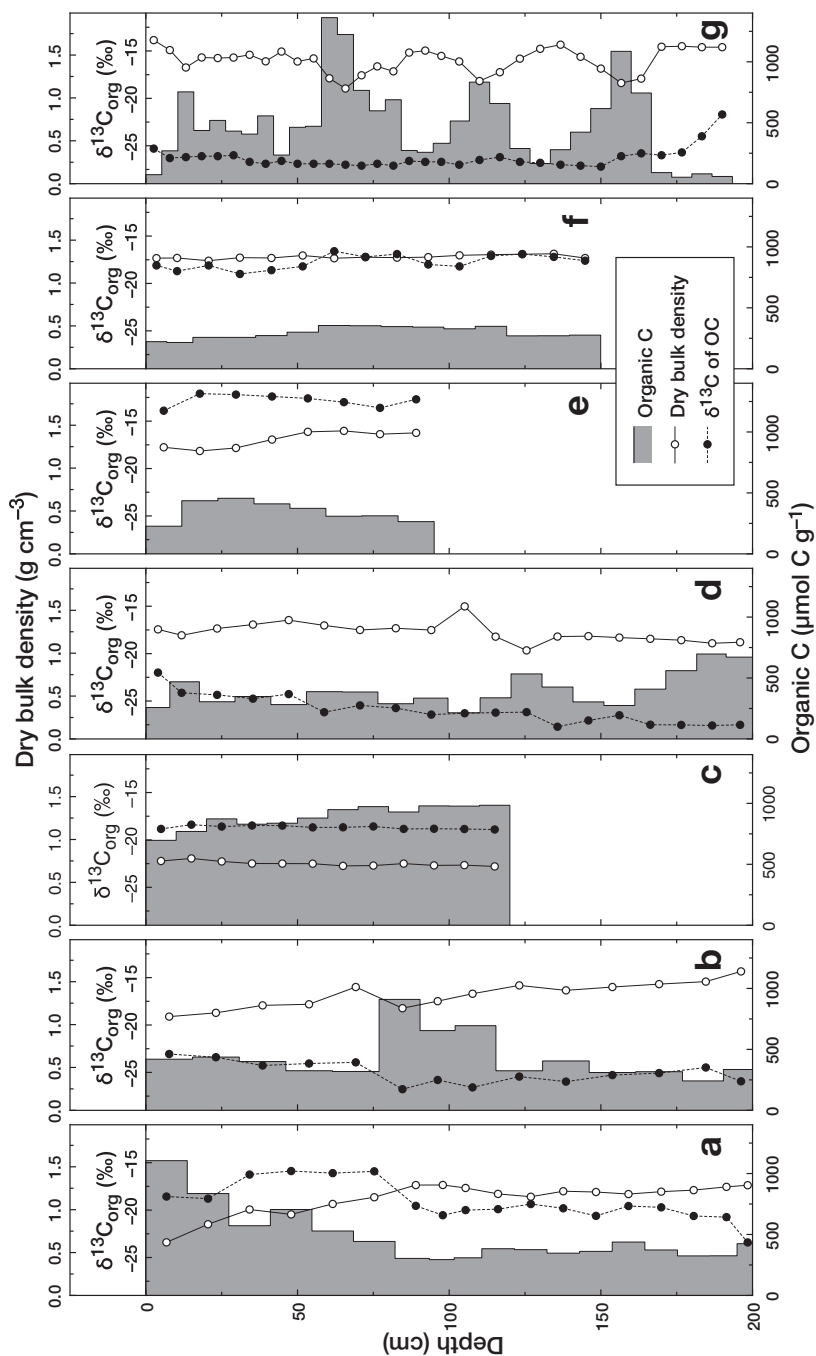
Fig. 2.3 Examples of vertical profiles of OC in seagrass meadow sediment cores up to 200 cm long. The dry bulk density of sediment and the carbon isotope ratio ($\delta^{13}C$) of OC are also shown. Sampling locations: (**a**) *Zostera marina* meadow in the Seto Inland Sea, central Japan; (**b**) unvegetated area adjacent to the meadow in (**a**); (**c**) another *Z. marina* meadow in the Seto Inland Sea; (**d**) *Z. japonica* meadow in the Seto Inland Sea; (**e**) *Cymodocea serrulata*–dominated mixed-species meadow on carbonate sediment of Ishigaki Island, southwestern Japan; (**f**) *Enhalus acoroides* meadow on carbonate sediment of Ishigaki Island; (**g**) *E. acoroides* meadow near mangroves on the Andaman Sea coast of Thailand. (Data source: Miyajima et al. (2015))

of decomposition, microorganisms produce secondary organic matter, including various cellular components, extracellular polymers, and organic metabolic waste. The fraction of OC carried over to secondary organic products as the proportion of OC in the initial substrate consumed by microorganisms is referred to as the conversion factor. The conversion factor varies among substrates, microorganisms, and available electron acceptors and ranges between 10% and 50% for many aerobic bacteria (Del Giorgio and Cole 1998). The secondary organic products of microorganisms may be utilized by other microorganisms, which produce their own secondary products based on their own conversion factor. Thus, the overall process of early diagenesis of degradable organic matter can be regarded as a microbial food web. Among the OC initially supplied to the sediment, the degradable fraction is processed through this diagenetic food web and eventually either remineralized to inorganic carbon or temporarily stored as microbial secondary products (e.g., Lomstein et al. 2009; Cyle et al. 2016), while inherently recalcitrant fractions tend to remain intact in the sediment for a long time.

An important factor influencing the stability of organic molecules in the sediment is the role of the mineral matrix as an adsorbent for organic matter (Keil and Mayer 2014). The majority of OC in marine sediments exists in close association with the surface of sediment mineral particles. This association is demonstrated by the fact that most of the OC in bulk coastal sediments is associated with relatively heavy density fractions (e.g., >2.0 g cm^{-3}) when sediment grains are sorted by density (Bock and Mayer 2000; Arnarson and Keil 2007). Since the density range of most natural organic matter is 1.0–1.5 g cm^{-3} and those of clastic aluminosilicates and biogenic carbonates are 2.3–2.7 g cm^{-3} and 2.7–2.9 g cm^{-3}, respectively, the accumulation of OC in the density fraction >2.0 g cm^{-3} indicates that most OC is bound to clastic and/or carbonate sediment minerals. Another line of indirect evidence for the close association between OC and mineral surfaces is the positive correlation between the OC concentration and specific surface area (SSA) commonly found for continental shelf sediments (Keil et al. 1994a; Mayer 1994; Bergamaschi et al. 1997) and coastal carbonate sediments (Suess 1973). The amount of OC preserved per unit surface area of sediment particles is referred to as OC loading. OC loading converges within a narrow range of ~60 μmol C m^{-2} for typical continental shelf sediments (Mayer 1994) and a slightly higher range for carbonate sediments (Suess 1973). The accumulation of OC in heavier (>2.0 g cm^{-3}) density fractions (Fig. 2.4) and the close correlation between OC and SSA (Fig. 2.5; average OC loading of 61.5 μmol m^{-2}) have been demonstrated for temperate seagrass (*Zostera marina*) meadow sediments as well as coastal sediments near these meadows (Miyajima et al. 2017). Thus, it can be assumed that the sediment in seagrass meadows shares a common OC sequestration mechanism with pelagic continental shelf sediments.

The above empirical relationships imply that (i) OC can be preserved in sediments via adsorption to mineral surfaces even if it is not inherently recalcitrant, and (ii) the maximal amount of adsorbed OC per unit area of mineral surface is limited based on the mineralogy of the sediment matrix. As a corollary of (ii), it may be expected that when the rate of OC supply to the sediment exceeds the supply rate of
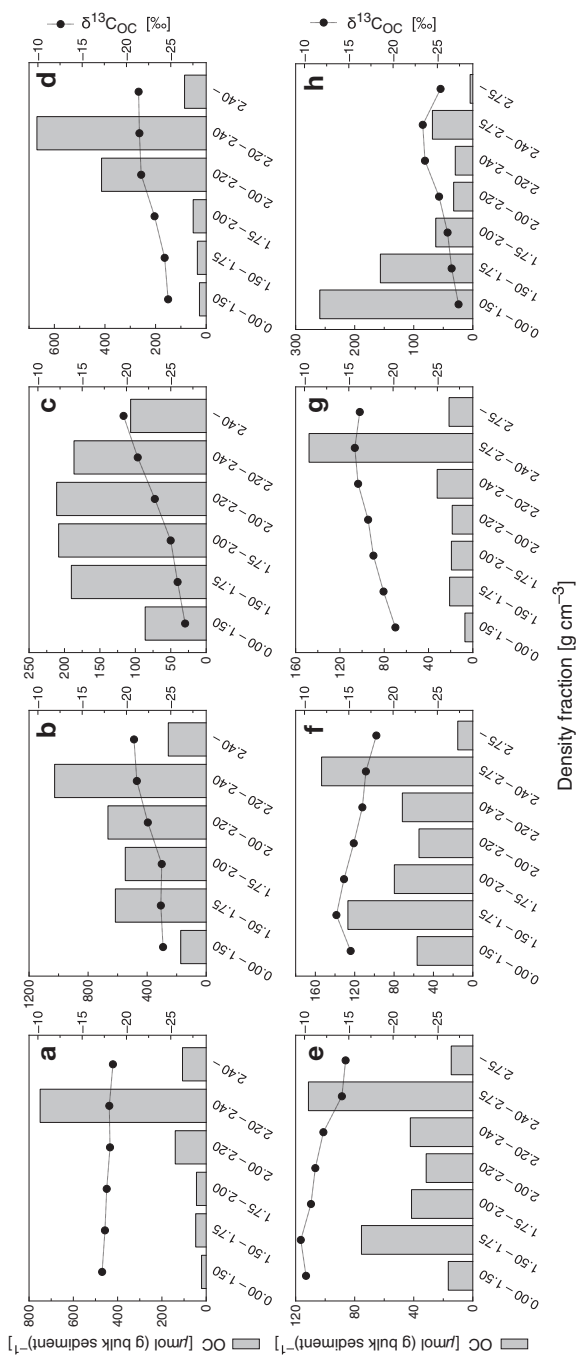
Fig. 2.4 The concentration and δ^{13}C of sediment OC in particle density fractions. (**a**) Temperate, non-estuarine *Zostera marina* meadow, (**b**) estuarine *Z. marina* meadow; (**c**) unvegetated area among *Z. marina* meadows, and (**d**) shallow (16 m) pelagic sediment of the Seto Inland Sea, Japan; (**e**) Subtropical *Thalassia hemprichii* meadow on carbonate sediment, (**f**) *Enhalus acoroides* meadow on carbonate sediment, (**g**) *E. acoroides* meadow on clastic sediment around Ishigaki Island, southwestern Japan; and (**h**) mangrove-fringed, tropical *E. acoroides* meadow on clastic sediment near Kuraburi, southern Thailand. Note that the scale of the OC concentration axis differs among the panels. (Data source: (**a–d**) Miyajima et al. (2017); (**e–h**) Miyajima et al., unpublished data)
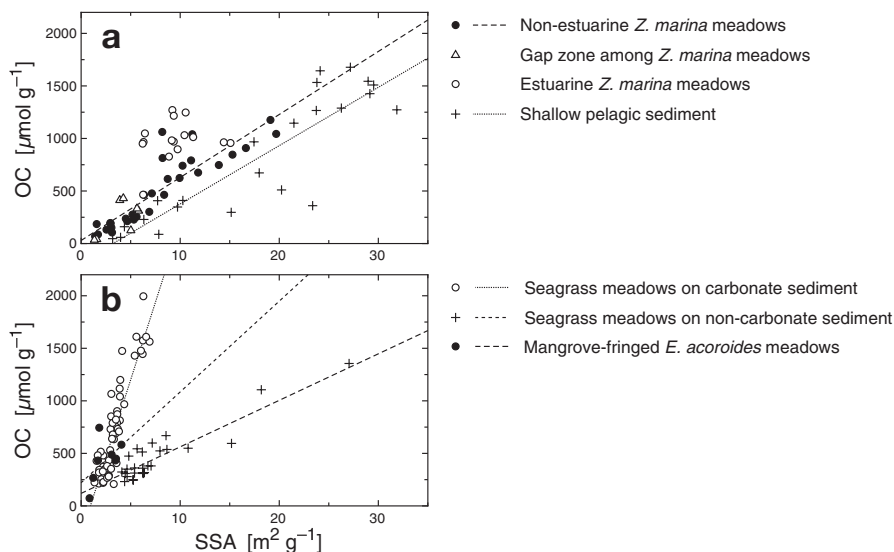
Fig. 2.5 Correlation between the OC concentration and specific surface area (SSA) of sediment in various types of seagrass meadows. (**a**) Temperate seagrass meadow and pelagic sediments collected from the Seto Inland Sea (central Japan); (**b**) subtropical and tropical seagrass meadow sediments collected from Ishigaki Island (southwestern Japan), Bolinao (northern Philippines), and Kuraburi (southern Thailand). Average OC loading was estimated by linear regression as 60.0 (non-estuarine *Z. marina* meadows), 55.5 (pelagic sediment of the Seto Inland Sea), 295 (tropical and subtropical seagrass meadows on carbonate sediment), 44.3 (tropical and subtropical seagrass meadows on non-carbonate sediment), and 86.4 μmol OC m^{-2} (mangrove-fringed *E. acoroides* meadows). (Data source: (**a**) Miyajima et al. (2017); (**b**) Miyajima et al., unpublished data)

available mineral surfaces multiplied by the typical OC loading, the excess OC will not be preserved long term but will eventually remineralize unless it is structurally recalcitrant. It has been demonstrated experimentally that OC tightly associated with a sediment mineral surface can be rapidly remineralized by bacteria once it physically detaches from the mineral surface (Keil et al. 1994b), and conversely, that the enzymatic degradation rate of simple soluble organic molecules can be drastically retarded by adsorption to a mesoporous mineral matrix (Zimmerman et al. 2004). The nature and origin of organic matter adsorbed onto sediment mineral surfaces, the exact mechanism of stability enhancement by adsorption, and the factors leading to maximal OC loading are currently unknown. One of the most likely sources of adsorbed organic matter is extracellular polymeric substances, such as acidic heteropolysaccharides, produced by indigenous bacteria, which can bind to mineral surfaces via mechanisms such as ligand exchange, hydrogen bonding, van der Waals forces, and cation bridges (Chenu 1993; Decho 2000; Lünsdorf et al. 2000; Nguyen and Harvey 2001). In fact, most organic matter detached from sediment minerals by ultrasonic and/or chemical treatments exhibits molecular weights >10,000 (Miyajima et al. 2001a; Nunn and Keil 2005). It may be hypothesized that the stereochemical structure of these macromolecules is determined by multiple

adsorptive interactions with the mineral surface, such that microbial hydrolytic enzymes may not easily access the substrates, resulting in inhibition or extensive retardation of degradation (Kaiser and Guggenberger 2007). Regardless of the internal mechanism, the adsorption process enhances preservation of OC in sediment, which apparently leads to a strong correlation between OC and SSA in clastic coastal sediments. The mechanism assumed to drive this correlation is often referred to as sorptive preservation of organic matter. Because SSA is generally greater for fine-grained sediments, ecosystems like seagrass meadows with a high capacity to accumulate fine-grained sediment also have a high potential to sequester OC.

2.5   Influence of Exposure to Molecular Oxygen on the Preservation of Organic Matter

Another major factor that influences the burial efficiency of OC in sediment is the availability of metabolic electron acceptors, especially O_2. This is because the remineralization rate of OC by sediment microorganisms depends strongly on the availability of electron acceptors, and O_2 is the most energetically favorable electron acceptor for the microbial electron transport system. Moreover, O_2 is a precursor of highly reactive intermediates such as reactive oxygen species, peroxides, and Mn^{3+}, which are produced by certain microbial enzymes, initiating autocatalytic oxidation of OC and degrading even inherently recalcitrant organic matter such as lignin (Raghukumar et al. 1999; Hammel et al. 2002; Galeron et al. 2018).

When the overlying seawater contains O_2, the surface layer of sediment contains O_2 in its pore water (oxic layer). The concentration of O_2 in the pore water decreases exponentially as sediment depth increases due to consumption by the respiration of microorganisms. The O_2 concentration eventually drops below the detection limit at a certain depth, referred to as the oxic/anoxic interface (Fig. 2.2). The thickness of the oxic layer, also referred to as the oxygen penetration depth, varies widely depending on the balance between supply and consumption of O_2. The supply rate of O_2 is constrained by the O_2 concentration in the overlying water and the advective or diffusive supply rate of O_2 into sediment, with the latter depending on sediment texture and the intensity of turbulence in the overlying water. The consumption rate of O_2 depends principally on the availability of degradable organic matter as microbial substrates and on water temperature. In the fine-grained sediment of sheltered eutrophic embayments, the oxic layer is generally very thin, often <1 mm. In contrast, the oxic layer of carbon-limited, oligotrophic open ocean sediment is much thicker, sometimes reaching several meters (Wilson et al. 1985; Emerson and Hedges 2003).

The time required for newly deposited surface sediment to reach the oxic/anoxic interface through burial is referred to as the oxygen exposure time (OET). It is evaluated based on the thickness of the oxic layer (in mm) divided by the sedimentation rate (in mm year^{-1}) and ranges geographically from <1 to >1000 years. The OET is one of the principal factors constraining the OC burial efficiency in

pelagic sediments, with longer OETs allowing more extensive degradation of OC, resulting in lower OC burial efficiencies. Previous studies have demonstrated that the OC burial efficiency (Hartnett et al. 1998) and the OC/SSA ratio (Hedges et al. 1999) in continental margin sediments of the eastern North Pacific have negative correlations with the logarithm of OET. These relationships imply that (i) remineralization of OC (in particular, mineral-associated OC) proceeds during the OET but not significantly after burial in anoxic layers, and that (ii) the rate constant of OC remineralization during the OET does not depend significantly on the thickness of the oxic layer or OET.

In terms of remineralization during early diagenesis, OC in sediment may be conceptually categorized into three groups, as shown in Table 2.4; these are mineral-free labile (degradable), mineral-associated labile, and inherently refractory (undegradable) OC. Based on this classification, the conditions for long-term sequestration of OC in sediments can be summarized as follows. OC that can be sequestered long term in marine sediment is carbon contained in either mineral-associated labile organic carbon (LOC) or inherently refractory organic carbon (ROC). The supply rate of ROC is controlled primarily by the supply rate of woody organic substances from land and mangroves and therefore depends on the hydrological proximity to these habitats. For LOC to be sequestered in sediment, the mineral surfaces required for adsorption of LOC must be supplied simultaneously with LOC. In highly productive environments such as seagrass meadows, overall sequestration of OC may be limited by the supply of available mineral surfaces rather than the supply of organic matter. As mineral-adsorbed LOC may be remineralized slowly in the oxic layer, the burial efficiency of LOC is constrained by the OET.

2.6 Significance of Seagrass Meadows in Coastal Ecosystem Function

The factors outlined in Sects. 2.4 and 2.5 have important implications in relation to the significance of seagrass meadows in shallow coastal ocean functions. Oceanographic conditions that prevail over shallow coastal sediments are generally unfavorable for sequestration of OC (Aller 1998). In such environments, wave action and tidal currents often reach the bottom, causing frequent resuspension and removal of fine-grained sediment, such as clay, silt and organic detritus. As explained in Sect. 2.4, fine-grained sediment has a greater capacity to store OC by sorptive preservation per unit weight than does coarse-grained sediment. Therefore, removal of fine-grained sediment results in net loss of OC from shallow coastal sediments. Furthermore, penetration of wave-induced oscillation flows and tidal pumping cause intrusion of O_2 into deeper sediment layers, resulting in elongation of the OET. As noted in Sect. 2.5, longer OET may cause gradual loss of mineral-adsorbed LOC, and as a result, the OC loading of sediment particles may decrease from

Table 2.4 Empirical classification of sediment organic matter based on the susceptibility to remineralization during early diagenesis

Class	Definition	Main sources	Examples	Stability in	
				Oxic layer	Anoxic layer
Mineral-free labile organic matter	Organic materials that can be enzymatically hydrolyzed and consumed by microorganisms and are not protected by sorptive interactions with sediment minerals	Detrital particles derived from plankton, seagrasses, macroalgae, coral mucus, microphytobenthos, terrestrial plants, etc.	Low-molecular-weight carbohydrates and proteins, short-chain hydrocarbons and fatty acids	Remineralized within a relatively short period	Remineralized into inorganic carbon or decomposed into simple organic molecules
Mineral-associated labile organic matter	Organic materials that are essentially degradable by microorganisms but are protected by sorptive interactions with sediment minerals	Secondary organic products produced from primary organic matter by microorganisms	High-molecular-weight polysaccharides and polypeptides, DNA, long-chain lipids	Relatively resistant to decomposition but slowly and constantly remineralized over a long period	Somewhat stable
Refractory organic matter	Structurally recalcitrant organic matter that strongly resists against biodegradation	Lignin and other phenolic polymers contained in vascular plants, especially xylem, bark, and cones of arborous species; artificial durable polymers such as plastics	Lignin, plastics, kerogens	Degraded only conditionally and very slowly	Stable

saturation levels of ~60 μmol C m^{-2} to undersaturation levels of ~10 μmol C m^{-2} in shallow exposed sediments (Mayer 1994; Aller and Blair 2006).

Once seagrass meadows are formed on shallow coastal sediments, accumulation of fine-grained sediment is enhanced due to the energy-dissipating and sediment-stabilizing functions of the meadows. This facilitates long-term sequestration of OC through sorptive preservation. The supply rate of OC to sediment also increases due to autochthonous OC production by seagrasses and associated algae as well as increased input of allochthonous organic seston such as pelagic plankton and river-borne terrestrial detritus trapped by seagrasses. On the other hand, accumulation of fine-grained sediment reduces the mobility of O_2 in the pore water, resulting in a thinner surface oxic layer. The increased OC supply stimulates microbial consumption of O_2 in the sediment. These effects, acting synergistically with the increase in the sediment accumulation rate, drastically shorten the OET compared with unvegetated sediment. A portion of the O_2 produced by seagrasses through photosynthesis is translocated to the rhizomes and excreted from the roots to the surrounding sediment (Iizumi et al. 1980; Hemminga 1998). Simultaneously, soluble LOC is excreted from the roots, stimulating microbial activity (Moriarty et al. 1986; Bouillon and Boschker 2006) and resulting in the development of a microbial community specific to the seagrass rhizosphere (Jensen et al. 2007). Such an active microbial community could produce copious secondary metabolites including extracellular polymers, providing precursors for mineral-associated LOC (Cyle et al. 2016) and elevating the mineral surface OC loading to saturation levels. These characteristic functions of seagrass meadows act cooperatively to enhance the OC sequestration rate in the sediment.

From a historical perspective, the role of seagrass meadows (and probably also salt marshes and mangroves) described above may be viewed as an emergent ecosystem function of the sediment source–sink system (Fig. 2.6). According to this hypothesis, recruitment and proliferation of seagrasses can render previously OC-depleted coastal sediments into hot spots of OC accumulation and sequestration. If such habitat changes occur worldwide, it would significantly alter the global inventories and cycling of carbon, resulting in secular reduction of atmospheric CO_2. Quantitative evidence supporting this hypothesis is introduced in the following sections.

2.7   Organic Carbon Storage in Seagrass Meadow Sediments

Kennedy et al. (2010) investigated the variability in sediment OC concentrations in 32 individual seagrass beds (predominantly *Z. marina* and *P. oceanica*) and adjacent non-vegetated areas from temperate coastal environments. They reported that the average OC concentration in seagrass sediments was approximately twice as high as that in corresponding barren sediments, and this difference was statistically significant. Our data also showed similar patterns not only in OC, but also in total nitrogen   and   organic   phosphorus   concentrations,   between   subtropical
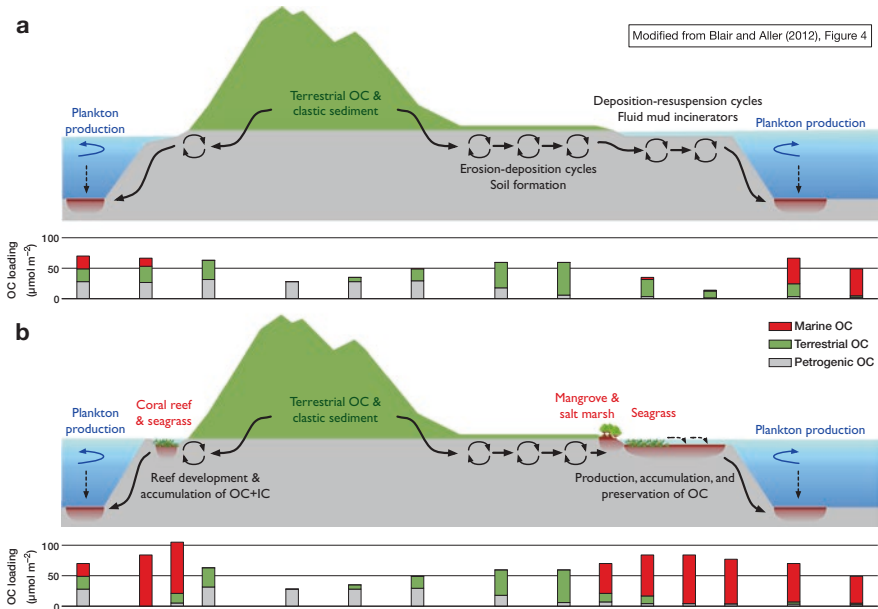
Fig. 2.6 Carbon sequestration as an ecosystem function of coastal vegetated ecosystems (CVEs) from a sediment source-sink perspective (Blair and Aller 2012). (**a**) Schematic representation of the serial transport-reaction system from the watershed to the coastal ocean in the absence of the CVEs. The shallow coastal sedimentary system plays a role as a "fluid mud incinerator", in which OC delivered from the watershed is efficiently oxidized and remineralized via deposition–resuspension cycling (modified from Fig. 4 of Blair and Aller (2012)). (**b**) Establishment of CVEs converts a portion of the coastal sedimentary system into a site of efficient OC sequestration via their own primary production and sediment accumulation/stabilization functions. Development of coral reefs also enhances OC sequestration by providing favorable habitats for CVEs (Watanabe and Nakamura (2018) in this volume). Bar graphs below the diagrams show the typical spatial changes in OC loading of surface sediment and the fractions of OC attributed to marine, terrestrial, and "petrogenic" (ancient crustal) organic matter. The advent of CVEs is thus assumed to have considerably altered the global carbon cycle

mixed-species seagrass beds and adjacent barren areas of back-reef carbonate sediments (Miyajima et al. 1998, 2001b). Thus, seagrass meadows may generally have an ecosystem function of increasing the storage of OC in sediment to at least twice the extent of storage observed under the same oceanographic conditions in the absence of seagrass. It should be noted that sediment in unvegetated zones neighboring seagrass meadows often contains a significant amount of OC exported from the seagrass meadow (Kennedy et al. 2010) and cannot be considered equivalent to sediment prior to colonization by seagrasses. The OC concentration in the original unvegetated sediment would have been even lower than that in sediment in zones adjacent to meadows. Therefore, the influence of seagrass meadows on sediment OC stock would be greater than expected from the comparison described above.

Based on a compilation of more than 200 datasets from 88 seagrass meadows worldwide, Kennedy et al. (2010) also reported that the actual OC concentration in

seagrass bed sediments varied widely, from 0.1% to 11% of dry weight depending on the sampling site, and did not correlate with seagrass biomass. The average OC concentration in seagrass bed sediments was 1.8%, although the frequency distribution of the observations was clearly skewed, with most data confined in a range of 0–2.0%. For this reason, the authors recommend using the median OC value of 1.2% rather than the average as the representative OC concentration for seagrass bed sediments worldwide. Similar results based on a more comprehensive dataset (219 core sites) were published by Fourqurean et al. (2012), who found average and median OC concentrations in seagrass bed sediments of 2.0 and 1.4% of dry weight, respectively. They also estimated the OC stock in the upper 1 m of sediment, which was in the range 9–830 Mg C ha^{-1} with a median value of 140 Mg C ha^{-1}. According to their online supplementary dataset, the OC concentration in surface sediments does not correlate with the aboveground biomass of seagrasses, even when the correlation is limited to seagrass meadows with similar species compositions. Alongi et al. (2016) also found that the average OC concentration in 82 sediment samples from Indonesian tropical seagrass meadows was 1.3% of dry weight (ranging from 0.2% to 3.0%) and that, on average, the detrital OC stock in the upper 1 m of sediment was equivalent to ~400 times the average OC stock in aboveground seagrass biomass and ~100 times that in belowground biomass. However, according to their data, there was no correlation between aboveground seagrass biomass and the OC stock in the sediment.

These findings suggest that despite the fact that the presence of seagrass meadows actually enhances sediment OC storage at a local scale, the degree of enhancement depends not only on biological factors such as biomass and species composition, but on some non-biological factor or factors that significantly influence sediment OC accumulation at regional and global scales. It follows that estimating the aboveground biomass or coverage of seagrasses using remote-sensing techniques, which has been undertaken in many ongoing survey projects to constrain "blue carbon" stocks worldwide, is not necessarily an appropriate way to quantify total blue carbon in seagrass meadows.

In the case of *Z. marina* meadows in the Seto Inland Sea (central Japan), the OC concentration in the top 30 cm of sediment varies widely from 0.1% to 1.6% of dry weight, with a strong positive correlation with the SSA of mineral sediments (Miyajima et al. 2017). This OC concentration range is consistent with those of the previous reports noted above. The average OC loading (OC/SSA ratio) was 61.5 ± 5.5 µmol C m^{-2} (Fig. 2.5a), in accordance with known saturated OC loading values for continental shelf sediments (63.3 ± 2.5 µmol C m^{-2}; Keil et al. 1994a). Most of the OC in these sediments was found in >2.0 g cm^{-3} density fractions (Fig. 2.4a as an example), indicating a close association between OC and sediment minerals. The carbon isotope ratio (δ^{13}C) implied that approximately half of the OC in these heavy fractions was derived from seagrasses. Furthermore, the OC concentration and SSA were correlated with the patch size of the seagrass meadows, with larger patches having larger mineral surface areas and storing more OC per unit weight of sediment (Miyajima et al. 2017). These findings suggest that the capacity of seagrass meadows to capture fine-grained sediment and thereby to

increase the availability of sediment mineral surfaces, which is expected to be higher in larger patches, is a principal constraint on OC storage in these sediments. The importance of the context of landscape in sediment OC storage for tropical and subtropical seagrass habitats was also recently suggested (Gullström et al. 2017).

However, the OC concentration in some estuarine seagrass meadow sediments clearly exceeded the value predicted by the typical OC–SSA relationship (Fig. 2.5a), indicating inclusion of OC that is not adsorbed to a mineral surface. In fact, a significant fraction of OC was found in density fractions <2.0 g cm^{-3} in estuarine seagrass meadow samples (e.g., Fig. 2.4b), and the δ^{13}C indicated that the OC in these lighter fractions originated mainly from terrestrial C_3 plants. This result implies that terrestrial refractory OC transported by rivers can be effectively trapped and stored in estuarine seagrass meadows in excess of the OC concentration expected from the normal OC–SSA relationship. Sediments from seagrass-free estuarine tidal flats and sandy macroalgal beds in the Seto Inland Sea were generally depleted of OC and showed lower OC loading compared with seagrass meadow sediments. Sediments from bare areas adjacent to seagrass meadows usually showed similar OC loading but lower OC concentrations compared with the nearest seagrass meadow sediments. OC in these seagrass-free sediments was divided almost equally between the mineral-associated (>2.0 g cm^{-3}) and mineral-free (<2.0 g cm^{-3}) density fractions (e.g., Fig. 2.4c).

The implications of these results can be summarized as follows: (i) *Z. marina* meadows in the Seto Inland Sea have the capacity to increase the OC loading of sediments from depleted values to near saturation; (ii) seagrass meadow sediments vary widely in OC concentration but often have similar saturated OC loading values; (iii) the rate of OC accumulation in seagrass meadow sediments is constrained mainly by the supply of mineral surfaces available for sorptive preservation of OC, rather than by the supply of OC itself, unless refractory OC is supplied from allochthonous (terrestrial) sources; and (iv) the capacity of seagrass meadows to accumulate available mineral surfaces and therefore to store OC in sediments, depends on spatial factors such as the patch size of individual meadows, which is presumably related to enhanced sediment stability. These characteristics are generally consistent with the hypothesis proposed in Sect. 2.6.

2.8 Factors That Influence the Carbon Storage Capacity of Seagrass Meadows

The conclusions of the previous section regarding *Z. marina* meadows in temperate Japan are thought to be generally applicable to perennial seagrass meadows growing on clastic sediments. However, the sources of OC supplied to seagrass meadows are highly variable depending on the oceanographic setting, and the source-specific characteristics of OC can influence its long-term stability when stored in sediment. Various types of OC supplied to seagrass meadows are conceptually categorized into allochthonous and autochthonous OC, and allochthonous OC can be further divided into two groups based on an association with minerals (Table 2.5).

Table 2.5 Major sources of organic carbon (OC) and the pathways of transportation to coastal seagrass meadows

Classification		Main sources	Degradability	Isotopic characteristics
(I) Allochthonous OC transported as independent suspended organic particles	(I-1) Sestonic organic particles transported from the oceanic pelagic zone	Live and dead plankton	Generally labile	Typical $\delta^{13}C$: –24‰ to –18‰
	(I-2) Detrital organic particles resuspended and transported from neighboring benthic ecosystems	Seagrasses, macroalgae, microphytobenthos, coral mucus	Generally labile	Typical $\delta^{13}C$: –12‰ to –5‰ (seagrass); –20‰ to –10‰ (others)
	(I-3) Detrital organic particles transported from terrestrial or mangrove ecosystems by river flow or tidal exchange	Terrestrial or mangrove plants	Mostly refractory	Typical $\delta^{13}C$: –30‰ to –25‰
(II) Allochthonous OC transported in the form of mineral-associated organic matter	(II-1) Soil and sediment organic matter resuspended and transported from land, mangroves, or seagrass meadows	Microbial secondary organic products	Essentially labile but protected by minerals	Typical $\delta^{13}C$: –30‰ to –25‰ (soil organic matter); –25‰ to –10‰ (seagrass sediment organic matter)
	(II-2) Ancient organic matter included originally in sedimentary bedrocks and transported as rock weathering products (clastic particles)	Aged organic matter of various sources	Refractory	Various $\delta^{13}C$ values; typically depleted in radiocarbon (^{14}C)
	(II-3) Organic remains in biogenic carbonate minerals	Carbonate-producing organisms (corals, foraminifera, calcareous algae, etc.)	Essentially labile but protected by minerals	Typical $\delta^{13}C$: –18‰ to –12‰ (corals)
(III) Autochthonous OC	(III-1) Live and dead fragments of seagrass tissues	Seagrasses	Generally labile	Typical $\delta^{13}C$: –12‰ to –5‰
	(III-2) Dissolved organic matter produced by seagrasses and excreted from their roots into sediment	Seagrasses	Labile	Unknown (putatively same as above)
	(III-3) Organic matter derived from algae	Seagrass-associated macro- and microalgae, microphytobenthos	Labile	Typical $\delta^{13}C$: –20‰ to –10‰

Allochthonous OC transported to seagrass meadows as independent (i.e., mineral-free) organic particles (Category I) may be derived from either marine (I-1,2) or terrestrial (I-3) primary production; OC derived from terrestrial plants, including mangroves, is generally more structurally resistant against degradation compared with OC of marine origin. Allochthonous organic particles are hydrodynamically transported to coastal ecosystems, where they are effectively trapped and accumulated by seagrass blades (Dauby et al. 1995; Miyajima et al. 1998; Kennedy et al. 2004). Some invertebrate residents of seagrass meadows, such as bivalves and epibenthic particle feeders, actively capture floating nutrient-rich organic particles such as living microalgae and coral mucus (Morimoto et al. 2017). A portion of the suspended OC captured by these animals may be incorporated into sediments in their excreta and carrion.

Mineral-associated allochthonous OC (Category II) can be supplied to seagrass meadows as soil or sediment OC that has been resuspended and transported from distant ecosystems including land, mangroves, and other soft-bottom communities, including seagrass meadows. As explained in Sect. 2.4, mineral-associated soil (sediment) organic matter (II-1) presumably originates from microbial secondary products, such as extracellular polymeric materials (Decho 2000; Cyle et al. 2016). Although it may not be intrinsically refractory, adsorption to a mineral surface significantly retards remineralization. Clastic sediment particles generated through physical weathering of sedimentary rocks, especially in tectonically active continental margins, contain ancient organic matter (II-2), which may be transported by rivers to coastal areas (Blair et al. 2003; Leithold et al. 2006; Rosenheim and Galy 2012; Fig. 2.6). Such fossil organic matter, also referred to as petrogenic OC, is generally highly altered and considered resistant against enzymatic decomposition, but it is not totally undegradable (Petsch et al. 2001). Biogenic carbonate sediment contains a significant amount of OC in a carbonate matrix (II-3) that may be solubilized into dissolved OC upon acid decarbonation (Froelich 1980). This fraction can be as large as 40% of the total OC in carbonate sediments of seagrass meadows (Miyajima et al. 1998). This OC is putatively derived from tissues of carbonate-bearing organisms such as reef corals, foraminifera, and calcareous algae and is therefore generally labile once exposed to microbial hydrolytic enzymes.

Autochthonous organic matter produced within seagrass ecosystems (Category III) is also an important source of OC stored in sediment. Organic matter is produced by seagrasses, epiphytic algae, and epibenthic algae (including microphytobenthos). Algal species in seagrass meadows are highly diverse, ranging from unicellular diatoms and cyanobacteria to multicellular macroalgae. Microalgal primary production in meadows can be comparable with that of seagrasses (Pollard and Kogure 1993) and more important than the latter as an energy source for food webs (Moncreiff and Sullivan 2001). The most important autochthonous source of sedimentary OC storage can vary. However, it is often evident that the OC concentration in the top few centimeters of seagrass meadow sediment is more or less depleted compared with the subsurface layer (5–30 cm; Fig. 2.1f, Fig. 2.3c–g), implying that belowground production by seagrasses (rhizomes, roots, and root exudates), which is usually concentrated in the subsurface layer, is the predominant source of autochthonous OC stored in the sediment.

The relative contributions of different OC sources to the sedimentary OC pool in seagrass meadows can vary widely depending on their ecological and oceanographic settings. In typical temperate seagrass meadows growing on clastic sediment, approximately half of the total OC stored in sediment is derived from primary production by seagrasses (Kennedy et al. 2010; Miyajima et al. 2015; Oreska et al. 2018), and most exists as mineral-associated OC (Miyajima et al. 2017). On the other hand, in estuarine *Z. marina* meadows (e.g., Fig. 2.4b; see also Watanabe and Kuwae 2015) and mangrove-fringed tropical seagrass meadows (e.g., Fig. 2.4h; see also Hemminga et al. 1994; Chen et al. 2017), the majority of sediment OC is often of terrestrial or mangrove origin, as suggested by a low $\delta^{13}C$, and is present as mineral-free detrital particles (see Sect. 2.9 for the use of $\delta^{13}C$ as a source proxy). In tropical and subtropical seagrass meadows on carbonate sediments, mineral-free OC and mineral-associated OC contribute roughly equally to the sediment OC stock (e.g., Fig. 2.4e, f), and in the absence of OC input from mangroves, mineral-free OC exhibits an elevated $\delta^{13}C$ ($\geq -15‰$), indicating that it is almost exclusively derived from seagrasses and possibly microphytobenthos (Fig. 2.4e, f). Carbonate sediment slowly undergoes dissolution via reaction with CO_2 produced by microbial respiration (Eldridge and Morse 2000; Hu and Burdige 2007), which may inhibit accumulation of OC on carbonate mineral surfaces and consequently result in a low relative abundance of mineral-associated OC compared with clastic sediment. Although OC loading in carbonate seagrass meadow sediments is apparently very high (Fig. 2.5b), this could be partly explained by the coexistence with mineral-free OC. Another remarkable case involves meadows of *P. oceanica*, a large Mediterranean seagrass species. This species forms a robust belowground structure of rhizomes and roots, which can persist in the sediment for thousands of years after death (Mateo et al. 1997; Lo Iacono et al. 2008). In this case, belowground seagrass production is apparently the most important OC source to the sediment by far (Serrano et al. 2016). A similar but less extensive belowground structure formed by rhizomes and roots is also found in seagrass meadows of subtropical *Thalassia* spp. (Wanless 1981; Fig. 2.1e).

As such, the provenance of OC in seagrass meadow sediments can differ greatly depending on sediment mineralogy, seagrass species composition, and connectivity with neighboring habitats. Estimating global carbon inventory without considering habitat-specific variability of OC sources is likely to introduce a large bias in the case of seagrass meadow sediments.

2.9 Methods for Provenance Analysis of Sediment OC

Many seagrass species do not leave any visible remains that persist long term in sediments (Reich et al. 2015). Most OC in seagrass meadow sediments is either mineral-adsorbed OC or amorphous detrital OC, and the morphological characteristics of these types of organic matter provide few clues as to their origin. Three methods are currently used to infer the primary producers that originally produced OC: isotopic signatures, molecular biomarkers, and environmental DNA

(eDNA). Among these methods, isotope-based techniques, particularly those using $\delta^{13}C$, are the easiest to perform and most straightforward and reliable methods. The major groups of primary producers have specific and distinct $\delta^{13}C$ ranges (Table 2.5), and it has been empirically supported that the $\delta^{13}C$ of organic matter is conserved during diagenetic processes, even when the OC is converted into secondary organic products (except lipids and hydrocarbons) by microorganisms. The $\delta^{13}C$ signature is particularly convenient for tracing seagrass-derived OC, because seagrasses have the highest $\delta^{13}C$ range among major marine and terrestrial primary producers (Table 2.5). When sediment receives OC from multiple sources, the $\delta^{13}C$ may be used to evaluate the relative importance of each source using mixing models and stochastic simulation (e.g., Minagawa 1992; Phillips et al. 2005; Parnell et al. 2010). Typical applications of this approach have been reported by Kennedy et al. (2010) and Miyajima et al. (2015). It should be noted that the reliability of estimates using isotope mixing models may be reduced when the sources are too great in number or not clearly distinguished from each other by the $\delta^{13}C$. Although the isotope ratios of other biogenic elements, such as nitrogen ($\delta^{15}N$) and sulfur ($\delta^{34}S$), have been used in combination with $\delta^{13}C$ for source evaluation in food webs (Kharlamenko et al. 2001; Tewfik et al. 2005), these signatures are not conservative enough to be used for source determination of sediment organic matter, as they are readily altered by selective remineralization, immobilization, oxidation–reduction, and isotope exchange reactions during early diagenetic processes (e.g., Francois 1987; Kohzu et al. 2011; Möbius 2013).

Molecular biomarker approaches are generally not as convenient as isotope signatures for source estimation of OC stored in sediments long term, because many molecular biomarkers are relatively unstable in an oxygenated aquatic environment or easily degraded by the natural bacterial assemblage. Nonetheless, a few potential biomarkers specific to seagrasses have been proposed, including dihydroxy fatty acids (de Leeuw et al. 1995), *n*-alkane-2-ones (Hernandez et al. 2001; Xu et al. 2006), and *p*-hydroxybenzoic acid (as a pyrolysis product; Kaal et al. 2016). Lignin and lignin phenols contained in sediment provide a good proxy for OC derived from vascular plants. Seagrasses also contain lignin, especially in their belowground parts (Klap et al. 2000). A combination of molecular biomarkers and compound-specific isotope analysis would have much greater potential for provenance analysis of sediment OC, because the use of isotopic signatures such as $\delta^{13}C$ allows a wider range of organic molecules to be used as seagrass-specific tracers, including common fatty acids, sterols, and hydrocarbons. However, application of this technique in seagrass meadow sediments is currently limited to microbial trophic studies (Boschker et al. 2000; Bouillon and Boschker 2006).

The use of eDNA is more promising (Parducci et al. 2015), because short fragments of DNA can persist over a long period in sediments due to the sorptive preservation mechanism (Cai et al. 2006). Recently, eDNA techniques were applied successfully in the source evaluation of OC in seagrass meadows (Reef et al. 2017; Hamaguchi et al. 2018). Also, Hamaguchi et al. (unpublished data) demonstrated that their eDNA technique can be used to trace the fate of seagrass-derived OC exported from seagrass habitats to the open ocean and deposited in pelagic sediment.
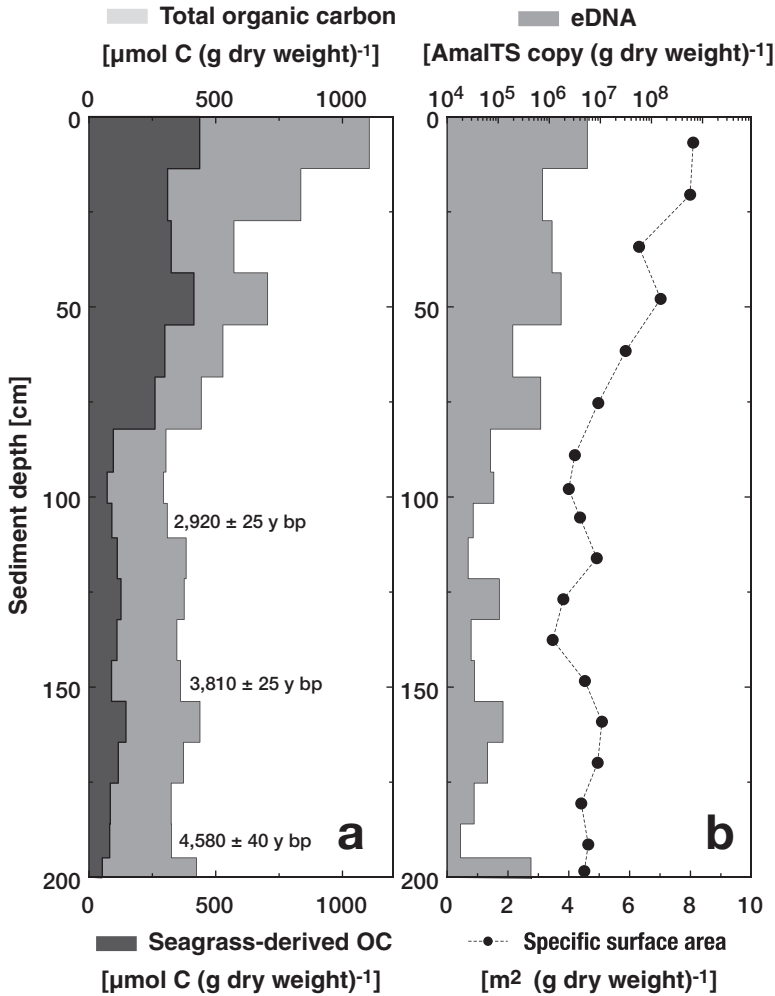
Fig. 2.7 Vertical profiles of total OC (**a**, thin gray) and seagrass-derived OC as determined using δ^{13}C-based provenance analysis (**a**, dark gray), seagrass-derived eDNA (logarithmic copy number of AmaITS gene fragments; **b**, gray area) and SSA (**b**, closed circle) in a sediment core collected from a seagrass bed in the Seto Inland Sea, Japan. [14]C ages of several layers are shown in (**a**). See Hamaguchi et al. (2018) for technical details

When employing the molecular biomarker and eDNA techniques for evaluation of the contributions of specific OC sources in sediment, the most challenging step is establishing the quantitative relationship between the concentration of a biomarker or eDNA and that of total OC derived from the same primary producers. Hamaguchi et al. (2018) explored this relationship and found that the concentration of DNA fragments from *Z. marina* in modern and ancient (up to 4500 years BP) eelgrass meadow sediments varied consistently with the concentration of seagrass-derived OC, as evaluated using the isotope mass balance method (Fig. 2.7). The coefficient

of determination between the logarithm of the eDNA copy number and seagrass-derived OC (excluding the sample from the deepest layer that was apparently subject to eDNA contamination) is as high as 0.89. This example shows that eDNA is a promising tool for quantitative evaluation of sediment OC derived from various plant species. However, the quantitative relationship between eDNA and OC from seagrasses appears to depend on the age of the samples and also on the environmental settings of the meadows, which poses a challenge to the broader applicability of this technique. This discrepancy may be partially related to differences in the specificity to seagrasses of eDNA- and δ^{13}C-based techniques. At present, more comprehensive studies are required to understand which factors control the preservation of molecular biomarkers and eDNA in the diverse sediments of coastal vegetated ecosystems.

2.10 Global Significance of Carbon Sequestration in Seagrass Meadow Sediments

An obvious condition for a marine ecosystem to sequester carbon long term is that the sediment mass accumulation rate in that ecosystem is greater than zero. The rate of long-term carbon sequestration (μmol C m^{-2} year^{-1}) can then be defined as the product of the sediment mass accumulation rate (g dry weight m^{-2} year^{-1}), the OC concentration of surface sediment (μmol C (g dry weight)$^{-1}$), and the OC burial efficiency (dimensionless). However, estimation of the OC burial efficiency in seagrass meadows is often problematic, because the OC concentration in anoxic sediment does not necessarily decrease with increasing depth and may show a subsurface maximum due to belowground seagrass production (see Sect. 2.4.1). For this reason, the OC sequestration rate in seagrass meadows is usually estimated as the product of the average OC concentration in the top 20–100 cm sediment core and the mass accumulation rate. The mass accumulation rate is the product of the sedimentation rate (mm year^{-1}) and the dry bulk density of the sediment core (g dry weight cm^{-3}) times 1000.

Two methods have been conventionally used to determine the sedimentation rate from intact sediment cores: radioactive carbon (^{14}C) dating by accelerator mass spectrometry and ^{210}Pb/^{137}Cs dating by γ-spectroscopy. However, caution is required to interpret the dating results obtained from each of these methods. Although the ^{14}C method is, in principle, more straightforward for use in carbon sequestration studies, it requires core samples covering a much longer time span (hundreds to thousands of years) than does the ^{210}Pb/^{137}Cs method (<100 years). In addition, ^{14}C dating is affected by spatiotemporal variability in the influence of aged OC, such as old terrestrial OC and deep-sea dissolved inorganic carbon (referred to as the reservoir effect). On the other hand, the ^{210}Pb/^{137}Cs method often provides higher sedimentation rates than those of the ^{14}C method, presumably due to sediment compaction and physical and biological vertical mixing of the top layers of sediment causing overestimation of sedimentation rates in the ^{210}Pb/^{137}Cs dating. Many available data

regarding OC burial in seagrass meadows rely on sedimentation rates measured using the ^{14}C method (Table 2.6). It should be noted that these data generally do not represent instantaneous rates, but rather average rates over the previous hundreds of years.

Quite a few studies have evaluated the sedimentation rate in seagrass meadows (Table 2.6). Most of these studies (except Jankowska et al. 2016) used ^{14}C dating, and the measured sedimentation rates generally ranged from 0.3 to 1.4 mm year^{-1}, except in meadows of the large Mediterranean seagrass species *P. oceanica* (average, 2.1 mm year^{-1}). The OC sequestration rate is even more variable among different seagrass species, with that in *P. oceanica* meadows (average, 5820 mmol C m^{-2} year^{-1}) being an order of magnitude greater than that in seagrass meadows of other species (420 mmol C m^{-2} year^{-1}). This is due to both higher sedimentation rates and greater OC concentrations in the sediment of *P. oceanica* meadows than in other meadows. It is very difficult to estimate the contribution of OC sequestration in seagrass meadows to the global carbon budget, because the available information is still far from sufficient for evaluating geographic variability in the sedimentation and OC sequestration rates in seagrass meadows (see also Sect. 2.8). With this in

Table 2.6 Examples of sedimentation rates and OC sequestration rate measured for seagrass meadow sediments

Geographic region	Latitude	Dominant seagrass	n	Sedimentation rate (mm year^{-1})	OC sequestration rate (mmol C m^{-2} year^{-1})	References
Baltic Sea	54.23°–54.42°N	*Zostera marina*	3	1.3	210 ± 130	Jankowska et al. (2016)
Northern Japan	43.33°N	*Zostera marina*	3	0.37 ± 0.18	458 ± 156	Tokoro et al. (2014)
Southeastern Spain	38.16°–42.30°N	*Posidonia oceanica*	7	1.75 ± 1.18	4800 ± 3500	Mateo et al. (1997)
Northwestern Mediterranean	38.72°–38.91°N	*Posidonia oceanica*	2	2.4 – 4.2	7100 – 11700	Serrano et al. (2014)
Central Japan	33.60°–34.32°N	*Zostera marina*	3	0.37 – 1.34	570 ± 290	Miyajima et al. (2015)
Southwestern Japan	24.49°N	*Enhalus acoroides*	1	1.23	447	Miyajima et al. (2015)
Southern Thailand	7.39°N	*Thalassia hemprichii*	1	0.82	203	Miyajima et al. (2015)
Western Australia	32.16°S	*Posidonia sinuosa*	4	0.6 – 1.3	530 ± 430	Serrano et al. (2014)
Southwestern Australia	34.98°S	*Posidonia australis*	1	0.49	287	Rozaimi et al. (2016)
Average			25		2450 ± 3450	
Average excluding *Posidonia oceanica* meadows			16		420 ± 270	

mind, a tentative minimal estimation of long-term OC sequestration by global seagrass meadows may be 1.6 Tg C year^{-1}, based on the average OC sequestration rate excluding *P. oceanica* meadows and a global extent of seagrass meadows of 320,000 km^2. If the average OC sequestration rate including *P. oceanica* meadows is used, the global OC sequestration by seagrass meadows is estimated to be 9.4 Tg C year $^{-1}$.

It should be noted that these estimates represent the amount of OC expected to be sequestered in sediment for hundreds to thousands of years, because millennial-scale sediment cores were used to draw them. In the literature, several different estimates of global carbon sequestration in seagrass meadows have been reported, and these estimates are much larger than those described above: 27.4 Tg C year^{-1} (based on sediment delivery partitioning; Duarte et al. 2005; see also Table 2.3), 44 Tg C year^{-1} (derived from community metabolic balancing; Duarte et al. 2005), and 48–112 Tg C year^{-1} (based on a compilation of various direct estimates of net primary production and allochthonous carbon accumulation; Kennedy et al. 2010). Such discrepancies among estimates are principally derived from differences in the time span covered by the methods used (Miyajima et al. 2015). The shorter the time span used for estimation of OC sequestration, the greater the resulting estimates are. Therefore, when the OC sequestration rate of seagrass meadows is compared with the corresponding rates in other ecosystems or global carbon emissions flux, the time span over which the rate is evaluated should be carefully chosen and clearly defined.

The overall potential of seagrass meadows and other coastal vegetated ecosystems for carbon sequestration may be considerably greater than the estimates noted above, because these estimates focused solely on OC sequestered within the ecosystems' own sediments. In fact, seagrass meadows often export as large a fraction of their net primary production to the pelagic ocean as that stored in their own sediments (Duarte and Cebrián 1996). After OC is exported to the open ocean, a portion of it may be sequestered within the ocean via several different mechanisms (Fig. 2.8). Firstly, particulate OC (POC) exported from seagrass meadows as detached seagrass leaves or resuspended organic sediment may settle onto pelagic sediments and be stored for long term therein. For example, the export of detached blades from the seagrass meadows of the Seto Inland Sea, Japan, to surrounding pelagic sediment and further to the open Pacific Ocean has been estimated by numerical hydrodynamic simulations (see Abo et al. (2018) in this volume). The presence of seagrass-derived OC in the pelagic sediment of the Seto Inland Sea has been observed directly using the eDNA approach (Hamaguchi et al., unpublished data). Secondly, seagrasses excrete photosynthetic products as dissolved OC (DOC) to the surrounding seawater (Wetzel and Penhale 1979; Ziegler and Benner 1999; Barrón and Duarte 2009). Such DOC is presumably exported outside the meadows to reside temporarily in the water column, where a portion of the DOC may be converted to long-lived refractory DOC (RDOC) through complex microbial reactions (Ogawa et al. 2001; see also Kuwae et al. (2018) in this volume). This mechanism can be regarded as a type of carbon sequestration in the ocean, insofar as the turnover time of the RDOC produced is sufficiently long. Thirdly, under some conditions, dissolved inorganic carbon produced from remineralization of seagrass-
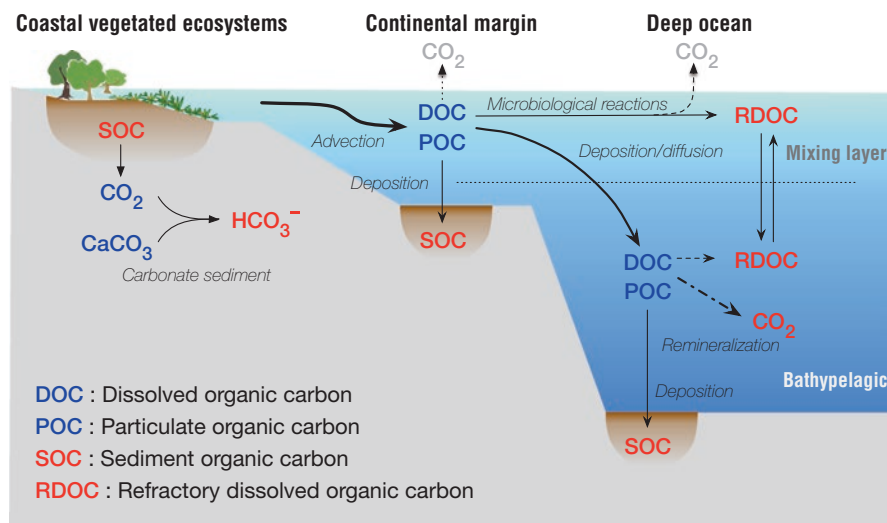
Fig. 2.8 Carbon export pathways from coastal vegetated ecosystems. OC produced in seagrass ecosystems may be potentially sequestered long term in the reservoirs marked by red letters, i.e., pelagic sediment OC (SOC), water-column bicarbonate (HCO_3^-) and refractory dissolved OC (RDOC), and dissolved carbon dioxide (CO_2) in the bathypelagic water column

derived POC and DOC may be considered long-term sequestered carbon. For example, a portion of the POC exported from seagrass meadows located at the edge of the continental shelf may settle rapidly in the deep ocean and undergo remineralization into CO_2 below the pycnocline (Fig. 2.8). As CO_2 generated below the pycnocline is expected to be isolated from the atmosphere for hundreds of years, it can be regarded as sequestered carbon. Another example occurs when belowground seagrass OC is remineralized within carbonate sediment. CO_2 generated in carbonate sediment instantly reacts with ambient $CaCO_3$ and is converted to HCO_3^-. As HCO_3^- can no longer outgas from the ocean to the atmosphere, it can also be regarded as sequestered carbon in terms of the atmospheric CO_2 budget. Similarly, when remineralization of OC occurs in anoxic sediment via denitrification and sulfate reduction, a portion of the remineralized carbon is formed as HCO_3^- rather than as CO_2, although the ratio of HCO_3^- to CO_2 in the final product depends on environmental conditions such as the availability of reactive iron. Production of HCO_3^- in seagrass meadow sediments has been demonstrated in several case studies (Hu and Burdige 2007; Higuchi et al. 2014). The global contribution of each of these processes to carbon sequestration remains unclear. To fully evaluate the significance of ecosystem functions of seagrass meadows and other coastal vegetated systems in the biogeochemical carbon cycle, the roles of all the above processes should be adequately described and included in the global analysis.

To understand geographical variability and predict future trends in the carbon sequestration potential of seagrass meadows, the following aspects should also be

considered: (i) the vulnerability and resilience of seagrass meadows to catastrophic physical disturbances (e.g., tropical storms and tsunamis) and biological grazing pressure; (ii) their response to local anthropogenic influences on nutrient status and sediment discharge; and (iii) the effects of global changes such as elevated water temperature, ocean acidification, and sea-level rise. Although these topics are not addressed in this chapter, some important local and global anthropogenic influences are discussed elsewhere in this volume (Yoshida et al. (2018) and Kuwae et al. (2018) among others).

References

Abo K, Sugimatsu K, Hori M, Yoshida G, Shimabukuro H, Yagi H, Nakayama A, Tarutani K (2018) Chapter 9: Quantifying the fate of captured carbon: from seagrass meadow to deep sea. In: Kuwae T, Hori M (eds) Blue carbon in shallow coastal ecosystems: carbon dynamics, policy, and implementation. Springer, Singapore, pp 251–271

Aller RC (1998) Mobile deltaic and continental shelf muds as suboxic, fluidized bed reactors. Mar Chem 61:143–155. https://doi.org/10.1016/S0304-4203(98)00024-3

Aller RC, Blair NE (2006) Carbon remineralization in the Amazon–Guianas tropical mobile mudbelt: a sedimentary incinerator. Cont Shelf Res 26:2241–2259. https://doi.org/10.1016/j.csr.2006.07.016

Alongi DM (2012) Carbon sequestration in mangrove forests. Carbon Manag 3:313–322. https://doi.org/10.4155/cmt.12.20

Alongi DM, Murdiyarso D, Fourqurean JW, Kauffman JB, Hutahaean A, Crooks S, Lovelock CE, Howard J, Herr D, Fortes M (2016) Indonesia's blue carbon: a globally significant and vulnerable sink for seagrass and mangrove carbon. Wetl Ecol Manag 24:3–13. https://doi.org/10.1007/s11273-015-9446-y

Arnarson TS, Keil RG (2007) Changes in organic matter–mineral interactions for marine sediments with varying oxygen exposure times. Geochim Cosmochim Acta 71:3545–3556. https://doi.org/10.1016/j.gca.2007.04.027

Barrón C, Duarte CM (2009) Dissolved organic matter release in a *Posidonia oceanica* meadow. Mar Ecol Prog Ser 374:75–84. https://doi.org/10.3354/meps07715

Beer S, Björk M, Beardall J (2014) Photosynthesis in the marine environment. Wiley Blackwell, London

Bergamaschi BA, Tsamakis E, Keil RG, Eglinton TI, Montlucon DB, Hedges JI (1997) The effect of grain size and surface area on organic matter, lignin and carbohydrate concentration, and molecular compositions in Peru margin sediments. Geochim Cosmochim Acta 61:1247–1260. https://doi.org/10.1016/S0016-7037(96)00394-8

Berner RA (1982) Burial of organic carbon and pyrite sulfur in the modern ocean: its geochemical and environmental significance. Am J Sci 282:451–473. https://doi.org/10.2475/ajs.282.4.451

Bianchi TS, Cui X, Blair NE, Burdige DJ, Eglinton TI, Galy V (2018) Centers of organic carbon burial and oxidation at the land-ocean interface. Org Geochem 115:138–155. https://doi.org/10.1016/j.orggeochem.2017.09.008

Blair NE, Aller RC (2012) The fate of terrestrial organic carbon in the marine environment. Annu Rev Mar Sci 4:401–423. https://doi.org/10.1146/annurev-marine-120709-142717

Blair NE, Leithold EI, Ford ST, Peeler KA, Holmes JC, Perkey DW (2003) The persistence of memory: the fate of ancient sedimentary organic carbon in a modern sedimentary system. Geochim Cosmochim Acta 67:63–73. https://doi.org/10.1016/S0016-7037(02)01043-8

Bock MJ, Mayer LM (2000) Mesodensity organo–clay associations in a near-shore sediment. Mar Geol 163:65–75. https://doi.org/10.1016/S0025-3227(99)00105-X

Boden TA, Marland G, Andres RJ (2011) Global, regional, and national fossil-fuel CO_2 emissions, Carbon Dioxide Information Analysis Center, Oak Ridge National Laboratory, U.S. Department of Energy, Oak Ridge. doi:https://doi.org/10.3334/CDIAC/00001_V2011

Boschker HTS, Wielemaker A, Schaub BEM, Holmer M (2000) Limited coupling of macrophyte production and bacterial carbon cycling in the sediment of *Zostera* spp. meadows. Mar Ecol Prog Ser 203:181–189. https://doi.org/10.3354/meps203181

Bouillon S, Boschker HTS (2006) Bacterial carbon sources in coastal sediments: a cross-system analysis based on stable isotope data of biomarkers. Biogeosciences 3:175–185. https://doi.org/10.5194/bg-3-175-2006

Bouillon S, Borges AV, Castañeda-Moya E, Diele K, Dittmar T, Duke NC, Kristensen E, Lee SY, Marchand C, Middelburg JJ, Rivera-Monroy VH, Smith TJ, Twilley RR (2008) Mangrove production and carbon sinks: a revision of global budget estimates. Glob Biogeochem Cycles 22:GB2013. https://doi.org/10.1029/2007GB003052

Cabaço S, Santos R, Duarte CM (2008) The impact of sediment burial and erosion on seagrasses: a review. Estuar Coast Shelf Sci 79:354–366. https://doi.org/10.1016/j.ecss.2008.04.021

Cai P, Huang Q-Y, Zhang X-W (2006) Interactions of DNA with clay minerals and soil colloidal particles and protection against degradation by DNase. Environ Sci Technol 40:2971–2976. https://doi.org/10.1021/es0522985

Chen G, Azkab MH, Chmura GL, Chen S, Sastrosuwondo P, Ma Z, Dharmawan IWE, Yin X, Chen B (2017) Mangroves as a major source of soil carbon storage in adjacent seagrass meadows. Sci Rep 7:42406. https://doi.org/10.1038/srep42406

Chenu C (1993) Clay- or sand-polysaccharide associations as models for the interface between micro-organisms and soil: water related properties and microstructure. Geoderma 56:143–156. https://doi.org/10.1016/0016-7061(93)90106-U

Ciais P, Sabine CL, Bala G, Bopp L, Brovkin V, Canadell J, Chhabra A, DeFries R, Galloway J, Heimann M, Jones C, Le Quéré C, Myneni RB, Piao S, Thornton P (2013) 6. Carbon and other biogeochemical cycles. In: Stocker TF, Qin D, Plattner G-K, Tignor M, Allen SK, Boschung J, Nauels A, Xia Y, Bex V, Midgley PM (eds) Climate change 2013: the physical science basis. Contribution of Working Group I to the fifth assessment report of the intergovernmental panel on climate change. Cambridge University Press, Cambridge

Cyle KT, Hill N, Young K, Jenkins T, Hancock D, Schroeder PA, Thompson A (2016) Substrate quality influences organic matter accumulation in the soil silt and clay fraction. Soil Biol Biochem 103:138–148. https://doi.org/10.1016/j.soilbio.2016.08.014

Dauby P, Bale AJ, Bloomer N, Canon C, Ling RD, Norro A, Robertson JE, Simon A, Theate J-M, Watson AJ, Frankignoulle M (1995) Particle fluxes over a Mediterranean seagrass bed: a one year case study. Mar Ecol Prog Ser 126:233–246. https://doi.org/10.3354/meps126223

De Leeuw JW, Rijpstra WIC, Nienhuis PH (1995) Free and bound fatty acids and hydroxy fatty acids in the living and decomposing eelgrass *Zostera marina* L. Org Geochem 23:721–728. https://doi.org/10.1016/0146-6380(95)00062-J

Decho AW (2000) Microbial biofilms in intertidal systems: an overview. Cont Shelf Res 20:1257–1273. https://doi.org/10.1016/S0278-4343(00)00022-4

Del Giorgio PA, Cole JJ (1998) Bacterial growth efficiency in natural aquatic systems. Annu Rev Ecol Syst 29:503–541. https://doi.org/10.1146/annurev.ecolsys.29.1.503

Donato DC, Kauffman JB, Murdiyarso D, Kurnianto S, Stidham M, Kanninen M (2011) Mangroves among the most carbon-rich forests in the tropics. Nat Geosci 4:293–297. https://doi.org/10.1038/NGEO1123

Duarte CM (1991) Seagrass depth limits. Aquat Bot 40:363–377. https://doi.org/10.1016/0304-3770(91)90081-F

Duarte CM, Cebrián J (1996) The fate of marine autotrophic production. Limnol Oceanogr 41:1758–1766. https://doi.org/10.4319/lo.1996.41.8.1758

Duarte CM, Middelburg JJ, Caraco N (2005) Major role of marine vegetation on the oceanic carbon cycle. Biogeosciences 2:1–8. https://doi.org/10.5194/bg-2-1-2005

Eldridge PM, Morse JW (2000) A diagenetic model for sediment-seagrass interactions. Mar Chem 70:89–103. https://doi.org/10.1016/S0304-4203(00)00018-9

Emerson S, Hedges J (2003) Chapter 6.11. Sediment diagenesis and benthic flux. In: Elderfield H (ed) The oceans and marine geochemistry, treatise on geochemistry, vol 6. Elsevier, Oxford, pp 293–319

Emerson S, Fischer K, Reimers C, Heggie D (1985) Organic carbon dynamics and preservation in deep-sea sediments. Deep-Sea Res A 32:1–21. https://doi.org/10.1016/0198-0149(85)90014-7

Fonseca MS (1989) Sediment stabilization by *Halophila decipiens* in comparison to other seagrasses. Estuar Coast Shelf Sci 29:501–507. https://doi.org/10.1016/0272-7714(89)90083-8

Fonseca MS, Fisher JS (1986) A comparison of canopy friction and sediment movement between four species of seagrasses with reference to their ecology and restoration. Mar Ecol Prog Ser 29:15–22

Fonseca MS, Fisher JS, Zieman JC, Thayer GW (1982) Influence of the seagrass, *Zostera marina* L., on current flow. Estuar Coast Shelf Sci 15:351–364. https://doi.org/10.1016/0272-7714(82)90046-4

Fourqurean JW, Duarte CM, Kennedy H, Marbà N, Holmer M, Mateo MA, Apostolaki ET, Kendrick GA, Krause-Jensen D, McGlathery KJ (2012) Seagrass ecosystems as a globally significant carbon stock. Nat Geosci 5:505–509. https://doi.org/10.1038/ngeo1477

Francois R (1987) A study of sulphur enrichment in the humic fraction of marine sediments during early diagenesis. Geochim Cosmochim Acta 51:17–27. https://doi.org/10.1016/0016-7037(87)90003-2

Froelich PN (1980) Analysis of organic carbon in marine sediments. Limnol Oceanogr 25:564–572. https://doi.org/10.4319/lo.1980.25.3.0564

Fujimoto K, Miyagi T, Murofushi T, Mochida Y, Umitsu M, Adachi H, Pramojanee P (1999) Mangrove habitat dynamics and Holocene sea-level changes in the southwestern coast of Thailand. Tropics 8:239–255. https://doi.org/10.3759/tropics.8.239

Gacia E, Duarte CM (2001) Sediment retention by a Mediterranean *Posidonia oceanica* meadow: the balance between deposition and resuspension. Estuar Coast Shelf Sci 52:505–514. https://doi.org/10.1006/ecss.2000.0753

Gacia E, Granata TC, Duarte CM (1999) An approach to measurement of particle flux and sediment retention within seagrass (*Posidonia oceanic*a) meadows. Aquat Bot 65:255–268. https://doi.org/10.1016/S0304-3770(99)00044-3

Galeron M-A, Radakovitch O, Charrière B, Vaultier F, Volkman JK, Bianchi TS, Ward ND, Medeiros PM, Sawakuchi HO, Tank S, Kerhervé P, Rontani J-F (2018) Lipoxygenase-induced autoxidative degradation of terrestrial particulate organic matter in estuaries: a widespread process enhanced at high and low latitude. Org Geochem 115:78–92. https://doi.org/10.1016/j.orggeochem.2017.10.013

Gibbs RJ (1981) Sites of river-derived sedimentation in the oceans. Geology 9:77–80. https://doi.org/10.1130/0091-7613(1981)9<77:SORSIT>2.0.CO;2

Gorham E, Vitousek PM, Reiners WA (1979) The regulation of chemical budgets over the course of terrestrial ecosystem succession. Annu Rev Ecol Syst 10:53–84

Gullström M, Lyimo LD, Dahl M, Samuelsson GS, Eggertsen M, Anderberg E, Rasmusson LM, Linderholm HW, Knudby A, Bandeira S, Nordlund LM, Björk M (2017) Blue carbon storage in tropical seagrass meadows relates to carbonate stock dynamics, plant–sediment processes, and landscape context: insights from the Western Indian Ocean. Ecosystems 21:551. https://doi.org/10.1007/s10021-017-0170-8

Hamaguchi M, Shimabukuro H, Hori M, Yoshida G, Terada T, Miyajima T (2018) Quantitative real-time PCR and droplet digital PCR duplex assays for detecting *Zostera marina* DNA in coastal sediments. Limnol Oceanogr Methods 16:253. https://doi.org/10.1002/lom3.10242

Hammel KE, Kapich AN, Jensen KA, Ryan ZC (2002) Reactive oxygen species as agents of wood decay by fungi. Enzym Microb Technol 30:445–453. https://doi.org/10.1016/S0141-0229(02)00011-X

Hartnett HE, Keil RG, Hedges JI, Devol AH (1998) Influence of oxygen exposure time on organic carbon preservation in continental margin sediments. Nature 391:572–574. https://doi.org/10.1038/35351

Hedges JI, Keil RG (1995) Sedimentary organic matter preservation: an assessment and speculative synthesis. Mar Chem 49:81–115. https://doi.org/10.1016/0304-4203(95)00008-F

Hedges JI, Hu FS, Devol AH, Hartnett HE, Tsamakis E, Keil RG (1999) Sedimentary organic matter preservation: a test for selective degradation under oxic conditions. Am J Sci 299:529–555. https://doi.org/10.2475/ajs.299.7-9.529

Hemminga MA (1998) The root/rhizome system of seagrasses: an asset and a burden. J Sea Res 39:183–196. https://doi.org/10.1016/S1385-1101(98)00004-5

Hemminga MA, Slim FJ, Kazungu J, Ganssen GM, Nieuwenhuize J, Kruyt NM (1994) Carbon outwelling from a mangrove forest with adjacent seagrass beds and coral reefs (Gazi Bay, Kenya). Mar Ecol Prog Ser 106:291–301. https://doi.org/10.3354/meps106291

Hendriks IE, Sintes T, Bouma TJ, Duarte CM (2008) Experimental assessment and modeling evaluation of the effects of the seagrass *Posidonia oceanica* on flow and particle trapping. Mar Ecol Prog Ser 356:163–173. https://doi.org/10.3354/meps07316

Hernandez ME, Mead R, Peralba MC, Jaffé R (2001) Origin and transport of *n*-alkane-2-ones in a subtropical estuary: potential biomarkers for seagrass-derived organic matter. Org Geochem 32:21–32. https://doi.org/10.1016/S0146-6380(00)00157-1

Higuchi T, Takagi KK, Matoba K, Kobayashi S, Tsurumi R, Arakaki S, Nakano Y, Fujimura H, Oomori T, Tsuchiya M (2014) The nutrient and carbon dynamics that mutually benefit coral and seagrass in mixed habitats under the influence of groundwater at Bise coral reef, Okinawa, Japan. Int J Mar Sci 4:1–15. https://doi.org/10.5376/ijms.2014.04.0001

Hori M, Kuwae T (2018) Chapter 1: Blue carbon: characteristics of the ocean's sequestration and storage ability of carbon dioxide. In: Kuwae T, Hori M (eds) Blue carbon in shallow coastal ecosystems: carbon dynamics, policy, and implementation. Springer, Singapore, pp 1–31

Hori M, Hamaoka H, Hirota M, Lagarde F, Vaz S, Hamaguchi M, Hori J, Makino M (2018) Application of the coastal ecosystem complex concept toward integrated management for sustainable coastal fisheries under oligotrophication. Fish Sci 84:283–292. https://doi.org/10.1007/s12562-017-1173-2

Houghton RA (2014) 10.10 – the contemporary carbon cycle. In: Karl D, Schlesinger WH (eds) Biogeochemistry, treatise on geochemistry, vol 9, 2nd edn. Elsevier, Oxford, pp 399–435. https://doi.org/10.1016/B978-0-08-095975-7.00810-X

Hu X, Burdige DJ (2007) Enriched stable carbon isotopes in the pore waters of carbonate sediments dominated by seagrasses: evidence for coupled carbonate dissolution and reprecipitation. Geochim Cosmochim Acta 71:129–144. https://doi.org/10.1016/j.gca.2006.08.043

Iizumi H, Hattori A, McRoy CP (1980) Nitrate and nitrite in interstitial waters of eelgrass beds in relation to the rhizosphere. J Exp Mar Biol Ecol 47:191–201. https://doi.org/10.1016/0022-0981(80)90112-4

Inoue T (2018) Chapter 3: Carbon sequestration in mangroves. In: Kuwae T, Hori M (eds) Blue carbon in shallow coastal ecosystems: carbon dynamics, policy, and implementation. Springer, Singapore, pp 73–99

Jackson RB, Canadell J, Ehleringer JR, Mooney HA, Sala OE, Schulze ED (1996) A global analysis of root distributions for terrestrial biomes. Oecologia 108:389–411. https://doi.org/10.1007/BF00333714

Jankowska E, Michel LN, Zaborska A, Włodarska-Kowalczuk M (2016) Sediment carbon sink in low-density temperate eelgrass meadows (Baltic Sea). J Geophys Res Biogeosci 121:2918. https://doi.org/10.1002/2016JG003424

Jensen SI, Kühl M, Priemé A (2007) Different bacterial communities associated with the roots and bulk sediment of the seagrass *Zostera marina*. FEMS Microbiol Ecol 62:108–117. https://doi.org/10.1111/j.1574-6941.2007.00373.x

Jobbágy EG, Jackson RB (2000) The vertical distribution of soil organic carbon and its relation to climate and vegetation. Ecol Appl 10:423–436. https://doi.org/10.1890/1051-0761(2000)010[0423:TVDOSO]2.0.CO;2

Kaal J, Serrano O, Nierop KGJ, Schellekens J, Martínez Cortizas A, Mateo M-Á (2016) Molecular composition of plant parts and sediment organic matter in a Mediterranean seagrass (*Posidonia oceanica*) mat. Aquat Bot 133:50–61. https://doi.org/10.1016/j.aquabot.2016.05.009

Kaiser K, Guggenberger G (2007) Sorptive stabilization of organic matter by microporous goethite: sorption into small pores vs. surface complexation. Eur J Soil Sci 58:45–59. https://doi.org/10.1111/j.1365-2389.2006.00799.x

Keil RG, Mayer LM (2014) Mineral matrices and organic matter. In: Falkowski PG, Freeman KH (eds) Organic geochemistry, Treatise on geochemistry, vol 12, 2nd edn. Elsevier, Oxford, pp 337–359. https://doi.org/10.1016/B978-0-08-095975-7.01024-X

Keil RG, Tsamakis E, Fuh CB, Giddings JC, Hedges JI (1994a) Mineralogical and textural controls on the organic composition of coastal marine sediments: hydrodynamic separation using SPLITT-fractionation. Geochim Cosmochim Acta 58:879–893. https://doi.org/10.1016/0016-7037(94)90512-6

Keil RG, Montluçon DB, Prahl FG, Hedges JI (1994b) Sorptive preservation of labile organic matter in marine sediments. Nature 370:549–552. https://doi.org/10.1038/370549a0

Kennedy H, Gacia E, Kennedy DP, Papadimitriou S, Duarte CM (2004) Organic carbon sources to SE Asian coastal sediments. Estuar Coast Shelf Sci 60:59–68. https://doi.org/10.1016/j.ecss.2003.11.019

Kennedy H, Beggins J, Duarte CM, Fourqurean JW, Holmer M, Marbà N, Middelburg JJ (2010) Seagrass sediments as a global carbon sink: isotopic constraints. Glob Biogeochem Cycles 24:1–8. https://doi.org/10.1029/2010GB003848

Kharlamenko VI, Kiyashko SI, Imbs AB, Vyshkvarzev DI (2001) Identification of food sources of invertebrates from the seagrass *Zostera marina* community using carbon and sulfur stable isotope ratio and fatty acid analysis. Mar Ecol Prog Ser 220:103–117. https://doi.org/10.3354/meps220103

Klap VA, Hemminga MA, Boon JJ (2000) Retention of lignin in seagrasses: angiosperms that returned to the sea. Mar Ecol Prog Ser 194:1–11. https://doi.org/10.3354/meps194001

Klee RJ, Graedel TE (2004) ELEMENTAL CYCLES: A status report on human or natural dominance. Annu Rev Environ Resour 29:69–107. https://doi.org/10.1146/annurev.energy.29.042203.104034

Koch EW (2001) Beyond light: physical, geological, and geochemical parameters as possible submersed aquatic vegetation habitat requirements. Estuaries 24:1–17. https://doi.org/10.2307/1352808

Kohzu A, Imai A, Miyajima T, Fukushima T, Matsushige K, Komatsu K, Kawasaki N, Miura S, Sato T (2011) Direct evidence for nitrogen isotope discrimination during sedimentation and early diagenesis in Lake Kasumigaura, Japan. Org Geochem 42:173–183. https://doi.org/10.1016/j.orggeochem.2010.10.010

Kuwae T, Kanda J, Kubo A, Nakajima F, Ogawa H, Sohma A, Suzumura M (2018) Chapter 11: CO₂ uptake in the shallow coastal ecosystems affected by anthropogenic impacts. In: Kuwae T, Hori M (eds) Blue carbon in shallow coastal ecosystems: carbon dynamics, policy, and implementation. Springer, Singapore, pp 295–319

Leithold EL, Blair NE, Perkey DW (2006) Geomorphologic controls on the age of particulate organic carbon from small mountainous and upland rivers. Glob Biogeochem Cycles 20:GB3022. https://doi.org/10.1029/2005GB002677

Les DH, Cleland MA, Waycott M (1997) Phylogenetic studies in Alismatidae, II: evolution of marine angiosperms (seagrasses) and hydrophily. Syst Bot 22:443–463. https://doi.org/10.2307/2419820

Lo Iacono C, Mateo MA, Gràcia E, Guasch L, Carbonell R, Serrano L, Serrano O, Dañobeitia J (2008) Very high-resolution seismo-acoustic imaging of seagrass meadows (Mediterranean

Sea): implications for carbon sink estimates. Geophys Res Lett 35:L18601. https://doi.org/10.1029/2008GL034773

Lomstein BA, Niggemann J, Jørgensen BB, Langerhuusa AT (2009) Accumulation of prokaryotic remains during organic matter diagenesis in surface sediments off Peru. Limnol Oceanogr 54:1139–1151. https://doi.org/10.4319/lo.2009.54.4.1139

Lünsdorf H, Erb R, Abraham W, Timmis K (2000) 'Clay hutches': a novel interaction between bacteria and clay minerals. Environ Microbiol 2:161–168. https://doi.org/10.1046/j.1462-2920.2000.00086.x

Manzello DP, Enochs IC, Melo N, Gledhill DK, Johns EM (2012) Ocean acidification refugia of the Florida reef tract. PLoS One 7:e41715. https://doi.org/10.1371/journal.pone.0041715

Mateo MA, Romero J, Perez M, Littler MM, Littler DS (1997) Dynamics of millenary organic deposits resulting from the growth of the Mediterranean seagrass *Posidonia oceanica*. Estuar Coast Shelf Sci 44:103–110. https://doi.org/10.1006/ecss.1996.0116

Mayer LM (1994) Surface area control of organic carbon accumulation in continental shelf sediments. Geochim Cosmochim Acta 58:1271–1284. https://doi.org/10.1016/0016-7037(94)90381-6

Middelburg JJ, Nieuwenhuize J, Lubberts RK, van de Plassche O (1997) Organic carbon isotope systematics of coastal marshes. Estuar Coast Shelf Sci 45:681–687. https://doi.org/10.1006/ecss.1997.0247

Minagawa M (1992) Reconstruction of human diet from $\delta^{13}C$ and $\delta^{15}N$ in contemporary Japanese hair: a stochastic method for estimating multi-source contribution by double isotopic tracers. Appl Geochem 7:145–158. https://doi.org/10.1016/0883-2927(92)90033-Y

Miyajima T, Koike I, Yamano H, Iizumi H (1998) Accumulation and transport of seagrass-derived organic matter in reef flat sediment of Green Island, Great Barrier Reef. Mar Ecol Prog Ser 175:251–259. https://doi.org/10.3354/meps175251

Miyajima T, Ogawa H, Koike I (2001a) Alkali-extractable polysaccharides in marine sediments: abundance, molecular size distribution, and monosaccharide composition. Geochim Cosmochim Acta 65:1455–1466. https://doi.org/10.1016/S0016-7037(00)00612-8

Miyajima T, Suzumura M, Umezawa Y, Koike I (2001b) Microbiological nitrogen transformation in carbonate sediments of a coral-reef lagoon and associated seagrass beds. Mar Ecol Prog Ser 217:273–286. https://doi.org/10.3354/meps217273

Miyajima T, Hori M, Hamaguchi M, Shimabukuro H, Adachi H, Yamano H, Nakaoka M (2015) Geographic variability in organic carbon stock and accumulation rate in sediments of East and Southeast Asian seagrass meadows. Glob Biogeochem Cycles 29:397–415. https://doi.org/10.1002/2014GB004979

Miyajima T, Hori M, Hamaguchi M, Shimabukuro H, Yoshida G (2017) Geophysical constraints for organic carbon sequestration capacity of *Zostera marina* seagrass meadows and surrounding habitats. Limnol Oceanogr 62:954–972. https://doi.org/10.1002/lno.10478

Möbius J (2013) Isotope fractionation during nitrogen remineralization (ammonification): implications for nitrogen isotope biogeochemistry. Geochim Cosmochim Acta 105:422–432. https://doi.org/10.1016/j.gca.2012.11.048

Moncreiff CA, Sullivan MJ (2001) Trophic importance of epiphytic algae in subtropical seagrass beds: evidence from multiple stable isotope analyses. Mar Ecol Prog Ser 215:93–106. https://doi.org/10.3354/meps215093

Moriarty DJW, Iverson RL, Pollard PC (1986) Exudation of organic carbon by the seagrass *Halodule wrightii* Aschers. And its effect on bacterial growth in the sediment. J Exp Mar Biol Ecol 96:115–126. https://doi.org/10.1016/0022-0981(86)90237-6

Morimoto N, Umezawa Y, San Diego-McGlone ML, Watanabe A, Siringan FP, Tanaka Y, Regino GL, Miyajima T (2017) Spatial dietary shift in bivalves from embayment with river discharge and mariculture activities to outer seagrass beds in northwestern Philippines. Mar Biol 164:1. https://doi.org/10.1007/s00227-016-3063-z

Nakaoka M, Aioi K (2001) Ecology of seagrasses *Zostera* spp. (Zosteraceae) in Japanese waters: a review. Otsuchi Mar Sci 26:7–22

Nakaoka M, Tanaka Y, Watanabe M (2004) Species diversity and abundance of seagrasses in southwestern Thailand under different influence of river discharge. Coast Mar Sci 29:75–80

Nguyen RT, Harvey HR (2001) Preservation of protein in marine systems: hydrophobic and other noncovalent associations as major stabilizing forces. Geochim Cosmochim Acta 65:1467–1480. https://doi.org/10.1016/S0016-7037(00)00621-9

Nunn BL, Keil RG (2005) Size distribution and amino acid chemistry of base-extractable proteins from Washington coast sediments. Biogeochemistry 75:177–200. https://doi.org/10.1007/s10533-004-6546-9

Ogawa H, Amagai Y, Koike I, Kaiser K, Benner R (2001) Production of refractory dissolved organic matter by bacteria. Science 292:917–920. https://doi.org/10.1126/science.1057627

Ono K, Hiradate S, Morita S, Hiraide M, Hirata Y, Fujimoto K, Tabuchi R, Lihpai S (2015) Assessing the carbon compositions and sources of mangrove peat in a tropical mangrove forest on Pohnpei Island, Federated States of Micronesia. Geoderma 245–246:11–20. https://doi.org/10.1016/j.geoderma.2015.01.008

Oreska MPJ, Wilkinson GM, McGlathery KJ, Bost M, McKee BA (2018) Non-seagrass carbon contributions to seagrass sediment blue carbon. Limnol Oceanogr 63:S3–S18. https://doi.org/10.1002/lno.10718

Parducci L, Väliranta M, Salonen JS, Ronkainen T, Matetovici I, Fontana SL, Eskola T, Sarala P, Suyama Y (2015) Proxy comparison in ancient peat sediments: pollen, macrofossil and plant DNA. Philos Trans R Soc Lond B 370:20130382. https://doi.org/10.1098/rstb.2013.0382

Parnell AC, Inger R, Bearhop S, Jackson AL (2010) Source partitioning using stable isotopes: coping with too much variation. PLoS One 5:e9672. https://doi.org/10.1371/journal.pone.0009672

Petsch ST, Eglinton TI, Edwards KJ (2001) ^{14}C-dead living biomass: evidence for microbial assimilation of ancient organic carbon during shale weathering. Science 292:1127–1131. https://doi.org/10.1126/science.1058332

Phillips DL, Newsome SD, Gregg JW (2005) Combining sources in stable isotope mixing models: alternative methods. Oecologia 144:520–527. https://doi.org/10.1007/s00442-004-1816-8

Pollard PC, Kogure K (1993) The role of epiphytic and epibenthic algal productivity in a tropical seagrass, *Syringodium isoetifolium* (Aschers.) Dandy, community. Aust J Mar Freshw Res 44:141–154. https://doi.org/10.1071/MF9930141

Premuzic ET, Benkovitz CM, Gaffney JS, Walsh JJ (1982) The nature and distribution of organic matter in the surface sediments of world oceans and seas. Org Geochem 4:63–77. https://doi.org/10.1016/0146-6380(82)90009-2

Raghukumar C, D'Souza TM, Thorn RG, Reddy CA (1999) Lignin-modifying enzymes of Flavodon flavus, a basidiomycete isolated from a coastal marine environment. Appl Environ Microbiol 65:2103–2111

Reef R, Atwood TB, Samper-Villarreal J, Adame MF, Sampayo EM, Lovelook CE (2017) Using eDNA to determine the source of organic carbon in seagrass meadows. Limnol Oceanogr 62:1254–1265. https://doi.org/10.1002/lno.10499

Reich S, Di Martino E, Todd JA, Wesselingh FP, Renema W (2015) Indirect paleo-seagrass indicators (IPSIs): a review. Earth-Sci Rev 143:161–186. https://doi.org/10.1016/j.earscirev.2015.01.009

Röhr ME, Boström C, Canal-Vergés P, Holmer M (2016) Blue carbon stocks in Baltic Sea eelgrass (*Zostera marina*) meadows. Biogeosciences 13:6139–6153. https://doi.org/10.5194/bg-13-6139-2016

Romankevich EA, Vetrov AA, Peresypkin VI (2009) Organic matter of the World Ocean. Russ Geol Geophys 50:299–307. https://doi.org/10.1016/j.rgg.2009.03.013

Rosenheim BE, Galy V (2012) Direct measurement of riverine particulate organic carbon age structure. Geophys Res Lett 39:L19703. https://doi.org/10.1029/2012GL052883

Rozaimi M, Lavery PS, Serrano O, Kyrwood D (2016) Long-term carbon storage and its recent loss in an estuarine *Posidonia australis* meadow (Albany, Western Australia). Estuar Coast Shelf Sci 171:585–565. https://doi.org/10.1016/j.ecss.2016.01.001

Schlünz B, Schneider RR (2000) Transport of terrestrial organic carbon to the oceans by rivers: re-estimating flux- and burial rates. Int J Earth Sci 88:599–606. https://doi.org/10.1007/s005310050

Serrano O, Lavery PS, Rozaimi M, Mateo MÁ (2014) Influence of water depth on the carbon sequestration capacity of seagrasses. Glob Biogeochem Cycles 28:950–961. https://doi.org/10.1002/2014GB004872

Serrano O, Lavery PS, Duarte CM, Kendrick GA, Calafat A, York PH, Steven A, Macreadie PI (2016) Can mud (silt and clay) concentration be used to predict soil organic carbon content within seagrass ecosystems. Biogeosciences 13:4915–4926. https://doi.org/10.5194/bg-13-4915-2016

Siikamäki J, Sanchirico JN, McLaughlin D, Morris DF (2012) Blue carbon: global options for reducing emissions from the degradation and development of coastal ecosystems. Resources for the future. http://www.rff.org/research/publications/blue-carbon-global-options-reducing-emissions-degradation-and-development. Accessed 23 Mar 2018

Suess E (1973) Interaction of organic compounds with calcium carbonate - II. Organo-carbonate association in recent sediments. Geochim Cosmochim Acta 37:2435–2447. https://doi.org/10.1016/0016-7037(73)90290-1

Sundquist ET (1985) Geological perspectives on carbon dioxide and the carbon cycle. In: Sundquist ET, Broecker WS (eds) The carbon cycle and atmospheric CO_2: natural variations from archean to present, Geophysical monograph series, vol 32. American Geophysical Union, pp 5–59. https://doi.org/10.1029/GM032p0005

Sundquist ET, Visser Ackerman K (2014) The geologic history of carbon cycle. In: Karl DM, Schlesinger WH (eds) Biogeochemistry, Treatise on geochemistry, vol 10, 2nd edn. Elsevier, Oxford, pp 361–398. https://doi.org/10.1016/B978-0-08-095975-7.00809-3

Tanaka Y, Kayanne H (2007) Relationship of species composition of tropical seagrass meadows to multiple physical environmental factors. Ecol Res 22:87–96. https://doi.org/10.1007/s11284-006-0189-3

Tanaka Y, Nakaoka M (2007) Interspecific variation in photosynthesis and respiration balance of three seagrasses in relation to light availability. Mar Ecol Prog Ser 350:63–70. https://doi.org/10.3354/meps07103

Tewfik A, Rasmussen JB, McCann KS (2005) Anthropogenic enrichment alters a marine benthic food web. Ecology 86:2726–2736. https://doi.org/10.1890/04-1537

Tokoro T, Hosokawa S, Miyoshi E, Tada K, Watanabe K, Montani S, Kayanne H, Kuwae T (2014) Net uptake of atmospheric CO_2 by coastal submerged aquatic vegetation. Glob Chang Biol 20:1873–1884. https://doi.org/10.1111/gcb.12543

Unsworth RKF, Collier CJ, Henderson GM, McKenzie LJ (2012) Tropical seagrass meadows modify seawater carbon chemistry: implications for coral reefs impacted by ocean acidification. Environ Res Lett 7:024026. https://doi.org/10.1088/1748-9326/7/2/024026

Wanless HR (1981) Fining-upwards sedimentary sequences generated in seagrass beds. J Sediment Petrol 51:445–454

Ward LG, Kemp WM, Boynton WR (1984) The influence of waves and seagrass communities on suspended particulates in an estuarine embayment. Mar Geol 59:85–103. https://doi.org/10.1016/0025-3227(84)90089-6

Watanabe K, Kuwae T (2015) How organic carbon derived from multiple sources contributes to carbon sequestration processes in a shallow coastal system? Glob Chang Biol 21:2612–2623. https://doi.org/10.1111/gcb.12924

Watanabe A, Nakamura T (2018) Chapter 10: Carbon dynamics in coral reefs. In: Kuwae T, Hori M (eds) Blue carbon in shallow coastal ecosystems: carbon dynamics, policy, and implementation. Springer, Singapore, pp 271–273

Wetzel RG, Penhale PA (1979) Transport of carbon and excretion of dissolved organic carbon by leaves and roots/rhizomes in seagrasses and their epiphytes. Aquat Bot 6:149–158. https://doi.org/10.1016/0304-3770(79)90058-5

Wilson TRS, Thomson J, Colley S, Hydes DJ, Higgs NC, Sørensen J (1985) Early organic diagenesis: the significance of progressive subsurface oxidation fronts in pelagic sediments. Geochim Cosmochim Acta 49:811–822. https://doi.org/10.1016/0016-7037(85)90174-7

Xu Y, Mead RN, Jaffé R (2006) A molecular marker-based assessment of sedimentary organic matter sources and distributions in Florida Bay. Hydrobiologia 569:179–192. https://doi.org/10.1007/s10750-006-0131-2

Yoshida G, Hori M, Shimabukuro H, Hamaoka H, Onitsuka T, Hasegawa N, Muraoka D, Yatsuya K, Watanabe K, Nakaoka M (2018) Chapter 4: Carbon sequestration by seagrass and macroalgae in Japan: estimates and future needs. In: Kuwae T, Hori M (eds) Blue carbon in shallow coastal ecosystems: carbon dynamics, policy, and implementation. Springer, Singapore, pp 101–127

Ziegler S, Benner R (1999) Dissolved organic carbon cycling in a subtropical seagrass-dominated lagoon. Mar Ecol Prog Ser 180:149–160. https://doi.org/10.3354/meps180149

Zimmerman AR, Chorover J, Goyne KW, Brantley SL (2004) Protection of mesopore-adsorbed organic matter from enzymatic degradation. Environ Sci Technol 38:4542–4548. https://doi.org/10.1021/es035340

Chapter 3
Carbon Sequestration in Mangroves

Tomomi Inoue

Abstract Mangrove ecosystems are widely regarded as highly productive, and the high ability of mangroves to store carbon is currently receiving much attention in the context of climate change. Globally, mangroves are estimated to occupy an area of 152,361 km^2. A model relating mangrove biomass to temperature and precipitation has been used, together with global mangrove distribution maps, to estimate the total aboveground biomass worldwide as 2.83 Pg dry weight (95% confidence interval 2.18–3.40 Pg), and the base area average as 184.8 t dry weight ha^{-1} (95% CI 142.1–222.0 t ha^{-1}). Almost half of the total global mangrove biomass is in Southeast Asia. The global mangrove belowground biomass has been estimated to be 1.11 Pg dry weight (95% CI 0.74–1.64 Pg). Thus, the total estimated biomass (aboveground + belowground) is 3.94 Pg dry weight. Estimates of carbon storage as necromass (dead organic matter) in mangrove soils differ. By one estimate, 5.00 Pg C is stored globally as necromass. By another estimate, ~2.6 Pg C is stored globally, and the whole mangrove ecosystem stores ~4.4 Pg C.

3.1 Introduction

Although mangrove ecosystems are confined to coastal areas of the tropics and subtropics, they are now being widely and frequently discussed, especially in an environmental context, in part because they are being seriously threatened around the world by loss of area and degradation. In the Indo-West Pacific region, where the species diversity of mangroves is highest, the area occupied by mangrove ecosystems has decreased by approximately 1% a year during the past 30 years (FAO 2007). At this rate, mangrove ecosystems in this region are likely to disappear within a hundred years. This possibility highlights how precious mangroves are to us.

The astonishing mangrove trees have intrigued mangrove researchers for many years. Mangrove plants grow in the intertidal environment. To survive and flourish

T. Inoue (✉)
National Institute for Environmental Studies, Japan, Onogawa, Tsukuba, Ibaraki, Japan
e-mail: tomomi.inoue@nies.go.jp

in this physically and chemically harsh environment, mangroves have developed adaptations that allow them to cope with the high salinity, lack of oxygen, and tidal turbulence. When you make your way into a mangrove forest, you are likely to encounter many living things (Fig. 3.1). At low tide, mudskippers hop and colorful crabs dance and wave their claws while waterfowl peck at them. If you are lucky, you may observe a simultaneous spawning event of sea snails. At high tide, fish swim swiftly through the intertwining roots of the partly submerged forest. If you look up, you might see the brilliant blue of a kingfisher as it flies from branch to branch. You might also notice monkeys watching you. Large mammals such as deer and tigers also inhabit mangrove forests. Moreover, people who live around mangrove forests have been enjoying their blessings for countless years while handing down from generation to generation their knowledge and philosophy of coexisting with mangroves. Mangrove plants supply energy, in the form of food and other materials, to these many living things, including human beings, through their production of organic matter. Another significant function of mangrove forest ecosystems is the absorption of carbon dioxide. In this chapter, I focus on carbon sequestration in mangrove forests and examine the environmental factors that influence carbon regulation in mangrove ecosystems.

3.2 Global Mangrove Distribution

First, before discussing carbon sequestration itself, I would like to touch on the wide distribution and diverse environmental settings of mangrove ecosystems. Given the variety of mangrove forests around the world and their diverse features, it would be surprising indeed if all mangrove ecosystems had the same carbon sequestration ability.

   If you want to see mangroves, two keys should guide your search. First, mangroves occur in mostly warm regions, the tropics and subtropics. More specifically, they are confined to regions between about 35° north latitude and about 40° south latitude: The most northerly mangroves are in Bermuda (32°20′N), and the most southerly are found in Corner Inlet, Australia (38°45′S). These latitudinal limits reflect water temperature, corresponding to the 20 °C winter water temperature isotherm (Duke 1992). My own research experience suggests that most mangrove plants have difficulty surviving at water temperatures below 10 °C. Second, mangroves grow only in intertidal zones along coasts, where tidal fluctuations subject them to repeated inundation and exposure. Numerous observations indicate that mangroves grow mainly on tidal flats that lie above mean sea level. Although these two environmental settings are key elements of mangrove distributions, it is actually very difficult to obtain accurate data on mangrove distributions at the global scale, because other factors also determine where mangroves grow, including local topography, micro-environmental characteristics, and human land use. Nevertheless, several global distribution maps of mangroves have been drawn (Spalding et al. 1997, 2010: Giri et al. 2011). One map (Fig. 3.2), which can be downloaded from
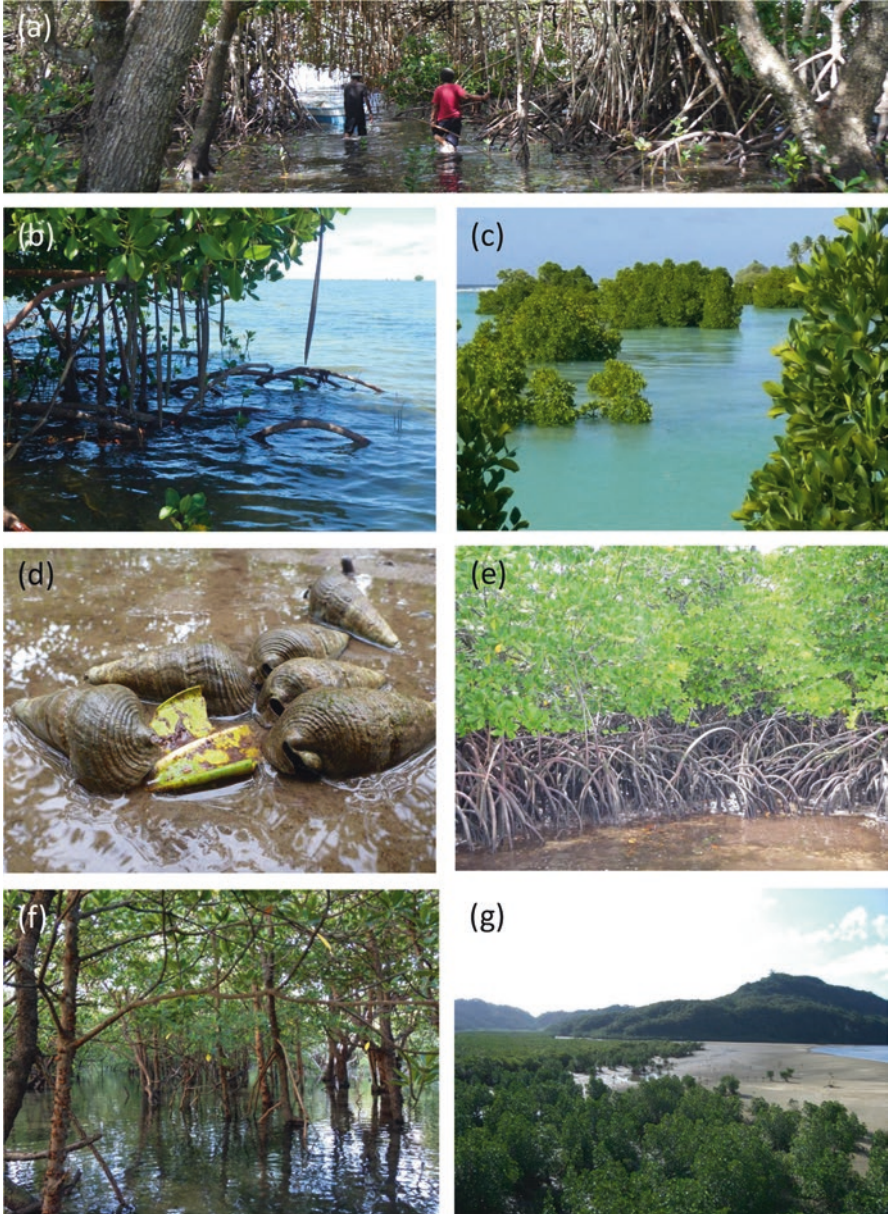
Fig. 3.1 Mangrove forest views: (**a**) People have benefited from mangrove forests for countless years. *Rhizophora* forest in Fiji. (**b**) Mangrove (*Rhizophora stylosa*) diaspores (fruit) may hang on the mother tree for several months. Rewa delta in Fiji. (**c**) When the tide comes in, the mangrove forest is flooded. *Rhizopgora stylosa* in Kiribati. (**d**) Snails (*Terebralia palustris*) feeding on fallen mangrove leaves. Mangrove forest on Iriomote island, Japan. (**e**) Dense aerial roots. *Rhizophora stylosa* in Federated states of Micronesia (**f**) Mangrove plants (*Bruguiera gymnorrhiza*) standing in the sea. Iriomote island, Japan. (**g**) Mangrove forest in Iriomote, Japan. (Photos were taken by Tomomi Inoue)

Fig. 3.2 Global distribution of mangrove ecosystems. Map from the Tropical Coastal Ecosystems Portal. (http://www.nies.go.jp/TroCEP/index.html)

Table 3.1 Mangrove areas by region

Region	Area (km^2)	Proportion of global total (%)
East and South Africa	7917	5.2
Middle East	624	0.4
South Asia	10,344	6.8
Southeast Asia	51,049	33.5
East Asia	215	0.1
Australia	10,171	6.7
Pacific Ocean	5717	3.8
North and Central America	22,402	14.7
South America	23,882	15.7
West and Central Africa	20,040	13.1
Total	152,361	

From Spalding et al. (2010)

the Tropical Coastal Ecosystems Portal (TroCEP 2017), is an updated version of a map originally published in the *World Atlas of Mangroves* (Spalding et al. 2010). The original GIS dataset for this map was produced mainly by analyzing Landsat imagery acquired during 2000–2003 that covered over 50% of the global mangrove area. Data for the remaining coverage area were generously contributed by multiple national and international organizations and mangrove experts, typically at a resolution of at least 1:250,000. This map shows that all mangrove ecosystems are located in warm coastal zones satisfying the two key conditions mentioned above. The total area occupied by mangroves globally has been estimated to be 152,361 km^2 (Table 3.1). Globally, mangroves account for <1% of the total area of tropical forests and for <0.4% of the total forested area. Most mangrove forests are found in South and Central America, West and Central Africa, and in a broad region stretching from northeast India through Southeast Asia into northern Australia. Over 65% of the world's total mangrove forest area is located in 12 countries (Table 3.2), and 20% of the total area is in Indonesia. The largest mangrove tracts are found on wet

Table 3.2 Top 12 countries by mangrove area

Country	Area (km^2)	Proportion of global total (%)
Indonesia	31,894	20.9
Brazil	13,000	8.5
Australia	9910	6.5
Mexico	7701	5.1
Nigeria	7356	4.8
Malaysia	7097	4.7
Myanmar	5029	3.3
Bangladesh	4951	3.2
Cuba	4944	3.2
India	4326	2.8
Papua New Guinea	4265	2.8
Colombia	4079	2.7
Total	104,552	68.5

From Spalding et al. (2010)

deltaic coasts, where they may extend inland for several tens of kilometers and include large, massive forest trees over 20 m tall. The Sundarbans of India and Bangladesh, the best-known mangrove forests, have a total area of 6500 km^2 and extend up to 85 km inland (Akhand et al. 2018). Large mangrove tracts are also found in northern Brazil (6500 km^2) and the Gulf of Papua (5400 km^2). The mangrove distribution is comparatively sparse in East Africa, the Middle East, South Asia, and Australia. Accurate global distribution maps are essential for assessing carbon sequestration and other ecosystem functions at global scale.

Although there are no accurate data on the past distribution of mangroves, in almost all countries where they are found, there has been a considerable decline in the area occupied, especially during the past 40 years, as a result of human activities. According to the Food and Agriculture Organization of the United Nations (FAO 2007), in the 25 years from 1980 to 2005, the area declined at an average rate of 0.7% per year, from 187,940 km^2 in 1980 to 169,250 km^2 in 1990, 157,400 km^2 in 2000, and 152,310 km^2 in 2005 (Fig. 3.3). By combining data from three datasets—the global forest cover dataset (Hansen et al. 2013), the global mangrove forest dataset (Giri et al. 2011), and the global terrestrial ecoregions dataset (Olson et al. 2001)—Hamilton and Casey (2016) estimated that the global mangrove forest area decreased by 4.73% from 2000 to 2012 by deforestation, an annual rate of loss of 0.39%. In Southeast Asia, where most mangrove forests are found, the area declined by 8.08% on average from 2000 to 2012. When mangrove ecosystems disappear, all of the living things that depend on them disappear as well. What would be the consequences of a world without mangroves? Now is the time to seriously think about the future of this unique and rare ecosystem.
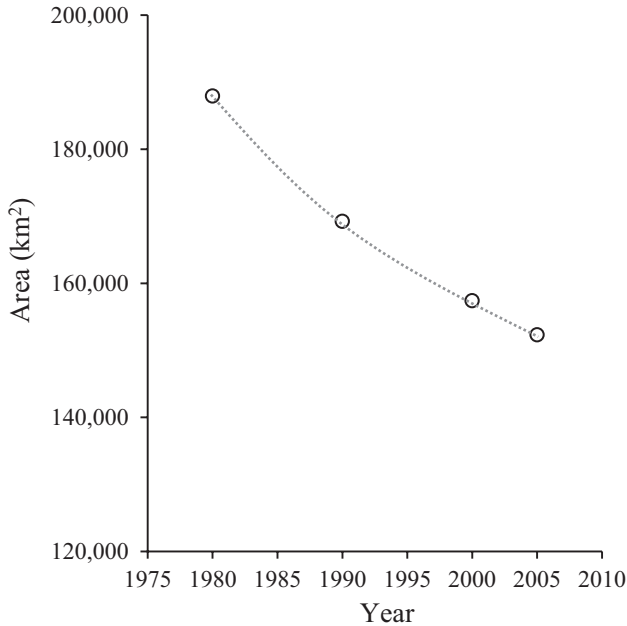
Fig. 3.3 Change in the global area of mangrove ecosystems from 1980 to 2005. (Data from FAO 2007)

3.3 Mangrove Species and Distribution Patterns

3.3.1 Mangrove Plant Species

From time to time I meet someone who thinks that "mangrove" refers to a certain plant species that "looks like an octopus." In actuality, there are about a hundred species of mangroves worldwide, although because there is not general agreement on what is and what is not a mangrove, reports of the number of mangrove species do not agree. For example, in their *Atlas*, Spalding et al. (2010) listed a total of 74 mangrove species and hybrids, whereas according to Tomlinson (1986) there are 54 species, according to Saenger (2002) there are 84 species, and Duke et al. (1998) mention 70 species. Because mangrove ecosystems lie in the ecotone between sea and land ecosystems, many mangroves have a broad habitat range, which makes it difficult to distinguish between mangrove and upland species. Furthermore, there are taxonomic uncertainties about some mangrove taxa. For example, in the genus *Rhizophora*, *R. mucronata* in East Africa is morphologically similar to *R. stylosa* in the Asia-Pacific region. The application of recently developed molecular genetic techniques to mangroves will lead to advances in mangrove taxonomy.
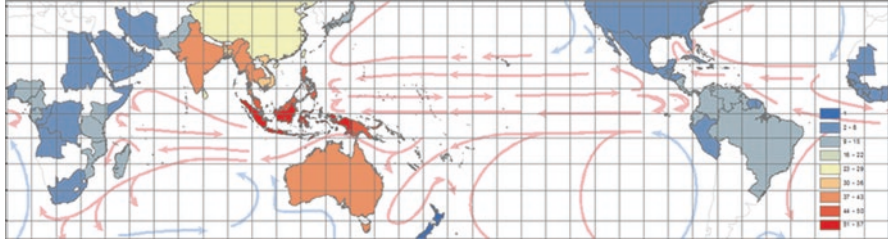
Fig. 3.4 Worldwide mangrove plant species diversity. The colors indicate the number of mangrove plant species recorded in each country. The blue and pink arrows indicate ocean current. Data were obtained from Tropical Coastal Ecosystems Portal. (http://www.nies.go.jp/TroCEP/index.html)

3.3.2   Species Distribution Pattern in Global Scale

When mangrove species distributions among countries are considered (e.g., TroCEP 2017), two distinct floristic regions can be recognized. In the Indo-West Pacific region, which extends from East Africa eastward to the islands of the Central Pacific, there are 63 species, whereas the Atlantic-East Pacific region, which includes all of the Americas as well as West and Central Africa, has 12 species. The only species found in mangrove ecosystems in both these regions is the mangrove fern, *Acrostichum aureum*. The global center of mangrove diversity is Southeast Asia, and the highest species diversity is found in Indonesia and Malaysia, with 53 and 47 species, respectively (Fig. 3.4).

Many factors may be responsible for the observed variation in the number of species in different parts of the global distribution range. For example, there are more species where temperatures are higher and where there are long estuaries with large catchments and a high volume of freshwater runoff, whereas there are fewer species where intra-annual rainfall variability is high (Smith and Duke 1987).

3.3.3   Local Zonation Patterns

Ecotone ecosystems such as wetlands are often characterized by plant species zonation, which is commonly observed in mangroves (Watson 1928; Macnae 1968, 1969; Semeniuk 1980; Elsol and Saenger 1983; Johnstone 1983; Van Steenis 1957). For example, mangrove species zonation is seen in the intertidal zone on Iriomote Island, Japan (Fig. 3.5), as one moves inland from the seashore. Zonation can also be seen along rivers as one moves upstream from the mouth. In the Indo-West Pacific region, the dominant mangrove genera near the shore (in the lower intertidal zone) are typically *Aegiceras*, *Avicennia*, and *Sonneratia*; in the middle intertidal zone, *Rhizophora* and *Bruguiera* species dominate; and in the higher intertidal zone,
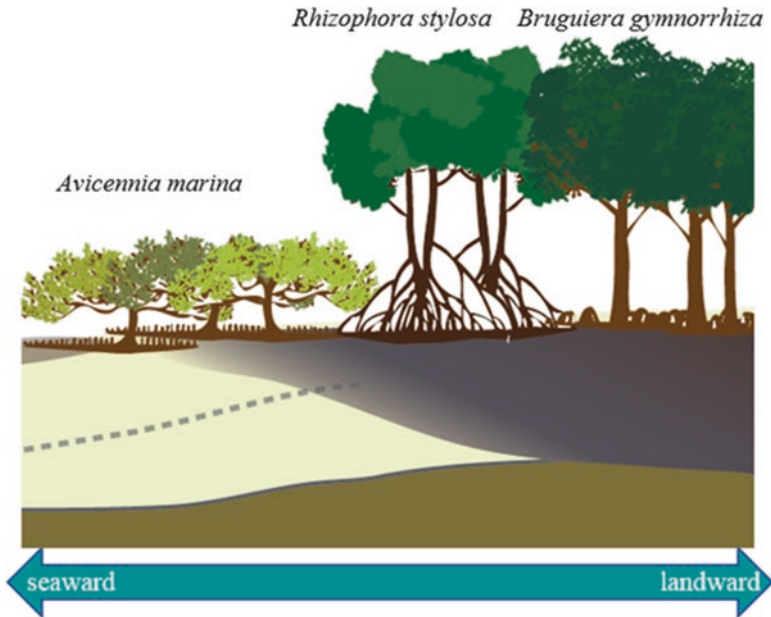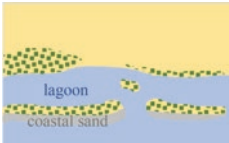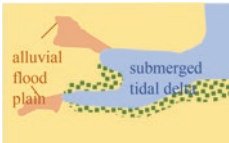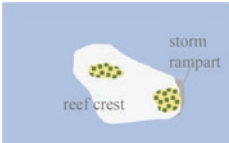
Fig. 3.5 A typical mangrove species zonation pattern in the Indo-West Pacific region, observed on Iriomote Island, Japan

Heritiera and *Xylocarpus* are often found. There are many exceptions, however; for example, *Avicennia* species are often observed at inland sites. The distribution pattern presumably reflects differences in tolerance to waterlogging, drought, and salinity among species. Therefore, the zonation pattern, including the species composition of each zone and the order or arrangement of the species zones, can vary from site to site, depending, for example, on topography, whether a river is present and its catchment size, and local climatic patterns.

3.4 Environmental Settings of Mangroves
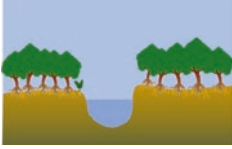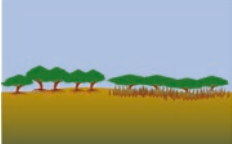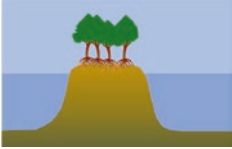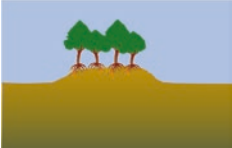
Mangroves occur in various environmental settings, and many ways of characterizing mangrove habitats have been suggested. Mangrove ecosystems have been classified broadly into six settings (Table 3.3) (e.g., Thom 1982, 1984; Semeniuk 1985; Woodroff 1992) on the basis of geomorphic and physical factors such as river flow, tides, and waves. These factors relate to the past development of each setting and also reflect forest structure and zonation dynamics; thus, this geomorphic classification system is useful for large-scale assessment of ecosystem functions such as carbon accumulation. Mangrove ecosystems have also been classified into six settings on the basis of the functional relationship between mangroves and hydrogeological features (Table 3.4; Lugo and Snedaker 1974). This functional classification

Table 3.3 Geomorphic mangrove settings

(i) River dominated	Mangroves in a river-dominated setting are situated on the large delta of a large river, where the input of sediment from upstream is high. The distribution of mangrove plants on the delta depends on environmental factors such as microtopography and inundation frequency.
(ii) Tide dominated	Mangroves in a tide-dominated setting grow on tidal flats exposed to the open ocean where the tidal fluctuation is >4 m. Freshwater input from upstream is very small. Mangrove plants are distributed on tidal flats and along river banks.
(iii) Wave dominated	Mangroves in a wave-dominated setting grow on sandy coasts where they experience strong wave energy. Both strong waves and sandy sediments make it hard for mangrove plants to become established and grow; thus, mangroves are found mainly along the shores of protected lagoons. A large amount of carbon tends to be stored below ground as peat.
(iv) Composite river and wave dominated	This setting is a composite of (i) and (iii); it is characterized by a sandy coast, strong wave energy, and sediment input from a large river. Mangroves tend to grow on the shores of protected lagoons and along the river banks. Similar to (iii), a large amount of carbon is stored as peat.
(v) Drowned bedrock valley	Mangroves in this setting grow along the shores of coastal embayments, known as rias, which formed in river valleys as a result of the post-glacial rise in sea level. In southeastern Australia, these drowned valleys are commonly incised in bedrock.
(vi) Carbonate settings	Mangroves in carbonate settings grow on oceanic islands and coral reefs where the soils are mostly of calcareous origin. The tidal range is generally small, and little or no sediment is supplied from inland areas. Peat develops underground in these settings.

Illustrations redrawn from Woodroffe (1992) by Tomomi Inoue

Table 3.4 Functional mangrove settings

(a) Fringe mangroves	Fringe mangroves grow along open coastlines where they experience repeated daily inundations caused by tidal fluctuations. Plant species zonation based on the amount of sea influence is observed. Despite the tidal currents, mangrove litter accumulates on the forest floor.
(b) Riverine mangroves	Riverine mangroves grow along the banks of rivers and creeks in river-dominated deltas. Nutrient and freshwater inputs from upstream are large, and the mangroves are therefore highly productive and grow into tall trees. Plant species zonation is observed as one moves away from river edges.
(c) Basin mangroves	Basin mangroves grow in interior regions lacking outlets, where water gathers in depressions. Water flow is minimal, and organic matter tends to accumulate in the soils. The mangrove species composition depends on local physical and chemical conditions.
(d) Dwarf mangroves	Dwarf and scrub mangroves have a tree height of <1.5 m because they grow where the nutrient supply is low or salinity is high (or both). Such mangroves sometimes grow along the inland edge of forests where the salinity is very high because of strong water evaporation. Although the aboveground parts of the trees are small, there is a thick mat of peat and roots underground.
(e) Overwash mangroves	Overwash mangroves grow on small islands that are completely submerged at high tide. They are typically found growing on river-mouth shoals in tide-dominated settings or on incipient islands in river-dominated settings. Peat derived from mangrove roots accumulates underground.
(f) Hummock mangroves	Hummock mangroves grown on a raised layer of peat above a limestone base. This type of mangrove is observed in basins in the Florida Everglades.

Illustrations redrawn from Woodroffe (1992) by Tomomi Inoue

system is often utilized in the New World but not very much in the Old World (Indo-West Pacific region), where the species richness is much higher (Woodroff 1992).

3.5 Organic Materials As an Energy Source for the Inhabitants of Mangrove Ecosystems

When plant seeds germinate in soil and start to grow, the organic matter content in that location is changed. As they grow, green plants photosynthesize and produce organic materials, including leaves, twigs, stems, trunks, and roots, thus increasing the accumulation of organic matter. Furthermore, plants continuously drop leaves and twigs as litter onto the forest floor, and as the litter decays it enriches the organic matter content of the soil. Below ground, plants continuously produce new roots, and as old roots die, they become detached from the plant and also enrich the soil organic matter content. Plant litter, dead roots, and other detrital organic matter is decomposed in the soil by organisms such as bacteria and fungi. Under aerobic conditions, carbon contained in the organic matter is converted by decomposition into gaseous CO_2, and under anaerobic conditions, it is converted into CH_4 and HCO_3^-. In wet environments such as mangrove forest, conditions in the submerged soil are typically anoxic, and the decomposition rate is extremely low. As a result, the rate at which organic materials are supplied usually exceeds the rate at which they decompose. For this reason, wetland ecosystems can store large amounts of carbon in their soils. Carbon that remains in the soil is referred to as sequestered (Fig. 3.6). Some of the organic matter produced by mangrove plants provides energy to the various ecosystem inhabitants (Fig. 3.7), which can include both terrestrial and marine organisms.

Fig. 3.6 Schematic diagram of carbon sequestration in a mangrove forest. Sequestration occurs when the input of carbon into the soil exceeds the loss
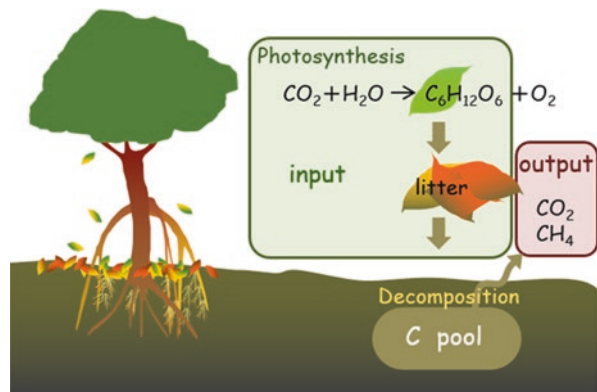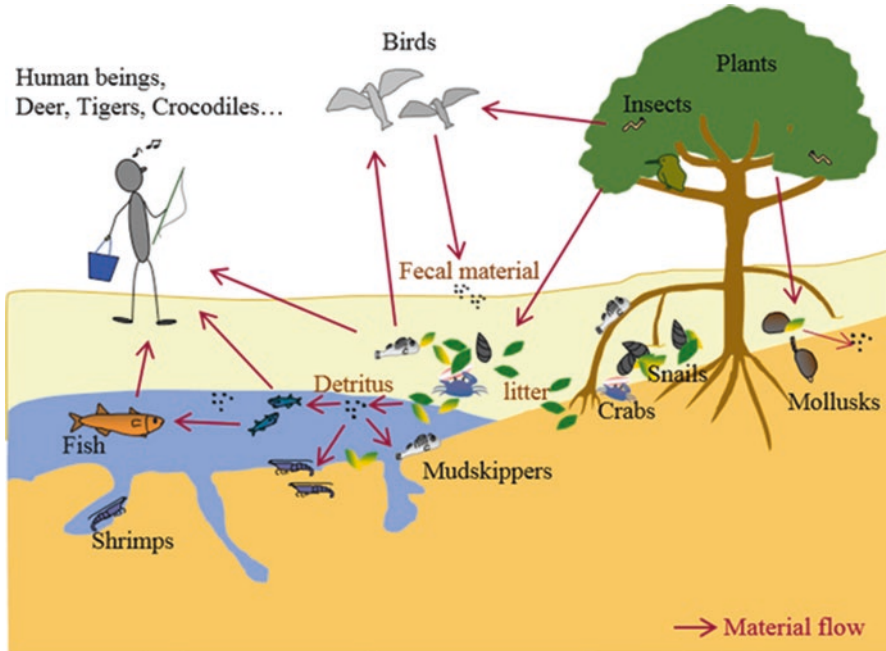
Fig. 3.7 The food web in a mangrove ecosystem showing material and energy flows

3.5.1 Biomass in Mangrove Ecosystems

"Biomass" is the mass of living biological organisms in a given ecosystem at a given time. It may include microorganisms, plants, and animals, and can be expressed as the average mass per unit area or as the total mass in the ecological community. About half of the biomass of plants (in dry weight) is attributable to carbon, although the amount differs among species.

3.5.1.1 Biomass Increments and Decrements

The main primary producers in mangrove ecosystems are vascular plants such as trees and shrubs. These plants use solar energy to produce organic materials (leaves, twigs, trunks, and roots) from carbon dioxide and water by the process of photosynthesis. Although mangrove ecosystems are widely considered to be highly productive, that does not necessarily mean that mangrove plant leaves have high photosynthetic ability. Generally, plant photosynthesis rates range from 0 to 40 micromoles (µmol) of CO_2 per square meter of leaf area per second (m^{-2} s^{-1}). Gong et al. (1992) reported that the net photosynthesis rate of a 20-year-old *Rhizophora apiculata* in Malaysian mangrove forests varies between 5.6 and 11.0 µmol CO_2 m^{-2} s^{-1}, within the general range of reported rates. At the forest scale, estimated

annual growth increments of aboveground biomass range from 4 t ha^{-1} year^{-1} in an *Avicennia* mangrove forest in Mexico (Day et al. 1996) to 26.7 t ha^{-1} year^{-1} in a *Rhizophora* forest in Thailand (Christensen 1978). Although very little information is available about annual belowground biomass increments in mangrove ecosystems, Ong et al. (1995) reported growth increments in a *Rhizophora apiculata* stand in Malaysia of 0.08 t C ha^{-1} year^{-1} for leaves, 0.44 t C ha^{-1} year^{-1} for branches, 5.56 t C ha^{-1} year^{-1} for trunk, 0.64 t C ha^{-1} year^{-1} for (aerially exposed) stilt roots, and 0.42 t C ha^{-1} year^{-1} for roots buried in the soil (total, 7.14 t C ha^{-1} year^{-1}).

Mangrove ecosystems typically include multiple waterways. The primary producers in these waterways include periphyton, benthic algae (microphytobenthos), and phytoplankton. Production of periphyton on mangrove aerial roots ranges from 0.14 to 1.1 g C m^{-2} day^{-1} (Lugo et al. 1975; Hoffman and Dawes 1980). Benthic algal production was 0.11–0.18 g C m^{-2} day^{-1} in a forest in Thailand, in which the production from trees was 1.90–2.75 g C m^{-2} day^{-1} (Kristensen et al. 1988); the production of benthic algae thus accounted for <10% of the total plant production. The net primary productivity of phytoplankton in most mangrove ecosystems is essentially nil, because very little light penetrates into the turbid waters (Ong et al. 1984).

Figure 3.7 illustrates the food web in a mangrove ecosystem. The living parts of primary producers are eaten by herbivores, including primary consumers such as insects. These primary consumers extract energy from the organic materials that they eat. Secondary consumers—carnivores—eat primary consumers and extract energy from their biomass. These carnivores then pass on this energy to the next trophic level, tertiary consumers, which are carnivores that feed only on secondary consumers. The ecosystem also has a detrital chain, which starts with dead material from the primary producers, namely plant litter such as leaves and woody tissues, and dead roots. Organisms such as crabs, snails, and mudskippers are detritivores, which extract energy from these dead organic materials and are subsequently eaten by carnivores (the detrital food chain is describe in more detail in Sect. 3.5.2.1).

Although many leaves in a mangrove forest typically show insect damage, the resulting plant production loss is not very high. Robertson and Duke (1987) reported that direct grazing by herbivores accounted for a loss of only 0.3–3.5% of the total expanded leaf area in a mangrove forest in Australia. However, the loss from grazing can differ substantially depending on what kinds of herbivores inhabit the forest. For example, mangrove forests of Southeast Asia probably suffer a large biomass loss from leaf-eating monkeys, which like to eat young buds of mangrove trees.

3.5.1.2 Biomass Stocks

Biomass in mangroves, as in upland forests, is estimated by measuring trunk diameter and height and other physical parameters and then substituting the measured values into an allometric equation which relates these measurements to biomass (Table 3.5). Many studies have estimated aboveground biomass in mangrove forests, but very few have estimated belowground biomass, probably because of the

Table 3.5 Mangrove biomass estimated as $W_{above\ or\ below} = A\ DBH^B$, where W is biomass (kg dry weight) and DBH is diameter at breast height

	Species	DBH (cm)	n	A	B	r^2	References
Aboveground							
	Avicennia germinans	<4	45	0.140	2.40	0.97	1
		nd	21	0.094	2.52	0.99	2
	Avicennia marina	<35	22	0.308	2.11	0.97	3
	Rhizophora apiculate	<28	57	0.235	2.42	0.98	4
		nd	nd	0.171	2.52	0.98	5
	Rhizophora mangle	nd	17	0.178	2.47	0.98	2
	Bruguiera gymnorrhiza	2–21	17	0.186	2.31	0.99	6
	Bruguiera parviflora	2–21	16	0.168	2.42	0.99	6
	Ceriops australis	2–18	26	0.189	2.34	0.99	6
	Xylocarpus granatum	3–17	15	0.082	2.59	0.99	6
Belowground							
	Avicennia marina	<35	14	1.28	1.17	0.80	3
	Rhizophora apiculate	<28	11	0.00698	2.61	0.99	4
	Rhizophora stylosa	<15	5	0.261	1.86	0.92	3
	Bruguiera exaristata	<10	9	0.302	2.15	0.88	3
	Xylocarpus granatum	<8	6	0.145	2.55	0.99	7

References: 1, Fromard et al. (1998); 2, Imbert and Rollet (1989); 3, Comley and McGuinness (2005); 4, Ong et al. (2004); 5, Putz and Chan (1986); 6, Clough and Scott (1989); 7, Poungparn et al. (2002)

nd no data

difficulty of extracting roots from the muddy soils. Different allometric equations for aboveground biomass are used for different mangrove species (Tam et al. 1995; Ong et al. 2004; Comley and McGuinness 2005) and sometimes at different forest sites (Clough et al. 1997), although Ong et al. (2004) applied similar equations to two different *Rhizophora apiculata* forest sites. Komiyama et al. (2005) developed the following universal allometric equation for mangrove trees with a trunk diameter of <49 cm:

$$W_{above} = 0.251\rho DBH^{2.46} \tag{3.1}$$

where W_{above} (kg dry weight) is the aboveground biomass, ρ is wood density (g cm^{-3}), and DBH is the trunk diameter at breast height (cm). They based this equation on the pipe model, which relates biomass to the cross-sectional area of stems and branches (Shinozaki et al. 1964), and the static plant form model, an extension of the pipe model (Oohata and Shinozaki 1979). Wood density of mangroves varies, depending on the species, from 0.486 to 0.980 g cm^{-3} (Putz and Chan 1986; Clough and Scott 1989). A comparative analysis of reported allometric equations (using mainly data obtained in Southeast Asia) showed that estimates of aboveground biomass obtained by using the universal equation are the same, within a 10% relative error, as estimates obtained by using site-specific equations (Komiyama et al. 2008).

We can infer from these results that allometric equations for mangrove plants in Southeast Asia are highly species-specific but less site-specific.

Published estimates of mangrove aboveground biomass vary from <10 t ha^{-1} to >600 t ha^{-1} (Paijmans and Rollet 1977; Putz and Chan 1986; Komiyama et al. 1988; Donato et al. 2011). This wide range of values reflects the fact that mangrove plants have a great deal of form plasticity depending on their environment. Further, analyses of mangrove biomass data from forests growing at various latitudes (Twilley et al. 1992; Saenger and Snedaker 1993; Hutchison et al. 2014) have reported a more or less linear decline in aboveground biomass with increasing latitude. Hutchison et al. (2014) derived the following linear regression of biomass against latitude:

$$\text{Aboveground Biomass}\left(\text{t ha}^{-1}\right) = -4.617\,\text{Latitude}\left(\text{decimal degrees}\right) + 298.5 \quad (3.2)$$

Komiyama et al. (2008) also reported that the aboveground biomass tends to be low in temperate areas and suggested that the low values may be related to climatic conditions such as temperature, solar radiation, precipitation, and storm frequency. To obtain insight into the factors behind these observations, Hutchison et al. (2014) used bioclimatic data from the WorldClim Bioclim 30 arc-second dataset (http://www.worldclim.org/bioclim), a globally interpolated dataset of 19 bioclimatic variables derived from monthly temperature and rainfall data (Hijmans et al. 2005), to develop the following model (Eq. 3.3):

$$\text{Aboveground Biomass}\left(\text{t ha}^{-1}\right) = 0.295\,A + 0.658\,B + 0.0234\,C \\ +0.195\,D - 120.3 \quad (3.3)$$

where A is mean air temperature during the warmest quarter of the year (°C), B is mean air temperature during the coldest quarter (°C), C is precipitation during the wettest quarter (mm), and D is precipitation during the driest quarter (mm).

This equation suggests that biomass is higher in areas where the air temperature (especially in the coldest quarter) and rainfall (especially in driest quarter) are high. Hutchison et al. (2014) used this model, along with the mangrove global maps of Spalding et al. (2010), to estimate the total worldwide aboveground biomass of mangroves as 2.83 Pg dry weight (95% confidence interval [CI] 2.18–3.40 Pg) and the base area average as 184.8 t ha^{-1} (95% CI 142.1–222.0 t ha^{-1}). They also reported that almost half of the total global mangrove biomass is in Southeast Asia (Table 3.6).

The partitioning of biomass among the aboveground parts of the mangrove plant is also important. In *Rhizophora* stands, about 80% of the biomass is allocated to the trunk and <20% is allocated to aerial roots and leaves (Golley et al. 1962; Lugo and Snedaker 1974; Aksornkoae 1975; Christensen 1978; Tamai et al. 1986; Komiyama et al. 1988; Kusmana et al. 1992; Ong et al. 1995). My personal observation is that *Rhizophora* species in the Pacific region seem to allocate more biomass to aerial roots than those in Southeast Asia.

Apart from these large-scale tendencies, mangrove plant forms show local variations. For example, mangrove trees tend to be shorter at sites with low precipitation,

Table 3.6 Aboveground biomass (AGB) of mangroves (dry weight) predicted by the model equation of Hutchison et al. (2014)

Region	AGB (10^6 t)	Mean AGB (t ha^{-1})
East and south Africa	143.33	136.4
Middle East	14.75	110.4
South Asia	136.60	136.4
Southeast Asia	1131.56	230.9
East Asia	2.54	107.2
Australia and New Zealand	87.51	132.9
Pacific Islands	133.47	233.3
North and Central America and the Caribbean	356.29	145.3
South America	465.91	185.7
West and Central Africa	357.44	177.8
Global Total	2829.39	184.8

high evaporation, and a low freshwater supply, probably because of plant physiological responses to high salinity. Cintrón et al. (1978) developed the following equation for the effect of salinity on mangrove tree height in Puerto Rico:

$$\text{Tree height}(m) = -0.20\,\text{Soil salinity}(ppt) + 16.58\,(r^2 = 0.72) \qquad (3.4)$$

Other factors such as soil nutrients and flooding conditions can also influence plant morphology and biomass amount. Donato et al. (2011) measured mangrove biomass in 25 forests in the Indo-West Pacific region and compared the data between oceanic mangroves, situated in marine-edge settings, often on the coasts of islands with fringing coral reefs, and estuarine mangroves, situated on large alluvial deltas, often within a protected lagoon. They found that the area-based aboveground biomass carbon of oceanic mangroves was higher than that of estuarine mangroves, and attributed this difference to differences in nutrient and physical conditions between the settings. They also reported that the area-based aboveground biomass tended to increase with distance inland from the coast, particularly so in estuarine settings.

The biomass of the belowground parts, here including aerial root systems, has been estimated to be large in some mangrove forests in Indonesia: 196.1 t ha^{-1} in a *Rhizophora apiculata* stand and 180.7 t ha^{-1} in a *Bruguiera gymnorrhiza* stand (Komiyama et al. 1988). These estimates are higher than belowground estimates for most upland forests (<150 t ha^{-1}) (Cairns et al. 1997). Most upland forest trees partition <30% of their biomass to belowground parts (Ulrich et al. 1974), whereas mangrove trees may partition 40–60% of the total to belowground biomass (Saenger 1982; Lugo 1990). Several explanations have been proposed for the high percentage of root mass of mangroves. Komiyama et al. (1988) suggested that a high belowground biomass may be needed to physically support the plant body in unstable muds. But the belowground biomass of mangroves is not invariably high: for example, Gong and Ong (1990) reported that in mangroves in Malaysia, it represents

only 8.5% of the total biomass. There are several possible reasons for the large variation in reported belowground biomass values: (i) the mangrove root mass percentage may truly vary among sites and species; (ii) belowground biomass has been examined by few studies; (iii) aerial root systems may be reported as belowground or aboveground biomass, depending on the study; and (iv) it can be difficult to distinguish between live and dead roots, depending on the measurement procedure used.

Hutchison et al. (2014) analyzed 41 datasets that included both aboveground and belowground biomass data and suggested the following allometric relationship:

$$\text{Belowground Biomass} \left(t\,ha^{-1} \right) = 0.073\,\text{Aboveground Biomass}^{1.32} \left(t\,ha^{-1} \right) \qquad (3.5)$$

This equation predicts a global mangrove belowground biomass of 1.11 Pg (95% CI 0.74–1.64 Pg), based on an estimated aboveground biomass of 2.83 Pg, and thus a total biomass (aboveground + belowground) of 3.95 Pg.

3.5.2 Necromass in Mangrove Ecosystems

"Necromass" is the mass ("weight") of dead materials of biological origin in a given ecosystem at a given time, and includes dead microorganisms, plants, and animals. Plant-derived necromass is the sum of coarse woody debris, plant litter, and soil humus. Necromass is expressed either as the average mass per unit area or as the total mass in the community. In biology, "detritus" refers mostly to dead particulate organic material: fragments of dead organisms as well as fecal material. If biomass is expressed as "current income by the organisms living in an ecosystem", then necromass can be regarded as "property constructed by ancestors throughout the long history of the ecosystem (sometimes >1000 years)". The amount of necromass carbon stored in ecosystems is generally about three times the amount of carbon stored in living plant bodies (Eswaran et al. 1993; see also Table 2.1 in Chap. 2 of this volume). In wetland soils such as mangrove forest soils, the oxygen concentration within the soil sometimes drops to zero, with the result that bacterial decomposition of organic matter tends to be low (Miyajima and Hamagichi 2018). This means that the rate at which organic matter is supplied to the soil (in the form of plant litter and detached dead roots) is likely to exceed the rate at which it is decomposed. Thus, in mangrove soils, the amount of carbon stored in necromass is large. Cebrián and Duarte (1995) compiled data on aboveground biomass, primary production of biomass, and production of detrital carbon for a broad range of ecosystems (forests, grasslands, seagrass meadows, freshwater macrophyte meadows, macroalgal beds, and benthic microalgae and plankton) and found that the detrital carbon mass cannot be predicted by either primary production or the carbon flux into the detrital pool. In contrast, it is strongly related to the plant turnover rate: the higher the plant turnover rate, the lower the detrital carbon mass. It follows from

these observations that in ecosystems dominated by slow-growing plants such as trees, large, slowly decomposing detrital pools accumulate. Mangrove forest ecosystems are dominated by slow-growing trees growing on intertidal flats where the soil is anoxic because it is constantly inundated by brackish water. Thus, mangrove ecosystems satisfy the conditions for large necromass accumulation.

3.5.2.1 Necromass Increments and Decrements

Litter, such as leaves, flowers, twigs, and small branches, falls continuously in mangrove forests. According to Bouillon et al. (2008), litter input in mangrove forests ranges from 4 to 13 t ha^{-1} year^{-1} by dry weight. They also reported a latitudinal difference in litter production, from an average of 10.4 t ha^{-1} year^{-1} (dry weight) at 0° to 10° of latitude to an average of 4.7 t ha^{-1} year^{-1} (dry weight) at latitudes of >30°.

In the soil, plants continuously produce fine roots for nutrient and water uptake and shed old roots. The production of root litter by mangrove plants is thought to be considerable, so the organic matter content of mangrove soils may be high, but evaluation of root litter production is difficult. Thus, information on the mangrove necromass increment from dead roots is lacking. In addition to materials produced in the mangrove ecosystem itself, litter may also be transported into the ecosystem from surrounding areas. For example, leaves and branches may be carried from upland areas by river flow, and materials from the sea such as algae, sea grasses, and dead fish carried by waves and tidal currents can contribute further necromass. At the same time, dead organic materials in mangrove ecosystems may be exported to nearby waters (Gong and Ong 1990; Alongi et al. 1998). In fact, large masses of dead wood from a mangrove forest are sometimes observed floating in the sea. The dead materials remaining in mangrove ecosystems become fragmented by physical processes such as tidal fluctuations and wind, and by animal activities, and soluble organic matter may be leached from the dead materials into the water. Cundell et al. (1979) suggested that 30–50% of mangrove leaf biomass can be lost by leaching. The leached compounds can serve as energy sources for organisms in the water. On the floor of a mangrove forest, macrofauna (crabs, snails, mudskippers, prawns, snakes, and so on) are often observed busily feeding on litter (Chong and Sasekumar 1981; Rodelli et al. 1984). Leaf-consuming crabs sometimes have carbon stable isotopic ratios, which can be used to trace carbon sources, close to the ratio of mangrove litter, an indication that mangrove litter is their main food source. According to Robertson et al. (1992), who compiled data on macrofaunal feeding in mangrove forests, crabs consumed 28–71% of the litter in mangrove forests. Moreover, various prawn species that live in mangrove waterways also feed on dead organic materials derived from mangrove plants (Chong and Sasekumar 1981; Rodelli et al. 1984; Chong et al. 2001). The species that feed on the litter and the intensity of their feeding depend on factors such the macrofaunal species composition and physicochemical conditions in the forest. At smaller scales, bacteria and fungi are major decomposers in mangrove ecosystems. These organisms extract electrons from organic materials in the soil and obtain energy from the electron flow for their

Table 3.7 Centennial-scale organic carbon burial rates in mangrove ecosystems

Organic C burial rate (g C m^{-2} year^{-1})	Authors	Publication year
100	Twilley et al.	1992
115	Jennerjahn and Ittekkot	2002
210	Chmura et al.	2003
139	Duarte et al.	2005
115	Bouillon et al.	2008
181	Alongi	2009
226	Mcleod et al.	2011
163	Breithaupt et al.	2012

biological activities. If oxygen is available, it can act as an electron acceptor and the decomposition products are CO_2 and H_2O. In wetland soils where oxygen is scarce, other electron acceptors such as nitrates, manganese and iron oxides, sulfates, and the organic matter itself are used, and compounds such as CH_4 and HCO_3^- are produced.

All processes that affect necromass increments and decrements are reflected in the ecosystem organic carbon burial rate (g C m^{-2} year^{-1}). Organic carbon burial rates in an ecosystem are generally obtained by measuring the concentration of organic carbon in the soil and estimating the time interval during which the carbon in all or part of the soil profile accumulated. The rate is then calculated by dividing the measured amount of organic carbon by the estimated time interval. Time intervals at the millennial scale can be determined by ^{14}C dating; those at the centennial scale by ^{210}Pb and ^{137}Cs dating; and those at the sub-annual scale by using markers for past surface elevations (e.g., Cahoon and Lynch 1997). A number of studies have used various methods to estimate centennial-scale organic carbon burial rates (Table 3.7). Twilley et al. (1992), Chmura et al. (2003), and Breithaupt et al. (2012) estimated global mean annual burial rates from primary measured burial rates. Jennerjahn and Ittekkot (2002) used a mass balance approach to estimate the organic carbon burial rate from plant production, litterfall, export, and remineralization data. Duarte et al. (2005) recalculated the rate for the dataset of Chmura et al. (2003) using a top-down approach. Alongi (2009) and Mcleod et al. (2011) both reported rates that were higher than most earlier estimates. In the most recent of these studies, Breithaupt et al. (2012) analyzed 16 sets of primary centennial-scale organic carbon burial data for mangrove ecosystems, including data from 65 sediment cores collected in Australia, Brazil, China, Indonesia, Japan, Malaysia, Mexico, Thailand, the USA, and Vietnam (data from 22 of these 65 cores had been used by Chmura et al. 2003). The primary burial rates ranged from 22 g organic carbon (OC) m^{-2} year^{-1} in Fukido Estuary, Ishigaki Island, Japan (Tateda et al. 2005), to 1020 g OC m^{-2} year^{-1} in Jiulongjiang Estuary, China (Alongi et al. 2005), but Breithaupt et al. (2012) found no latitudinal pattern. Moreover, at a local level, reported burial rates show large variation: 26–336 g OC m^{-2} year^{-1} in Hinchinbrook Channel, Australia (Brunskill et al. 2002); 148–410 g OC m^{-2} year^{-1} in Matang, Malaysia (Alongi et al. 2004); 149–1020 g OC m^{-2} year^{-1} in Jiulongjiang Estuary, China

(Alongi et al. 2005); 22–230 g OC m^{-2} year^{-1} in Fukido Estuary, Japan (Tateda et al. 2005); and 100–600 g OC m^{-2} year^{-1} in Trat, Thailand (Tateda et al. 2005). Such local variation probably reflects site-specific biological and physicochemical factors (Amundson 2001; Davidson and Janssens 2006; De Deyn et al. 2008; Kristensen 2008; Smith et al. 1991). Breithaupt et al. (2012) compared rates between core sites with and without river inputs and reported a mean rate of 268 ± 227 g OC m^{-2} year^{-1} for sites with rivers and 114 ± g OC m^{-2} year^{-1} for sites without rivers. They attributed the higher burial rates at sites with rivers to high organic carbon input rates from riverine or tidal sources, in addition to input from autochthonous production. For example, in Hinchinbrook Channel, Australia (Alongi et al. 1999), mangrove carbon accounted for only 56% of the total organic carbon input, and the contribution of mangrove materials varied widely both over time and at different coring locations (Gonneea et al. 2004).

Not only do area-based mangrove OC burial rates vary widely depending on site characteristics, but estimates of the global mangrove area also differ (see Sect. 3.2.). At present, the global amount of buried mangrove OC can be estimated only by multiplying the mean global OC burial rate by the global mangrove area. Breithaupt et al. (2012) used 163 g m^{-2} year^{-1} as the mean global OC burial rate and 160,000 km^2 as the global mangrove area and estimated the mean global mangrove OC burial rate as 26.1 Tg C year^{-1} (95% CI 21.0–32.4 Tg C year^{-1}). This corresponds to 9.6–14.9% of the global annual mangrove production (218 ± 72 Tg C year^{-1}) estimated by Bouillon et al. (2008), and to 8.3–15% of the total annual marine OC burial rate (213.7–252.4 Tg C year^{-1}) estimated by Duarte et al. (2005) and recalculated by Breithaupt et al. (2012).

3.5.2.2 Necromass Stocks

Published data suggest that mangrove soils contain large carbon stocks (Donato et al. 2011; Atwood et al. 2017; Sanderman et al. 2018). Donato et al. (2011) measured whole-ecosystem carbon storage in mangrove ecosystems in the Indo-West Pacific region and found that the carbon was stored mainly as necromass in soils (49–98% of the whole-ecosystem carbon storage). The amount of carbon stored in mangrove soils is extremely high compared with that in upland forest soils (Fig. 3.8; see also Table 2.1 in Chap. 2 of this volume). Donato et al. (2011) also found that necromass carbon was higher in estuarine than in oceanic mangrove ecosystems (Fig. 3.9). In both types of ecosystems, the carbon concentration (% dry mass) in the top 100 cm of soil was high and gradually decreased with depth, but the mean soil carbon density in oceanic settings (0.061 g C cm^{-3}) was larger than that in estuarine settings (0.038 g C cm^{-3}). This density difference might reflect autochthonous versus allochthonous sources of sediment or litter. Despite the greater soil carbon density in oceanic settings, the thicker organic (peat) soils in estuarine settings (usually >3 m) than in oceanic settings (<2 m) mean that estuarine soils store more carbon per unit area than oceanic soils. Donato et al. (2011) reported that belowground carbon storage was positively but only weakly correlated with aboveground carbon
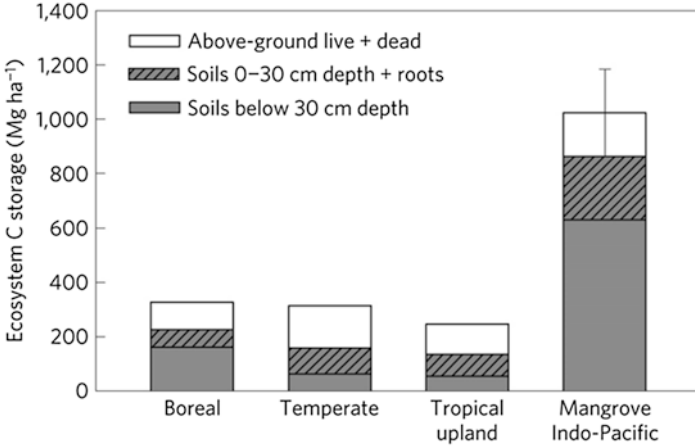
Fig. 3.8 Comparison of carbon storage (mean ± 95% CI) between mangrove and other major global forest domains. (The figure is reproduced from Donato et al. (2011) and is reprinted with permission from the publisher)
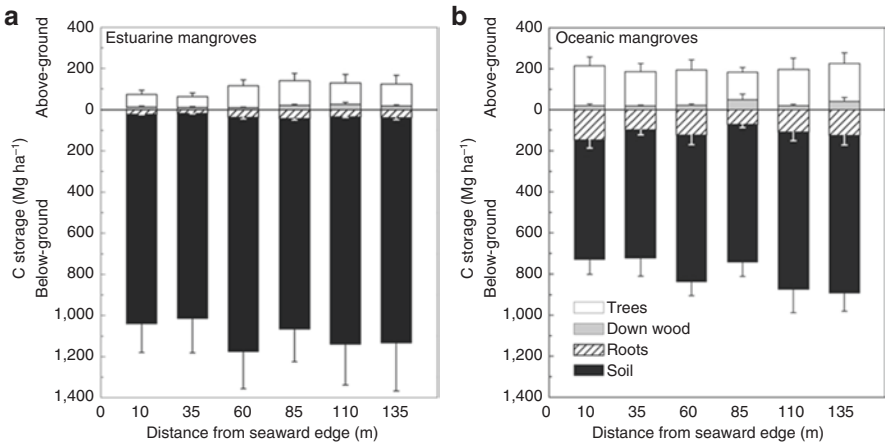
Fig. 3.9 Above- and belowground carbon pools in Indo-West Pacific mangroves, assessed by distance from the seaward edge of the mangrove forest in (A) estuarine mangrove forests situated on large alluvial deltas and (B) oceanic mangroves situated in marine-edge environments (for example, on island coasts). Belowground carbon accounts for 71–98% of ecosystem carbon at estuarine sites and 49–90% at oceanic sites. Overall carbon storage does not vary significantly with distance from the seaward edge in either setting over the sampled range ($P > 0.10$ for aboveground, belowground, and total carbon storage by functional data analysis; 95% CIs for rates of change were between −1.2 and +3.9 Mg C ha^{-1} per m distance from the seaward edge, and all overlapped zero). (The figures are reproduced from Donato et al. (2011) and are reprinted with permission from the publisher)

storage ($r^2 = 0.21$ at estuarine sites, and $r^2 = 0.50$ at oceanic sites). Therefore, below-ground necromass cannot be reliably estimated from aboveground data.

Atwood et al. (2017) analyzed mangrove soil carbon data from 48 countries and found no difference in soil carbon storage per unit area between the northern and southern hemispheres. They did find, however, that soil carbon storage (per unit area) was 20% higher in mixed mangrove stands than it was in stands composed of a single genus. They examined stands with various numbers of mangrove taxa, ranging from single genus to as many as 7 genera, and reported that soil carbon storage per unit area was 70–90% higher in stands with 5 genera than it was in stands with either more or fewer genera. Atwood et al. (2017) also found that forests composed of *Laguncularia*, *Rhizophora*, and *Bruguiera* had higher soil carbon storage per unit area than those composed of other genera (in order of decreasing magnitude of carbon storage, *Xylocarpus*, *Lumnitzera*, *Avicennia*, *Kandelia*, *Ceriops*, *Heritiera*, *Sonneratia*, *Excoecaria*, *Nypa*, *Conocarpus*, and *Aegiceras*). Thus, estimated soil carbon storage per unit area seems to vary greatly among mangrove forests (Jardine and Siikamäki 2014; Atwood et al. 2017), probably because of differences in climate, species composition, hydrology, and topography.

From a global perspective, Jardine and Siikamäki (2014) estimated that the total amount of carbon storage in mangrove soils is 5.00 Pg C, but Atwood et al. (2017) estimated <2.6 Pg C. The large difference between these two estimates is due mainly to the use of different mangrove areal distribution data. Jardine and Siikamäki (2014) used the *World Atlas of Mangroves* (Spalding et al. 2010), whereas Atwood et al. (2017) used data published by Hamilton and Casey (2016). Continuous monitoring and updating of global mangrove distribution data is clearly important. Both of these estimates were made under the assumptions that carbon storage per unit area is constant worldwide, and carbon is stored only to a soil depth of 100 cm. The second assumption is made for practical reasons, because of the difficulty of measuring carbon storage in the entire soil profile (from the surface to underlying rock). In fact, the amount of carbon stored at soil depths below 100 cm may be non-negligible; thus, more carbon storage data in deep soil are needed to improve estimates of soil carbon storage in mangrove forests.

3.6   Conclusion

Donato et al. (2011) quantified whole-ecosystem carbon storage in 25 mangrove forests in the Indo-West Pacific region (Kosrae Island in eastern Micronesia; Yap and Palau islands in western Micronesia; Sulawesi, Java, and Borneo in Indonesia; and the Sundarbans, in the Ganges–Brahmaputra delta in Bangladesh) and estimated that mangrove ecosystems in that region store an average of 1023 Mg C ha^{-1} (Fig. 3.8). This number is extremely high compared with carbon storage in upland forest ecosystems; boreal, temperate and tropical uplands (Fig. 3.8). Atwood et al. (2017) estimated that whole-ecosystem carbon storage in mangrove ecosystems was ~4.4 Pg C globally. Breithaupt et al. (2012) estimated the mean global

mangrove organic carbon burial rate to be 26.1 Tg C year^{-1}, which corresponds to 9.6–14.9% of the global annual mangrove production (Bouillon et al. 2008) and 8.3–15% of the total annual marine organic carbon burial rate (Duarte et al. 2005, as recalculated by Breithaupt et al. 2012).

The high ability of mangroves to sequester carbon is attracting much attention, and more precise estimates of this ecosystem function of mangrove forests are required. In particular, information on belowground biomass and necromass is lacking. For more accurate global-scale evaluation of carbon storage, more precise distribution maps of mangroves and the use of updated monitoring and measurement techniques are needed.

References

Akhand A, Chanda A, Das S, Hazra S, Kuwae T (2018) CO$_2$ fluxes from mangrove ecosystems. In: Kuwae T, Hori M (eds) Blue carbon in shallow coastal ecosystems: carbon dynamics, policy, and implementation. Springer, Singapore, pp 185–221

Aksornkoae S (1975) Structure, regeneration and productivity of mangroves in Thailand. Ph. D. dissertation, Michigan University, 109 pp

Alongi DM (2009) The energetics of mangrove forests. Springer, New York

Alongi D, Ayukai T, Brunskill G, Clough B, Wolanski E (1998) Sources, sinks, and export of organic carbon through a tropical, semi-enclosed delta (Hinchinbrook Channel, Australia). Mangrove Salt Marshes 2:237–242

Alongi DM, Tirendi F, Dixon P, Trott LA, Brunskill GJ (1999) Mineralization of organic matter in intertidal sediments of a tropical semienclosed delta. Estuar Coast Shelf Sci 48:451–467

Alongi DM, Sasekumar A, Chong VC, Pfitzner J, Trott LA, Tirendi F, Dixon P, Brunskill GJ (2004) Sediment accumulation and organic material flux in a managed mangrove ecosystem: estimates of land–ocean–atmosphere exchange in peninsular Malaysia. Mar Geol 208:383–402

Alongi DM, Pfitzner J, Trott LA, Tirendi F, Dixon P, Klumpp DW (2005) Rapid sediment accumulation and microbial mineralization in forests of the mangrove *Kandelia candel* in the Jiulongjiang Estuary, China. Estuar Coast Shelf Sci 63:605–618

Amundson R (2001) The carbon budget in soils. Annu Rev Earth Planet Sci 29:535–562

Atwood TB, Connolly RM, Almahasheer H, Carnell PE, Duarte CM, Lewis CJE, Irigoien X, Kelleway JJ, Lavery PS, Macreadie PI, Serrano O, Sanders CJ, Santos I, Steven ADL, Lovelock CE (2017) Global patterns in mangrove soil carbon stocks and losses. Nat Clim Chang 7:523–528

Bouillon S, Borges AV, Castañeda-Moya E, Diele K, Dittmar T, Duke NC, Kristensen E, Lee SY, Marchand C, Middelburg JJ, Rivera-Monroy VH, Smith TJ III, Twilley R (2008) Mangrove production and carbon sinks: a revision of global budget estimates. Glob Biogeochem Cycles 22:GB2013. https://doi.org/10.1029/2007GB003052

Breithaupt JL, Smoak JM, Smith TJ, Sanders CJ, Hoare A (2012) Organic carbon burial rate in mangrove sediments: strengthening to global budget. Glob Biogeochem Cycles 26:GB3011

Brunskill GJ, Zagorskis I, Pfitzner J (2002) Carbon burial rates in sediments and a carbon mass balance for the Herbert River region of the Great Barrier Reef continental shelf, North Queensland, Australia. Estuar Coast Shelf Sci 54:677–700

Cahoon DR, Lynch JC (1997) Vertical accretion and shallow subsidence in a mangrove forest of southwestern Florida, USA. Mangrove Salt Marshes 1:173–186

Cairns MA, Brown S, Helmer EH, Baumgardner GA (1997) Root biomass allocation in the world's upland forests. Oecologia 111:1–11

Cebrián J, Duarte CM (1995) Plant growth-rate dependence of detrital carbon storage in ecosystems. Science 268:1606–1608

Chmura GL, Anisfeld SC, Cahoon DR, Lynch JC (2003) Global carbon sequestration in tidal, saline wetland soils. Glob Biogeochem Cycles 17:1111. https://doi.org/10.1029/2002GB001917

Chong VC, Sasekumar A (1981) Food and feeding habits of the white prawn *Penaeus merguiensis*. Mar Ecol Prog Ser 5:185–191

Chong VC, Low CB, Ichikawa T (2001) Contribution of mangrove detritus to juvenile prawn nutrition: a dual stable isotope study in Malaysian mangrove forest. Mar Biol 138:77–86

Christensen B (1978) Biomass and productivity of Rhizophora apiculata B1 in a mangrove in southern Thailand. Aquat Bot 4:43–52

Cintrón G, Lugo AE, Pool DJ, Morris G (1978) Mangroves of arid environments in Puerto Rico and adjacent islands. Biotropica 10:110–121

Clough BF, Scott K (1989) Allometric relationships for estimating aboveground biomass in six mangrove species. For Ecol Manag 27:117–127

Clough BF, Dixon P, Dalhaus O (1997) Allometric relationship for estimating biomass in multi-stemmed mangrove trees. Aust J Bot 45:1023–1031

Comley BWT, McGuinness KA (2005) Above- and below-ground biomass and allometry of four common northern Australian mangroves. Aust J Bot 53:431–436

Cundell AM, Brown MS, Stanford R, Mitchell R (1979) Microbial degradation of Rhizophora mangle leaves immersed in the sea. Estuar Coast Shelf Sci 9:281–286

Davidson EA, Janssens IA (2006) Temperature sensitivity of soil carbon decomposition and feedbacks to climate change. Nature 440:165–173

Day JW, Coronado-Molina C, Vera-Herrera FR, Twilley R, Rivera-Monroy VH, Alvarez-Guillen H, Day R, Conner W (1996) A 7-year record of above-ground net primary production in a southeastern Mexican mangrove forest. Aquat Bot 55:39–60

De Deyn GB, Cornelissen JHC, Bardgett RD (2008) Plant functional traits and soil carbon sequestration in contrasting biomes. Ecol Lett 11:516–531

Donato DC, Kauffman JB, Murdiyarso D, Kurnianto S, Stidham M, Kanninen M (2011) Mangroves among the most carbon-rich forests in the tropics. Nat Geosci 4:293–297

Duarte CM, Middelburg JJ, Caraco N (2005) Major role of marine vegetation on the oceanic carbon cycle. Biogeosciences 2:1–8

Duke NC (1992) Mangrove floristics and biogeography. Tropical mangrove ecosystems. In: Robertson AI, Alongio DM (eds) Tropical mangrove ecosystems. American Geophysical Union, Washington, DC, pp 63–100

Duke NC, Benzie JAH, Goodall JA, Ballment ER (1998) Genetic structure and evolution of species in the mangrove genus *Avicennia* (Avicenniaceae) in the Indo-West Pacific. Evolution 52:1612–1626

Elsol JA, Saenger P (1983) A general account of the mangroves of Princess Charlotte Bay with particular reference to zonation along the open shoreline. In: Teas HJ (ed) Biology and ecology of mangroves, tasks for vegetation science. Dr. W. Junk Publishers, The Hague, pp 37–48

Eswaran H, Van Den Berg E, Reich P (1993) Organic carbon in soils of the world. Soil Sci Soc Am J 57:192–194

FAO (2007) The world's mangroves 1980–2005. FAO Forestry Paper. FAO, Rome

Fromard F, Puig H, Mougin E, Marty G, Betoulle JL, Cadamuro L (1998) Structure above-ground biomass and dynamics of mangrove ecosystems: new data from French Guiana. Oecologia 115:39–53

Giri C, Ochieng E, Tieszen LL, Zhu Z, Singh A, Loveland T, Masek J, Duke N (2011) Status and distribution of mangrove forests of the world using earth observation satellite data. Glob Ecol Biogeogr 20:154–159

Golley F, Odum HT, Wilson R (1962) The structure and metabolism of a Puerto Rican red mangrove forest in May. Ecology 43:9–19

Gong WK, Ong JE (1990) Plant biomass and nutrient flux in a managed mangrove forest in Malaysia. Estuar Coast Shelf Sci 31:519–530

Gong WK, Ong JE, Clough B (1992) Photosynthesis in different aged stands of mangrove forest in Malaysia. In: Chou LM, Wilkinson CR (eds) Marine science: living coastal resources, 3rd ASEAN science and technology week conference proceedings, vol 6. National University of Singapore and National Science and Technology Board, Singapore, pp 345–352

Gonneea ME, Paytan A, Herrera-Silveira JA (2004) Tracing organic matter sources and carbon burial in mangrove sediments over the past 160 years. Estuar Coast Shelf Sci 61:211–227

Hamilton S, Casey D (2016) Creation of a high spatio-temporal resolution global database of continuous mangrove forest cover for the 21st century (CGMFC-21). Glob Ecol Biogeogr 25:729–738

Hansen MC, Potapov PV, Moore R, Hancher M, Turubanova SA, Tyukavina A, Thau D, Stehman SV, Goetz SJ, Loveland TR, Kommareddy A, Egorov A, Chini L, Justice CO, Townshend JRG (2013) High-resolution global maps of 21st-century forest cover change. Science 344:981

Hijmans RJ, Cameron SE, Parra JL, Jones PG, Jarvis A (2005) Very high resolution interpolated climate surfaces for global land areas. Int J Climatol 25:1965–1978

Hoffman WE, Dawes CJ (1980) Photosynthetic rates and primary production by two Florida red algae species from a salt marsh and a mangrove community. Bull Mar Sci 30:358–364

Hutchison J, Manica A, Swetnam R, Balmfold A, Spalding M (2014) Predicting global patterns in mangrove forest biomass. Conserv Lett 7(3):233–240

Imbert D, Rollet B (1989) Phytomassaerinne et production primaire dans la mangrove du Grand Cul-de-sac Marine (Guadeloupe, Antilles francaises). Bull Ecol 20:27–39

Jardine SL, Siikamäki JV (2014) A global predictive model of carbon in mangrove soils. Environ Res Lett 9:10403

Jennerjahn TC, Ittekkot V (2002) Relevance of mangroves for the production and deposition of organic matter along tropical continental margins. Naturwissenschaften 89:23–30

Johnstone IM (1983) Succession in zoned mangrove communities: where is the climax? In: Teas HJ (ed) Biology and ecology of mangroves, tasks for vegetation science. Dr. W. Junk Publishers, The Hague, pp 131–139

Komiyama A, Moriya H, Prawiroatmodjo S, Toma T, Ogino K (1988) Forest primary productivity. In: Ogino K, Chihara M (eds) Biological system of mangrove. Ehime University, Ehime, pp 97–117

Komiyama A, Poungparn S, Kato S (2005) Common allometric equations for estimating the tree weight of mangroves. J Trop Ecol 21:471–477

Komiyama A, Ong JE, Poungparn S (2008) Allometry, biomass, and productivity of mangrove forests: a review. Aquat Bot 89:128–137

Kristensen E (2008) Mangrove crabs as ecosystem engineers; with emphasis on sediment processes. J Sea Res 59:30–43

Kristensen E, Andersen FO, Kofoed LH (1988) Preliminary assessment of benthic community metabolism in a south-east Asian mangrove swamp. Mar Ecol Prog Ser 48:137–145

Kusmana C, Sabiham S, Abe K, Watanabe H (1992) An estimation of above ground tree biomass of a mangrove forest in east Sumatra, Indonesia. Tropics 1:243–257

Lugo AE (1990) Fringe wetlands. In: Lugo AE, Brinson M, Brown S (eds) Ecosystems of the world, 15, Forested Wetlands. Elsevier, Amsterdam, pp 143–169

Lugo AE, Snedaker SC (1974) The ecology of mangroves. Annu Rev Ecol Syst 5:39–64

Lugo AE, Evink G, Brinson M, Broce A, Snedaker SC (1975) Diurnal rates of photosynthesis, respiration and transpiration in mangrove forests of south Florida. In: Golley FB, Medina E (eds) Tropical ecological systems, vol 22. Springer, New York, pp 335–350

Macnae W (1968) A general account of the flora and fauna of mangrove swamps in the Indo-Pacific region. Adv Mar Biol 6:73–270

Macnae W (1969) Zonation within mangroves associated with estuaries in north Queensland. In: Lauf GH (ed) Estuaries. American Association for the Advancement of Science, Washington, DC, pp 432–441

Mcleod E, Chmura GL, Bouillon S, Salm R, Björk M, Duarte CM, Lovelock CE, Schlesinger WH, Silliman BR (2011) A blueprint for blue carbon: toward an improved understanding of the role of vegetated coastal habitats in sequestering CO_2. Front Ecol Environ 9:552–560

Miyajima T, Hamagichi M (2018) Carbon sequestration in sediment as an ecosystem function of seagrass meadows. In: Kuwae T, Hori M (eds) Blue carbon in shallow coastal ecosystems: carbon dynamics, policy, and implementation. Springer, Singapore, pp 33–71

Olson DM, Dinerstein E, Wikramanayake ED, Burgess ND, Ppwell GVN, Underwood EC, D'amico JA, Itoua I, Strand HE, Morrison JC, Loucks CJ, Allnutt TF, Ricketts TH, Kura Y, Lamoreux JF, Wettengel WW, Hedao P, Kassem KR (2001) Terrestrial ecoregions of the world: a new map of life on earth: a new global map of terrestrial ecoregions provides an innovative tool for conserving biodiversity. Bioscience 51:933–938

Ong JE, Gong WK, Wong CH, Dhanarajan G (1984) Contribution of aquatic productivity in a managed mangrove ecosystem in Malaysia. In: Soepadmo E, Rao AN, Macintosh DJ (eds) Proceedings of the Asian symposium on mangrove environment: research and management. University of Malaysia and UNESCO, Kuala Lumpur, pp 209–215

Ong JE, Gong WK, Clough BF (1995) Structure and productivity of a 20-year-old stand of Rhizophora apiculata B1 Mangrove forests. J Biogeogr 22:417–427

Ong JE, Gong WK, Wong CH (2004) Allometry and partitioning of the mangrove, Rhizophora apiculata. For Ecol Manag 188:395–408

Oohata S, Shinozaki K (1979) A statical model of plant form – further analysis of the pipe model theory. Jpn J Ecol 29:323–335

Paijmans K, Rollet B (1977) The mangroves of Galley Reach, Papua New Guinea. Forest Ecol Manage 1:141–147

Poungparn S, Komiyama A, Jintana V, Piriyayaota S, Sangtiean T, Tanapermpool P, Patanaponpaiboon P, Kato S (2002) A quantitative analysis on the root system of a mangrove, *Xylocarpus granatum* Koenig. Tropics 12:35–42

Putz F, Chan HT (1986) Tree growth, dynamics, and productivity in a mature mangrove forest in Malaysia. For Ecol Manag 17:211–230

Robertson AI, Duke NC (1987) Insect herbivory in mangrove leaves in north Queensland. Aust J Ecol 12:1–7

Robertson AI, Alongi DM, Boto KG (1992) Food chains and carbon fluxes. In: Robertson AI, Alongi DM (eds) Tropical mangrove ecosystems. American Geophysical Union, Washington, DC, pp 293–326

Rodelli MR, Gearing JN, Gearing PJ, Marshall N, Sasekumar A (1984) Stable isotope ratio as a tracer of mangrove carbon in Malaysian ecosystems. Oecologia 61:326–333

Saenger P (1982) Morphological, anatomical and reproductive adaptations of Australian mangroves. In: Clough BF (ed) Mangrove ecosystems in Australia: structure, function and management. Australian National University Press, Canberra, pp 153–191

Saenger P (2002) Mangrove ecology, silviculture and conservation. Kluwer Academic Publishers, Dordrecht

Saenger P, Snedaker SC (1993) Pantropical trends in mangrove above-ground biomass and annual litterfall. Oecologia 96:293–299

Sanderman J, Hengl T, Fiske G, Solvik K, Adame MF, Benson L, Bukoski JJ, Carnell P, Cifuentes-Jara M, Donato D, Duncan C, Eid EM, Ermgassen P, Lewis CJE, Macreadie PI, Glass L, Gress S, Jardine SL, Jones TG, Nsombo EN, Rahman MM, Sanders CJ, Spalding M, Landis E (2018) A global map of mangrove forest soil carbon at 30m spatial resolution. Environ Res Lett 13:055002

Semeniuk V (1980) Mangrove zonation along an eroding coastline in King Sound, north-western Australia. J Ecol 68:789–812

Semeniuk V (1985) Development of mangrove habitats along ria shorelines in north and north-western tropical Australia. Vegetatio 53:11–31

Shinozaki K, Yoda K, Hozumi K, Kira T (1964) A quantitative analysis of plant form – the pipe model theory. II Further evidence of the theory and its application in forest ecology. Jpn J Ecol 14:133–139

Smith TJI, Duke NC (1987) Physical determinants of inter-estuary variation in mangrove species richness around the tropical coastline of Australia. J Biogeogr 14:9–19

Smith TJ, Boto KG, Frusher S, Giddins RL (1991) Keystone species and mangrove forest dynamics: the influence of burrowing by crabs on soil nutrient status and forest productivity. Estuar Coast Shelf Sci 33:419–432

Spalding MD, Blasco F, Field CD (1997) World mangrove atlas. International Society for Mangrove Ecosystems, Okinawa

Spalding MD, Kainuma M, Collins L (2010) World atlas of mangroves. Earthscan, London

Tam NFY, Wong YS, Lan CY, Chen GZ (1995) Community structure and standing crop biomass of a mangrove forest in Futian Nature Reserve, Shenzhen, China. Hydrobiologia 295:193–201

Tamai S, Nakasuga T, Tabuchi R, Ogino K (1986) Standing biomass of mangrove forests in southern Thailand. J Jpn Forest Soc 68:384–388

Tateda Y, Nhan DD, Wattayakorn G, Toriumi H (2005) Preliminary evaluation of organic carbon sedimentation rates in Asian mangrove coastal ecosystems estimated by ^{210}Pb chronology. Radioprotection 40(suppl):S527–S532. https://doi.org/10.1051/radiopro/2005s1-077

Thom BG (1982) Mangrove ecology: a geomorphological perspective. In: Clough BF (ed) Mangrove ecosystems in Australia, structure, function and management. Australian National University Press, Canberra, pp 3–17

Thom BG (1984) Coastal landforms and geomorphic processes. In: Snedaker SC, Snedaker JG (eds) The mangrove ecosystem: research methods. UNESCO, Paris, pp 3–17

Tomlinson PB (1986) The botany of mangroves. University of Cambridge, New York, pp 25–39

TroCEP (Tropical Coastal Ecosystems Portal) 2017 Available from http://www.nies.go.jp/TroCEP/index.html. Accessed 22 Dec 2017

Twilley RR, Chen RH, Hargis T (1992) Carbon sinks in mangroves and their implications to carbon budget of tropical coastal ecosystems. Water Air Soil Pollut 64:265–288

Ulrich B, Mayer R, Heller H (eds) (1974) Data analysis and data synthesis of forest ecosystems. Göttinger Bodenkundliche Berichte 30:459 pp

Van Steenis CJJG (1957) Outline of vegetation types in Indonesia and some adjacent regions. Proc Pac Sci Congr 8:61–97

Watson JG (1928) Mangrove forests of the Malay Peninsula. Malayan For Rec 6:1–275

Woodroffe C (1992) Mangrove sediments and geomorphology. In: Robertson AI, Alongi DM (eds) Tropical mangrove ecosystems. American Geophysical Union, Washington, DC, pp 7–41

Chapter 4
Carbon Sequestration by Seagrass and Macroalgae in Japan: Estimates and Future Needs

Goro Yoshida, Masakazu Hori, Hiromori Shimabukuro, Hideki Hamaoka, Toshihiro Onitsuka, Natsuki Hasegawa, Daisuke Muraoka, Kousuke Yatsuya, Kentaro Watanabe, and Masahiro Nakaoka

Abstract In this chapter, we estimated carbon sequestration by seagrass and macroalgal beds, defined as the integration of annual plant tissue (organic carbon) production, in Japan. Each of the main four beds, eelgrass beds (*Amamo-ba*), *Sargassum* beds (*Garamo-ba*), warm-temperate kelp beds (*Arame-ba*), and cold-temperate kelp beds (*Kombu-ba*), exhibited a distinctive geographic distributional pattern along Japan's coasts that depended on regional climate and topographic characteristics. The total area of the four beds was approximately 230,000 ha nationwide, based on an analysis of the latest satellite images and information on past distributions of the beds. Carbon sequestration of each seagrass or macroalgal bed was evaluated as

G. Yoshida (✉) · M. Hori · H. Shimabukuro
National Research Institute of Fisheries and Environment of Inland Sea, Japan Fisheries Research and Education Agency, Hatsukaichi, Hiroshima, Japan
e-mail: gorogoro@affrc.go.jp

H. Hamaoka
Niigata Prefectural Fisheries and Marine Research Institute, Niigata, Japan

T. Onitsuka
Kushiro Laboratory, Hokkaido National Fisheries Research Institute, Japan Fisheries Research and Education Agency, Japan Fisheries Research and Education Agency, Kushiro, Hokkaido, Japan

N. Hasegawa
National Research Institute of Aquaculture, Fisheries Research and Education Agency, Minami-ise, Mie, Japan

D. Muraoka · K. Yatsuya
Miyako Laboratory, Tohoku National Fisheries Research Institute, Japan Fisheries Research and Education Agency, Miyako, Iwate, Japan

K. Watanabe
Waterfront Vitalization and Environmental Research Foundation, Naha, Okinawa, Japan

M. Nakaoka
Akkeshi Marine Station, Field Science Center for Northern Biosphere, Hokkaido University, Akkeshi, Hokkaido, Japan

integrated annual plant tissue production converted to organic carbon, which was defined by subtracting dissolved organic matter production from net primary production. Plant tissue production of the main constituent macrophyte of the seagrass and macroalgal beds was directly measured in each coastal region, and production values from past reports were also collected and utilized. Annual carbon sequestration by seagrass and macroalgal beds in Japan, expressed in a CO_2-converted base, was about 4.7 million tons per year, which is comparable to the CO_2 emissions of the industrial sectors of agriculture and fisheries.

4.1   Introduction

The Japanese archipelago is long from south to north and lies within a wide climatic range, from subarctic to subtropical. Warm and cold currents flow near the Japanese coast, affecting and characterizing the local climate of coastal habitats. In addition, topographic characteristics along the coast are also diverse, from rocky shores struck by waves to gentle coves with sandy beaches or tidal flats. Many species of seagrass and macroalgae with diverse physiological and ecological features inhabit these diverse climatic and physical environments along the coast. As a result, various forms of seagrass and macroalgal beds are distributed throughout Japan.

As discussed in other chapters in this volume, blue carbon ecosystems store substantial amounts of carbon, and it has become clear that they make a great contribution to carbon sequestration and storage on a global scale (Endo and Otani 2018; Inoue 2018; Miyajima and Hamagichi 2018). UNEP's "Blue Carbon "report (Nellemann et al. 2009) suggested that seagrass beds such as eelgrass meadows deposit considerable amounts of organic carbon of biological origin in the soft sediment within the beds and store it for long periods. Since publication of the report, increasing attention has been paid to the potential of seagrass beds as carbon sinks, which could be an effective measure against global warming.

Macroalgal beds formed mainly of large brown algae on rocky shores do not share the same depositional function as the seagrass beds, so there has been little discussion of their contribution in terms of blue carbon and carbon sequestration in the UNEP's "Blue Carbon" report. However, a considerable amount of macroalgae may flow out from their beds and be transported and deposited to the deep seafloor (Krause-Jensen and Duarte 2016). If this is the case, macroalgal beds also serve as a source of long-term stored organic carbon, even though it is stored in different locations from its origin.

Seagrass and macroalgal beds have high primary production (and carbon sequestration potential), which is comparable to that of forests (Kurashima 2010). In shallow coastal waters, seagrass and macroalgae are often more abundant than other primary producers such as phytoplankton and benthic microalgae. Therefore, seagrass and macroalgae are the major ecosystem members responsible for sequestration and storage of carbon in shallow coastal waters.

To estimate how much carbon dioxide is absorbed and sequestered from the atmosphere by seagrass and macroalgal beds in Japan, we first need to determine how much seagrass and macroalgae actually grow in Japan. Organic carbon, consti-
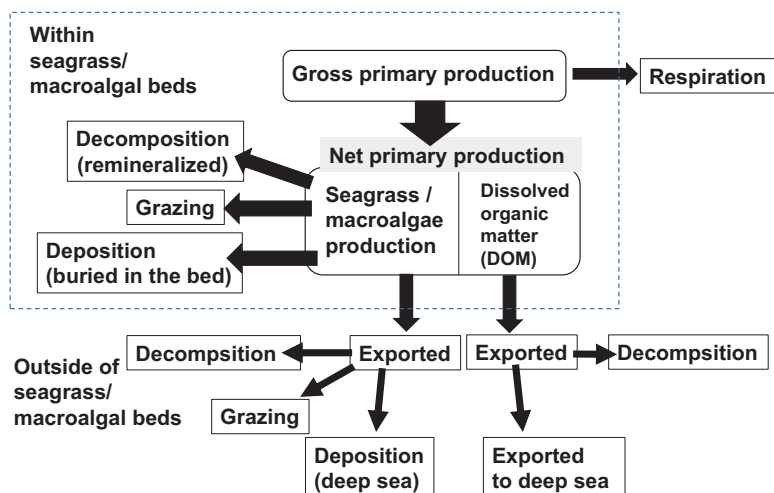
Fig. 4.1 Carbon pathway via primary production of seagrass and macroalgae. (Modified from Krause-Jensen and Duarte 2016)

tuting the plant body of seagrass and macroalgae, has several fates. It can be consumed and circulate in the ecosystem through the food web, it can be deposited and accumulate on the seafloor in beds for a long period, and it can flow out of the beds as seagrass and macroalgal drift (Fig. 4.1) (Abo et al. 2018). To understand the entire route and amount of carbon flow, it is essential to quantitatively evaluate the amount of carbon sequestred by seagrass and macroalgae as part of the carbon flow baseline. Also, as in the case of forests, if carbon sequestration and storage by seagrass and macroalgal beds is recognized as an effective measure to reduce greenhouse gas emissions in the future, activities related to conservation and reconstruction of seagrass and macroalgal beds will become more socially significant. Gathering basic information about the amount of carbon sequestration and storage by seagrass and macroalgae in Japan will also enable us to obtain fundamental knowledge important for promoting such social measures. Further, seagrass and macroalgae have been used traditionally as industrial materials or food in Japan. Even this use may sometimes conflict with sequestering and storing carbon, and it will most likely continue to be an important use in the future. A quantitative assessment of seagrass and macroalgae growth on the coast of Japan is necessary for the sustained and wise use of the ecosystem services offered by seagrass and macroalgal beds.

For this purpose, we estimated the amount of seagrass and macroalgae produced along the entire coast of Japan on a dry weight basis. This amount was converted into an equivalent amount of organic carbon and expressed as the amount annually sequestered by seagrass and macroalgal beds. In addition, we compared these values with those from areas in other countries and examined the geographic characteristics of the production of seagrass and macroalgal beds. The available data that can be used for this calculation are still limited, and there are uncertainties in the estimates, which we also discuss in the chapter. It should be noted that the estimates in this chapter should be updated as research on the topic progresses in the future.

First, however, we introduce some points of discussion and terms used in the chapter. Seagrass and macroalgae produce organic matter through photosynthesis. The total amount of this organic matter is gross primary production. Part of the gross primary production is mineralized by respiration and released as carbon dioxide. Gross primary production minus respiration is net primary production, which is split between that used to form the tissues of seagrass and macroalgae and that released into surrounding water as dissolved organic matter (DOM) (Fig. 4.1). In the past researches on the production of seagrass and macroalgae in Japan, the amount of DOM relative to total net primary production has been assumed to be negligible, and only the amount of seagrass and macroalgal tissue production is usually considered as net primary production. However, recent studies have suggested that the released DOM cannot necessarily be neglected quantitatively and that some of the DOM is also refractory, which may greatly contribute to carbon storage in the ocean (Wada et al. 2008; Kuwae et al. 2018). In this chapter, we only focus on the production of seagrass and macroalgal tissues, which are the main pathways of carbon sequestration by these macrophyte. To avoid confusion, we simply use the term "production" for this tissue production instead of the term net primary production.

4.2 The Area and Distributional Characteristics of Seagrass and Macroalgal Beds in Japan

To estimate the total amount of production by seagrass and macroalgae along the entire coast of Japan, data on their bed area are required. To ascertain the current status of seagrass and macroalgal beds, nationwide and (more frequently) regional surveys on the area and distribution of seagrass and macroalgal beds have been conducted in Japan. However, the available data are spatiotemporally discrete, and the last nationwide research by the Ministry of the Environment was conducted in the early 1990s.

As was mentioned in the Introduction, there are many seagrass and macroalgal species in Japan. Therefore, for convenience, seagrass and macroalgal beds have often been classified into several types, depending on the main constituent species. In this section, we first describe the classification types of seagrass and macroalgal beds generally used in research in Japan. We then outline the area and distributional characteristics of each type of bed along the Japanese coast obtained in the latest survey in which the authors were involved recently (in 2009–2013).

4.2.1 Types of Seagrass and Macroalgal Beds

In research conducted by the Ministry of the Environment and the Fisheries Agency of Japan, seagrass and macroalgal beds have generally been classified as *Amamo-ba* (which contains all kinds of seagrass) and seven types of macroalgal
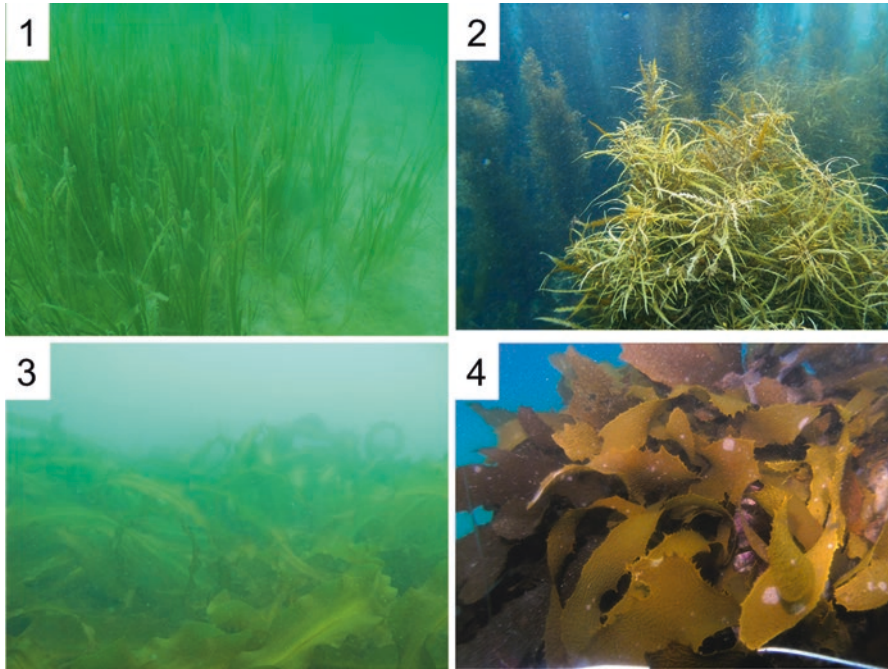
Fig. 4.2 Main seagrass and macroalgal beds in Japan: (1) eelgrass, (2) *Sargassum*, (3) cold-temperate kelp (*Saccharina*), and (4) warm-temperate kelp (*Ecklonia* and *Eisenia*)

beds: *Garamo-ba*, *Arame-ba*, *Kombu-ba*, *Tengusa-ba*, *Wakame-ba*, *Aosa-Aonori-ba*, and other macroalgal bed, according to their main constituent macroalgal species (Environmental Agency, Marine Parks Center of Japan 1994). The classification type depends on taxa levels higher than species, so the constituents of a bed type generally include several species that are taxonomically closely related. Because these constituent species exhibit similar morphology, life cycles, and other ecological properties characterized by the taxa, each bed has characteristic landscapes and specific functions in coastal ecosystems.

In general, of these eight types of seagrass and macroalgal beds, *Amamo-ba*, *Garamo-ba*, *Arame-ba*, and *Kombu-ba* (Fig. 4.2) are considered to be more important than the other beds from the viewpoint of ecological function. Seagrass and macroalgae comprising these beds have large thalli that grow upright and are mostly perennial. Therefore, these beds form remarkable stands that are maintained throughout the year and have a large influence on the surrounding environment and other organisms. In addition, the combined area of these four main types of beds occupied approximately 75% of the total area of all beds in Japan, as evaluated in the 4th National Survey on the Natural Environment (Environmental Agency, Marine Parks Center of Japan 1994). Most of the carbon sequestration contribution by seagrass and macroalgal beds in Japan is therefore attributed to these four main types, and we use them in this chapter to estimate production in Japan.

Amamo means eelgrass in Japanese, mainly *Zostera marina*, which is distributed in temperate regions in the northern hemisphere. This is the most common species of seagrass in Japan and is widely distributed from Hokkaido to the Satsuma Peninsula in southern Kyushu, forming vast beds in shallow areas of sandy to muddy sea bottom (Nakaoka and Aioi 2001). Around the Nansei Islands, which have a subtropical climate, numerous other seagrass species distribute, and in temperate regions, species other than *Z. marina*, such as *Z. japonica* and *Z. caulescens,* also exist. Because of its wide distribution, however, *Amamo* (i.e., *Z. marina*) is the most representative seagrass in Japan, and in many cases seagrass beds are simply referred to as *Amamo-ba* by researchers in Japan.

Garamo-ba is a bed composed of macroalgae belonging to the family Sargassaceae, order Fucales (Phaeophyceae, brown algae). Macroalgae belonging to Sargassaceae are widely distributed from temperate to tropical regions, and about 70 species have been described in Japan (Yoshida et al. 2015). Each species shows slightly different physiological and ecological characteristics, and *Garamo-ba* has diverse constituents, depending on differences in water depth, current flow conditions, and characteristics of the substrate where the beds are formed.

Both *Kombu-ba* and *Arame-ba* consist of various kinds of macroalgae belonging to the order Laminariales (Phaeophyceae). The kelp forming *Kombu-ba* contains many commercially important species, mainly of the genus *Saccharina*, and are distributed from Hokkaido to the Pacific coast of the Tohoku region, where the cold current affects the coastal environment (Kawashima 2004). Kelp forming *Arame-ba* belong to the genera *Ecklonia* and *Eisenia* in the family Lessoniaceae. They are mainly distributed on the coast in temperate regions affected by warm currents and are sometimes called "warm temperate kelp." The constituent species are limited to two species of the genus *Eisenia* (*E. bicyclis* and *E. arborea*) and three species of the genus *Ecklonia* (*E. cava, E. kurome*, and *E. stolonifera*), but each species forms beds on a large scale and *Arame-ba* is commonly found on the rocky shores in temperate Japan, often along with *Garamo-ba. Arame* is a Japanese name for *E. bicyclis* in a narrow sense, but species of *Eisenia* and *Ecklonia* share similar morphology and ecological features, so they are often collectively referred to as *Arame* in many local areas (Terawaki and Arai 2004).

Hereafter, *Amamo-ba* will be referred to as "eelgrass bed". *Garamo-ba, Arame-ba*, and *Kombu-ba* will be referred to as "*Sargassum* bed," "warm-temperate kelp bed," and "cold-temperate kelp bed," respectively.

4.2.2   Areas and Geographic Distribution Patterns of Seagrass and Macroalgal Beds in Japan

The nationwide area and distribution of seagrass and macroalgal beds in Japan has been surveyed in various ways such as scuba, shipboard observation or interviews, etc., in the National Survey of Natural Environment led by the Ministry of

Environment, Japan. The last and most detailed survey before 2000 was conducted in the early 1990s (the 4th National Survey). No similar nationwide survey has been conducted until recently, and the area surveyed in the 4th National Survey (201,212 ha) has been used as the total area of seagrass and macroalgal bed in Japan, often even now. Given that more than 20 years has passed since the survey was conducted, an update is needed to determine the current nationwide status of seagrass and macroalgal beds.

Against this background, a survey project was conducted by the Fisheries Agency of Japan (2009–2013) that attempted to evaluate the nationwide area of seagrass and macroalgal beds in Japan based on an analysis of satellite images (Hori et al. 2014). The area of each type of seagrass and macroalgal beds was estimated from an analysis of images taken by the Earth Observation Satellite ALOS of the Japan Aerospace Exploration Agency starting in 2000 (Hori et al. 2014). Here, we use the area obtained by this project to estimate the carbon sequestration by seagrass and macroalgae.

In the survey project in 2009–2013, estimated areas were 61,667 ha of eelgrass bed, 88,041 ha of *Sargassum* bed, 63,120 ha of warm-temperate kelp bed, and 20,356 ha of cold-temperate kelp bed. These values are similar to the areas reported in the previous survey in the 4th National Survey (49,464 ha, 85,682 ha, 64,483 ha, and 35,724 ha, respectively; Environment Agency, Marine Parks Center of Japan 1994), although larger differences were observed in eelgrass and cold-temperate kelp beds. However, there were differences in methodology and processes used for the estimations between the 4th National Survey and the latest survey by the Fisheries Agency, so it is not practical to simply compare the area values obtained in the two surveys. In the 4th National Survey, the area was estimated only for seagrass and macroalgal beds with an area of at least 1 ha and a depth of less than 20 m, whereas higher resolution data from satellite images were obtained in the survey led by the Fisheries Agency.

Figure 4.3 shows the coastal area of Japan divided into seven regions according to the characteristics of the water temperature environment, which is mainly influenced by warm and cold ocean currents. It also shows the area of each type of seagrass and macroalgal bed in each region, which were obtained in the latest survey by the Fisheries Agency. As can be readily seen, each type of seagrass and macroalgal bed exhibits a very characteristic geographic distribution pattern along the Japanese coastline.

More eelgrass beds are distributed in the coastal areas of Hokkaido and the Seto Inland Sea than in other regions (Fig. 4.3). Generally, seagrasses including *Z. marina* grow rhizomes in sediment composed of sand and mud. Therefore, it is difficult for them to form and maintain beds in environments where the bottom sediment is disturbed by strong waves and currents. In Hokkaido, where relatively natural coastlines remain highly intact, many lagoons are sheltered from the waves of the open sea and suitable for eelgrass bed development. For example, there are vast eelgrass beds in Lake Furen and Lake Akkeshi, which are large lagoons in eastern Hokkaido. The Seto Inland Sea is the largest semi-enclosed sea area in Japan and with many islands, so there are many places that escape the influence of intense
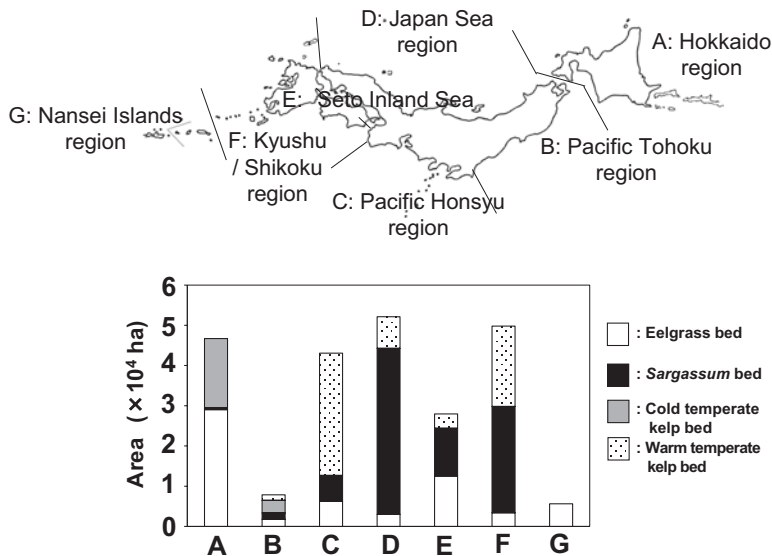
Fig. 4.3 Division of Japanese coastal regions according to sea water temperature, and seagrass and macroalgal bed areas in each region. (Modified from Hori et al. 2014)

waves induced by winds and are suitable for eelgrass bed development. Vast areas (23,000 ha) of eelgrass beds were present in the Seto Inland Sea before 1960, but that area was reduced by as much as 30% by landfill and water pollution during the period of rapid economic growth from the 1960s to the early 1970s in Japan (Yoshida et al. 2010).

The distribution of the cold-temperate kelp beds is limited to the coastal areas of Hokkaido and the Pacific coast of the Tohoku region that are affected by cold currents (Fig. 4.3). On the contrary, *Sargassum* beds and warm-temperate kelp beds distribute along the coasts of central and western Japan in which the climate is temperate. Though the two beds often coexist in rocky shores, the dominance patterns are different among the regions. Warm-temperate kelp beds are dominant in coastal regions of the Pacific Honshu region, whereas *Sargassum* beds are quite abundant in coastal regions of the Japan Sea region. Although both plants of *Sargassum* and kelps (*Eisenia* and *Ecklonia*) grow in the rocky shore, their beds are formed under different physical conditions depending on depth, wave effects, and substrate properties (Terawaki and Arai 2004). Therefore, the physical conditions related to macroalgal bed establishment are different between the Pacific Ocean and Japan Sea sides of Honshu. Unlike these two regions of Honshu, *Sargassum* beds and warm-temperate kelp beds are distributed evenly in the open coastal region of Kyushu and Shikoku. In the Seto Inland Sea region, *Sargassum* beds on the rocky shores are distributed almost equally as the eelgrass beds developed on the soft sediments (Fig. 4.3). As noted above, there are many islands in the Seto Inland Sea, each

of which has complex intricate coastlines made up both of rocky reefs protruding into the sea and calm coves with intrinsic beaches or tidal flats. The diversity in environments allows the formation and coexistence of both eelgrass and *Sargassum* beds (Yoshida et al. 2010).

Only eelgrass beds have been detected in the Nansei Islands region (Fig. 4.3). Though *Z. marina* is not distributed in this region, many tropical seagrass species exist, including *Thalassia hemprichii* and *Cymodocea rotundata*. Although some *Sargassum* species are also distributed in the Nansei Islands, the distribution of *Sargassum* beds was not also reported in the 4th National Survey. There are many coral reefs in the rocky shores of the Nansei Islands, and large stands of *Sargassum* may not develop and have not been perceptible as a bed.

4.3 Estimation of Carbon Sequestration by Seagrass/ Macroalgae

To calculate the production of seagrass and macroalgae for the entire coastal area of Japan, the area and estimated production per unit area of each type of seagrass and macroalgal bed is needed. Here, we introduce the production rate directly measured from those beds throughout Japan and compare the rates with those obtained worldwide to clarify the characteristics of seagrass and macroalgal production in Japan. We then calculate the total nationwide production rate in seagrass and macroalgal bed areas and convert that to an organic carbon sequestration rate on a yearly basis.

The amount of seagrass and macroalgae existing in their beds at some point in time is called its biomass. Seagrass and macroalgae exhibit seasonal growth and withering as land plants do, and the fluctuations appear as seasonal changes in biomass. Generally, plant biomass increases with the accumulation of newly-formed tissues and organs during the growth season and reaches a peak with the peak of growth. However, the tissues and organs of seagrass and macroalgae are relatively short-lived and generally do not persist for long periods, unlike tree trunks, for example, which grow gradually from year to year and accumulate biomass with age. That means that, in seagrass and macroalgae, new formation and loss of tissues or organs proceed simultaneously throughout the year. Biomass increases as the total amount of newly formed tissues and organs exceeds the total amount of their loss, and it decreases when the opposite phenomenon occurs. Consequently, it is generally not possible to grasp the annual amount of seagrass and macroalgal production simply by investigating biomass. It is also necessary to investigate the temporal amounts of new tissue formation and to acquire the annual net totals.

Fortunately, direct measurement methods of production corresponding to *in situ* growth characteristics have been developed for eelgrass, *Sargassum*, and kelps, respectively. We used these methods in our estimations as detailed in the following sections.
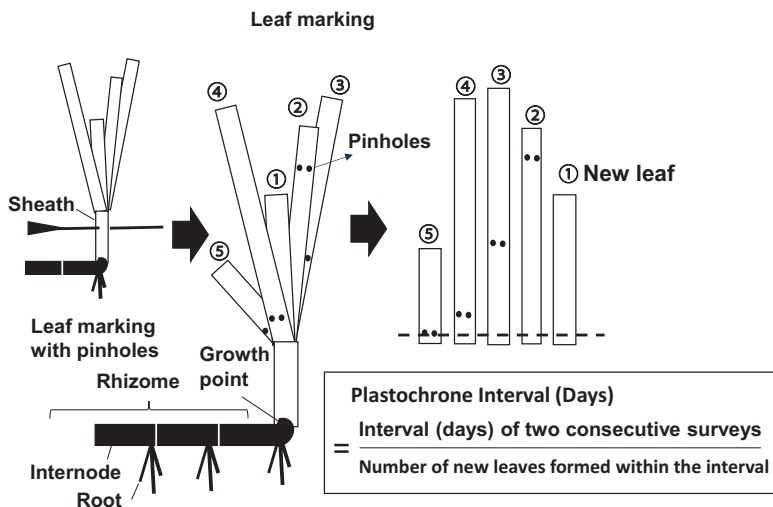
Fig. 4.4 Production measurement of *Zostera marina* leaves by the leaf-marking method (Zieman 1974) and plastochrone interval. Modified from Short and Duarte (2001)

4.3.1 Eelgrass Bed (Amamo-ba)

4.3.1.1 Measurement of Production by the Leaf-Marking Method

Seagrasses including *Z. marina* generally develop the rhizomes in the soft sediments of sand or mud. Leafy thalli or, depending on the species, upright stems arise from the rhizomes above the sediments (Fig. 4.4). Propagation is carried out not only by sexual reproduction (i.e., by seeds) but also by active branching of the rhizome (vegetative propagation). Therefore, the aboveground part (i.e., the "shoot") can be connected with other shoots near it by their rhizomes, meaning they are clones.

Each *Z. marina* shoot consists of two to six leaves bundled into a leaf sheath at the lower part of the shoot, the base of which transits to the rhizome. The rhizome has root bundles arising from each of its nodes, and the rhizome body between two adjacent nodes is called an internode (Fig. 4.4). A growth point exists in the transition between the shoot and the rhizome and new leaves are formed alternately at the growth point. Each node is also formed simultaneously with the formation of each leaf, that is, nodes and leaves are formed at the same rate. The newly formed leaves are gradually pushed to the outside of the shoot as they grow, because new leaves are formed successively inside the shoot. The leaves fall off the shoot after growth has been accomplished and stopped. The formation rate of new leaves varies with the season.

Several methods have been devised to measure the production of seagrass including *Z. marina*, but the leaf-marking method by Zieman (1974) (Fig. 4.4) is the most common. With this method, pinholes are made through a leaf bundle in a leaf sheath

of a shoot with a needle, and the shoot is then collected after a certain period of time. The pinhole-free leaves inside the recovered shoots are new leaves that formed during this period. Because the outermost leaf of the shoot has almost stopped growing when the pinhole was made, the pinhole on this outer leaf is considered to have not moved. Using this position as a starting point, the new formation of leaf tissue of each leaf is estimated from the movement of the pinhole (Fig. 4.4). The sum of the weight of newly formed tissues on each leaf with pinholes and new leaves is considered to be the production by the shoot within the period. With this method, however, production may be underestimated by missing the maturation of leaf tissue above the pinholes. Therefore, Short and Duarte (2001) recommended an alternative method to evaluate production based on the formation rate of new leaves. In this method, a period of observation (days) is divided by the number of newly formed leaves within the period to obtain the plastochrone interval (days) (Fig. 4.4). The plastochrone interval is therefore an interval between consecutive new leaf formations, and the reciprocal of this value shows the leaf formation rate, that is, the number of newly formed leaves in a certain period (generally, per day). By dividing the weight of an individual fully-grown leaf (usually using the third to fourth leaf from the inside, which is the longest in the shoot) by the plastochrone interval, the daily leaf production of the shoot can be approximated.

In the case of *Z. marina*, the nodes of the rhizomes are formed at the growth point at the same rate as the leaves, so the production of the underground part can be estimated in the same way. By dividing the weight of a fully-grown internode with its root by the plastochrone interval, the daily underground production of the shoot can be estimated. The sum of the production of the aboveground part (leaves) and underground part (rhizome and roots) is the total production of the shoot. Furthermore, by multiplying the mean density of shoots, the production amount per unit area can be calculated.

4.3.1.2 Production of Eelgrass Along the Coast of Japan

Zostera marina exhibits seasonal changes in its growth. In Japan, vigorous growth and active vegetative propagation generally occur after spring, and shoot size, shoot density, and biomass reach their annual peak in late spring to summer. After summer, shoot density decreases, and from late autumn to early winter, *Z. marina* exhibits senescence, with the shortest annual shoot size and smallest biomass.

Shoot density in the peak growing season of eelgrass beds in Japan has been reported to be from less than 100 shoots/m^2 to 1500 shoots/m^2, and the biomass of the aboveground part from about 50 g dry weight/m^2 to about 700 g dry weight/m^2 (Hasegawa et al. 2013; Fig. 4.5). The modes for the frequency distributions of these values were found to be about 200 shoots/m^2 and 100–200 g dry weight/m^2, respectively, but large variations exist among beds. Also, no clear relationship has been found between shoot density and aboveground biomass (Hasegawa et al. 2013). The lack of a relationship between density and biomass seems to be due to the fact that the morphological variation of *Z. marina* is extremely large among the beds; for
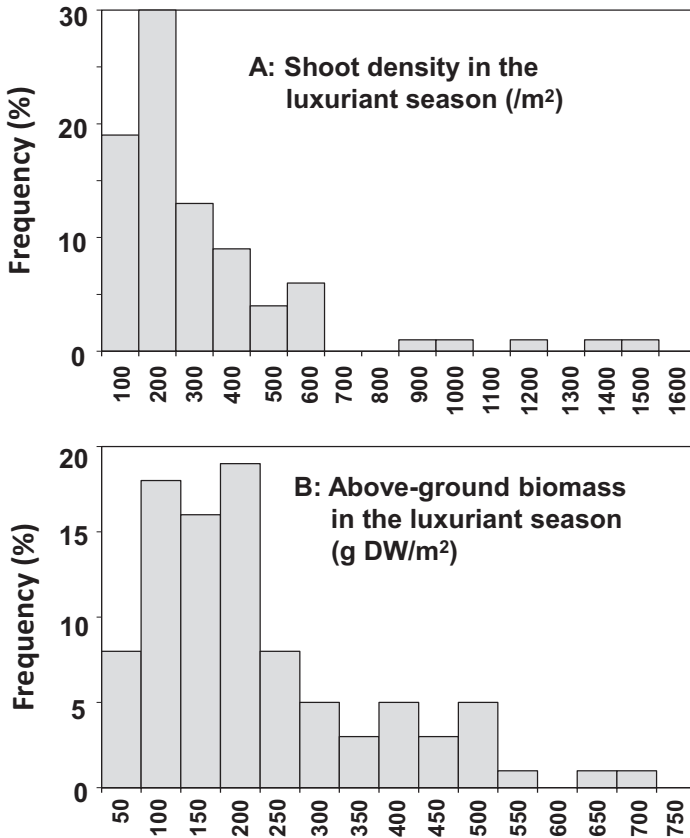
Fig. 4.5 Frequency of shoot density (**a**) and aboveground biomass of *Zostera marina* in the peak growing season in Japan (**b**). *DW* dry weight. (Modified from Hasegawa et al. 2013)

example, there are beds where small shoots grow densely and ones where relatively large shoots grow more sparsely. Furthermore, no clear difference or tendency has been observed in shoot density and biomass of *Z. marina* among coastal regions or along a latitudinal gradient in Japan (Nakaoka and Aioi 2001; Hasegawa et al. 2013).

In the nationwide survey in 2010 and 2011, *Z. marina* production was measured by the leaf-marking method in representative eelgrass beds in each coastal region (Hori et al. 2014). The survey was conducted at Lake Akkeshi (Hokkaido), Sameno-ura Bay and Mangoku-ura (Miyagi Prefecture, Pacific Tohoku region), Futtsu (Tokyo Bay, Pacific Honshu region), Ikuno Island (Seto Inland Sea region), and Tachibana Bay (Nagasaki Prefecture, Kyushyu region). During the survey, the site in the Pacific Tohoku region was forced to move from Sameno-ura Bay to Mangoku-ura because of the impact of the Great East Japan Earthquake in 2011 (Muraoka 2012). All of the surveyed eelgrass beds were formed under sheltered conditions in lagoons or bays. The average shoot densities of these five eelgrass beds during the

Fig. 4.6 Mean production of *Zostera marina* in the representative eelgrass bed of each region (mean value of the peak growing and senescent seasons). Production values in the 2010 senescent season and the 2011 peak growing season are also shown. *DW* dry weight
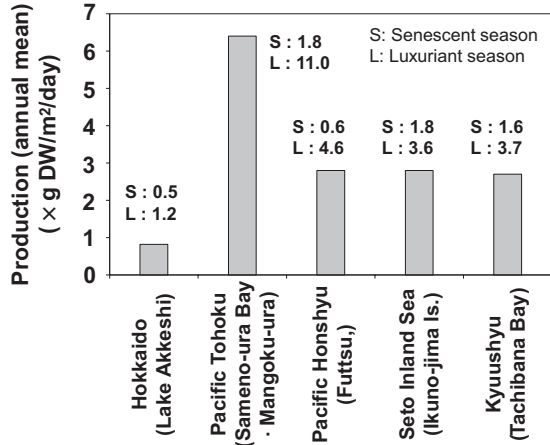
peak growing season ranged from 60 to 250 shoots/m², and the biomass (aboveground and underground) ranged from 64 to 430 g dry weight/m². Figure 4.6 shows the mean daily production of the five eelgrass beds during the senescent and the peak growing seasons; the production in the peak growing season was from 2.0 to 7.7 times larger than that of the senescent season.

Production was notably high in the peak growing season in the Pacific Tohoku region (Mangoku-ura) (11.0 g dry weight/m²/day, Fig. 4.6). The plastochrone interval of *Z. marina* in Mangoku-ura was extremely short (5.5 days) compared with those in the other regions (about 10 days; Muraoka 2012). It is unknown whether higher production is a general characteristic of the eelgrass beds in the Pacific Tohoku region or of this specific area. In Otsuchi Bay, which is also located in the Pacific Tohoku region, a maximum of 13.0 g dry weight/m²/day was recorded for the aboveground part in the peak growing season by the leaf-marking method (Nakaoka and Aioi 2001). Although it is difficult to compare the values because of the different measurement methods used, the aboveground production of *Z. marina* was 5.2 g dry weight/m²/day at Nabeta Bay (Shizuoka Prefecture) located in the Pacific Honshu region and 7.4 g dry weight/m²/day at Yanai (Yamaguchi Prefecture) in the Seto Inland Sea region (Nakaoka and Aioi 2001). Therefore, it is possible that the production of *Z. marina* in the Pacific Tohoku region is higher than those in other regions. The range of water temperature suitable for growth of *Z. marina* ranges from 12 to 21 °C; it becomes senescent at 22 °C or higher (Fisheries Agency and Marino-Forum 21 2007). In the Pacific Tohoku region, the summer water temperature rarely exceeds 20 °C, whereas summer coastal water temperatures in central and western Japan reach >25 °C. The longer period with a suitable water temperature for *Z. marina* growth may explain the higher production in the Pacific Tohoku region.

In Lake Akkeshi in Hokkaido, lower production was observed (Fig. 4.6). Because the plastochrone interval was longer here than in the other regions and because the leaves can persist and remain on shoots after being fully grown due to the low water

Fig. 4.7 Frequency distribution of maximum seagrass production reported worldwide (Modified from Duarte and Chiscano 1999). Arrows indicate the mean values of *Zostera marina* obtained in the review of Nakaoka and Aioi (2001). *DW* dry weight
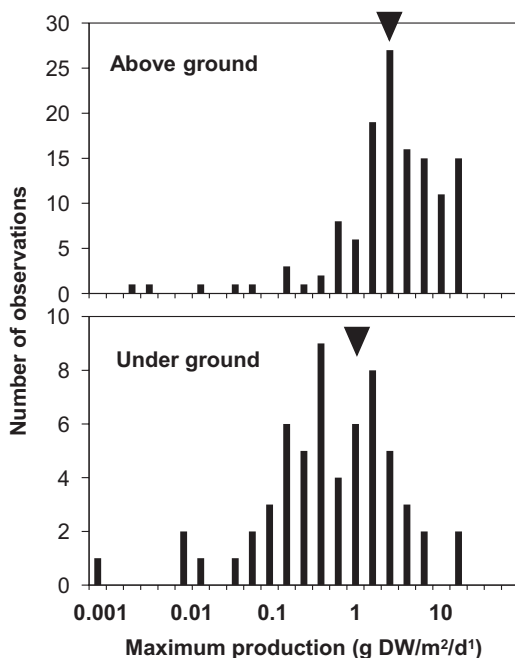
temperature, the biomass can remain high (close to the maximum) longer, which in turn inhibits growth. In addition, in Lake Akkeshi, abundant microalgae were found to adhere to eelgrass leaves (Hasegawa et al. 2007), which could also inhibit *Z. marina* growth, so multiple factors may interact to influence production in Lake Akkeshi.

Duarte and Chiscano (1999) reviewed many studies that reported seagrass production including *Z. marina* in countries other than Japan. Production of seagrass in various regions of the world has been reported to vary depending on species, but its average is about 5 g dry weight/m^2/day (3.8 g aboveground +1.2 g underground; Duarte and Chiscano 1999) in the peak growing season. Although *Z. marina* production varies depending on beds and regions, its mean value (5.2 g aboveground +1.7 g underground; Duarte and Chiscano 1999) is a somewhat larger than the mean of all seagrass. If we compile all past data of *Z. marina* production measured in the peak growing season in Japan, which were reviewed by Nakaoka and Aioi (2001), the mean value (about 4 g aboveground +1.2 g underground) is near the mode of values obtained globally (Fig. 4.7). The annual production of *Z. marina* at the survey sites in Fig. 4.6, calculated by accumulating the mean daily production in the peak growing and senescent seasons for 1 year, production in the Pacific Tohoku region was 2.3 kg dry weight/m^2/year, which is still large compared with any of the three sites in central and western Japan, where the annual production was about 1.0 kg dry weight/m^2/year. This latter value is approximately equal to the mean annual production of seagrass in the world (1012 g dry weight/m^2/year; Duarte and Chiscano 1999).

In northern Japan, many species of the genus *Zostera* other than *Z. marina* (e.g., *Z. caulescens*, *Z. caespitosa*, and *Z. asiatica*) are often dominant (Nakaoka and Aioi 2001). In general, these species form their beds in deeper zones than *Z. marina*, and there has been little information available on biomass and production for these species. For *Z. caulescens* in Otsuchi Bay off the Sanriku coast, annual production was estimated to be 0.47 kg dry weight/m²/year (Nakaoka et al. 2003). On the other hand, in Akkeshi Bay in eastern Hokkaido, *Z. asiatica* had a mean production of 2.03 kg dry weight/m²/year, which exceeded the value (1.35 kg dry weight/m²/year) of the sympatric *Z. marina* (Watanabe et al. 2005). The latter case points out the possibility of over- or underestimation of the production of eelgrass beds composed of multiple species when the values are extrapolated from production data of only *Z. marina*.

Until now, data on the actual production of seagrass in Japan have been still few. To clarify the mechanism of the spatiotemporal variation of production of eelgrass beds, continuous surveys of beds exhibiting various characteristics are necessary, as is monitoring of the fluctuation of environmental parameters related to production.

4.3.2   Sargassum *Bed (Garamo-ba)*

4.3.2.1   Measurement of Production by Productive Structure Analysis

Thalli of *Sargassum* adheres to hard substrata such as rocks or boulders by holdfasts as it grows. A short axis (a stem or stipe) arises from the holdfast, and several main branches are formed at the top of the axis and elongate. Thalli develop from 1 m to several meters in length, but the length differs among species. Lateral branches and leaves are formed on the main branches, and buoyant vesicles transformed from leaves are formed to allow the thalli to stand upright (Fig. 4.2). The presence of the complex morphological features of the constituent thalli means that *Sargassum* beds present an extremely complex three-dimensional structure that offers an important habitat for many organisms.

Sargassum exhibits extremely clear seasonal growth, and after the growth season in which the main branches rapidly elongate, reproductive organs (receptacles) are formed on the branches in the maturation season. Generally, the maturation season of many species in Japan is in spring, and the biomass also reaches the yearly maximum during this season. Most *Sargassum* species (e.g., *S. macrocarpum*, *S. patens*, and *S. siliquastrum*) are perennial, but a few are annual (e.g., *S. horneri*). Whole thalli of *S. horneri* die back after maturation, so beds of *S. horneri* temporarily disappear in summer. On the other hand, although the old main branches of perennial species also wither after maturation, newly formed main branches sprout out from the persistent perennial systems of holdfasts and stipes. Therefore, beds of perennial *Sargassum* are maintained throughout the year.

Sargassum beds often develop to be large in scale and offer important fishing grounds in Japan. Therefore, there have been numerous ecological investigations of
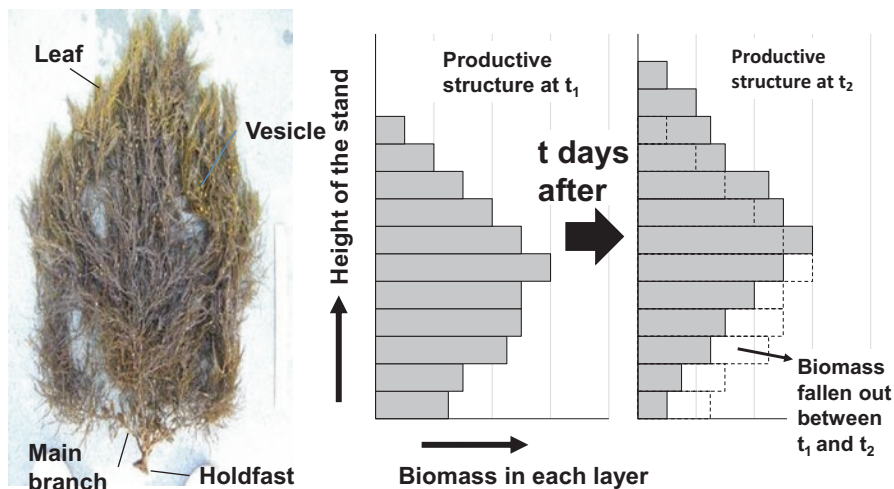
Fig. 4.8 Estimation scheme of *Sargassum* thalli by productive structure analysis. After vertical distribution of thallus biomass is obtained by stratified clipping, the decreased biomass in each layer is assumed to be organs that have fallen off. (Modified from Murase 2010)

them, including of their biomass and more rarely of production. Production measurements have been conducted on beds composed of single species, mainly by the productive structure analysis method. We outline of the methodology below; and for details, see Murase (2010).

Unlike eelgrass or kelps, which have meristems at the base of the shoots or thalli, the growth point of *Sargassum* is at the top of thalli (the tip of the main branch). Therefore, as the thalli grow, the newly produced organs develop upward (Fig. 4.8). Simultaneously, thallus organs such as the leaves in the lower part of thalli gradually die back and fall off due to insufficient light availability caused by shading. In the productive structure analysis method of determining *Sargassum* production, quadrat sampling of thalli is conducted in beds at a given frequency (at least once a month), and the amount of organs that fell out in each interval is estimated by temporal changes in the vertical biomass distribution in the thallus stand (called the "production structure") which are obtained by cutting thalli into stratified for each certain height (Fig. 4.8). For annual species such as *S. horneri*, annual production is equal to the sum of all organs that fell off in a year. In the case of perennial species, the main branches show annual growth and dropout every year, and seasonal changes of biomass of *Sargassum* is largely affected by the fluctuation of main branches. On the other hand, development of perennial parts such as holdfasts and stipes is extremely slow. Therefore, it can be assumed that annual new production is responsible for the new growth of the main branches and formation of organs (i.e., leaves, vesicles, and receptacles) on the branches. With this assumption, as in the case of annual species, the annual production of perennial species can be estimated from the total sum of drop-offs of the main branch and associated organs in a year.

To date, the annual maximum biomass of *Sargassum* species in Japan has been reported to be <1 to >4 kg dry weight/m^2, and annual production to be 1 to >5 kg dry weight/m^2/year, but the amount varies depending on the species (and within the same species) and habitat. However, the ratio of annual production to maximum biomass (P/B$_{MAX}$ ratio) has been reported in the range of 1.0–1.9 for all *Sargassum* species, and mostly within the narrower range of 1.0–1.5. Therefore, we can only roughly estimate the annual production by determining the annual maximum biomass in the peak growing season of a *Sargassum* bed of a target species and multiplying it by the average P/B$_{MAX}$ ratio (Murase 2010).

However, we need to recognize the possibility of underestimating the production of *Sargassum* with the productive structure analysis. This method is based on the premise that newly produced tissues or organs are persistent, at least over the duration of the survey interval, and they accumulate on the upper part of the thallus. If some or all of that part is subject to destruction through grazing by herbivorous animals or through wave action, the lost part will not be accounted for in the production estimate (Murase 2010). Also, it is highly likely that, when rapid regeneration of tissues and organs occurs after any partial loss of thalli, it will be overlooked in the evaluation. In this case, the true P/B$_{MAX}$ ratio should be larger than the value obtained in the survey. In past cases, production has been measured on the premise that excessive grazing by animals or physical damage to thalli does not occur. However, in recent years, the environment in coastal areas of Japan has been changing, and the grazing effects of herbivorous fish and invertebrates on macroalgal beds cannot be ignored.

4.3.2.2 Biomass and Characteristics of *Sargassum* Species Along the Coast of Japan

Unlike eelgrass beds where *Z. marina* is the sole constituent in most cases, many species form *Sargassum* beds, and there are significant differences in biomass between the species. Therefore, it is impossible to represent the biomass of *Sargassum* beds in some regions with the biomass of a single species. Fortunately, relatively large amounts of data on the biomass and species composition are available from ecological surveys of *Sargassum* beds. We collected biomass data of *Sargassum* beds gathered from past surveys done during the peak growing season (mainly, from winter to spring). Some of these data include biomass of macroalgae other than *Sargassum* mixed in the beds (mostly small green and red algae), but it was assumed that these "undergrowth" algae are quantitatively negligible. For the biomass, 20% of the wet weight was used as the dry weight of *Sargassum*.

Figure 4.9 shows the biomass distribution of *Sargassum* beds in the Japan Sea, Pacific Honshu, Seto Inland Sea, and open Kyushu-Shikoku regions. Data for beds of both single and mixed species were available. The mean biomass was 1.2 kg dry weight/m^2 in the Seto Inland Sea, 0.7 kg dry weight/m^2 in the Pacific Honshu region, and about 1.0 kg dry weight/m^2 in the other two regions. There was a large variation in the biomass in every region, and it was difficult to identify clear differences

Fig. 4.9 Biomass of
sargassaceous macroalgae
in the peak growing season
in four Japanese coastal
regions in which
Sargassum beds are
abundantly distributed. *DW*
dry weight
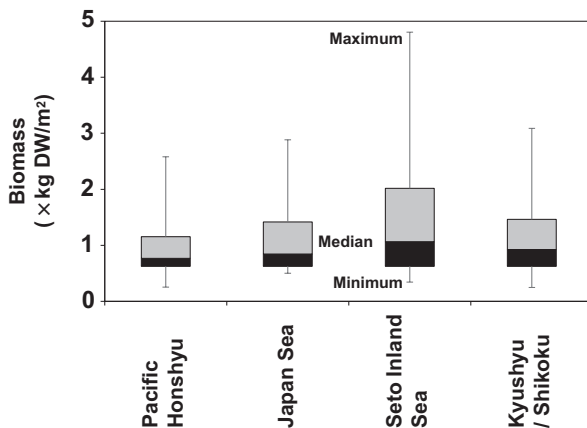
among the regions (Fig. 4.9). In the Seto Inland Sea, maximum biomasses exceeding 4 kg dry weight/m^2 were recorded, but in the other regions, the maximum was around 3 kg dry weight/m^2.

Sargassum beds exceeding 3–4 kg dry weight/m^2 of biomass in the Seto Inland Sea were mainly composed of *S. horneri* and *S. siliquastrum* (Nansei Regional Fisheries Research Laboratory 1979). Although *S. horneri* is an annual species, it has a large biomass that has been report to exceed 3 kg dry weight/m^2 in the Yatsushiro Sea of Kyushu (Kumamoto Prefectural Fisheries Research Center 2010). *Sargassum* bed biomass tends to be greater when the bed is located in the inner area of bays, such as Kagoshima Bay (e.g., *S. patens*) in the Kyushu region and Maizuru Bay (*S. autumnale*) in the Japan Sea region, each of which has a biomass of greater than 3 kg dry weight/m^2 (Seikai Regional Fisheries Research Laboratory 1981; Yatsuya et al. 2007). On the other hand, in the Pacific Honshu region, *S. nipponicum*, which forms highly dense beds that are influenced by waves of open seas, had a reported biomass of 2.5 kg dry weight/m^2 (Takase and Tanaka 2008).

In coastal areas of Hokkaido and the Pacific Tohoku region, where cold-temperate kelps of the genus *Saccharina* are the main macroalgae, data about *Sargassum* beds has been scarce. Biomass values of up to 2–3 kg dry weight/m^2 have been recorded for *S. horneri* and *S. yezoense* along the coast of Miyagi Prefecture in the Pacific Tohoku region (Muraoka 2003, 2013), which are similar to those found in central and western Japan. Along the coast of Hokkaido, which is the northern distribution limit of the family Sargassaceae, a biomass of 1 kg dry weight/m^2 was recorded for *S. confusum* and *Cystoseira hakodatensis* (Tsuda and Akaike 2001; Onitsuka and Hasegawa 2013), although it is difficult to determine whether these values are representative of the area because of a lack of comparable data.

Macroalgae belonging to the family Sargassaceae are distributed in temperate to tropical climate zones on a global scale. Using data from the literature, the maximum biomass values of Sargassaceous macroalgae reported are plotted against latitude in Fig. 4.10. The biomass values in latitudes from 30 to 40°N, which correspond to the temperate region of Japan, tend to be larger than those of the lower latitudinal

Fig. 4.10 Relationship between biomass of sargassaceous macroalgae in the peak growing season and latitude. *DW* dry weight
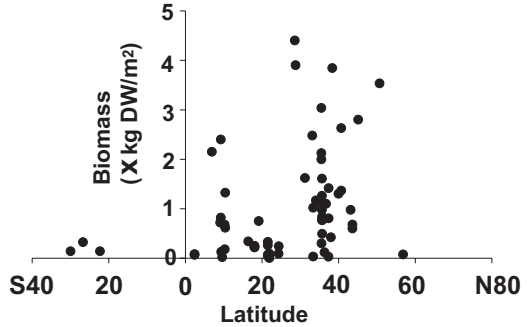
zones, although there are variations. This does not necessarily indicate, however, that the production of tropical and subtropical species of Sargassaceae growing in the lower latitudinal zones is lower than that of temperate species. According to a literature survey, there was no statistical difference between the temperate and tropical species in the maximum rates of photosynthesis and respiration (Yoshida et al. unpublished). In tropical and subtropical regions, the consumption of macroalgae by herbivorous fish and invertebrates is known to be large (Littler et al. 1991). In that case, the P/B_{MAX} ratio of tropical and subtropical species of Sargassaceae should be greater than that of the temperate species. Conversely, production loss due to heavy grazing by herbivorous animals is considered to be small in Japan, especially in the temperate zone. Therefore, since new tissue production can be accumulated throughout the year, the biomass of temperate *Sargassum* is considered to be large and the P/B_{MAX} ratio is considered to be near 1.

Data on production of Sargassaceous macroalgae are globally scarce. The production structure analysis adopted in Japan has not been recognized worldwide, probably because of uncertainties in the estimate of annual production of *Sargassum*. More reliable methods that can be commonly used should be developed, and global comparisons of production among Sargassaceae are needed.

4.3.3 Warm-and Cold-Temperate Kelp Beds (Arame-ba and Kombu-ba)

Kelps forming *Arame-ba* and *Kombu-ba* attach to hard substrates with a branched holdfast (haptera) arising from the base of the stipe, and a blade arises from the tip of the stipe. Kelps of the genus *Saccharina* have a simple blade morphology, which is subulate to lanceolate, but the blade of *Ecklonia* and *Eisenia* has a more complicated morphology, in which a center blade has numerous lateral blades arising at its margin. All these kelps develop large thalli of 1 to several meters, and some species reach >10 m in size.

The growth point of thalli of Laminariales exists at the junction of the stipe and blade, where new blade tissue is produced. The newly formed tissue of the blade

moves upwardly along a thallus, similar to the action of a conveyor belt. Therefore, by marking a hole with a cork borer at an appropriate position on the blade and tracing the temporal movement of the hole on the thallus, it is possible to estimate the new growth of the blade or the number of newly formed lateral blades in the case of *Ecklonia* and *Eisenia*, within a given period. Kurashima (2010) and Sakanishi (2010) describe the method of measuring the production of these kelps by this punch-hole marking method in their reviews.

Both warm- and cold- temperate kelps also show clear seasonal fluctuations, and the thallus size and biomass are generally maximized in late spring to summer. From summer onward, senescence and withering of blade tissues rapidly progress at the tip of thalli (called *Sue-gare*), and the biomass decreases. Formation of new blade tissue is activated again in seasons with lower water temperature. At the Iki Islands in Nagasaki Prefecture, the production of *Ecklonia kurome* is extremely small in the summer, when the water temperature can reach a maximum of 28 °C, but it recovers rapidly as the water temperature declines after autumn (Yatsuya et al. 2014a).

Reported annual production of *Ecklonia* species was 2.8 kg dry weight/m^2/year at Izu peninsula, Pacific Honshu region (Yokohama et al. 1987); 2.7 kg dry weight/m^2/year at Tosa Bay, Shikoku region (Tominaga et al. 2004); and 2.8 kg dry weight/m^2/year at Iki Islands, Kyushyu region (Yatsuya et al. 2014a). In addition, we obtained a similar value (2.5 kg dry weight/m^2/year) in Iyo-nada, Seto Inland Sea region (Yoshida et al. unpublished). Reported production of species of *Eisenia* was 3.0 kg dry weight/m^2/year at Matsushima Bay, Pacific Tohoku region (Yoshida 1970) and 3.6 kg dry weight/m^2/year at Miura Peninsula, Pacific Honshu region (Terawaki et al. 1991; converted to dry weight as 15% of wet weight). The annual production of *Ecklonia* and *Eisenia* in Japan ranged from 1.4 to 3.6 kg dry weight/m^2/year regardless of region (Kurashima 2010; Yatsuya et al. 2014a).

Cold-temperate kelps in Japan, mostly species belonging to genus *Saccharina* and called *Kombu* in general, are commercially very important. *Kombu* fisheries in Japan are almost dependent on harvest of natural resources. However, whereas many data about catch statistics are available, information on the biomass and production of natural kelp beds has been scarce. Even with this small amount of information, some studies have reported the biomass and production of some species at some locations. In *S. japonica*, the maximum biomass was 2.6 kg dry weight/m^2 in Tsugaru Peninsula (Pacific Tohoku region) and 0.8 kg dry weight/m^2 in Onagawa Bay (Pacific Tohoku region). In *S. japonica* var. *religiosa*, it was 1.0 kg dry weight/m^2 in Otaru (Hokkaido region) and 4–18.4 kg dry weight/m^2 in Kadonohama Bay (Pacific Tohoku region). On the northern coast of Hokkaido such as in Rausu and Akkeshi, *S. japonica* var. *diabolica* showed biomass values of <1 to 8.7 kg dry weight/m^2 (Onitsuka and Hasegawa 2013; converted to dry weight as 20% of the wet weight). Although data on annual production are quite limited, it was recorded as 1.3 kg dry weight/m^2/year for *S. japonica* in Onagawa Bay and 1.4 kg dry weight/m^2/year for *S. angustata* in Urakawa Town in Hokkaido. In addition, production of 20 kg dry weight/m^2/year or more has been reported for *S. japonica* var. *diabolica* in the eastern coast of Hokkaido (Sakanishi 2010; Onitsuka and Hasegawa 2013).

As described above, variation in the production of cold-temperate kelps is extremely large among species and locations. Elsewhere, production as high as 6 kg dry weight/m²/year was reported in Nova Scotia, Canada (Mann 1972). Therefore, it seems that cold-temperate kelps can exhibit extremely high production under certain environmental conditions of their habitats. To explain why kelp can demonstrate such high production, Sakanishi (2010) considered water motion conditions in habitats are responsible because thallus undulation under moderate water motions can promote the supply of dissolved inorganic carbon and nutrients to the kelp. In addition, it seems that the biomass and production of *Saccharina* species tend to be higher on the coast in Japan with the cold current (Oyashio Current), which carries abundant nutrients and may be a contributing factor for the high production of kelps. Comparisons of the production of kelp among habitats with different environmental conditions are needed, as well as on a global scale that includes climate variation.

4.3.4   Estimation of Carbon Sequestration by Seagrass and Macroalgae on the Coast of Japan

Here, annual production, which is defined by subtracting DOM production from net primary production (see Fig. 4.1), by seagrass and macroalgae in Japan is calculated on a dry weight basis from the area of each of the seagrass and macroalgal beds and the production per unit area of each bed shown in the previous sections. The annual production is then converted into amounts of organic carbon and carbon dioxide, and defined as the carbon sequestration potential of seagrass and macroalgal beds in Japan. The basic procedure is as follows.

1. *Amamo-ba*: The daily production per unit area of eelgrass in each sea area shown in Fig. 4.6 was integrated for 1 year to calculate annual production output. This value was multiplied by each area of the eelgrass beds in each region and summed as the nationwide total. For the Japan Sea region, which has no actual measured production, we used the production value from the Seto Inland Sea region, which has similar water temperature conditions. For the Nansei Islands region where *Z. marina* is not distributed, the measured values of *Thalassia hemprichii* and *Cymodocea serrulata* we obtained in our research (Hori unpublished) were used.
2. *Garamo-ba*: The mean value of maximum biomass in each of the four regions shown in Fig. 4.9 was used and multiplied by the mean P/B$_{MAX}$ ratio of *Sargassum* species (1.4; Murase 2010). For the maximum biomass in the Hokkaido and Pacific Tohoku regions, we used the average of all values collected from past studies of those respective areas and multiplied them by the *Sargassum* bed area of each region.
3. *Arame-ba*: The mean annual production per unit area of *Ecklonia* and *Eisenia* in each region, which was obtained from previous research or direct *in situ* measurements conducted in our survey, was multiplied by the warm-temperate kelp bed area in each region. For the Japan Sea region for which no data were avail-

Table 4.1 Estimation of carbon sequestration by seagrass and macroalgal beds in Japan (overall summary)

	Areal seagrass/ macroalgae production (kg DW/m^2/year)	Carbon content (% DW)	Areal carbon sequestration as CO$_2$ (tons CO$_2$/ha/ year)	Area (ha)	Total carbon sequestration as CO$_2$ (tons CO$_2$/ year)
Eelgrass bed (*Amamo-ba*)	1.0 ± 0.7	35.0	12.6 ± 8.9	61,667	508,459
Sargassum bed (*Garamo-ba*)	1.4 ± 0.2	32.0	16.0 ± 2.6	88,041	1,413,685
Cold- temperate kelp bed (*Kombu-ba*)	6.2 ± 6.8	30.0	60.5 ± 71.8	20,356	1,159,836
Warm temperate kelp bed (*Arame-ba*)	2.1 ± 0.4	32.5	24.6 ± 4.7	63,120	1,631,851
Total					4,713,831

able, the mean value of production data of the other regions of central and western Japan was used.

4. ***Kombu-ba***: Because there were large variations in production reported among species and locations in the Hokkaido and Pacific Tohoku regions in which cold-temperate kelp beds are distributed, these areas were further divided into several subregions depending on dominant species of *kombu* and their geographic distributions. These included *S. japonica* var. *diabolica* (northeastern Hokkaido region), *S. longissima* (Pacific coastal area of the eastern Hokkaido region), *S. japonica* var. *ochotensis* (Okhotsk Sea coastal area in the northern Hokkaido region), *S. japonica* var. *religiosa* (Japan Sea coastal area of the western Hokkaido region), and *S. japonica* (the southern Hokkaido and Tohoku regions). Annual production of cold-temperate kelp beds was represented by these dominant species in each subregion, based on published and measured values. Annual production in each subregion was calculated and summed (Onitsuka et al. 2014).

5. **Conversion to carbon sequestration amount:** Depending on the species, 30% to 35% of the annual production (dry weight) of seagrass and macroalgae in each bed was assumed to be the mean organic carbon content (Table 4.1; Onitsuka et al. 2014). These mean values of organic carbon were then converted into equivalent amount of carbon dioxide.

The results are shown in Table 4.1. The annual organic carbon sequestered in the plant tissue of seagrass and macroalgae in Japan was estimated to be equivalent to about 4.7 million tons CO$_2$/year. The contribution of macroalgae was large, especially that of cold-temperate kelp beds, which have a very high mean value of the production, and also, variation in the production. We are not certain that these are general characteristics of cold-temperate kelp beds, however, because basic information on production of these kelps remains inadequate. It is therefore necessary to

continue research on spatiotemporal changes in production of each seagrass and macroalgal bed to improve the accuracy of estimated values.

4.4 Conclusion: Future Issues and Concerns

In this chapter, we estimated the area of the main seagrass and macroalgal beds (i.e., *Amamo-ba*, *Garamo-ba*, *Arame-ba*, and *Kombu-ba*) in Japan to be approximately 230,000 ha. Through the production of seaweed and macroalgae in these beds, about 4.7 million tons CO_2/year was estimated to be sequestered annually. For comparison, Japan's reported forested area is about 25 million ha and absorbed approximately 49.9 million tons of carbon dioxide in 2014 (Forestry Agency 2015). On a unit area basis, the carbon sequestration function of seagrass and macroalgal beds is higher than that of forests, most likely because the turnover rates of seagrasses and macroalgae are larger than those of trees. Therefore, the production of seagrass and macroalgal beds is higher than that of trees.

Japan was the fifth largest greenhouse gas emitting country in the world in 2014, and in the same year, it emitted approximately 1.3 billion tons of carbon dioxide (Ministry of the Environment 2016). In comparison, the production of seagrass and macroalgae (4.7 million tons CO_2/year) may be considered small. However, among industrial sectors, the amounts of carbon dioxide emitted annually by the agriculture and fisheries sectors are approximately 5.65 million tons and 5.74 million tons, respectively (National Institute for Environmental Studies 2010). Each of these amounts is approximately equal to the amount of carbon dioxide estimated to be sequestered by seagrass and macroalgae.

However, for seagrass and macroalgal beds to be recognized as carbon sinks that contribute to measures to reduce greenhouse gas emissions, more fundamental research is needed. Seagrass and macroalgae produced within a bed follow numerous fates, for example, decomposition, consumption by animals, sedimentation at the sea bottom, and outflow from coastal areas (Fig. 4.1) (Abo et al. 2018). In Japan, however, few studies have quantified each carbon flow path. Particularly, sedimentation at the sea bottom needs to be quantitatively evaluated from the viewpoint of contribution to carbon storage. In particular for macroalgae, research on a large scale, along with the development of effective equipment and technology, is necessary to elucidate the outflow and transportation from the bed to sedimentation in the deep sea. Also, it is becoming clear that DOM released by seagrasses and macroalgae, which was not discussed in detail in this chapter, should not be ignored (Krause-Jensen and Duarte 2016). It is necessary to understand the quantitative values and dynamics of DOM in the ocean to further justify the function of carbon sequestration and the storage potential of seagrass and macroalgae.

Although seagrass and macroalgal beds are expected to contribute to the mitigation of global warming through sequestration and storage of organic carbon, future concerns about the beds themselves exist because they are extremely vulnerable to global warming. Since the latter half of the 1990s, *Iso-yake* (or sea desertification),

which is the sudden and unusual disappearance and decline of macroalgal beds, has been expanding, mainly in the coastal areas of western Japan. A reported 18,538 ha of macroalgal beds have disappeared (Akimoto and Matsumura 2010) since then. Assuming that the disappearance caused by *Iso-yake* has occurred mainly in *Garamo-ba* and *Arame-ba*, the carbon sequestration function by these macroalgal beds, which corresponds to about 300,000–500,000 tons CO_2/year, has already been lost in coastal areas (Remember though, as noted previously in this chapter, the latest seagrass and macroalgal bed area shown in Fig. 4.3 cannot be simply compared with an area from past surveys because of differences in methodologies).

The expansion of *Iso-yake* has occurred concurrently with the rise of seawater temperature in coastal areas. Along the northern coast of Kyushu, massive deaths of *Ecklonia* and *Eisenia* were recorded due to abnormally high water temperature over a wide area in the summer of 2013 (Yatsuya et al. 2014b). Grazing activity by herbivorous fish and invertebrates such as sea urchins, which is a major factor for *Iso-yake*, has also been suggested to be associated with an increase in water temperature. In the coastal areas of Kyushu and Shikoku, in addition to the shrinking of the macroalgal beds due to *Iso-yake*, changes in the constituent species of *Garamo-ba* have been occurring as invasive tropical *Sargassum* species have been replacing temperate species (Yoshimura et al. 2010; Tanaka et al. 2012). In the tropical and subtropical macroalgal bed ecosystem, the grazing pressure of herbivorous animals tends to be large and the biomass of macroalgae tends to be small. The expansion of *Iso-yake* and changes in the constituent species of the beds may indicate that tropicalization of the temperate coastal zone in Japan is ongoing.

In local areas where fishery grounds have been devastated due to *Iso-yake*, countermeasures such as the principal method of protecting the macroalgal beds from grazing have been implemented. For example, activities related to the removal and control of sea urchins in *Iso-yake* zones have been conducted by fishermen, and successful recovery of beds has been observed in some areas (Fisheries Agency 2015). To make these measures against *Iso-yake* sustainable, it will be necessary to provide social incentives to these activities. If macroalgal beds are institutionally recognized as a sink of carbon dioxide similar to forests, fishermen's activities to combat *Iso-yake* may be viewed as having the same significance as forest maintenance activities, some of which have already been approved as contributing to carbon sequestration.

On the other hand, if global warming progresses according to current predictions, changes in seagrass and macroalgal beds will unfortunately become irreversible in the long run. If that becomes the case, it will then be necessary to take the viewpoint of adaptive use of the ecosystem services provided by 'new' coastal ecosystems. Tropical and subtropical seagrass and macroalgal beds can be used as a model for this scenario, but it will require the comparison of various ecological functions including carbon sequestration and storage with temperate seagrass and macroalgal beds.

References

Abo K, Sugimatsu K, Hori M, Yoshida G, Shimabukuro H, Yagi H, Nakayama A, Tarutani K (2018) Quantifying the fate of captured carbon: from seagrass meadow to deep sea. In: Kuwae T, Hori M (eds) Blue carbon in shallow coastal ecosystems: carbon dynamics, policy, and implementation. Springer, Singapore, pp 251–271

Akimoto Y, Matsumura T (2010) Available past information on seaweed bed distribution and changes in seaweed bed area in Japanese coastal waters. In: Fujita D, Murase N, Kuwahara H (eds) Monitoring and maintenance of seaweed beds. Seizando-Shoten, Tokyo, pp 17–24 (in Japanese)

Duarte CM, Chiscano CL (1999) Seagrass biomass and production: a reassessment. Aquat Bot 65:159–174

Endo T, Otani S (2018) Chapter 8. Carbon storage in tidal flats. In: Kuwae T, Hori M (eds) Blue carbon in shallow coastal ecosystems: carbon dynamics, policy, and implementation. Springer, Singapore, pp 129–151

Environmental Agency, Marine Parks Center of Japan (1994) The report of the marine biotic environment survey in the 4th National Survey on the Natural Environment, vol 2. Algal and seagrass beds (in Japanese)

Fisheries Agency (2015) *Isoyake Taisaku* Guidelines (Revised edition) http://www.jfa.maff.go.jp/j/gyoko_gyozyo/g_hourei/pdf/isoyake1.pdf. Accessed 1 Apr 2017 (in Japanese)

Fisheries Agency, Marino-Forum 21 (2007) Natural regeneration guidelines for eelgrass (in Japanese)

Forestry Agency (2015) http://www.rinya.maff.go.jp/j/kikaku/hakusho/26hakusyo/pdf/1hyousi.pdf. Accessed 1 Apr 2017 (in Japanese)

Hasegawa N, Hori M, Mukai H (2007) Seasonal shifts in seagrass bed primary producers in a cold-temperate estuary: dynamics of eelgrass *Zostera marina* and associated epiphytic algae. Aquat Bot 86:337–345

Hasegawa N, Yoshida G, Hori M, Tarutani K, Nakaoka M, Watanabe, K (2013) Supplementary information: collection and arrangement of past findings concerning eelgrass. Project report "Development of technology for improving carbon sinks and absorption capacity of seaweed beds and tidal flats". Fisheries Research Agency, Atmosphere and Ocean Research Institute of the University of Tokyo, Field Science Center for Northern Biosphere of Hokkaido University, pp 99–103 (in Japanese)

Hori M, Hamaoka H, Yoshida G (2014) Survey and implementation of national evaluation of carbon absorption amount of seaweed bed/tidal flat. Project report "Development of technology for improving carbon sinks and absorption capacity of seaweed beds and tidal flats". Fisheries Research Agency, Atmosphere and Ocean Research Institute of the University of Tokyo, Field Science Center for Northern Biosphere of Hokkaido University, pp 51–59 (in Japanese)

Inoue T (2018) Carbon sequestration in mangroves. In: Kuwae T, Hori M (eds) Blue carbon in shallow coastal ecosystems: carbon dynamics, policy, and implementation. Springer, Singapore, pp 73–99

Kawashima S (2004) *Kombu*. In: Ohno M (ed) Biology and technology of economic seaweeds. Uchida Rokakuho Publishing Co Ltd, Tokyo, pp 59–85 (in Japanese)

Krause-Jensen D, Duarte CM (2016) Substantial role of macroalgae in marine carbon sequestration. Nat Geosci 9:737–742

Kumamoto Prefectural Fisheries Research Center (2010) Technical report for fiscal 2009. Kumamoto Prefectural Fisheries Research Center (in Japanese)

Kurashima A (2010) Productivity of *Eisenia* and *Ecklonia* bed. In: Fujita D, Murase N, Kuwahara H (eds) Monitoring and maintenance of seaweed beds. Seizando-Shoten, Tokyo, pp 115–120 (in Japanese)

Kuwae T, Kanda J, Kubo A, Nakajima F, Ogawa H, Sohma A, Suzumura M (2018) CO_2 uptake in the shallow coastal ecosystems affected by anthropogenic impacts. In: Kuwae T, Hori M (eds) Blue carbon in shallow coastal ecosystems: carbon dynamics, policy, and implementation. Springer, Singapore, pp 295–319

Littler MM, Littler DS, Titlyanov EA (1991) Comparisons of N- and P-limited productivity between high granitic islands vs. low carbonate atolls in the Seychelles Archipelago: a test of the relative dominance paradigm. Coral Reefs 10:199–209

Mann KH (1972) Ecological energetics of the seaweed zone in a marine bay on the Atlantic coast of Canada. II Productivity of the seaweeds. Mar Biol 14:199–209

Ministry of the Environment (2016) http://www.env.go.jp/earth/ondanka/ghg/2014_kakuho_gaiyo.pdf. Accessed 1 Apr 2017 (in Japanese)

Miyajima T, Hamagichi M (2018) Carbon sequestration in sediment as an ecosystem function of seagrass meadows. In: Kuwae T, Hori M (eds) Blue carbon in shallow coastal ecosystems: carbon dynamics, policy, and implementation. Springer, Singapore, pp 33–71

Muraoka D (2003) *Ezo-no-Nejimoku*. In: Notoya M (ed) Seaweed of marine forest and its developmental technology. Seizando-Shoten, Tokyo, pp 75–81 (in Japanese)

Muraoka D (2012) Collection of information on macroalgal bed area in Tohoku region, and survey of its production and biomass. Project report "Development of technology for improving carbon sinks and absorption capacity of seaweed beds and tidal flats". Fisheries Research Agency, Atmosphere and Ocean Research Institute of the University of Tokyo, Field Science Center for Northern Biosphere of Hokkaido University, pp 73–75 (in Japanese)

Muraoka D (2013) Collection of information on macroalgal bed area in Tohoku region, and survey of its production and biomass. Project report "Development of technology for improving carbon sinks and absorption capacity of seaweed beds and tidal flats". Fisheries Research Agency, Atmosphere and Ocean Research Institute of the University of Tokyo, Field Science Center for Northern Biosphere of Hokkaido University, pp 79–81 (in Japanese)

Murase N (2010) Productivity of *Sargassum* bed. In: Fujita D, Murase N, Kuwahara H (eds) Monitoring and maintenance of seaweed beds. Seizando-Shoten, Tokyo, pp 109–115 (in Japanese)

Nakaoka M, Aioi K (2001) Ecology of seagrasses *Zostera* spp. (Zosteraceae) in Japanese waters. Otsuchi Mar Sci 26:7–22

Nakaoka M, Aioi K, Kouchi K, Omori N, Tanaka Y, Tatsukawa K (2003) Distribution, productivity, life history and biodiversity of seagrass community along Sanriku Coast: a review. Otsuchi Mar Sci 28:31–38

Nansei Regional Fisheries Research Laboratory (1979) Survey on coastal seaweed beds. Report on distribution of seaweed beds related to Seto Inland Sea: Distribution of seaweed beds. (in Japanese)

National Institute for Environmental Studies (2010) http://www-gio.nies.go.jp/aboutghg/data/2010/. Accessed 1 Apr 2017 (in Japanese)

Nellemann C, Corcoran E, Duarte CM, Valdes L, DeYoung C, Fonseca L, Grimsditch G. (2009) Blue carbon. A rapid response assessment. United Nation Environment Programme, GRID-Arendal (http://www.grida.no)

Onitsuka T, Hasegawa N (2013) Collection of information on macroalgal bed area in the Hokkaido region, and survey of its production and biomass. Project report "Development of technology for improving carbon sinks and absorption capacity of seaweed beds and tidal flats". Fisheries Research Agency, Atmosphere and Ocean Research Institute of the University of Tokyo, Field Science Center for Northern Biosphere of Hokkaido University, pp 73–79 (in Japanese)

Onitsuka T, Muraoka T, Hasegawa N, Kurogi H, Yoshida G, Hori M, Yatsuya K (2014) Field survey for nationwide evaluation (Overall summary). Project report "Development of technology for improving carbon sinks and absorption capacity of seaweed beds and tidal flats". Fisheries Research Agency, Atmosphere and Ocean Research Institute of the University of Tokyo, Field Science Center for Northern Biosphere of Hokkaido University, pp 75–90 (in Japanese)

Sakanishi Y (2010) Productivity of *Kombu-ba*. In: Fujita D, Murase N, Kuwahara H (eds) Monitoring and maintenance of seaweed beds. Seizando-Shoten, Tokyo, pp 120–124 (in Japanese)

Seikai Regional Fisheries Research Laboratory (1981) Survey on coastal seaweed beds. Report on distribution of seaweed beds along the western coast of Kyushyu (in Japanese)

Short FT, Duarte CM (2001) Methods for the measurement of seagrass growth and production. In: Short FT, Coles RG, Duarte CM (eds) Global seagrass research methods. Elsevier, Amsterdam, pp 155–182

Takase T, Tanaka Y (2008) Growth, maturation of *Sargassum nipponicum* and oceanographic conditions on the coast of Sokodo in Hachijyo-jima Island, Central Japan. Aquac Sci 56:369–374 (in Japanese with English abstract)

Tanaka K, Taino S, Haraguchi H, Prendergast G, Hiraoka M (2012) Warming off southwestern Japan linked to distributional shifts of subtidal canopy-forming seaweeds. Ecol Evol 2:2854–2865

Terawaki T, Arai S (2004) Kelps of the genus *Eisenia* and *Ecklonia*. In: Ohno M (ed) Biology and technology of economic seaweeds. Uchida Rokakuho Publishing Co Ltd, Tokyo, pp 133–158 (in Japanese)

Terawaki T, Kawasaki Y, Honda M, Yamada S, Maruyama K, Igarashi Y (1991) Verification of technologies for kelp forest creation on sandy sea beds. II Ecology and growing characteristics of *Eisenia bicyclis* and *Ecklonia cava* at western sea coast of Miura Peninsula, central Japan. CRIEPI Research Report U91022: 1–69 (in Japanese with English abstract)

Tominaga H, Serisawa Y, Ohno M (2004) Seasonal changes in net production of the bladelets and size of the proximal blade of *Ecklonia cava* in Tosa Bay, Kochi Prefecture. Jpn J Phycol 52:13–19 (in Japanese with English Abstract)

Tsuda F, Akaike S (2001) Annual life cycle and productivity of *Sargassum confusum* population off the coast of western Shakotan Peninsula in southwestern Hokkaido, Japan. SUISANZOSHOKU 49:143–149 (in Japanese with English Abstract)

Wada S, Aoki MN, Mikami A, Komatsu T, Tsuchiya Y, Sato T, Shinagawa H, Hama T (2008) Bioavailability of macroalgal dissolved organic matter in seawater. Mar Ecol Prog Ser 370:33–44

Watanabe M, Nakaoka M, Mukai H (2005) Seasonal variation in vegetative growth and production of the endemic Japanese seagrass *Zostera asiatica*: a comparison with sympatric *Zostera marina*. Bot Mar 48:266–273

Yatsuya K, Nishigaki T, Douke A, Itani M, Wada Y (2007) Annual net productions of Sargassacean species in coastal areas with different environmental characteristics in Kyoto Prefecture, the Sea of Japan. Nippon Suisan Gakkaishi 73:880–890 (in Japanese with English Abstract)

Yatsuya K, Kiyomoto S, Yoshimura T (2014a) Seasonal changes in biomass and net production of *Ecklonia kurome* Okamura community off Gounoura, Iki Island, northern Kyushyu, Japan. Algal Resour 7:67–77 (in Japanese with English Abstract)

Yatsuya K, Kiriyama T, Kiyomoto S, Taneda T, Yoshimura T (2014b) On the deterioration process of *Ecklonia* and *Eisenia* beds observed in 2013 at Gounoura, Iki Island, Nagasaki Prefecture, Japan. Initiation of the bed degradation due to high water temperature in summer and subsequent cascading effect by the grazing of herbivorous fish in autumn. Algal Resour 7:79–94 (in Japanese with English Abstract)

Yokohama Y, Tanaka J, Chihara M (1987) Productivity of the *Ecklonia cava* community in a bay of Izu Peninsula on the Pacific Coast. Bot Mag Tokyo 100:129–141

Yoshida T (1970) On the productivity of the *Eisenia bicyclis* community. Bull Tohoku Reg Fish Res Lab 30:107–112 (in Japanese with English abstract)

Yoshida G, Hori M, Sakiyama K, Hamaguchi M, Kajita A, Nishimura K, Shoji J (2010) Distribution of seaweed bed and tidal flat, and their correlations with fisheries catches in the nine sea areas of the Seto Inland Sea. Fish Eng 47:19–29 (in Japanese with English abstract)

Yoshida T, Suzuki M, Yoshinaga K (2015) Checklist of marine algae of Japan (revised in 2015). Jpn J Phycol 63:129–189 (in Japanese)

Yoshimura T, Morinaga K, Kiyomoto S (2010) Is it really the effect of global warming? long-term fluctuation of a seaweed bed in Nagasaki city. In: Fujita D, Murase N, Kuwahara H (eds) Monitoring and maintenance of seaweed beds. Seizando-Shoten, Tokyo, pp 161–167 (in Japanese)

Zieman JC (1974) Methods for the study of the growth and production of turtle grass, *Thalassia testudinum* Köning. Aquaculture 4:139–143

Chapter 5
Carbon Storage in Tidal Flats

Toru Endo and Sosuke Otani

Abstract Tidal flat ecosystems are important habitats in shallow coastal waters. In this chapter, carbon storage in a bivalve (*Corbicula japonica*), phytoplankton, and sediment is estimated at two tidal flats in a eutrophic coastal area of Osaka Bay in Japan. First, we estimate the carbon storage of the bivalve from the rate of organic carbon production and shell production measured by monthly field investigations. We then estimate the carbon storage of phytoplankton based on phytoplankton biomass measurements and a model of gross primary production and respiration based on incubation experiments. To assess carbon storage in sediment, biodegradation tests of sedimentary organic carbon taken from the intertidal zone and the subtidal zone were carried out for 100 days; the residual sedimentary organic carbon is considered to represent long-term storage of carbon in sediment. Finally, the carbon storage functions of bivalves, phytoplankton, and sedimentary organic matter in tidal flat ecosystems are summarized.

5.1   Introduction

Over half of the biological carbon in the world is captured by marine living organisms (Nellemann et al. 2009). Furthermore, 50–71% of all carbon storage in ocean sediments occurs within coastal vegetated habitats, despite the area of the ocean's vegetated habitats such as mangroves, salt marshes, and seagrass meadows (blue carbon ecosystems) representing less than 0.5% of the sea bed and their plant biomass accounting for only 0.05% of the global total (Nellemann et al. 2009). Atwood et al. (2015) have also noted the importance of food web structures in blue carbon ecosystems for carbon storage.

T. Endo (✉)
Graduate School of Engineering, Osaka City University, Sugimoto, Sumiyoshi-ku, Osaka, Japan
e-mail: t.endo@eng.osaka-cu.ac.jp

S. Otani
Civil Engineering and Environment Course, Department of Technological Systems, Osaka Prefecture University College of Technology, Saiwaicho, Neyagawa, Osaka, Japan

Many studies have estimated the carbon storage capacity of blue carbon ecosystems around the world, particularly in mangroves (Donato et al. 2012; Wang et al. 2013; Rahman et al. 2015; Inoue 2018) and seagrass meadows (Fourqurean et al. 2012; Lavery et al. 2013; Miyajima et al. 2015; Watanabe and Kuwae 2015; Miyajima and Hamaguchi 2018; Yoshida et al. 2018). However, little is known about carbon storage in tidal flat ecosystems, despite their importance as shallow coastal habitats.

Because the conditions in tidal flats are distinct, they are inhabited by a unique set of organisms. For example, crustaceans such as crabs and aquatic plants such as reeds live in the supratidal zone, benthic microalgae (microphytobenthos) and polychaetes such as sandworms live in the intertidal zone, and algae such as phytoplankton and seaweeds and filter feeders such as clams live in the subtidal zone. Figure 5.1 shows the carbon cycle in a typical tidal flat ecosystem. Phytoplankton take up carbon dioxide (CO_2) and produce organic matter by photosynthesis, so carbon is stored in their cells. Through food webs, consumers take in organic matter and store carbon in their bodies. Both producers and consumers emit CO_2 to seawater by respiration. Detritus and excrement are accumulated on the surface of the sediment. If these materials are not decomposed for a long time, then the carbon accumulated on the sea floor is regarded as carbon stored in tidal flats.

In this chapter, we review the literature on carbon storage in tidal flat ecosystems worldwide and describe our case studies of carbon storage in bivalves, phytoplankton, and sediment conducted at tidal flats in an urban coastal area of Japan.
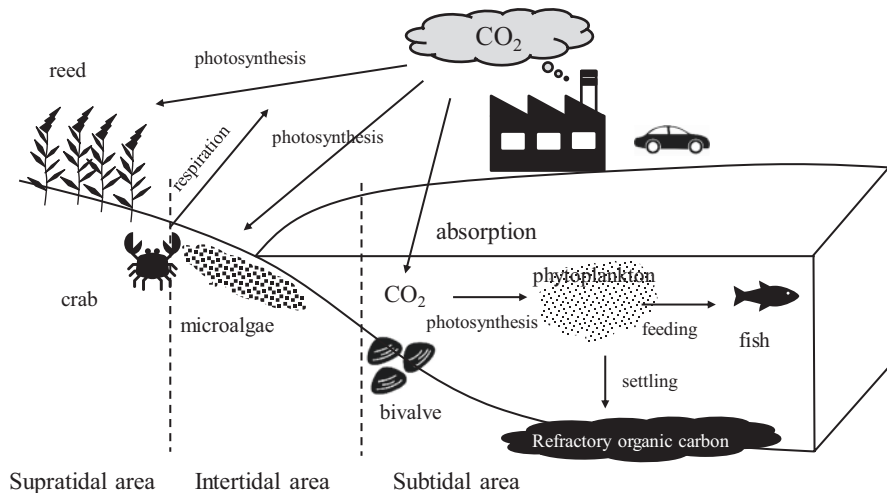
Fig. 5.1 Representative carbon cycle in tidal flats

5.2 Literature Review of Carbon Storage Functioning in Tidal Flats

Carbon storage functioning can be evaluated with regard to carbon stocks and flows. Primary and secondary producers and sediment have all been the subjects of carbon stock and flow studies in tidal flat ecosystems. Table 5.1 lists some of the reported carbon flows related to microalgae, macrofauna, and sediment in tidal flats and salt

Table 5.1 Summary of primary production by microalgae, secondary production and calcification by macrofauna, and sedimentary carbon accumulation rate in tidal flats

Subject	Station	Species/site	Rate (g $C\ m^{-2}\ year^{-1}$)	References
Microalgae		Microphytobenthos temperate intertidal ($n = 41$)	111 ± 99	Cahoon (1999)
		Microphytobenthos	29–234	Underwood and Kromkamp (1999)
	U.S. and Europe estuaries	Microphytobenthos	80–150	Colijn and de Jonge (1984)
		Phytoplankton	7–875	Underwood and Kromkamp (1999)
	24 U.S. estuaries	Phytoplankton	251	Heip et al. (1995)
	16 Europe estuaries	Phytoplankton	195	Heip et al. (1995)
	Seto Inland Sea, Japan	Phytoplankton	218	Tada et al. (1998)
Macroalgae	Venice lagoon	*Ulva rigida*	132–358	Sfriso et al. (1993)
	Mudflat Coos Bay estuary	*Enteromorpha* spp.	1110	Pregnall and Rudy (1985)
Vascular plant	Salt marsh Mar Menor lagoon	*Phragmites australis*	2610	González-Alcaraz et al. (2012)
	Salt marsh Tagus estuary	*Sarcocornia fruticosa*	1298	Sousa et al. (2010)
	Yangtze estuary	*Spartina alterniflora*	2160	Liao et al. (2007)
Macrofaunal secondary production	Marennes-Oléron Bay, France	*Cerastoderma edule*	11.4	Sauriau and Kang (2000)
	Hichirippu Lagoon, Japan	*Ruditapes philippinarum*	96.5	Komorita et al. (2014)

Table 5.1 (continued)

Subject	Station	Species/site	Rate (g C m^{-2} year^{-1})	References
Macrofaunal calcification	San Francisco Bay, USA	*Potamocorbula amurens* (shell)	26.5	Chauvaud et al. (2003)
	Adriatic Sea, Italy	*Arcuatula senhousia* (shell)	46.0	Mistri and Munari (2013)
Sediment	The Molenplaat, Netherlands	Tidal flat	10–105	Widdows et al. (2004)
	Tamandaré, Brazil	Tidal flat	112.9[a]	Sanders et al. (2010)
	84 tidal marsh sites, Australia	Salt marsh	55 ± 2.0	Macreadie et al. (2017)
	Big bend of Florida, USA	Salt marsh	49.5–109.5	Arriola and Cable (2017)
	San Francisco Bay, USA	Salt marsh	79	Callaway et al. (2012)
	Mangroves and salt marshes in the world	Mangroves salt marshes	21[a]	Chmura et al. (2003)
	$n = 143$	Salt marsh	244.7 ± 26.1	Ouyang and Lee (2014)
	$n = 96$	Salt marsh	151.0	Duarte et al. (2005)
	Northern Florida, USA	Salt marsh	42–193	Choi and Wang (2004)
	$n = 24$	Estuaries	45.0	Duarte et al. (2005)

[a]Organic carbon content was calculated as 10%

marshes. The primary production rates was reported to be 29–234 g C m^{-2} year^{-1} for benthic microalgae (Colijn and de Jonge 1984; Cahoon 1999; Underwood and Kromkamp 1999), 7–875 g C m^{-2} year^{-1} for phytoplankton (Heip et al. 1995; Tada et al. 1998; Underwood and Kromkamp 1999), 132–1110 g C m^{-2} year^{-1} for macroalgae such as *Ulva rigida* and *Enteromorpha* spp. (Pregnall and Rudy 1985; Sfriso et al. 1993), and 1298–2610 g C m^{-2} year^{-1} for vascular plants (Liao et al. 2007; Sousa et al. 2010; González-Alcaraz et al. 2012). Studies show that the production rate increases as the individual becomes larger. The secondary production rates of bivalves were reported to be 11.4 g C m^{-2} year^{-1} for *Cerastoderma edule* (Sauriau and Kang 2000) and 96.5 g C m^{-2} year^{-1} for *Ruditapes philippinarum* (Komorita et al. 2014). The calcification rate of bivalves was reported to be 26.5 g C m^{-2} year^{-1} for *Potamocorbula amurensis* (Chauvaud et al. 2003) and 46 g C m^{-2} year^{-1} for *Arcuatula senhousia* (Mistri and Munari 2013). The carbon storage rates of consumers were smaller than those of the primary producers. The accumulation rate of sedimentary carbon was reported to be 10–112.9 g C m^{-2} year^{-1} in tidal flats

Table 5.2 Carbon stock within top 1 m of sediment in tidal flats and salt marshes

Method/station	Site	Carbon stock (t C ha⁻¹)	References
Tidal flat	Jiangsu Province, China	18.2	Yuan et al. (2015)
	Ise Bay, Japan	29.5–35.7	Kokubu et al. (2017)
Salt marsh	84 tidal marsh sites, Australia	165.41	Macreadie et al. (2017)
	Reviewed 154 sites globally	390 ± 30	Chmura et al. (2003)
	Jiangsu Province, China (*Phragmites australis*)	29.0	Yuan et al. (2015)

(Widdows et al. 2004; Sanders et al. 2010), 21–244.7 g C m^{-2} year^{-1} in salt marshes (Chmura et al. 2003; Choi and Wang 2004; Duarte et al. 2005; Callaway et al. 2012; Ouyang and Lee 2014; Arriola and Cable 2017; Macreadie et al. 2017), and 45 g C m^{-2} year^{-1} in estuaries (Duarte et al. 2005). Thus, the accumulation rate of sedimentary carbon in tidal flats is comparable with that in salt marshes and estuaries.

Table 5.2 provides a summary of the reported sedimentary carbon stocks in tidal flats, tidal marshes, and salt marshes. Here, we calculated the stock as the amount of carbon accumulated within the top 1 m of sediment based on reported data. The sedimentary carbon stock was reported to be 18.2–35.7 t C ha^{-1} in tidal flats (Yuan et al. 2015; Kokubu et al. 2017) and 29–390 t C ha^{-1} in salt marshes (Chmura et al. 2003; Yuan et al. 2015).

5.3 Sites of Field Investigation

Osaka Bay is an inner bay located in the eastern part of the Seto Inland Sea, Japan, and it is connected to the open sea by two narrow straits, the Akashi Strait and Kitan Strait (Fig. 5.2). The area of the bay is 1400 km², and the average water depth is about 28 m. The monthly average air temperature of this region ranges from about 6.0–28.8 °C, and the climate is temperate. In addition, Osaka Bay is affected by external nutrient loading from the Yodo River, the annual average discharge of which was 193 m³ s^{-1} at Hirakata observatory from 1952 to 2003 (Lake Biwa-Yodo River Water Quality Preservation Organization 2008). Therefore, the water quality in the closed-off section of Osaka Bay is chronically eutrophic.

The field surveys were conducted at the Yodo River mouth tidal flat (Fig. 5.2: Area 1) and the Osaka Nanko bird sanctuary (Area 2), which are located in the innermost region of Osaka Bay. The two surveyed areas are only about 13 km apart in a straight-line distance. The Yodo River mouth tidal flat is a natural estuary, whereas the Osaka Nanko bird sanctuary is an artificial salt marsh constructed in a landfill site.
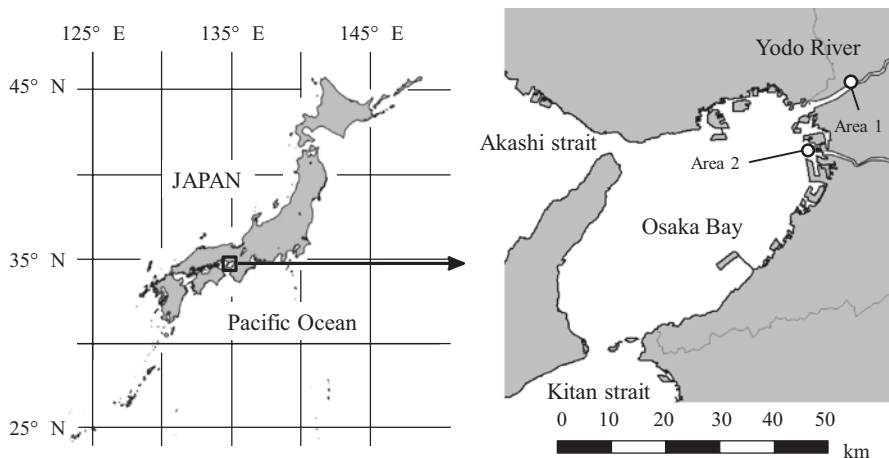
Fig. 5.2 Location of field investigation sites in Osaka Bay. Area 1: Yodo River mouth tidal flat. Area 2: Osaka Nanko bird sanctuary

5.3.1   *Yodo River Mouth Tidal Flat*

The Yodo River tidal flat and salt marsh are located about 8 km upstream from the river mouth (Fig. 5.2). The tidal flat covers about 3000 m^2 (Fig. 5.3a), and the salt marsh area is about 42,000 m^2. The salinity at the tidal flat fluctuated between 0 and 22.9, but values in winter and fall tended to be in the range of 0–10. The sediment is sandy mud (gravel content ~0%, sand content 80%, and silt and clay ~20%, with ignition loss being 6–13%).

5.3.2   *Osaka Nanko Bird Sanctuary*

Osaka Nanko bird sanctuary is an artificial salt marsh constructed in 1983 in the port area of Osaka Bay (135°23′58.9″E, 34°38′05.4″N) for protecting wild bird habitat. The total area of this site is 19.3 ha, including the terrestrial area of 6.5 ha and the wetland area of 12.8 ha. The wetland area is composed of the north salt marsh flat (about 4.6 ha), west salt marsh (about 1.4 ha), and south salt marsh (about 3.8 ha). The north salt marsh has a lagoon-type tidal flat because the seawater can be exchanged between the salt marsh and the open sea through conduit pipes. At this north salt marsh, we conducted a field survey on the carbon storage capacity of the phytoplankton and carbon accumulation in the sedimentary layer.

   An overview of the north salt marsh is shown in Figure 5.3b. The salinity is usually about 25, but sometimes it declines to 7.5 because the north salt marsh is located in the Yodo River estuary area. The salt marsh is also strongly affected by external nutrient loads, and the biological production rate is high. The sediment is sandy

Area (ha)	4.5
-Salt marsh area	4.2
-Tidal flat area	0.3
Water qualities	
-Water temperature (ºC)	2.62 – 36.5
-Salinity	0 – 22.9
-Dissolved Oxygen (mg/l)	0.01 –17.42
Grain size distribution (tidal flat)	
-Gravel content (%)	0
-Sand content (%)	80
-Clay content (%)	20
Ignition loss (%) (tidal flat)	6 - 13

(a) Yodo River mouth tidal flat

Area (ha)	19.3
-Green area	6.5
-Wetland area	12.8
-North salt marsh	4.6
-West salt marsh	1.4
-South salt marsh	3.8
Averaged ground level (m)	L.W.L. +0.72
Averaged exposure rate to air (%)	17.3
Water qualities	
-Water temperature (ºC)	7.5 – 30.6
-Salinity	13.2 – 30.0
-DIN (mg-N/l)	0.11 – 0.62
Grain size distribution	
-Gravel content (%)	18
-Sand content (%)	70
-Clay content (%)	12
Ignition loss (%)	6 - 9

(b) the north salt marsh in Osaka Nanko bird sanctuary

Fig. 5.3 Profiles of two investigation sites. (**a**) Yodo River mouth tidal flat, and (**b**) north salt marsh in the Osaka Nanko bird sanctuary. These maps are reproductions of the Digital Map 25,000 (Map Image) published by the Geospatial Information Authority of Japan

mud (gravel content is ~18%, sand content is 70%, and silt and clay content is ~12%, with ignition loss being about 6–9%).

5.4 Carbon Storage of a Bivalve

We quantified the biomass and secondary production separately for the organic carbon and inorganic carbon fractions of the bivalve *Corbicula japonica*, which is dominant in Osaka Bay and distributed in brackish lakes and estuarine tidal flats in Japan. A field investigation was carried out on the 3000-m^2 muddy tidal flat in the Yodo River (Fig. 5.3a). From June 2012 to May 2015, samples of *C. japonica* were collected using a 1-mm-mesh sieve from quadrats (50 × 50 × 10 cm) at eight stations to examine abundance. The shell length and number of individuals in the collected samples were measured in the laboratory.

Cohort analysis was performed with the frequency distribution of shell lengths for production using Eq. (5.1):

$$P = \sum \left(W_{t+1} - W_t \right) \times \left(N_{t+1} + N_t \right) / 2, \qquad (5.1)$$

where P represents production, W_t is the average dry weight of the cohort at sampling month t, and N_t is the average population density of the cohort at t.

Production of the population was calculated by performing cohort analysis using the population density measured during the field investigation (340–1240 ind. m^{-2}; Fig. 5.4a). Population density increased sharply beginning in June and then tended to decrease from November onward. Each year, three or four cohorts were produced. Shell length increased greatly in summer (Fig. 5.4b).

The carbon concentrations of the body and the shell were measured with an element analyzer (FLASH EA 1112, Thermo Finnigan, San Jose, CA, USA). Organic carbon biomass was 2–35 g C m^{-2}, and inorganic carbon biomass of shell was 12–176 g C m^{-2} (Fig. 5.5). The ratio of inorganic carbon biomass to the total carbon biomass was 85%. Together, organic and inorganic carbon biomass in tidal flats ranged from 12 to 176 g C m^{-2}, with an average value of 95 g C m^{-2}.

Organic carbon production was 28 g C m^{-2} year^{-1} (range, 11–41 g C m^{-2} year^{-1}), and inorganic carbon shell production was 131 g C m^{-2} year^{-1} (58–192 g C m^{-2} year^{-1}) (Table 5.3). Thus, inorganic carbon production was 4.7 times that of organic carbon, accounting for 82% of the total production. Furthermore, the production/biomass ratio (P/B ratio) of organic carbon was 1.88 and that of inorganic carbon was 1.65, respectively. The ratio of inorganic to organic carbon production was reported for seven major shells, including the clam *Ruditapes philippinarum* and the oyster *Cassostrea gigas*, as 1.8–3.5 (Nakamura et al. 2003). That of *C. japonica* was higher than these values, meaning that inorganic carbon production by shell formation in this bivalve is large.
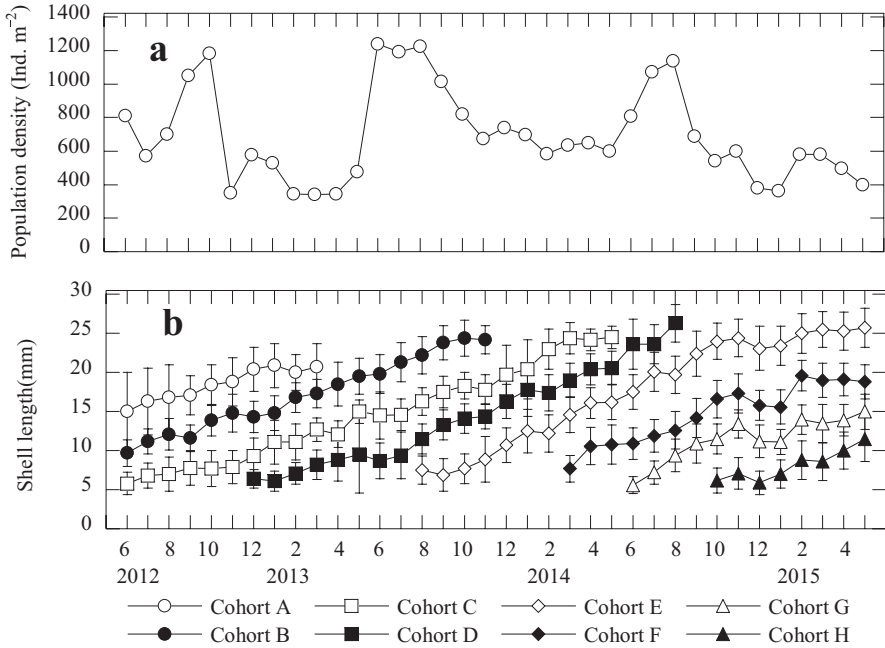
Fig. 5.4 (**a**) Monthly change of population density in *Corbicula japonica*, and (**b**) monthly change of shell length of each cohort in *C. japonica* (Otani et al. unpublished data)
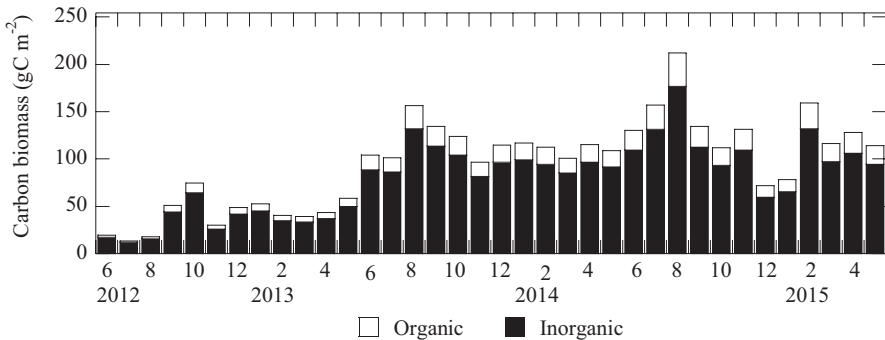
Fig. 5.5 Monthly change of carbon biomass in *Corbicula japonica* (Otani et al. unpublished data)

However, calcification generates CO_2 during the shell formation process, as shown by the following chemical equation:

$$Ca^{2+} + 2HCO_3^- \rightarrow CaCO_3 + CO_2 + H_2O. \tag{5.2}$$
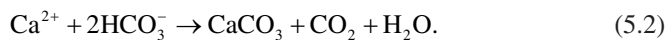
Table 5.3 Annual fluctuations of carbon stock and flow in *Corbicula japonica*

Period	Biomass of organic carbon (body) (g C m^{-2})	Biomass of inorganic carbon (shell) (g C m^{-2})	Production organic carbon (body) (g C m^{-2} year^{-1})	Production of inorganic carbon (shell) (g C m^{-2} year^{-1})
June 2012–May 2013	6	35	11	58
June 2013–May 2014	18	97	41	192
June 2014–May 2015	21	107	32	144
Average	15	80	28	131

The ratio of CO_2 released to $CaCO_3$ precipitated was estimated as 76 g C m^{-2} year^{-1} by Frankignoulle et al. (1994).

Although respiration was not measured in this study, by considering the biomass it is possible to estimate secondary production of *C. japonica*. Bivalves are CO_2 generators (Chauvaud et al. 2003; Mistri and Munari 2013). Organic matter of the bivalve body and CO_2 absorbed by photosynthesis of consumed vegetation is stocked as organic carbon, and most of it decomposes in a short time and is released as CO_2 after death. In turn, inorganic carbon of the shell after death is buried in sediment in tidal flats (Fodrie et al. 2017). That is, bivalves play a role in immobilizing carbon, although inorganic carbon production by bivalves is small compared to that produced by vegetation.

To date, organic carbon in sediment and algae has been the focus of carbon storage research in aquatic systems, but it is necessary to consider the storage of inorganic carbon as well. The relationship between organic and inorganic carbon affects the carbonate cycle, such as the rates of calcification and dissolution in water, and it also affects CO_2 gas flux between the atmosphere and seawater.

5.5 Carbon Storage of Phytoplankton

In the sea, carbon is circulating continuously via complex biological processes such as photosynthesis, respiration, and decomposition of organic matter, chemical processes such as chemical equilibration of the carbonate system, and physical processes such as advection along with water exchange. In this section, we describe the carbon absorption of phytoplankton in the carbon budget of the tidal flat at Osaka Nanko bird sanctuary.

(a)

(b)
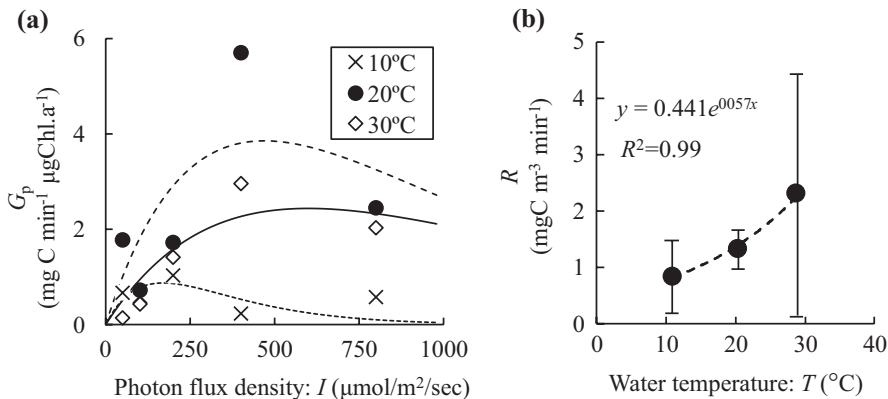
Fig. 5.6 Relationships between (**a**) gross primary production per chlorophyll a (G_p) and photon flux density, and (**b**) respiration/decomposition (R) of seawater and water temperature. (From Endo and Kawasaki 2017)

5.5.1 Calculation of Gross Primary Production, Decomposition, and Respiration in Seawater

We performed an incubation experiment using seawater sampled in the north salt marsh of the bird sanctuary site to model gross primary production (GPP) of phytoplankton and the respiration/decomposition in the water column by using the light and dark bottle method. Although both GPP and respiration/decomposition occur in the light bottles, it is assumed that only respiration/decomposition occurs in the dark bottles. Therefore, rate of GPP and respiration/decomposition were calculated based on the changes in dissolved inorganic carbon (DIC) concentration in the light and dark bottles:

$$G = \left[\left(C_{l1} - C_{l2} \right) - \left(C_{d1} - C_{d2} \right) \right] / t \qquad (5.3)$$

$$R = \left(C_{d2} - C_{d1} \right) / t, \qquad (5.4)$$

where G is the rate of GPP, C_{l1} and C_{d1} represent the DIC concentrations in the light and dark bottles at the beginning of incubation, R is the rate of respiration/decomposition, C_{l2} and C_{d2} are those at the end of incubation, and t is incubation time. Generally, G has been estimated by the change in dissolved oxygen concentration, but this is merely an estimate calculated by using an arbitrary respiratory quotient. So, in this study, G was evaluated by measuring DIC changes directly.

Figure 5.6a shows the relationship between G per unit chlorophyll a (G_p) and photon flux density (I). At each water temperature, G_p increases as photon flux density increases until I is around 200–600 µmol m^{-2} s^{-1}, but then G_p decreases at higher photon flux densities. In addition, under the same photon flux density
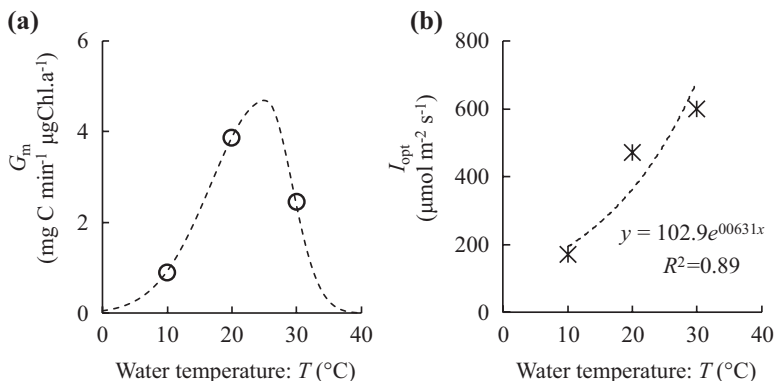
Fig. 5.7 Relationships between water temperature and (**a**) maximum G_P (G_m) and (**b**) optical photon flux density (I_{opt}). (From Endo and Kawasaki 2017)

conditions, G_p is highest when water temperature is around 20 °C. These data confirm that G_p depends on light intensity and water temperature.

Steele (1962) proposed the following model of the relationship between photosynthetic rate of phytoplankton and light intensity:

$$G_p = G_m \cdot I / I_{opt} \exp\left(1 - I / I_{opt}\right), \tag{5.5}$$

where G_m is the maximum value of G_p and I_{opt} is the optimum photon flux density. G_p at each water temperature was approximated by Eq. (5.5) by the method of least squares, resulting in G_m of 0.87, 3.85, and 2.44 mg C min^{-1} µg Chl.a^{-1} and I_{opt} of 170, 470, and 600 µmol m^{-2} s^{-1} at water temperatures of 10, 20, and 30 °C, respectively.

Figure 5.7a shows the relationship between G_m and water temperature. The relationship seemed to reach a peak at an optimal water temperature rather than obey the Arrhenius equation. Therefore, the relationship between G_m and water temperature was calculated using Eq. (5.6):

$$G_m = G'_m \exp\left\{-\beta_1 \left(T - T_{opt}\right)^2\right\} \cdots T \le T_{opt}$$

$$G_m = G'_m \exp\left\{-\beta_2 \left(T_{opt} - T\right)^2\right\} \cdots T > T_{opt}, \tag{5.6}$$

where β_1 and β_2 represent the degree of kurtosis of the function versus water temperature, G'_m is the maximum value of G_m, and T_{opt} is the optimum temperature of G_m. When these parameters were obtained from the experimental results by the method of least squares, β_1 and β_2 were 0.007 and 0.03, P'_m was 4.7 mg C min^{-1} µg Chl.a^{-1}, and T_{opt} was 25.2 °C.

Table 5.4 Monthly changes of carbon flow and stock of phytoplankton in the north salt marsh of Osaka Nanko bird sanctuary

Date	C_{chl} (µg L^{-1})	Carbon stock (g C m^{-2})	$\overline{GPP}$ (g C m^{-3} day^{-1})	$\overline{R}$ (g C m^{-3} day^{-1})	$\overline{NEP}$ (g C m^{-3} day^{-1})
15 July 2015	1.47	0.094	1.78	3.37	−1.59
16 September 2015 (red tide)	23.81	1.524	18.95	2.30	16.65
25 November 2015	2.30	0.148	0.77	1.51	−0.74
27 January 2016	3.74	0.239	0.90	0.99	−0.09
9 March 2016	1.51	0.097	0.30	1.07	−0.76
25 May 2016	3.98	0.255	6.59	1.99	4.60
Average[a]		0.167	2.07	1.78	0.28

[a]Average value was calculated without the data of 16 September 2015

Figure 5.7b shows the relationship between I_{opt} and the water temperature. I_{opt} was calculated by using Eq. (5.7), assuming that it follows the Arrhenius equation (e.g., Robarts and Zohary 1987):

$$I_{opt} = 102.9\exp(0.063T).\qquad(5.7)$$

Figure 5.6b shows the relationship between the respiration/decomposition rate in seawater (R) and the water temperature. Note that there is great variability in R when water temperature is 30 °C, because data measured on different days are included in this figure. Like I_{opt}, however, the average value of R increases with increasing water temperature, so R was calculated by using Eq. (5.8), where T is water temperature, assuming that the respiration rate follows the Arrhenius equation as well (e.g., Hirche 1987):

$$R = 0.407\exp(0.056T).\qquad(5.8)$$

Q_{10}, which represents the change in metabolic rate associated with a temperature rise of 10 °C, was 1.75. Q_{10} of this experiment was a bit lower than the generally reported value of 2 to 3, but it was judged to be appropriate.

5.5.2 Carbon Flow and Stock of Phytoplankton

Table 5.4 shows the carbon stock and flow of phytoplankton at this site. Carbon stock (CS_p) was estimated as the carbon stored in the phytoplankton body and was calculated by using Eq. (5.9):

$$CS_p = (C_{chl} \times V \times r)/A,\qquad(5.9)$$

where C_{chl} is the chlorophyll a concentration of phytoplankton on the measurement day, V is the average water volume of the north salt marsh (45,700 m³), r is the conversion ratio of phytoplankton biomass carbon to chlorophyll a (= 56; Lü et al. 2009), and A is the average water surface area of the north salt marsh (40,000 m²). C_{chl} ranged from 1.47 to 23.81 μg L⁻¹, and C_{chl} was higher in September because of a red tide. CS_{p} ranged from 0.094 to 1.524 g C m⁻². Excluding the data gathered during the red tide, the average carbon stock of phytoplankton at this bird sanctuary site was estimated to be 0.167 g C m⁻².

The carbon flow by phytoplankton was estimated as the net ecosystem production (NEP) of the water column including phytoplankton and bacteria, because the net primary production of phytoplankton alone could not be estimated. Water quality parameters and phytoplankton biomass were measured at 17 sites corresponding to a 50 m × 50 m mesh covering the north salt marsh, and the daily net ecosystem production ($\overline{NEP}$) of the water column at each site was calculated by using Eqs. (5.10), (5.11) and (5.12):

$$\overline{GPP} = \sum_{i=1}^{n} \int_0^h G(z_i) dz / h_i \cdot t_g \tag{5.10}$$

$$\overline{R} = \sum_{i=1}^{n} \int_0^h R(z_i) dz / h_i \cdot t_r \tag{5.11}$$

$$\overline{NEP} = \overline{GPP} - \overline{R}, \tag{5.12}$$

where $\overline{GPP}$ is the daily gross production rate in the north salt marsh, n is the total number of measurement sections (= 17), $G(z)$ is G at the depth z estimated by using Eqs. (5.5), (5.6) and (5.7), h is water depth in each measurement section, i is the measurement section, t_g is photosynthesis time (8 h), $\overline{R}$ is the daily respiration/decomposition rate in seawater, $R(z)$ is the respiration/decomposition rate at depth z estimated by using Eq. (5.9), and t_r is respiration time (24 h). The $\overline{NEP}$ values were estimated as -1.59 g C m⁻³ day⁻¹ on 15 July 2015, 16.6 g C m⁻³ day⁻¹ on 16 September 2015, -0.74 g C m⁻³ day⁻¹ on 25 November 2015, -0.09 g C m⁻³ day⁻¹ on 27 January 2016, -0.76 g C m⁻³ day⁻¹ on 9 March 2016, and 4.60 g C m⁻³ day⁻¹ on 25 May 2016. A large amount of carbon was absorbed by phytoplankton on 16 September 2015 due to the red tide. $\overline{NEP}$ was negative in the season of low water temperature because $\overline{R}$ was larger than $\overline{GPP}$. However, the averaged value of $\overline{NEP}$ without including the red tide data implied a net uptake of inorganic carbon. These findings suggest that the photosynthesis of phytoplankton affects the carbon cycle of the tidal flat. The average annual carbon flow of phytoplankton per area was estimated as 118.3 g C m⁻² year⁻¹ based on $\overline{GPP}$, which is likely smaller than that of previously reported carbon flow of phytoplankton (see Table 5.1) because this value includes not only respiration of phytoplankton but also that of bacteria in the water column.

Table 5.5 Carbon balance in the north salt marsh of Osaka Nanko bird sanctuary

Measurement time		Change of water carbon storage (kg C)	Sea water exchange (kg C)	GPP (kg C)	R	NEP	Contribution rate (%)
Daily	25 October 2016 at 18:00–26 October 2016 at 17:00	91.8	66.4	74.1	87.9	31.9	–
Nighttime	25 October 2016 at 18:00–26 October 2016 at 06:00	−243.3	−326.8	0.0	45.8	0.0	0
Daytime	26 October 2016 07:00–17:00	335.2	393.2	74.1	42.2	31.9	55

GPP gross primary production, *R* respiration/decomposition, *NEP* net ecosystem production

5.5.3   Effect of Water Column NEP on Carbon Cycling

To clarify the contribution of carbon storage by phytoplankton on the carbon cycle in a tidal flat, the carbon balance at the bird sanctuary was estimated. Table 5.5 shows the balance of the amount of carbon storage change in the water column (estimated from DIC concentration measurements and water volume), carbon inflow or outflow along with seawater exchange, NEP, GPP, and respiration/decomposition on 25–26 October 2016.

Carbon storage in seawater increased 91.7 kg C in 1 day, and 66.4 kg C flowed into the salt marsh from the open sea by seawater exchange. Thus, it appears that there was a 25.3 kg C increase caused by factors other than those measured in this study, such as CO_2 sedimentary emission or respiration by aquatic organisms. We could not evaluate the contribution because carbon increased in the water column despite 31.9 kg C being absorbed by phytoplankton. On the other hand, during only the daytime, carbon storage in water increased by 335.2 kg C, and 393.2 kg C flowed into the salt marsh, meaning that 58 kg C was absorbed in the water column. NEP was 31.9 kg C, so the percent contribution to carbon storage by phytoplankton was about 55%. These results suggest that the carbon storage effect of phytoplankton was about half that of carbon absorption in the water during the daytime.

5.6   Carbon Storage in Sediment

5.6.1   Methods

Detritus of organisms is deposited in the sedimentary layer. The deposited organic matter is decomposed by bacteria or fed on by benthos, but some of it accumulates without being decomposed or consumed. This organic matter was originally carbon

Table 5.6 Monthly changes of acid-volatile sulfide (AVS: mg g-dry^{-1}) in the intertidal and subtidal zones

Date		Intertidal zone	Subtidal zone
2014	14 May	0.00	0.26
	4 June	0.05	0.38
	9 July	0.00	0.36
	6 August	0.11	0.18
	10 September	0.23	0.54
	Average	0.08	0.34

taken up by organisms through the process of photosynthesis and the food web, so it can be thought as the carbon storage of the salt marsh. Here, we investigated the carbon accumulated into the sedimentary layer of the intertidal and subtidal zones at the bird sanctuary. Biodegradation tests of sediment taken from the salt marsh were carried out for 100 days, and the remaining organic matter was evaluated as the carbon accumulation of the sediment layer.

Table 5.6 shows the monthly change of concentration of acid-volatile sulfide (AVS) per dry weight of sediments in the intertidal and subtidal zones. AVS is an index of the sulfide concentration in the sediment, and if the concentration is high, it indicates that anaerobic decomposition of organic matter is occurring. The average concentration of AVS in the intertidal zone was 0.08 mg g-dry^{-1}, a value that is relatively low. In contrast, the concentration of AVS in the subtidal zone was high, with an average value of 0.34 mg g-dry^{-1}. These estimates indicate that aerobic decomposition occurred in the intertidal zone, whereas anaerobic decomposition occurred in the subtidal zone. Thus, 100-day biodegradation tests of sediments from the intertidal zone were carried out under aerobic conditions, and sediments in the subtidal zone were incubated under anaerobic conditions.

Figure 5.8 shows the experimental apparatus of the sediment biodegradation tests. A 100-ml flask with 10 g of sediment and 100 ml of filtered seawater was placed on a shaker table at 50 rpm for 100 days for the case of aerobic incubation, and a 50-ml sealed vial bottle with 5 g of sediment and 50 ml of filtered seawater was shaken in anaerobic jar substituted nitrogen gas at 50 rpm for 100 days for the case of anaerobic incubation. The sedimentary organic carbon (SOC) was measured with a CHN analyzer (MT-6, Yanaco Co. Kyoto, Japan.) before and after the experiment, and residual SOC (R-SOC) after 100 days was defined as sequestered SOC.

5.6.2 Remaining Organic Matter in Sediment

The amount of SOC in the intertidal zone ranged from 1.24 to 3.29 mg C g-dry^{-1}, and that of the subtidal zone ranged from 2.64 to 4.27 mg C g-dry^{-1} (Fig. 5.9). Thus, sedimentary organic carbon was higher in the subtidal zone.
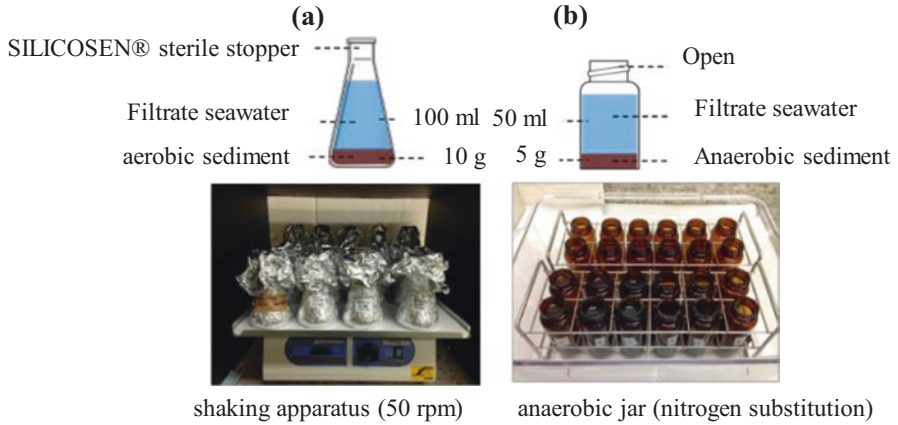
Fig. 5.8 Experimental apparatus for the biodegradation tests
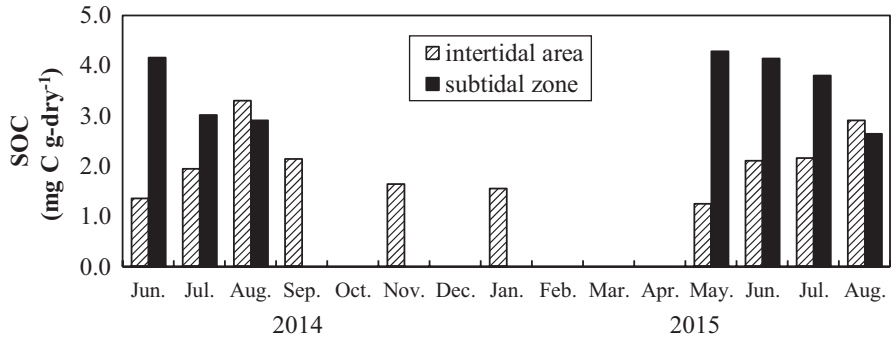
Fig. 5.9 Monthly changes of sedimentary organic carbon (SOC) at the intertidal zone and the subtidal zone. (Modified from Nishio et al. 2016)

Figure 5.10 shows the percentage of the decomposed and residual organic carbon (R-SOC) after 100 days. The percentage of residual organic carbon ranged from 46% to 77% of the total SOC in the intertidal zone, with about half the organic matter decomposed. In contrast, this range was 77–98% in the subtidal zone, and most organic carbon remained in the sedimentary layer. Thus, the carbon storage effect is higher in the subtidal zone than in the intertidal zone. In other words, 20–50% of the organic matter accumulated on sediment decomposes in the intertidal zone, whereas only 20–25% of it decomposes in the subtidal zone. Although the subtidal area serves a carbon storage function in the benthic ecosystem, deposited organic matter continues to accumulate as sludge, and it could be a source of hypoxia in some cases.
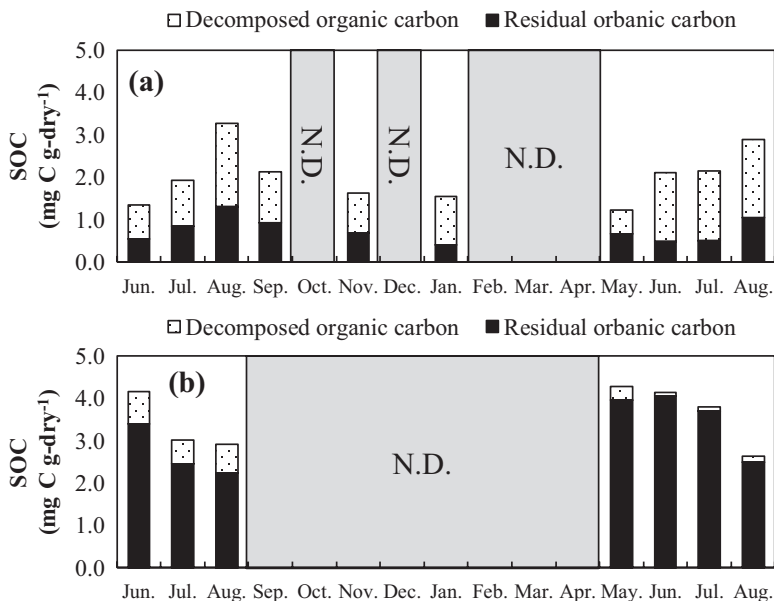
Fig. 5.10 Concentration of decomposed organic carbon and residual organic carbon of the sediment in (**a**) the intertidal flat and (**b**) the subtidal flat. (Modified from Nishio et al. 2016)

Fig. 5.11 Changes in SOC biodegradation over time. (Modified from Nishio et al. 2016)
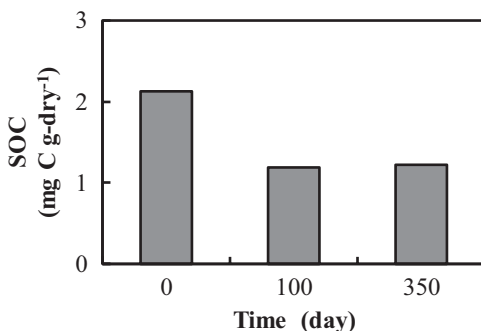
We also performed biodegradation tests for 350 days under aerobic conditions to check the degree of SOC decomposition (Fig. 5.11). SOC was 2.1 mg C g-dry^{-1} at the start of the test and decreased to 1.2 mg C g-dry^{-1} after 100 days, but it remained unchanged at 350 days. These results confirmed that it is valid to estimate the R-SOC based on 100-day biodegradation tests.
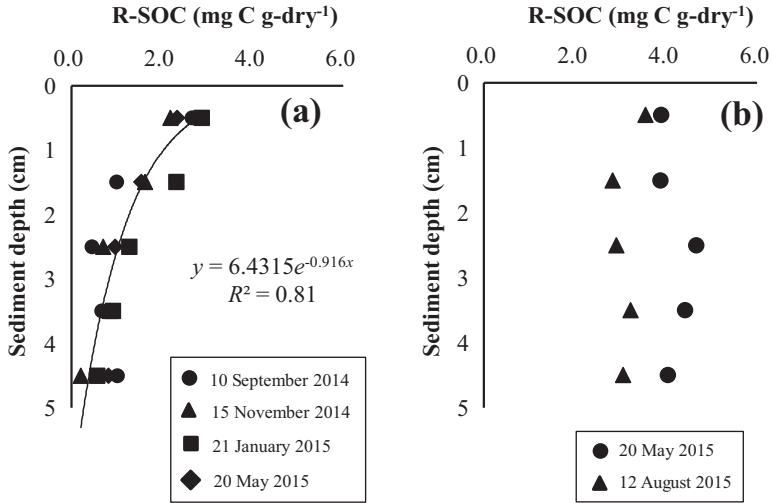
Fig. 5.12 Vertical distributions of R-SOC at the (**a**) aerobic area and (**b**) anaerobic area. (Modified from Nishio et al. 2016)

5.6.3   Vertical Distribution of Residual Organic Carbon in Sediment

Figure 5.12 shows the vertical distributions of R-SOC in the intertidal and subtidal area. In the intertidal area, R-SOC at 0.5 cm depth ranged from 2.19 to 2.84 mg C g-dry^{-1} and decreased with increasing depth from 0 to 5 cm (Fig. 5.12a). The vertical distribution of R-SOC could be approximated by using Eq. (5.12) in the intertidal area:

$$RSOC_a = 6.4315e^{-0.916z}, \tag{5.12}$$

where $RSOC_a$ is residual sedimentary organic carbon under aerobic conditions and z is sediment depth.

The R-SOC at 0.5 cm depth was 3.5–3.9 mg C g-dry^{-1} in the subtidal area under anaerobic conditions, which was larger than that in the intertidal area (Fig. 5.12b). Furthermore, R-SOC in the subtidal area remained about the same across the 0–5 cm depth range. Therefore, it appears that the carbon storage capacity in the subtidal area was higher than that in the intertidal area.

Table 5.7 Carbon stock in the upper 1 m of sediment at the Osaka Nanko bird sanctuary

Site	Area of seafloor (m^2)	Sedimentary carbon concentration (mg C g-dry^{-1})	Carbon stock (t C)
Aerobic area	30,040	0.35	14.7
Anaerobic area	7225	3.65	37.1
Total			51.8
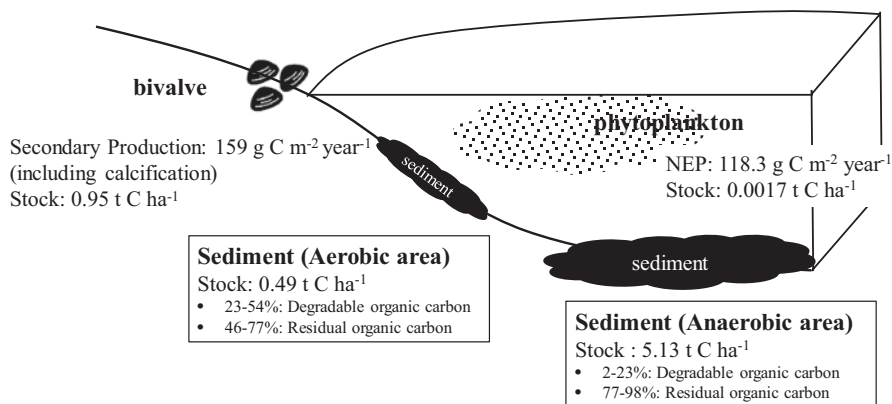
Fig. 5.13 Summary of carbon stocks and flows of the tidal flat ecosystem in this study

5.6.4 Carbon Storage in Sediment at Osaka Nanko Bird Sanctuary

Table 5.7 shows the carbon storage in sediment of 1 m depth estimated from the data reported here. The SOC concentration was calculated under the assumption that vertical distribution of R-SOC followed Eq. (5.12) from 0 to 5 cm depth and remained constant from 5 to 100 cm depth. The average concentration of R-SOC for the top 1 m was 0.35 mg C g-dry^{-1} in the aerobic (intertidal) area and 3.65 mg C g-dry^{-1} in the anaerobic (subtidal) area. The carbon storage was 14.7 t C in the aerobic zone and 37.1 t C in the anaerobic zone, such that total carbon storage was estimated to be 51.8 t C at the bird sanctuary site.

5.7 Summary

In this chapter, we estimated the carbon flows and stocks of bivalves, phytoplankton, and sediments in a tidal flat and salt marsh of a eutrophic area. Figure 5.13 illustrates the estimated carbon stock and flow in this study. The secondary carbon production including calcification was 159 g C m^{-2} year^{-1} for bivalves and NEP was

118.3 g C m^{-2} year^{-1} for phytoplankton, which were similar to previously reported values (Table 5.1). This carbon flow was smaller than that of seagrass meadows, which is 344 g C m^{-2} year^{-1} (see Table 4.1 in Chap. 4).

On the other hand, the carbon stock was 0.95 t C ha^{-1} for bivalves and 0.0017 t C ha^{-1} for phytoplankton. Residual organic carbon was 45.9–77.0% in the intertidal sediment and 92.5–98.3% in the subtidal sediment for the top 5 cm. The sedimentary carbon stock to 1 m depth was 5.13 t C ha^{-1} in the subtidal area and 0.49 t C ha^{-1} in the intertidal area. This carbon stock is less than that reported for seagrass meadows (47.7–48.5 t C ha^{-1}; Kokubu et al. 2017) and mangrove forest (170.1–336.1 t C ha^{-1}; Rahman et al. 2015).

Generally, tidal flats have been recognized as carbon sources due to their decomposing organic matter and respiration. Therefore, mangroves, seagrass meadows, and wetlands are regarded as blue carbon resources of coastal ecosystems according to the United Nations Environment Programme (Nellemann et al. 2009). However, this study revealed both carbon stocks and flows for a bivalve, phytoplankton, and sediment in the tidal flats. Although tidal flat ecosystems are composed of relatively short-lived species, the existence of these components over several generations is important for carbon storage. Our analyses suggest that tidal flat ecosystems also can be expected to serve a carbon storage function as repositories of blue carbon.

References

Arriola JM, Cable JE (2017) Variations in carbon burial and sediment accretion along a tidal creek in a Florida salt marsh. Limnol Oceanogr 62:S15–S28

Atwood TB, Connolly RM, Ritchie EG, Lovelock CE, Heithaus MR, Hays GC, Fourqurean JW, Macreadie PI (2015) Predators help protect carbon stocks in blue carbon ecosystems. Nat Clim Chang 5:1038–1045

Cahoon LB (1999) The role of benthic microalgae in neritic ecosystems. Oceanogr Mar Biol Annu Rev 37:47–86

Callaway JC, Borgnis EL, Turner RE, Milan CS (2012) Carbon sequestration and sediment accretion in San Francisco Bay tidal wetlands. Estuar Coasts 35:1163–1181

Chauvaud L, Thompson JK, Cloern JE, Thouzeau GL (2003) Clams as CO$_2$ generators: the *Potamocorbula amurensis* example in San Francisco Bay. Limnol Oceanogr 48:2086–2092

Chmura GL, Anisfeld SC, Cahoon DR, Lynch JC (2003) Global carbon sequestration in tidal, saline wetland soils. Glob Biogeochem Cycles 17:1111

Choi Y, Wang Y (2004) Dynamics of carbon sequestration in a coastal wetland using radiocarbon measurements. Glob Biogeochem Cycles 18:GB4016

Colijn F, de Jonge V (1984) Primary production of microphytobenthos in the Ems-Dollard estuary. Mar Ecol Prog Ser 14:185–196

Donato DC, Kauffman JB, Mackenzie RA, Ainsworth A, Pfleeger AZ (2012) Whole-island carbon stocks in the tropical Pacific: implications for mangrove conservation and upland restoration. J Environ Manag 97:89–96

Duarte CM, Middelburg JJ, Caraco N (2005) Major role of marine vegetation on the oceanic carbon cycle. Biogeosciences 2:1–8

Endo T, Kawasaki T (2017) Evaluation of carbon absorption of phytoplankton at the north salt marsh of Osaka Nanko bird sanctuary. J Jpn Soc Civil Eng Ser B2 Coast Eng 73:1369–1374 (in Japanese)

Fodrie FJ, Rodriguez AB, Gittman RK, Grabowski JH, Lindquist NL, Peterson CH, Piehler MF, Ridge JT (2017) Oyster reefs as carbon sources and sinks. Proc Biol Sci B 284:20170891

Fourqurean JW, Duarte CM, Kennedy H, Marbà N, Holmer M, Mateo MA, Apostolaki ET, Kendrick GA, Krause-Jensen D, McGlathery KJ, Serrano O (2012) Seagrass ecosystems as a globally significant carbon stock. Nat Geosci 5:505–509

Frankignoulle M, Canon C, Gattuso JP (1994) Marine calcification as a source of carbon dioxide: positive feedback of increasing atmospheric CO_2. Limnol Oceanogr 39:458–462

González-Alcaraz MN, Egea C, Jiménez-Cárceles FJ, Párraga I, María-Cervantes A, Delgado MJ, Álvarez-Rogel J (2012) Storage of organic carbon, nitrogen and phosphorus in the soil-plant system of *Phragmites australis* stands from a eutrophicated Mediterranean salt marsh. Geoderma 185:61–72

Heip C, Goosen NK, Herman PMJ, Kromkamp J, Middelburg JJ, Soetaert K (1995) Production and consumption of biological particles in temperate tidal estuaries. Oceanogr Mar Biol Annu Rev 33:1–149

Hirche HJ (1987) Temperature and plankton. II. Effect on respiration and swimming activity in copepods from the Greenland Sea. Mar Biol 94:347–356

Inoue T (2018) Carbon sequestration in mangroves. In: Kuwae T, Hori M (eds) Blue carbon in shallow coastal ecosystems: carbon dynamics, policy, and implementation. Springer, Singapore, pp 73–99

Kokubu H, Ishii Y, Miyazaki H, Yabe T (2017) Estimation of carbon storage in tidal flat and *Zostera marine* bed in Ise Bay, toward a blue carbon evaluation. Journal of Japan Society of Civil Engineers, Ser B2 (Coastal Engineering) 73:1261–1266 (in Japanese)

Komorita T, Kajihara R, Tsutsumi H, Shibanuma S, Yamada T, Montani S (2014) Food sources for *Ruditapes philippinarum* in a coastal lagoon determined by mass balance and stable isotope approaches. PLoS One 9:e86732

Lake Biwa-Yodo River Water Quality Preservation Organization (2008) BYQ Report on water environment in Biwa Lake-Yodo River System, FY 2007 Version (in Japanese)

Lavery PS, Mateo MA, Serrano O, Rozaimi M (2013) Variability in the carbon storage of seagrass habitats and its implications for global estimates of blue carbon ecosystem service. PLoS One 8(9):e73748

Liao C, Luo Y, Jiang L, Zhou X, Wu X, Fang C, Chen J, Li B (2007) Invasion of *Spartina alterniflora* enhanced ecosystem carbon and nitrogen stocks in the Yangtze estuary, China. Ecosystems 10:1351–1361

Lü S, Wang X, Han B (2009) A field study on the conversion ratio of phytoplankton biomass carbon to chlorophyll-a in Jiaozhou Bay, China. Chin J Oceanol Limnol 27:793–805

Macreadie PI, Ollivier QR, Kelleway JJ, Serrano O, Carnell PE, Lewis CJE, Atwood TB, Sanderman J, Baldock J, Connolly RM, Duarte CM, Lavery PS, Steven A, Lovelock CE (2017) Carbon sequestration by Australian tidal marshes. Sci Rep 7:44071

Mistri M, Munari C (2013) The invasive bag mussel *Arcuatula senhousia* is a CO_2 generator in near-shore coastal ecosystems. J Exp Mar Biol Ecol 440:164–168

Miyajima T, Hamaguchi M (2018) Carbon sequestration in sediment as an ecosystem function of seagrass meadows. In: Kuwae T, Hori M (eds) Blue carbon in shallow coastal ecosystems: carbon dynamics, policy, and implementation. Springer, Singapore, pp 33–71

Miyajima T, Hori M, Hamaguchi M, Shimabukuro H, Adachi H, Yamano H, Nakaoka M (2015) Geographic variability in organic carbon stock and accumulation rate in sediments of east and southeast Asian seagrass meadows. Glob Biogeochem Cycles 29:397–415

Nakamura Y, Kanetsuna K, Isono R, Mimura N (2003) Characteristics distribution of biomass and biological functions on the shellfish in Japan. Proc Coast Eng 50:1296–1300 (in Japanese)

Nellemann C, Corcoran E, Duarte CM, Valdés L, De Young C, Fonseca L, Grimsditch G (2009) Blue carbon: a rapid response assessment. United Nations Environment Programme, GRID-Arendal (www.grida.no)

Nishio N, Endo T, Yamochi S (2016) A research on the dynamics of refractory organic carbon in the sediment of an artificial salt marsh. J Jpn Soc Civil Eng Ser B2 Coast Eng 72:1315–1320 (in Japanese)

Ouyang X, Lee SY (2014) Updated estimates of carbon accumulation rates in coastal marsh sediments. Biogeosciences 11:5057–5071

Pregnall AM, Rudy PP (1985) Contribution of green macroalgal mats (*Enteromorpha* spp.) to seasonal production in an estuary. Mar Ecol Prog Ser 24:167–176

Rahman MM, Khan MNI, Hoque AKF, Imra A (2015) Carbon stock in the Sundarbans mangrove forest: spatial variations in vegetation types and salinity zones. Wetl Ecol Manag 23:269–283

Robarts RD, Zohary T (1987) Temperature effects on photosynthetic capacity, respiration, and growth rates of bloom-forming cyanobacteria. New NZ J Mar Freshwater Res 21:391–399

Sanders CJ, Smoak JM, Naidu AS, Sanders LM, Patchineelam SR (2010) Organic carbon burial in a mangrove forest, margin and intertidal mud flat. Estuar Coast Shelf Sci 90:168–172

Sauriau PG, Kang CK (2000) Stable isotope evidence of benthic microalgae-based growth and secondary production in the suspension feeder *Cerastoderma edule* (Mollusca, Bivalvia) in the Marennes-Oléron Bay. Hydrobiologia 440:317–329

Sfriso A, Marcomini A, Pavoni B, Orio AA (1993) Species composition, biomass, and net primary production in shallow coastal waters: the Venice lagoon. Bioresour Technol 44:235–249

Sousa AI, Lillebo AI, Pardal MA, Caçador I (2010) Productivity and nutrient cycling in salt marshes: contribution to ecosystem health. Estuar Coast Shelf Sci 87:640–646

Steele JG (1962) Environmental control of photosynthesis in the sea. Limnol Oceanogr 7:137–150

Tada K, Monaka K, Morishita M, Hashimoto T (1998) Standing stocks and production rates of phytoplankton and abundance of bacteria in the Seto Inland Sea, Japan. J Oceanogr 54:285–295

Underwood GJC, Kromkamp J (1999) Primary production by phytoplankton and microphytobenthos in estuaries. Adv Ecol Res 29:93–153

Wang G, Guan D, Peart MR, Chen Y, Peng Y (2013) Ecosystem carbon stocks of mangrove forest in Yingluo Bay, Guangdong Province of South China. For Ecol Manag 310:539–546

Watanabe K, Kuwae T (2015) How organic carbon derived from multiple sources contributes to carbon sequestration processes in a shallow coastal system? Glob Chang Biol 21:2612–2623

Widdows J, Blauw A, Heip CHR, Herman PMJ, Lucas CH, Middelburg JJ, Schmidt S, Brinsley MD, Twisk F, Verbeek H (2004) Role of physical and biological processes in sediment dynamics of a tidal flat in Westerschelde estuary, SW Netherlands. Mar Ecol Prog Ser 274:41–56

Yoshida G, Hori M, Shimabukuro H, Hamaoka H, Onitsuka T, Hasegawa N, Muraoka D, Yatsuya K, Watanabe K, Nakaoka M (2018) Carbon sequestration by seagrass and macroalgae in Japan: estimates and future needs. In: Kuwae T, Hori M (eds) Blue carbon in shallow coastal ecosystems: carbon dynamics, policy, and implementation. Springer, Singapore, pp 101–127

Yuan J, Ding W, Liu D, Kang H, Freeman C, Xiang J, Lin Y (2015) Exotic *Spartina alterniflora* invasion alters ecosystem-atmosphere exchange of CH_4 and N_2O and carbon sequestration in a coastal salt marsh in China. Glob Chang Biol 21:1567–1580

Chapter 6
Air–Water CO$_2$ Flux in Shallow Coastal Waters: Theory, Methods, and Empirical Studies

Check for updates

Tatsuki Tokoro, Kenta Watanabe, Kazufumi Tada, and Tomohiro Kuwae

Abstract The fact that the ocean is one of the largest sinks of atmospheric CO$_2$ on Earth is an important consideration in the prediction of future climate changes and identification of possible mitigation strategies for global climate change. Recently, carbon storage in vegetated coastal habitats (blue carbon ecosystems) has been explored as a new option to mitigate climate change. However, the complexity of the mechanisms that control air–water CO$_2$ fluxes in shallow coastal ecosystems has precluded their adequate quantification. Spatiotemporal extension of accurate values of these fluxes will be an important milestone for assessing the contribution of blue carbon ecosystems to mitigation of climate change. In this chapter, we explain the theoretical understanding of air–water CO$_2$ fluxes and methods for their measurement. We then discuss results of empirical measurements of air–water CO$_2$ fluxes in shallow coastal waters. We conclude that statistical analyses of augmented air–coastal-water CO$_2$ flux data based on long-term measurements and multiple methods should lead to a quantitative understanding of the current status and future air–water CO$_2$ fluxes in shallow coastal waters at national and global scales.

6.1 Introduction

CO$_2$ is a very soluble gas in water. At 25 °C and 1 atmosphere pressure, approximately 1.4 g of CO$_2$ are dissolved in 1 L of freshwater, about 100 times the amount of dissolved N$_2$. CO$_2$ is more soluble in seawater than in freshwater (except for very hard water) because the capacity of CO$_2$ dissociation into bicarbonate ions (HCO$_3^-$) and carbonate ions (CO$_3^{2-}$) in seawater is larger than that in freshwater.

The amount of carbon stored in the global ocean is estimated to be about 38,000 Pg-C (about 50 times the amount of carbon present as CO$_2$ in the atmosphere), and the ocean is the largest carbon reservoir on the Earth's surface (Ciais et al. 2013).

T. Tokoro · K. Watanabe · K. Tada · T. Kuwae (✉)
Coastal and Estuarine Environment Research Group, Port and Airport Research Institute, Yokosuka, Japan
e-mail: kuwae@p.mpat.go.jp

In the long history of Earth, the ocean has had a strong influence on atmospheric CO_2 concentrations and the global climate system. Examples can be seen during times of global warming in the Jurassic and Cretaceous periods as well as during Snowball Earth events in the Proterozoic Eon. Excessive increases or decreases of atmospheric CO_2 concentrations due to volcanic activities and ecosystem metabolism are among the main causes of extreme climates. The ocean absorbs or releases excess CO_2 over millennial time scales and thereby mitigates the extreme climate change.

During the period of history before the Industrial Revolution, the absorption and release of atmospheric CO_2 by the ocean were in balance. However, atmospheric CO_2 concentrations have recently increased, mainly as a result of the combustion of fossil fuels (Ciais et al. 2013). This increase of atmospheric CO_2 concentrations has led to an imbalance between atmospheric and oceanic CO_2; the ocean is now a net sink of atmospheric CO_2. Takahashi et al. (2009) have estimated that about 1.42 Pg-C were absorbed in 2000 (Fig. 6.1). The latest global summary shows that the net influx of CO_2 into the ocean has increased to 2.4 ± 0.5 Pg-C year^{-1} (Le Quéré et al. 2018), which is about 27% of the annual releases of CO_2 due to anthropogenic activities.

In contrast, the air–water CO_2 flux in shallow coastal waters has not been as well quantified as the fluxes in the open ocean and continental shelves. Air–water CO_2 fluxes in continental shelves have been estimated to be about half the global oceanic absorption by the "continental shelf pump" system (Tsunogai et al. 1999). The
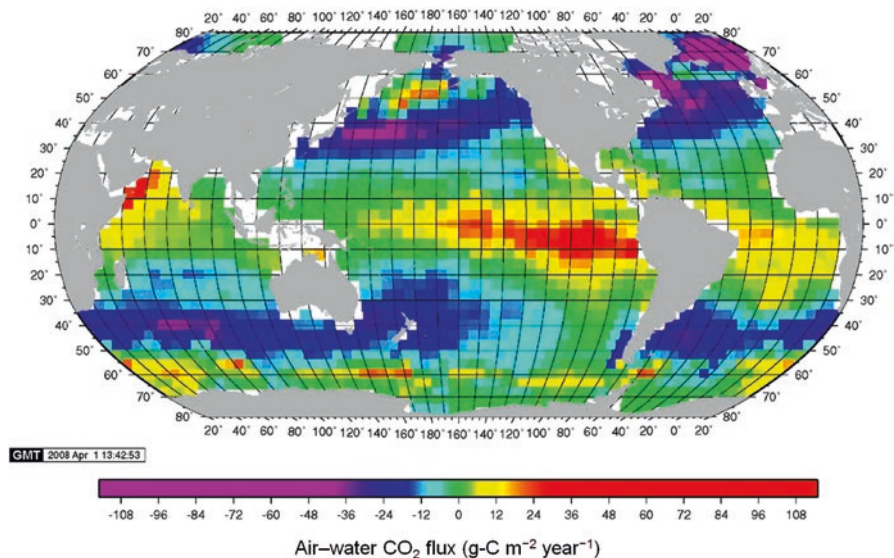
Fig. 6.1 Global estimates of mean annual air–water CO_2 fluxes (g-C m^{-2} year^{-1}) for the reference year 2000. Positive values show areas that are sources of CO_2, and negative values show areas that are CO_2 sinks. The difference yields a net global air–water CO_2 flux of 1.42 Pg-C year^{-1} (Takahashi et al. 2009)

uncertainty in the estimates for shallow coastal waters reflects the fact that environments in coastal waters are far more diverse than those in the open ocean and continental shelves. Although results of several studies of air–water CO$_2$ fluxes in shallow coastal waters have recently been reported, the estimates are far from constrained, and the mechanisms are now under discussion (Akhand et al. 2018; Kuwae et al. 2016; Otani and Endo 2018; Watanabe and Nakamura 2018). Because the absorption and release of atmospheric CO$_2$ in shallow coastal waters undergo extreme temporal and spatial fluctuations, a database of more extensive and intensive measurements in shallow coastal waters is needed to guide effective climate change mitigation using blue carbon ecosystems.

In this chapter, we first explain the theoretical background of air–water CO$_2$ flux measurements and methods for making those measurements. We then introduce examples of in situ measurements made in shallow coastal waters and analyses thereof, and we show that these waters can be sinks of atmospheric CO$_2$.

6.2   Theoretical Background of Air–Water CO$_2$ Fluxes

The methods of measuring air–water CO$_2$ fluxes can be assigned to one or the other of the following two approaches. The first approach is the direct measurement of the CO$_2$ flux, such as by a tracer method (e.g., Sweeney et al. 2007), the floating chamber method (e.g., Frankignoulle 1988), or the eddy covariance method (e.g., Lee et al. 2004). The other is indirect estimation using a theoretical model (Danckwerts 1951). The bulk formula method is the most general theoretical model. Although indirect estimation may be inaccurate in shallow coastal waters, indirect estimation has been used more than direct measurement methods because it is easy and less expensive. Furthermore, indirect estimation can reveal the environmental factors that affect the gas flux. We therefore first explain the theoretical background relevant to air–water gas fluxes. We then assess the bulk formula method as a representative indirect estimation method.

6.2.1   Thin–Film Model

There are several theoretical models of air–water CO$_2$ fluxes. Here, we describe a simple model called the "thin-film model". According to this model, just below the water surface there is a thin film, within which there is a CO$_2$ concentration gradient. That concentration gradient is used to determine the CO$_2$ flux (Fig. 6.2).

In this chapter, the terms "concentration" and "partial pressure" are frequently used; we briefly define them here. The former is the amount of a substance per unit volume, and the latter is the pressure of a gas. In the case of water, the concentration of a gas divided by its solubility equals the partial pressure. The air–water CO$_2$ flux can be determined from the difference between the partial pressures of CO$_2$ (pCO$_2$)
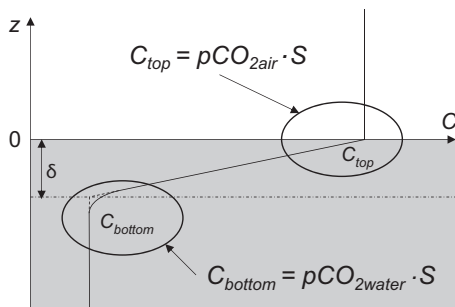
Fig. 6.2 Schematic diagram of the thin-film model. The horizontal axis shows the CO_2 concentration (C), and the vertical axis shows the vertical depth ($z = 0$ at water surface). This figure illustrates the case where the CO_2 concentration in water is lower than that in the atmosphere. In the thin-film model, the air–water CO_2 flux (F) is determined by multiplying the molecular diffusion coefficient of CO_2 (D) by the concentration gradient ($\partial C_{water}/\partial z$) in the boundary layer just below the water surface (Fick's law). This gradient is calculated from both the thickness (δ) of the boundary layer and the difference between C at the top of the layer (C_{top}) and C at the bottom of the layer (C_{bottom}). This model assumes that the top and bottom of the layer are in equilibrium with the partial pressure of CO_2 (pCO_2) in the atmosphere and water, respectively ($C_{top} = pCO_{2air} \cdot S$, $C_{bottom} = pCO_{2water} \cdot S$; where S is the solubility of CO_2). Whether the atmospheric CO_2 concentration and C_{top} are equal depends on the water temperature and salinity. This figure illustrates the case where their concentrations are equal

in the air and water. Strictly speaking, the air–water CO_2 flux should be calculated from the fugacity of CO_2 (fCO_2), which is the partial pressure of an ideal gas with the same chemical potential as the real gas. However, for the sake of simplicity no distinction between pCO_2 and fCO_2 has been made in this chapter. The difference in the estimated CO_2 fluxes would be very small (Weiss 1974).

The following assumptions are made in the thin-film model (Fig. 6.2): (1) pCO_2 at the top of the film is the same as atmospheric pCO_2, (2) pCO_2 at the bottom of the film is the same as that in water, and (3) the concentration gradient within the film is linear. Using these assumptions, the air–water CO_2 flux can be determined from the thickness of the film and the difference in pCO_2 between the air and water.

If the CO_2 concentrations at the top and bottom of the film are C_{top} and C_{bottom}, respectively, assumptions (1) and (2) lead to Eqs. 6.1 and 6.2.

$$C_{top} = pCO_{2top} \times S = pCO_{2air} \times S \tag{6.1}$$

$$C_{bottom} = pCO_{2bottom} \times S = pCO_{2water} \times S \tag{6.2}$$

In these equations, pCO_{2top} and $pCO_{2bottom}$ are the pCO_2 at the top and bottom of the film, respectively, and pCO_{2air} and pCO_{2water} are the pCO_2 in the atmosphere and in water deeper than the film, respectively. S is the CO_2 solubility in the water.

Under assumption (3), introduction of Fick's law and Eqs. 6.1 and 6.2 into the thin-film model gives the following equation.

$$F = -D\frac{\partial C_{water}}{\partial z} = -D\frac{\left(C_{top} - C_{bottom}\right)}{\delta} = -\frac{D}{\delta}S\left(pCO_{2air} - pCO_{2water}\right) \quad (6.3)$$
$$= -kS\left(pCO_{2air} - pCO_{2water}\right) = kS\left(pCO_{2water} - pCO_{2air}\right)$$

In this equation, F is the air–water CO$_2$ flux; a positive value indicates an efflux from the water into the atmosphere, and a negative value indicates an influx from the atmosphere into the water. D is the molecular diffusion coefficient of CO$_2$; δ is the thickness of the film; and k is called the "transfer velocity", which has dimensions of velocity and equals the ratio of the molecular diffusion coefficient D and the film thickness δ (i.e., $k = D/\delta$). Because the transfer velocity is strongly correlated with the wind speed at the water surface (see below), this parameter has frequently been estimated from wind speed in the bulk formula method.

Two aspects of Eq. 6.3 are noteworthy. First, because the solubility and transfer velocity are always positive, the direction of the CO$_2$ flux (efflux or influx) depends only on the difference in pCO$_2$ between air and water. In other words, whether seawater is a sink or source of atmospheric CO$_2$ can be determined by knowing only whether pCO_{2water} is lower or higher than pCO_{2air}, respectively. In most non-urban areas, atmospheric pCO$_2$ is around 400 μatm and is stable. This value can therefore be used as a threshold for the direction of the CO$_2$ flux.

Second, to estimate the magnitude of the CO$_2$ flux, it is necessary to determine the transfer velocity. In Eq. 6.3, the solubility and molecular diffusion coefficient of CO$_2$ can be calculated from the water temperature and salinity (Jähne et al. 1987; Weiss 1974). However, the film thickness is a hypothetical parameter of the thin-film model, and there is no practical measurement method. Therefore, a more advanced fluid dynamics model or an empirical estimation using directly measured CO$_2$ fluxes and other related parameters are required to calculate the transfer velocity. It is difficult to develop an advanced fluid dynamics model that is applicable to shallow coastal waters because there is no practical method for measuring the required turbulence parameter just below the water surface. In contrast, numerous empirical equations that use wind speed to estimate the transfer velocity have been proposed. Those equations have been applied mainly in the open ocean. Although the assumptions of the thin-film model do not apply under strong-wind conditions that cause whitecaps and direct CO$_2$ intrusion into water, a wind-dependent equation for estimating gas transfer velocity has been applied even under such conditions. The validity of such estimates is a subject of current discussions.

Interestingly, even models other than the thin-film model (such as the surface renewal model: Danckwerts 1951) eventually lead to an equation with the same form as Eq. 6.3. In these models, the transfer velocity is defined using other parameters, but the CO$_2$ flux can still be determined using the pCO$_2$ difference, the CO$_2$ solubility, and the transfer velocity.

In the following sections, we explain the determinants of the pCO_{2water} and transfer velocity, both of which are key parameters for the bulk formula method.

6.2.2   *pCO$_2$ and Carbonate Chemistry in Water*

The pCO_{2water} is influenced by several factors. First, even if the CO_2 concentration in water is constant, pCO_2 changes when the CO_2 solubility changes (Eq. 6.2). The solubility of a gas in water is the amount of the gas that can be dissolved in water under specified conditions, and it tends to decrease as the water temperature rises. This behavior reflects the fact that the dissolved gas molecules have higher kinetic energy (pressure) in warmer water, and a higher percentage of the molecules is able to escape from the water. This tendency applies to CO_2. The solubility therefore decreases and pCO_2 increases as the temperature increases (Fig. 6.3). The kinetic energy of atmospheric CO_2 also rises as the temperature rises, but the effect is not as great as the temperature effect on the kinetic energy of CO_2 molecules in water because CO_2 molecules in air already have a much higher kinetic energy than CO_2 molecules dissolved in water.

Changes of salinity also affect CO_2 solubility, but the influence of salinity is smaller than the effect of temperature in normal seawater. However salinity indirectly influences pCO_2 via changes of carbonate system equilibria; that effect (see below) is much stronger than the direct effect of salinity on solubility. This indirect salinity effect complicates carbonate chemistry in shallow coastal waters.

It is important to note here that HCO_3^- and CO_3^{2-} are present in water in addition to dissolved CO_2, and these ions partially compensate for changes of pCO_{2water}. There are two parameters related to the compensation process, dissolved inorganic carbon (DIC) and total alkalinity (TA). DIC is the sum of all inorganic carbon species dissolved in water: dissolved CO_2, HCO_3^-, and CO_3^{2-}. In the case of seawater, HCO_3^- accounts for more than 90% of DIC at typical seawater pH values. TA is determined by mineral components such as calcium ion (Ca^{2+}) and magnesium ion (Mg^{2+}) in water. Dickson et al. (2007) give an accurate and precise definition of TA. TA gives a rough indication of the potential amount of dissolved CO_2 that can dissociate into bicarbonate or carbonate ions. To be more specific, TA indicates the excess positive electrical charge contributed by the conservative cations (e.g., Ca^{2+}, Mg^{2+}, K^+, and Na^+) versus the conservative anions (e.g., Cl^- and SO_4^{2-}). When the excess positive charge is large, a greater percentage of DIC is in the form of negative bicarbonate and carbonate ions so that positive and negative charges are in balance. As a result, the pCO_2 in high-TA water tends to decrease (Fig. 6.3). Furthermore, the buffer capacity against changes of pCO_2 is greater in high-TA water. The pCO_2 affects the air–water CO_2 flux, but carbonate and bicarbonate ions do not because they are electrically isolated in water. Water therefore tends to be an atmospheric sink for CO_2 if the TA is high, even if the DIC is also high.

Biological processes such as photosynthesis, respiration, and remineralization also change pCO_{2water} by changing the distribution of carbonate species in the water. Photosynthesis and respiration/remineralization basically change only DIC, but calcification (i.e., formation of the calcium carbonate that makes up the hard parts of organisms such as corals, foraminifera, pteropods, and coccolithophores) changes
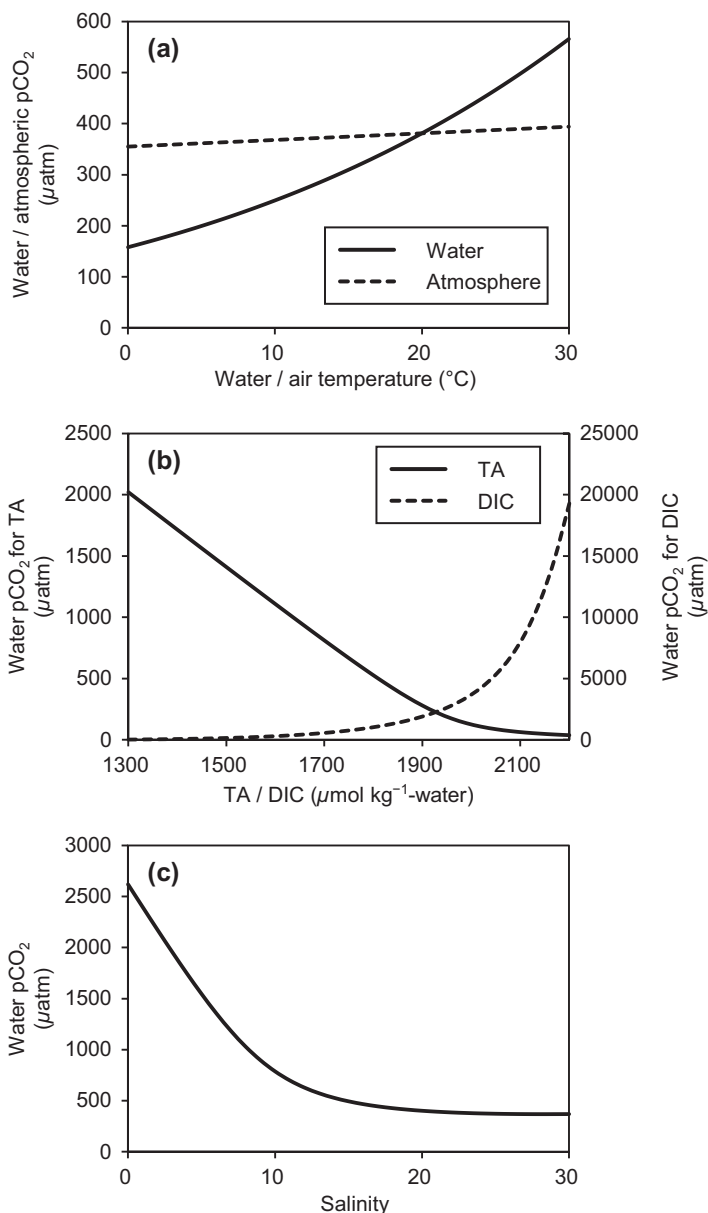
Fig. 6.3 Physical and chemical parameters used to determine CO_2 partial pressure (pCO_2) in water. (**a**) Changes in pCO_2 due to changes in water or atmospheric temperature assuming that CO_2 concentration is constant. Computational conditions: water temperature, variable; TA, 2200 μmol kg^{-1}-water; DIC, 1950 μmol kg^{-1}-water; salinity, 35; air temperature, variable; atmospheric CO_2 concentration, 15.85 mmol m^{-3}; atmospheric pressure, 1 atm. (**b**) Change in pCO_2 in water due to changes in total alkalinity (TA) and dissolved inorganic carbon concentration (DIC). Computational conditions: DIC, variable; TA, 2200 μmol kg^{-1}-water; water temperature, 20 °C; salinity, 35; TA, variable; DIC, 1950 μmol kg^{-1}-water; water temperature, 20 °C; salinity, 35. (**c**) Changes in pCO_2 in water due to changes in salinity assuming that TA and DIC also change because of salinity. Computational conditions: water temperature, 20 °C; river end member: salinity, 0; TA, 800 μmol kg^{-1}-water; DIC, 850 μmol kg^{-1}-water; marine end member: salinity, 35; TA, 2200 μmol kg^{-1}-water; DIC, 1950 μmol kg^{-1}-water

both DIC and TA. Because the influence of calcification on pCO_2 is very complicated, we elaborate on calcification effects in Sect. 6.4.3.

Salinity is closely correlated with DIC and TA and thus has a strong indirect effect on pCO_{2water}. The correlation reflects the fact that bicarbonate, which is the major contributor to both DIC and TA, is among the major anions in seawater. Freshwater with low concentrations of calcium and magnesium cations is characterized as soft water and, in order to maintain charge neutrality, contains low concentrations of bicarbonate and carbonate anions. Hence, DIC and TA of soft water arelow. Conversely, DIC and TA of hard water are high, because hard water contains high concentrations of calcium and magnesium ions. In shallow coastal waters where freshwater and seawater are mixed, changes of salinity and hence pCO_{2water} reflect dynamic environmental factors such as tides and river discharge. The pCO_{2water} in shallow coastal waters is also affected by temporal and spatial variations of both DIC and TA of freshwater.

In summary, pCO_{2water} is determined by complex interactions involving the carbonate system, which is affected by parameters such as water temperature and salinity as well as by processes such as photosynthesis, respiration, calcification, terrestrial runoff, and tidal exchange. Because it is very difficult to precisely determine pCO_{2water} via indirect methods, pCO_{2water} is generally measured directly with specialized sensors or determined on the basis of chemical analyses of water samples (see Sect. 6.3).

6.2.3 Transfer Velocity

The transfer velocity is the ratio of the CO_2 molecular diffusion coefficient to the film thickness in the thin-film model. The correlation between the transfer velocity and the wind speed at the water surface has been investigated by using direct measurements of CO_2 fluxes in the ocean and in large lakes such as the Great Lakes. The following is the most commonly used empirical equation for the transfer velocity as a function of wind speed (Wanninkhof 1992).

$$k = 0.39 \times U_{10}{}^2 \times \left(Sc \big/ 660 \right)^{-0.5} \tag{6.4}$$

In Eq. 6.4, U_{10} is the wind speed at an altitude of 10 m above the water surface. Because the vertical profile of wind speed near the water surface can be approximated by a logarithmic relationship (e.g., Kondo 2000), U_{10} can be calculated with observational data recorded by an anemometer at the site or obtained from a public database. The parameter Sc, called the "Schmidt number", is defined by the relationship between the turbulence near the water surface and the thickness of the boundary layer of solute concentrations. In Eq. 6.4, the gas transfer velocity is expressed under the assumption that the temperature of seawater is 20 °C, at which the Sc is 660, before the correction by on-site Sc. In the case of freshwater and sea-

water, an empirical equation for *Sc* as a function of water temperature has been proposed for various gases, including CO$_2$ (Jähne et al. 1987). The transfer velocity for gases other than CO$_2$ (e.g., O$_2$) can also be calculated with Eq. 6.4.

Some problems have also been pointed out with the estimates of gas transfer velocity. One problem is their reliability under strong-wind conditions. The thin-film model should obviously not be applied under strong-wind conditions when whitecaps occur on the water surface. The bulk formula method has been used under such conditions because empirical observations have revealed a high correlation between wind speed and gas transfer velocity. However, the correlation between the transfer velocity and wind speed under extremely strong wind conditions, when the field survey is difficult to be performed, has not been sufficiently evaluated, and the gas transfer velocity estimates are unreliable because the gas flux is difficult to measure directly. Although such strong wind conditions occur infrequently, the CO$_2$ flux under such conditions would be expected to have a significant influence on the global CO$_2$ flux because the transfer velocity would be very high.

Another problem is that most empirical equations (e.g., Eq. 6.4) have been constructed by using data from observations made in the open ocean and large lakes. Wind and current effects on the surfaces of coastal waters are likely to differ from those on open-water surfaces (Tokoro et al. 2007, 2008).

6.3 Methods for CO$_2$ Flux Measurements

6.3.1 Bulk Formula Method

Estimates of air–water CO$_2$ fluxes can be made with the bulk formula method once values have been assigned to the parameters in Eq. 6.3. Because pCO_{2water} can be modeled with parameters such as water temperature and chlorophyll *a* concentrations that are easy to obtain for the open ocean, the bulk formula method has become the standard way to estimate global CO$_2$ fluxes between the atmosphere and ocean (Fig. 6.1, Takahashi et al. 2009). Although CO$_2$ fluxes are more difficult to estimate in shallow coastal areas, the bulk formula method has also been used in many previous studies in such areas because of its simplicity and low cost. However, because the bulk formula method can provide estimates only at fixed points and in the instant of time, much effort is required to evaluate temporal and spatial variations. Unlike direct measurement methods, the bulk formula method can be used to infer the factors that regulate air–water CO$_2$ fluxes because it uses an equation that includes biochemical (pCO_{2water}) and physical (transfer velocity) terms.

The value of pCO_{2water}, which is a key parameter in the bulk formula method, can be determined from in situ measurements using sensors or from chemical analyses of water samples (Fig. 6.4). The non-dispersive infrared (NDIR) method is the infrared absorptiometry, and commonly used with sensors. With NDIR, the value of pCO_{2water} is determined from the extent of infrared (IR) absorption of an equilibrated
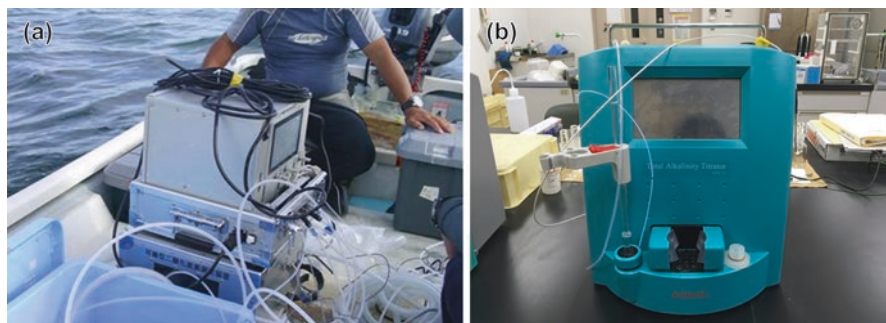
Fig. 6.4 Methods for measuring the CO_2 partial pressure (pCO_2) in water for indirectly estimating air–water CO_2 flux using the bulk formula method. (**a**) pCO_2 meter with a nondispersive infrared sensor. (**b**): instrument for chemical analysis of water samples

air sample. Because the NDIR method can be used only for a sample of gas (water itself absorbs IR strongly), an atomizer or equilibration device such as a membrane filter that passes air must be used to generate gas with the same pCO_2 as the water sample. A problem with this method is that a sensor with sufficient precision (several microatmospheres or less) is expensive.

There are roughly two approaches to calculating pCO_{2water} using the chemical parameters of a water sample. The first approach is to calculate pCO_{2water} from DIC, TA, and pH (Zeebe and Wolf-Gladrow 2001). Water samples for DIC and TA analyses should be collected in hermetically sealed, gas-impermeable, thick glass bottles. DIC and TA are determined via a potentiometric titration procedure with a solution of hydrochloric acid (Dickson et al. 2007). The value of pCO_{2water} is calculated using the chemical equilibrium relationships between DIC and TA. The value of pCO_{2water} can also be calculated from the combination of pH with either DIC or TA. The pH can be measured with a pH probe. However, a highly accurate pH sensor is necessary because the pH measurement must be accurate to ±0.001 or less. In addition, the pH sensors should be based on the Total pH scale, not NBS scale (Hansson 1973). In other words, the pH sensor should be calibrated by saline standards (e.g., Tris-buffered saline or seawater samples of which the TA and DIC are known), not by common unsalted standards like phosphate buffers. The second approach is to estimate pCO_{2water} from salinity and pH. This method can be applied in places where TA is strongly correlated with salinity because under such conditions calcification and dissolution processes are negligible. The first approach yields highly accurate estimates of pCO_{2water}, but the cost and effort required for water sampling are disadvantages. The second approach enables a long time series of measurements via installation of salinity and pH sensors in situ, but it is less accurate than the first approach.

The value of pCO_{2air} can be directly measured in situ with a sensor using the NDIR method. Representative values from the literature can also be adopted because pCO_{2air} does not fluctuate greatly in less than decadal scales. During the 1980s and 1990s, it was common to use approximately 360 ppm as a representative value, but

recent studies have used higher values (approximately 400 ppm) because atmospheric CO_2 concentrations have been increasing at 10–15 ppm per decade as a result of anthropogenic releases of CO_2.

6.3.2   Direct Measurement Methods for Air–Water CO_2 Fluxes

There are advantages to using direct methods for measuring CO_2 fluxes in shallow coastal waters because the accuracies of indirect methods such as the bulk-formula method are compromised by the difficulty of accurately estimating transfer velocities in shallow coastal waters (see Sect. 6.2.3). However, most of the direct measurement methods require more expensive instruments and greater technical expertise than the bulk formula method. The cost and spatiotemporal coverage of the fluxes vary among the direct measurement methods.

The tracer method uses chemical tracers to provide estimates of air–water gas fluxes that are easily quantifiable and recalcitrant to decomposition. A commonly used tracer is ^{14}C. Prior to atmospheric bomb testing during the 1950s, ^{14}C was a very small fraction of naturally occurring carbon. In recent years, however, ^{14}C has been widely used as a tracer of atmospheric CO_2 and has been used to estimate regional and global CO_2 fluxes in the ocean (e.g., Sweeney et al. 2007; Wanninkhof 1992). Sulfur hexafluoride (SF_6) has also been used as a gas tracer in the ocean (e.g., Watson et al. 1991). SF_6 is artificially injected into the water, and the CO_2 flux is calculated from the rate of change of the SF_6 concentration. Correction for the dilution effect of the water mass is made by using another concurrently injected gas (e.g., ^3He) that has a different transfer velocity. The relationship between the transfer velocity and wind speed (Eq. 6.4) has been determined mainly from gas tracer studies. A disadvantage of the tracer method is that CO_2 gas fluxes can be measured only as long-term and area-wide average values. The tracer method is therefore not suitable for detecting diurnal fluctuations of CO_2 fluxes. Application of the tracer method to shallow coastal waters is also limited by the fact that shallow coastal waters consist of heterogeneous water bodies.

The floating chamber method estimates CO_2 fluxes from continuous measurements of CO_2 concentrations made inside a chamber floating on the water surface (Fig. 6.5). This method is designed to directly measure CO_2 fluxes in shallow coastal waters (e.g., Frankignoulle 1988; Tokoro et al. 2007). However, there is no wind inside the chamber, and although the wind blowing against the chamber may cause the chamber to move relative to the water and thereby generate artificial turbulence, the measured flux may be biased from the true flux. Unlike other direct methods, this method is poor at measuring long-term fluxes over wide areas. Despite acknowledging these problems, some authors have concluded that the floating chamber method is suitable for shallow coastal waters (Tokoro et al. 2007, 2014).

The eddy covariance method is one meteorological method for measuring the transfers of gas and heat by atmospheric turbulence (Fig. 6.6). This method has been used mainly to measure CO_2 fluxes between the air and terrestrial ecosystems
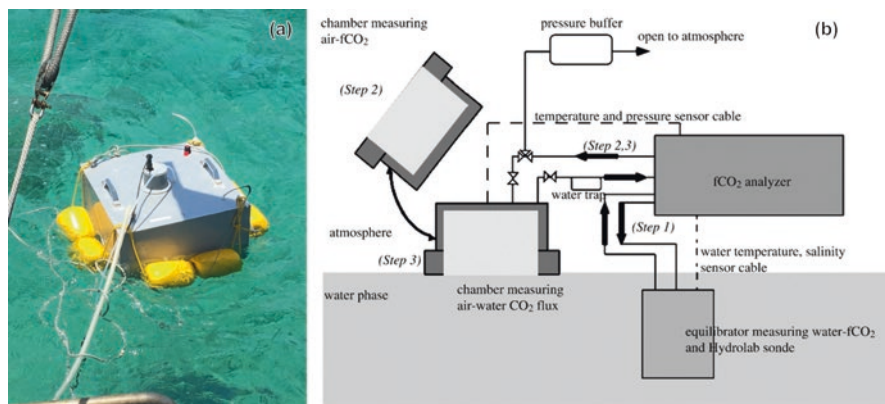
Fig. 6.5 The floating chamber method for directly measuring air–water CO_2 fluxes. (**a**) Photograph of a floating chamber. (**b**) Flow diagram of the chamber system (Tokoro et al. 2007). The air in the chamber is circulated through a pCO_2 meter with a nondispersive infrared sensor on the ship (same as in Fig. 6.4a); pCO_2 can be continuously measured. (*Step 1*) Ambient water pCO_2 is measured using an equilibrator. (*Step 2*) The atmospheric pCO_2 is measured using a chamber that is open to the atmosphere. (*Step 3*) Air–water CO_2 flux is measured using a chamber floating on the water surface. The measurement time should be set to about 20–30 min because the internal temperature and pressure change over time. The internal temperature and pressure are simultaneously monitored and are used to correct the CO_2 concentration inside the chamber

(Baldocchi 2008) and O_2 fluxes between the water and benthic systems (Berg et al. 2003; Kuwae et al. 2006). The CO_2 flux at the atmospheric interface can be quantified by measuring the CO_2 concentration and wind velocity at very high frequencies (more than 10 Hz). Details of the procedures can be found in Lee et al. (2004). The measurement length (footprint) of the eddy covariance method is on the order of several hundred meters to several kilometers in the windward direction, although the length depends on the installation altitude and environmental conditions such as wind speed and roughness at the interface. The wide area of the footprint and the unmanned nature of the operation enable long-term measurements to be made over wide areas. However, the eddy covariance method requires very expensive instruments and advanced post-processing techniques. Especially in aquatic environments, the raw data may contain low quality signals because of the spatiotemporal variations of the water and air masses (e.g., the heterogeneity of water and atmosphere). The post-processing procedure for quality control of the data has been improved to address these issues (e.g, Tokoro and Kuwae 2015, 2018).

Other meteorological methods have been proposed to measure long-term CO_2 fluxes over wide areas. Although they have not been used as much as the eddy covariance method, they are potentially easy-to-use alternatives to the eddy covariance method. The relaxed eddy accumulation method, which was derived from the eddy accumulation method, can potentially be applied to atmospheric species for which fast-response sensors are unavailable (Baldocchi 2014; Businger and Oncley 1990). The concentrations are measured separately in updraft and downdraft reservoirs
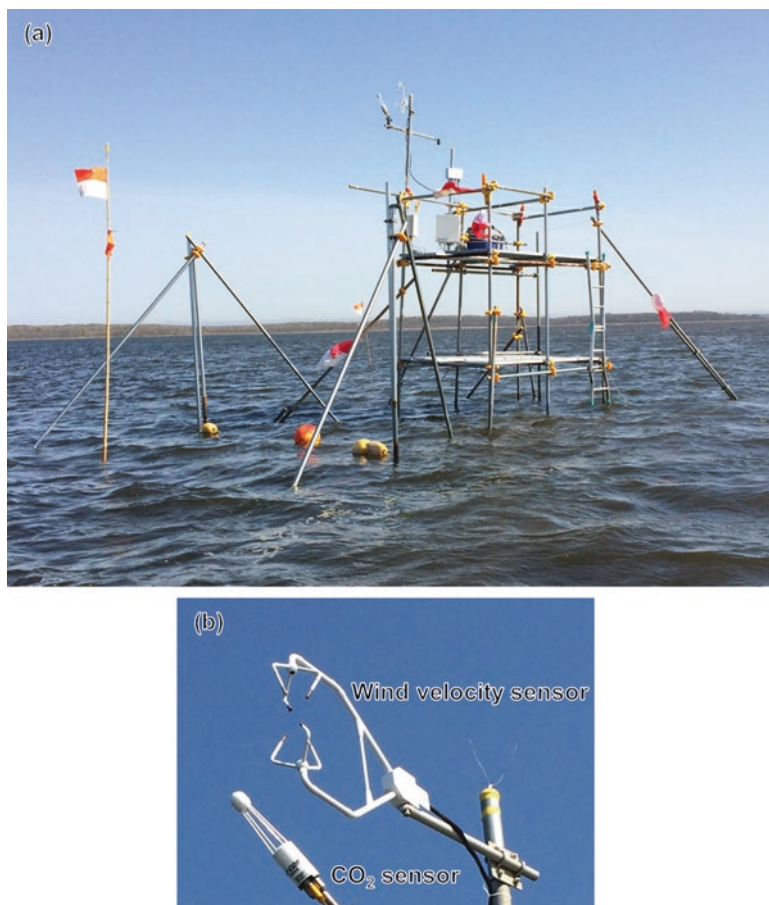
Fig. 6.6 Eddy covariance method for directly measuring air–water CO$_2$ flux. (**a**) Platform for installing the measurement system. In the photograph, the CO$_2$ sensor, wind velocimeter, data loggers, batteries, and solar panels have been installed. (**b**) The sensors for measuring atmospheric CO$_2$ concentration and wind velocity. Both devices can collect high-frequency data (10–20 Hz). The CO$_2$ gas flux is determined from the covariance between the atmospheric CO$_2$ concentration and the vertical wind speed with technical corrections

based on the vertical direction of the wind velocity, and then the flux is calculated from the difference of the average concentrations in the downdrafts and updrafts. Although the calculation and sampling methodologies need to be refined for highly precise estimates, this method has merit because it is relatively inexpensive compared to the cost of most fast-response sensors. In addition, Lemaire et al. (2017) have evaluated the possibility of its application to sediment–water fluxes.

The flux gradient method (e.g., Meyers et al. 1996) calculates the gas flux from the vertical gradient of atmospheric CO$_2$ concentrations and a parameter that characterizes turbulence. The instrumentation required for this method is inexpensive

because there is no need for fast-response sensors. However, the eddy diffusion coefficient, which is the metric of turbulence for this method, is difficult to estimate accurately.

Because there are advantages and disadvantages to each method, there is no perfect method for determining the true values of air–water CO_2 fluxes over any spatial and temporal scales. It is thus important to apply multiple methods to estimate air–water CO_2 fluxes in shallow coastal waters. When a discrepancy between fluxes measured by these different methods is reported, especially in aquatic environments, elucidation of the causes of the discrepancy will be an important subject of future research.

6.3.3 Direct Measurement Methods of Air–Ecosystem CO_2 Flux

Although we focus on the air–water CO_2 flux in this chapter, we also briefly introduce methods for measuring air–non-water (ecosystem) CO_2 fluxes because of their relevance to some blue carbon ecosystems such as mangroves and saltmarshes. CO_2 fluxes between the air and mangrove/saltmarsh ecosystems, which are exposed to the atmosphere, obviously cannot be estimated by the bulk formula method. Direct measurement methods have therefore been applied to determine the fluxes (Akhand et al. 2018; Otani and Endo 2018).

The benthic chamber method is a common method for measuring air–ecosystem CO_2 fluxes. The floating chamber method is analogous to this method, and the two methods are based on a common principle. The methodology of the benthic chamber is more established than the floating chamber methodology, and benthic chambers are commercially available (e.g., Li-8100A, LI-COR, Nebraska, USA).

The eddy covariance method and other micro-meteorological methods have also been applied to air–terrestrial ecosystem CO_2 fluxes (e.g., FLUXNET, Baldocchi 2008). The terrestrial application was somewhat earlier than the aquatic application. The methodology is the same for estimating air–terrestrial ecosystem and air–water fluxes. Because terrestrial CO_2 fluxes are generally more than an order of magnitude larger than air–water fluxes, the post-processing procedures for terrestrial CO_2 fluxes tend to be easier than those for air–water fluxes.

Like the methods for air–water fluxes, the methods for air–ecosystem fluxes cover different spatial and temporal scales and should be applied in combination. The eddy covariance method can be used to measure the net flux from all components of a mangrove/saltmarsh ecosystem. Although the air–vegetation CO_2 flux and air–soil CO_2 flux should be quite different, the eddy covariance method cannot quantify the contributions of soils and vegetation separately. In this case, the benthic chamber method should also be used to measure the air–soil flux, and the contribution of vegetation can be estimated from the difference between the fluxes estimated by the eddy covariance and benthic chamber methods.

6.4   Air–Water CO$_2$ Flux in Shallow Coastal Waters

An increasing number of measurements of CO$_2$ fluxes between the atmosphere and shallow coastal waters have recently been made in seagrass meadows (Kone et al. 2009; Maher and Eyre 2012; Tokoro et al. 2014; Tokoro and Kuwae 2018), macroalgal beds (Ikawa and Oechel 2014), mangroves (Borges et al. 2003; Akhand et al. 2016, 2018), tidal flats (Otani and Endo 2018), saltmarshes (Otani and Endo 2018), and coral reefs (Watanabe et al. 2013; Watanabe and Nakamura 2018). Additional measurements will be necessary to reveal the factors that regulate CO$_2$ fluxes and to predict future changes in those fluxes. In this section, we discuss results of some studies of air–water CO$_2$ fluxes in shallow coastal waters as practical examples of the measurement methods.

6.4.1   Air–Water CO$_2$ Fluxes in Seagrass Meadows: Combined Measurements Using Multiple Methods

Here, we show empirical studies of air–water CO$_2$ fluxes and the factors that regulate them in seagrass meadows based on the use of multiple methods (Tokoro et al. 2014, Tokoro and Kuwae 2015, 2018). These studies were conducted in Furen Lagoon, which is located on the east coast of Hokkaido, Japan (Fig. 6.7). Furen Lagoon has an area of 57.4 km^2, and its water is brackish. Most of the lagoon is shallower than 1 m, and eelgrass meadows (dominant species: *Zostera marina*) cover 70% of the bottom. Organic carbon dynamics in the lagoon have been reported elsewhere (Watanabe and Kuwae 2015b). Three methods (bulk formula method, floating chamber method, and eddy covariance method) were used to measure the air–water CO$_2$ fluxes.

The results showed that the air–water CO$_2$ fluxes varied seasonally (Figs. 6.8, 6.9, and 6.10). The system was a sink of atmospheric CO$_2$ during the summer and a small source during the winter. The annual average CO$_2$ flux was negative, i.e., the eelgrass meadows functioned as a net CO$_2$ sink over the course of 1 year (Fig. 6.10).

Diurnal changes of air–water CO$_2$ fluxes were clearly identified by both the bulk formula and floating chamber methods (Fig. 6.8), whereas the seasonal variations were recorded by the eddy covariance method and bulk formula method (Figs. 6.9 and 6.10). The results of the eddy covariance method included some time intervals when data were lacking because the post processing filtered out some low quality data. The post-processing procedure for the eddy covariance method is still in the development stage (Tokoro and Kuwae 2018).

Results of conventional studies have indicated that estuarine systems are net sources of CO$_2$ to the atmosphere because of the input of DIC and organic carbon from terrestrial systems (e.g., Cai 2011; Laruelle et al. 2010; Regnier et al. 2013). However, air–water CO$_2$ fluxes estimated with multiple methods in this case showed that seagrass meadows were atmospheric CO$_2$ sinks. As mentioned in Sect. 6.2, the
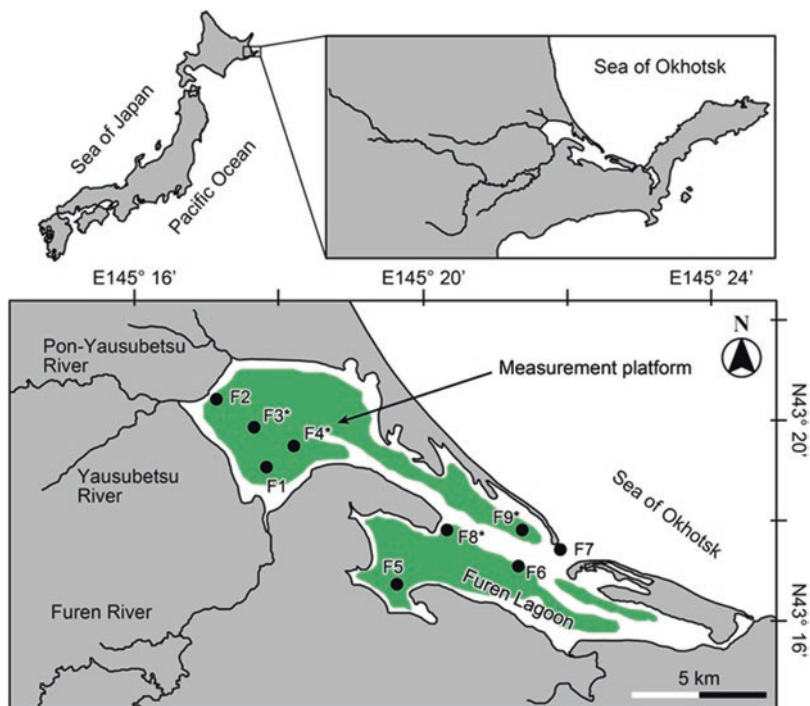
Fig. 6.7 Location of Furen Lagoon in eastern Hokkaido, Japan, and observation sites. The green-shaded areas indicate eelgrass meadows. The western part of the lagoon receives freshwater from several rivers. Long-term measurement by the eddy covariance system was performed at station F4. Direct uptake of atmospheric CO_2 by eelgrass was demonstrated using the samples collected at stations F1–F7. Eelgrass samples were collected at stations F3, F4, F8, and F9 (marked with *)

value of pCO_{2water} determines whether the system is a sink or source of atmospheric CO_2. Factors that control the pCO_{2water} therefore have a major effect on the sink/source behavior.

In Furen Lagoon, net ecosystem production (NEP) is the key factor that controls the air–water CO_2 flux (Fig. 6.11). Observed values of DIC, which is changed by the NEP and regulates the pCO_{2water}, have been compared with the DIC estimated from the conservative mixing line (determined from salinity) of both the riverine and coastal endmembers. The estimated value can be assumed to be DIC when the NEP is zero, and the pCO_{2water} without NEP can be calculated by the estimated DIC (the TA can be assumed to be independent from any ecosystem activities in this site). The pCO_{2water} without NEP was higher than both the observed pCO_2 and atmospheric pCO_2. This result shows that the seagrass ecosystem changed the lagoon from a source to a sink of CO_2. The fact that the decrease of DIC with NEP continued at night indicates that the reduction of DIC by photosynthesis during the day exceeded the increase of DIC due to respiration and decomposition at night. The significant correlation between the air–water CO_2 flux and the change of DIC

Fig. 6.8 Diurnal air–water CO_2 fluxes measured by bulk formula method and floating chamber method. (**a**) Furen Lagoon in summer (bulk formula: -0.12 ± 0.09 μmol-C m^2 s^{-1}; floating chamber: -0.07 ± 0.03 μmol-C m^2 s^{-1}, mean $\pm$ 95% confidence interval). (**b**) Furen Lagoon in winter (bulk formula: 0.01 ± 0.01 μmol-C m^2 s^{-1}; floating chamber: 0.06 ± 0.10 μmol-C m^2 s^{-1}, mean $\pm$ 95% confidence interval). Negative fluxes indicate CO_2 uptake, and positive fluxes indicate CO_2 emission. Shading indicates nighttime. (Tokoro et al. 2014)
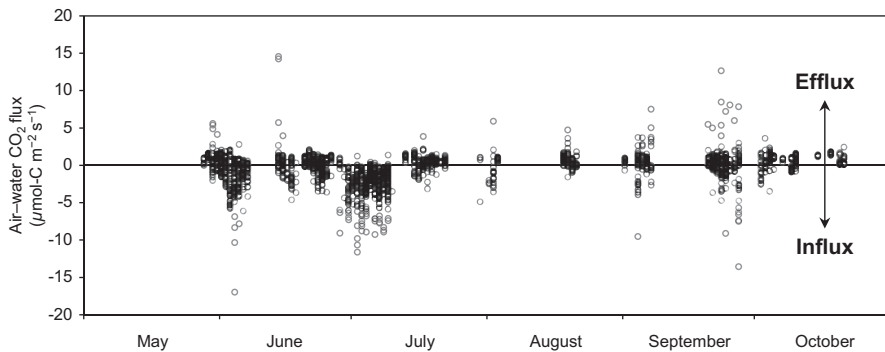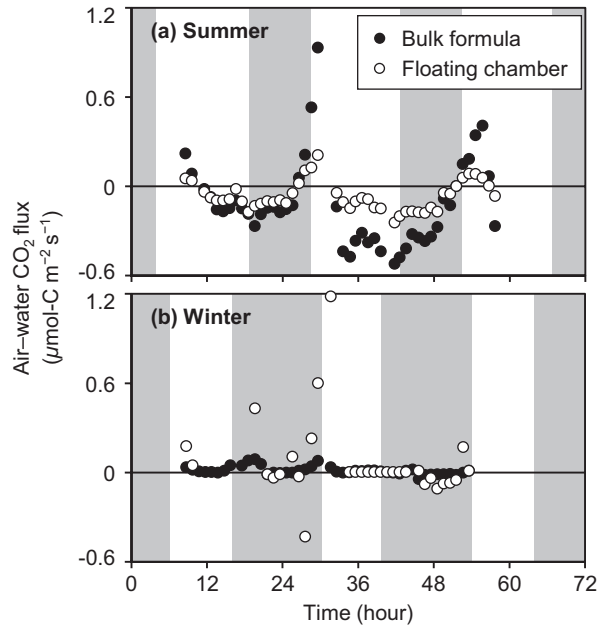
Fig. 6.9 Air–water CO_2 flux measured by the eddy covariance method in Furen Lagoon from 28 May to 21 October 2014 except for the ice-covered period from November to April. Negative fluxes indicate CO_2 uptake, and positive fluxes indicate CO_2 emission. Calculation processing was applied to correct for long-term fluctuations. (Tokoro and Kuwae 2018)

(ΔDIC) due to biogeochemical processes such as ecosystem production and respiration (positive ΔDIC, heterotrophy; negative ΔDIC, autotrophy) also supports the importance of NEP as a key regulating factor (Fig. 6.12).

These results imply that conservation and restoration of strongly autotrophic coastal vegetated habitats have the potential to serve as an effective way to mitigate the adverse effects of anthropogenic CO_2 emissions.
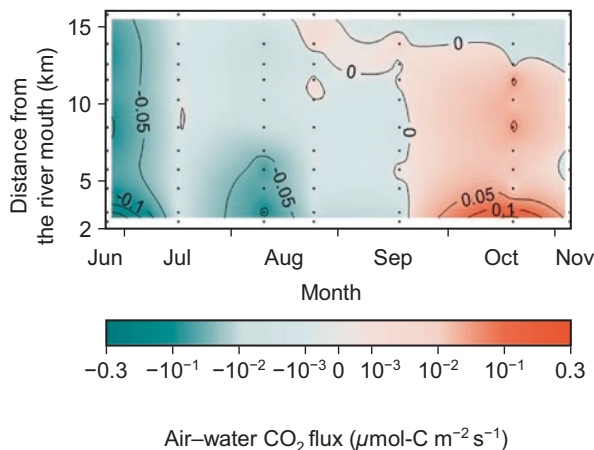
Fig. 6.10 Seasonal changes in air–water CO_2 flux in Furen Lagoon. Seasonal measurements by the bulk formula method were conducted from June to November 2011. Negative fluxes (uptake of CO_2 into water) are indicated by blue, and positive fluxes (efflux of CO_2 from water) by red. The fact that the annual average of the air–water CO_2 flux was negative ($-1.76 \times 10^{-2} \pm 1.50 \times 10^{-2}$ μ mol-C m^{-2} s^{-1}) indicates that the lagoon was a net sink of atmospheric CO_2. (Tokoro et al. 2014)

6.4.2 Air–Water CO_2 Fluxes in Macroalgal Beds

Beds of macroalgae such as *Sargassum* and kelp have limited capacity to store organic carbon in their substrata because they do not develop their own organic-rich sediment. However, recent studies have suggested that they act as "carbon donors" to receiver sites, where the organic carbon accumulates (Duarte et al. 2017; Hill et al. 2015; Krause-Jensen and Duarte 2016). The fact that macroalgal beds are among the most productive of shallow coastal ecosystems (Yoshida et al., 2018) indicates that macroalgal beds have the potential to serve as a direct sink of atmospheric CO_2 (Krause-Jensen and Duarte 2016). However, few empirical measurements have been made of the sink/source behavior of macroalgal beds (Ikawa and Oechel, 2014). Here, we demonstrate that macroalgal beds can contribute to the absorption of atmospheric CO_2 based on in situ measurement in the Seto Inland Sea in western Japan.

To examine the sink/source behavior of the macroalgal bed, pCO_{2water}, DIC, and dissolved organic carbon (DOC) were measured in the *Sargassum* bed and in adjacent waters without vegetation. The DIC concentration was lower in the *Sargassum* bed than in the adjacent waters (Fig. 6.13). Conversely, the DOC concentration was higher in the *Sargassum* bed. These results indicate that the *Sargassum* bed was autotrophic and that DOC was released by the *Sargassum* bed. The pCO_{2water} was

Fig. 6.11 Diurnal cycle of (**a**) observed pCO$_2$ (strictly, fCO$_2$) in the water and estimated pCO$_2$ in the water under the assumption that the net ecosystem production (NEP) was zero (pCO$_2$ without NEP) in Furen Lagoon in summer 2010. Parameters related to pCO$_2$ in the water, such as (**b**) DIC (observed DIC and DIC without NEP), and (**c**) water temperature and salinity are also presented. Shading indicates nighttime. (Tokoro et al. 2014)
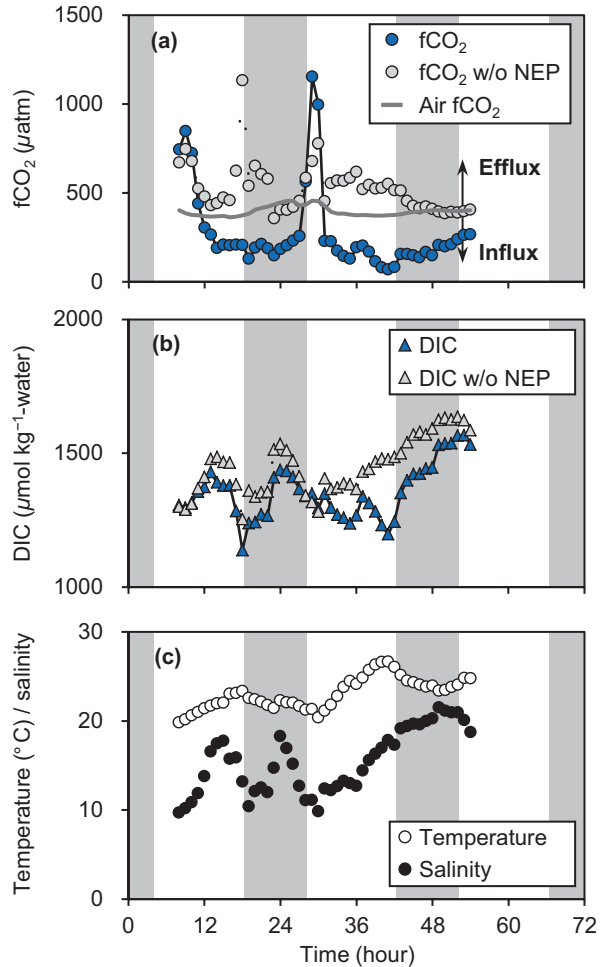
lower in the *Sargassum* bed than in the adjacent waters. Given that the atmospheric pCO$_2$ ranged from 360 to 400 μatm, the adjacent waters, which were originally CO$_2$ neutral to the atmosphere, changed to CO$_2$ sinks over the *Sargassum* bed.

A previous study also demonstrated using the eddy covariance method that a giant kelp bed off the Californian coast absorbs atmospheric CO$_2$ (Ikawa and Oechel 2014). Future studies should fill the spatial and temporal gaps in the observations and will contribute to a better understanding of the role of macroalgal beds as CO$_2$ sinks.
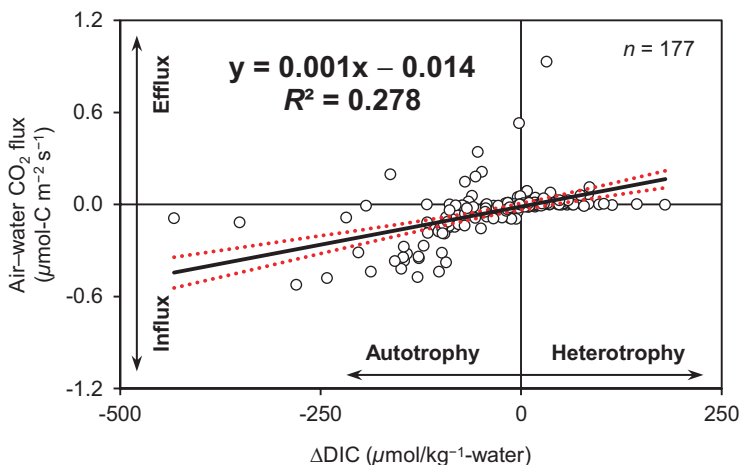
Fig. 6.12 Relationship between air–water CO_2 flux and ΔDIC ($n = 170$) at boreal and temperate sites in Japan. ΔDIC is the difference between the observed DIC value and the value estimated from the mixing ratio and the effect of calcification. ΔDIC thus indicates the extent of biogeochemical processes such as ecosystem production and respiration (positive, heterotrophy; negative, autotrophy). Air–water CO_2 fluxes, including both the monthly and diurnal data, were measured by using the bulk formula method. The 95% confidence limits to the regression line are indicated by the red dashed curves. (Tokoro et al. 2014)

6.4.3 Air–Water CO_2 Fluxes over Coral Reefs: Effects of Calcification and Dissolution Processes

The calcification and dissolution of calcium carbonate (e.g., coral skeletons, foraminiferal tests, pteropod shells, coccolithophores) exert a substantial control on pCO_{2water} in addition to photosynthesis, respiration, and remineralization, especially on coral reefs. Recent studies have proposed that calcium carbonate cycling should be accounted for in evaluating the carbon sequestration potential of blue carbon ecosystems (Howard et al. 2017; Macreadie et al. 2017). In this section, basic concepts concerned with air–water CO_2 fluxes and pCO_{2water} over coral reefs are briefly explained. For a comprehensive review, see Chap. 10 (Watanabe and Nakamura, 2018).

The calcification process increases pCO_{2water} according to the following equation.

$$Ca^{2+} + 2HCO_3^- \rightarrow CaCO_3 + CO_2 + H_2O \qquad (6.5)$$

The calcification process consumes calcium ions in water and decreases TA. As already noted (Sect. 6.2.2), TA is a parameter that reflects the potential of dissolved CO_2 to convert into bicarbonate and carbonate ions. A decrease of TA thus reflects a conversion of these ions into dissolved CO_2 and an increase of pCO_{2water}. This
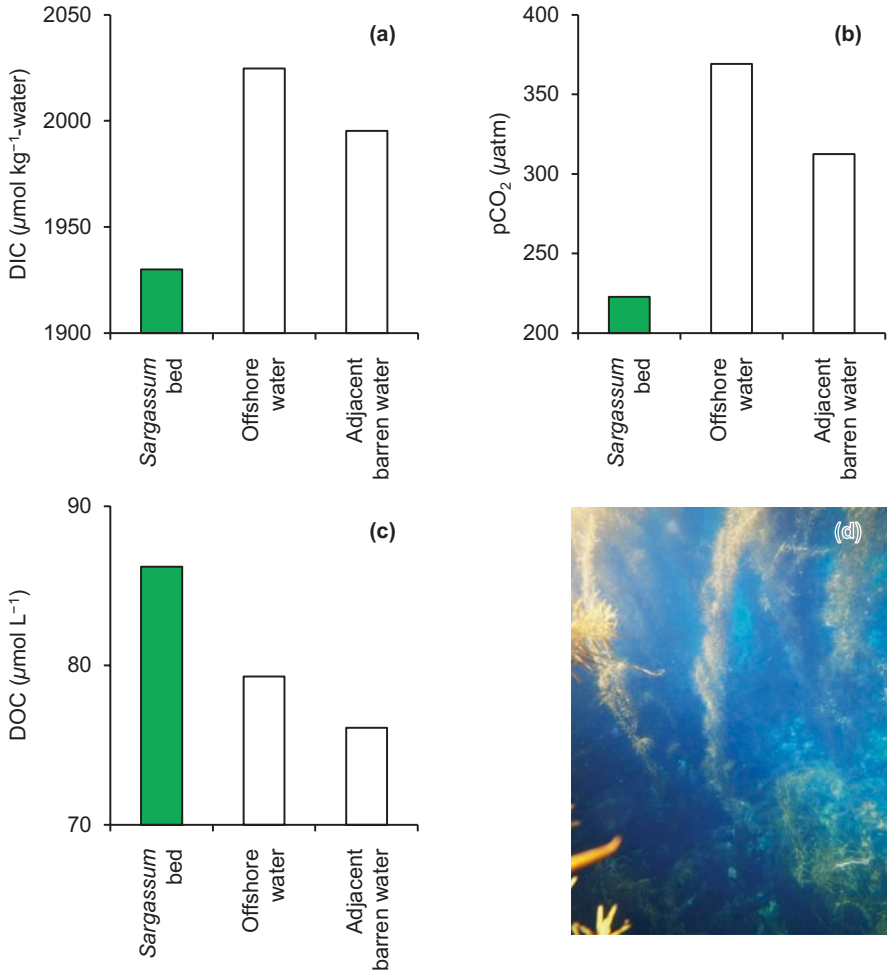
Fig. 6.13 (**a**) DIC, (**b**) pCO$_2$, and (**c**) DOC in a *Sargassum* bed, adjacent barren (no *Sargassum*) water, and offshore water in the Seto Inland Sea, Japan. In the *Sargassum* bed (depth of water: 2.7 m), *Sargassum horneri* was the dominant species and reached a length of more than 3 m (**d**). The adjacent barren water was located 200 m away from the *Sargassum* bed, and the water depth was comparable to the bed. The offshore water (depth of water, 12.7 m) was located 5 km from the bed

effect on pCO_{2water} is greater than the effect of the DIC decrease due to calcification.

In contrast, primary producers (zooxanthellae, seagrasses, and algae) consume DIC via photosynthesis and thus reduce pCO_{2water}. The balance between calcification/dissolution and photosynthesis/remineralization determines whether the ecosystem is a CO$_2$ sink or source. Previous studies have suggested that a photosynthesis/calcification ratio of about 0.6 is the boundary between an increase or decrease of

Fig. 6.14 The balance between photosynthesis (organic carbon production) and calcification (inorganic carbon production) regulates the CO_2 sink/source behavior of coral reefs. The white area indicates the sink, and the shaded area indicates the source. R_{OI} represents the photosynthesis/calcification ratio. (Suzuki and Kawahata 2004)
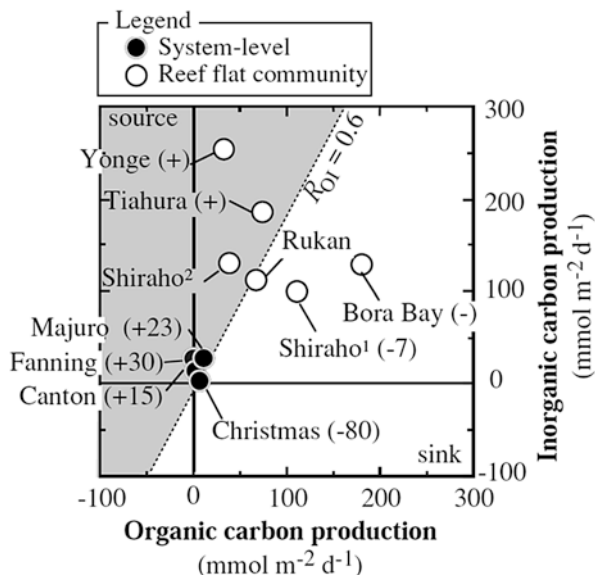
pCO_{2water} (Frankignoulle et al. 1994; Suzuki and Kawahata 2004; Ware et al. 1992). The exact value of the ratio is a function of water temperature, salinity, and other carbonate parameters (Watanabe and Nakamura, 2018).

The sink/source behavior of coral reefs varies between sites. In French Polynesia and the Great Barrier Reef, pCO_{2water} is higher around coral reefs than in the surrounding area (Gattuso et al. 1996). In contrast, a coral reef in the Yaeyama Islands (Okinawa, Japan) is a sink for atmospheric CO_2 (Kayanne et al. 1995). In addition to the balance of biological activities, the residence time of water over a coral reef and riverine inputs affect the sink/source characteristics of a reef (Fig. 6.14, Suzuki and Kawahata 2004).

Coral bleaching is the release of the zooxanthellae symbionts from corals and may result in the death of the coral. Coral bleaching was induced by the high temperatures during the El Niño event. This event is reported to have changed the Yaeyama coral reef to an atmospheric CO_2 source (Kayanne et al. 2005). We should pay close attention to the effects of climate change on coral reef ecosystems and the valuable ecosystem services they perform with respect to CO_2 absorption, coastal protection, biodiversity, and tourism resources.

6.5 Statistical Prediction of pCO_2 in Water

The value of pCO_{2water} is an important parameter for calculating air–water CO_2 fluxes and is measured by specialized sensors or via water sampling (see Sect. 6.3 and 6.4). These methods generally require considerable expense and effort to expand
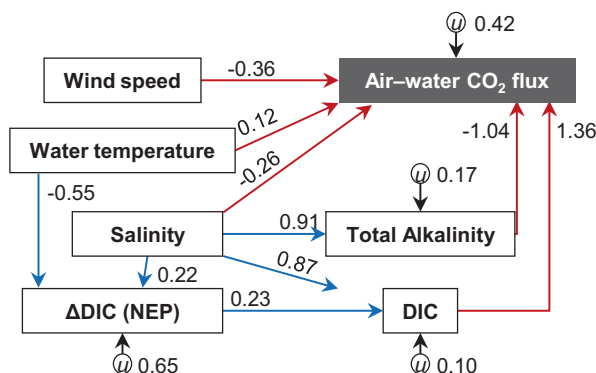
Fig. 6.15 A structured equation model showing direct factors (red arrows) and indirect factors (blue arrows) that affect the air–water CO_2 fluxes in boreal and temperate seagrass meadows. The value of a coefficient indicates the relative influence of the path. All of the path coefficients are statistically significant ($p < 0.05$). The parameter u represents unknown factors. (Tokoro et al. 2014)

the spatial and temporal coverage of pCO_{2water} data, and the methods are hard for non-specialists and organizations to use. Statistical models aimed at predicting pCO_{2water} may overcome these limitations. The global efflux of CO_2 from river networks has been estimated with a statistical model (Lauerwald et al. 2015), but there have been few similar estimates in shallow coastal waters. Here, we discuss studies based on statistical analyses of air–water CO_2 exchanges in shallow coastal waters in Japan.

The factors that control the variability of air–water CO_2 fluxes have been analyzed using structured equation models (SEMs) in boreal and temperate seagrass meadows (Tada et al. 2014a, 2014b; Tokoro et al. 2014). SEMs can quantify the relationships among the controlling factors and their relative influence. Tokoro et al. (2014) have shown that the extent and direction of the air–water CO_2 flux is determined by geophysical (wind speed, water temperature, and salinity) and biogeochemical factors (DIC, TA, and NEP) in boreal and temperate seagrass meadows (Fig. 6.15). The fact that these variables have also been identified as controlling factors by SEMs in other seagrass meadows (Tada et al. 2014a, 2014b) suggests that they are important parameters for predicting in situ air–water CO_2 exchange.

A generalized linear models (GLM) has been used to predict the pCO_{2water} from biogeochemical parameters (water temperature, salinity, DIC, and TA) and ecosystem type (seagrass, tidal flat, or coral reef) (Tada et al. 2015). A GLM model has shown that biological factors such as ΔDIC and ΔTA exert significant control over pCO_{2water} (Fig. 6.16). Here, ΔDIC and ΔTA are defined as the differences between the measured DIC and TA, respectively, and those estimated by a conservative dilution model based on salinity. The values of ΔDIC and ΔTA represent changes of DIC and TA due to biological metabolism. According to the GLM results, both a decrease of ΔDIC (autotrophy) and an increase of ΔTA (dissolution of calcium carbonate) induce lower pCO_{2water} and make the system a CO_2 sink (see also Sect. 6.4).
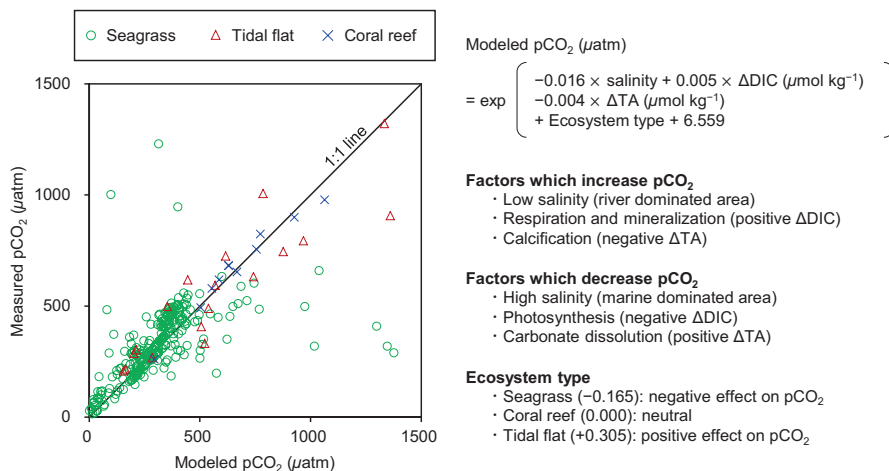
Fig. 6.16 Prediction of pCO_2 in water according to a generalized linear model. The left graph compares the modeled pCO_2 values with the observed values. The right side shows the model equation and the interpretation of the model. (Tada et al. 2015)

The GLM indicated a negative correlation between salinity and pCO_{2water}, but water temperature was not an important factor (Fig. 6.16). Although the type of ecosystem has relatively less influence than the above parameters, pCO_{2water} tends to decrease in the following order: seagrass meadow, coral reef, and tidal flat. These relationships are consistent with previous findings (see Fig. 6.3; Otani and Endo 2018; Watanabe and Nakamura 2018). This statistical model can be used to predict pCO_{2water} from salinity, ΔDIC, ΔTA, and the type of ecosystem. However, ΔDIC and ΔTA are not readily accessible parameters. To improve the utility of the statistical model, other easily accessible parameters (e.g., geographical setting, population density, precipitation, Lauerwald et al. 2015) should be used in future studies.

6.6 Direct Uptake of Atmospheric CO₂ by Seagrass Meadows

In seagrass meadows with shallow water depths (~1 m), the seagrass leaves are often exposed to the air at low tide (Fig. 6.17). Under such conditions, seagrasses may utilize atmospheric CO_2 in addition to dissolved DIC for photosynthesis. Although previous studies have pointed out the possibility of direct use of atmospheric CO_2 by seagrasses (Clavier et al. 2011; Jiang et al. 2014; Leuschner and Rees 1993), it is difficult to quantify their direct use by conventional methods.

Stable isotope analyses have been used to evaluate the behavior of a variety of substances. Different isotopes of an element differ only in terms of the number of neutrons in their nuclei and hence their mass number. For example, ^{12}C and ^{13}C, two
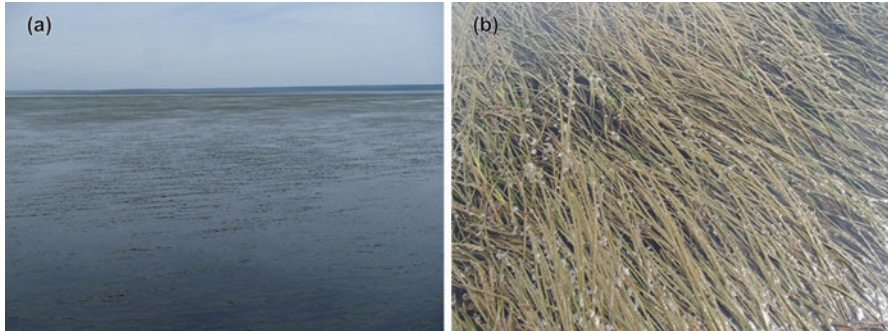
Fig. 6.17 (**a**) Distant and (**b**) close-up views of eelgrass leaves exposed to the air during low tide in Furen Lagoon, Japan. Direct uptake of atmospheric CO$_2$ by eelgrass (*Zostera marina*) was demonstrated using ^{14}C. (Watanabe and Kuwae 2015a)

isotopes of carbon, have mass numbers of 12 and 13, respectively. ^{12}C and ^{13}C account for approximately 99% and 1%, respectively, of naturally occurring carbon. The metric of their relative abundance is called δ^{13}C, which is the ^{13}C/^{12}C ratio normalized to an arbitrary standard and expressed on a per mil (i.e., parts per thousand) basis. Stable isotope ratios change during various processes, a change referred to as "isotope fractionation". Therefore, the δ^{13}C value, for example, reflects the history of carbon transformations in an ecosystem. When seagrasses take up atmospheric CO$_2$, isotope fractionation occurs because atmospheric CO$_2$ is dissolved in the water and then assimilated by the seagrasses. The origin and fate of substances can therefore be evaluated by using the differences in their stable isotope ratios. δ^{13}C is conventionally used in the study of carbon cycling in ecosystems.

It is possible to evaluate whether seagrasses actually assimilate atmospheric CO$_2$ in addition to DIC by comparing the δ^{13}C values of their carbon sources with that of the seagrass itself. However, this approach is not applicable unless there is a difference in δ^{13}C among the carbon sources (Fig. 6.18). In this case, because the δ^{13}C value of DIC (especially in low-salinity water) and that of atmospheric CO$_2$ overlap, it is impossible to distinguish between these contributions. In addition, the fact that isotope fractionation occurs during the process of carbon assimilation confounds the use of this method to infer carbon sources (Hemminga and Mateo 1996).

The radioactive form of carbon, ^{14}C, is also a useful tracer of carbon, but its natural abundance is very small. Roughly one of every 10^{12} carbon atoms is ^{14}C. ^{14}C is produced by collisions between nitrogen atoms (^{14}N) and neutrons generated by cosmic rays in the upper atmosphere. The amount of ^{14}C is almost constant in the atmosphere (Fig. 6.19). However, ^{14}C is released into the atmosphere by nuclear tests and other anthropogenic activities (see Sect. 6.3.2). ^{14}C is oxidized to ^{14}CO$_2$ in the atmosphere and may then be transferred to the biosphere via photosynthesis. Because ^{14}C decays with a half-life of approximately 5730 years, the ^{14}C concentration decreases with time, and the change of ^{14}C (Δ^{14}C) is therefore a powerful method for dating in various fields such as paleoenvironmental studies and archeology. Accelerator mass spectrometry is used for ^{14}C analysis, and recently
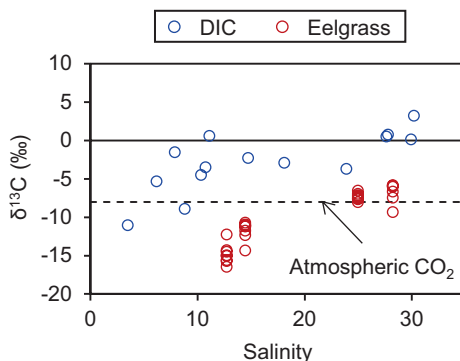
Fig. 6.18 Spatial distribution of the $\delta^{13}C$ values of DIC (blue circles) and eelgrass (red circles) along a salinity gradient in Furen Lagoon. The dashed line shows the $\delta^{13}C$ value of atmospheric CO_2. It was not possible to distinguish the contribution of atmospheric CO_2 from that of DIC because the $\delta^{13}C$ values of atmospheric CO_2 overlapped those of DIC. (Watanabe and Kuwae 2015a)
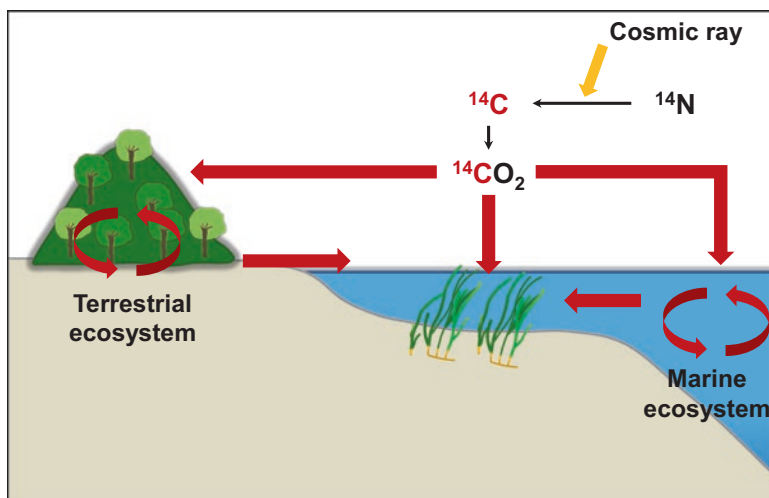
Fig. 6.19 Dynamics of radiocarbon (^{14}C) in ecosystems. ^{14}C produced by cosmic rays combines with oxygen and becomes $^{14}CO_2$, which is taken up by terrestrial and marine ecosystems. ^{14}C is circulated in the systems and then flows into coastal waters. DIC originating from terrestrial and offshore sources is therefore generally old, and the ^{14}C concentration is lower than that of atmospheric CO_2

this technique has become commercially available at a cost similar to that of $\delta^{13}C$ analysis.

The following two points concern the merits of using $\Delta^{14}C$ to estimate the origin and fate of carbon. First, $\Delta^{14}C$ values provide information about time scales. We can distinguish carbon sources using $\Delta^{14}C$ that could not be separated on the basis of $\delta^{13}C$ values. For example, both modern-day plants and plants that inhabited Earth
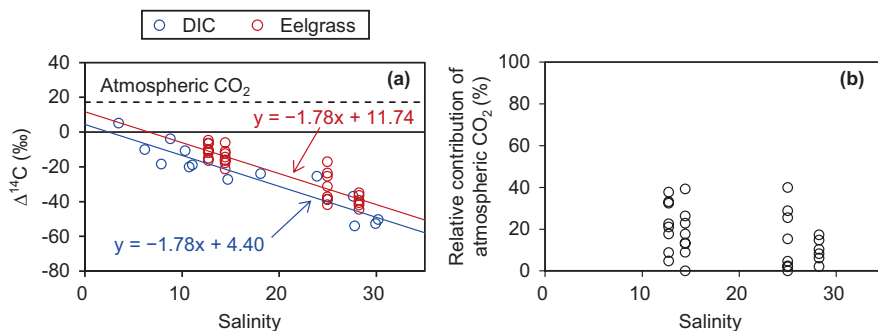
Fig. 6.20 (**a**) Spatial distribution of the $\Delta^{14}C$ values of dissolved inorganic carbon (DIC) (blue circles) and eelgrass (red circles) along a salinity gradient in May and July 2014 in Furen Lagoon, Japan. Blue and red solid lines represent the linear models for DIC and eelgrass, respectively, fitted via analysis of covariance (ANCOVA). The dashed line shows the $\Delta^{14}C$ value of atmospheric CO$_2$. (**b**) The relative contribution of atmospheric CO$_2$ to total inorganic carbon assimilated by eelgrass along the salinity gradient, as calculated by the two-carbon-source mixing model. The fact that the $\Delta^{14}C$ of eelgrass was significantly higher than that of DIC shows that the eelgrass assimilates ^{14}C-rich atmospheric CO$_2$. The relative contribution of atmospheric CO$_2$ was estimated to be from 0 to 40%, and the average was 17%. (Watanabe and Kuwae 2015a)

5000 years ago have almost the same $\delta^{13}C$ values because the mechanism of carbon assimilation has remained constant; however, their $\Delta^{14}C$ values can easily be distinguished. Secondly, the calculation of $\Delta^{14}C$ by internal correction using $\delta^{13}C$ values eliminates any effects from isotope fractionation (Stuiver and Polach 1977). For these two reasons, it is possible to overcome the above-described problems with the conventional $\delta^{13}C$ approach by combining $\delta^{13}C$ and $\Delta^{14}C$ measurements.

The results of $\Delta^{14}C$ analyses of seagrass (eelgrass, *Zostera marina*) and DIC along a salinity gradient demonstrate that eelgrass is significantly higher in $\Delta^{14}C$ than DIC (Fig. 6.20). This significant difference shows that the seagrass assimilates ^{14}C-rich atmospheric CO$_2$. In addition to the conventional idea that eelgrass uses dissolved DIC as its main carbon source, this result quantitatively showed that eelgrass directly takes up and assimilates atmospheric CO$_2$ when the leaves are exposed to air (Watanabe and Kuwae 2015a). The contribution of atmospheric CO$_2$ varied from 0 to 40%, and the average was 17% (Fig. 6.20). The average assimilation rate of atmospheric CO$_2$ was estimated to be 35 mmol-C m^{-2} day^{-1}, assuming that the average net primary production rate of eelgrass was 200 mmol-C m^{-2} day^{-1}, a value that was computed with a numerical model (Moki et al. 2016). This estimate is comparable to the air–water CO$_2$ gas flux (Tokoro et al. 2014, Tokoro and Kuwae 2018). This direct CO$_2$ uptake should be a universal carbon pathway in many shallow waters because exposure of leaves to air at low tide level is widely observed in submerged aquatic vegetation.

The mechanism of direct CO$_2$ uptake is still unknown, but the following scenario is likely (Fig. 6.21). Eelgrass is a marine angiosperm that has evolved from a terrestrial plant, but eelgrass lost their stomata when they expanded their habitat to marine ecosystems. Seagrasses take up dissolved CO$_2$ across their thin cuticle layer
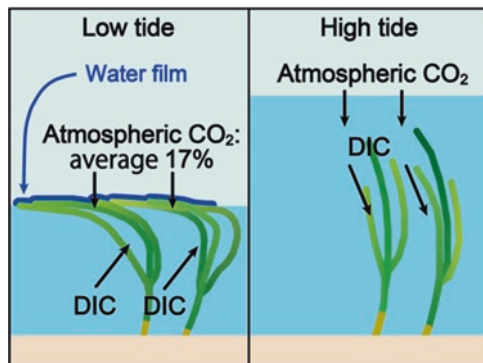
Fig. 6.21 Conceptual scheme for the direct uptake of atmospheric CO_2 by eelgrass. Conventionally, eelgrass has been considered to use inorganic carbon in water as its only carbon source. However, the ^{14}C approach demonstrated that atmospheric CO_2 utilization by eelgrass is also important. The atmospheric CO_2 is hypothesized to be taken up through a thin film of water left on the leaves at low tide. (Watanabe and Kuwae 2015a)

because they cannot take up gaseous CO_2 for photosynthesis. A thin film of water remains on eelgrass leaves when the leaves are exposed to air during low tide. Atmospheric CO_2 may be taken up by eelgrass through the thin aqueous film, in which the pCO_{2water} would be reduced much more rapidly by photosynthesis than it would be in the bulk water. The reduction of pCO_{2water} would enhance the net passive uptake of atmospheric CO_2 by diffusion.

Direct CO_2 uptake cannot be measured by the bulk formula method, and the relative contribution of the flux of CO_2 gas via the air–seagrass water film to the total flux should be addressed in the future. In fact, the carbon flux via this direct uptake process may explain the fact that the CO_2 flux is generally larger when measured by the eddy covariance method than by other methods (Tokoro and Kuwae 2018).

6.7   Summary

The ocean is one of the largest sinks of atmospheric CO_2 and will play an important role in future climate change. The absorption of atmospheric CO_2 and carbon storage by blue carbon ecosystems have attracted attention as mitigation measures in recent years. However, the air–water CO_2 flux is a completely different process from storage of organic carbon in ecosystems. The air–water CO_2 flux is determined by complicated processes within the water. To evaluate the role of ecosystems as sinks of atmospheric CO_2, air–water CO_2 gas fluxes should be appropriately measured. Because there are advantages and disadvantages to each measurement method (e.g., the bulk formula method, the floating chamber method, and the eddy covariance method), a combined analysis based on multiple methods should produce the most reliable results.

In this chapter, we discussed previous investigations of air–water CO$_2$ fluxes that used several methods in shallow coastal ecosystems. Empirical measurements using multiple methods revealed that autotrophic seagrass meadows can be a sink of atmospheric CO$_2$ over the course of a year. Also, macroalgal beds can directly absorb atmospheric CO$_2$. In coral reefs, the relative rate of photosynthesis and calcification is the key factor that determines whether these ecosystems are net sinks or sources of atmospheric CO$_2$.

Statistical prediction methods may be practical for quantifying the effect of the interactions between regulating factors on the air–water CO$_2$ flux and also provide information on the spatial and temporal variability of the fluxes.

Studies exploiting carbon isotopes have demonstrated that the CO$_2$ flux between the atmosphere and seagrass water-films may contribute to the uptake of atmospheric CO$_2$ by eelgrass beds. Determining the pathways of CO$_2$ absorption via this process should be addressed in future studies of air–aquatic ecosystem CO$_2$ fluxes.

Accurate quantification of air–aquatic ecosystem CO$_2$ fluxes over local, regional, and global scales is essential for assessing the role of shallow coastal ecosystems in mitigating the effects of anthropogenic CO$_2$ emissions. Fluxes should be measured at dense spatiotemporal scales in various types of shallow coastal ecosystems for this purpose. We propose two strategies for this extensive data collection.

The first approach is to build observation facilities based mainly on the eddy covariance method around the world and to conduct long-term measurements over annual and decadal time scales (e.g., FLUXNET in terrestrial ecosystems). The observation facilities should be deployed in various types of ecosystem (i.e., seagrass meadows, mangroves, saltmarshes, macroalgal beds, coral reefs, tidal flats, and urbanized systems). A combination of multiple methods such as the bulk formula method and the floating chamber method will be necessary to complement the eddy-covariance CO$_2$ flux estimates by assessing details of the pertinent mechanisms.

The second approach is to develop simple, low-cost, and easy-to-use methods for non-specialists and organizations. This approach will facilitate filling gaps in the spatial and temporal coverage of the data. Statistical prediction is a candidate method in this respect, although the accuracy of statistical predictions should be enhanced in future studies. Because the accuracy of statistical predictions can be improved with empirical data, the concurrent use of both of these approaches will promote the quantification of CO$_2$ exchanges in blue carbon ecosystems at national and global scales.

References

Akhand A, Chanda A, Manna S et al (2016) A comparison of CO$_2$ dynamics and air-water fluxes in a river-dominated estuary and a mangrove-dominated marine estuary. Geophys Res Lett 43:726–735

Akhand A, Chanda A, Das S, Hazra S, Kuwae T (2018) CO$_2$ fluxes in mangrove ecosystems. In: Kuwae T, Hori M (eds) Blue carbon in shallow coastal ecosystems: carbon dynamics, policy, and implementation. Springer, Singapore, pp 185–221

Baldocchi D (2008) 'Breathing' of the terrestrial biosphere: lessons learned from a global network of carbon dioxide flux measurement systems. Aust J Bot 56:1–26. https://doi.org/10.1071/BT07151

Baldocchi D (2014) Measuring fluxes of trace gases and energy between ecosystems and the atmosphere—the state and future of the eddy covariance method. Glob Chang Biol 20:3600–3609

Berg P, Røy H, Janssen F et al (2003) Oxygen uptake by aquatic sediments measured with a novel non-invasive eddy-correlation technique. Mar Ecol Prog Ser 261:75–83

Borges AV, Djenidi S, Lacroix G et al (2003) Atmospheric CO_2 flux from mangrove surrounding waters. Geophys Res Lett 30:1558. https://doi.org/10.1029/2003GL017143

Businger JA, Oncley SP (1990) Flux measurement with conditional sampling. J Atmos Ocean Technol 7:349–335

Cai WJ (2011) Estuarine and coastal ocean carbon paradox: CO_2 sinks or sites of terrestrial carbon incineration? Annu Rev Mar Sci 3:123–145

Ciais P, Sabine C, Bala G et al (2013) Carbon and other biogeochemical cycles. In: Stocker TF, Qin D, Plattner GK (eds) Climate change 2013: the physical science basis, Contribution of Working Group I to the Fifth Assessment Report of the Intergovernmental Panel on Climate Change. Cambridge University Press, Cambridge, pp 465–570

Clavier J, Chauvaud L, Carlier A et al (2011) Aerial and underwater carbon metabolism of a *Zostera noltii* seagrass bed in the Banc d'Arguin, Mauritania. Aquat Bot 95:24–30

Danckwerts PV (1951) Significance of liquid-film coefficients in gas absorption. Ind Eng Chem 43:1460–1467

Dickson AG, Sabine CL, Christian JR (eds) (2007) Guide to best practice for ocean CO_2 measurement, PICES special publication, vol 3. North Pacific Marine Science Organization, Sidney

Duarte CM, Wu J, Xiao X et al (2017) Can seaweed farming play a role in climate change mitigation and adaptation? Front Mar Sci 4:100. https://doi.org/10.3389/fmars.2017.00100

Frankignoulle M (1988) Field measurements of air–sea CO_2 exchange. Limnol Oceanogr 33:313–322

Frankignoulle M, Canon C, Gattuso JP (1994) Marine calcification as a source of carbon dioxide: positive feedback of increasing atmospheric CO_2. Limnol Oceanogr 39:458–462

Gattuso JP, Pichon MR, Delesalle B et al (1996) Carbon fluxes in coral reefs. I. Lagrangian measurements of community metabolism and resulting air-sea CO_2 disequilibrium. Mar Ecol Prog Ser 145:109–121

Hansson I (1973) A new set of pH-scales and standard buffers for sea water. Deep Sea Res Oceanogr Abstr 20:479–491

Hemminga MA, Mateo MA (1996) Stable carbon isotopes in seagrasses: variability in ratios and use in ecological studies. Mar Ecol Prog Ser 140:285–298

Hill R, Bellgrove A, Macreadie PI et al (2015) Can macroalgae contribute to blue carbon? An Australian perspective. Limnol Oceanogr 60:1689–1706

Howard JL, Creed JC, Aguiar MV et al (2017) CO_2 released by carbonate sediment production in some coastal areas may offset the benefits of seagrass "Blue Carbon" storage. Limnol Oceanogr 63:160–172. https://doi.org/10.1002/lno.10621

Ikawa H, Oechel WC (2014) Temporal variations in air-water CO_2 exchange near large kelp beds near San Diego, California. J Gephys Res Oceans 120:50–63

Jähne B, Heinz G, Dietrich W (1987) Measurement of the diffusion-coefficients of sparingly soluble gases in water. J Geophys Res Oceans 92:10767–10776

Jiang Z, Huang X, Zhang J et al (2014) The effects of air exposure on the desiccation rate and photosynthetic activity of *Thalassia hemprichii* and *Enhalus acoroides*. Mar Biol 161:1051–1061

Kayanne H, Suzuki A, Saito H (1995) Diurnal changes in the partial pressure of carbon dioxide in coral reef water. Science 269:214–216

Kayanne H, Hata H, Kudo S et al (2005) Seasonal and bleaching-induced changes in coral reef metabolism and CO_2 flux. Glob Biogeochem Cycles 19:GB3015. https://doi.org/10.1029/2004GB002400

Kondo J (2000) Atmosphere science near the ground surface. University of Tokyo Press, Tokyo

Kone YJM, Abril G, Kouadio KN, Delille B, Borges AV (2009) Seasonal variability of carbon dioxide in the rivers and lagoons of Ivory Coast (West Africa). Estuar Coast 32:246–260

Krause-Jensen D, Duarte CM (2016) Substantial role of macroalgae in marine carbon sequestration. Nat Geosci 9:737–742

Kuwae T, Kamio K, Inoue T et al (2006) Oxygen exchange flux between sediment and water in an intertidal sandflat, measured *in situ* by the eddy-correlation method. Mar Ecol Prog Ser 307:59–68

Kuwae T, Kanda J, Kubo A et al (2016) Blue carbon in human-dominated estuarine and shallow coastal systems. Ambio 45:290–301

Kuwae T, Kanda J, Kubo A, Nakajima F, Ogawa H, Sohma A, Suzumura M (2018) CO$_2$ uptake in the shallow coastal ecosystems affected by anthropogenic impacts. In: Kuwae T, Hori M (eds) Blue carbon in shallow coastal ecosystems: carbon dynamics, policy, and implementation. Springer, Singapore, pp 295–319

Laruelle GG, Dürr HH, Slomp CP et al (2010) Evaluation of sinks and sources of CO$_2$ in the global coastal ocean using a spatially-explicit typology of estuaries and continental shelves. Geophys Res Lett 37:L15607. https://doi.org/10.1029/2010GL043691

Lauerwald R, Laruelle GG, Hartmann J et al (2015) Spatial patterns in CO$_2$ evasion from the global river network. Glob Biogeochem Cycles 29:534–554

Le Quéré C, Andrew RM, Friedlingstein P et al (2018) Global carbon budget 2017. Earth Syst Sci Data 10:405–448. https://doi.org/10.5194/essd-10-405-2018

Lee X, Massman W, Law B (eds) (2004) Coordinate system and flux bias error, handbook of micrometeorology. Kluwer Academic Publishers, Dordrecht

Lemaire BJ, Noss C, Lorke A (2017) Toward relaxed eddy accumulation measurements of sediment-water exchange in aquatic ecosystems. Geophys Res Lett 44:8901–8909

Leuschner C, Rees U (1993) CO$_2$ gas flux of two intertidal seagrass species, *Zostera marina* L. a. Aquat Bot 45(1):53–62

Macreadie PI, Serrano O, Maher DT et al (2017) Addressing calcium carbonate cycling in blue carbon accounting. Limnol Oceanogr Lett 2:195–201. https://doi.org/10.1002/lol2.10052

Maher DT, Eyre BD (2012) Carbon budgets for three autotrophic Australian estuaries: implications for global estimates of the coastal air-water CO$_2$ flux. Glob Biogeochem Cycles 26:GB1032. https://doi.org/10.1029/2011GB004075

Meyers TP, Hall ME, Lindberg SE et al (1996) Use of the modified Bowen-ratio technique to measure fluxes of trace gases. Atmos Environ 30:3321–3329

Moki H, Nakagawa Y, Watanabe K et al (2016) Field observations and numerical analyses on the effect of vegetation on the hydrodynamics of a shallow water using a new hydrodynamic model. Report of the Port and Airport Research Institute 55(2):35–59 (in Japanese with English abstract)

Otani S, Endo T (2018) CO$_2$ flux in tidal flats and salt marshes. In: Kuwae T, Hori M (eds) Blue carbon in shallow coastal ecosystems: carbon dynamics, policy, and implementation. Springer, Singapore, pp 223–250

Regnier P, Friedlingstein P, Ciais P et al (2013) Anthropogenic perturbation of the carbon fluxes from land to ocean. Nat Geosci 6:597–607

Stuiver M, Polach HA (1977) Discussion: reporting of ^{14}C data. Radiocarbon 19:355–363

Suzuki A, Kawahata H (2004) Reef water CO$_2$ system and carbon production of coral reefs: topographic control of system-level performance. In: Shiyomi M et al (eds) Global environmental change in the ocean and on land. TERRAPUB, Tokyo, pp 229–248

Sweeney C, Gloor E, Jacobson AR et al (2007) Constraining global air-sea gas exchange for CO$_2$ with recent bomb ^{14}C measurements. Glob Biogeochem Cycles 21:GB2015. https://doi.org/10.1029/2006GB002784

Tada K, Tokoro T, Watanabe K et al (2014a) Spatial distribution of air-sea CO$_2$ flux and its influencing factors at the Lake Komuke, Hokkaido. J Jpn Soc Civ Eng Ser B3 70:I_1188–I_1193 (in Japanese with English abstract)

Tada K, Tokoro T, Watanabe K et al (2014b) Continuous measurements of air-sea CO_2 flux in an eelgrass meadow. J Jpn Soc Civ Eng Ser B2 70:I_1191–I_1195 (in Japanese with English abstract)

Tada K, Tokoro T, Watanabe K et al (2015) Observation and statistical predictions of CO_2 fugacity shallow waters in Japan. J Jpn Soc Civ Eng Ser B2 71:I_1333–I_1338 (in Japanese with English abstract)

Takahashi T, Sutherland S, Wanninkhof R et al (2009) Climatological mean and decadal change in surface ocean pCO_2, and net sea–air CO_2 flux over the global oceans. Deep Sea Res II 56:554–577

Tokoro T, Kuwae T (2015) Data management of air-sea CO_2 gas exchanges by the eddy covariance technique. J Jpn Soc Civ Eng Ser B2 71:I_1747–I_1752 (in Japanese with English abstract)

Tokoro T, Kuwae T (2018) Improved post-processing of eddy-covariance data to quantify atmosphere-aquatic ecosystem CO_2 exchanges. Front Mar Sci 5: 286. doi: 10.3389/fmars.2018.00286

Tokoro T, Watanabe A, Kayanne H et al (2007) Measurement of air-water CO_2 transfer at four coastal sites using a chamber method. J Mar Syst 66:140–149

Tokoro T, Kayanne H, Watanabe A et al (2008) High gas-transfer velocity in coastal regions with high energy-dissipation rates. J Geophys Res Oceans 113:C11006. https://doi.org/10.1029/2007JC004528

Tokoro T, Hosokawa S, Miyoshi E et al (2014) Net uptake of atmospheric CO_2 by coastal submerged aquatic vegetation. Glob Chang Biol 20:1873–1884

Tsunogai S, Watanabe S, Sato T (1999) Is there a continental shelf pump for the absorption of atmospheric CO_2? Tellus 51:701–712

Wanninkhof R (1992) Relationship between wind-speed and gas-flux over the ocean. J Geophys Res Oceans 97:7373–7382

Ware JR, Smith SV, Reaka-Kudla ML (1992) Coral reefs: sources or sinks of atmospheric CO_2? Coral Reefs 11:127–130

Watanabe K, Kuwae T (2015a) Radiocarbon isotopic evidence for assimilation of atmospheric CO_2 by the seagrass *Zostera marina*. Biogeosciences 12:6251–6258

Watanabe K, Kuwae T (2015b) How organic carbon derived from multiple sources contributes to carbon sequestration processes in a shallow coastal system? Glob Chang Biol 21:2612–2623

Watanabe A, Nakamura T (2018) Carbon dynamics in coral reefs, Kuwae T, Hori M Blue carbon in shallow coastal ecosystems: carbon dynamics, policy, and implementation. Springer, Singapore, pp 273-293

Watanabe A, Yamamoto T, Nadaoka K et al (2013) Spatiotemporal variations in CO_2 flux in a fringing reef simulated using a novel carbonate system dynamics model. Coral Reefs 32:239–254

Watson AJ, Upstill-Goddard RC, Liss PS (1991) Air–sea gas flux in rough and stormy seas measured by a dual-tracer technique. Nature 349:145–147

Weiss RF (1974) Carbon dioxide in water and seawater: the solubility of a nonideal gas. Mar Chem 2:203–215

Yoshida G, Hori M, Shimabukuro H, Hamaoka H, Onitsuka T, Hasegawa N, Muraoka D, Yatsuya K, Watanabe K, Nakaoka M (2018) Carbon sequestration by seagrass and macroalgae in Japan: estimates and future needs. In: Kuwae T, Hori M (eds) Blue carbon in shallow coastal ecosystems: carbon dynamics, policy, and implementation. Springer, Singapore, pp 101–127

Zeebe RE, Wolf-Gladrow D (2001) CO_2 in seawater: equilibrium, kinetics, isotopes. Elsevier, Amsterdam

Chapter 7
CO$_2$ Fluxes in Mangrove Ecosystems

Anirban Akhand, Abhra Chanda, Sourav Das, Sugata Hazra, and Tomohiro Kuwae

Abstract Mangroves have long been recognized as a potential sink of carbon owing to their high productivity and carbon sequestration potential. The short term CO$_2$ dynamics of mangroves are often put under lenses to examine their potential to combat the human induced CO$_2$ emission. Mainly three types of CO$_2$ fluxes take place within a mangrove ecosystem namely (i) atmosphere-biosphere CO$_2$ exchange, (ii) soil CO$_2$ efflux and (iii) air-water CO$_2$ flux. In this chapter, we have compiled all types of the CO$_2$ flux data from mangrove ecosystems with special emphasis on the Sundarban, the world's largest mangrove forest and analyzed the regulating factors of these fluxes. Summarizing all the studies, it can be inferred that the terrestrial compartments of mangroves acts as net sink for CO$_2$, though the soil continually emit CO$_2$ (apart from few exceptions). Almost all the mangrove surrounding waters act as source of CO$_2$, however, the magnitude of air-water CO$_2$ fluxes are much less than the inward fluxes of CO$_2$ towards the canopy, hence the ecosystem as a whole acts as a net sink for CO$_2$. Light conditions, air temperature, salinity, tidal cycle and so forth are mainly found to regulate the atmosphere-biosphere CO$_2$ flux, whereas, soil temperature, moisture and waterlogging are the principal factors regulating the soil CO$_2$fluxes. In case of air-water fluxes, the main governing factors are the variation in salinity, pore-water flushing during ebb tide and wind speed.

A. Akhand (✉) · T. Kuwae
Coastal and Estuarine Environment Research Group, Port and Airport Research Institute, Yokosuka, Japan

A. Chanda · S. Das · S. Hazra
School of Oceanographic Studies, Jadavpur University, Kolkata, West Bengal, India

7.1 Introduction

7.1.1 *The Menace of Ever-Increasing Atmospheric CO$_2$*

Carbon dioxide (CO_2) and its dynamics in the natural ecosystems are perhaps the most studied and discussed issues of the last few decades. Ever since the greenhouse gas potential (GWP) of CO_2, its rapid increase in concentration in the atmosphere (mostly due to anthropogenic activities) and its contribution to global warming and climate change were realized, quantification of the source and/or sink strength of various ecosystems (both natural and man-made) became the 'need of the hour' (IPCC 2007). The partial pressure of CO_2 (pCO_2) in the pre-industrial era used to be ~280 μatm, which increased to ~367 μatm in 1999, ~379 μatm in 2005 (IPCC 2007) and at present it has just crossed 400 μatm according to the observations made in Mauna Loa Observatory, Hawaii. A group of scientists strongly believe that in near future we can witness an atmosphere having double the CO_2 concentration than the present levels (IPCC 2012). Owing to such predictions and the ongoing trends, it has become imperative to understand the functioning and characteristics of various crucial ecosystems found throughout the globe which has the potential to play a significant role in maintaining the carbon equilibrium. In this regard, the importance of terrestrial biomes like forest ecosystems is unambiguously appreciated.

7.1.2 *The Role of Forests to Mitigate CO$_2$ Emission*

Forests are usually a complex ecosystem by virtue of their variability in structure and composition (Noe et al. 2011). The forest ecosystems have the potential to play a decisive role in governing the atmospheric composition and in turn the global climate, through exchanging trace gases between the biosphere and the atmosphere (Magnani et al. 2007; Misson et al. 2007). Dixon et al. (1994) estimated forests to represent a carbon pool of 1146 PgC shared by their above ground biomass (31%) and by the soils (69%) mostly as soil organic carbon and belowground biomass; however, recent estimates of Liu et al. (2015) showed that at present forest carbon stock ranges between 652 and 952 PgC. Terrestrial gross primary production (GPP) is at present known to be the largest global CO_2 flux [∼123 ± 8 Pg C year^{-1} estimated by Beer et al. (2010); 107–152 Pg C year^{-1} estimated by Campbell et al. (2017)] which in turn drives several ecosystem functions (Reich 2010).

7.1.3 *Mangroves and Their Specialty*

Among the several types of forests found in the globe, mangroves are considered as one of the most important forested ecosystems from the perspective of their carbon sequestration potential and blue carbon standing stock (Pendleton et al. 2012). The

term 'Mangroves' came into existence from the Portuguese word 'Mangue' meaning 'community' and the English word 'Grove' meaning trees or bushes. Macnae (1968) coined the term 'Mangal' to define these set of tidal halophytic species which are found to thrive luxuriantly in saline habitats like estuaries, and coastal regions like bays, lagoons etc. throughout the tropics and subtropics of the globe. Later on, Lear and Turner (1977) expressed the word 'mangrove' while depicting the entire ecosystem comprising the floral and faunal communities of these specialized coastal communities, and subsequently the works of Mepham and Mepham (1984) and Tomlinson (1986) firmly established the definition of mangrove ecosystems. Usually mangroves are characterized by morphological adaptation/specialization such as aerial roots, viviparous germination etc. along with physiological mechanisms like salt exclusion and/or salt excretion which enables them to inhabit regions which are physiologically dry in nature or otherwise not suitable for sustaining any floral life (Parani et al. 1998; Lacerda et al. 2002). However, the aspect of mangrove ecosystems that drew the attention of the environmental scientists and climate change experts is their remarkable ability to sequester carbon. Mangrove forests are one of the most highly productive and bio-diverse ecosystems known to exist on earth having productivity rate almost 20 times higher than average oceanic production (Gouda and Panigrahy 1996). In order to adapt with harsh conditions like saline habitat, mangroves developed an advantageous physiological mechanism of maximizing carbon gain and minimizing water loss with high water-use and nutrient-use efficiencies and low transpiration rates (Alongi 2014). Despite thriving in saline waterlogged soils, mangroves exhibit rapid CO_2 uptake and respiratory release (Ball 1988) and owing to these unique ecological characteristics of mangroves they are capable of competently make use of limiting nutrients and store substantial quantities of carbon (Alongi 2009; Feller et al. 2010). Contrary to other terrestrial forests, mangroves have the option of exchanging inorganic and organic materials, nutrients and solutes through tidal mixing with the adjacent coastal water bodies and it usually lead to net sedimentation as well as carbon burial (Adame and Lovelock 2011).

7.1.3.1 The Global Coverage of Mangroves and Carbon Storage

According to a recent high resolution estimate, mangroves occupy about 0.1% of the total continental surface of the earth (Hamilton and Casey 2016) covering an area of 137,760 km² (Giri et al. 2011) and yet they comprise one of the most carbon rich sectors of the world (Bouillon et al. 2008; Donato et al. 2011) owing to a high above-ground primary productivity (Alongi et al. 2004), rich below ground carbon content compared to other tropical forests (Komiyama et al. 2008; Lovelock 2008) and high litter degradation rate accompanied by efficient recycling of autochthonous and allochthonous nutrients (Bouillon et al. 2002). Globally, total aboveground carbon stock of mangroves have been estimated at present to be 2.83 Pg and together with the belowground carbon and soil carbon stock it can reach up to 8.95 Pg (Inoue 2018). Other blue carbon ecosystems, like seagrass have an

estimated global carbon stock of 4.2–8.4 Pg (Fourqurean et al. 2012). The carbon stock in mangroves is much higher than that observed in tidal marshes (Hinson et al. 2017). Factors like intricate root systems up to great depths, high sedimentation rates, and waterlogged soils free from risk of fires, along with anoxic soils in mangroves result in substantially high rate of net carbon burial compared to any other terrestrial forests (Mcleod et al. 2011; Alongi 2012; Breithaupt et al. 2012). Due to these intrinsic features of the mangrove ecosystems, these ecosystems are eyed as one of the cheapest options towards mitigating climate change (Siikamäki et al. 2012; Murdiyarso et al. 2015) by means of two approaches. A school of thought insists that successful and effective reforestation of mangroves can substantially offset the effects of increase in greenhouse gas concentrations in the atmosphere (Pendleton et al. 2012; Van Lavieren et al. 2012), whereas, some scientists opined that restoration of existing mangroves can also serve the climate by preventing a substantial quantity of carbon being emitted to the atmosphere by various natural biogeochemical pathways during natural or man-made degradation of mangroves (Alongi and Mukhopadhyay 2015). In recent days, these ideas in turn have renewed interest on topics like carbon sequestration and biogeochemical cycles of the mangrove forest with special emphasis on their CO_2 flux characteristics and net carbon capture (Bouillon et al. 2008; Breithaupt et al. 2012).

7.1.3.2 CO_2 Flux in the Mangrove Ecosystem

CO_2 flux denotes the rate of exchange of carbon in the form of CO_2 per unit time per unit area amongst the several pools of an ecosystem or between ecospheres, by means of physico-chemical, biological or anthropogenic activities. The CO_2 trapped by photosynthetic activities of mangroves remains as the live biomass in the mangrove trees which might have different fates like (i) part of the biomass produced can be consumed by fauna, either directly or after export to the aquatic system, (ii) carbon can be deposited deep into the sediment, where it is stored for longer periods of time, (iii) carbon can be re-mineralized and either emitted back to the atmosphere as CO_2, or can be exported as dissolved inorganic carbon (DIC), (iv) carbon can be exported to adjacent ecosystems in organic form (dissolved or particulate) where it can either be deposited in sediments, mineralized, or used as a food source by faunal communities (IUCN 2009) (Fig. 7.1). Thus several biogeochemical processes take place within the mangrove ecosystem which completes the dynamics of carbon and all the pathways leading to its different speciation (like organic carbon, carbonate ion, bicarbonate ion, aqueous CO_2 etc.). However, in this chapter we have concentrated exclusively on the CO_2 flux mechanisms that take place within a mangrove ecosystem. The term 'CO_2 flux within mangroves' can be broadly classified into three categories, namely: (i) air-vegetation/atmosphere-biosphere CO_2 flux (which mainly denotes the CO_2 exchange between the mangrove canopy and the overlying atmosphere); (ii) soil CO_2 flux/air-soil CO_2 exchange (which denotes the CO_2
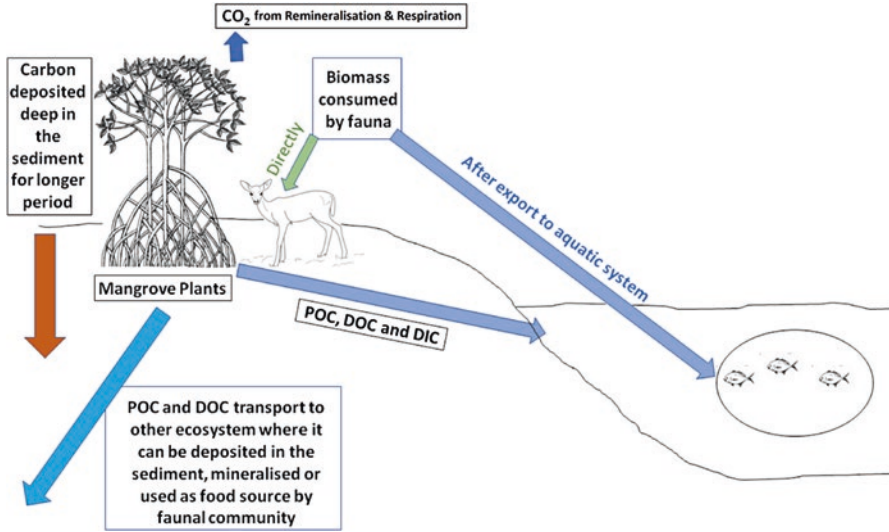
Fig. 7.1 The fate of CO$_2$ trapped by photosynthetic activity (live mangrove biomass) in a typical mangrove forest. (Prepared up on IUCN 2009)
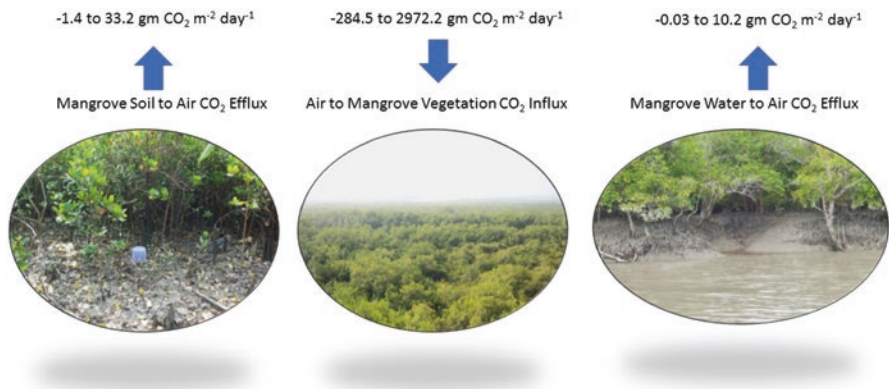
Fig. 7.2 Three type of fluxes from the mangrove ecosystems and their estimated range (positive value indicates towards atmosphere and vice-versa)

exchange, mostly effluxes from the pedosphere towards the atmosphere below the canopy when the soil is exposed to air) and (iii) air-water/atmosphere-hydrosphere CO$_2$ flux (which covers all the CO$_2$ exchange taking place at the interface between the mangrove surrounding waters like estuaries or tidal bays and the atmosphere) (Fig. 7.2).

7.1.3.2.1   Atmosphere-Biosphere CO_2 Fluxes in Mangroves

The 'Atmosphere-biosphere' CO_2 fluxes mainly take place due to photosynthetic activities during the day time and respiration activities during the night time above the canopy of any forest. Various kinds of micrometeorological techniques are deployed to measure this kind of gaseous exchange; however, comparatively lesser attention has been paid to the marine-terrestrial interface regimes like mangrove forests till date (Wofsy and Harris 2002; Barr et al. 2010). Among the different types of micrometeorological methods two approaches are commonly used namely: 'Flux-gradient method' and 'Eddy covariance method'. The Flux-gradient theory is based on the assumption that any turbulent transfer of any trace gas is analogous to molecular diffusion and that the turbulent flux is directly proportional to mean vertical mixing ratio gradient and constant known as eddy diffusivity (Baldocchi et al. 1988). These eddy diffusivities in turn are usually computed by either aerodynamic method or the Bowen ratio energy balance technique (Kanemasu et al. 1979). However, now-a-days the eddy covariance technique is being unanimously implemented throughout the globe to measure the CO_2 exchange above the canopy by using 3D sonic anemometers and open path CO_2/H_2O gas analyzer (Baldocchi 2008). Owing to the simplicity of this approach and feasibility to monitor fluxes continuously over diurnal to annual scale, a network of more than 140 sites has been established throughout the world under the umbrella named FLUXNET (Baldocchi et al. 2001). In all these sites continuous measurement of CO_2, water vapor and heat fluxes are being monitored to develop an intercomparable data set and provide a platform of ground-truth data to validate the satellite sensors mounted on the NASA Terra Satellite (Baldocchi et al. 2001).

7.1.3.2.2   Soil CO_2 Fluxes in Mangroves

Soil CO_2 fluxes mainly results due to production of CO_2 in mangrove soils by means of mostly microbial activity during organic matter mineralization and root respiration (Chen et al. 2012; Lovelock et al. 2011). The organic compounds that enter the pedosphere as decaying roots, root exudates, litter, microbial biomass etc. undergoes decomposition by a multitude of micro- and meso-fauna (Oades 1998). Due to regular flushing of seawater, this decomposition in the mangroves mainly takes place by reducing other electron acceptors substituting the O_2 (i.e., $O_2 \rightarrow NO_3^- \rightarrow Mn$ oxyhydroxides $\rightarrow Fe$ oxyhydroxides $\rightarrow SO_4^{2-} \rightarrow CO_2$) and leading to a decreased rate of decomposition due to lower energetic yield (Alongi et al. 2001; Neue et al. 1997). In other words, when the microorganisms oxidize the organic C using O_2, NO_3^-, Mn^{4+}, Fe^{3+}, and SO_4^{2-} as electron acceptors the CO_2 flux to the atmosphere takes place from the soils surface (Kristensen et al. 2008).The soil respired CO_2 is considered to be the second largest terrestrial carbon flux (Raich and Schlesinger 1992), out of which forest soils may account for 30–80% of the total ecosystem respiration (Luo and Zhou 2006). Soil temperature, moisture and various other

edaphic factors govern and regulate the saptio-temporal variability of soil CO$_2$ fluxes (Joffre et al. 2003; Rustad et al. 2000).

7.1.3.2.3   Air-Water CO$_2$ Fluxes in Mangrove Surrounding Aquatic Bodies

It is almost unequivocally accepted that the entire mangrove ecosystem acts as a sink for CO$_2$ (i.e. net autotrophic), however, the aquatic bodies adjacent to the mangroves are mostly heterotrophic in nature (Borges et al. 2003), though few exceptions are there. This heterotrophic character is mainly attributed to the factors like low primary production due to highly turbid waters, a vast spectrum of changing salinity, immense re-mineralization of leaf and wood litter from the canopy and export of labile organic carbon from mangroves (Jennerjahn and Ittekkot 2002). Due to these factors, measurement of the air-water CO$_2$ exchange in the mangrove waters has become an utmost necessity for a holistic quantification of the carbon budget of any mangrove ecosystem. The air-water CO$_2$ flux is either measured directly by means of deploying closed chamber at the air-water interface or by the bulk formula method (Chap. 2) (Tokoro et al. 2018); both these methods are applicable at present (Wanninkhof and Triñanes 2017). In the bulk formulation method, the CO$_2$ fluxes are computed from the product of the air-water pCO$_2$ gradient, the gas transfer velocity and the solubility of CO$_2$ in water (Takahashi et al. 2009). The main challenge was to accurately quantify the gas exchange coefficient which is based on the parameterization of wind velocity, however, several studies conducted by purposeful tracers showed excellent correspondence with the global estimates (Sweeney et al. 2007). The gas exchange parameterizations formulated by Ho et al. (2011) and Wanninkhof (2014) are the newest estimations and these formulations have shown least possible uncertainty (< 15%) in computing gas transfer velocities and bulk CO$_2$ fluxes.

7.1.4   Objectives

The principal purpose of writing the present chapter is to provide a broad overview about the present scenario and current knowledge on the quantitative aspects of the different types of CO$_2$ fluxes that takes place in and around a mangrove ecosystem giving special emphasis on the world's largest mangrove of Sundarbans. An exhaustive literature survey was conducted to compile the data of three types of fluxes introduced above (recorded in any mangroves of the world and Sundarbans), i.e., atmosphere-biosphere CO$_2$ fluxes above the canopy, soil CO$_2$ fluxes and air-water fluxes in the mangrove surrounding waters. Apart from delineating a global picture from the perspective of quantification of the CO$_2$ fluxes, this chapter also intended to assimilate and discuss all the factors controlling and governing these fluxes (Fig. 7.3). Most of the research works considered in this chapter is being carried out within the last two decades, except a few which dates back to the 1980s. Keywords
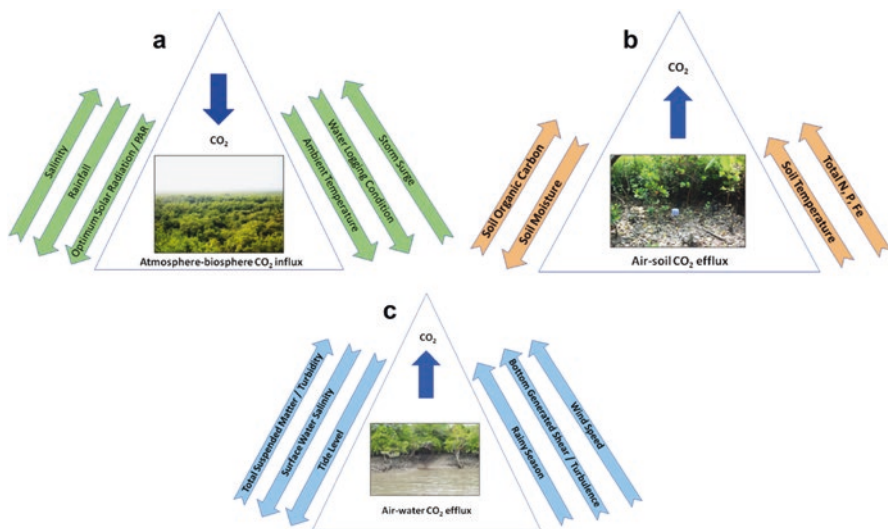
Fig. 7.3 The controlling factors of (**a**) atmosphere-biosphere CO_2 flux (**b**) air-soil CO_2 efflux and (**c**) air-water CO_2 efflux (the slanted upward arrows beside the triangles indicate directly proportional relationship with CO_2 effluxes from biosphere, soil and water and the downward arrows indicate inversely proportional relationship)

like 'mangrove', 'CO_2 flux', 'net ecosystem exchange', 'atmosphere-biosphere CO_2 fluxes', 'soil CO_2 fluxes', 'soil respiration', 'air-water CO_2 exchange', 'mangrove estuaries' and so forth were used in search engines like 'Google scholar' and 'Science direct' to download the papers taken into account in this chapter. The CO_2 fluxes from the mangrove forests all around the world (except Sundarban) are discussed separately and at last a comparative assessment was carried out with fluxes observed in the Sundarbans.

7.2   Atmosphere-Biosphere CO_2 Exchange – The Global Scenario at Present

7.2.1   The Overview of Research Work in a Nutshell

It is evident from Table 7.1 that only a handful number of work has been done on the mangroves from the perspective of characterizing the atmosphere-biosphere CO_2 exchange (by means of micrometeorological methods) above the canopy of mangrove forests. Moreover, most of these works are repeated in the same study sites in either different time period or different locations within the same study site. The sparsity and regional bias of studies on the CO_2 flux in the mangrove forests have limited reliable estimation of the capacity of mangrove ecosystem as a global CO_2 sink/source. Sundarbans mangrove forest has received the largest attention in

Table 7.1 Atmosphere-biosphere CO_2 fluxes recorded in various mangrove forests throughout the world

Site	Method	Time	NEE – CO_2 flux (g CO_2 m^{-2} day^{-1})[a]	Authors
Lothian Island, Sundarban, India	Flux gradient method	May, 1999	0.003	Mukhophadhya et al. (2001)
Lothian Island & Sagar Island, Sundarban, India	Flux gradient method	1998–2000 (Annual cycle)	−284.5–2972.2	Mukhopadhyay et al. (2002)
Lothian Island &Sajnekhali, Sundarban, India	Flux gradient method	2006 (Annual cycle)	−48.3	Ganguly et al. (2008)
Lothian Island and Bonnie Camp, Sundarban, India	Flux gradient method	September, 2009–2010	−86.4 ± 57.0(day) 79.5 ± 38.0 (night)	Ray et al. (2011)
Jharkhali (JK), Henry Island (HI) & Bonnie Camp (BC), Sundarban, India	Flux gradient method	April & May, 2011	−51.1(JK) −18.9 (HI) −1.5 (BC)	Chanda et al. (2013a)
Jharkhali (JK), Henry Island (HI) & Bonnie Camp (BC), Sundarban, India	Flux gradient method	April, 2011– March, 2012 (Annual cycle)	−114.9 (JK) −76 (HI) −33 (BC)	Chanda et al. (2013b)
Bonnie Camp, Sundarban, India	Eddy covariance	April (2012)– March (2012)	−2.5 ± 0.2	Rodda et al. (2016)
Lothian Island, Sundarban, India	Flux gradient method	December, 2011	−31.1	Ray and Jana (2017)
Phangnga National Park Mangroves, Thailand	Eddy covariance	July & August, 1994	−86.4–1.7	Monji et al. (1996)
Phangnga National Park Mangroves, Thailand	Eddy covariance	March & April, 1995	−172.8–518.4	Monji et al. (1997)
Phangnga National Park Mangroves, Thailand	Eddy covariance	December &January, 1996–97; July & August, 1997; August & September, 1998	−151.2–86.4	Monji et al. (2002)
Guangzhou Mangroves, China	NA	NA	−81.2	Kang et al. (2008)
Everglades National Park, USA	Eddy covariance	January, 2004 – August, 2005	−11.8 ± 1.3	Barr et al. (2010)

Table 7.1 (continued)

Site	Method	Time	NEE – CO_2 flux (g CO_2 m^{-2} day^{-1})[a]	Authors
Everglades National Park, USA	Eddy covariance	2007 (Annual cycle)	−8.3 ± 0.8	Barr et al. (2012)
		2008 (Annual cycle)	−8.0 ± 0.6	
		2009 (Annual cycle)	−9.3 ± 0.7	
Zhangjiangkou & Zhanjiang Mangrove National Nature Reserve, China	Eddy covariance	2010 (Annual cycle)	−38.1 to −76.0 (day)	Li et al. (2014)
			~15.2 (night)	

[a]The CO_2 flux magnitudes are converted to a single unit for the sake of comparison; few data are given in the Mean ± standard deviation format, whereas, the others are given in the minimum to maximum format (as retrieved from the respective papers); positive values indicate biosphere to atmosphere fluxes (source) and negative values indicates atmosphere to biosphere fluxes (sink)

this regard as seven papers are published on the atmosphere-biosphere CO_2 exchange (Mukhophadhya et al. 2001, 2002; Ganguly et al. 2008; Ray et al. 2011; Chanda et al. 2013a, b; Rodda et al. 2016) observed in various sites of Sundarbans between the time window of the years 2001 and 2016 (the details are discussed later in Sect. 7.5.2). Followed by Sundarbans, few works are reported on the Phangnga National Park Mangroves of Thailand; however, these works were carried out 15–20 years ago (Monji et al. 1996, 1997, 2002). Apart from these two sites, in the last decade, a few works have been done on the Everglades National Park (Barr et al. 2010, 2012) and three mangrove forests of China (Guangzhou, Zhangjiangkou & Zhanjiang) (Kang et al. 2008; Li et al. 2014).

7.2.2 Net Ecosystem Exchange (NEE) Above Mangrove Canopy and the Role of Light

The studies conducted so far throughout the world found a negative net ecosystem exchange (NEE) (i.e. the forests acted as a net sink for CO_2) (Table 7.1). The magnitude of NEE observed in these mangroves was substantially higher than NEE values observed in other terrestrial ecosystems (Baldocchi et al. 2001; Luyssaert et al. 2007; Hirata et al. 2008). In most cases the downward fluxes during day time in the mangroves was significantly higher than the night time upward fluxes (respiration). Barr et al. (2010) accounted this phenomenon to be one of the principal factors behind such a high NEE in the mangroves. Monji et al. (1996) also made similar observations in the Phangnga National Park Mangroves of Thailand during a short term study in the wet season. They also observed that higher magnitude of negative fluxes was recorded during optimum solar radiation range of 400–800 W m^{-2}. They inferred from their study that the photosynthetic activity of the

mangroves would be no less than any typical tropical and/or temperate (exclusively terrestrial forest) provided the solar radiation remains optimum.

Monji et al. (1997) repeated another short term work in the same Phangnga National Park Mangroves of Thailand during a dry season. The relationship obtained between the solar radiation and the day time downward fluxes were the same, however, significant changes were observed in the magnitude of fluxes. In the dry season, the mean day time fluxes were almost similar to the mean night time fluxes, hence making the forest neither act as sink nor source of CO$_2$.Thus it was established for the first time that mangroves exhibit significant seasonality in terms of atmosphere-biosphere fluxes. In order to verify the observations from the two short term works, 2 years later Monji et al. (2002) carried out a comparatively long term work in the dry and wet seasons in the Phangnga National Park Mangroves. Even in this study, the previous observations of seasonal differences in CO$_2$ fluxes held true; i.e. wet season exhibited larger –NEE than dry season. In addition to these findings they also found that a substantial quantity of CO$_2$ was getting stored inside the canopy during the night time (with larger amount of storage during low wind condition and vice-versa), however, the stored CO$_2$ was getting utilized in the first hours of morning with the initiation of photosynthetic activities.

7.2.3 NEE and Water Logging in Mangroves

Kang et al. (2008) recoded similar magnitudes of CO$_2$ fluxes in the Guangzhou Mangroves of China. They also made a crucial observation that under water logged conditions, the CO$_2$ sink strength of the mangroves was substantially high, whereas, higher emissions were observed when the forest floor was not all logged with water. This observation was later explained by Barr et al. (2010) (during their prolonged study in the Everglades National Park Mangroves of USA) as under waterlogged conditions most of the soil and pneumatophore respired CO$_2$ came into direct contact with the water column and it was eventually tidally exported to the adjacent water bodies as dissolved inorganic carbon (DIC) instead of being emitted straight away as CO$_2$.

7.2.4 Observations from Everglades National Park – Longest Continuous Flux Monitoring in Mangrove

The results published in Barr et al. (2010) and Barr et al. (2012) are perhaps the longest continuous micrometeorological measurements carried out over a mangrove forest by means of eddy covariance technique. Barr et al. (2010) found a strong correlation between NEE and the ambient temperature both in diurnal as well as seasonal scale. Higher inward fluxes always coexisted with high ambient temperature

during the mid day and in terms of season, during the dry season. During the cloudless skies, when the high temperature conditions coincided with highest photosynthetically active radiation (PAR), the peak –NEE values were recorded. On the contrary, during October, when the frequency of thunderstorms increase, it lead to a decrease in solar irradiance and hence the ambient temperature as well which eventually lead to lower NEE values during day time. They also observed a steep decrease in light use efficiency of mangroves with a sharp increase of salinity at the end of dry season due to lowest water column depth. This in turn showed that the photosynthetic potential or light use efficiency of mangroves depends substantially on the salinity stress and its response to factors like temperature and solar irradiance under varying salinity profile in the adjacent water column and extent of inundation. Barr et al. (2010) also observed significant month to month inter-annual variability in CO_2 fluxes and they attributed differences in the mean temperature, rainfall, solar irradiance to be the principal driving factors behind such variability.

7.2.5   Impact on NEE of a Mangrove Ecosystem Post a Cyclonic Disaster

It is worth mentioning that in 24th October, 2005, Hurricane Wilma made landfall in the very study site of Barr et al. (2010) and it enabled the authors to carry out a natural disturbance experiment as they resumed measurements from the end of the year 2006 (Barr et al. 2012). The hurricane brought upon a substantial damage to the mangroves of those regions leading to widespread mortality of mangroves (Smith et al. 2009). Barr et al. (2012) observed a significant reduction in the NEE for five consecutive years after the hurricane. They attributed the complex leaf generation dynamics behind the reduced day time NEE and enhanced decomposition of litter and coarse woody debris behind the enhanced night time NEE. Thus it can be inferred that apart from anthropogenic encroachment towards mangrove forests witnessed throughout the world, natural disasters like cyclone, hurricane, storm surges and so forth, are also capable of altering the sink strength of mangroves substantially and that too for a long period of time.

7.2.6   NEE of Mangroves and Tidal Cycles

Alike Barr et al. (2010), Li et al. (2014) also carried out NEE measurements in the Zhangjiangkou & Zhanjiang Mangrove National Nature Reserve of China and they mainly observed that magnitudes of NEE as well as soil respired CO_2 vary significantly between the spring and the neap tides. Maximum photosynthetic rate and minimum soil CO_2 effluxes were recorded during spring tide and vice-versa.

Moreover, the dependency of soil CO$_2$ effluxes on the soil temperature was much less during the spring tide. Thus Li et al. (2014) on the whole pointed out these aspects which should be kept in mind while budgeting or modeling the mangrove ecosystems' carbon dynamics under future sea level rise scenarios.

7.2.7   Factors Controlling Atmosphere-Biosphere CO$_2$ Exchange – Summing up

Salinity of the ambient water mass that is coming in contact with the forest floor was found to potentially alter both the day time as well night time CO$_2$ fluxes between the canopy and the atmosphere (Fig. 7.3a). The light use efficiency of the mangroves drastically reduced to half of its potential under high saline conditions compared to low saline conditions. Rainfall and freshwater discharge indirectly plays a role in the atmosphere-biosphere CO$_2$ exchange by lowering the soil salinity. Under low soil saline conditions the atmosphere-biosphere CO$_2$ exchanges increases to a great extent and vice versa. Higher solar radiation or PAR led to more uptake of CO$_2$ in the canopy (i.e. more negative NEE), however, a threshold was observed in many studies, i.e. beyond a certain value of PAR the ─ NEE did not increase equally.

Solar radiation is long known to be one of the principal factors regulating canopy photosynthesis or atmosphere-biosphere CO$_2$ exchange during day time (Fig. 7.3a). Ambient temperature also played a crucial role in atmosphere-biosphere CO$_2$ exchange (Fig. 7.3a). Increase in temperature which incidentally happened with increasing photosynthetically active radiation led to increase in carbon uptake by the canopy. In addition to these, factors like storm surges and water logging ultimately leads to increase in salinity in the forest floor which eventually leads to decrease in light use efficiency and hence lesser CO$_2$ uptake is observed during day time.

7.3   Soil CO$_2$ Fluxes from the Mangroves Around the World

7.3.1   The Area Coverage of Research Work

Table 7.2 reflects that compared to atmosphere-biosphere CO$_2$ exchange, soil CO$_2$ fluxes have received more attention in different parts of the world. Quite a many works have been done covering the mangroves situated in China, Australia, New Zealand, Caribbean Islands, Thailand, Indonesia, Brazil, USA and so forth, whereas very few soil CO$_2$ flux related work have been done in Sundarban mangroves (discussed later in Sect. 7.5.2). Most of the studies are conducted in few seasons only; however, some of the works are carried out throughout the year.

Table 7.2 Soil CO_2 fluxes recorded in various mangrove forests throughout the world

Site	Method	Time	CO_2 flux (g CO_2 m^{-2} day^{-1})*	Authors
Henry Island, Sundarban, India	Static closed chamber	April & May, 2011	5.8 ± 0.6	Chanda et al. (2011)
Jharkhali& Henry Island, Sundarban, India	Static closed chamber	April, 2011–March, 2012 (Annual cycle)	0.6–8.9	Chanda et al. (2014)
Jiulongjiang Estuary, Fujian Province, China	Semi-closed chamber	July, 2002	0.7–5.3	Alongi et al. (2005)
Three sites from Caribbean; six sites from Australia; two sites from New Zealand	Static closed chamber	Between April, 2004 and July, 2006	−0.9–11.3	Lovelock (2008)
Mtoni and Ras Dege Mangroves, Tanzania	Ex-situ soil core	September, 2005	1.2–5.1	Kristensen et al. (2008)
Gazi Bay, Kenya	Soda-lime method	October 2004–January 2006	16.9–33.2	Kirui et al. (2009)
Trat River Mangroves, Eastern Thailand	Static closed chamber	Dry and Wet Season of 2006 and 2007	1.7–3.3	Poungparn et al. (2009)
Shenzhen and Hong Kong Mangroves, South China	Static closed chamber	July & August, 2008	0.7–21.7	Chen et al. (2010)
Island of Twin Cays Mangroves, Belize	Static closed chamber	A span of 20 years (year not specified)	7.9	Lovelock et al. (2011)
Mai Po Mangroves, Hong Kong, South China	Static closed chamber	April, 2009 – January, 2010	0.01–1.3	Chen et al. (2012)
New Caledonia Mangroves, French Territory	Static closed chamber	September, 2010–2011	−1.2–13.5	Leopold et al. (2013)
Teremaal, Likupang and Kema Mangroves, Indonesia	Static closed chamber	April (year not specified)	−1.4–4.1	Chen et al. (2014)
New Zealand Mangroves	Static closed chamber	November 2013–January 2014	7.4 ± 2.0 (intact mangrove) 5.9 ± 1.6 (cleared mangrove)	Bulmer et al. (2015)
Everglades National Park, USA	Static closed chamber	2010 (Annual cycle) 2011 (Annual cycle)	4.8 ± 0.2 (only soil) 12.1 ± 0.4 (soil and pneumatophores)	Troxler et al. (2015)

Table 7.2 (continued)

Site	Method	Time	CO$_2$ flux (g CO$_2$ m^{-2} day^{-1})*	Authors
Jiulong River Estuary, South China	Static closed chamber	Winter, spring, summer, autumn (year not specified)	−0.7–12.3	Chen et al. (2016)
Ceará state, NE-Brazil	Static closed chamber	April (2012)	1.1 ± 0.1	Nóbrega et al. (2016)
			(Timonha Mangroves)	
			0.5 ± 0.02	
			(Jaguaribe Mangroves)	
			0.4 ± 0.1	
			(Cocó Mangroves)	

*The CO$_2$ flux magnitudes are converted to a single unit for the sake of comparison; few data are given in the Mean ± standard deviation format, whereas, the others are given in the minimum to maximum format (as retrieved from the respective papers); positive values indicate efflux towards atmosphere (source) and negative values indicates influx towards soil (sink)

7.3.2 Magnitude of Soil CO$_2$ Fluxes in Comparison with Atmosphere-Biosphere CO$_2$ Exchange

First of all it is worth mentioning that the magnitudes of CO$_2$ fluxes from the soils are substantially less than that observed for the atmosphere-biosphere fluxes as has been shown in salt marsh ecosystems (Otani and Endo 2018). Moreover, the range of fluxes (or in terms of standard deviation) is quite small compared to the atmosphere-biosphere fluxes. Negative fluxes of CO$_2$, i.e. towards the soil from atmosphere are scarcely observed (Lovelock 2008; Leopold et al. 2013; Chen et al. 2014, 2016). Most of the studies observed only effluxes of CO$_2$ from the soil; i.e. the soils only emitted CO$_2$; however, in some instances where the authors witnessed algal mat cover or biofilms in the study regions negative fluxes were observed [like Leopold et al. (2013) in New Caledonia Mangroves; Chen et al. (2014) in Indonesian mangroves].

7.3.3 Sulphate Reducers

Alongi et al. (2005) observed that a major part of the organic carbon ending up in the upper layer of pedosphere was oxidized by sulphate reducers followed by aerobic bacteria, denitrifiers, metal-reducing bacteria and methanogens. The magnitude of fluxes observed in this study site was on the lower end compared to the other reports of CO$_2$ fluxes tabulated in Table 7.2; which implies that substantial sulphate reduction in the mangrove soils up to a depth of 1 m has eventually led to lower magnitude of fluxes.

7.3.4   Leaf Area Index, Litter Fall and Benthic Microbial Community

Lovelock (2008) carried out an exhaustive work covering 11 mangrove sites in Caribbean, Australia and New Zealand spread over a latitudinal range of 27°N to 37°S. One of the most crucial observations made in this study was that the magnitude of soil CO_2 effluxes was similar to that observed in terrestrial forest soils which are mostly due to enhanced microbial activities in the mangrove soils. Lovelock (2008) examined that soil CO_2 flux significantly correlated (positive correlation) with leaf area index (LAI), litter fall rate as well as magnitude and above ground primary productivity (especially in case of dwarf mangrove patches).

7.3.5   Biogenic Structures

Kristensen et al. (2008) observed that sediments with biogenic structures like pneumatophores and crab burrows showed significantly higher effluxes (especially during the dark hours) compared to those mangrove sediments which are devoid of those structures. They also observed that the CO_2 efflux from pneumatophores varied significantly from species to species and has a strong relation with the shape and size of the pneumatophores. On the contrary, the authors argued that CO_2 flux estimation in a crab burrow might slightly overestimate the soil CO_2 fluxes as most of the crab burrows are inhabited by crabs (Skov et al. 2002) and depending upon their size they may respire CO_2 substantially which is erroneously considered as soil respired CO_2.

Troxler et al. (2015) observed that soil CO_2 flux from soils rich in pneumatophores emitted CO_2 substantially higher than soils without any pneumatophores as emphasized by earlier studies of Kristensen et al. (2008). All these observations made the authors to conclude that site specific measurement of soil CO_2 fluxes only in places without any biogenic structures might underestimate the global soil respiration to a large extent.

7.3.6   Soil Temperature and Moisture

Soil temperature and moisture were found to be the main covariates responsible for regulating the seasonal fluxes (Fig. 7.3b). A similar dependency of soil temperature on the soil CO_2 fluxes was observed by Poungparn et al. (2009) while working in the Trat River Mangroves of Eastern Thailand. Most of the studies observed an exponential relationship between the magnitude of soil CO_2 efflux and soil temperature. Lovelock (2008) observed an increase in soil respiration with increasing soil temperature, however, in most cases the soil respiration rate was found to decline at

temperatures higher than 26 °C. Lovelock (2008) attributed the benthic photosynthetic microbial community behind the reduction of this soil respired CO$_2$. On the contrary, Kirui et al. (2009) observed substantially high range of effluxes (a minimum magnitude of 16.9 g CO$_2$ m^{-2} day^{-1}; the highest tabulated amongst all the observations of Table 7.2). It should be noted that most of the time in the study area the soil temperature was significantly high (~36 °C) and they observed a statistically significant relationship (positive) between the soil CO$_2$ effluxes and the soil moisture.

7.3.7 Inundation of Forest Floor

The magnitude of fluxes was quite low and they examined a critical relationship between the fluxes and the time of inundation of the mangrove forest floor. They observed that the more the soils were inundated the lesser was the temperature and consequently lower fluxes were observed. In this regard, they inferred that the spatial change in elevation of the mangroves from the vicinity of the river/estuary to the inshore lands could play a deciding role in the magnitude of fluxes. In this regard, Troxler et al. (2015) also observed low CO$_2$ emissions from the sediment surface of the mangroves of Everglades National Park, USA during inundated conditions, however, they inferred that during inundated phases a substantial increase in the pCO$_2$ is also observed in the overlying water mass and it is subject to tidally driven export mainly in the form of HCO$_3^-$.

7.3.8 Soil Chemistry

Chen et al. (2010, 2012, 2016) carried out many short term and long term studies in several mangrove forests of South China and made many crucial observations. Scarcely had they observed negative fluxes due to photosynthetic activities in the soil surface, however, the range of fluxes varied significantly depending upon the duration and season during which the respective studies were undertaken.

Chen et al. (2010) observed that CO$_2$ fluxes exhibit a positive correlation with soil organic carbon, total phosphate, total nitrogen and total iron concentration of the top soil. Leopold et al. (2013) further added that the redox conditions of the sediments, which in turn is controlled by the physiological activities of the root system along with the position and elevation of the mangrove stands, could play a significant role in governing the soil CO$_2$ fluxes. Chen et al. (2012) also reconfirmed higher magnitude of fluxes in the landward sites where soil organic carbon, total Kjeldahl nitrogen, nitrate and phosphate concentration was significantly high compared to foreshore bare mudflats where the abundance of ammonium ions superseded the other nutrients.

However, observations contrary to these regulating factors were also made by Chen et al. (2014). They observed that despite having high organic carbon content, the soil CO_2 fluxes were very low suggesting an extremely slow metabolic rate in the soil microbial community, which actually leads to higher stock of organic carbon accompanied by low emission of CO_2. Chen et al. (2016) inferred that a substantial part of the soil respired CO_2 was consumed by the mangrove canopy during day time as a part of photosynthetic process and hence they recommended to reconsider the measurement of net soil CO_2 efflux from the perspective of total CO_2 budgeting in the terrestrial compartments of mangroves.

7.3.9   Anthropogenic Disturbance

Anthropogenic impacts especially clearing of mangroves for various activities like aquaculture and shrimp farming has become widespread throughout the world. Few studies in the recent past intended to see the effect of such anthropogenic disturbances on the rate of soil CO_2 fluxes but several interesting findings were recorded from such studies. Lovelock et al. (2011) investigated the soil CO_2 flux rates from a cleared mangrove patch and observed that initially after the clearing the CO_2 effluxes from the soils were substantially high; however, after 20 years of the clearing the magnitude was almost 4 times lesser than that observed initially. They also experimented by artificially disturbing the mangrove peat soils and observed that the soils could emit CO_2 at a rate as high as 102 g CO_2 m^{-2} day^{-1}, however, it came back to the normal rate within 2 days. Despite these observations, Lovelock et al. (2011) estimated that almost 10,600 tonnes CO_2 km^{-2} was lost annually due to the clearing of the forest. Hence they inferred that simply preventing deforestation can serve as an excellent approach towards preservation of threatened carbon stocks.

Bulmer et al. (2015) observed that the rate of CO_2 efflux from soils in the temperate regions [only 1.4% of the global mangrove cover falls under temperate region, the rest being in tropics and subtropics (Morrisey et al. 2010)] was comparable to the tropical mangroves. Furthermore they also observed that there was practically no difference between the rate of soil CO_2 efflux between the cleared and the intact mangrove site and that the soil CO_2 efflux in the cleared sites was mainly controlled by sediment organic carbon concentration, nitrogen concentration and sediment grain size.

Contrary to these observations, Nóbrega et al. (2016) observed that intact mangroves emitted more CO_2 compared to the sites which were anthropogenically disturbed. They argued that higher degree of labile organic carbon stock along with lower degree of pyritization, (i.e. lesser degree of iron sulphide formation during decay) in the intact mangrove soils was principally responsible for the higher magnitude of fluxes.

7.3.10 Factors Controlling the Soil CO$_2$ Fluxes – Summing up

Soil temperature and soil moisture are the main factors that control the soil CO$_2$ fluxes. Higher soil temperature facilitates enhanced microbial activity in the pedo-sphere and leads to higher soil CO$_2$ effluxes. Soil moisture in most of the studies has been found to play a negative role on the soil CO$_2$ effluxes (Fig. 7.3b). Lesser magnitude of soil CO$_2$ fluxes were observed during high tide sessions and vice-versa. The higher the residence time of the tidal water the lower was the CO$_2$ fluxes as during this time sediment-water CO$_2$ exchange took place at a higher rate than the soil to atmosphere CO$_2$ exchange. Soil rich in organic carbon are usually found to emit more CO$_2$ as this organic carbon was used as resource by the microbial community to feed upon and release CO$_2$ (Fig. 7.3b). Higher nutrients like N, P, Fe usually led to higher effluxes of CO$_2$, however, exceptions were observed in rare cases where slow metabolic rate of the microbes are held accountable for lower fluxes despite having higher nutrients.

7.4 Air-Water CO$_2$ Fluxes from the Adjacent Water Bodies of Mangroves

7.4.1 Basic Global Scenario

Amongst the three types of CO$_2$ fluxes taken into consideration in this chapter, quantification of air-water CO$_2$ flux is perhaps one of the most challenging endeavors due to several intrinsic complicacies in delineating the bio-physical factors driving these fluxes. A substantial part of the carbon assimilated by the mangrove vegetation finds its way to the adjacent water bodies by phenomenon like tidal flushing, pore water drainage, litter fall and so forth. More than 50% of the fixed carbon in the terrestrial compartment of mangroves enters the adjacent water bodies either in the form of dissolved inorganic carbon (DIC) or dissolved organic carbon (DOC) and particulate organic carbon (POC) as well (Bouillon et al. 2008). Again, a major part of these DOCs are also re-mineralized to DIC (Bouillon et al. 2008). Tidal export of DIC, DOC and POC to the near shore sea waters accounts for a considerable amount of carbon trapped in the mangroves, out of which a fair share of DIC is converted to CO$_2$ and they are eventually emitted to the atmosphere back again (Bouillon et al. 2008).

In this chapter, we have only taken into account those studies which directly measured the CO$_2$ flux in the air-water interface (the lateral flux of DIC or DOC from the mangrove waters to the coastal seas is kept outside the ambit of this chapter). Table 7.3 shows that quite a many works have been done in the estuarine and

Table 7.3 Air-water CO_2 fluxes recorded in various mangrove forests throughout the world

Site	Method	Time	CO_2 flux (g CO_2 m^{-2} day^{-1})*	Authors
Estuarine mouth of Mooriganga, Saptamukhi, and Thakuran, Sundarbans, India	Bulk formula	2001 (Annual cycle)	−0.02–0.05 Mean: 0.01	Biswas et al. (2004)
Mouth of the Edwards Creek, Thakuran River, Herobhanga River, Sundarbans, India	Bulk formula	April and May, 2011	−0.03–0.03	Akhand et al. (2013)
Matla Estuary, Sundarbans, India	Bulk formula	August 2013–July 2014	Mean: 0.3	Akhand et al. (2016)
Nagada Creek, Papua New Guinea; Gaderu Creek, India; Norman's Pond, Bahamas	Bulk formula	December, 2000; June, 2001	Mean: 2.2	Borges et al. (2003)
Gautami-Godavari mangrove Estuary	Bulk formula	Pre-monsoon season, 2001	3.1 ± 5.5	Bouillon et al. (2003)
Mtoni and Ras Dege Mangroves, Tanzania	Bulk formula	September, 2005	0.04–3.5	Kristensen et al. (2008)
Tam Giang and KiênVàng Mangroves, Ca Mau Province, Vietnam	Bulk formula	April & October, 2005	1.2–6.8	Konè and Borges (2008)
Ishigaki Island, Japan	Floating chamber	August 2003–July2006	3.6 ± 2.2	Tokoro et al. (2008)
Mangrove Bay, Bermuda	Bulk formula	October, 2007	2.6 ± 0.8	Zablocki et al. (2011)
Shark River, Everglades National Park, USA	SF_6 tracer	November, 2011	10.2 ± 1.0	Ho et al. (2014)
Wright Myo; Kalighat, Andaman Islands	Bulk formula	Dry season (2005); Wet season (2006)	1.0–7.6	Linto et al. (2014)
Moreton Bay, Australia	Bulk formula	November, 2013	0.4–27.7	Call et al. (2015)
Shark River, Everglades National Park, USA	Bulk formula	August and November, 2011	3.9 ± 0.4	Troxler et al. (2015)
Shark River, Everglades National Park, USA	^{3}He/SF_6 dual tracer	October, 2014	4.6 ± 0.4	Ho et al. (2016)
6 mangrove sites of Australia	Bulk formula	2013 & 2014	1.5 ± 0.7	Sippo et al. (2016)
Iriomote Island, Japan	Bulk formula	July, 2017	0.4 ± 0.5	Akhand et al. (unpublished data)

*The CO_2 flux magnitudes are converted to a single unit for the sake of comparison; few data are given in the Mean ± standard deviation format, whereas, the others are given in the minimum to maximum format (as retrieved from the respective papers); positive values indicate efflux towards atmosphere (source) and negative values indicates influx towards water (sink)

river bodies adjacent to mangroves situated in countries like Australia, USA, Bermuda, Papua New Guinea, Tanzania, Vietnam and India. Notably three works have been reported from the Indian part of Sundarbans which will be discussed later.

7.4.2   Quantification of Air-Water CO$_2$ Fluxes – Role of Tracers

Until the recent advancements regarding quantification of air-water CO$_2$ exchange with the help of tracers were made (Ho et al. 2014; Wanninkhof 2014; Wanninkhof and Triñanes 2017), the most challenging part in the quantification of air-water CO$_2$ exchange in any aquatic ecosystem was to accurately estimate the gas transfer velocity. However, the bulk formula method has been applied in many eminent works carried out in the last two decades.

Glancing through the magnitudes of air-water CO$_2$ fluxes observed throughout the world (Table 7.3), it can be observed that the fluxes are much less than that observed in case of atmosphere-biosphere CO$_2$ fluxes, however, quite similar to the soil CO$_2$ effluxes. Borges et al. (2003) was among the first few comprehensive works in this field that measured and analyzed the air-water CO$_2$ fluxes in the mangrove waters of Papua New Guinea, India and Bahamas. They pointed out that the mangrove waters usually remain oversaturated with CO$_2$ (having a varying extent in terms of pCO$_2$ of 380–4800 μatm) and can prove to be potential source of CO$_2$ to the atmosphere. Up-scaling their observed mean magnitude to the global expanse of mangrove adjacent water mass, they assessed that the emission can be up to 50×10^6 t C year^{-1}.

They also stressed that the seasonal variability of these fluxes should be thoroughly studied to properly estimate the global budget. However, it is evident from Table 7.3 that most of the studies that followed, were done in short term scale and very few studies attempted the annual cycle or at least in seasonal scale.

7.4.3   Spatial Variability Within an Estuary

Bouillon et al. (2003) observed that in the oligohaline and the mesohaline sections substantial production of DIC and total alkalinity (TAlk) was recorded, and the pCO$_2$ in water varied over a range of 293–500 ppm only. Whereas, in the outward fringes of the estuaries where extensive mangrove cover was crisscrossed by many tidal creeks rapid mineralization of organic carbon was found to take place (reflected from a wide range of pCO$_2$ in water from 1375 to 6437 ppm), eventually leading to high magnitude of effluxes.

7.4.4 Role of Tides in Short Term Variation

Kristensen et al. (2008) carried out a short term monitoring in two Tanzanian mangrove forests. However, they emphasized on one of the crucial most phenomenon that is unambiguously accepted to play a deciding role in regulating the short term variation in fluxes of CO_2, i.e. the effect of tides. They observed a wide range of fluxes from the water column depending upon the water level; lower effluxes were observed during the high tide sessions and the lower effluxes were observed during the low tide sessions. It is worth mentioning that the fluxes during low tide were almost 5–16 times higher than that observed during the high tides. Pore-water seepage along with the supersaturated runoff the forest floor was mainly held accountable for this hike in flux rate during the low tide, whereas, during the high tide, the dilution of the water column with pCO_2 lean water from the sea led to the decrease in fluxes.

7.4.5 Seasonal Variability

Very few works have ever been performed on the seasonal dynamics of air-water CO_2 exchange in the mangrove dominated waters. Konè and Borges (2008) carried out in two mangrove forests namely Tam Giang and KiênVàng Mangroves during the dry and the rainy season. In one of these mangrove forests, i.e. KiênVàng Mangroves, they observed a CO_2 flux rate 5 times higher during the rainy season compared to dry season, however, in the other mangrove forest, i.e. Tam Giang, no such seasonal differences were observed. This contrast was explained by the authors mainly in terms of the ΔpCO_2 and wind speed both of which were substantially high in the KiênVàng Mangroves during rainy season but no seasonal difference of these aspects were seen in Tam Giang Mangroves.

A noticeable enrichment of total suspended matter (TSM) indicating in turn substantial increase in the organic load and leading to net heterotrophic conditions was observed in KiênVàng Mangroves, however, such a phenomenon was found to take place in the Tam Giang Mangroves. Thus this observation teaches us that seasonality should not be expected to behave in a similar fashion in all the mangroves of the world.

Linto et al. (2014) carried out a seasonal study in the Wright Myo and Kalighat mangrove forests of Andaman Islands and their observations were mostly similar to that of Konè and Borges (2008). Two to five fold rise in air-water CO_2 fluxes were observed during the wet season (i.e. during the peak of southwest monsoon) accompanied by four fold rise in the turbidity of the water column leading to enhanced net heterotrophy. The range of the magnitude of fluxes was comparable to that observed in the other mangroves.

In the Everglades mangrove forest, Ho et al. (2014) observed the largest flux rates (10.2 ± 1.0 g CO_2 m^{-2} day^{-1}) compared to all the magnitudes tabulated in Table 7.3. However, Troxler et al. (2015) while working in the same region in the

months of August and November, 2011 observed a much lesser mean CO$_2$ flux (3.88 ± 0.38 g CO$_2$ m^{-2} day^{-1}) signifying the large scale seasonal variability of these fluxes.

7.4.6   Short Term Variability of CO$_2$ Fluxes

Zablocki et al. (2011) gave stress on the fact that large uncertainties could be hidden in the global estimates due to not considering the dramatic changes in wind speed within one diel cycle. They inferred from their short term study, that extremely precise flux estimates computed on any given day can be tremendously influenced by the wind condition of that particular day. As an example they noted that taking into consideration the wind speed measured during their study of 1 day, the mean CO$_2$ flux amounted to 13.1 ± 4.8 mmol m^{-2} day^{-1}, however, if they tried to extrapolate the data in a monthly scale taking into consideration the monthly average wind data, the flux estimate would become 59.8 ± 17.3 mmol m^{-2} day^{-1}.The mangrove waters lying in the periphery of the Australian landmass has received substantial attention with respect to quantifying the air-water CO$_2$ fluxes. Call et al. (2015) carried out an investigation in a mangrove creek near Moreton Bay of Australia in order to examine the spring-neap-spring air-water CO$_2$ flux variability. Earlier it was observed that lower fluxes were observed during high tide phase and vice-versa, however, the tidal amplitude varies to a great extent during the lunar cycle depending upon the shift from spring to neap phase. Call et al. (2015) observed lower fluxes during the spring phase and vice versa and depending upon the location of the sampling station in the creek and gas transfer models used the effluxes within a small creek through a complete spring-neap-spring cycle varied from 0.41 to 27.68 g CO$_2$ m^{-2} day^{-1}. This observation again signifies the necessity of long term monitoring of these types of fluxes in order to up-scale and compute large scale estimates.

7.4.7   Advancements in the Field of Gas Exchange Parameterizations

The gas exchange parameterizations were carried out with a help of a tracer named sulphur hexafluoride (SF$_6$) (Ho et al. 2014) and a dual tracer of SF$_6$ along with ^{3}He (Ho et al. 2016). Both the studies revealed that the gas exchange taking place in the air-water interface can be regulated by both wind speed and the bottom generated shear/turbulence along with the residence time of the water. However, for large estuaries, where wind flow is not obstructed by the mangrove canopy, wind speed alone can serve as the deciding parameter to compute gas transfer velocity. Though both of these short term studies were conducted with the main intention to compute a universally acceptable formulation of gas transfer velocity, it gave us an idea about the air-water CO$_2$ fluxes in this crucial mangrove waters.

7.4.8   Soil Surface Topography

Sippo et al. (2016) pointed out that earlier study like Bouillon et al. (2008) assumed a constant ratio between mangrove soil surface and water or even study like Borges et al. (2003) assumed the total water area to the total mangrove area, however, in reality the area of water-air interface varies substantially within a tidal cycle. Thus Sippo et al. (2016) inferred that high resolution digital elevation model (DEM) measurements of water surface should be also performed to reduce the uncertainties in the global estimates of air-water CO_2 fluxes from the mangrove adjacent water bodies.

7.4.9   Factors Controlling the Air-Water CO_2 Fluxes – Summing up

Salinity is one of the principal factors that govern the air-water CO_2 fluxes. Usually higher salinity implies higher dominance of seawater which is lean in pCO_2 and hence leads to lower effluxes of CO_2 from water surface. On the other hand, lower salinity value indicates more freshwater abundance or mangrove pore water which is rich in pCO_2 and leads to higher effluxes of CO_2 (Fig. 7.3c). Higher total suspended matter or turbidity of the water column usually prevents the penetration of PAR within the water mass and hence delimits photosynthetic activity which in turn leads to heterotrophy or enhances the CO_2 source potential of the water body. Tidal cycle is another important factor as it regulates the mixing of freshwater and sea water in the mangrove adjoining areas. Usually high tide phases experience lesser abundance of pCO_2(water) leading to lesser magnitude of water to air CO_2 flux and vice-versa. Among the physical forcing factors, wind speed plays one of the most important roles in regulating the magnitude of fluxes. Higher wind speed always facilitates higher exchange of any gas in the air-water interface, hence higher CO_2 flux is observed in high wind conditions and vice-versa (Fig. 7.3c). Bottom generated shear and turbulence usually leads to good mixing of the entire water column and it brings organic material rich water to the surface which in turn leads to higher mineralization and higher air-water CO_2 fluxes towards the atmosphere. Lastly the effect of rain has been also found to play a crucial role. Rain usually facilitates more runoff and more draining mangrove pore water to the estuarine systems. Thus, usually during rainy season or monsoon phase, higher effluxes of CO_2 is observed to take place towards atmosphere.

7.5   Sundarban Mangroves

7.5.1   Area Description

Sundarban happens to be the world's largest single tract of contiguous mangrove forest covering a total area of 9630 km^2 situated at the border of two countries namely India and Bangladesh. Out of which an area of ~4264 km^2 encompasses dense mangrove cover, whereas, water ways cover ~1781 km^2 (Biswas et al. 2004). Roughly the Sundarban mangroves cover ~3% of the global mangrove cover.

This forest lies on the lower end of the world's largest delta as well known as the Ganges-Brahmaputra-Meghna (GBM) Delta. The tail end of River Ganges known as Hugli River serves as the main source of freshwater in the Indian part of Sundarban; however, several distributaries like Matla, Saptamukhi, and Bidya have presently lost its connection in their upper reaches (Sarkar et al. 2004). In the Sundarban's counterpart of Bangladesh (which comprises 60% of total Sundarban's areal coverage), comparatively more freshwater flow is still being maintained through Rivers like Padma and Meghna.

Sundarban experiences a typical tropical climate and it is grossly demarcated as monsoon (June–September), post-monsoon (October–January) and pre-monsoon(February–May). This region experiences an average annual rainfall of ~1770 mm and 75% of it is poured during the monsoon season. The estuaries surrounding the mangroves are semidiurnal and meso-macro tidal in nature. The spring tidal amplitude ranges between 4.3 and 4.8 m and in case of neap tide it is found to vary between 1.8 and 2.8 m (Biswas et al. 2007). The texture of the soil varies from clayey to sandy loam to silty owing to the deposition of inundated materials in the deltaic formation.

Sundarban is blessed with a rich biodiversity both in terms of flora as well as fauna. Sanyal et al. (2008) reported 25 species of true mangroves, 9 semi-mangroves (grasses), 37 mangrove associates and 22 mangrove commensals from the Indian part of Sundarban. *Avicennia* spp., *Excoecaria agallocha*, *Bruguiera* spp., *Ceriops* spp., *Phoenix paludosa* are some of the abundant mangrove species available in Sundarbans. According to the local belief the term 'Sundarban' originated from the name of the *Heritiera* spp. (colloquially called as Sundari tree – meaning beautiful); however, at present very few naturally occurring *Heritiera* spp. is found to thrive in the Indian part of Sundarbans. Besides mangroves, a multitude of faunal, microbial and algal species are reported to thrive in the Sundarbans.

7.5.2 *CO₂ Flux Scenario*

7.5.2.1 Research Gap in Bangladesh Counterpart of Sundarban

Being the world's largest mangrove forest, Sundarbans undoubtedly demands a special attention and several works have been done regarding characterization of the atmosphere-biosphere, soil derived and air-water CO_2 fluxes (Tables 7.1, 7.2 and 7.3). However, all of these works were carried out in the Indian part of Sundarbans. Though several works based on the assessment of carbon stock and delineating mangrove cover with respect to climate change and sea level rise have been undertaken in the Bangladesh part of Sundarbans (Rahman et al. 2011; Rahman et al. 2015; Chanda et al. 2016), none of them directly measured CO_2 fluxes.

7.5.2.2 Atmosphere-Biosphere CO₂ Flux – Initial Short Term Studies

Endeavors attempting to quantify the atmosphere-biosphere CO_2 flux in Sundarbans began since the year 1999. Mukhophadhya et al. (2001) in their short term study found the marine compartments of the mangrove canopy to be a mild source of CO_2. However, surprisingly in the following study by Mukhopadhyay et al. (2002) which was conducted every month and completed an annual cycle throughout the years 1998–2000 also found the terrestrial compartments of Sundarbans to be a net source for CO_2. None of the other studies in other mangroves of the world recorded this kind of atmosphere-biosphere CO_2 fluxes. They concluded that net source character exhibited by the mangroves could be due to the regional micrometeorological conditions and slow turnover of biomass accumulation in the young stands as well as the CO_2 flux character of the Sundarban mangroves is transient in nature.

Almost all the studies carried out in the Sundarban during this phase and more studies that followed were based on discrete data sets acquired in hourly intervals throughout one particular day of each month. Moreover, the fluxes were computed by means of flux gradient method which is known to have a limitation of depicting the CO_2 exchange of a low footprint, whereas, eddy covariance technique usually acquires data continuously and depending upon the height of the flux towers it can give a broad picture of the gaseous exchange. Thus uncertainties in up-scaling the fluxes for the entire Sundarban was much high in these studies.

7.5.2.3 Atmosphere-Biosphere CO₂ Flux – Spatial and Temporal Variability

Ganguly et al. (2008) and Ray et al. (2011) carried out comprehensive works and found the Sundarban to be net sink for CO_2 having flux magnitudes (negative NEE) very much comparable or sometimes much higher than that observed in the other studies around the world.

In all the above four studies, sampling was done in the Lothian Island of Sundarban, however, in the later two studies of Ganguly et al. (2008) and Ray et al. (2011), study sites like Sajnekhali Sanctuary and Bonnie Camp which are located amidst the dense mangrove cover of Sundarbans were covered under the ambit of sampling. This observation gave a strong indication that the atmosphere-biosphere CO$_2$ fluxes could exhibit high spatial as well as temporal variability.

Moreover, since the method adopted was flux gradient technique (in these studies), it was quite reasonable to argue that regional fluxes within the Sundarban might vary substantially depending upon the site and the mangrove vegetation in its surrounding. Based on these hints, Chanda et al. (2013a, b) carried out their measurements in three sites of the Sundarban mangroves, especially to delineate the spatial variability of CO$_2$ fluxes throughout the Indian part of Sundarbans. Both in the short term study of Chanda et al. (2013a) and the study over a complete annual cycle (Chanda et al. 2013b), significant spatial variability in the atmosphere-biosphere CO$_2$ fluxes were observed. The variability in the species composition along with the canopy density was found to be the principal regulating factors of the fluxes. However, the relationship between the atmosphere-biosphere CO$_2$ fluxes and photosynthetically active radiation (PAR) was found to be same in all the three sites.

7.5.2.4 Sundarbans Acting As a Strong Sink for CO$_2$

In order to characterize the fluxes above the canopy with more certainty, a flux tower has been set up beside the station Bonnie camp and it was fitted with sensors and sonic anemometers to measure CO$_2$ flux by eddy covariance technique. Rodda et al. (2016) reported the annual mean flux to be -2.5 ± 0.2 g CO$_2$ m^{-2} day^{-1} from this tower, which was comparable to the short term observations of Chanda et al. (2013a) but much less than that observed by the year round data of Chanda et al. (2013b). Thus it can be inferred that discrete data sets taken in certain specific days of each month cannot necessarily portray the true scenario and it can substantially overestimate or underestimate the fluxes.

However, the findings of Rodda et al. (2016) affirmed that Sundarbans at present is acting as a strong sink for CO$_2$ and its efficient management and prevention of forest encroachment can enable the policymakers to combat substantially the effect of anthropogenic emissions. In this regard, Ray and Jana (2017) carried out a significant work as they simultaneously measured the CO$_2$ fluxes over the metropolis of Kolkata, a thermal power plant belt (both lying close to Sundarbans) and the Sundarban mangroves. They observed that almost 95% of the emissions made by the thermal power plant belt was consumed by Sundarban's net photosynthetic uptake rate, hence, proving again the potential of Sundarban mangroves to combat CO$_2$ emission.

7.5.2.5   Factors Regulating Atmosphere-Biosphere CO_2 Exchange

The atmosphere-biosphere CO_2 flux observed from the various studies carried out in Sundarbans portrayed that the magnitude of fluxes were 8–10 times higher than that observed in Everglades National Park. However, it was at par with the values observed in the mangroves of China and Thailand. Only two studies analyzed the relationship of NEE and PAR in Sundarbans (Chanda et al. 2013a, b; Rodda et al. 2016). Both the studies observed an exponential relationship between PAR and NEE.

Rodda et al. (2016) plotted the NEE vs PAR for two different sessions (one session being September to December and the other comprising January to August). Notably during the September to December session, despite having lower temperature as well as lower PAR values compared to summer months of April and May, the study showed higher NEE values. This observation was unique as most of the other studies reported higher NEE during higher temperature conditions. Barr et al. (2013) mentioned that the light use efficiency of mangroves sometimes get saturated beyond a certain threshold of PAR, which might have taken place in Sundarbans as well during the peak of summer. The effect of salinity and tides on the atmosphere-biosphere CO_2 exchange was not taken into account in any of the studies on Sundarbans yet.

7.5.2.6   Soil CO_2 Flux Studies

Compared to eight published papers on atmosphere-biosphere CO_2 fluxover Sundarban mangroves, only two papers are published until yet on the soil CO_2 effluxes of mangroves (Chanda et al. 2011; Chanda et al. 2014).The soil CO_2 effluxes varied between 0.6 and 8.9 g m^{-2} day^{-1} throughout the year and the mean efflux was much less than the NEE observed in Sundarban, thus it can be inferred that Sundarban's terrestrial compartment at present is acting as a net sink for CO_2.

The soil CO_2 effluxes mainly varied with the varying soil temperature and seasonally a mild effect of soil moisture was found to play a regulating role (Chanda et al. 2011; Chanda et al. 2014). Excessive soil moisture was found to reduce the effluxes as the top soil was virtually super saturated with water, especially during the spring tide phase. The inward sites of the mangrove forest floor which exhibited high organic carbon content showed higher magnitude of fluxes, whereas, the near shore sites showed lower emission of CO_2.

7.5.2.7   Factors Regulating Soil CO_2 Flux

The magnitude of soil CO_2 fluxes observed were very much comparable to the findings in other mangroves of the world. The principal regulating factors were soil temperature and soil moisture, which is also found to be more or less the same in all

other mangroves. However, it is worth mentioning that the soil temperature in Sundarbans varied between 13.9 and 36.8 °C, and throughout this entire range, soil CO$_2$ fluxes were found to increase, i.e. a positive exponential relationship was observed between the soil CO$_2$ effluxes and soil temperature.

Lovelock (2008) on the contrary mentioned about a drop in soil CO$_2$ fluxes above 26 °C in many of the Australian mangroves. Such phenomenon did not take place in Sundarbans. In many studies (Leopold et al. 2013; Chen et al. 2014) negative fluxes, i.e. CO$_2$ fluxes towards the soil were observed due to the presence of biofilms. However, in Sundarbans no such biofilms were noted to exist in the selected study sites at least.

The effect of tides was the same in Sundarbans as observed in other mangroves i.e., higher soil CO$_2$ effluxes during low tides and vice-versa.

7.5.2.8   Spatial Variability of Air-Water CO$_2$ Flux

Like soil CO$_2$ effluxes, very few air-water CO$_2$ flux oriented studies have been conducted in Sundarbans. Biswas et al. (2004) reported the air-water CO$_2$ fluxes for the first time in the year 2004. They chose the study sites to be the sea mouths of three main distributaries flowing in the Sundarbans. The fluxes ranged from -0.02 to 0.05 g CO$_2$ m^{-2} day^{-1} (having a mean of 0.01 g CO$_2$ m^{-2} day^{-1}), which was several orders less than that observed in the forest floor or above canopy fluxes. Thus the sink strength of the Sundarban mangrove ecosystem as a whole was not compromised due to the air-water CO$_2$ fluxes. However, in this study the spatial variability was not discussed in details.

In order to address this issue, Akhand et al. (2013) carried out a short term work and a long term work throughout one complete annual cycle (Akhand et al. 2016) trying to characterize the spatial variability of air-water CO$_2$ fluxes in the inner, middle and outer estuarine stations. Both these studies observed that the inner estuarine stations were substantial sources of CO$_2$, whereas, the outer estuarine stations behaved as sinks of carbon, leading to lower mean effluxes from the air-water interface. It was found that the organic matter rich waters leading to re-mineralization to CO$_2$ was abundant in inner estuarine stations, whereas, in the outer estuarine stations, where the seawater lean in organic matter content diluted the mangrove exported water mass ultimately resulting in lower water pCO$_2$.

Incidentally the air-water CO$_2$ fluxes observed in the Sundarban waterways were fairly low compared to the results obtained in other mangrove waters of the world. It is worth mentioning that the estuary (namely Matla Estuary) where the study was undertaken happened to be an enclosed estuary, with very limited perennial supply of freshwater. This might have led to the greater dominance of sea water in the Sundarban mangroves (Indian part), however, observations like this emphasizes to take into account the spatial variability of CO$_2$ fluxes within a mangrove adjacent water mass, as up-scaling a single stationed data from any mangrove water body might highly overestimate the fluxes taking place at the air-water interface.

7.5.2.9 Factors Regulating Air-Water CO₂ Fluxes

Upon doing a comparative analysis between the air-water CO_2 fluxes observed in the Sundarbans and the other mangroves throughout the world, it can be seen that the magnitude of fluxes are quite low in Sundarbans. One of the main reasons behind such a contrasting finding may be that Sundarbans happen to be one of the rarest examples where the estuary is almost enclosed on the landward end and the freshwater flow is substantially less. Moreover, the area and volume of the estuaries are fairly large which allows a huge quantity of seawater to approach during high tide and recede during the low tide.

Very recently Rosentreter et al. (2018) after carrying out a holistic review mentioned that Sundarbans happen to be the only mangrove site in the world, where the water mass acts as a sink for CO_2. However, the study of Akhand et al. (2013) showed that was a significant spatial variability in CO_2 fluxes from the inward stations towards the outward stations; the inward stations acted as mild source of CO_2 whereas the outward stations acted as sinks. Usually a strong relation between the salinity and pCO_2 in water is seen in the mangrove waters especially while analyzing the spatial variability. However, in Sundarban (Indian part) since there is no significant freshwater supply from the landward end such spatial relation was not observed.

Apart from these the effect of tides were observed to be the same as in case of other mangroves of the world; i.e., higher fluxes during low tides and vice-versa.

7.6 Summary and Conclusion

Scrutinizing the findings of all the studies related to the atmosphere-biosphere CO_2 fluxes, soil CO_2 fluxes and air-water CO_2 fluxes conducted in the global mangroves, it can be summed up that almost all the mangrove forests that are studied throughout the world are at present acting as significant sinks of CO_2. However, still a lot of endeavor needs to be taken to estimate the year round global budgets of these fluxes and to reduce the uncertainties in the computation of these fluxes.

In this chapter we came to see that there could be various factors regulating atmosphere-biosphere CO_2 fluxes like canopy cover, species composition, age of the trees, ambient temperature near the canopy, rainfall, salinity regime in the forest floor and so forth, however, all the studies did not take into account each of these factors in the respective study sites. Much more data characterizing the fluxes with respect to all these factors in many more mangrove sites than what could be found at present is required to understand the CO_2 dynamics between the atmosphere and the mangrove canopy.

The research conducted in the Sundarban mangroves highlighted that for a vast stretch of mangroves like that of Sundarbans and especially where there lies a substantial heterogeneity in species assemblage, spatially explicit sampling is badly needed to properly up-scale the CO_2 flux data for the entire forest stretch. However,

most of the studies in this regard are carried out in single sites, which might significantly impose errors in global estimates.

On the contrary, soil CO$_2$ fluxes are studied in many mangrove forests and at various inter-tidal sites to examine the variability of fluxes. On the whole it can be inferred that the magnitude of fluxes reported from the forest floor was much less than the canopy uptake, implementing the net sink character of the mangroves to be intact. Soil temperature, soil moisture, organic carbon content, and presence of soil nutrients were the main regulating factors of soil CO$_2$ effluxes. However, much more emphasis needs to be given to the processes undergoing in the soil surface during inundated conditions, i.e. the pore water dynamics and the mineralization of CO$_2$ to DIC should be properly characterized or else the soil CO$_2$ efflux could significantly underestimated throughout the world.

The studies conducted in Sundarban though covered all the regulating factors like soil temperature, moisture, organic carbon content, soil texture and so forth. However, compared to the stretch of Sundarbans the sampling sites were limited. Thus Sundarban despite being the largest mangrove forest of the world cannot serve as a suitable proxy to upscale the fluxes to global level.

Air-water CO$_2$ fluxes, though measured in many mangrove sites, most of them are carried out in short term scales. It was evident from the present analysis that tidal dynamics, spatial variation in salinity and organic carbon, along with the effect of seasonality can substantially alter the air-water CO$_2$ fluxes. These aspects are still to a large extent neglected in most of the studies. Mangroves being such an ecosystem which constantly experiences a change in soil exposed area and adjacent water surface area, due to the dynamic encroachment and receding of tidally influenced water regime, more effort needs to be taken to quantify properly the area of soil and water surface.

The studies conducted in Sundarban further highlighted that based on the type of estuary, i.e. enclosed or perennially open and depending upon the position of the chosen sampling stations throughout the extent of the water ways the fluxes might vary to a great extent. This aspect should be dealt with more importance in the future studies to be carried out in different other mangroves of the world so as to reduce the uncertainties in air-water CO$_2$ fluxes from the mangrove adjacent water bodies. Keeping in mind all these factors and lessons learnt from the previous studies, a more holistic approach should be taken to quantify these fluxes taking place in the mangrove ecosystems of the world.

A global model to up-scale the annual budget of these fluxes and a model applicable to all the mangroves of world can only be prepared if all the constraints and regulating factors can be taken into account altogether vis-à-vis the changing regional sea level rise and anthropogenic rate of destruction of mangroves. As a concluding remark it can be stated further, that mangroves still prove to be an excellent option to combat the ongoing anthropogenic CO$_2$ emission. Hence, widespread awareness and endeavors to restore, prevention of destruction, afforestation and reforestation of degraded mangroves should be taken up globally to safeguard this unique ecosystem and the services they provide to the mankind and the environment.

References

Adame ME, Lovelock CE (2011) Carbon and nutrient exchange of mangrove forests with the coastal ocean. Hydrobiologia 663:23–50

Akhand A, Chanda A, Dutta S, Manna S, Sanyal P, Hazra S, Rao KH, Dadhwal VK (2013) Dual character of Sundarban estuary as a source and sink of CO_2 during summer: an investigation of spatial dynamics. Environ Monit Assess 185(8):6505–6515

Akhand A, Chanda A, Manna S, Das S, Hazra S, Roy R, Choudhury SB, Rao KH, Dadhwal VK, Chakraborty K, Mostofa KMG, Tokoro T, Kuwae T, Wanninkhof R (2016) A comparison of CO_2 dynamics and air-water fluxes in a river-dominated estuary and a mangrove-dominated marine estuary. Geophys Res Lett 43(22). https://doi.org/10.1002/2016GL070716

Alongi DM (2009) The energetics of mangrove forests. Springer Science, Dordrecht, 216 pp

Alongi DM (2012) Carbon sequestration in mangrove forests. Carbon Manag 3:313–322

Alongi DM (2014) Carbon cycling and storage in mangrove forests. Annu Rev Mar Sci 6:195–219

Alongi DM, Mukhopadhyay SK (2015) Contribution of mangroves to coastal carbon cycling in low latitude seas. Agric For Meteorol 213:266–272

Alongi DM, Wattayakorn G, Pfitzner J, Tirendi F, Zagorskis I, Brunskill GJ, Clough BF (2001) Organic carbon accumulation and metabolic pathways in sediments of mangrove forests in southern Thailand. Mar Geol 179(1):85–103

Alongi DM, Sasekumar A, Chong VC, Pfitzner J, Trott LA, Tirendi F, Dixon P, Brunskill GJ (2004) Sediment accumulation and organic material flux in a managed mangrove ecosystem: estimates of land-ocean-atmosphere exchange in peninsular Malaysia. Mar Geol 208:383–402

Alongi DM, Pfitzner J, Trott LA, Tirendi F, Dixon P, Klumpp DW (2005) Rapid sediment accumulation and microbial mineralization in forests of the mangrove *Kandeliacandel* in the Jiulongjiang Estuary, China. Estuar Coast Shelf Sci 63(4):605–618

Baldocchi DD (2008) 'Breathing' of the terrestrial biosphere: lessons learned from a global network of carbon dioxide flux measurement systems. Aust J Bot 56:1–26. https://doi.org/10.1071/BT07151

Baldocchi DD, Hicks BB, Meyers TP (1988) Measuring biosphere–atmosphere exchanges of biologically related gases with micrometeorological methods. Ecology 69:1331–1340

Baldocchi DD et al (2001) FLUXNET: a new tool to study the temporal and spatial variability of ecosystem-scale carbon dioxide, water vapor, and energy flux densities. Bull Am Meteorol Soc 82:2415–2434. https://doi.org/10.1175/1520-0477(2001)082<2415:FANTTS>2.3.CO;2

Ball MC (1988) Ecophysiology of mangroves. Trees 2:129–142

Barr JG, Engel V, Fuentes JD, Zieman JC, O'Halloran TL, Smith TJ, Anderson GH (2010) Controls on mangrove forest-atmosphere carbon dioxide exchanges in western Everglades National Park. J Geophys Res Biogeosci 115(G2). https://doi.org/10.1029/2009JG001186

Barr JG, Engel V, Smith TJ, Fuentes JD (2012) Hurricane disturbance and recovery of energy balance, CO_2 fluxes and canopy structure in a mangrove forest of the Florida Everglades. Agric For Meteor 153:54–66

Barr JG, Engel V, Fuentes JD, Fuller D, Kwon H-H (2013) Modeling light use efficiency in a subtropical mangrove forest equipped with CO_2 eddy covariance. Biogeosciences 10:2145–2158

Beer C, Reichstein M, Tomelleri E, Ciais P, Jung M, Carvalhais N, R¨odenbeck C, AltafArain M, Baldocchi D, Bonan GB, Bondeau A, Cescatti A, Lasslop G, Lindroth A, Lomas M, Luyssaert S, Margolis H, Oleson KW, Roupsard O, Veenendaal E, Viovy N, Williams C, IanWoodward F, Papale D (2010) Terrestrial gross carbon dioxide uptake: global distribution and covariation with climate. Science 329:834–838

Biswas H, Mukhopadhyay SK, De TK, Sen S, Jana TK (2004) Biogenic controls on the air—water carbon dioxide exchange in the Sundarban mangrove environment, northeast coast of Bay of Bengal, India. Limnol Oceanogr 49(1):95–101

Biswas H, Mukhophadhya SK, Sen S, Jana TK (2007) Spatial and temporal patterns of methane dynamics in the tropical mangrove dominated estuary, NE coast of Bay of Bengal, India. J Mar Syst 68:55–64

Borges AV, Djenidi S, Lacroix G, Theate G, Delille B, Frankignoulle M (2003) Atmospheric CO$_2$ flux from mangrove surrounding waters. Geophys Res Lett 30(11):1558. https://doi.org/10.1029/2003GL017143

Bouillon S, Koedam N, Raman AV, Dehairs F (2002) Primary producers sustaining macro-invertebrate communities in intertidal mangrove forests. Oecologia 130:441–448

Bouillon S, Frankignoulle M, Dehairs F, Velimirov B, Eiler A, Abril G, Etcheber H, Borges AV (2003) Inorganic and organic carbon biogeochemistry in the Gautami Godavari estuary (Andhra Pradesh, India) during pre-monsoon: the local impact of extensive mangrove forests. Global Biogeochem Cycles 17(4). https://doi.org/10.1029/2002GB002026

Bouillon S, Borges AV, Castañeda-Moya E, Diele K, Dittmar T, Duke NC, Kristensen E, Lee SY, Marchand C, Middleburg JJ, Rivera-Monroy VH, Smith TJ III, Twilley RR (2008) Mangrove production and carbon sinks: A revision of global budget estimates. Global Biogeochem Cycles 22:GB2013. https://doi.org/10.1029/2007GB003052

Breithaupt JL, Smoak JM, Smith TJ, Sanders CJ, Hoare A (2012) Organic carbon burial rates in mangrove sediments: strengthening the global budget. Global Biogeochem Cycles 26(3). https://doi.org/10.1029/2012GB004375

Bulmer R, Lundquist C, Schwendenmann L (2015) Sediment properties and CO$_2$ efflux from intact and cleared temperate mangrove forests. Biogeosciences 12:6169–6180

Call M, Maher DT, Santos IR, Ruiz-Halpern S, Mangion P, Sanders CJ, Erler DV, Oakes JM, Rosentreter J, Murray R, Eyre BD (2015) Spatial and temporal variability of carbon dioxide and methane fluxes over semi-diurnal and spring–neap–spring timescales in a mangrove creek. Geochim Cosmochim Acta 150:211–225

Campbell JE, Berry JA, Seibt U, Smith SJ, Montzka SA, Launois T, Belviso S, Bopp L, Laine M (2017) Large historical growth in global terrestrial gross primary production. Nature 544(7648):84

Chanda A, Akhand A, Dutta S, Hazra S (2011) Summer fluxes of CO$_2$ from soil, in the coastal margin of world's largest mangrove patch of Sundarbans–first report. J Basic Appl Sci Res 1:2137–2141

Chanda A, Akhand A, Manna S, Dutta S, Das I, Hazra S (2013a) Spatial variability of atmosphere-biosphere CO$_2$ and H$_2$O exchange in selected sites of Indian Sundarbans during summer. Trop Ecol 54(2):167–178

Chanda A, Akhand A, Manna S, Dutta S, Hazra S, Das I, Dadhwal VK (2013b) Characterizing spatial and seasonal variability of carbon dioxide and water vapour fluxes above a tropical mixed mangrove forest canopy, India. J Earth Syst Sci 122(2):503–513

Chanda A, Akhand A, Manna S, Dutta S, Das I, Hazra S, Rao KH, Dadhwal VK (2014) Measuring daytime CO$_2$ fluxes from the inter-tidal mangrove soils of Indian Sundarbans. Environ Earth Sci 72(2):417–427

Chanda A, Mukhopadhyay A, Ghosh T, Akhand A, Mondal P, Ghosh S, Mukherjee S, Wolf J, Lázár AN, Rahman MM, Salehin M, Chowdhury SM, Hazra S (2016) Blue carbon stock of the Bangladesh Sundarban mangroves: what could be the scenario after a century? Wetlands 36(6):1033–1045

Chen GC, Tam NFY, Ye Y (2010) Summer fluxes of atmospheric greenhouse gases N$_2$O, CH$_4$ and CO$_2$ from mangrove soil in South China. Sci Total Environ 408(13):2761–2767

Chen GC, Tam NFY, Ye Y (2012) Spatial and seasonal variations of atmospheric N$_2$O and CO$_2$ fluxes from a subtropical mangrove swamp and their relationships with soil characteristics. Soil Biol Biochem 48:175–181

Chen GC, Ulumuddin YI, Pramudji S, Chen SY, Chen B, Ye Y, Ou DY, Ma ZY, Huang H, Wang JK (2014) Rich soil carbon and nitrogen but low atmospheric greenhouse gas fluxes from North Sulawesi mangrove swamps in Indonesia. Sci Total Environ 487:91–96

Chen G, Chen B, Yu D, Tam NFY, Ye Y, Chen S (2016) Soil greenhouse gas emissions reduce the contribution of mangrove plants to the atmospheric cooling effect. Environ Res Lett 11(12):124019. https://doi.org/10.1088/1748-9326/11/12/124019

Dixon RK, Brown S, Houghton RA, Solornon AM, Trexler MC, Wisniewski J (1994) Carbon pools and flux of global forest ecosystems. Science 263:185–190

Donato DC, Kauffman JB, Murdiyarso D, Kurnianto K, Stidham M, Kanninen M (2011) Mangroves among the most carbon-rich forests in the tropics. Nat Geosci 4:293–297

Feller IC, Lovelock CE, Berger U, McKee KL, Joye SB, Ball MC (2010) Bio-complexity in mangrove ecosystems. Annu Rev Mar Sci 2:395–417

Fourqurean JW, Duarte CM, Kennedy H, Marbà N, Holmer M, Mateo MA et al (2012) Seagrass ecosystems as a globally significant carbon stock. Nat Geosci 5(7):505–509

Ganguly D, Dey M, Mandal SK, De TK, Jana TK (2008) Energy dynamics and its implication to biosphere–atmosphere exchange of CO_2, H_2O and CH_4 in a tropical mangrove forest canopy. Atmos Environ 42(18):4172–4184

Giri C, Ochieng E, Tieszen LL, Zhu Z, Singh A, Loveland T, Masek J, Duke N (2011) Status and distribution of mangrove forests of the world using earth observation satellite data. Glob Ecol Biogeogr 20(1):154–159

Gouda R, Panigrahy RC (1996) The mangroves of Orissa. J Indian Ocean Stud 3(3):228–237

Hamilton S, Casey D (2016) Creation of high spatiotemporal resolution global database of continuous mangrove forest cover for the 21st century: a big-data fusion approach. Glob Ecol Biogeogr 25:729–738

Hinson AL, Feagin RA, Eriksson M, Najjar RG, Herrmann M, Bianchi TS, Kemp M, Hutchings JA, Crooks S, Boutton T (2017) The spatial distribution of soil organic carbon in tidal wetland soils of the continental United States. Glob Chang Biol 23(12):5468–5480

Hirata R, Saigusa N, Yamamoto S, Ohtani Y, Ide R, Asanuma J, Gamo M, Hirano T, Kondo H, Kosugi Y, Li SG, Nakai Y, Takagi K, Tani M, Wang H (2008) Spatial distribution of carbon balance in forest ecosystems across East Asia. Agric For Meteorol 148(5):761–775

Ho DT, Coffineau N, Hickman B, Chow N, Koffman T, Schlosser P (2016) Influence of current velocity and wind speed on air-water gas exchange in a mangrove estuary. Geophys Res Lett 43:3813–3821

Ho DT, Wanninkhof R, Schlosser P, Ullman DS, Hebert D, Sullivan KF (2011) Towards a universal relationship between wind speed and gas exchange: gas transfer velocities measured with 3He/SF6 during the Southern Ocean gas exchange experiment. J Geophys Res 116:C00F04. https://doi.org/10.1029/2010JC006854

Ho DT, Ferrón S, Engel VC, Larsen LG, Barr JG (2014) Air-water gas exchange and CO_2 flux in a mangrove-dominated estuary. Geophys Res Lett 41:108–113. https://doi.org/10.1002/2013GL058785

Inoue T (2018) Carbon sequestration in mangroves. In: Kuwae T, Hori M (eds) Blue carbon in shallow coastal ecosystems: carbon dynamics, policy, and implementation. Springer, Singapore, pp 73–99

IPCC (2007) Climate change 2007: the physical science basis. Contribution of Working Group I to the fourth assessment report of the Intergovernmental Panel on Climate Change. In: Solomon S, Qin D, Manning M, Chen Z, Marquis M, Tignor KBM, Miller HL (eds) Cambridge University Press, Cambridge/New York

IPCC (2012) Summary for policymakers, in managing the risks of extreme events and disasters to advance climate change adaptation: a special report of Working Groups I and II of the Intergovernmental Panel On Climate Change, In: Field CB, Barros V, Stocker TF, Qin D, Dokken DJ, Ebi KL, Mastrandrea MD, Mach KJ, Plattner G-K, Allen SK, Tignor M, Midgley PM (eds) Cambridge University Press, Cambridge/New York, pp 1–19

IUCN (2009) The management of natural coastal carbon sink. In: Laffoley D, GrimsditchG (eds) IUCN World Commission on Protected Areas; Natural England; UNEP

Jennerjahn TC, Ittekkot V (2002) Relevance of mangroves for the production and deposition of organic matter along tropical continental margins. Naturwissenschaften 89:23–30

Joffre R, Ourcival JM, Rambal S, Rocheteau A (2003) The key-role of topsoil moisture on CO_2 efflux from a Mediterranean *quercus ilex* forest. Ann For Sci 60:519–526

Kanemasu ET, Wesely ML, Hicks BB, Heilman JL (1979) Techniques for calculating energy and mass fluxes. In: Barfield BL, Gerber JF (eds) Modification of the aerial environment of crops. American Society of Agricultural Engineering, St. Joseph

Kang WX, Zhao ZH, Tian DL, He JN, Deng XW (2008) CO$_2$ exchanges between mangrove- and shoal wetland ecosystems and atmosphere in Guangzhou. Ying Yong Sheng Tai Xue Bao 19(12):2605–2610 (Article in Chinese)

Kirui B, Huxham M, Kairo JG, Mencuccini M, Skov MW (2009) Seasonal dynamics of soil carbon dioxide flux in a restored young mangrove plantation at Gazi Bay. In: Hoorweg J, Muthiga N (eds) Advances in coastal ecology. African Studies Centre Publisher, Leiden, pp 122–130

Komiyama A, Ong JE, Poungparn S (2008) Allometry, biomass, and productivity of mangrove forests: a review. Aquat Bot 89:128–137

Koné YM, Borges AV (2008) Dissolved inorganic carbon dynamics in the waters surrounding forested mangroves of the Ca Mau Province (Vietnam). Estuar Coast Shelf Sci 77(3):409–421

Kristensen E, Flindt MR, Ulomi S, Borges AV, Abril G, Bouillon S (2008) Emission of CO$_2$ and CH$_4$ to the atmosphere by sediments and open waters in two Tanzanian mangrove forests. Mar Ecol Prog Ser 370:53–67

Lacerda LD, Conde JE, Kjerfve B, Alvarez-León R, Alarcón J, Polanía J (2002) American mangroves. In: Lacerda LD (ed) Mangrove ecosystems: function and management. Springer, Berlin, pp 1–62

Lear R, Turner T (1977) Mangrove of Australia. University of Queensland Press, St. Lucia

Leopold A, Marchand C, Deborde J, Chaduteau C, Allenbach M (2013) Influence of mangrove zonation on CO$_2$ fluxes at the sediment–air interface (New Caledonia). Geoderma 202:62–70

Li Q, Lu W, Chen H, Luo Y, Lin G (2014) Differential responses of net ecosystem exchange of carbon dioxide to light and temperature between spring and neap tides in subtropical mangrove forests. Sci World J https://doi.org/10.1155/2014/943697

Linto N, Barnes J, Ramachandran R, Divia J, Ramachandran P, Upstill-Goddard RC (2014) Carbon dioxide and methane emissions from mangrove-associated waters of the Andaman Islands, Bay of Bengal. Estuar Coasts 37:381–398

Liu WW, Wang XK, Lu F, Ouyang ZY (2015) Regional and global estimates of carbon stocks and carbon sequestration capacity in forest ecosystems: a review. J Appl Ecol 26(9):2881–2890

Lovelock CE (2008) Soil respiration and belowground carbon allocation in mangrove forests. Ecosystems 11:342–354

Lovelock CE, Ruess RW, Feller IC (2011) CO$_2$ efflux from cleared mangrove peat. PLoS One 6(6):e21279

Luo Y, Zhou X (2006) Soil respiration and the environment. Elsevier, Amsterdam

Luyssaert S, Inglima I, Jung M, Richardson AD, Reichstein M, Papale D et al (2007) CO$_2$ balance of boreal, temperate, and tropical forests derived from a global database. Glob Chang Biol 13(12):2509–2537

Macnae W (1968) A general account of the flora and fauna of mangrove swamps in the Indo-Western Pacific region. Adv Mar Biol 6:73–270

Magnani F, Mencuccini M, Borghetti M, Berbigier P, Berninger F, Delzon S, Grelle A, Hari P, Jarvis PG, Kolari P, Kowalski AS, Lankreijer H, Law BE, Lindroth A, Loustau D, Manca G, Moncrieff JB, Rayment M, Tedeschi V, Valentini R, Grace J (2007) The human footprint in the carbon cycle of temperate and boreal forests. Nature 447:849–851

McLeod E, Chmura GL, Bouillon S, Salm R, Björk M, Duarte CM, Lovelock CE, Schlesinger WH, Silliman BR (2011) A blueprint for blue carbon: toward an improved understanding of the role of vegetated coastal habitats in sequestering CO$_2$. Front Ecol Environ 9:552–560

Mepham R, Mepham JS (1984) The flora of tidal forests—a rationalization of the use of term mangrove. South African J Bot 51:77–79

Misson L, Baldocchi DD, Black TA, Blanken PD, Brunet Y, Curiel Yuste J, Dorsey JR, Falk M, Granier A, Irvine MR, Jarosz N, Lamaud E, Launiainen S, Law BE, Longdoz B, Loustau D, McKay M, Paw UKT, Vesala T, Vickers D, Wilson KB, Goldstein AH (2007) Partitioning forest carbon fluxes with overstory and understory eddy-covariance measurements: a synthesis based on FLUXNET data. Agric For Meteorol 144:14–31

Monji N, Hamotani K, Hirano T, Yabuki K, Jintana V (1996) Characteristics of CO$_2$ flux over a mangrove forest of southern Thailand in rainy season. J Agric Meteorol 52(5):149–154

Monji N, Hamotani K, Hirano T, Fukagawa T, Yabuki K, Jintana V (1997) CO_2 and heat exchange of mangrove forest in Thailand. J Agric Meteorol 52(5):489–492

Monji N, Hamotani K, Hamada Y, Agata Y, Hirano T, Jintana V, Piriyayota S, Nishimiya A, Iwasaki M (2002) Exchange of CO_2 and heat between mangrove forest and the atmosphere in wet and dry seasons in Southern Thailand. J Agric Meteorol 58(2):71–77

Morrisey DJ, Swales A, Dittmann S, Morrison M, Lovelock C, Beard C (2010) The ecology and management of temperate mangroves. Oceanogr Mar Biol 48:43–160. https://doi.org/10.1201/EBK1439821169-c2

Mukhophadhya SK, Biswas H, Das KL, De TK, Jana TK (2001) Diurnal variation of carbon dioxide and methane exchange above Sundarbans mangrove forest, in NW coast of India. Indian J Mar Sci 30:70–74

Mukhophadhya SK, Biswas H, De TK, Sen BK, Sen S, Jana TK (2002) Impact of Sundarban mangrove biosphere on the carbon dioxide and methane mixing ratios at the NE Coast of Bay of Bengal, India. Atmos Environ 36(4):629–638

Murdiyarso D et al (2015) The potential of Indonesian mangrove forests for global climate change mitigation. Nat Clim Chang 5:8–11

Neue HU, Gaunt JL, Wang ZP, Becker-Heidmann P, Quijano C (1997) Carbon in tropical wetlands. Geoderma 79(1):163–185

Nóbrega GN, Ferreira TO, Neto MS, Queiroz HM, Artur AG, Mendonça EDS, Silva EDO, Otero XL (2016) Edaphic factors controlling summer (rainy season) greenhouse gas emissions (CO_2 and CH_4) from semiarid mangrove soils (NE-Brazil). Sci Total Environ 542:685–693

Noe SM, Kimmel V, Hüve K, Copolovici L, Portillo-Estrada M, Püttsepp Ü, Jõgiste K, Niinemets Ü, Hörtnagl L, Wohlfahrt G (2011) Ecosystem-scale biosphere–atmosphere interactions of a hemiboreal mixed forest stand at Järvselja, Estonia. Forest Ecol Manag 262:71–81

Oades JM (1998) The retention of organic matter in soils. Biogeochemistry 5(1):35–70. https://doi.org/10.1007/BF02180317

Otani S, Endo T (2018) CO_2 flux in tidal flats and salt marshes. In: Kuwae T, Hori M (eds) Blue carbon in shallow coastal ecosystems: carbon dynamics, policy, and implementation. Springer, Singapore, pp 223–250

Parani M, Lakshmi M, Senthilkumar P, Ram N, Parida A (1998) Molecular phylogeny of mangroves V. Analysis of genome relationships in mangrove species using RAPD and RFLP markers. Theor Appl Genet 97:617–625

Pendleton L, Donato DC, Murray BC, Crooks S, Jenkins WA, Sifleet S et al (2012) Estimating global 'blue carbon' emissions from conversion and degradation of vegetated coastal ecosystems. PLoS One 7:e43542. https://doi.org/10.1371/journal.pone.0043542

Poungparn S, Komiyama A, Tanaka A, Sangtiean T, Maknual C, Kato S, Tanapermpool P, Patanaponpaiboon P (2009) Carbon dioxide emission through soil respiration in a secondary mangrove forest of eastern Thailand. J Trop Ecol 25(4):393–400

Rahman AF, Dragoni D, El-Masri B (2011) Response of the Sundarbans coastline to sea level rise and decreased sediment flow: a remote sensing assessment. Remote Sens Environ 115(12):3121–3128

Rahman MM, Khan MNI, Hoque AF, Ahmed I (2015) Carbon stock in the Sundarban mangrove forest: spatial variations in vegetation types and salinity zones. Wetl Ecol Manag 23:269–283

Raich JW, Schlesinger WH (1992) The global carbon dioxide flux in soil respiration and its relationship to vegetation and climate. Tellus 44B:81–99

Ray R, Jana TK (2017) Carbon sequestration by mangrove forest: one approach for managing carbon dioxide emission from coal-based power plant. Atmos Environ 171:149–154

Ray R, Ganguly D, Chowdhury C, Dey M, Das S, Dutta MK, Mandal SK, Majumdar N, De TK, Mukhopadhyay SK, Jana TK (2011) Carbon sequestration and annual increase of carbon stock in a mangrove forest. Atmos Environ 45(28):5016–5024

Reich PB (2010) The carbon dioxide exchange. Science 329:774–775

Rodda SR, Thumaty KC, Jha CS, Dadhwal VK (2016) Seasonal variations of carbon dioxide, water vapor and energy fluxes in tropical Indian mangroves. Forests 7(2):35–41. https://doi.org/10.3390/f7020035

Rosentreter JA, Maher DT, Erler DV, Murray R, Eyre BD (2018) Seasonal and temporal CO$_2$ dynamics in three tropical mangrove creeks–A revision of global mangrove CO$_2$ emissions. Geochim Cosmochim Acta 222:729–745

Rustad LE, Huntington TG, Boone RD (2000) Controls on soil respiration: implications for climate change. Biogeochemistry 48:1–6

Sanyal P, Mukhopadhyay A, Das I (2008) Sundarban – the greatest Mangal diversity of the planet. J Indian Soc Coastal Agric Res 26(2):132–134

Sarkar SK, Frančišković-Bilinski S, Bhattacharya A, Saha M, Bilinski H (2004) Levels of elements in the surficial estuarine sediments of the Hugli River, northeast India and their environmental implications. Environ Int 30:1089–1098

Siikamäki J, Sanchirico JN, Jardine SL (2012) Global economic potential for reducing carbon dioxide emissions from mangrove loss. Proc Natl Acad Sci U S A 109:14369–14374

Sippo JZ, Maher DT, Tait DR, Holloway C, Santos IR (2016) Are mangroves drivers or buffers of coastal acidification? insights from alkalinity and dissolved inorganic carbon export estimates across a latitudinal transect. Global Biogeochem Cycles 30:753–766. https://doi.org/10.1002/2015GB005324

Skov MW, Vannini M, Shunula PJ, Hartnoll GR (2002) Quantifying the density of mangrove crabs: Ocypodidae and Grapsidae. Mar Biol 141:725–732

Smith TJ III, Anderson GH, Balentine K, Tiling G, Ward GA, Whelan KRT (2009) Cumulative impacts of hurricanes on Florida mangrove ecosystems: sediment deposition, storm surges and vegetation. Wetlands 29:24–34

Sweeney C, Gloor E, Jacobson AR, Key RM, McKinley G, Sarmiento JL, Wanninkhof R (2007) Constraining global air-sea gas exchange for CO$_2$ with recent bomb ^{14}C measurements. Global Biogeochem Cycles 21:GB2015. https://doi.org/10.1029/2006GB002784

Takahashi T et al (2009) Climatological mean and decadal change in surface ocean pCO$_2$, and net sea-air CO$_2$ flux over the global oceans. Deep-Sea Res II Top Stud Oceanogr 56:554–577. https://doi.org/10.1016/j.dsr2.2008.12.009

Tokoro T, Kayanne H, Watanabe A, Nadaoka K, Tamura H, Nozaki K, Kato K, Negishi A (2008) High gas-transfer velocity in coastal regions with high energy-dissipation rates. J Geophys Res Oceans 113(C11)

Tokoro T, Watanabe K, Tada K, Kuwae T (2018) Air–water CO$_2$ flux in shallow coastal waters:theoretical background, measurement methods, andmechanisms. In: Kuwae T, Hori M (eds) Blue carbon in shallow coastal ecosystems: carbon dynamics, policy, and implementation. Springer, Singapore, pp 153–184

Tomlinson PB (1986) The botany of mangroves. Cambridge University Press, Cambridge

Troxler TG, Barr JG, Fuentes JD, Engel V, Anderson G, Sanchez C, Lagomasino D, Price R, Davis SE (2015) Component-specific dynamics of riverine mangrove CO$_2$ efflux in the Florida coastal Everglades. Agric For Meteorol 213:273–282

Van Lavieren H, Spalding M, Alongi DM, Kainuma M, Clüsener-Godt M, Adeel Z (2012) Securing the future of mangroves. A policy brief. UNU-INWEH,UNESCO-MAB with ISME, ITTO, FAO, UNEP-WCMC and TNC, 53pp

Wanninkhof R (2014) Relationship between wind speed and gas exchange over the ocean revisited. Limnol Oceanogr Methods 12:351–362. https://doi.org/10.4319/lom.2014.12.351

Wanninkhof R, Triñanes J (2017) The impact of changing wind speeds on gas transfer and its effect on global air-sea CO$_2$ fluxes, Global Biogeochem Cycles 31. https://doi.org/10.1002/2016GB005592

Wofsy SC, Harris RC (2002) The North American carbon program (NACP), report of the NACP Committee of the U.S. Interagency Carbon Cycle Science Program, 56 pp, U.S. Global Change Res. Program, Washington, DC

Zablocki JA, Andersson AJ, Bates NR (2011) Diel aquatic CO$_2$ system dynamics of a Bermudian mangrove environment. Aquat Geochem 17(6):841–859

Chapter 8
CO$_2$ Flux in Tidal Flats and Salt Marshes

Sosuke Otani and Toru Endo

Abstract Tidal flats and salt marshes are sites where CO$_2$ is released to the environment by decomposing organic matter and CO$_2$ is absorbed by vegetation through photosynthesis. It is thought that on balance, carbon is stored in tidal flats and salt marshes. To explore this topic, we reviewed published estimates of air–water, air–sediment, water–sediment, and air–marsh fluxes of CO$_2$ in tidal flats and salt marshes. We also carried out multiyear measurements of CO$_2$ flux and related parameters at two field sites in Osaka Bay, Japan, having flat intertidal and salt marsh areas. The CO$_2$ fluxes were measured using the eddy correlation and chamber methods. The air–sediment CO$_2$ flux data from tidal flats indicated net absorption of atmospheric CO$_2$ into the sediment during daytime hours. The air–water CO$_2$ flux data indicated that CO$_2$ was emitted from the water surface in small amounts, with temporal fluctuations and seasonal changes that were strongly related to salinity, as has been documented in the literature. We found that CO$_2$ was absorbed into salt marsh and intertidal sediment and that CO$_2$ was emitted from subtidal sediment as well as from the water surface of the tidal flat ecosystem during periods of submersion. The air–sediment CO$_2$ flux and its temporal fluctuation at the field sites appear to be regulated by vegetation such as the reed *Phragmites australis* and microphytobenthos.

S. Otani (✉)
Civil Engineering and Environment Course, Department of Technological Systems, Osaka Prefecture University College of Technology, Saiwaicho, Neyagawa, Osaka, Japan
e-mail: otani@osaka-pct.ac.jp

T. Endo
Graduate School of Engineering, Osaka City University,
Sugimoto, Sumiyoshi-ku, Osaka, Japan

8.1   Introduction

Estuarine Tidal flats and marshes are influenced by freshwater from rivers and sea-water from offshore and are also sites where tides cause large environmental fluc-tuations. Because they serve as places of decomposition of organic matter inflowing from the watershed, these ecosystems have typically been regarded as CO_2 sources (Laruelle et al. 2013; Regnier et al. 2013). However, salt marshes are drawing atten-tion for their role in blue carbon storage (Nellemann et al. 2009). Researchers are investigating the plants that directly and indirectly absorb atmospheric CO_2 as well as the animals and soils that store carbon.

Besides hosting vigorous biogenic production and consumption, tidal flats and marshes display wide variations in CO_2 absorption and emission in response to carbon influx driven by tides. Primary producers in these settings include large veg-etation and benthic microalgae (microphytobenthos), and all participate in the cycling of material through the food web. The macroalgae and seagrass are con-sumed by fish (Yoshida et al. 2015), mangrove leaves are a food source of crabs (Robertson 1986; Skov and Hartnoll 2002), and microphytobenthos are major food sources for macrobenthos.

The strong influence of tides means that tidal flats and salt marshes fluctuate between being CO_2 sources and sinks over the course of a day. Therefore, it is nec-essary to evaluate CO_2 and carbon fluxes on a detailed temporal and seasonal scale. However, compared with data from land areas and the open ocean, CO_2 gas flux data from shallow coastal waters are scarce (Laruelle et al. 2013).

In this study, we sought to review the published CO_2 gas flux data from tidal flats and salt marshes and to quantitatively evaluate CO_2 flux at two field sites near Osaka, Japan, as model cases. Our main focus was CO_2 fluxes across the air–water and air–sediment interfaces. Positive values of CO_2 flux and heat flux indicate sources to the atmosphere and negative values indicate sinks from the atmosphere. CO_2 fluxes in tidal flat and salt marsh ecosystems are shown schematically in Fig. 8.1.

8.2   Literature Review on CO_2 Flux in Tidal Flats and Marshes

Direct ways to measure air–water CO_2 flux include the eddy correlation method and the chamber method, but the indirect bulk method is widely used because of the ease in obtaining the necessary parameters such as wind speed and temperature (Tokoro et al. 2018). Table 8.1 lists representative studies of CO_2 flux using these three methods in intertidal and subtidal areas.

More studies of air–ecosystem CO_2 flux using the eddy correlation method have been conducted in salt marshes than in tidal flats, and these focused on absorption of CO_2 flux throughout the year. In particular, much research has targeted the common
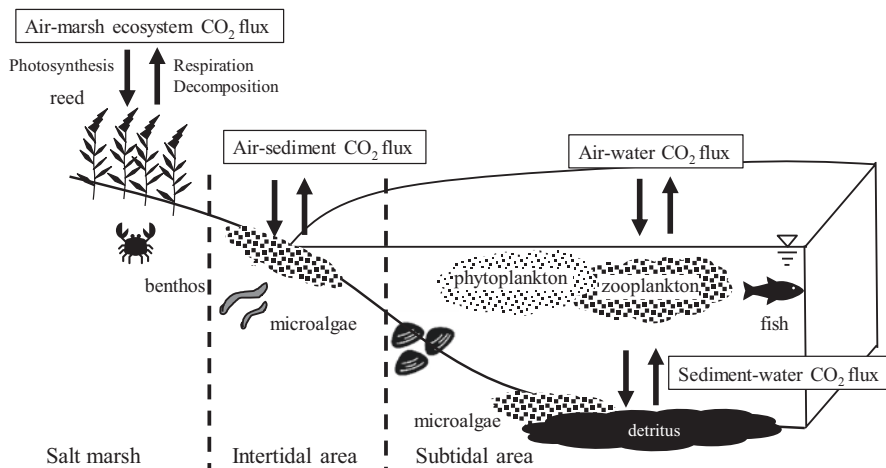
Fig. 8.1 Diagram showing representative CO_2 fluxes in tidal flat ecosystems

Table 8.1 Representative studies of CO_2 flux using one of three major measurement methods in tidal flat and salt marsh ecosystems

Subject	Object[a]	Measurement method[b]	Station	CO_2 flux (mmol C/m²/ day)	Measurement period and notes	References
Air–tidal flat	T	E	Ariake Bay, Japan	−417 to −83	April	Tanaka and Takikawa (2006)
	T	E	Ariake Bay, Japan	83–833	May–June	Tanaka and Takikawa (2006)
	T	E	Wadden Sea	−158	Spring average	Zemmelink et al. (2009)
	T	E	Arcahon Bay, France	42	September–October *Zostera noltii*	Polsenaere et al. (2012)
	T	E	Arcahon Bay, France	−200–8	April, September–October, July *Z. noltii*	Polsenaere et al. (2012)
Air–salt marsh	S	E	Yangtze River, China	−285	Year *Spartina alterniflora*	Guo et al.(2009)
	S	E	Yangtze River, China	−1037	Year *Phragmites australis*	Guo et al.(2009)

Table 8.1 (continued)

Subject	Object[a]	Measurement method[b]	Station	CO_2 flux (mmol C/m²/day)	Measurement period and notes	References
	S	E	Panjin wetland, China	−309 to −170	July–October *P. australis*	Zhou et al. (2009)
	S	E	Yellow River, China	−252 to −20	July–October *P. australis*	Han et al. (2013)
	S	E	Hudson-Raritan estuary, USA	−67– 225	Year *P. australis, S. alterniflora*	Schäfer et al. (2014)
	S	E	New Jersey wetland, USA	−306	Year, max value *P. australis*	Artigas et al. (2015)
	S	E	Yangtze River, China	−129	Year *P. australis*	Zhong et al. (2016)
	S	E	Yodo River, Japan	−341– 139	Year *P. australis*	Otani and Marikawa (2017)
Air– sediment	S	C	Dipper harbour, Canada	57	July– September *S. alterniflora* and other plant community Dark condition	Magenheimer et al. (1996)
	S	C	Ribble estuary, England	182	Year *Festuca rubra* Dark condition	Ford et al. (2012)
	S	C	Ribble estuary, England	229	Year *Elytrigia repens* Dark condition	Ford et al. (2012)
	T	C	Westerschelde estuary, Netherlands	22–381	Year Dark condition	Middelburg et al. (1996)
	T	C	Kurose River, Japan	30–135	Summer dark condition	Sasaki et al. (2012)
	T	C	Somme River, France	−87	August Light and dark condition	Migné et al. (2002)
	T	C	Eastern English Channel, France	−35	Year Light and dark condition	Spilmont et al. (2005)
	T	C	Wadden Sea, northern Europe	−16–4	Year Light and dark condition	Klaassen and Spilmont (2012)

Table 8.1 (continued)

Subject	Object[a]	Measurement method[b]	Station	CO$_2$ flux (mmol C/m²/day)	Measurement period and notes	References
	T	C	Arcahon Bay, France	−237	Winter, spring, fall, max value	Migné et al. (2016)
					Light and dark condition	
	T	C	Yodo River, Japan	−36.3	Year average	Otani et al. (2017)
					Light and dark condition	
	T	C	Yodo River, Japan	25.5	Year average	Otani et al. (2017)
					Dark condition	
	T	C	Nanko bird sanctuary, Japan	2.0	Spring	Endo et al. (2016)
	T	C		−133.9	Summer	Endo et al. (2016)
	T	C		−78.5	Fall	Endo et al. (2016)
	T	C		−7.5	Winter	Endo et al. (2016)
Water–sediment	T	C	Nanko bird sanctuary, Japan	−16.4– 46.5	May	Tanaka et al. (2016) and Yamochi et al. (2017)
					Submerged subtidal area	
	T	C		−26.2– 26.2	July	Tanaka et al. (2016) and Yamochi et al. (2017)
					Submerged subtidal area	
Air–water		B	Guadalquivir River, Spain	67	Year average	Flecha et al. (2015)
					Salinity, 1.1 ± 0.6	
		B	Guadalquivir River, Spain	20	Year average	Flecha et al. (2015)
					Salinity, 9.2 ± 6.8	
		B	Guadalquivir River, Spain	3	Year average	Flecha et al. (2015)
					Salinity, 30.0 ± 6.4	
		C	Scheldt estuary, northern Europe	65–925	April salinity, 0.57–19.29	Borges et al. (2004b)
		C	Scheldt estuary, northern Europe	259– 1377	November salinity, 0.41–13.31	Borges et al. (2004b)

Table 8.1 (continued)

Subject	Object[a]	Measurement method[b]	Station	CO_2 flux (mmol $C/m^2/$ day)	Measurement period and notes	References
		C	Gironde estuary, France	12–331	May salinity, 0.3–5.3	Abril et al. (2009)
		C	Gironde estuary, France	28–194	November salinity, 5.4–10.7	Abril et al. (2009)
			26 cases inner estuaries	50–760		Frankignoulle et al. (1998)
			11 stations inner estuaries	6.1–211		Borges et al. (2006)
			165 estuaries and 87 continental shelves	108	Salinity, <2	Chen et al. (2013)
			165 estuaries and 87 continental shelves	49	Salinity, 2–25	Chen et al. (2013)
			165 estuaries and 87 continental shelves	23	Salinity, >25	Chen et al. (2013)
	T	C	Yodo River, Japan	101.8	Year average Daytime	Otani et al. (2017)
	T	C	Nanko bird sanctuary, Japan	2.9	Spring	Endo et al. (2016)
	T	C		1.0	Summer	Endo et al. (2016)
	T	C		0.3	Fall	Endo et al. (2016)
	T	C		−7.5	Winter	Endo et al. (2016)

[a]*T* tidal flat, *S* salt marsh or wetland
[b]*E* eddy correlation method, *C* chamber method, *B* bulk method

reed *Phragmites australis*; for example, the CO_2 flux between the air and the salt marsh ecosystem (air–salt marsh CO_2 flux hereafter) was found to be −1037 mmol $C/m^2/day$ in the Yangtze River estuary (Guo et al. 2009). Also, the CO_2 flux between the air and the tidal flat ecosystem (air–tidal flat CO_2 flux hereafter) was measured in a tidal flat area in Japan where an observation tower was constructed (Tanaka and Takikawa 2006), and CO_2 was found to be absorbed largely during daytime emersion periods, which suggested a significant contribution by microphytobenthos.

The air–sediment CO$_2$ flux has been measured in two field studies using a closed dark chamber system during emersion periods. One study, in the tidal flat of the Westerschelde estuary, Netherlands, measured a maximum flux of 381 mmol C/m^2/day (Middelburg et al. 1996) and the other, in the salt marsh of the Ribble estuary, England, measured a flux of 229 mmol C/m^2/day (Ford et al. 2012). These areas were considered to be CO$_2$ emission sites dominated by decomposition of organic matter. Primary production in these tidal flats was also estimated for the submerged sediments, using in situ data for temporal O$_2$ concentration changes. Migné et al. (2002, 2016) and Spilmont et al. (2005) measured CO$_2$ flux by monitoring changes of CO$_2$ concentration in situ in benthic light and dark chambers, and found that CO$_2$ was absorbed by microphytobenthos in the light chamber. Gross primary production appeared to be larger than respiration and decomposition in these intertidal sediments, and the researchers suggested that CO$_2$ absorption by microphytobenthos on the sediment surface was important in the carbon cycle of the tidal flat ecosystem.

In many cases the air–water CO$_2$ flux has been measured by the bulk method, and the water surface has been shown to be a place of CO$_2$ emission in tidal flats and salt marshes. The air–water CO$_2$ flux in estuaries indicates overall emission of CO$_2$, given the influx of dissolved inorganic carbon and organic carbon from the basin and the excess of mineralization and respiration over primary production (Raymond and Cole 2001; Borges et al. 2004a, 2005; Jiang et al. 2008; Laruelle et al. 2010; Cai 2011; Chen et al. 2013; Regnier et al. 2013). For example, in a summary of published CO$_2$ flux emissions for about 165 estuaries and 87 continental shelves, Chen et al. (2013) found that upper estuaries with salinities less than 2 are strong sources of atmospheric CO$_2$ (39 ± 56 mol C/m^2/year); middle estuaries with salinities between 2 and 25 are moderate sources (17.5 ± 34 mol C/m^2/year); and lower estuaries with salinities more than 25 are weak sources (8.4 ± 14 mol C/m^2/year). Flecha et al. (2015) found that the air–water CO$_2$ flux in the Guadalquivir estuary, Spain, fluctuates due to differences in salinity and emitters in the upstream part of the estuary. And Frankignoulle et al. (1998) and Borges et al. (2006) reported that CO$_2$ emissions from European estuaries (averaging 0.05 mmol C/m^2/year) are significant in the regional CO$_2$ budget.

8.3 Materials and Methods

8.3.1 Study Sites

The two study sites were near the city of Osaka in a eutrophicated area. The sites were characterized in terms of their CO$_2$ flux in the atmosphere, water surface, sediments of supratidal area, intertidal area, and subtidal area in tidal benthic ecosystems. Further details are presented (Endo and Otani 2018).

8.3.1.1 Yodo River-Mouth Site

The Yodo river-mouth site near Osaka Bay has both an intertidal flat area (without large vegetation) and a salt marsh area (with reed vegetation). Salinity here ranges from 0 to 23 (Otani et al. 2017). We measured the air–marsh CO_2 fluxes at Station 1 by the eddy correlation method and the air–sediment and air–water CO_2 fluxes at Station 2 by the chamber method (Fig. 8.2a).

   We conducted 10 observation campaigns, each lasting 2–6 days, in the supratidal zone dominated by reeds during the months of May, August, and November of 2014 and February and April through September of 2015. Atmospheric CO_2 concentration was measured at 10 Hz (LI-COR Co. LI-7500), as was the three-dimensional wind speed (Sonic Co. SAT-540), and other weather conditions such as air temperature were measured at the same stations (Fig. 8.2b). The air–salt marsh CO_2 flux, latent heat flux, and sensible heat flux were calculated from the data every 30 min using the eddy correlation method (see Chap. 6) (Tokoro et al. 2018).

   Air–sediment CO_2 fluxes during emersion periods in the intertidal zone were measured on a monthly basis from July 2013 to March 2015 using light and dark chambers (inner diameter 12 cm, height 21 cm) with an NDIR Carbon Dioxide Probe (Vaisala Co. GMP: 343) (Fig. 8.2c). During submersion periods from April 2014 to March 2015, air–water CO_2 fluxes were measured using a chamber floating on the water surface using a light chamber (diameter 19.5 cm, height 12.5 cm) with the same probe.

8.3.1.2 Bird Sanctuary Site

At the bird sanctuary site, on the shore of Osaka Bay, the artificial salt marsh includes intertidal and subtidal flat areas. Salinity ranges from 13 to 30 (Yamochi et al. 2017). About 17% of the north salt marsh is in the intertidal zone (tidal flat area). This surface is covered with abundant microphytobenthos, thus photosynthesis contributes to the air–sediment CO_2 exchange. However, the CO_2 exchanges at the air–water interface and the water–sediment interface affect the carbon cycle of the north salt marsh because the rest of the north salt marsh is subtidal. We measured the air–sediment CO_2 flux in the intertidal area and the water–sediment and air–water CO_2 fluxes in the subtidal area (Fig. 8.3a).

   Figure 8.3b is a schematic diagram of the CO_2 flux measurements. The air–sediment and air–water CO_2 fluxes were measured every hour for 24-h periods in spring (13–14 May 2014), summer (5–6 August 2014), fall (4–5 November 2014) and winter (2–3 February 2015). In the intertidal area, a light chamber and a dark chamber (volume 1.27×10^{-2} m³, bottom area 5.72×10^{-2} m²) were placed on the sediment. The CO_2 concentrations inside them were measured by using a CO_2 data logger (T&D Co.: Tr-76Ui), and the air–sediment CO_2 flux was calculated from the changes in CO_2 concentration. For the air–sea CO_2 flux, a light chamber (volume 1.43×10^{-2} m³, bottom area 5.74×10^{-2} m²) was floated on the sea surface and the

flux was calculated from the changes in CO$_2$ concentration inside the chamber. The photon density flux was measured by using a pocket-sized PAR logger (JFE advantec Co.: DEFI2-L), and the atmospheric CO$_2$ concentration and temperature were measured by using a CO$_2$ data logger (T&D Co.: Tr-76Ui). The sediment temperature in air was measured by using a temperature data logger (Onset Computer Co.: Tidbit v2), and the chlorophyll *a* (Chl-a) concentration of sediment was measured by the acetone extraction analysis method. In the water column, we measured water temperature, salinity, fluorescence intensity of phytoplankton Chl-a (JFE advantec Co.: Compact CTD), pH (TOA DKK Co.:MM-43X), and dissolved oxygen (Hack Co.: HQ40d) and dissolved inorganic carbon concentrations.

In the subtidal area, we measured the water–sediment CO$_2$ flux during daytime on 22 May and 9 July 2013 and 14 May and 24 July 2014. A light chamber and a dark chamber (volume 1.51×10^{-2} m^3, bottom area 7.21×10^{-2} m^2) were placed on the sea bottom, and the time series of CO$_2$ partial pressure (pCO$_2$) inside the chambers was measured by using a gas-liquid equilibrium sensor made of PTFE tubing (Sumitomo Electric Fine Polymer, Inc.; inner diameter 4.0 mm, porosity 60%) in which pCO$_2$ inside the tube was pumped and measured by a flow-through type CO$_2$ gas analyzer (Vaisala Co.: GMP-343).

8.3.2 Measurement Methods

Four different CO$_2$ fluxes (air–marsh, air–sediment, air–water, and water–sediment) were measured at the two field sites in Japan (Figs. 8.2 and 8.3).

The air–marsh CO$_2$ flux F_c (mg CO$_2$/m^2/s), measured by the eddy correlation method, was calculated using Eq. 8.1, including the Webb-Pearman-Leuning (WPL) correction (Webb et al. 1980):

$$F_c = \overline{w'\rho_c'} + \mu \frac{\overline{\rho_c}}{\rho_a} \overline{w'\rho_v'} + \left(1 + \mu\sigma\right)\frac{\overline{\rho_c}}{T} \overline{w'T'}, \tag{8.1}$$

where w is vertical wind velocity, T is air temperature, ρ_c is the density of CO$_2$, ρ_a is the density of dry air, ρ_v is the density of water vapor, μ is the ratio of the molecular weights of dry air and water vapor, and σ is the ratio of water vapor and dry air densities. The overbars indicate averages, and the prime symbols (′) indicate variations from the mean. The first term on the right side of Eq. 8.1 is the raw flux directly obtained, and the second and third terms are the WPL correction terms for latent heat and sensible heat, respectively. The sensible heat flux H (W/m^2) and the latent heat flux lE (W/m^2) were obtained by Eqs. 8.2 and 8.3:
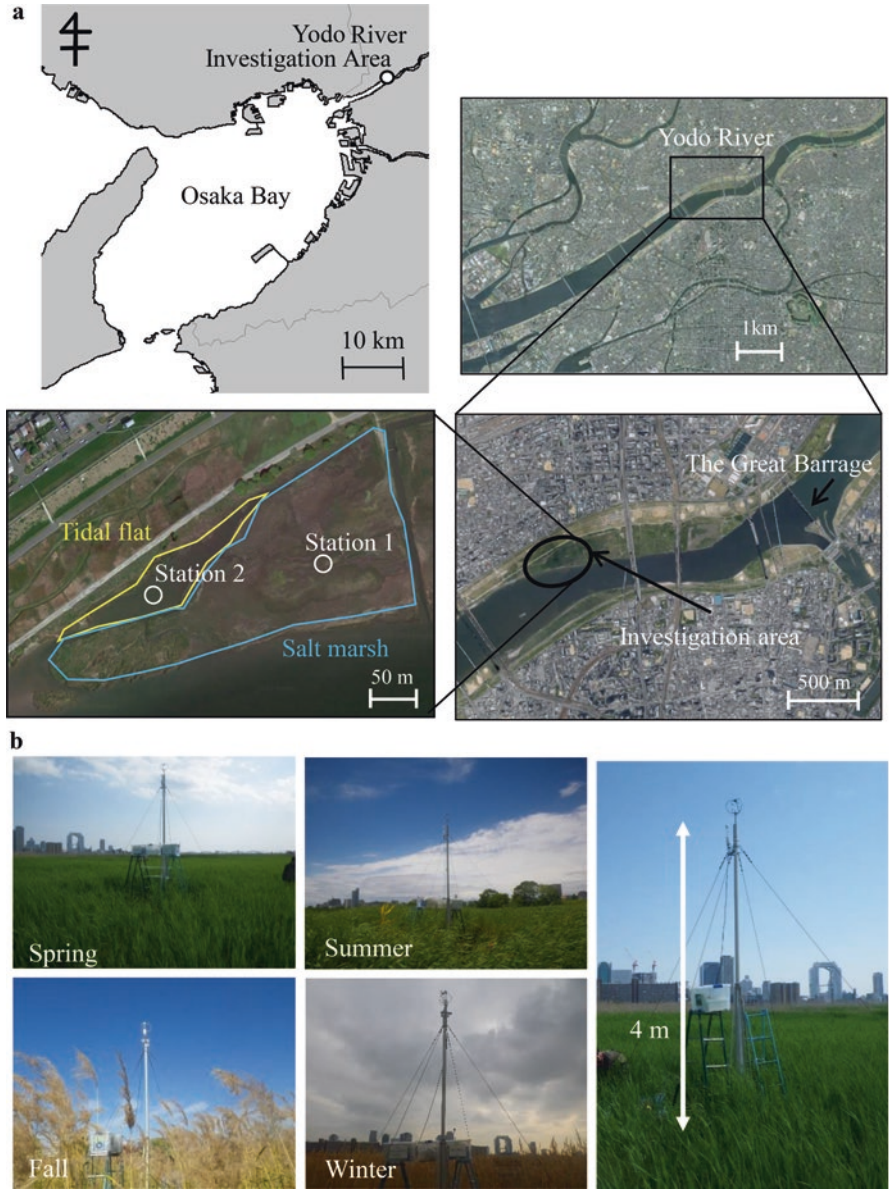
$$H = C_p \rho_a \overline{w'T'} \tag{8.2}$$

Fig. 8.2 Location and instrumentation of the Yodo river-mouth field site. (**a**) Measurement sites of CO_2 fluxes (Station 1, air–salt marsh CO_2 flux; Station 2, air–water and water–sediment CO_2 fluxes), (**b**) Photos of the eddy correlation system, (**c**) Schematic diagram of the CO_2 flux measurements in the field site
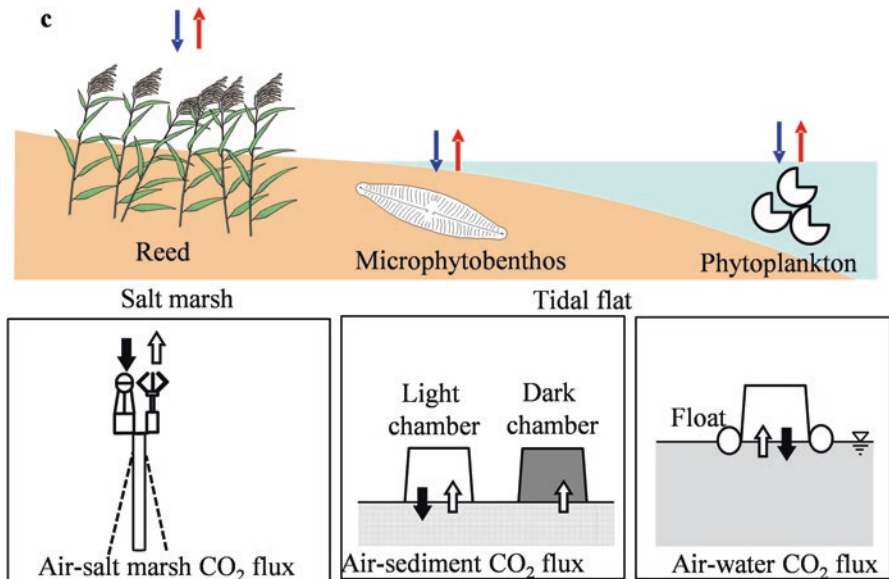
Fig. 2 (continued)

and

$$lE = l\overline{w'\rho_v'}, \tag{8.3}$$

where C_p is specific heat, l is latent heat of vaporization, and E is the amount of water evaporated.

The air–sediment CO$_2$ flux in intertidal and subtidal areas and the air–water CO$_2$ flux were measured by the chamber technique. In intertidal and subtidal areas, atmospheric CO$_2$ or aqueous CO$_2$ above the sediment are exchanged directly at the sediment surface by biological processes such as CO$_2$ absorption by photosynthesis of microphytobenthos or CO$_2$ emission by respiration of benthic animals and decomposition of organic matter. Therefore, the air–sediment and water–sediment CO$_2$ fluxes were measured by using a dark chamber and a light chamber. Net primary production (NPP), sedimentary respiration, and gross primary production (GPP) at the interface of the sediment were calculated by using Eqs. 8.4, 8.5 and 8.6:

$$NPP = \frac{C_L^{t+\Delta t} - C_L^t}{\Delta t} \cdot \frac{V_L}{A_L} \tag{8.4}$$

$$\text{Sedimentary respiration} = \frac{C_D^{t+\Delta t} - C_D^t}{\Delta t} \cdot \frac{V_D}{A_D} \tag{8.5}$$
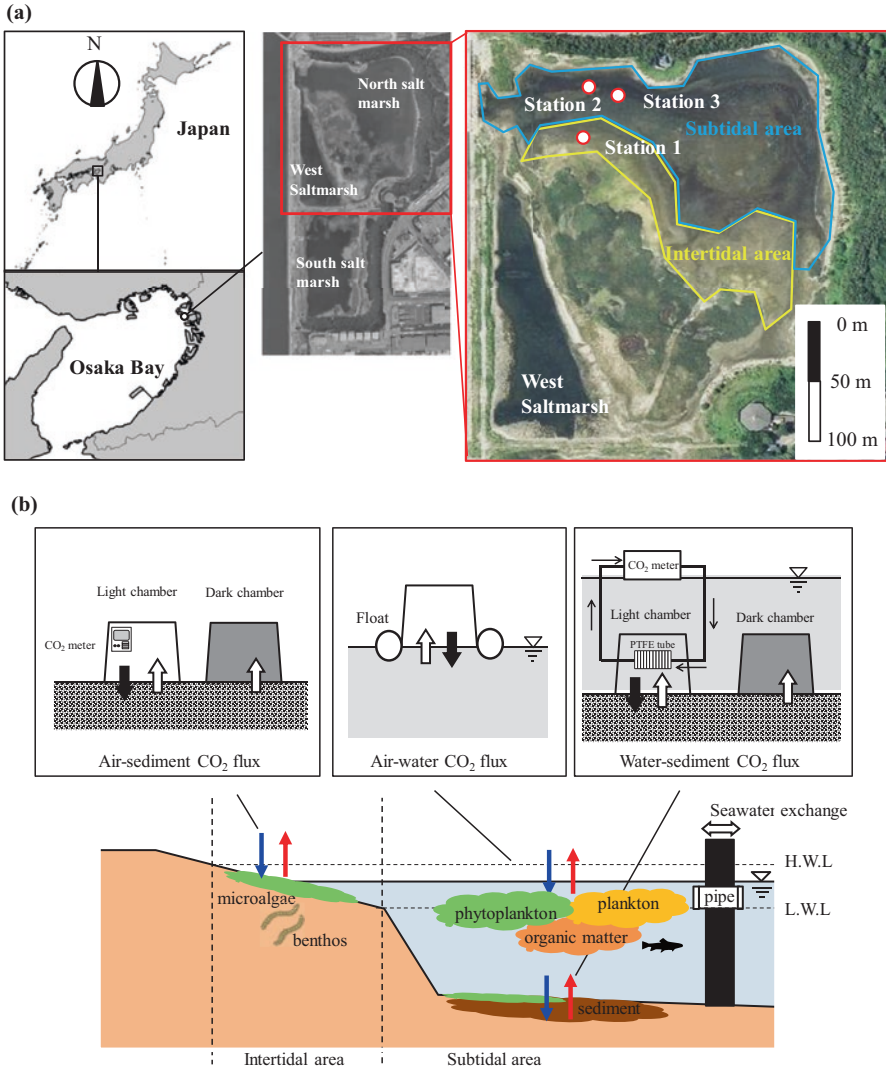
Fig. 8.3 Location and instrumentation of the Osaka bird sanctuary field site. (**a**) Measurement sites of CO_2 fluxes (Station 1, air–sediment CO_2 flux; Station 2, air–water CO_2 flux; Station 3, water–sediment CO_2 flux), (**b**) Schematic diagram of the CO_2 flux measurements in the field site. H.W.L., high water level; L.W.L., low water level

$$GPP = \left(\frac{C_D^{t+\Delta t} - C_D^t}{\Delta t} \cdot \frac{V_D}{A_D} \right) - \left(\frac{C_L^{t+\Delta t} - C_L^t}{\Delta t} \cdot \frac{V_L}{A_L} \right), \qquad (8.6)$$

where Δt is the measurement time interval; C_L and C_D are the CO_2 concentrations inside light and dark chambers, respectively; C^t and $C^{t+\Delta t}$ are the CO_2

Table 8.2 Measurement methods used in this study for CO$_2$ fluxes in the tidal flat and marsh ecosystems

Interface	Site		Method			Factor		
	River-mouth	Bird sanctuary	Eddy correlation	Light chamber	Dark chamber	NEP	Sedimentary respiration	GPP
Air–marsh	Yes		Yes			Yes		
Air–sediment	Yes	Yes		Yes	Yes	Yes	Yes	Yes
Air–water	Yes	Yes		Yes		Yes		
Water–sediment		Yes		Yes	Yes	Yes	Yes	Yes

concentrations at times t and $t + \Delta t$, respectively; V is the volume of the chamber; and A is the area of the base of the chamber. Subscripts L and D represent the light and dark chambers, respectively. The difference between the CO$_2$ fluxes of the light and dark chambers was defined as GPP of microphytobenthos on the sediment.

In contrast, air–water CO$_2$ exchange responds to temporal changes of CO$_2$ in water, which arise not only from biological process but also from changes in water quality. Because it is difficult to analyze these factors using data from light and dark chambers, we measured the air–water CO$_2$ flux with a light chamber.

Table 8.2 summarizes the measurement methods and factors (NPP, sedimentary respiration, and GPP) used in this study.

8.4 Results

8.4.1 River-Mouth Site

8.4.1.1 Air–Marsh CO$_2$ Flux in Salt Marsh

The CO$_2$ flux measurements indicated that the salt marsh site was an atmospheric CO$_2$ sink in May 2014 and June–September 2015, and a CO$_2$ source in August and November 2014 and February, April, and May 2015 (Fig. 8.4). The CO$_2$ flux ranged from −0.12 to 0.072 mg CO$_2$/m^2/s and tended to be negative in spring and summer. The latent heat flux and sensible heat flux were positive, showing that water vapor and heat were released from the salt marsh.

We classified the CO$_2$ flux of the 10 monthly observation results into three groups (Fig. 8.5). Group A was defined as months when the daytime CO$_2$ flux was negative (May 2014 and June, August, and September 2015). During daytime in this group, the latent heat flux was largely positive and the air temperature was higher than the sediment temperature. At night, the sediment temperature was higher than the air temperature. Group B was defined as months when the daytime CO$_2$ flux was positive (August 2014 and April and May 2015). During daytime, the sensible heat flux

Fig. 8.4 Times series of monthly air–salt marsh fluxes at the river-mouth site. (Otani and Marikawa 2017). (a) Latent heat, (b) Sensible heat, (c) CO_2. Extensions of histogram bars indicate standard errors
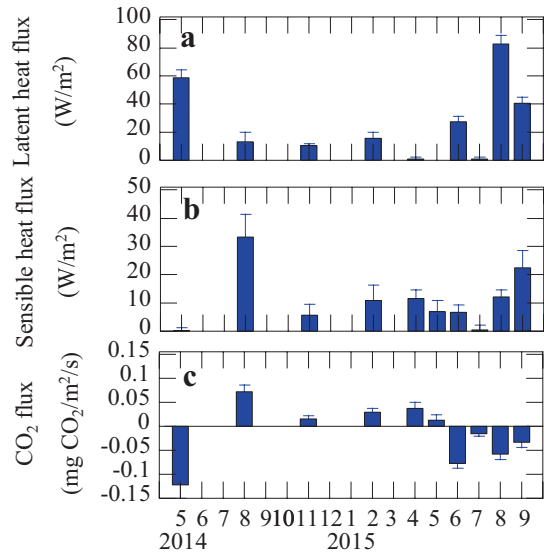
was positive and the air temperature was lower than the sediment temperature. At night, the sediment temperature was lower than the air temperature. Group C was defined as months with no clear fluctuations in the CO_2 flux (November 2014 and February and July 2015). The characteristics of the CO_2 flux are summarized in Fig. 8.6.

During the Group A months, CO_2 was absorbed by photosynthesis with increasing air temperature during daytime, and latent heat was released by transpiration of water vapor. A statistically significant negative relationship was found between the latent heat flux and the CO_2 flux. In other words, the material cycle was driven by the reed marsh.

During the Group B months, because the sediment temperature was higher than the air temperature during daytime, both the CO_2 and sensible heat flux were positive during daytime. On the other hand, the air temperature was higher than the sediment temperature at night. These temperature differences contributed to fluctuations in the CO_2 flux.

During two of the Group C months, November and February, the reed marsh was withered and inactive, thus fluctuations in the CO_2 flux caused by plant respiration and photosynthesis were small. Moreover, even though precipitation caused a temperature difference, it has been suggested that the CO_2 flux would have small fluctuations because the photon flux density was low (Tokoro and Kuwae 2017).

In summary, the CO_2 flux tended to be negative from spring to summer in the reed marsh zone owing to the photosynthetic activity of reeds. Furthermore, the CO_2 flux appeared to vary with the temperature difference between air and sediment.
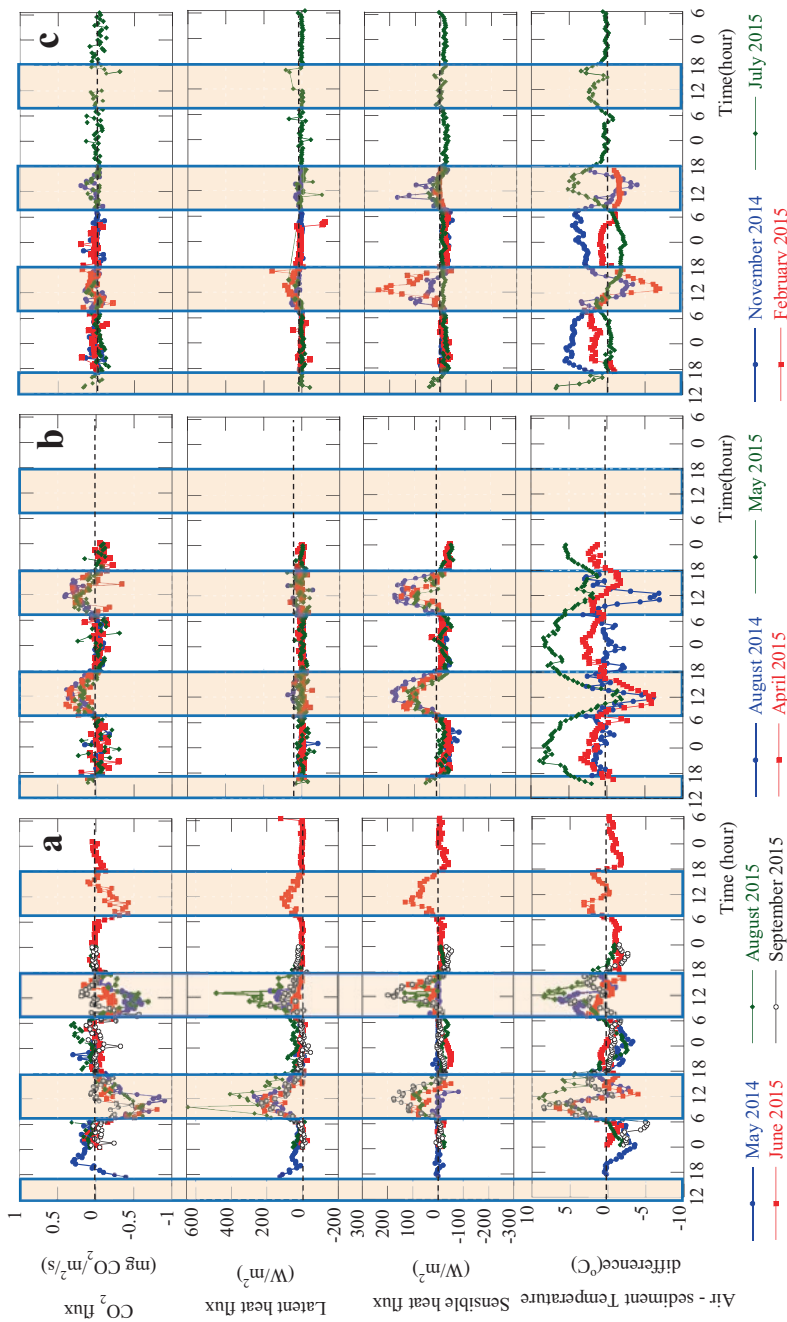
Fig. 8.5 Detailed time series of air–salt marsh CO$_2$ flux at the river-mouth site (Otani and Marikawa 2017). (**a**) CO$_2$ absorption in daytime (Group A), (**b**) CO$_2$ emission in daytime (Group B), (**c**) No clear fluctuation (Group C). Shading indicates daytime hours

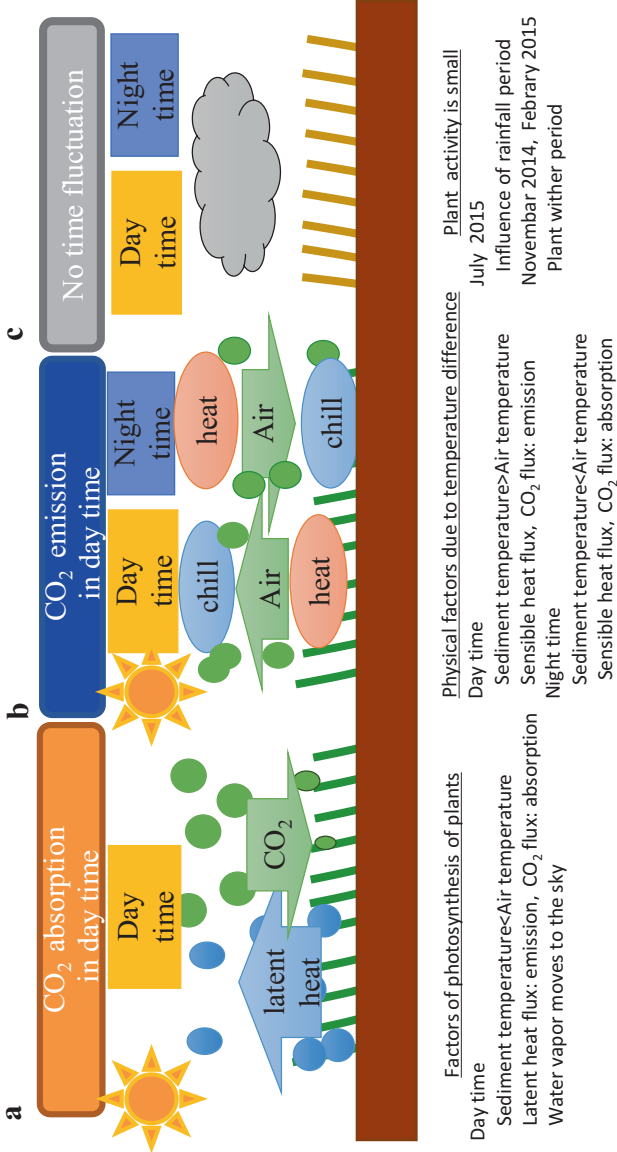**Fig. 8.6** Diagram showing characteristics of the air–salt marsh CO_2 flux at the river-mouth site (Otani and Marikawa 2017). (**a**) Group A, (**b**) Group B, (**c**) Group C

Fig. 8.7 Time series of monthly air–sediment CO$_2$ flux during emersion periods in the tidal flat area at the river-mouth site (modified from Otani et al. 2017). Extensions of histogram bars indicate standard deviations
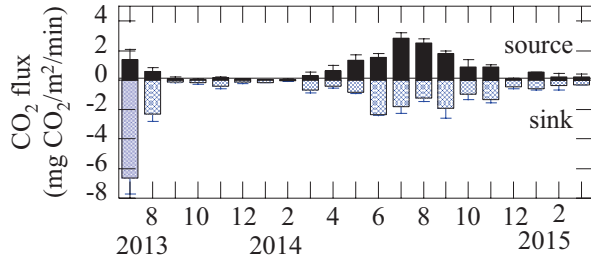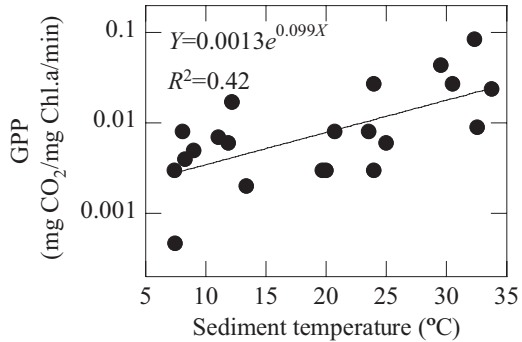

Fig. 8.8 Relationship between air–sediment CO$_2$ flux per Chl-a and sediment temperature in the tidal flat area of the river-mouth site. (Otani et al. 2017)

8.4.1.2   Air–Sediment CO$_2$ Flux in Tidal Flat

In the tidal flat, dominated by microphytobenthos, air–sediment CO$_2$ fluxes fluctuated from 0.0675 to 6.63 mg CO$_2$/m^2/min, and the CO$_2$ emission rate was 0.038–2.82 mg CO$_2$/m^2/min (Fig. 8.7). These rates were highest in summer and were strongly positively correlated with sediment temperature and oxidation reduction potential (ORP). In addition, the GPP, measured as CO$_2$ absorption rate per Chl-a (mg CO$_2$/Chl.a/min), had a statistically significant positive correlation with sediment temperature (Fig. 8.8), increasing logarithmically with increasing sediment temperature. Thus, it appears that microphytobenthos activity contributes to the CO$_2$ absorption rate.

The bivalve *Corbicula japonica* was the dominant species in the tidal flat, and the CO$_2$ emission rate had a statistically significant positive correlation with the biomass of *C. japonica* as reported by Otani et al. (2017) (r = 0.55, P < 0.01, Fig. 8.9). It appears that macrobenthos respiration also contributed to the CO$_2$ emission rate from the sediment.

8.4.1.3   Air–Seawater CO$_2$ Flux in Tidal Flat

The air–seawater CO$_2$ flux in the tidal flat was positive throughout the year (Fig. 8.10). The CO$_2$ emission rate ranged from 0.242 ± 0.05 to 12.5 ± 5.61 mg CO$_2$/m^2/min. A significant positive correlation was found between the air–seawater CO$_2$

Fig. 8.9 Relationship between air–sediment CO_2 flux and biomass of *Corbicula japonica* in the tidal flat area of the river-mouth site. (Otani et al. 2017)

$$Y=0.0973X-1.21$$
$$R^2=0.37$$

CO$_2$ emission (mg CO_2/m^2/min)

Biomass of *C.japonicus* (gC/m^2)
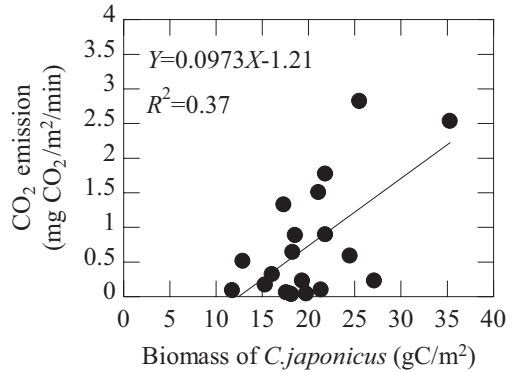
Fig. 8.10 Time series of monthly air–water CO_2 flux during submersion periods in the tidal flat area of the river-mouth site. (Otani et al. 2017). Extensions of histogram bars indicate standard deviations

CO$_2$ emission (mg CO_2/m^2/min)

2014   2015
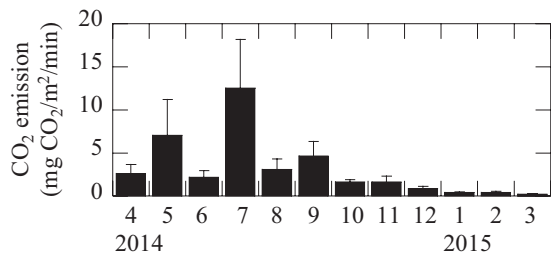
Fig. 8.11 Relationship between air–water and air–sediment CO_2 fluxes in the tidal flat area of the river-mouth site. (Otani et al. 2017)

$$Y=3.078X-0.347$$
$$R^2=0.60$$

1:1

(mg CO_2/m^2/min)

CO$_2$ emission in surface water (mg CO_2/m^2/min)
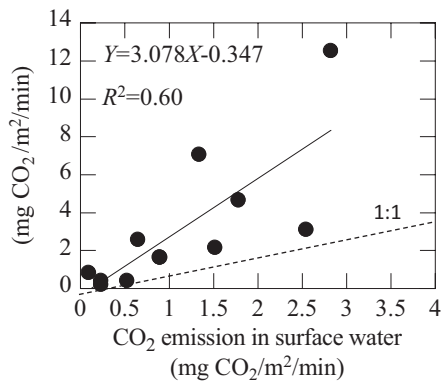
flux during emersion periods and the air–sediment CO_2 flux during submersion periods ($r = 0.77$, $P < 0.01$, $n = 12$, Fig. 8.11). The values of the air–seawater CO_2 flux ranged from 0.84 to 9.4, on average 3.0 times the air–sediment CO_2 flux. During emersion periods in the daytime, CO_2 was taken up by microphytobenthos, but CO_2 was released into the atmosphere during submersion periods.
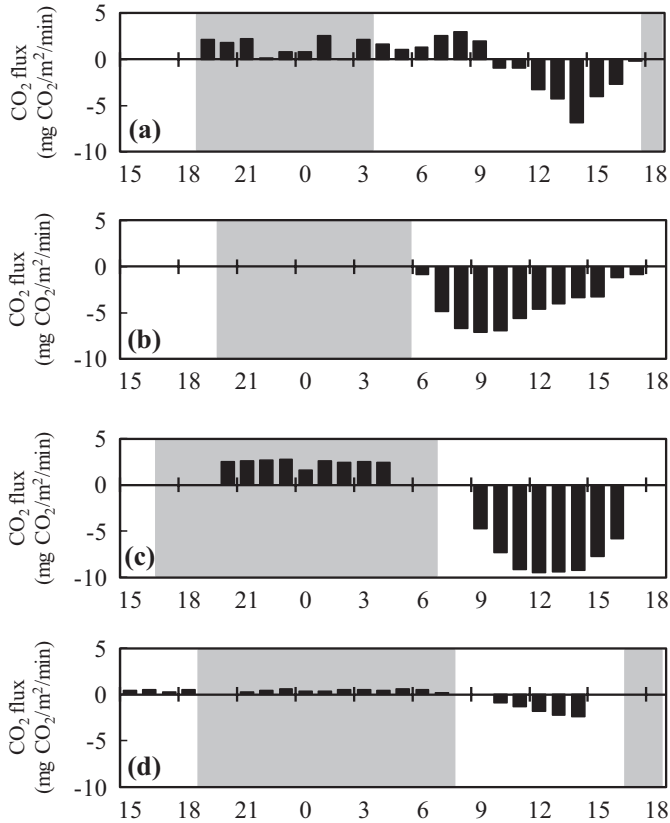
Fig. 8.12 Time series of hourly air–sediment CO$_2$ fluxes in the intertidal area of the bird sanctuary site (Endo et al. 2015). (**a**) Spring (13–14 May 2014), (**b**) Summer (5–6 August 2014), (**c**) Fall (4–5 November 2014), (**d**) Winter (3–4 February 2015). Positive values represent CO$_2$ emission from the sediment and negative values represent CO$_2$ absorption. Shaded area represent night hours. Gaps represent times when CO$_2$ fluxes could not be measured

8.4.2   Bird Sanctuary Site

8.4.2.1   Air–Sediment CO$_2$ Flux in Intertidal Area

Figure 8.12 shows the diurnal changes in the air–sediment CO$_2$ flux at different seasons in the intertidal area, which was dominated by microphytobenthos. In spring the air–sediment CO$_2$ flux ranged from −6.84 to 2.97 mg CO$_2$/m^2/min and averaged 0.06 mg CO$_2$/m^2/min, meaning the intertidal area was a CO$_2$ source. In the summer, the air–sediment CO$_2$ flux ranged from −7.07 to −0.84 mg CO$_2$/m^2/min during the daytime (CO$_2$ flux could not be measured at night because the area was submerged), and in the fall it ranged from −9.50 to 2.74 mg CO$_2$/m^2/min. CO$_2$ was strongly absorbed during the daytime during summer and fall, seasons with strong
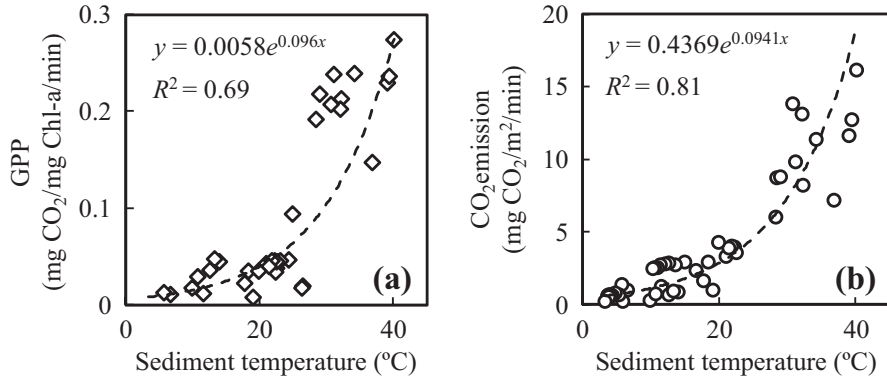
Fig. 8.13 Relationships between sediment temperature and (**a**) GPP of microphytobenthos in the intertidal area and (**b**) CO_2 emission from sediment in the intertidal area. (Endo et al. 2016)

sunlight. In winter, the CO_2 flux ranged from −2.39 to 0.62 mg $CO_2/m^2/min$ and averaged −0.23 mg $CO_2/m^2/min$, making the area a CO_2 sink.

CO_2 was absorbed during daytime at all times of year except during spring mornings, indicating that daytime CO_2 absorption by microalgal photosynthesis usually exceeded CO_2 emission by decomposition of organic matter or respiration. Our estimates of total CO_2 budgets also showed that the intertidal area mainly acted as a CO_2 sink except in spring. During the warmer seasons, CO_2 emissions at night increased as did CO_2 absorption during the daytime, the result being that on a net basis CO_2 was absorbed. In winter, biological activities were weaker as inferred from the low CO_2 emissions at night, thus on a net basis CO_2 was absorbed during the cold season.

The relationship between GPP of microphytobenthos and sediment temperature, and the relationship between CO_2 emission from sediment by respiration and decomposition and sediment temperature, are shown in Fig. 8.13. The GPP of microphytobenthos ranged from 0.01 to 0.27 mgCO_2/mgChl.a/min, and the respiration rate ranged from 0.04 to 16.14 mg$CO_2/m^2/min$. Because both GPP and respiration are dependent on water temperature, they can be approximated by

$$F_{CO_2} = a \cdot e^{bT},$$ (8.7)

where F_{CO_2} is the rate of GPP or respiration, a is the rate at a sediment temperature of 0 °C, b is the temperature coefficient, and T is the sediment temperature. The determination coefficients (R^2) were 0.69 for GPP and 0.81 for respiration rate, both of which indicate a good fit to the model within the observed temperature range. The Q_{10} values resulting from this calculation are 2.62 for GPP and 2.56 for the respiration rate. These values, indicating a typical temperature response to bioactivity, are comparable to those reported by Hofman et al. (1991) and Migné et al. (2004).

Our results show that microphytobenthos has a substantial effect on the air–sediment CO_2 flux, making the intertidal area a net CO_2 sink.
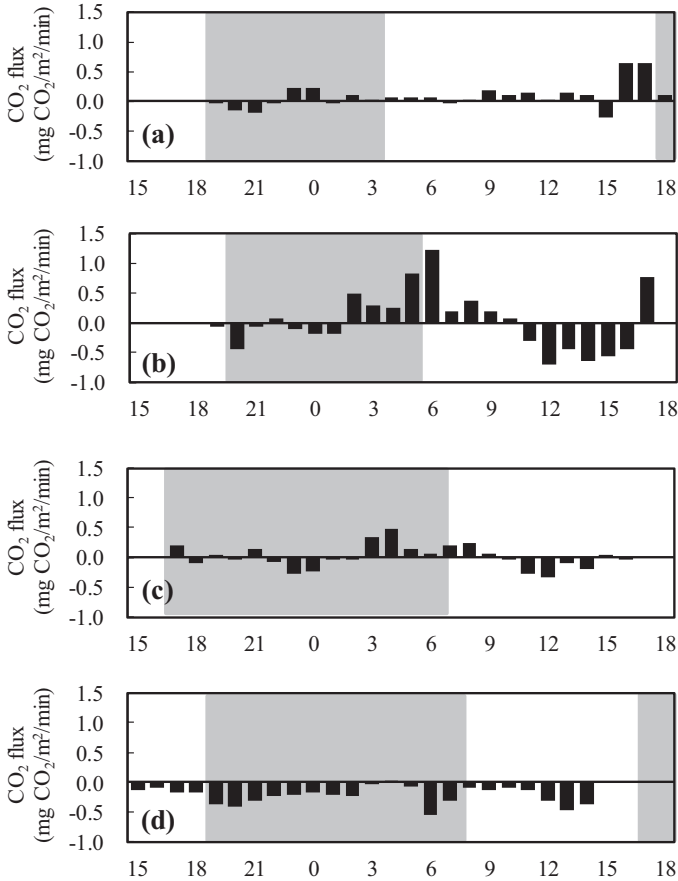
**Fig. 8.14** Time series of hourly air–water CO$_2$ flux at the bird sanctuary site. (**a**) Spring (13–14 May 2014), (**b**) Summer (5–6 August 2014), (**c**) Fall (4–5 November 2014), and (**d**) Winter (3–4 February 2015) (Endo et al. 2015). Positive values represent CO$_2$ emissions from sediment and negative values represent CO$_2$ absorption by sediment. Shaded area represents night hours

8.4.2.2   Air–Water CO$_2$ Flux in Subtidal Area

We determined the diurnal pattern of air–water CO$_2$ flux at the subtidal area during each season (Fig. 8.14). In spring, this flux ranged from −0.26 to 0.64 mg CO$_2$/m^2/min and averaged 0.09 mg CO$_2$/m^2/min. Its daily variation was smaller than in other seasons. In summer, the flux ranged from −0.71 to 1.23 mg CO$_2$/m^2/min and averaged 0.03 mg CO$_2$/m^2/min. Its daily variation was larger than in other seasons. In fall, the flux ranged from −0.34 to 0.48 mg CO$_2$/m^2/min and averaged 0.01 mg CO$_2$/m^2/min. The CO$_2$ balance was almost zero. In winter, the flux ranged from −0.54 to 0.03 mg CO$_2$/m^2/min and averaged −0.25 mg CO$_2$/m^2/min. The daily variation was

comparatively small in winter because biological activity is suppressed at low temperatures and adds little CO_2 to seawater, such that the CO_2 concentration in seawater becomes lower than the atmospheric concentration. The CO_2 balance was negative in winter because atmospheric CO_2 is more readily absorbed owing to its increased solubility in colder water.

Correlation coefficients between the air–water flux, the air–sediment flux, photon density flux, and different measured water qualities are listed in Table 8.3. The air–water flux is weakly related to the air–sediment flux because their CO_2 exchange processes differ. Atmospheric CO_2 gas is exchanged directly with sediment by biological processes during the emersion periods. On the other hand, air–water CO_2 exchange is governed by physical processes that depend on the gradient of CO_2 concentration between air and water, along with changes in CO_2 concentrations in water from biological activity as well as chemical effects related to solubility and aqueous carbonate equilibrium. Therefore, air–water CO_2 flux is related to the difference in CO_2 concentrations between air and seawater (ΔpCO_2). The table also shows that there is a negative correlation between air–water CO_2 flux and photon density flux, showing an effect arising from photosynthesis by phytoplankton.

8.4.2.3   Water–Sediment CO_2 Flux in Subtidal Area

Water–sediment CO_2 fluxes in the subtidal area during daytime are listed in Table 8.4. In spring, the averaged water–sediment CO_2 flux was 1.11 mg CO_2/m²/min, signifying net release of CO_2 from sediment to seawater. In summer, the average flux was −0.65 mg CO_2/m²/min, signifying net absorption by sediment. The water–sediment CO_2 flux was smaller than the air–sediment CO_2 flux and the same as the air–water CO_2 flux. The water–sediment CO_2 flux had seasonal trends similar to those of the air–sediment CO_2 flux.

We found that both absorption and emission of CO_2 from subtidal sediment were strongly correlated with sediment temperature in a relationship that could be approximated by Eq. 8.6 because they were for the intertidal zone at this site (Fig. 8.15). However, the values of CO_2 absorption and emission at the water–sediment interface in the subtidal area were about one-tenth of those in the intertidal area. The Q_{10} value was 3.0 for CO_2 absorption and 3.3 for CO_2 emission. These values are larger than those for the intertidal area, suggesting that CO_2 exchange at the water–sediment interface in the subtidal area was strongly influenced by sediment temperature, unlike the case in the intertidal area.

8.4.2.4 CO_2 Budget at the Bird Sanctuary Site

We used the air–sediment and air–water CO_2 flux data to estimate the daily CO_2 budget at the bird sanctuary site. We calculated the daily CO_2 budget in the intertidal and subtidal areas considering the temporal changes of their CO_2 fluxes and the changes in their respective surface areas caused by the tides. The results are shown schematically in Fig. 8.16.

Table 8.3 Correlation coefficients (R) between air–water CO$_2$ flux and other parameters

		x_1	x_2	x_3	x_4	x_5	x_6	x_7	x_8	x_9	x_{10}
x_1	Air–sea flux	1									
x_2	Air–sediment flux	0.12	1								
x_3	Photon density flux	−0.50**	−0.21	1							
x_4	Water temperature	0.25*	−0.40**	0.41**	1						
x_5	Salinity	−0.18	0.17	−0.07	−0.35	1					
x_6	pH	−0.34**	−0.06	0.51**	0.00	−0.09	1				
x_7	Fluorescence intensity of Chl.a	0.22	−0.09	0.30	0.64**	−0.65**	−0.02	1			
x_8	Dissolved inorganic carbon	−0.28*	0.02	−0.37*	−0.78**	0.68**	0.03	−0.69**	1		
x_9	pCO$_2$ of water	0.48**	−0.11	−0.50**	0.07	−0.16	−0.95**	0.35	0.09	1	
x_{10}	ΔpCO$_2$	0.44**	−0.09	−0.51**	0.01	−0.19	−0.95**	0.35	0.10	0.99**	1

R values between 0.4 and 0.7 indicate moderately strong relationships and R values greater than 0.7 indicate very strong relationships
*$P < 0.01$; **$P < 0.005$

Table 8.4 Monthly values of water–sediment CO_2 flux, sediment temperature, and chlorophyll *a* of microphytobenthos in the subtidal area

Date		Water–sediment CO_2 flux (mg $CO_2/m^2/min$)	Sediment temperature (°C)	Chlorophyll *a* (mg/m²)
2013	22 May	1.42 ± 0.16	21.0	56.7
	24 July	-0.5 ± 0.2	31.0–32.0	167.3
2014	14 May	0.8 ± 0.6	20.6–20.9	87.4
	9 July	-0.8 ± 0.1	26.9–27.9	156.1
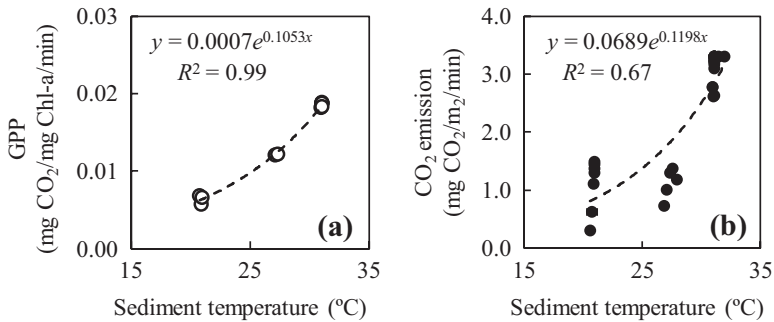
Fig. 8.15 Relationships between sediment temperature and (**a**) CO_2 absorption (GPP) by microphytobenthos and (**b**) CO_2 emission at the water–sediment interface in the subtidal area at the bird sanctuary site. (Tanaka et al. 2016; Yamochi et al. 2017)
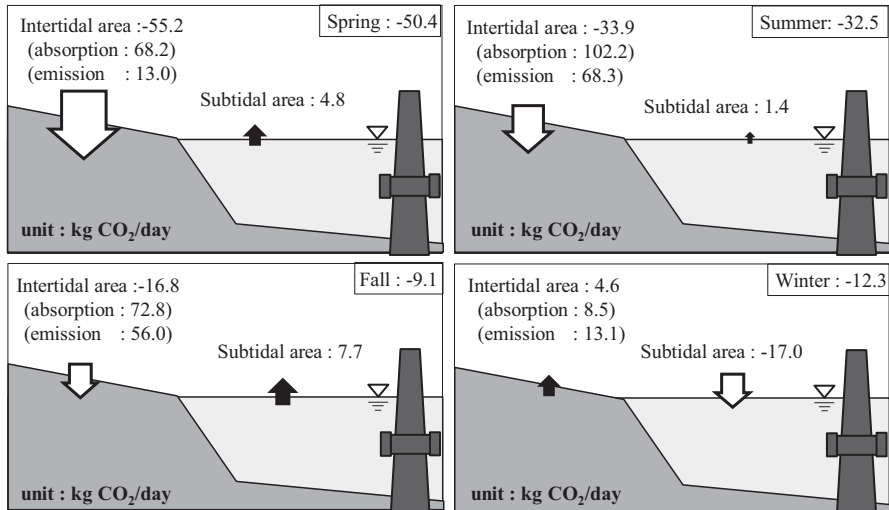
Fig. 8.16 Schematic diagram showing estimated daily CO_2 balance (in kg CO_2/day) at the bird sanctuary site. Negative values indicate CO_2 sinks and positive values indicate CO_2 sources. (Modified from Endo et al. 2016)

In the intertidal area, the CO$_2$ budget ranged from -50.4 to 4.7 kg CO$_2$/day, thus this area was a CO$_2$ sink in every season except winter. Both CO$_2$ absorption and emissions were largest in summer. In the subtidal area, the CO$_2$ budget ranged from -17.0 to 4.8 kg CO$_2$/day, thus this area was a CO$_2$ source in every season except winter. The total CO$_2$ budget for the bird sanctuary site ranged from -50.4 to -9.1 kg CO$_2$/day, constituting a carbon sink throughout the year. Both the intertidal and subtidal areas made important contributions to the CO$_2$ budget because while the air–water CO$_2$ flux in the subtidal area was smaller than the air–sediment CO$_2$ flux in the intertidal area, the subtidal area was larger than the intertidal area.

8.5 Summary

In this chapter, we showed that the air–water, air–sediment, water–sediment, and air–salt marsh CO$_2$ fluxes and their temporal variations are affected by different vegetation (Table 8.1). This is the case for our sites and for tidal flats and salt marshes throughout the world.

At our sites, the air–sediment and air–salt marsh CO$_2$ fluxes showed net absorption (Figs. 8.7 and 8.12). However, the air–water CO$_2$ flux showed net emission throughout the year, except in winter at the bird sanctuary site (Table 8.1). The water–sediment CO$_2$ flux showed net emission during the warm months of May and July (Table 8.4).

The air–sediment CO$_2$ fluxes at our sites were almost the similar value, especially GPP per Chl.a (Figs. 8.8 and 8.13a). The absorption of CO$_2$ by sediments is thought to be due to microphytobenthos, which has high primary production as summarized by Cahoon (1999) and Underwood and Kromkamp (1999). GPP and CO$_2$ emission from sediment in the subtidal area, where light levels are low, is an order of magnitude smaller than from sediment in the intertidal area (Figs. 8.13 and 8.15).

The air–water CO$_2$ flux at our sites may have been influenced by freshwater discharge in the water column. At the bird sanctuary site, where salinity is 13–30 (Yamochi et al. 2017), the air–water CO$_2$ flux tended to be smaller than the air-sediment CO$_2$ flux, but in the river-mouth site, where salinity is 0–23 (Otani et al. 2017), the opposite was true. Moreover, it has been shown that atmospheric CO$_2$ is absorbed into seawater in the eastern part of Osaka Bay (-8.3 mmol C/m^2/day; Fujii et al. 2013), which is affected by discharge from the Yodo River.

Air–salt marsh CO$_2$ flux measured by the eddy correlation method tended to be larger than air–sediment and water–sediment CO$_2$ fluxes at all sites (Table 8.1). One factor that may be significant is that CO$_2$ is absorbed during the growth period of *Phragmites australis* and *Spartina alterniflora*. It has also been reported that *Zostera marina* directly absorbs CO$_2$ (Watanabe and Kuwae 2015). Vegetation appears to be a major driver of air–ecosystem CO$_2$ flux and other carbon cycles in blue carbon ecosystems and tidal flats.

References

Abril G, Commarieu MV, Sottolichio A, Bretel P, Guérin F (2009) Turbidity limits gas exchange in a large macrotidal estuary. Estuar Coast Shelf Sci 83:342–348

Artigas F, Shin JY, Hobble C, Marti-Donati A, Schäfer KVR, Pechmann I (2015) Long term carbon storage potential and CO_2 sink strength of a restored salt marsh in New Jersey. Agric For Meteorol 200:313–321

Borges AV, Delille B, Schiettecatte LS, Gazeau F, Abril G, Frankignoulle M (2004a) Gas transfer velocities of CO_2 in three European estuaries (Randers Fjord, Scheldt, and Thames). Limnol Oceanogr 49:1630–1641

Borges AV, Vanderborght JP, Schiettecatte LS, Gazeau F, Ferrón-Smith S, Delille B, Frankignoulle M (2004b) Variability of the gas transfer velocity of CO_2 in a macrotidal estuary (the Scheldt). Estuaries 27:593–603

Borges AV, Delille B, Frankignoulle M (2005) Budgeting sinks and sources of CO_2 in the coastal ocean: diversity of ecosystem counts. Geophys Res Lett 32:L14601

Borges AV, Schiettecatte LS, Abril G, Delille B, Gazeau F (2006) Carbon dioxide in European coastal waters. Estuar Coast Shelf Sci 70:375–387

Cahoon LB (1999) The role of benthic microalgae in neritic ecosystems. Oceanogr Mar Biol Annu Rev 37:47–86

Cai WJ (2011) Estuarine and coastal ocean carbon paradox: CO_2 sinks or sites of terrestrial carbon incineration? Annu Rev Mar Sci 3:123–145

Chen CTA, Huang TH, Chen YC, Bai Y, He X, Kang Y (2013) Air-sea exchanges of CO_2 in the world's coastal seas. Biogeosciences 10:6509–6544

Endo T, Otani S (2018) Chapter 5. Carbon storage in tidal flats. In: Kuwae T, Hori M (eds) Blue carbon in shallow coastal ecosystems: carbon dynamics, policy, and implementation. Springer, Singapore, pp 129–159

Endo T, Nakano Y, Ikada N, Tanaka T, Shimano J, Miyawaki K, Yamochi S (2015) Estimation of CO_2 budget in the arttifical salt marsh developed at urban coastal zone by seasonal 24 hour field investigations of CO_2 fluxes. J Jpn Soc Civil Eng Ser B2 (Coastal Engineering) 71:1327–1332 (in Japanese)

Endo T, Nakano Y, Ikada N (2016) Evaluation method of CO_2 exchange at the intertidal flat, the sea surface and sea bottom of an artificial salt marsh in urban coastal zone. J Jpn Soc Civil Eng Ser. B2 (Coastal Engineering) 72:1447–1452 (in Japanese)

Flecha S, Huertas IE, Navarro G, Morris EP, Ruiz J (2015) Air-water CO_2 fluxes in a highly heterotrophic estuary. Estuar Coasts 38:2295–2309

Ford H, Garbutt A, Jones L, Jones DL (2012) Methane, carbon dioxide and nitrous oxide fluxes from a temperate salt marsh: grazing management does not alter global warming potential. Estuar Coast Shelf Sci 113:182–191

Frankignoulle M, Abril G, Borges A, Bourge I, Canon C, Delille B, Libert E, Théate JM (1998) Carbon dioxide emission from European estuaries. Science 282:434–436

Fujii T, Fujiwara T, Nakayama K (2013) Fluxes of carbon dioxide in the Eastern Regions of Osaka Bay. J Jpn Soc Civil Eng Ser. B2 (Coastal Engineering) 69:1111–1115. (in Japanese)

Guo H, Noormets A, Zhao B, Chen J, Sun G, Gu Y, Li B, Chen J (2009) Tidal effects on net ecosystem exchange of carbon in an estuarine wetland. Agric For Meteorol 149:1820–1828

Han G, Yang L, Yu J, Wang G, Mao P, Gao Y (2013) Environmental controls on net ecosystem CO_2 exchange over a reed (*Phragmites australis*) wetland in the Yellow River Delta. China Estuar Coasts 36:401–413

Hofman PAG, de Jong SA, Wagenvoort EJ, Sandee AJJ (1991) Apparent sediment diffusion coefficients for oxygen consumption rates measured with microelectrodes and bell jars: applications to oxygen budgets in estuarine intertidal sediments (Oosterschelde, SW Netherlands). Mar Ecol Prog Ser 69:261–272

Jiang LQ, Cai WJ, Wang Y (2008) A comparative study of carbon dioxide degassing in river- and marine-dominated estuaries. Limnol Oceanogr 53:2603–2615

Klaassen W, Spilmont N (2012) Inter-annual variability of CO$_2$ exchanges between an emersed tidal flat and the atmosphere. Estuar Coast Shelf Sci 100:18–25

Laruelle GG, Dürr HH, Slomp CP, Borges AV (2010) Evaluation of sinks and sources of CO$_2$ in the global coastal ocean using a spatially-explicit typology of estuaries and continental shelves. Geophys Res Lett 37:L15607

Laruelle GG, Durr HH, Lauerwald R, Hartmann J, Slomp CP, Goossens N, Regnier PAG (2013) Global multi-scale segmentation of continental and coastal waters from the watersheds to the continental margin. Hydrol Earth Syst Sci 17:2029–2051

Magenheimer JF, Moore TR, Chmura GL, Daoust RJ (1996) Methane and carbon flux from a macrotidal salt marsh, Bay of Fundy, New Brunswick. Estuaries 19:39–145

Middelburg JJ, Klaver G, Nieuwenhuize J, Wielemaker A, De Haas W, Vlug T, Van der Nat J (1996) Organic matter mineralization in intertidal sediments along an estuarine gradient. Mar Ecol Prog Ser 132:157–168

Migné A, Davoult D, Spilmont N, Menu D, Boucher G, Gattuso JP, Rybarczyk H (2002) A closed-chamber CO$_2$-flux method for estimating intertidal primary production and respiration under emersed conditions. Mar Biol 140:865–869

Migné A, Spilmont N, Davoult D (2004) In situ measurements of benthic primary production during emersion: seasonal variations and annual production in the Bay of Sommoe (eastern English Channel, France). Cont Shelf Res 24:1437–1449

Migné A, Davoult D, Spilmont N, Ouisse V, Boucher G (2016) Spatial and temporal variability of CO$_2$ fluxes at the sediment-air interface in a tidal flat of a temperate lagoon (arcachon bay, France). J Sea Res 109:13–19

Nellemann C, Corcoran E, Duarte C M, Valdés L, De Young C, Fonseca L, Grimsditch G (2009) Blue carbon. A rapid response assessment. United Nations Environment Programme, GRID-Arendal (www.grida.no)

Otani S, Marikawa J (2017) Elucidation dynamics of carbon dioxide flux on salt marsh. J Jpn Soc Civil Eng Ser B2 (Coastal Engineering) 73:1303–1308. (in Japanese)

Otani S, Kawasaki T, Endo T, Higashi K (2017) Seasonal change on characteristics of sediment and carbon dioxide absorption/emission rate at mud river mouth tidal flat. J Jpn Soc Civil Eng Ser B3 (Ocean Engineering) 73:630–635. (in Japanese)

Polsenaere P, Lamaud E, Lafon V, Bonnefond JM, Bretel P, Delille B, Deborde J, Loustau D, Abril G (2012) Spatial and temporal CO$_2$ exchanges measured by Eddy Covariance over a temperate intertidal flat and their relationships to net ecosystem production. Biogeosciences 9:249–268

Raymond PA, Cole JJ (2001) Gas exchange in rivers and estuaries: choosing a gas transfer velocity. Estuaries 24:312–317

Regnier P, Friedlingstein P, Ciais P, Mackenzie F, Gruber N, Janssens IA, Laruelle GG, Lauerwald R, Luyssaert S, Andersson AJ (2013) Anthropogenic perturbation of the carbon fluxes from land to ocean. Nat Geosci 6:597–607

Robertson AI (1986) Leaf-burying crabs: their influence on energy flow and export from mixed mangrove forests (*Rhizophora* spp.) in northeastern Australia. J Exp Mar Biol Ecol 102:237–248

Sasaki A, Hagimori Y, Yuasa I, Nakatsubo T (2012) Annual sediment respiration in estuarine sandy intertidal flats in the Seto Inland Sea. Japan Landscape Ecol Eng 8:107–114

Schäfer KVR, Tripathee R, Artigas F, Morin TH, Bohrer G (2014) Carbon dioxide fluxes of an urban tidal marsh in the Hudson-Raritan estuary. Biogeosciences 119:2065–2081

Skov MW, Hartnoll RG (2002) Paradoxical selective feeding on a low-nutrient diet: why do mangrove crabs eat leaves. Oecologia 131:1–7

Spilmont N, Migné A, Lefebvre A, Artigas LF, Rauch M, Davoult D (2005) Temporal variability of intertidal benthic metabolism under emersed conditions in an exposed sandy beach (Wimereux, eastern English Channel, France). J Sea Res 53:161–167

Tanaka K, Takikawa K (2006) Observational study on the CO$_2$ flux into atmosphere on the tidal zone in the Ariake Sea. Annu J Coast Eng 53:1136–1140 (in Japanese)

Tanaka T, Endo T, Ikada N, Yamochi S (2016) Characteristics of CO_2 absorption and emission in the high water temperature seasons at the north salt marsh of Osaka Nanko bird sanctuary. J Jpn Soc Civil Eng Ser B2 (Coastal Engineering) 72:1–11. (in Japanese)

Tokoro T, Kuwae T (2017) A new procedure for processing eddy-covariance data to better quantify atmosphere-aquatic ecosystem CO_2 exchanges, Biogeosci Discuss https://doi.org/10.5194/bg-2017-499

Tokoro T, Watanabe K, Tada K, Kuwae T (2018) Air–water CO_2 flux in shallow coastal waters: theoretical background, measurement methods, and mechanisms. In: Kuwae T, Hori M (eds) Blue carbon in shallow coastal ecosystems: carbon dynamics, policy, and implementation. Springer, Singapore, pp 153–184

Underwood GJC, Kromkamp J (1999) Primary production by phytoplankton and microphytobenthos in estuaries. Adv Ecol Res 29:93–153

Watanabe K, Kuwae T (2015) Radiocarbon isotopic evidence for assimilation of atmospheric CO_2 by the seagrass *Zostera marina*. Biogeosciences 12:6251–6258

Webb EK, Pearman GI, Leuning R (1980) Correction of flux measurements for density effects due to heat and water vapour transfer. Quart J Roy Meteorol Soc 106:85–100

Yamochi S, Tanaka T, Otani Y, Endo T (2017) Effects of light, temperature and ground water level on the CO_2 flux of the sediment in the high water temperature seasons at the artificial north salt marsh of Osaka Nanko bird sanctuary. Japan Ecol Eng 98:330–338

Yoshida G, Hori M, Shimabukuro H, Hamaoka H, Iwasaki S (2015) Production of *Zostera marina* with different shoot size and stand structures in the Seto Inland Sea, Japan – production in the luxuriant season in 2012. Biosphere Sci 54:29–44

Zemmelink HJ, Slagter HA, Van Slooten C, Snoek J, Heusinkveld B, Elbers J, Bink NJ, Klaassen W, Philippart CJM, HJW DB (2009) Primary production and eddy correlation measurements of CO_2 exchange over an intertidal estuary. Geophys Res Lett 36:L19606

Zhong Q, Wang K, Lai Q, Zhang C, Zheng L, Wang J (2016) Carbon dioxide fluxes and their environmental control in a reclaimed Coastal Wetland in the Yangtze estuary. Estuar Coasts 39:344–362

Zhou L, Zhou G, Jia Q (2009) Annual cycle of CO_2 exchange over a reed (*Phragmites australis*) Wetland in Northeast China. Aquat Bot 91:91–98

Chapter 9
Quantifying the Fate of Captured Carbon: From Seagrass Meadows to the Deep Sea

Katsuyuki Abo, Koichi Sugimatsu, Masakazu Hori, Goro Yoshida, Hiromori Shimabukuro, Hiroshi Yagi, Akiyoshi Nakayama, and Kenji Tarutani

Abstract To help evaluate the sequestration and carbon dioxide storage function of seagrass meadows, we describe the processes by which carbon is sequestered in eelgrass beds and transported from shallow coastal waters to the deep sea. A part of the carbon taken up by eelgrass is decomposed and returned to biological production or the water column's dissolved inorganic carbon pool, some is accumulated and stored in the shallow sea bottom, and the rest flows out into the deep sea. Here, we describe the growth of eelgrasses and the processes of decomposition, sedimentation, and transportation of eelgrass-derived organic carbon using the Seto Inland Sea as a model site. We estimated the amount of carbon sequestered and stored in eelgrass beds, the fate of eelgrass-derived organic carbon, and the amounts accumulated in the shallow coastal water and transported to the deep sea. According to our estimates based on calculations from tracking carbon over a 1-year period, of the 73,000 tons of carbon sequestered by eelgrass annually in the Seto Inland Sea, 40.9% is accumulated in the Seto Inland Sea and 8.3% flows out to the deep sea. In other words, the eelgrass beds in the Seto Inland Sea have an annual potential capacity of 36,000 tons of carbon storage. In addition, most of the organic carbon was accumulated in the shallow coastal waters rather than in the deep sea.

K. Abo (✉) · M. Hori · G. Yoshida · H. Shimabukuro
National Research Institute of Fisheries and Environment of Inland Sea, Japan Fisheries Research and Education Agency, Hatsukaichi, Hiroshima, Japan
e-mail: abo@fra.affrc.go.jp

K. Sugimatsu
National Research Institute of Fisheries Engineering, Fisheries Research Agency, Kamisu, Ibaraki, Japan

H. Yagi
School of Systems Engineering, National Defense Academy, Yokosuka, Japan

A. Nakayama
Alpha Hydraulic Engineering Consultants Co. Ltd., Chuoh-ku, Tokyo, Japan

K. Tarutani
Seikai National Fisheries Research Institute, Fisheries Research Agency, Nagasaki, Japan

9.1 Introduction

Global warming is caused by an increase in greenhouse gases such as carbon dioxide, and as such, carbon dioxide sinks and sources have been drawing attention. In addition to terrestrial forests, marine vegetation is also important for the sequestration and storage of carbon dioxide (Nellemann et al. 2009). Seagrass meadows, which are also called sea forests, are expected to act as a carbon dioxide sink. The broadly distributed eelgrass (*Zostera marina*) is expected to serve as a particularly large carbon sink (Rohr et al. 2016; Dahl et al. 2016; Miyajima and Hamagichi 2018). In this chapter, we focus on the process of sequestration of carbon dioxide in eelgrass beds. We also describe the transport of sequestered carbon from eelgrass beds in shallow coastal waters to the deep sea.

Eelgrass beds are expected to be an important carbon dioxide sink in shallow coastal waters (Tokoro et al. 2014, 2018). However, to prevent further global warming, it is not only necessary to sequester carbon dioxide from the atmosphere but also to accumulate the carbon as compounds in organisms or sediments over a prolonged period (Miyajima and Hamagichi 2018). Eelgrass grows from spring to summer. In autumn, the plants decline and the leaves fall off; some settle on the bottom sediment, while a portion of them flows out of the eelgrass bed (Aioi 1980; Douke et al. 2000; Nakaoka and Aioi 2001). Therefore, to evaluate the function of *Z. marina* in carbon sequestration and storage, it is necessary to estimate the amount of eelgrass-derived organic carbon that flows out of eelgrass beds and is deposited on the bottom of shallow coastal areas or the deep sea, as well as within the eelgrass beds (Duarte and Krause-Jensen 2017).

Figure 9.1 is a schematic diagram of the process by which carbon sequestered in an eelgrass bed is transported while changing its form. Inside the bed, eelgrass takes

(in eelgrass bed)   (outside eelgrass bed)
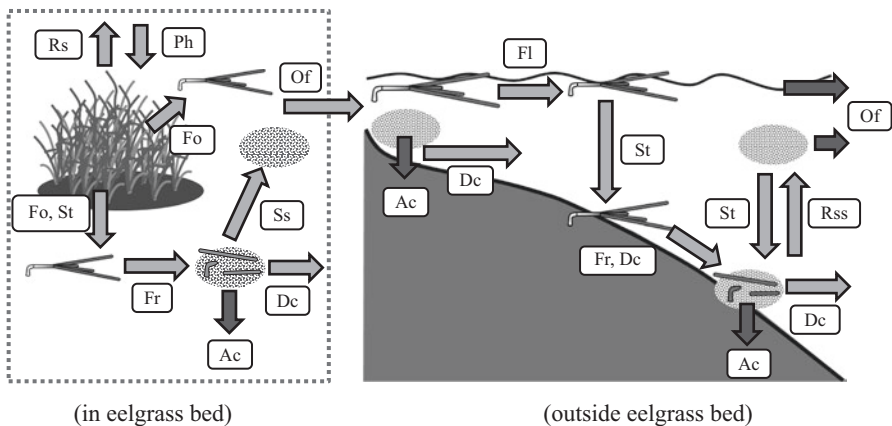
Rs: respiration, Ph: photosynthesis, Of: outflowing, Fo: falling off, St: settling, Fr: Fragmentation, Ss: suspension, Dc: decomposition, Ac: accumulation, Fl: floating, Rss: resuspension

Fig. 9.1 Processes involved in the transport of carbon originating in eelgrass beds
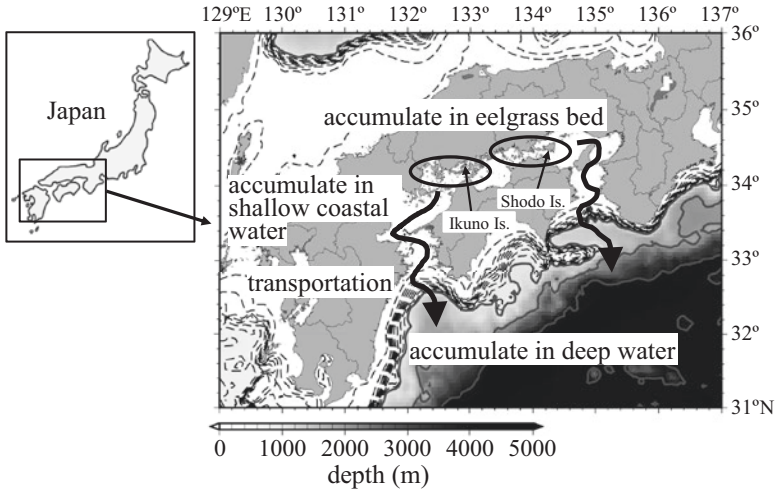
Fig. 9.2 Deposition and transport of carbon sequestered in eelgrass beds in the Seto Inland Sea

up dissolved inorganic carbon (DIC) in the water column and directly absorbs atmospheric carbon dioxide by photosynthesis (Watanabe and Kuwae 2015) and accumulates carbon as organic compounds in the leaves. After that, some of the fallen leaves settle in the eelgrass bed, while a portion of them flow out as drifting seagrass. The settled leaves are first fragmented by grazers such as small crustaceans, and then they are decomposed and mineralized by microorganisms. After that, the carbon compounds in the leaves are remineralized to DIC and released into the environment. In addition, the remaining eelgrass-derived organic carbon that settles on the bottom can flow out of the eelgrass bed due to tidal effects or meteorological disturbances such as typhoons. The leaves that flow out of the eelgrass beds drift for a while and settle in other locations. Some of the carbon compounds deposited on the sea bed are resuspended into the water column due to strong flow or disturbance and are transported even greater distances.

In this chapter, using the Seto Inland Sea as an example, we describe the transport of eelgrass-derived organic carbon inside and outside of eelgrass beds (Fig. 9.2). In addition, we present research based on a numerical ocean model used to express the cycling process of eelgrass-derived organic carbon. Based on our results, we then clarify the fate of carbon that is sequestered in eelgrass beds in the Seto Inland Sea.

9.2 Decomposition and Deposition of Leaves in Eelgrass Beds

A schematic illustration of the decomposition process of leaves in eelgrass beds is shown in Fig. 9.3. The mature leaves fall off mainly as the plants decline in autumn and settle onto the seabed. The settled leaves are fragmented by the action of small

Fig. 9.3 Decomposition
process of leaves in
eelgrass beds
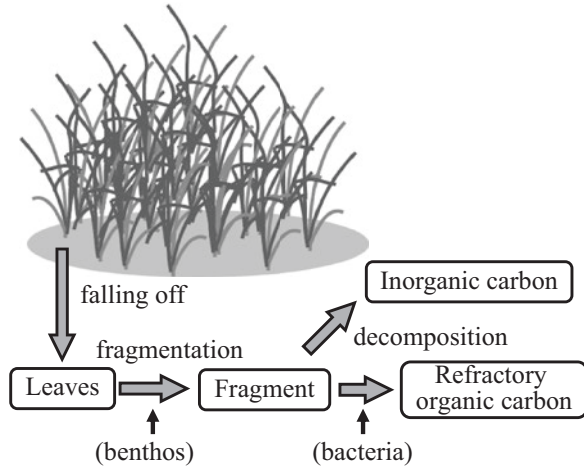
crustaceans and other organisms, and thereafter they are decomposed by microorganisms. Through this decomposition, the organic carbon compounds constituting the leaves are mineralized and released into the surrounding water as DIC. However, the refractory organic carbon decomposes slowly and remains for more than a couple of years. In this section, we describe the decomposition and deposition processes of the leaves and consider the roles that eelgrass beds play in carbon storage.

9.2.1 Falling Off and Settling of Leaves

Mature eelgrass leaves eventually fall off and then settle in the eelgrass bed or float away and settle on the sea bottom outside of the eelgrass bed. Eelgrass grows from spring to summer, and the leaves wither and fall off mainly in autumn. In eelgrass beds in the Seto Inland Sea, the number of fallen leaves increases from September to November, corresponding to the season of decline (Fujiwara et al. 2006). The leaves tend to fall off in locations susceptible to typhoons and strong waves, and after floating for a while, many leaves settle on the sea bottom in convergent areas where floating objects tend to gather. In the case of the Seto Inland Sea, the amount of fallen leaves was small in the inner part of the bay and large at the bay mouth, reflecting the strength of waves and water flow.

9.2.2 Fragmentation of the Settled Leaves

For fragmentation of the settled leaves, the presence of macrobenthos (benthic organisms of ≥1 mm) and meiobenthos (0.1–1 mm) in eelgrass beds is important, especially crustaceans, whose contribution to fragmentation is suggested to be large
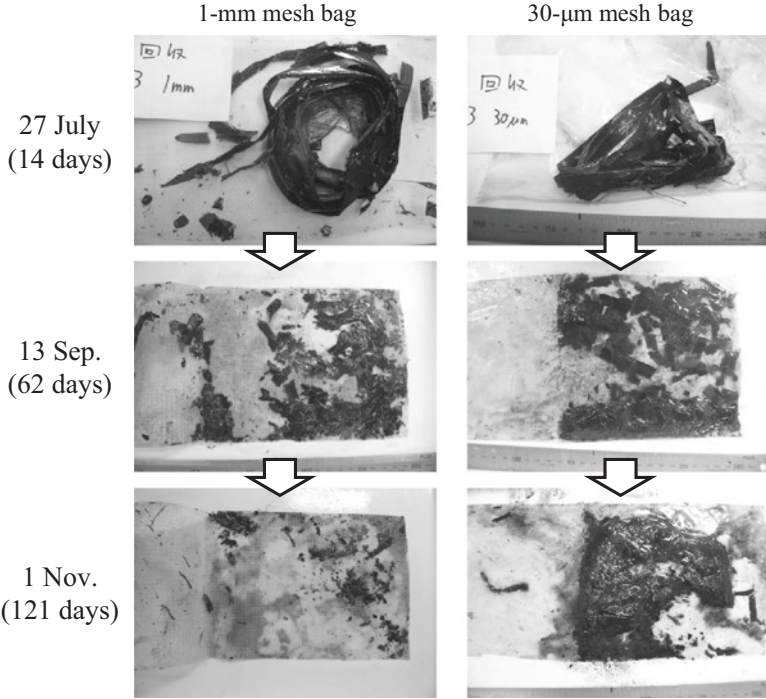
Fig. 9.4 Decomposition process of leaves in litter bags. (Hamaguchi et al. 2012)

(Zupo et al. 2001; Bostrom and Mattila 2005). Field experiments using litter bags (i.e., mesh bags that store fallen blades and leaves) are often performed to investigate the fragmentation and decomposition process of leaves. The litter bags are placed on the sediment of an eelgrass bed for a certain period, and then the leaves and remnants in the bag are observed periodically to investigate the fragmentation process.

Figure 9.4 shows states of leave decomposition in litter bags from an experiment performed in an eelgrass bed in Ikuno Island in the Seto Inland Sea (Hamaguchi et al. 2012). Leaves were placed in 1-mm and 30-µm mesh bags (20 × 17 cm), which are commonly used to prevent entry of macrobenthos larvae and meiobenthos, respectively (Opsahl and Benner 1993; Yamada and Toyohara 2012). At 2 weeks after installation, the leaves remained essentially intact but the decrease in their mass during this period was extremely large, from 40% to 50% of their initial mass in both mesh bags, the leaves lost. Fragmentation of the leaves then proceeded rapidly, and after 42 days, only 20% to 30% of the initial mass remained in the 1-mm mesh bag, whereas further reduction of the mass of the remnants in the 30-µm mesh bag was relatively small. The leave fragments seemed to move through the 1-mm mesh.

The rapid mass loss at the beginning of the experiment was mainly due to elution of soluble organic matter. It appears that the unstable and decomposable components

were lost first and then the fragmentation rapidly progressed. Although the contribution of grazers to the fragmentation process was expected to be very large, few grazers were present in the 1-mm mesh bag in this experiment. In addition, fragmentation progressed even in the 30-μm mesh bag, which meiofauna cannot invade. Therefore, these findings suggest that, after a certain period, fragmented leaves can decompose rapidly without the intervention of grazers.

9.2.3 Decomposition of Leaves

Organic matter is decomposed and mineralized by microorganisms, but the rates differ depending on the organic matter components. Starch, saccharides, and proteins are decomposed rapidly, cellulose is somewhat slower, and lignin is slow (Klap et al. 2000; Hemminga and Duarte 2000). With regard to decomposition rates of organic matter, three components are often considered: labile organic matter with rapid decomposition rates, semi-labile organic matter with intermediate decomposition rates, and refractory organic matter that is difficult to decompose and is continuously present as organic matter over a prolonged period. Eelgrass is made up of various components, and it contains a fixed amount of semi-labile organic matter such as cellulose and hemicellulose constituting the cell wall and refractory organic matter such as lignin that adheres and solidifies the cells (Opsahl and Benner 1993; Klap et al. 2000).

Figure 9.5 presents the results of the leave decomposition experiments, showing the change in the residual amount of the leaves. At the beginning of the experiment, the decomposition rate was fast because the labile organic matter decomposed first. About 20 days later, the decomposition rate slowed as the semi-labile organic matter decomposed. If the decomposition experiment was continued, only refractory organic matter would eventually remain. We often refer to the components that are not decomposed after more than a year as refractory organic matter (Opsahl and Benner 1993). Organic carbon compounds in eelgrass accumulate in bottom sediments or in the deep sea while they are decomposing, whereas a portion are not decomposed and are stored for a prolonged period. In this field experiment, the decomposition rates of labile and semi-labile organic matter were 0.116 (day^{-1}) and 0.004 (day^{-1}), respectively. In addition, the percentage of labile, semi-labile, and refractory organic matter of the leaves were 42%, 52%, and 6%, respectively (Tarutani et al. 2012). These values were obtained while assuming the value of the general lignin content (6%) was the proportion of refractory organic matter.

According to a review by Enriquez et al. (1993), the decomposition rate of eelgrass (*Z. marina*) was 0.0007–0.0357, and the average was 0.0114 (day^{-1}). However, these values were obtained without distinguishing between labile and semi-labile organic matter. Based on the field experiment presented here, the decomposition rate obtained without distinction between labile and semi-labile organic matter was
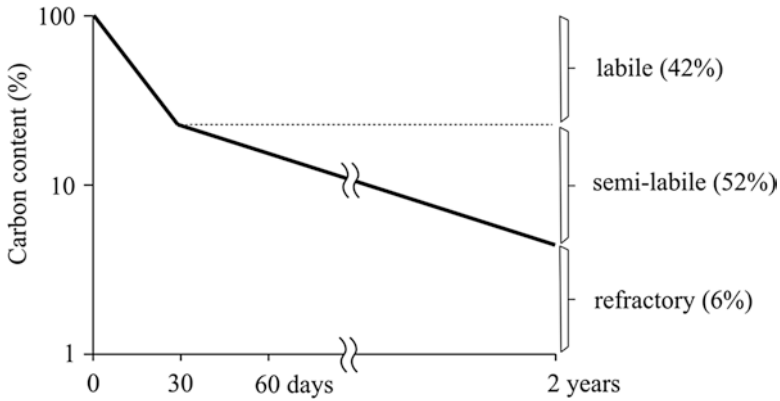
Fig. 9.5 Changes in the amount of carbon due to decomposition of the leaves. The remaining amount is indicated as the percentage of the initial amount of carbon. (Tarutani et al. 2012)
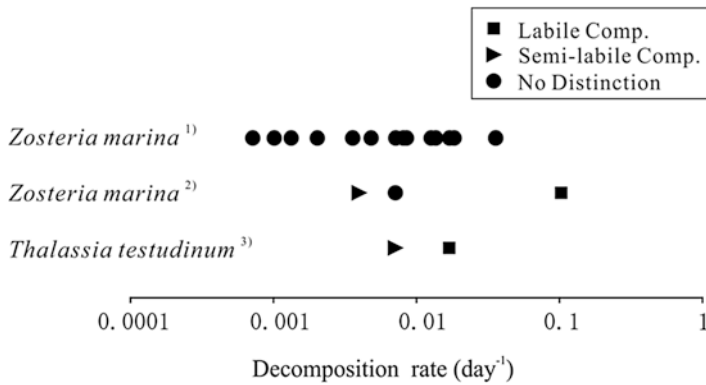
Fig. 9.6 Decomposition rate (day^{-1}) of seagrass leaves. Data from (1) Enriquez et al. (1993), (2) Tarutani et al. (2012), and (3) Fourqurean and Schrlau (2003)

0.008 (day^{-1}), which is within the previously reported range. Also, in the case of the seagrass *Thalassia testudinum*, the percentage of labile organic matter was 57% with a decomposition rate of 0.017 (day^{-1}), while the decomposition rate of semi-labile organic matter was 0.007 (day^{-1}) (Fourqurean and Schrlau 2003), which are comparable to the previously reported rates (Fig. 9.6). According to Trevathan-Tackett et al. (2017), who reviewed studies on seagrasses around the world, the leave content of semi-labile organic matter (cellulose and hemicellulose) is about 44% and the refractory organic matter (lignin) is about 5%, whereas these values in the rhizome are about 25% and 11%, respectively (Table 9.1). Thus, the results of the Tarutani et al. (2012) field experiment were in good agreement with other studies.

Table 9.1 The organic matter content (%) contained in seagrasses

Part of plant	Semi-labile organic matter (cellulose, hemicellulose)	Refractory organic matter (lignin)
Aboveground	43.85 ± 2.46	5.20 ± 0.90
Belowground	25.15 ± 1.47	11.33 ± 1.19

Values are mean ± SEM. Based on Trevathan-Tackett et al. (2017)

Table 9.2 Amount of eelgrass biomass in the Seto Inland Sea that is produced, falls as shoots, and outflows

	Dense eelgrass beds	Sparse eelgrass beds
Production (kg DW m^{-2} $year^{-1}$)	4.16	2.13
Fallen leaves (kg DW m^{-2} $year^{-1}$)	0.37	–
Fallen shoots (shoot m^{-2})	73.6	82.5
Production per shoot (g DW $shoot^{-1}$ $year^{-1}$)	24.2	11.1
Fallen leaves per shoot (g DW $shoot^{-1}$ $year^{-1}$)	2.2	1.0
Fallen shoots (kg DW m^{-2} $year^{-1}$)	1.62	0.83
Outflow from eelgrass beds (kg DW m^{-2} $year^{-1}$)	0.49	0.58

Values in dense and sparse eelgrass beds are estimated from Tarutani et al. (2012) and Fujiwara et al. (2009), respectively

9.3 Outflow of the Leaves and Eelgrass-Derived Organic Matter

To understand the size of the eelgrass-derived organic carbon stock, it is necessary to follow the ways in which organic carbon compounds in eelgrass decompose and disperse. Mature eelgrass leaves eventually wither and settle on the bottom in the eelgrass bed, settle in the eelgrass bed after floating for a while, or float and drift out of the eelgrass bed and settle at a distant location (drifting leaves). The leaves that settle in the eelgrass bed are fragmented and decomposed into fine particles, which can become resuspended in the water column due to turbulence and flow out of the eelgrass bed as particulate organic matter.

First, we consider the amount of leaves that flows out of eelgrass beds. Table 9.2 shows the estimated amounts of leaves produced, fallen, and flowing out of eelgrass beds on an annual basis. These values were estimated from field surveys in dense eelgrass beds around Ikuno Island (Tarutani et al. 2012) and in sparse eelgrass beds along Shodo Island (Fujiwara et al. 2009). The amounts of produced and fallen leaves from the dense beds were obtained by using the leaf-marking method, whereas those from the sparse beds were estimated from observed leave abundance. The amount of fallen shoot was estimated as the difference between the growing and declining seasons. Production in the dense and sparse eelgrass beds was 4.16 and 2.13 kg DW m^{-2} $year^{-1}$, respectively. The annual amount of fallen shoots from the dense and sparse eelgrass beds was 1.62 and 0.83 kg DW m^{-2} $year^{-1}$, respec-

tively. The amount of outflow has been reported to be about 30% of the fallen shoot in dense eelgrass beds and about 70% in sparse eelgrass beds (Hemminga and Duarte 2000). Therefore, the amounts of outflow shoots (drifting leaves) from the dense and sparse eelgrass beds are estimated to be 0.49 and 0.58 kg DW m^{-2} year^{-1}, respectively. Note that the rate of shoot flowing out is larger for the sparse eelgrass bed, whereas that of fallen shoot is larger in the dense eelgrass bed.

Next, we consider eelgrass-derived organic matter that flows out as suspended particles. Eelgrass-derived organic matter that has become fine particles due to fragmentation or decomposition is stirred up by water flow and resuspended in the water column. The suspended particles are transported by the currents and some flow out of the eelgrass bed, while the rest settle again within the eelgrass bed when conditions become calm. According to a sediment trap survey in the eelgrass beds around Ikuno Island, the amount of suspended organic matter (including small leave fragments) that flowed out of the eelgrass bed was 0.015 kg DW m^{-2} year^{-1}. This corresponds to 0.3% of the eelgrass production, or about 3% of the amount that flowed out as drifting leaves.

9.4 Fate of Eelgrass-Derived Organic Carbon in Eelgrass vBeds

In the previous sections, we described the sedimentation, decomposition, and outflow of eelgrass leaves. However, to evaluate carbon storage in eelgrass beds, it is necessary to quantify the development of eelgrass (including death and leave loss). In this section, we introduce a numerical model of the population dynamics of eelgrass and describe the mass balance within the eelgrass bed estimated by the model simulation.

9.4.1 Modeling the Growth and Withering Process of Eelgrass

The basic idea of the numerical eelgrass growth models is similar to low trophic ecosystem models targeting phytoplankton; they mathematically express that growth by photosynthesis depends on environmental factors such as solar radiation, water temperature, and nutrient concentrations. Because eelgrass is divided into an aboveground part composed of blades and a sheath and a belowground part composed of rhizomes and fibrous roots, most models calculate biomasses of the aboveground part and the belowground part (Verhagen and Nienhuis 1983, Bach 1993, Bocci et al. 1997, Zharova et al. 2001). Here, we introduce a model developed by Tarutani et al. (2011), which they modified from the relatively simple and highly versatile model of Bocci et al. (1997).

Figure 9.7 shows the outline of the eelgrass growth model. In this model, we calculate the biomasses of the aboveground and belowground parts, and the amount
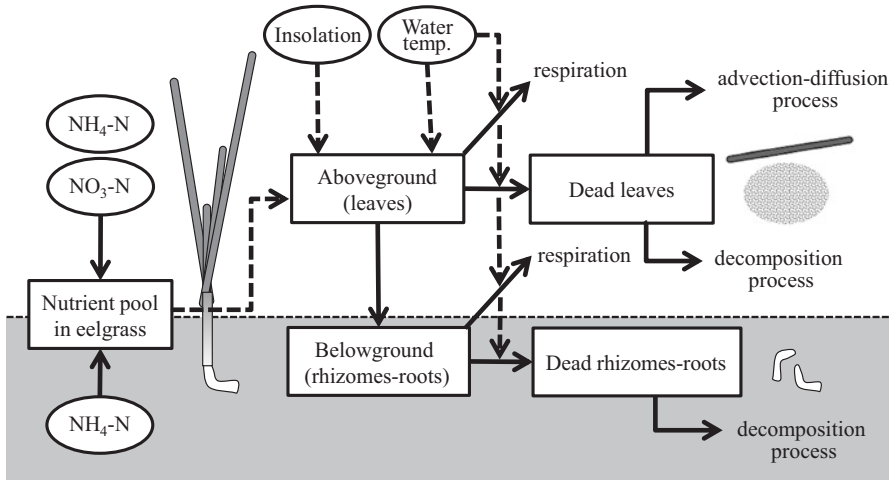
Fig. 9.7 Outline of the eelgrass growth model
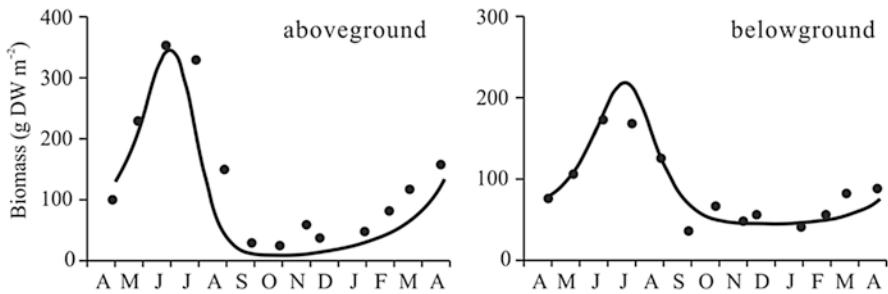
Fig. 9.8 Seasonal variation of the biomass of leaves (aboveground part) and rhizomes and roots (belowground part). Solid line: calculation result, black circle: measured value

of dead material derived from them. Eelgrass absorbs inorganic nutrients in sea water and in pore water from the muddy bottom by the aboveground and below-ground parts, respectively. In the aboveground part, carbon dioxide is absorbed and energy is obtained by photosynthesis using the nutrients in the grass body. Nitrogen uptake, photosynthesis, and respiration rates of the eelgrass are determined by solar radiation and water temperature. Figure 9.8 shows model calculation results of the aboveground and belowground parts in the eelgrass beds along Shodo Island. The biomass of the aboveground part increased with water temperature and reached a maximum in late June to early July, then decreased sharply. The biomass reached a minimum in October to early November and then again shifted to a growth phase in late November. The belowground biomass showed a similar seasonal fluctuation as that of the aboveground part, although the maximum was slightly delayed season-ally and the period of lower biomass was longer. The results of the model calculation

Fig. 9.9 Seasonal changes in biomass and net production in the aboveground and belowground parts of eelgrass (calculated value) in (**a**) a dense eelgrass bed, and (**b**) a sparse eelgrass bed

were in good agreement with observed values, and it was confirmed that the annual variations of eelgrass biomass can be reproduced by the model.

9.4.2   Mass Balance in Eelgrass Beds

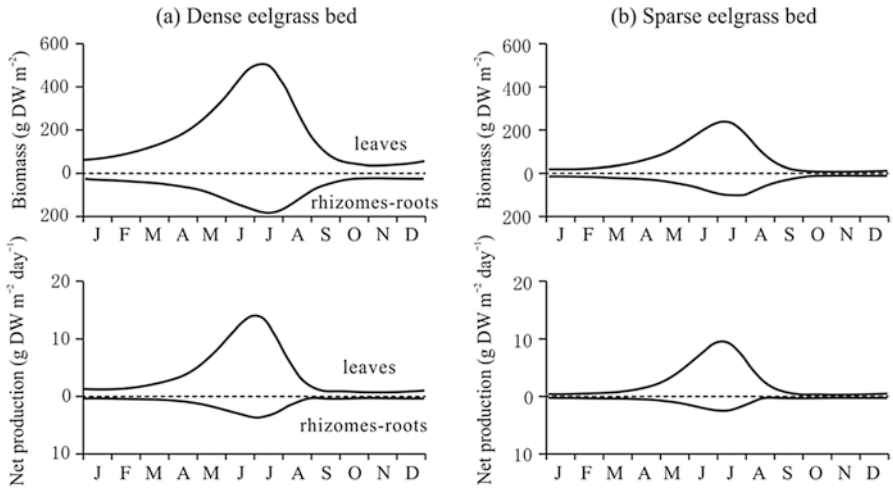As described in Sect. 9.3, both the production and the amount of fallen and drifting leaves differ between dense and sparse eelgrass beds. Therefore, the mass balance and the carbon sequestration and storage function of both types also differ. Figure 9.9 shows the results from the eelgrass growth model simulating the seasonal variations of biomass and the net primary production in dense and sparse eelgrass beds in the Seto Inland Sea. The net primary production of the aboveground and belowground parts of the dense eelgrass beds were in the range of 0.8–14 and 1–4 g DW m^{-2} day^{-1}, respectively, and the annual net primary production was 1240 g DW m^{-2} (440 g C m^{-2}). The net primary production of the sparse eelgrass beds were in the range of 0.3–10 and 0–2 g DW m^{-2} day^{-1}, respectively, and the annual net primary production was 786 g DW m^{-2} (279 g C m^{-2}).

Next, the mass balance of eelgrass-derived organic carbon was calculated by the eelgrass growth model. Figure 9.10 shows the fate of accumulated carbon in dense and sparse eelgrass beds from January to December in 2011. For this calculation, we used the ratio of the fallen leave amount to that of production, and the ratio of outflow amount of drifting leaves and suspended particle to that of production (Table 9.2). For the decomposition and sedimentation process of the fallen and withered leaves in the eelgrass bed, we assumed that only labile organic matter is decomposed while semi-labile and refractory organic matter are accumulated in the
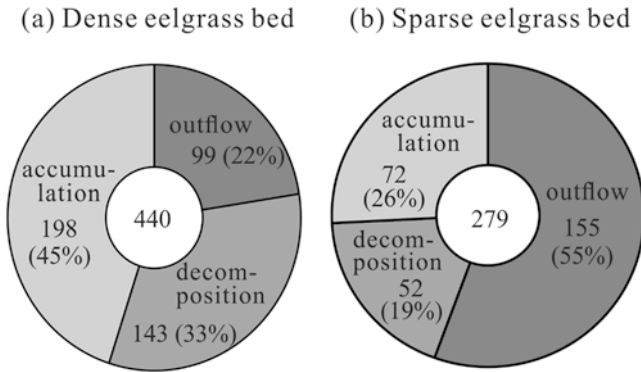
Fig. 9.10 Annual amounts of production, decomposition, outflow, and accumulation of carbon (g m^{-2}) in eelgrass beds in the Seto Inland Sea. Totals are given in the center of each circle

bottom sediment, within the 1-year time scale set for the calculation. In the dense eelgrass beds, 22% of the sequestered carbon amount flowed out, 33% was decomposed, and 45% was deposited. In the sparse eelgrass beds, 55% of the carbon amount flowed out, 19% was decomposed, and 26% was deposited (Fig. 9.10). The production and the deposition amounts per unit area were about 1.6 and 2.8 times higher in the dense eelgrass beds, whereas the outflow amount was 1.6 times higher in the sparse eelgrass beds.

9.5 Fate of Eelgrass Flowing Out of Eelgrass Beds

Here, we describe the numerical ocean model (Sugimatsu et al. 2015) capable of expressing the circulation process of eelgrass-derived organic carbon flowing out of eelgrass beds, and we present the simulation results of the fate of the eelgrass-derived organic carbon.

9.5.1 Numerical Ocean Model (Advection, Diffusion, Decomposition, and Deposition)

9.5.1.1 Hydrodynamics

Drifting leaves and suspended particles that flow out of eelgrass beds are transported toward distant areas by hydrodynamic force (i.e., physical transport). Therefore, to follow the fate of eelgrass-derived organic carbon, it is necessary to understand the system's hydrodynamics. In such ocean circulation models, the sea area is divided into cubic computational grids and currents are calculated by

considering the water temperature, salinity, outflow–inflow of heat and substances between the grids. To more accurately reproduce this system in detail, it is better for the computational grid to be smaller, but in that case the computation time becomes very long. In coastal areas, the size of the computational grid is often 1 km horizontally and 10–20 layers vertically.

The flow model used here to trace eelgrass-derived organic carbon is the Seto Inland Sea Model developed by the National Research Institute of Fisheries Engineering of Japan (Nakayama et al. 2009). The fundamental equation of the model uses motion, continuity, state of density, and transport of heat and salts (for details, see Nakayama et al. 2009). In this model, hydrodynamics in the sea area can be calculated by considering the tidal flow, density flow, and wind-induced flow. Using this model, the drifting leaves and suspended particles that flowed out of eelgrass beds were traced.

9.5.1.2 Outflow, Sedimentation, and Decomposition

We took two approaches to represent the behavior of eelgrass (drifting leaves) that flowed out of the eelgrass bed based on the Seto Inland Sea Model. One was to evaluate its behavior in the material circulation model by assuming drifting leaves are passive suspended organic matter (behavior of fine particles in water coincide with the behavior of water molecules), and the other was to track the drifting leaves as is (floating and settling while being reduced in size due to fragmentation and/or decomposition). By combining these two approaches, Sugimatsu et al. (2015) developed a drifting leave carbon circulation model that quantitatively expresses the material circulation including the behavior of the drifting leaves and decomposition process of the leaves after settling. Figure 9.11 shows the schematic view of the model for estimating the fate of drifting leaves and suspended particles.

Drifting leaves that flow out of the eelgrass bed begin to settle after drifting near the surface layer for a certain period; after settling on the seabed, they are fragmented into suspended organic matter. According to an experiment by Hamaguchi et al. (2012), in which eelgrass leaves were floated in a 10-ton running water tank to determine the number of days before settlement began, the drift period was 25.7 days and the settling velocity was 21.1 mm s^{-1}.

The leaves that settle on the sea bottom are fragmented and resuspended into the water column as particulate organic matter, or they are decomposed and resuspended as dissolved inorganic matter. The fragmentation rate of the leaves and the decomposition rate of the particulate organic matter can be obtained from the decomposition experiment using litter bags described in Sect. 9.2.2. The leaves comprise three components with different decomposition rates, with 42% being labile, 52% semi-labile, and 6% refractory organic matter. Because the labile organic matter has already been decomposed within the eelgrass bed, the suspended organic matter that flows out is assumed to be composed only of the semi-labile and refractory organic matter. Dissolved organic carbon (DOC) was not measured in the decomposition experiment above, so the model did not directly deal with
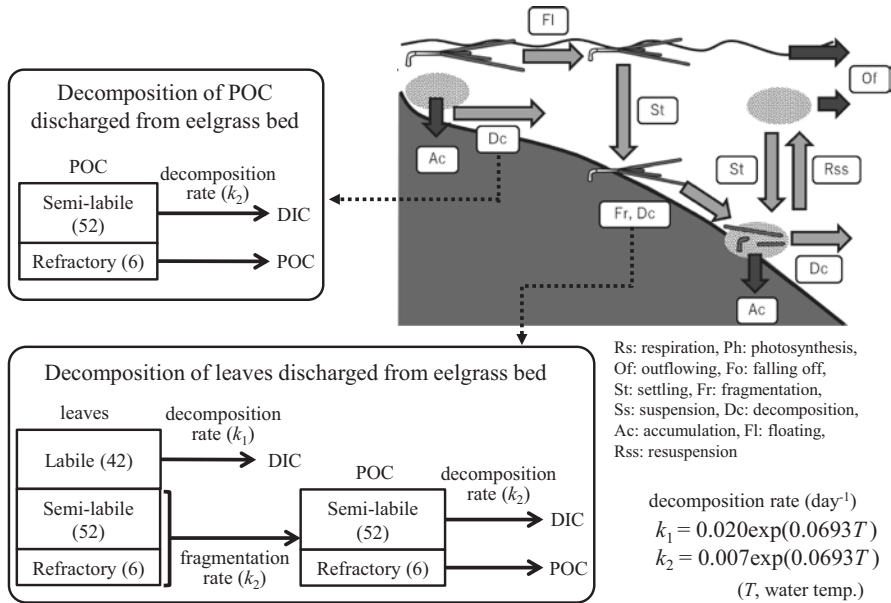
Fig. 9.11 Transport and decomposition processes of leaves and suspended organic matter that flow out of eelgrass beds. The numbers in parentheses are the percentages of total organic carbon

DOC. However, dissolved substances after decomposition include both DIC and DOC; therefore, in the model, DIC was considered to contain DOC as well.

Suspended organic matter that settles on the sea bottom is buried by means of sedimentation. However, if strong flow occurs due to a tidal current or a meteorological disturbance, the organic matter is resuspended into the water column (resuspension). The amount of resuspended matter can be estimated from the bottom shear stress calculated by the ocean flow model. Bottom shear stress is a force applied to the seabed driven by bottom currents, and if this stress is large, the amount of resuspended matter is increased. The suspended particles are decomposed while repeating the resuspension and settling, and those particles that are not decomposed eventually accumulate on the seabed and are buried. As a result, eelgrass-derived organic carbon is stored in the sediment. In addition, some particles are transported, settle, and are stored in the deep sea.

9.5.1.3 Outflow of Drifting Leaves and Particulate Organic Matter

The outflow points and amounts of drifting leaves and eelgrass-derived suspended organic matter are described here. Based on the distribution of eelgrass beds estimated from satellite image analysis (Hori et al. 2012), the outflow points were configured in the dense and sparse eelgrass beds in the computational grids of the model. Each eelgrass bed area was calculated by multiplying the resolution of the

Fig. 9.12 Time series of leaves and particulate organic carbon (POC) that flow out of eelgrass beds (setting value for the model)
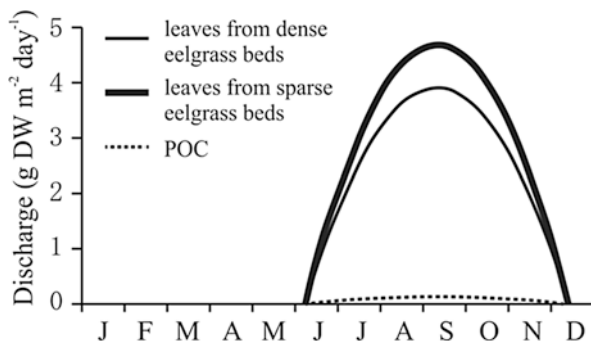
satellite data by the average value of the eelgrass cover ratio (dense eelgrass bed: 93%; sparse eelgrass bed: 47%) (Hori et al. 2012). The amounts of drifting leaves and suspended particles discharged from eelgrass beds were configured based on the results of the field survey (Tarutani et al. 2014), and the outflow was assumed to occur between June and December (Fig. 9.12).

9.5.2 Fate of Eelgrass-Derived Organic Matter That Flowed Out of Eelgrass Beds

The advection, diffusion, decomposition, and sedimentation of drifting leaves and eelgrass-derived suspended organic matter from eelgrass beds were calculated by the model and their fates were traced. The calculation period was from 1 May 2011 to 31 December 2012, a period for which field observation results were available. The purpose of the calculation was to estimate the decomposition and deposition amounts of the discharged eelgrass-derived organic carbon in a 1-year period. Referencing the outflow period of eelgrass (Fig. 9.12), the fate of the leaves and suspended particles discharged from July to December 2011 were traced. For the next year's calculation, from 1 January 2012 until 31 December 2012, the outflow conditions from the 1-year period were not considered.

Fluctuations in the eelgrass-derived organic carbon calculated by the model are shown in Fig. 9.13. The figure shows the time series of the content of each form (drifting leave, suspended particle, DIC, and marine sediment) and the total carbon amount existing in the Seto Inland Sea. The leave carbon content was highest in September 2011, and the total carbon content peaked in November. Thereafter, they decreased because the leaves became suspended particles and DIC due to fragmentation and decomposition and flowed out of the Seto Inland Sea. Then, the leave carbon content almost reached zero in January 2012, and the total carbon content continued to decrease moderately. In contrast, the DIC reached a maximum in January 2012, and organic carbon in the sediments peaked in February, then they
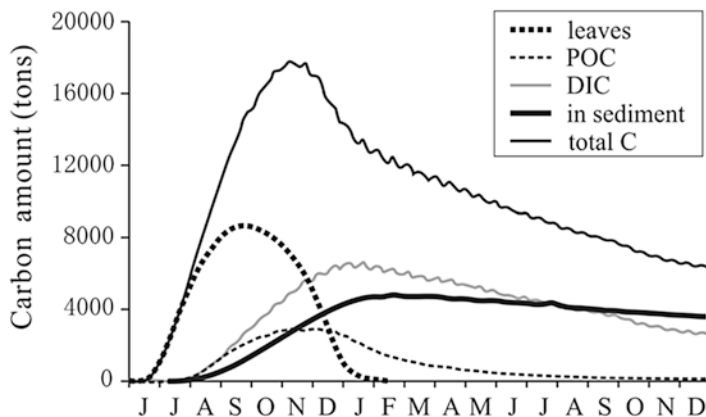
Fig. 9.13 Calculation result of the amount of eelgrass-derived carbon that flowed out of eelgrass beds (time series of each carbon component in the Seto Inland Sea). *POC* particulate organic carbon, *DIC* dissolved organic carbon

continued to moderately decrease until the end of the calculation period as they were resuspended and decomposed or flowed out of the area.

Figure 9.14 shows distributions of the leaves, suspended particles, and organic carbon accumulated in the sediment in September 2011 when the leave biomass was maximum, in February 2012 when the deposition amount was maximum, and at the end of the calculation period in December 2012. On 15 September, the leaves were distributed in most of the area, but particularly large numbers existed in the central part of the Seto Inland Sea. The leaves were assumed to diffuse from the eelgrass beds to the entire Seto Inland Sea. On 30 December, there were no leaves in the area because they settled on the sea bottom and fragmented. At the end of the calculation, the carbon in the sediment was distributed around Aki-nada in the central part of the sea area and in island coves where many eelgrass beds are distributed. In addition, sediment carbon was also distributed in the southern part of Hiuchi-nada and the central part of Aki-nada, where few eelgrass beds existed. These areas have low flow velocity, making resuspension difficult, and they are adjacent to many eelgrass beds. On the other hand, in the strait and other places with fast flow, the carbon content in the sediment was small. The eelgrass gene distribution in the sediment obtained from the field survey (Fisheries Agency of Japan) was qualitatively in good agreement with the carbon distribution in the sediment at the end of the calculation, which validates the results of the modal calculation.

Figure 9.15 shows the mass balance of the eelgrass-derived organic carbon in the Seto Inland Sea at the end of the model calculation. Of the eelgrass-derived organic carbon that flowed out of eelgrass beds, 97.4% was drifting leaves and 2.6% was suspended particles. After 1 year, 67% of the carbon was decomposed into DIC + DOC, and most of it flowed out of the Seto Inland Sea, with only 6.7% remaining in the sea. As for the organic carbon that flowed out of the Seto Inland Sea, 17.1% outflowed as suspended particles and 6.3% as drifting leaves. The
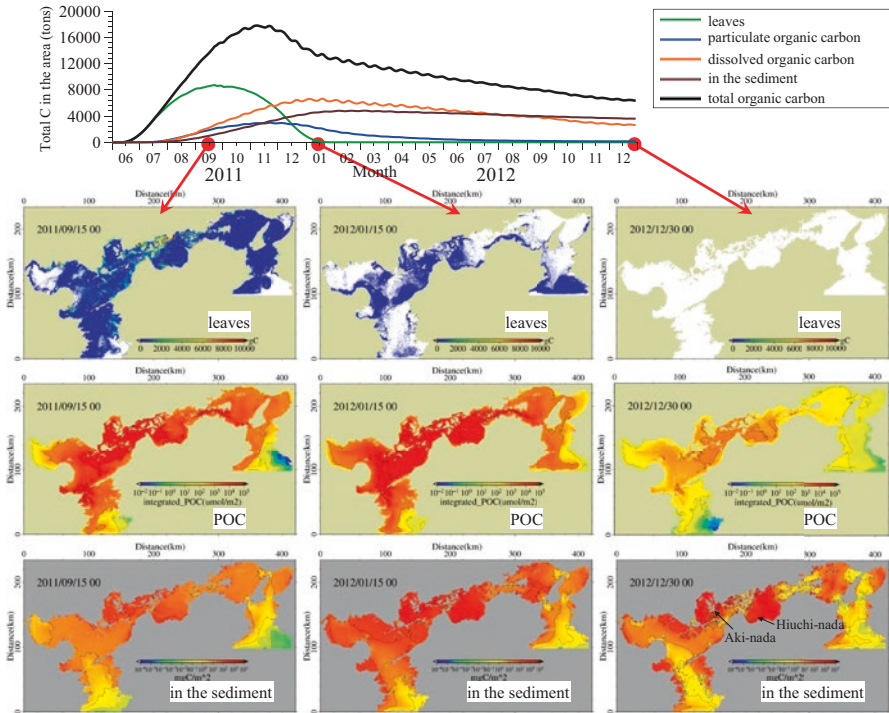
Fig. 9.14 Fate of eelgrass-derived organic carbon that flowed out of the eelgrass bed to the sea area (results of the model simulation). Above: seasonal variations of eelgrass-derived carbon amount in the Seto Inland Sea. Below: (upper) distribution of leaves floating and settling in the sea area; (middle) distribution of particulate organic carbon in sea water; (lower) distribution of organic carbon settled on the sea bottom
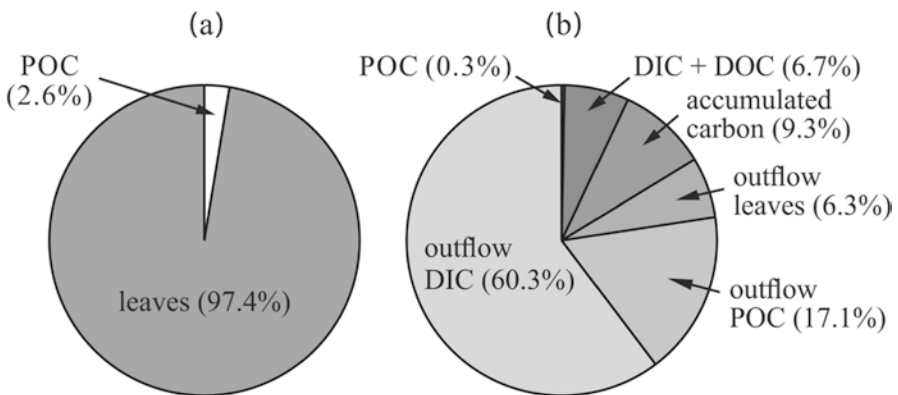
Fig. 9.15 Mass balance of the eelgrass-derived carbon in the entire Seto Inland Sea: (**a**) proportions of the total carbon discharged from the eelgrass bed, and (**b**) proportions of eelgrass-derived carbon at the end of the calculation. POC, particulate organic carbon; DIC, dissolved inorganic carbon; DOC, dissolved organic carbon

organic carbon that remained in the sea was mostly accumulated in the sediment, accounting for 9.3% of the total amount of carbon discharged from the eelgrass beds.

9.6 Carbon Storage Function of Eelgrass Beds in the Seto Inland Sea

To evaluate the carbon sequestration and storage function of eelgrass beds, it is necessary to clarify the amount of eelgrass-derived organic carbon accumulated in eelgrass beds and the amounts that flowed out and accumulated in the shallow coastal waters or deep sea. In Sect. 9.4, we described the growth and decomposition of eelgrass and the deposition and outflow processes of eelgrass-derived organic carbon, and we clarified the amount of carbon accumulated in eelgrass beds. In Sect. 9.5, we traced the fate of drifting leaves and eelgrass-derived suspended particles discharged from eelgrass beds, and we reported the amounts of carbon accumulated in the bottom of the Seto Inland Sea and that flowed out and accumulated in the deep sea.

From these results, we estimated the net primary production (potential carbon sequestration amount) during 2011 and the mass balance (decomposition, sedimentation, and outflow) after 1 year in the eelgrass beds of the Seto Inland Sea (Fig. 9.16). Among the annual net primary production (carbon sequestration) in the eelgrass beds, 37.6% was accumulated in the beds and 35.2% flowed out as drifting leaves or suspended particles. Furthermore, among the eelgrass-derived organic carbon discharged from eelgrass beds, 9.3% was accumulated in sediment in the Seto Inland Sea and 23.4% flowed out of the area to the deep sea. That is, of the 73,000 tons of carbon sequestered annually in the eelgrass beds of the Seto Inland Sea,

Fig. 9.16 Fate of carbon sequestered in eelgrass beds in the Seto Inland Sea. Numerals indicate annual amount of carbon (tons C year^{-1})

about 30,000 tons (40.9%) accumulated on the seabed in the Seto Inland Sea and about 6000 tons (8.3%) flowed out and accumulated in the deep sea.
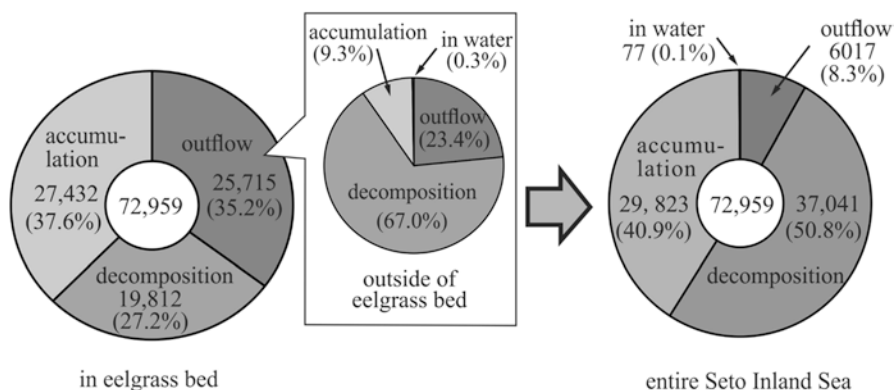
Thus, the total amount of carbon accumulated in the Seto Inland Sea and the deep sea is about 36,000 tons per year. We estimate that this amount accumulates yearly and is stored in the seabed, assuming that no additional mineralization occurs in the sediment after the first year. In other words, the eelgrass beds in the Seto Inland Sea can be regarded as having 36,000 tons of potential carbon storage capacity annually. The eelgrass bed area estimated from the satellite image used in the model was about 19,000 ha, so the carbon storage capacity of the eelgrass beds is about 1.9 tons ha^{-1}. The annual carbon uptake of artificial (reforested and afforested) *Cryptomeria japonica* forests was estimated to be about 2.3 tons ha^{-1} (Forestry Agency of Japan), so the eelgrass beds in the Seto Inland Sea have a potential carbon sequestration and storage capacity comparable to that of cedar plantations. In addition, most of the eelgrass-derived organic carbon was accumulated in the shallow water of the Seto Inland Sea, with only about one-sixth accumulated in the deep sea. Thus far, organic carbon sequestered in shallow coastal waters was not thought to be stored unless it settled in the deep sea, but our case study suggests that much more is stored in shallow coastal waters.

The carbon storage capacity of eelgrass beds described in this chapter was based on a value estimated over 1 year. However, some issues remain to be clarified, such as the storage period of organic carbon in the sediment. Therefore, it is necessary to improve our knowledge of the decomposition process of eelgrass-derived organic carbon accumulated in the sediment when we discuss the carbon storage function at longer time scales of several decades to a century. Moreover, the model calculations introduced here were based on various assumptions, and the reproducibility was not sufficiently verified due to the difficulty of acquiring data in the actual sea area. Thus, future research is needed to improve the accuracy of the estimates reported here.

To date, there were individual models that dealt with seagrass growth, material circulation in seagrass meadows, and tracking drifting leaves. The model presented in this chapter is a combination of these, using seagrass growth models, material circulation models, and drifting leave tracking models. This is the first model to estimate the carbon storage capacity of seagrass meadows by tracking seagrass-derived carbon from the meadows through shallow coastal waters to the deep sea.

References

Aioi K (1980) Seasonal changes in the standing crop of eelgrass (*Zostera marina* L.) in Odawa Bay, central Japan. Aquat Bot 8:343–354

Bach HK (1993) A dynamic model describing the seasonal variations in growth and the distribution of eelgrass (*Zostera marina L.*). I. Model theory. Ecol Model 65:31–50

Bocci M, Coffaro G, Bendoricchio G (1997) Modelling biomass and nutrient dynamics in eelgrass (*Zostera marina* L.): applications to the Lagoon of Venice (Italy) and Øresund (Denmark). Ecol Model 102:67–80

Bostrom C, Mattila J (2005) Effects of isopod grazing: an experimental comparison in temperate (*Idotea balthica*, Baltic Sea, Finland) and subtropical (*Erichsonella attenuata*, Gulf of Mexico, USA) ecosystems. Crustaceana 78:185–200

Dahl M, Deyanova DA, Gutschow S, Gullstrom M (2016) Sediment properties as important predictors of carbon storage in *Zostera marina* meadows: a comparison of four European areas. PLoS One 11:e0167493

Douke I, Itani M, Yoshiya M (2000) Some aspects of eelgrass (*Zostera marina*) communities in Maizuru Bay. I. Monthly variations of density, standing crop and frequency distribution of shoot length. Bull Kyoto Inst Oceanic Fish Sci 22:22–28. (In Japanese with English abstract)

Duarte CM, Krause-Jensen D (2017) Export from seagrass meadows contributes to marine carbon sequestration. Front Mar Sci 4:13

Enriquez S, Duarte CM, Sand-Jensen A (1993) Patterns in decomposition rates among photosynthetic organisms: the importance of detritus C:N:P content. Oecologia 94:457–471

Fisheries Agency of Japan. Mechanism of carbon dioxide sequestration and storage in seagrass beds and tidal flat. http://www.jfa.maff.go.jp/j/koho/pr/pamph/pdf/21-25mobahigatahyouka.pdf (in Japanese)

Forestry Agency of Japan How much carbon dioxide is sequestered by forests? www.rinya.maff.go.jp/j/sin_riyou/ondanka/20141113_topics2_2.html (in Japanese)

Fourqurean JW, Schrlau JE (2003) Changes in nutrient content and stable isotope ratios of C and N during decomposition of seagrass and mangrove leaves along a nutrient availability gradient in Florida Bay, USA. Chem Ecol 19:373–390

Fujiwara M, Yamaga K, Yoshida G, Terawaki T (2006) Long-term changes of eelgrass, *Zostera marina*, by using of artificial seeding behind offshore breakwater. Fish Eng 43:173–177 (In Japanese with English abstract)

Fujiwara M, Yamaga K, Kagawa K, Suenaga Y (2009) Horizonal distribution of seagrass and seasonal change of the *Zostera marina* population off Shodo-shima Island, eastern Seto Inland Sea. Bull Kagawa Prefect Fish Exp Station 10:9–15 (in Japanese)

Hamaguchi M, Yoshida G, Hori M, Tezuka N, Nakagawa N (2012) Field survey for validating carbon circulation model in seagrass bed. "Development of technology for improving carbon sinks and absorption capacity of seaweed bed and tidal flat" Out of the promotion expenses for global warming countermeasures in fiscal year 2011. Fisheries Research Agency, Atmosphere and Ocean Research Institute of the University of Tokyo, Field Science Center for Northern Biosphere, pp 23–41 (in Japanese)

Hemminga M, Duarte CM (2000) Seagrass ecology. Cambridge University Press, Cambridge

Hori M, Yoshida G, Hamaoka H, Miyashita T, Nakaoka M, Watanabe K (2012) Development of simplified area survey method for seagrass bed and tidal flat. "Development of technology for improving carbon sinks and absorption capacity of seaweed bed and tidal flat" Out of the promotion expenses for global warming countermeasures in fiscal year 2011. Fisheries Research Agency, Atmosphere and Ocean Research Institute of the University of Tokyo, Field Science Center for Northern Biosphere, pp 52–67 (in Japanese)

Klap VA, Hemminga MA, Boon JJ (2000) Retention of lignin in seagrasses: angiosperms that returned to the sea. Mar Ecol Prog Ser 194:1–11

Miyajima T, Hamagichi M (2018) Carbon sequestration in sediment as an ecosystem function of seagrass meadows. In: Kuwae T, Hori M (eds) Blue carbon in shallow coastal ecosystems: carbon dynamics, policy, and implementation. Springer, Singapore, pp 33–71

Nakaoka M, Aioi K (2001) Ecology of seagrasses *Zostera* spp. (Zosteraceae) in Japanese waters: a review. Otsuchi Mar Sci 26:7–22

Nakayama A, Yagi H, Fujii Y, Itou Y, Miura H, Yasunobu H, Sugino H, Yamada T (2009) Development of hydrodynamic-primary production coupled model on the whole area of the Seto Inland Sea and its application to the dispersion process of marbled flounder larvae. JJSCE, Ser. B2, Coastal Engineering 65:1126–1130 (in Japanese with English abstract)

Nellemann C, Corcoran E, Duarte CM, Valdés L, De Young C, Fonseca L, Grimsditch G (2009) Blue carbon: a rapid response assessment. United Nations Environment Programme, GRID-Arendal

Opsahl S, Benner R (1993) Decomposition of senescent blades of the seagrass *Halodule wrightii* in a subtropical lagoon. Mar Ecol Prog Ser 94:191–205

Rohr ME, Bostrom C, Canal-Verges P, Holmer M (2016) Blue carbon stocks in Baltic Sea eelgrass (*Zostera marina*) meadows. Biogeosciences 13:6139–6153

Sugimatsu K, Yagi H, Abo K, Tarutani K, Hori M, Yoshida G, Shimabukuro H, Nakayama A (2015) A coupled particle tracking–carbon cycle modeling system for sedimentary organic carbon derived from drifting seagrass in Seto Inland Sea. JJSCE, Ser. B2, Coastal Engineering 71:1-1387–1-1392 (in Japanese with English abstract)

Tarutani K, Abo K, Yagi H, Nakayama A (2011) Development and improvement of carbon cycle model for evaluating carbon absorption in seagrass bed and tidal flat. Project report "Development of technology for improving carbon sinks and absorption capacity of seaweed bed and tidal flat" Out of the promotion expenses for global warming countermeasures in fiscal year 2010. Fisheries Research Agency, Atmosphere and Ocean Research Institute of the University of Tokyo, Field Science Center for Northern Biosphere, pp 8–16 (in Japanese)

Tarutani K, Abo K, Yagi H, Sugimatsu K, Nakayama A (2012) Development and improvement of carbon cycle model for evaluating carbon absorption in seagrass bed and tidal flat. Project report "Development of technology for improving carbon sinks and absorption capacity of seaweed bed and tidal flat" Out of the promotion expenses for global warming countermeasures in fiscal year 2011. Fisheries Research Agency, Atmosphere and Ocean Research Institute of the University of Tokyo, Field Science Center for Northern Biosphere, pp 8–22 (in Japanese)

Tarutani K, Abo K, Yagi H, Sugimatsu K, Nakayama A (2014) Development and improvement of carbon cycle model for evaluating carbon absorption in seagrass bed and tidal flat. Project report "Development of technology for improving carbon sinks and absorption capacity of seaweed bed and tidalflat" Out of the promotion expenses for global warming countermeasures in fiscal year 2013. Fisheries Research Agency, Atmosphere and Ocean Research Institute of the University of Tokyo, Field Science Center for Northern Biosphere of Hokkaido University, pp 51–59 (in Japanese)

Tokoro T, Hosokawa S, Miyoshi E, Tada K, Watanabe K, Montani S, Kayanne H, Kuwae T (2014) Net uptake of atmospheric CO_2 by coastal submerged aquatic vegetation. Glob Chang Biol 20:1873–1884

Tokoro T, Watanabe K, Tada K, Kuwae T (2018) Air–water CO_2 flux in shallow coastal waters: theoretical background, measurement methods, and mechanisms. In: Kuwae T, Hori M (eds) Blue carbon in shallow coastal ecosystems: carbon dynamics, policy, and implementation. Springer, Singapore, pp 153–184

Trevathan-Tackett SM, Macreadie PI, Sanderman J, Baldock J, Howes JM, Ralph PJ (2017) A global assessment of the chemical recalcitrance of seagrass tissues: implications for long-term carbon sequestration. Front Plant Sci 8:925. https://doi.org/10.3389/fpls.2017.00925

Verhagen JHG, Nienhuis PH (1983) A simulation model of production, seasonal changes in biomass and distribution of eelgrass (*Zostera marina*) in Lake Grevelingen. Mar Ecol Prog Ser 10:187–195

Watanabe K, Kuwae T (2015) Radiocarbon isotopic evidence for assimilation of atmospheric CO_2 by the seagrass *Zostera marina*. Biogeosciences 12:6251–6258

Yamada K, Toyohara H (2012) Function of meiobenthos and microorganisms in cellulose breakdown in sediments of wetland with different origins in Hokkaido. Fish Sci 78:699–706

Zupo V, Nelson WG, Gambi MC (2001) Measuring invertebrate grazing on seagrasses and epiphytes. In: Short FT, Short CA, Coles RG (eds) Global seagrass research methods. Elsevier, Amsterdam, pp 271–292

Zharova N, Sfriso A, Voinov A, Pavoni B (2001) A simulation model for the annual fluctuation of *Zostera marina* biomass in the Venice lagoon. Aquat Bot 70:135–150

Chapter 10
Carbon Dynamics in Coral Reefs

Atsushi Watanabe and Takashi Nakamura

Abstract Coral reefs show high organic and inorganic carbon production and create unique landforms on tropical coastlines. The balance between organic and inorganic carbon production is determined by benthic organisms such as corals, macroalgae, and seagrasses, and also by reef hydrodynamics, which in turn determine CO_2 sinks and sources within the ecosystem. Many studies have shown that net organic carbon production in coral reef ecosystems is almost zero (balanced), with net positive calcification resulting in reefs acting as CO_2 sources. However, the relationships among productivity, benthic organisms, and hydrodynamics have not been well documented; more detailed information is required from both field observations and coupled physical–biological models. Reef sediments have low organic carbon content (median, 0.35% dry weight), approximately 50% those of tropical and subtropical seagrass beds (median, 0.67%) and 5% those of mangrove forests (median, 6.3%). Sedimentation rates do not vary significantly between these three ecosystems, so organic carbon input and decomposition in the surface sediments are key factors controlling organic carbon burial rates. Coral reefs provide calm conditions that enhance sedimentation of fine sediments, which facilitates the development of seagrass beds and mangrove forests. Seagrass meadows and mangrove forests in turn trap fine sediments from terrestrial sources and prevent high-turbidity water from reaching coral reefs. Coral reefs, seagrass meadows, and mangrove forests are thus interdependent ecosystems; to effectively store and export blue carbon in tropical coastal areas, it is necessary to maintain the health of these ecosystems.

A. Watanabe (✉)
Department of Transdisciplinary Science and Engineering, School of Environment and Society, Tokyo Institute of Technology, Meguro-ku, Tokyo 152-8550, Japan

Policy Ocean Policy Research Institute, The Sasakawa Peace Foundation, Minato-ku, Tokyo 105-8524, Japan

T. Nakamura
Department of Transdisciplinary Science and Engineering, School of Environment and Society, Tokyo Institute of Technology, Meguro-ku, Tokyo 152-8550, Japan

10.1 Introduction

Coral reefs are not explicitly included as part of the blue-carbon ecosystem, so you might wonder why coral reefs are included as a chapter in this book. In the tropics and subtropics, coral reefs often overlap seagrass beds and mangrove forests (Fig. 10.1) and are therefore strongly linked to blue-carbon ecosystems. Often there is also hydrodynamic connectivity or interaction among these tropical coastal habitats (Guannel et al. 2016).

This chapter briefly explains the general characteristics of coral reefs in terms of carbon-cycle components such as primary production and calcification. The resultant CO_2 sinks and sources, and carbon storage and export in coral reefs are then
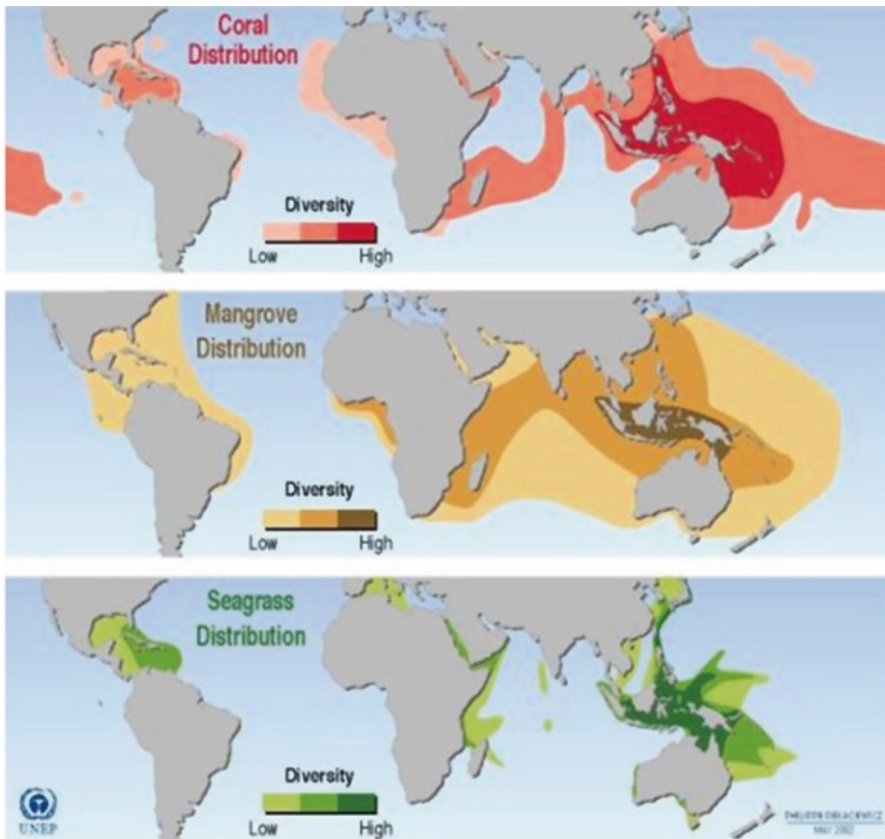
Source : UNEP-WCMC, 2001.

Fig. 10.1 World distribution of coral reefs, mangrove forests, and seagrass beds. The areas with high diversity for each ecosystem overlap, especially around Indonesia, Malaysia, Papua New Guinea, and the Philippines. (Source: https://www.grida.no/resources/7766 (credit: Hugo Ahlenius))

addressed. Finally the relationships between coral reefs and other ecosystems, especially with seagrass beds and mangrove forests, are discussed to highlight the necessity of regarding these connected ecosystems together as a blue-carbon ecosystem.

10.2 Carbon Cycling, Storage, and Export in Coral Reefs

10.2.1 Basic Carbonate-Chemistry Changes Due to Calcification and Primary Production

We first briefly explain the basics of carbonate chemistry alterations due to calcification and photosynthesis to provide the background necessary to understand this chapter. For further reading, please refer to Gattuso et al. (1999) or Zeebe and Wolf-Gladrow (2001).

The calcification reaction, which releases CO_2, is commonly expressed by the following equation:

$$Ca^{2+} + 2HCO_3^- \rightarrow CaCO_3 + H_2O + CO_2 - \qquad (10.1)$$

The reverse of Eq. (10.1) is the reaction for the dissolution of $CaCO_3$.

Photosynthesis fixes CO_2 and is expressed by the following equation:

$$CO_2 + H_2O \rightarrow CH_2O + O_2 \qquad (10.2)$$

The reverse of Eq. (10.2) is the reaction for aerobic respiration and decomposition.

There is a so-called "0.6 rule" for seawater, where about 0.6 moles of CO_2 is liberated (not the expected 1 mole) when 1 mole of $CaCO_3$ is produced by Eq. (10.1) (Ware et al. 1991; Frankignoulle et al. 1994). In contrast, 1 mole of CO_2 is fixed when 1 mole of organic C (CH_2O) is produced by Eq. (10.2). Therefore, when the rate of photosynthesis is greater (less) than 60% of the calcification rate, CO_2 is fixed (liberated) and the system acts as a sink (source) of CO_2. The value 0.6 in the 0.6 rule is due to the buffering capacity of seawater, and it changes with ocean acidification (the trend of increasing CO_2 in seawater). This value, termed Ψ (Frankignoulle et al. 1994), is 0.6 when pCO_2 (partial pressure of CO_2) in seawater is 350 µatm, salinity is 35, and water temperature is 25 °C, but it rapidly increases to 0.78 when pCO_2 reaches 1000 µatm under the same conditions. Ψ also changes with temperature (see Fig. 10.2). At constant pCO_2, Ψ decreases as water temperature increases. For example, seawater at higher latitudes generally has higher Ψ values and lower buffering capacity.
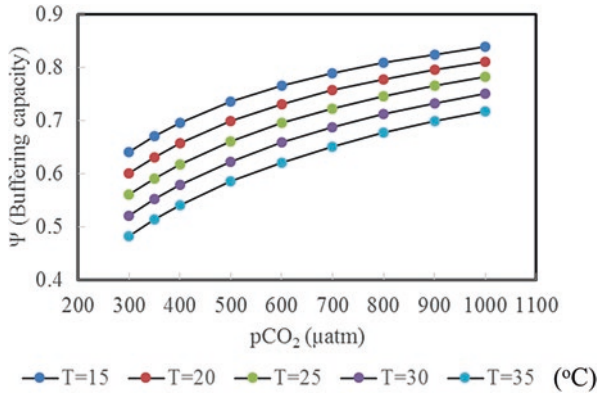
Fig. 10.2 Buffering capacity of seawater as a function of pCO_2 at varying water temperatures (salinity = 35 and the total alkalinity = 2300 μmol kg^{-1})
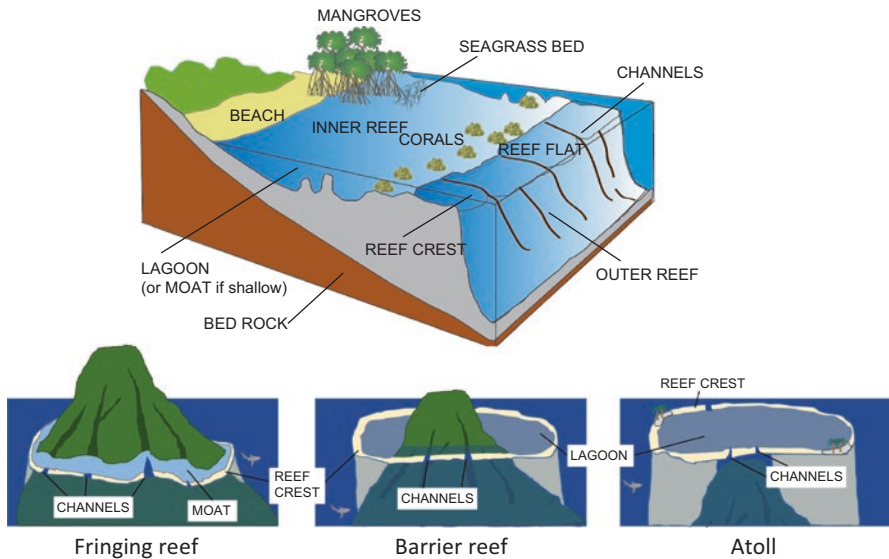
Fig. 10.3 General reef geomorphology and types (fringing reef, barrier reef, and atoll)

10.2.2 Calcification and Primary Production in Coral Reefs

One conspicuous characteristic of coral reefs is the huge production of $CaCO_3$ by which tiny corals build the world's largest living structures, such as the Great Barrier Reef in Australia, which is visible from space. Coral reef environments can be roughly divided into three parts: reef flat with reef crest, inner reef, and outer reef (upper panel in Fig. 10.3). The reef flat with reef crest is the shallowest part of a coral reef and is covered with either corals or macroalgae. Incoming wave energy is

effectively dissipated at the reef crest or reef flat. The inner reef is therefore calmer compared to the outer reef, and often has a lagoon (or "moat" when it is shallow [typically shallower than 5 m]), which can harbor corals, seagrasses, and mangroves. The outer reef is a high-energy environment and often covered with corals or coralline algae that are resistant to the high wave energy.

There are three major types of coral reefs: fringing reefs, barrier reefs, and atolls (lower panel in Fig. 10.3). A fringing reef develops right beside an island, whereas a barrier reef has a relatively deep lagoon between an island and the reef flat. Atolls are rings of reefs without a central island; sometimes the reef itself becomes exposed to air and forms a low-lying island.

The coral/algal reef flats display a wide range of calcification rates (5–126 mol $CaCO_3$ m^{-2} year^{-1} or 0.5–12.6 kg $CaCO_3$ m^{-2} year^{-1}; Gattuso et al. 1998). The value gets progressively higher as the water depths decrease over the reef flat zone (shallowest part of coral reefs) independent of domination by corals or coralline algae (Sorokin 1993). On average, the shallow seaward reef flat zone produces 40 moles (or 4 kg) of $CaCO_3$ m^{-2} year^{-1}. Considering the "0.6 rule" explained in Sect. 10.2.1, net primary production on the "average reef" would have to exceed 24 moles (or 288 g) C m^{-2} year^{-1} to act as a CO_2 sink. Gross primary production (GPP) on reef flats is quite high, varying from 79 to 584 moles (or 948–7008 g) C m^{-2} year^{-1} (Gattuso et al. 1998), but community respiration is also high and net primary production is thought to be close to zero. In this case, calcification overwhelms the net primary production on the reef flat, and the reef flat is believed to act as a source of CO_2.

10.2.3 CO_2 Sinks and Sources in Coral Reefs

The debate on whether coral reefs act as a sink or source of atmospheric CO_2 began in the 1990s. Gattuso's group (Gattuso et al. 1993, 1996b; Frankignoulle et al. 1996) reported that most coral reef flats are sources of CO_2 to the atmosphere. Their study sites were the Tiahura barrier reef (Moorea, French Polynesia) and Yonge Reef (northern Great Barrier Reef). Both sites are classified as barrier reef flats. Gattuso et al. (1996b) reported that the Tiahura reef supported abundant corals on the seaward side and abundant macroalgae on the back reef area, whereas the Yonge Reef flat was mainly dominated by a single community characterized by the coral species *Acropora palifera*. In contrast, Kayanne's group (Kayanne et al. 1995) reported that coral reef flats act as sinks for atmospheric CO_2. Their study site was the Shiraho reef (Ishigaki Island, Japan), which is a fringing reef flat. The dominant coral species around the monitoring site were *Montipora digitate*, *Porites cylindrica*, and *Heliopora coerulea* (Kayanne et al. 2002), and algal turf and brown algae were on the offshore side of the reef crest (Kayanne et al. 1995). Since Kayanne et al. (1995) indicated that coral reef flats are a net sink for atmospheric CO_2, there have been many comments and papers published regarding the CO_2 sink–source issue (Buddemeier 1996; Gattuso et al. 1996a, 1997; Kayanne 1996; Kraines et al. 1997; Ohde and van Woesik 1999; Bates et al. 2001; Bates 2002; Kayanne et al. 2005),

and the debate has been reviewed extensively (Gattuso et al. 1999; Suzuki and Kawahata 2004). Here we summarize the points of the debate and list some of the more recent literature published after those reviews.

Table 10.1 summarizes the CO_2 sinks and sources in coral reefs, separately listing reef flats and lagoons. Positive CO_2 flux values indicate sources and negative values indicate sinks. Although the values vary widely, the majority of reef flats studied acted as sources of CO_2, with a median CO_2 flux value of 2.2 mmol m^{-2} day^{-1}. The majority of relatively deep lagoons also act as sources of CO_2 with a median value of 0.7 mmol m^{-2} day^{-1}. These values are relatively small and comparable to the CO_2 flux for open ocean in most of the subtropical and tropical areas where coral reefs exist, which typically exhibit fluxes of -1 to 1 mol m^{-2} year^{-1} (or -2.7 to 2.7 mmol m^{-2} day^{-1}, Takahashi et al. 2009). Some reefs absorb CO_2 from the atmosphere, but many researchers insist that the reef flats absorbing CO_2 are mainly fringing reefs (see Fig. 10.3 and Sect. 10.2.2). The hypothesis is that fringing reefs receive substantial amounts of nutrients from adjacent lands, conditions more favorable for the growth of seagrasses or macroalgae than corals. With the reef area covered by these autotrophs, net primary production exceeds calcification and the system overall absorbs CO_2. Gattuso et al. (1997) tested this hypothesis by measuring community metabolism and air–sea CO_2 fluxes on a fringing reef at Moorea. The results showed that this reef flat was a sink for CO_2 up to 10 mmol m^{-2} day^{-1}, whereas the neighboring barrier reef flat was a CO_2 source (Gattuso et al. 1993, 1996b; Frankignoulle et al. 1996). These contrasting results from the fringing reef and the barrier reef of Moorea led to the concept that "algal" reefs absorb CO_2 whereas "coral" reefs emit CO_2 to the atmosphere.

More recently, different views have been offered regarding the air–sea CO_2 flux in coral reefs resulting from long-term or continuous monitoring at the same sites. For example, Kayanne et al. (2005) showed that the Shiraho fringing reef became a source of atmospheric CO_2 following coral bleaching[1] in 1998, although the reef was a CO_2 sink during other non-bleached periods. Massaro et al. (2012) presented continuous CO_2 data covering 2.5 years in southern Kaneohe Bay, Hawaii, a semi-enclosed tropical coral reef ecosystem. They showed that local climatic forcing strongly affected the biogeochemistry, water-column properties, and air–sea CO_2 gas exchange. Large drawdowns of CO_2 following storms occasionally caused the bay waters to switch from a CO_2 source to a sink. These results indicate that even the same reef can dynamically shift from sink to source depending on reef conditions (e.g. coral and macroalgal coverage) as well as on external forcing (e.g. storms and subsequent supply of nutrients). These kinds of dynamic features can be more important than the static sink–source views of coral reefs under rapidly changing reef conditions due to global climate change and local environmental changes.

---

[1] Coral bleaching: Corals have symbiotic algae called zooxanthellae inside their tissue. When corals are stressed from high water temperature or other causes, they release or digest their zooxanthellae and lose their color, making the white coral skeleton visible. This phenomenon is called coral bleaching.

Table 10.1 Summary of air–sea CO_2 flux data for coral reefs

Country (region)	Air–sea CO_2 flux (mmol CO_2 m^{-2} day^{-1})	Reference	Year
Reef flats (including moat or shallow lagoon)			
Barrier reef in Moorea, French Polynesia	1.5	Gattuso et al.	1993
Barrier reef in Moorea, French Polynesia	1.8	Frankignoulle et al.	1996
Yonge Reef, N. GBR[a], Australia	5.1	Frankignoulle et al.	1996
Barrier reef in Moorea, French Polynesia	31.0	Gattuso et al.	1996b
Yonge Reef, N. GBR, Australia	182.0	Gattuso et al.	1996b
Fringing reef in Moorea, French Polynesia	−10	Gattuso et al.	1997
Rukan-sho atoll, Okinawa, Japan	Neutral	Ohde & Van Woesik	1999
Hog Reef Flat, Bermuda	3.3	Bates et al.	2001
Xisha Islands, China	1.5	Dai et al.	2009
Nanwan, South China Sea, Taiwan	−0.56	Jiang et al.	2011
Yongxing Island, South China Sea	4.7	Yan et al.	2011
Luhuitou Reef, Hainan Island, China	9.8	Yan et al.	2011
Shiraho Reef, Ishigaki, Japan	0.0	Watanabe et al.	2013
Shiraho Reef, Ishigaki, Japan	−1.9	Watanabe et al.	2013
Heron Reef, southern GBR, Australia	2.5	Cyronak et al.	2014
Rarotonga, fringing reef in South Pacific	8.8	Cyronak et al.	2014
Coroa Vermelha, Brazil	0.3	Longhini et al.	2015
Heron Reef, southern GBR, Australia	172.8	McGowan	2016
Luhuitou Reef, Hainan Island, China	1.5	Yan et al.	2016
Median	**2.2**		
Lagoons (moderate to deep lagoons) or open ocean surrounding reefs			
Fanning Island	46.7	Smith & Pesret	1974
Christmas Island, Kiribati	−2.6	Smith et al.	1984
Rim and terrace reefs, Bermuda	−0.03	Bates	2002
Palau	1	Watanabe et al.	2006
Kaneohe Bay, Hawaii, USA	3.97	Fagan & Mackenzie	2007
Yongshu Reef atoll, Yongxiang Island reef flat, and Luhuitiou Fringing reef, South China Sea	0.4	Yan et al.	2011
Southern Kaneohe Bay, Hawaii, USA	4.93	Massaro et al.	2012
Kaneohe Bay, Hawaii, USA	4.0	Drupp et al.	2013
Mamala Bays, Hawaii, USA	0.06	Drupp et al.	2013
Lady Elliot Island, southern GBR, Australia	−1.82	Shaw & McNeil	2014
Median	**0.70**		

Positive values indicate a net CO_2 flux from the reef to the atmosphere

[a]Great Barrier Reef

More studies are needed for the mechanistic understanding of CO_2 dynamics in coral reefs. It is recommended that future works incorporate following points.

1. Measurements should include reef metabolisms (ecosystem primary production, respiration, calcification, and carbonate dissolution) and organic-matter flux along with air–sea CO_2 fluxes.
2. The benthic condition of reef areas of interest should be quantitatively monitored. The biomass balance between corals, macroalgae, and seagrasses can be especially important.
3. Monitoring should include terrestrial loads such as submarine ground water or river water inputs to the reefs, their chemistry (e.g. nutrients and carbonate chemistry), and their advection in the reef, together with hydrodynamic features of the reefs (e.g. residence time of seawater).
4. The reef as a CO_2 sink or source should be addressed by comparison with the CO_2 in the open ocean impinging on reefs, and not necessarily directly with atmospheric CO_2. The reason is simple: the open ocean is not necessarily in equilibrium with atmospheric CO_2, and the capacity of a coral reef as a CO_2 sink or source should be discussed relative to CO_2 levels in the source water (mainly open ocean seawater in many cases). This would require adequate monitoring of conditions offshore of the reefs as well.

Achieving these points will require a combination of hydrodynamic–biogeochemical modeling as well as the appropriate fieldwork to properly constrain the models. These topics are discussed in more detail in Sect. 10.4.

10.2.4 Carbon Storage in Coral Reefs

Coral reef sediments are known to contain small amounts of organic carbon (OC). Table 10.2 compiles data for the OC content of reef sediment. For example, Sorokin (1993) reviewed OC contents in reef bottom sediments and reported values ranging from 0.09% to 0.6% (% dry weight). The OC in reef sediments rarely exceeds 1%, and the mean and median values from previous studies are 0.46% and 0.35%, respectively. The low OC content of reef sands is thought to reflect background OC

Table 10.2 Summary of organic carbon content, burial rate, and sedimentation rate in reef, seagrass, and mangrove sediments

Ecosystem	Organic carbon content (% dry weight)			Organic carbon burial rate (g cm^{-2} year^{-1})			Sedimentation rate (g cm^{-2} year^{-1})		
	Mean	Median	n	Mean	Median	n	Mean	Median	n
Coral reefs	0.46	0.35	11	11.04	12.82	4	0.26	0.26	4
Seagrass meadows	0.73	0.67	6	65.76	83.00	3	0.12		1
Mangrove forests	8.7	6.3	14	149.98	139.00	9	0.28		2

contained in carbonates mainly originating from corals, foraminifera, and calcareous algae, which typically have values less than 0.2% to 0.4% (Miyajima et al. 1998).

Table 10.2 also summarizes the OC content of seagrass bed and mangrove forest sediments. Please also refer to Chaps. 2 and 3 for discussions of OC in seagrass beds (Miyajima and Hamaguchi 2018) and mangrove sediments (Inoue 2018), respectively. OC in seagrass sediments shows large variability, ranging from 0.1% to 11% (Kennedy et al. 2010). Most tropical and subtropical seagrass beds have a relatively low OC content of 0.6% or 0.7%; the median of the values surveyed here is 0.67%, which is about twice that of coral reef sediments (0.35%). Coral reef sands vegetated by seagrasses have OC contents 2–5 times those of unvegetated reef sands, possibly from the accumulation of detrital OC in seagrass beds (Miyajima et al. 2015). OC in mangrove sediments also shows large variability, ranging from 0.6% to 36% (Bouillon et al. 2003; Breithaupt et al. 2012). The median of values surveyed here is 6.3%, which is close to the median mangrove sediment OC content of 7.0% reported by Breithaupt et al. (2012) and about 18 times the OC content of reef sediments.

The differences between OC concentrations in coral reef, seagrass meadow, and mangrove sediments can be explained in terms of the supply and preservation of organic carbon in each ecosystem. The sedimentation rates compiled from previous studies are not very different across these ecosystems (Table 10.2): 0.26 g cm^{-2} year^{-1} for coral reefs, 0.12 g cm^{-2} year^{-1} for seagrass beds (although only limited data are reported), and 0.28 g cm^{-2} year^{-1} for mangrove forests. The OC burial rates, however, are much higher in mangroves and in seagrass beds than in coral reefs; the median values are 12.8 gC m^{-2} year^{-1} for coral reefs, 83.0 gC m^{-2} year^{-1} for seagrass beds, and 139 gC m^{-2} year^{-1} for mangrove forests. This difference results not only from the supply of organic matter, but also from the differences in decomposition and preservation of organic matter in the sediments. In coral reef sediments, the top several centimeters of sediments are usually supplied with oxygen (Werner et al. 2006; Yamamoto et al. 2015) mainly through pore-water advection due to highly permeable sediments with relatively large grain size (Werner et al. 2006). This oxygen supply can facilitate carbon mineralization in the surface sediments (Miyajima and Hamaguchi 2018). This mechanism can help maintain low OC content in reef sediments when the supply of organic matter is not too high.

10.2.5 Carbon Export from Coral Reefs

Coral reefs can export organic matter from primary production, either to their internal sediments or to the open ocean. As explained in Sect. 10.2.2, coral reefs have high GPP as well as respiration, but many reef flats are slightly autotrophic and show positive net primary production (NPP) (for example Gattuso et al. 1993, 1996b; Kayanne et al. 1995, 2005; Ohde and van Woesik 1999; Hata et al. 2002). Positive NPP means that OC can be either stored within the ecosystem or exported to adjacent systems such as the open ocean. Note that the pCO$_2$ decrease due to NPP

can often be offset by net calcification in coral reefs, which increases pCO_2. Corals release the excess primary production as mucus, either as dissolved organic carbon (DOC) or particulate organic carbon (POC) (Wild et al. 2004; Tanaka et al. 2008). According to Wild et al. (2004), much of the mucus released into seawater efficiently traps organic matter from the water column, which is rapidly carried to the lagoon sediment and filtered through the lagoon sands. Mucus transports energy to the lagoon sediments and then the sediments rapidly recycle the organic matter to nutrients, thus serving as a mechanism for retaining energy and nutrients within the reef ecosystem.

Some portion of the excess production can be transported offshore of the reef. Delesalle et al. (1998) studied the organic carbon and carbonate export for Tiahura reef, French Polynesia, and reported an offshore transport of about 47% and 21% of the excess organic and inorganic carbon production, respectively. Hata et al. (1998) studied the organic carbon flux around a barrier reef in Palau in the western Pacific. They estimated that 7% of carbon from GPP on the reef flat is deposited in the lagoon, 4% is exported to the open ocean, and 0.6% is transferred below the thermocline (150-m depth) of the inshore open ocean (Fig. 10.4). Hata et al. (2002) simultaneously studied organic carbon fluxes and community production rates on the Shiraho coral reef for a week. They found that 6–7% of GPP and a majority of NPP (almost 100%) were exported offshore as POC and DOC, and about 14–20% of the POC and 0.2% of GPP exported from the reef flat reached 1 km offshore and 40-m depth.
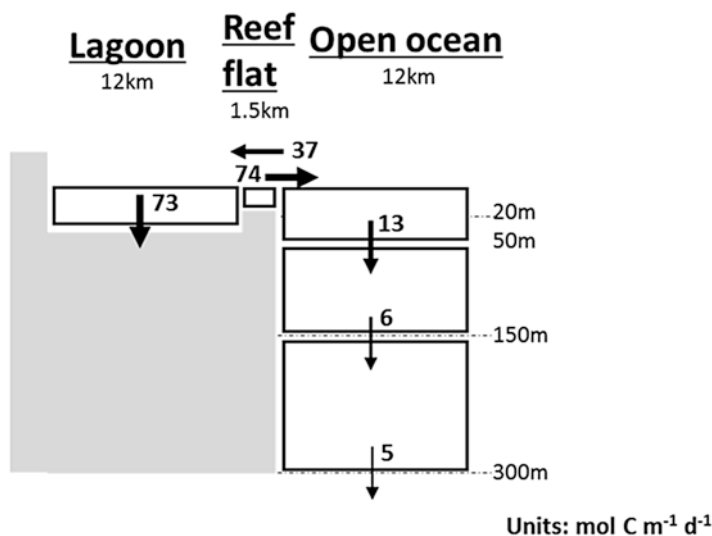
Fig. 10.4 Organic carbon flux around a coral reef (based on Hata et al. 1998). The organic carbon flux from the reef flat to the open ocean is estimated at 74 mol C m^{-1} day^{-1}, which is about 7% of the gross primary production (GPP) of the reef. The net export of organic carbon from the reef flat is 37 mol C m^{-1} day^{-1}, which is about 4% of the GPP, and about 6 mol C m^{-1} day^{-1} is carried to a depth of 150 m (below the thermocline) in the inshore open ocean, which is about 0.6% of the GPP

Carbon export studies from coral reefs are obviously limited and need a more integrated approach in the future. First, the carbon fluxes should be studied together with in-reef productivity measurements to understand their interrelationships. Seasonal variations as well as tidal effects on the carbon export should also be examined; a higher carbon flux can be anticipated during spring tide compared to neap tide. Characterization of the organic matter will also be required. The C/N ratios of the organic particles captured in sediment traps have been reported (Delesalle et al. 1998; Hata et al. 1998, 2002), but it will be necessary to know the fatty acid composition or isotopic signatures of the particles to determine the origins of the organic matter (Hata et al. 2002).

10.3   Relationships Between Coral Reefs and Other Tropical and Subtropical Coastal Ecosystems

As noted in the Introduction, the distribution of coral reefs overlaps with those of mangroves and tropical/subtropical seagrasses (Fig. 10.1), and we can expect close linkages among these ecosystems. Mangroves and seagrass beds interrupt freshwater discharge, are sinks for organic and inorganic materials as well as pollutants, and can generate an environment with clear, nutrient poor water that promotes the growth of coral reefs offshore (Fig. 10.5 and references such as Moberg and Folke 1999; Hemminga and Duarte 2000; Duke and Wolanski 2001; Unsworth and Cullen
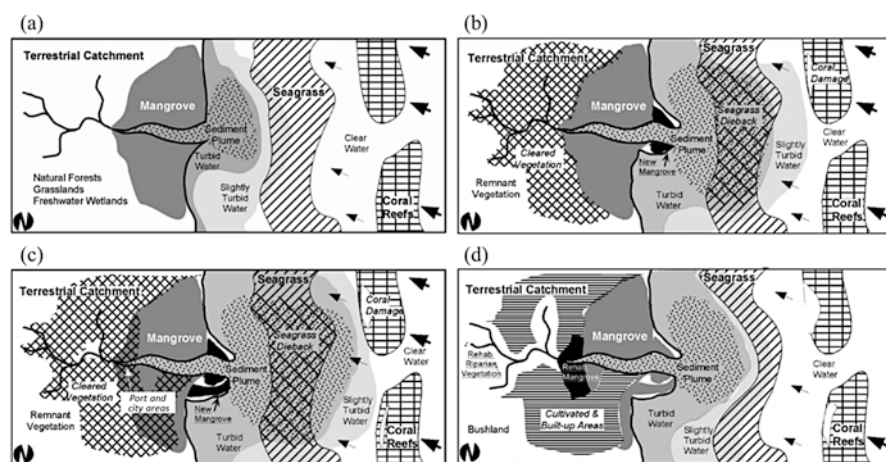
Fig. 10.5 Conceptual illustration showing the turbid waters and sediment plume from (**a**) an undisturbed terrestrial catchment, (**b**) a disturbed terrestrial catchment for a rural area only, (**c**) a terrestrial catchment including rural, port, and city areas disturbed by clearing mangrove vegetation, and (**d**) a catchment in a port and city area rehabilitated from the conditions in (**c**) with mangroves and riparian vegetation. Arrows indicate prevailing wave direction and relative strength. Figures are after Duke and Wolanski (2001) with slight modifications

2010). Coral reefs in turn dissipate wave energy and create favorable conditions for the growth of seagrasses and mangrove ecosystems (Birkeland 1985; Ogden 1988). Here we briefly summarize the physical and biogeochemical relationships between coral reefs and associated landscapes such as seagrass meadows and mangrove forests. We also explain the shift of reef flats from coral communities to macroalgal communities ("phase shift") and the implications of this shift to changes in biogeochemical cycles.

10.3.1   Relationship Between Coral Reefs and Seagrass Beds

Lamb et al. (2017) showed recently that when seagrass meadows are present in a reef ecosystem there is a 50% reduction in the relative abundance of pathogens potentially capable of causing diseases in humans and marine organisms. Their field surveys showed that disease levels in more than 8000 reef-building corals located adjacent to seagrass meadows were lower by a factor of two compared to corals at sites without adjacent seagrass meadows.

Biogeochemical interactions between seagrasses and corals have recently been proposed. Unsworth et al. (2012) found that 83% of seagrass meadows in the Indo-Pacific have a positive NPP and can increase seawater pH, which could buffer coral reef calcification against future ocean acidification. Future laboratory and field work should quantify the buffering capacity of seagrass relative to ocean acidification.

Coral reefs in turn serve as physical buffers against oceanic currents and waves, creating a suitable environment for seagrass beds over geologic time (Moberg and Folke 1999). However, as Saunders et al. (2014) suggested, this shelter effect can be threatened by increases of water depth in the lagoon (or moat) from sea-level rise. They indicate that the rates of carbonate accretion typical of modern reef flats (up to 3 mm year^{-1}) will not be sufficient to maintain suitable conditions for reef seagrasses in the future. These climate change (i.e. ocean acidification and sea-level rise) impacts on connected coral reef–seagrass landscapes should be considered when planning conservation efforts.

10.3.2   Relationships Between Coral Reefs and Mangrove Forests

Mangrove forests act as natural filters to trap fine sediments and improve water clarity (Fig. 10.5; Duke and Wolanski 2001). Mangrove forests typically occur in turbid waters where the turbidity mainly comes from a terrestrial catchment. When the catchment still has natural forests, grasslands, or freshwater wetlands, mangroves can filter the turbid water, and any remaining slightly turbid water does not reach

that far into the coastal areas, permitting the co-existence of offshore seagrass meadows and coral reefs (Fig. 10.5a). If a river catchment includes disturbances in rural areas from clearing vegetation for grazing and agriculture, the turbid waters and sediment plume can extend far offshore, resulting in seagrass dieback (Fig. 10.5b). Mangroves can be largely unaffected by these disturbances, or even become established on new depositional banks, achieving a net gain in areal extent. In cases where even the mangrove forests are cleared, slightly turbid water can extend farther toward reef areas (Fig. 10.5c). Seagrass dieback occurs in turbid waters and coral damage in slightly turbid water. In the Great Barrier Reef, there has been a shift from pristine conditions (Fig. 10.5a) to disturbed conditions (Fig. 10.5b, c) within the last 200 years, since European settlement. Rehabilitation of upstream ecosystems is considered the only way of restoring downstream marine ecosystems (Fig. 10.5d). The maintenance of healthy mangrove forests can therefore be seen as a prerequisite for keeping coral reefs (and seagrass meadows) productive, and thus they should be rehabilitated or conserved together as a connected seascape.

   Mangrove forests can enhance the biomass of coral reef fishes. Mumby et al. (2004) showed that mangroves in the Caribbean strongly influence the community structure of fish on neighboring coral reefs, and the biomass of some commercially important fish is more than doubled when the adult fish habitat is connected to mangroves. More recently, Serafy et al. (2015) pointed out that at a regional scale in the Caribbean, a greater expanse of mangrove forest generally functions to increase the densities on neighboring reefs of those fishes that use these shallow, vegetated habitats as nurseries.

10.3.3   Relationships Between Corals and Macroalgal Communities: Phase Shift

Several reefs around the world have been degraded and shifted from a coral-dominated phase to a macroalgae-dominated phase. This phase shift has been reported in Caribbean reefs and was attributed to increased nutrient loading as a result of changed land-use and intensive fishing, which reduced the numbers of herbivorous fish species (Scheffer et al. 2001).

   The phase shift toward macroalgae could influence the carbon cycle in the reefs. For example, Haas et al. (2013) found that macroalgae released more DOC than hermatypic corals, but the exudates from macroalgae and corals had different impacts on neighboring ecosystems. Coral exudates increased the net planktonic microbial community production and enhanced autotrophic benthic microbial community production, thus shifting toward a net autotrophic system. In contrast, macroalgal exudates stimulated heterotrophic organic carbon consumption rates by the planktonic and benthic microbial community, thus there was an overall shift toward a microbial community metabolism that was substantially more heterotrophic.

10.4   Directions for Future Study of Blue–Carbon Dynamics in Coral Reefs and Connected Ecosystems

Modeling can be a strong approach to understanding blue-carbon dynamics in coral reefs under both current and future conditions. Considering the large spatiotemporal variability of carbon dynamics caused by the heterogeneous distribution of benthic organisms and the resultant biogeochemical cycles in coral reefs, it is difficult to accurately represent blue-carbon dynamics solely from field data. Recently biogeochemical models have been coupled with hydrodynamic models for coral reefs (Zhang et al. 2011; Falter et al. 2013; Watanabe et al. 2013; Nakamura et al. 2017). For example, Watanabe et al. (2013) developed a carbonate-system dynamics model driven by coral and seagrass photosynthesis and calcification, and described the air–sea CO_2 fluxes under various hydrodynamic and benthic conditions. They clarified that the status of the fringing reef studied as a CO_2 sink or source was greatly influenced by neap and spring tides (Fig. 10.6). During neap tide, the tidal exchange becomes sluggish and the seawater residence time inside the reef increases, which allows the effects of reef metabolism to remain more within the reef.

The model by Watanabe et al. (2013) did not consider the feedback from water quality to coral metabolism, so Nakamura et al. (2017) further refined the model by
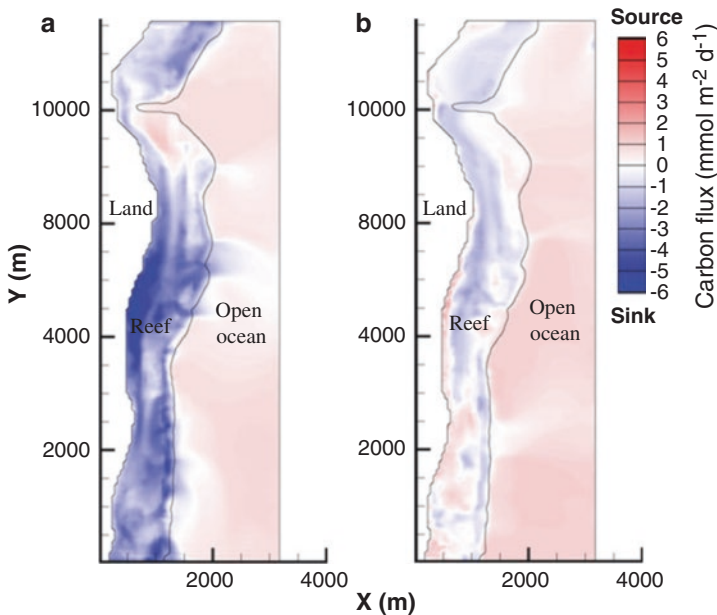

Fig. 10.6 Spatial distribution of CO_2 sinks and sources around a coral reef at Ishigaki Island, Japan during (**a**) neap tide and (**b**) spring tide, simulated using a carbonate-system dynamics model coupled with a three-dimensional hydrodynamics model (Watanabe et al. 2013). (Source: Watanabe et al. 2013 with slight modifications)
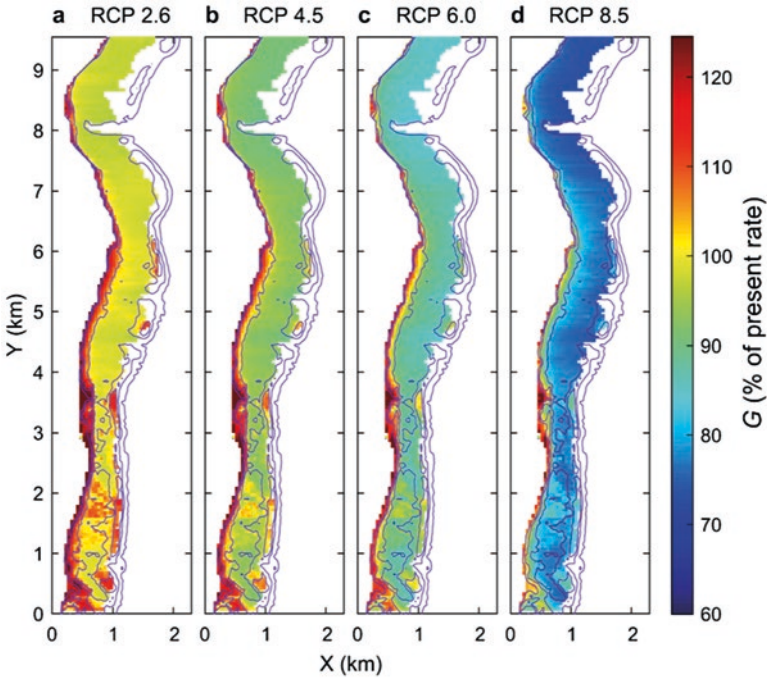
Fig. 10.7 Spatial distribution of coral polyp calcification rates (G, %) of inner-reef corals relative to the present rate under various future Intergovernmental Panel on Climate Change (IPCC) climate-change scenarios for the year 2100 around a coral reef at Ishigaki Island, Japan (Nakamura et al. 2017). (**a**) CO_2 421 ppm and sea level rise (SLR) 0.4 m (IPCC representative concentration pathway [RCP] 2.6); (**b**) CO_2 538 ppm, SLR 0.47 m (RCP 4.5); (**c**) CO_2 670 ppm, SLR 0.48 m (RCP 6.0); (**d**) CO_2 936 ppm, SLR 0.63 m (RCP 8.5). (Source: Nakamura et al. 2017)

incorporating these feedback interactions so that, for example, the modeled coral could respond to ocean acidification (OA). They also incorporated the effects of seawater flow over the reef on mass transfer in the model. Higher bottom velocity and hence higher bottom shear stress induces higher mass transfer velocity, which in turn enhances diffusive material exchange between corals and ambient seawater. Using their model, they examined coral calcification of inner reef corals under present conditions and under various future OA and sea-level-rise (SLR) scenarios in the year 2100 (Fig. 10.7). In general, calcification rates decreased as a result of OA, but increased in some nearshore reef flat areas because of enhanced mass exchange due to SLR. The more efficient water exchange due to SLR supplies more dissolved oxygen to corals and enhances respiration, which increases ATP synthesis and therefore increases calcification rates in the model.

Many things need to be improved or added for such ecosystem models to be applied to the analysis of blue-carbon dynamics (Fig. 10.8). First, it will be necessary to properly model organic matter production and decomposition. This is critically important to understanding whether the carbon produced within the blue-carbon
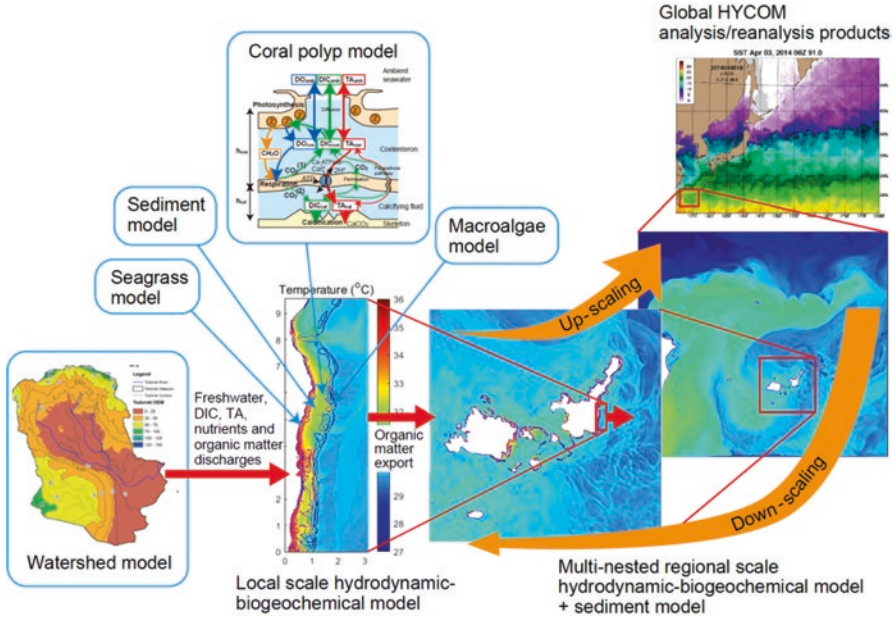
Fig. 10.8 Integrated model for describing blue-carbon dynamics at local and regional scales around a coral reef at Ishigaki Island, Japan. A coral polyp model, sediment model, seagrass model, and macroalgae model (and eventually mangrove) are incorporated into a local-scale hydrodynamic- biogeochemical model coupled with a watershed model which calculates green carbon flux. The model system calculates the local, reef scale primary production, calcification, and mucus release rate and then calculates dissolved and particulate organic carbon exports to the open ocean. A regional scale hydrodynamic model, which is downscaled from analysis/reanalysis products of global HYCOM (Hybrid Coordinate Ocean Model) using multi-nesting approach, is coupled with biogeochemical and sediment models to track the fate of organic C exported from the local scale model

ecosystem can be exported outside the system (i.e. to the deep layers of the open ocean or within reef sediments) (Abo et al. 2018; Kuwae et al. 2018). An initial simulation of DOC exports using the carbon dynamics model (Fig. 10.8) from a fringing coral reef is shown in Fig. 10.9. Second, interactions between sediment and water-column should be modeled. Carbon burial and sequestration in the sediments can be the key factor determining blue-carbon dynamics (Endo and Otani 2018; Inoue 2018; Miyajima and Hamaguchi 2018). Third, the model should properly address seagrass, macroalgae, and mangrove biogeochemical carbon cycles. Fourth, modeling should incorporate terrestrial carbon (so called "green carbon") dynamics in the coastal area, including the dynamics of suspended solids. The transport and accumulation of green carbon in coastal areas should be evaluated together with blue-carbon dynamics to quantify the relative importance of these carbons and to highlight the importance of the blue carbon. Fifth, regional three-dimensional models should incorporate horizontal and vertical carbon exports in the open ocean. Export of dissolved inorganic carbon, DOC, or POC from coastal ecosystems to the
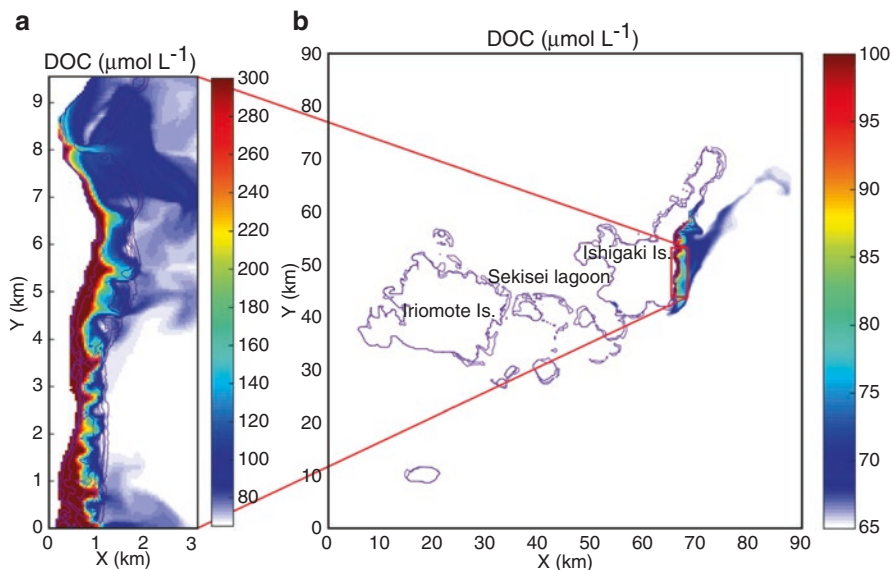
Fig. 10.9 Example of spatial variations in DOC around coral reefs at local and regional scales around a coral reef at Ishigaki Island, Japan

interior of the open ocean can be considered long-term storage of blue carbon, but is difficult to quantify solely from observations. We should therefore model the blue-carbon exports to the ocean interior, which can be validated from sediment-trap observations. All of these considerations can be challenging given the different time scales and models used, but they could be achieved through transdisciplinary approaches involving specialists in hydrology, geochemistry, oceanography, marine ecology, and ecological modeling.

Finally, field and experimental data are indispensable for verifying a blue-carbon dynamics model. The fate of organic matter should be assessed experimentally through decomposition experiments and empirically using sediment traps. Sediment organic carbon contents and sedimentation rates should be measured across different reef environments with and without mangrove forests and seagrass meadows.

References

Abo K, Sugimatsu K, Hori M, Yoshida G, Shimabukuro H, Yagi H, Nakayama A, Tarutani K (2018) Quantifying the fate of captured carbon: from seagrass meadow to deep sea. In: Kuwae T, Hori M (eds) Blue carbon in shallow coastal ecosystems: carbon dynamics, policy, and implementation. Springer, Singapore, pp 251–271

Bates NR (2002) Seasonal variability of the effect of coral reefs on seawater CO_2 and air–sea CO_2 exchange. Limnol Oceanogr 47:43–52

Bates NR, Samuels L, Merlivat L (2001) Biogeochemical and physical factors influencing seawater fCO_2 and air–sea CO_2 exchange on the Bermuda coral reef. Limnol Oceanogr 46:833–846

Birkeland C (1985) Ecological interactions between tropical coastal ecosystems. UNEP Reg Seas Rep Stud 73:1–26

Bouillon S, Dahdouh-Guebas F, Rao AVVS, Koedam N, Dehairs F (2003) Sources of organic carbon in mangrove sediments: variability and possible ecological implications. Hydrobiologia 495:33–39

Breithaupt JL, Smoak JM, Smith TJ III, Sanders CJ, Hoare A (2012) Organic carbon burial rates in mangrove sediments: strengthening the global budget. Glob Biogeochem Cycles 26:GB3011. https://doi.org/10.1029/2012GB004375

Buddemeier RW (1996) Coral reefs and carbon dioxide. Science 271:1298–1299

Cyronak T, Santos IR, Erler DV, Maher DT, Eyre BD (2014) Drivers of pCO_2 variability in two contrasting coral reef lagoons: the influence of submarine groundwater discharge. Glob Biogeochem Cycles 28:398–414

Dai M, Lu Z, Zhai W, Baoshan C, Zhimian C, Kuanbo Z, Wei-Jun C, Chen-Tung AC (2009) Diurnal variations of surface seawater pCO_2 in contrasting coastal environments. Limnol Oceanogr 54:735–745

Delesalle B, Buscail R, Carbonne J, Courp T, Dufour V, Heussner S, Monaco A, Schrimm M (1998) Direct measurements of carbon and carbonate export from a coral reef ecosystem (Moorea Island, French Polynesia). Coral Reefs 17:121–132

Drupp PS, De Carlo EH, Mackenzie FT, Sabine CL, Feely RA, Shamberger KE (2013) Comparison of CO_2 dynamics and air-sea gas exchange in differing tropical reef environments. Aquat Geochem 19:371–397

Duke NC, Wolanski E (2001) Muddy coastal waters and depleted mangrove coastlines – depleted seagrass and coral reefs. In: Wolanski E (ed) Oceanographic processes of coral reefs. Physical and biology links in the Great Barrier Reef. CRC Press, Washington, DC, pp 77–91

Endo T, Otani S (2018) Chapter 8. Carbon storage in tidal flats. In: Kuwae T, Hori M (eds) Blue carbon in shallow coastal ecosystems: carbon dynamics, policy, and implementation. Springer, Singapore, pp 129–151

Fagan KE, Mackenzie FT (2007) Air-sea CO_2 exchange in a subtropical estuarine-coral reef system, Kaneohe Bay, Oahu, Hawaii. Mar Chem 106:174–191

Falter JL, Lowe RJ, Zhang Z, McCulloch M (2013) Physical and biological controls on the carbonate chemistry of coral reef waters: effects of metabolism, wave forcing, sea level, and geomorphology. PLoS One 8:e53303

Frankignoulle M, Canon C, Gattuso J-P (1994) Marine calcification as a source of carbon dioxide: positive feedback of increasing atmospheric CO_2. Limnol Oceanogr 39(2):458–462

Frankignoulle M, Gattuso J-P, Biondo R, Bourge I, Copin-Montégut G, Pichon M (1996) Carbon fluxes in coral reefs. II. Eulerian study of inorganic carbon dynamics and measurement of air–sea CO_2 exchanges. Mar Ecol Prog Ser 145:123–132

Gattuso J-P, Pichon M, Delesalle B, Frankignoulle M (1993) Community metabolism and air–sea CO_2 fluxes in a coral reef ecosystem (Moorea, French Polynesia). Mar Ecol Prog Ser 96:259–267

Gattuso J-P, Frankignoulle M, Smith SV, Ware JR, Wollast R (1996a) Coral reefs and carbon dioxide. Science 271:1298

Gattuso J-P, Pichon M, Delesalle B, Canon C, Frankignoulle M (1996b) Carbon fluxes in coral reefs. I. Lagrangian measurement of community metabolism and resulting air–sea CO_2 disequilibrium. Mar Ecol Prog Ser 145:109–121

Gattuso J-P, Payri CE, Pichon M, Delesalle B, Frankignoulle M (1997) Primary production, calcification, and air–sea CO_2 fluxes of a macroalgal-dominated coral reef community (Moorea, French Polynesia). J Phycol 33:729–738

Gattuso J-P, Frankignoulle M, Wollast R (1998) Carbon and carbonate metabolism in coastal aquatic ecosystems. Annu Rev Ecol Syst 29:405–434

Gattuso J-P, Allemand D, Frankignoulle M (1999) Photosynthesis and calcification at cellular, organismal and community levels in coral reefs: a review on interactions and control by carbonate chemistry. Am Zool 39:160–183

Guannel G, Arkema K, Ruggiero P et al (2016) The power of three: coral reefs, seagrasses and mangroves protect coastal regions and increase their resilience. PLoS One 11(7):e0158094. https://doi.org/10.1371/journal.pone.0158094

Haas AF, Nelson CE, Rohwer F, Wegley-Kelly L, Quistad SD, Carlson CA, Leichter JJ, Hatay M, Smith JE (2013) Influence of coral and algal exudates on microbially mediated reef metabolism. PeerJ 1:e108. https://doi.org/10.7717/peerj.108

Hata H, Suzuki A, Maruyama T, Kurano N, Miyachi S, Ikeda Y, Kayanne H (1998) Carbon flux by suspended and sinking particles around the barrier reef of Palau, western Pacific. Limnol Oceanogr 43(8):1883–1893

Hata H, Kudo S, Yamano H, Kurano N, Kayanne H (2002) Organic carbon flux in Shiraho coral reef (Ishigaki Island, Japan). Mar Ecol Prog Ser 232:129–140

Hemminga MA, Duarte CM (2000) Seagrass ecology. Cambridge University Press, Cambridge

Inoue T (2018) Carbon sequestration in mangroves. In: Kuwae T, Hori M (eds) Blue carbon in shallow coastal ecosystems: carbon dynamics, policy, and implementation. Springer, Singapore, pp 73–99

Jiang ZP, Huang JC, Dai M, Kao SJ, Hydes DJ, Chou WC, Jan S (2011) Short-term dynamics of oxygen and carbon in productive nearshore shallow seawater systems off Taiwan: observations and modeling. Limnol Oceanogr 56:1832–1849

Kayanne H (1996) Coral reefs and carbon dioxide- reply. Science 271:1299–1300

Kayanne H, Suzuki A, Saito H (1995) Diurnal changes in the partial pressure of carbon dioxide in coral reef water. Science 269:214–216

Kayanne H, Harii S, Ide Y, Akimoto F (2002) Recovery of coral populations after the 1998 bleaching on Shiraho Reef, in the southern Ryukyus, NW pacific. Mar Ecol Prog Ser 239:93–103

Kayanne H, Hata H, Kudo S, Yamano H, Watanabe A, Ikeda Y, Nozaki K, Kato K, Negishi A, Saito H (2005) Seasonal and bleaching-induced changes in coral reef metabolism and CO_2 flux. Glob Biogeochem Cycles 19:GB3015. https://doi.org/10.1029/2004GB002400

Kennedy H, Beggins J, Duarte CM, Fourqurean JW, Holmer M, Marbà N, Middelburg JJ (2010) Seagrass sediments as a global carbon sink: isotopic constraints. Global Biogeochem Cycles 24:GB4026. https://doi.org/10.1029/2010GB003848

Kraines S, Suzuki Y, Omori T, Shitashima K, Kanahara S, Komiyama H (1997) Carbonate dynamics of the coral reef systems at Bora Bay, Miyako Island. Mar Ecol Prog Ser 156:1–16

Kuwae T, Kanda J, Kubo A, Nakajima F, Ogawa H, Sohma A, Suzumura M (2018) CO_2 uptake in the shallow coastal ecosystems affected by anthropogenic impacts. In: Kuwae T, Hori M (eds) Blue carbon in shallow coastal ecosystems: carbon dynamics, policy, and implementation. Springer, Singapore, pp 295–319

Lamb JB, van de Water JAJM, Bourne DG, Altier C, Hein MY, Fiorenza EA, Abu N, Jompa J, Harvell CD (2017) Seagrass ecosystems reduce exposure to bacterial pathogens of humans, fishes, and invertebrates. Science 355:731–733

Longhini CM, Souza MFL, Silva AM (2015) Net ecosystem production, calcification and CO_2 fluxes on a reef flat in Northeastern Brazil. Estuar Coast Shelf Sci 166:13–23

Massaro RFS, De Carlo EH, Drupp PS, Mackenzie FT, Jones SM, Shamberger KE, Sabine CL, Feely RA (2012) Multiple factors driving variability of CO_2 exchange between the ocean and atmosphere in a tropical coral reef environment. Aquat Geochem 18:357–386

McGowan HA, MacKellar MC, Gray MA (2016) Direct measurements of air-sea CO_2 exchange over a coral reef. Geophys Res Lett 43:4602–4608

Miyajima T, Hamaguchi M (2018) Carbon sequestration in sediment as an ecosystem function of seagrass meadows. In: Kuwae T, Hori M (eds) Blue carbon in shallow coastal ecosystems: carbon dynamics, policy, and implementation. Springer, Singapore, pp 33–71

Miyajima T, Koike I, Yamano H, Iizumi H (1998) Accumulation and transport of seagrass-derived organic matter in reef flat sediment of Green Island, Great Barrier Reef. Mar Ecol Prog Ser 175:251–259

Miyajima T, Hori M, Hamaguchi M, Shimabukuro H, Adachi H, Yamano H, Nakaoka M (2015) Geographic variability in organic carbon stock and accumulation rate in sediments of East and Southeast Asian seagrass meadows. Global Biogeochem Cycles 29:397–415. https://doi.org/10.1002/2014GB004979

Moberg F, Folke C (1999) Ecological goods and services of coral reef ecosystems. Ecol Econ 29:215–233

Mumby PJ, Edwards AJ, Ernesto Arias-González JE, Lindeman KC, Blackwell PG, Gall A, Gorczynska MI, Harborne AR, Pescod CL, Renken H, Wabnitz CCC, Llewellyn G (2004) Mangroves enhance the biomass of coral reef fish communities in the Caribbean. Nature 427:533–536

Nakamura T, Nadaoka K, Watanabe A, Yamamoto T, Miyajima T, Blanco AC (2017) Reef-scale modeling of coral calcification responses to ocean acidification and sea-level rise. Coral Reefs. https://doi.org/10.1007/s00338-017-1632-3

Ogden JC (1988) The influence of adjacent systems on the structure and function of coral reefs. Proceedings of the sixth international coral reef symposium. 1

Ohde S, van Woesik R (1999) Carbon dioxide flux and metabolic processes of a coral reef. Okinawa Bull Mar Sci 65:559–576

Saunders MI, Leon JX, Callaghan DP, Roelfsema CM, Hamylton S, Brown CJ, Baldock T, Golshani A, Phinn SR, Lovelock CE, Hoegh-Guldberg O, Woodroffe CD, Mumby PJ (2014) Interdependency of tropical marine ecosystems in response to climate change. Nat Clim Chang 4(8):724–729

Scheffer M, Carpenter S, Foley JA, Folke C, Walker B (2001) Catastrophic shifts in ecosystems. Nature 413:591–596

Serafy JE, Shideler GS, Araújo RJ, Nagelkerken I (2015) Mangroves enhance reef fish abundance at the Caribbean regional scale. PLoS One 10(11):e0142022. https://doi.org/10.1371/journal.pone.0142022

Shaw EC, McNeil BI (2014) Seasonal variability in carbonate chemistry and air-sea CO_2 fluxes in the southern Great Barrier Reef. Mar Chem 158:49–58

Smith SV, Pesret F (1974) Processes of carbon dioxide flux in the Fanning Island lagoon. Pac Sci 28:225–245

Smith SV, Chandra S, Kwitko L, Schneider RC, Schoonmaker J, Seeto J, Tebano T, Tribble GW (1984) Chemical stoichiometry of lagoon metabolism: preliminary report on an environmental chemistry survey of Christmas Island, Kiribati. University of Hawaii/University of South Pacific International Sea Grant Programme Cooperative Report. UNIHISEAGRANT-CR-84-02

Sorokin YI (1993) Coral reef ecology. Springer-Verlag (Ecological studies 102)

Suzuki A, Kawahata H (2004) Reef water CO_2 system and carbon production of coral reefs: topographic control of system-level performance. In: Global environmental change in the ocean and on land. pp 229–248

Takahashi T, Sutherland SC, Wanninkhof R, others (2009) Climatological mean and decadal change in surface ocean pCO_2, and net sea–air CO_2 flux over the global oceans. Deep-Sea Res II 56:554–577

Tanaka Y, Miyajima T, Koike I, Hayashibara T, Ogawa H (2008) Production of dissolved and particulate organic matter by the reef-building corals *Porites cylindrica* and *Acropora pulchra*. Bull Mar Sci 82:237–245

Unsworth RKF, Cullen LC (2010) Recognising the necessity for Indo-Pacific seagrass conservation. Conserv Lett 3:63–73

Unsworth RKF, Collier CJ, Henderson GM, McKenzie LJ (2012) Tropical seagrass meadows modify seawater carbon chemistry: implications for coral reefs impacted by ocean acidification. Environ Res Lett 7:024026

Ware JR, Smith SV, Reaka-Kudla ML (1991) Coral reefs: sources or sinks of atmospheric CO_2? Coral Reefs 11:127–130

Watanabe A, Yamamoto T, Nadaoka K, Maeda Y, Miyajima T, Tanaka Y, Blanco AC (2013) Spatiotemporal variations in CO_2 flux in a fringing reef simulated using a novel carbonate system dynamics model. Coral Reefs 32:239–254

Werner U, Bird P, Wild C, Ferdelman T, Polerecky L, Eickert G, Jonstone R, Hoegh-Guldberg O, de Beer D (2006) Spatial patterns of aerobic and anaerobic mineralization rates and oxygen penetration dynamics in coral reef sediments. Mar Ecol Prog Ser 309:93–105

Wild C, Huettel M, Klueter A, Kremb SG, Rasheed MYM, Jorgensen BB (2004) Coral mucus functions as an energy carrier and particle trap in the reef ecosystem. Nature 428:66–70

Yamamoto S, Kayanne H, Tokoro T, Kuwae T, Watanabe A (2015) Total alkalinity flux in coral reefs estimated from eddy covariance and sediment pore-water profiles. Limnol Oceanogr 60:229–241

Yan H, Yu K, Shi Q, Tan YH, Zhang HL, Zhao MX, Li S, Chen TR, Huang LY, Wang PX (2011) Coral reef ecosystems in the South China Sea as a source of atmospheric CO_2 in summer. Chin Sci Bull 56:676–684

Yan H, Yu K, Shi Q, Tan Y, Liu G, Zhao M, Li S, Chen T, Wang Y (2016) Seasonal variations of seawater pCO_2 and sea-air CO_2 fluxes in a fringing coral reef, northern South China Sea. J Geophys Res Oceans 121:998–1008

Zeebe RE, Wolf-Gladrow D (2001) CO_2 in seawater: equilibrium, kinetics, isotopes. Elsevier, Paperback ISBN: 9780444509468

Zhang Z, Lowe R, Falter J, Ivey G (2011) A numerical model of wave- and current-driven nutrient uptake by coral reef communities. Ecol Model 222:1456–1470

Chapter 11
CO$_2$ Uptake in the Shallow Coastal Ecosystems Affected by Anthropogenic Impacts

Tomohiro Kuwae, Jota Kanda, Atsushi Kubo, Fumiyuki Nakajima, Hiroshi Ogawa, Akio Sohma, and Masahiro Suzumura

Abstract Shallow coastal ecosystems (SCEs) are generally recognized as not only significant organic carbon reservoirs but also as sources for CO$_2$ emission to the atmosphere, thus posing a dilemma regarding their role in climate change mitigation measures. However, we argue that SCEs can act as sinks for atmospheric CO$_2$ under a given set of biogeochemical and socioeconomic conditions. The key properties of SCEs that show net uptake of atmospheric CO$_2$ are often characteristic of human-dominated systems, that is, high nutrient inputs from terrestrial systems, input of treated wastewater in which labile carbon has been mostly removed, and the presence of hypoxic waters. We propose a new perspective on the potential of human-dominated SCEs to contribute to climate change mitigation, both serving as

T. Kuwae (✉)
Coastal and Estuarine Environment Research Group, Port and Airport Research Institute, Yokosuka, Japan
e-mail: kuwae@p.mpat.go.jp

J. Kanda
Department of Ocean Sciences, Tokyo University of Marine Science and Technology, Minato-ku, Tokyo, Japan

A. Kubo
Department of Geoscience, Shizuoka University, Suruga-ku, Shizuoka-Shi, Shizuoka-Ken, Japan

F. Nakajima
Department of Urban Engineering, The University of Tokyo, Bunkyo-ku, Tokyo, Japan

H. Ogawa
Atmosphere and Ocean Research Institute, The University of Tokyo, Kashiwanoha, Kashiwa-shi, Chiba, Japan

A. Sohma
Graduate School of Engineering, Osaka City University, Sugimoto, Sumiyoshi-ku, Osaka, Japan

M. Suzumura
National Institute of Advanced Industrial Science and Technology, AIST Tsukuba West, Tsukuba, Japan

carbon reservoirs and providing direct net uptake of atmospheric CO_2, in light of human systems–ecosystem interactions. Namely, if we view the land and a SCE as an integrated system, with appropriate management of both wastewater treatment and SCE, we will be able to not only suppress CO_2 release but also capture and store carbon.

11.1 Introduction

Recent research has demonstrated that the sediment of shallow coastal ecosystems (SCEs), such as mangroves, salt marshes, tidal flats, seagrass meadows, estuaries, and embayment, is important as a marine carbon reservoir (e.g., Nellemann et al. 2009; McLeod et al. 2011; Fourqurean et al. 2012; Duarte et al. 2013; Miyajima et al. 2015, 2017; Endo and Otani 2018; Inoue 2018; Miyajima and Hamaguchi 2018). Moreover, coastal ecosystems with high primary productivity, such as seagrass meadows, can serve as net sinks for atmospheric CO_2 (i.e., total CO_2 uptake minus total CO_2 release is positive; Smith 1981; Tokoro et al. 2014).

From the viewpoint of mitigating climate change, the net uptake of atmospheric CO_2 through the exchange of CO_2 at the air–water interface is a direct process, whereas the suppression of CO_2 emission to the atmosphere by carbon storage in the marine ecosystem is an indirect process (Fig. 11.1). Although these are two completely different processes, both are effective for mitigating climate change. There is controversy as to which is more important, but ecosystems that show both net uptake of atmospheric CO_2 and long-term storage of carbon are desirable.

However, because ecosystems are dynamic natural systems characterized by complex fluctuations in biological communities and environmental conditions, atmospheric CO_2 uptake and carbon storage do not occur at constant rates. The CO_2 gas exchange at the air–water interface fluctuates through absorption and emission phases and the amount of carbon stored in the ecosystem increases and decreases over time (Tokoro et al. 2014, 2018). Therefore, in considering the effectiveness of ecosystem-based technology measures such as mitigation of climate change through the use of blue carbon ecosystems, setting a specified time and space of interest in advance is important to judge whether atmospheric CO_2 is taken up or whether carbon is stored. As the temporal and spatial scales of the processes increase, the measure becomes more effective and more reliable.

The effect of human activity cannot be ignored at longer time scales. The geophysical setting of SCEs is often at the boundary between land and sea, making them socioeconomically important features. As a result, the carbon cycle of many SCEs has changed significantly over time due to the load of nutrients and organic matter (green carbon), freshwater use, and topographic modification (Bauer et al. 2013; Regnier et al. 2013). In particular, because nutrient loading and wastewater
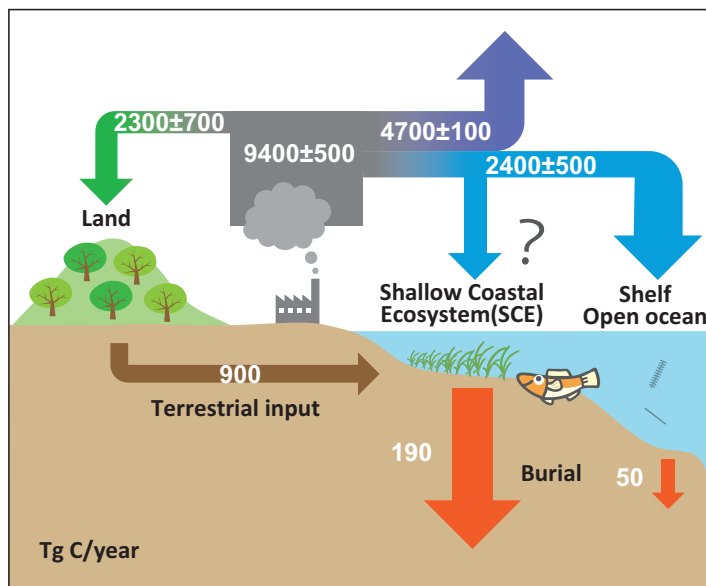
Fig. 11.1 Global carbon cycling. See Le Quéré et al. (2018) for atmosphere data (mean ± SD for 2007–2016), Nellemann et al. (2009) for the sedimentary accumulation rate, and IPCC (2013) for terrestrial input. SCE sediments accumulate 190 million tonnes of carbon (Tg C) every year, much faster than sediments in shelves and the open ocean

treatment have large impacts on the cycling of biogeochemical elements (e.g., carbon, nitrogen, and phosphorus) in the ecosystem (McIntyre et al. 2000), they may also have an impact on the uptake of atmospheric CO$_2$ and carbon storage within the ecosystem.

In comparison with the open ocean and shelves, SCEs are hotspots with a high rate of carbon accumulation to the sediment, although few measurements of CO$_2$ exchange at the air–water interface have been conducted, highlighting SCEs as largely unexplored places (but see Borges et al. 2005; Cai 2011; Chen et al. 2013; Laruelle et al. 2013; Regnier et al. 2013; Akhand et al. 2018; Otani and Endo 2018; Tokoro et al. 2018; Watanabe and Nakamura 2018). SCEs are characterized by diverse biogeochemical cycles and biota. Their complexity reflects their position at the boundaries between air and water, water and sediment, and atmosphere and sediment, with very different physical properties (such those of fresh water and salt water) and with rapid exchange rates at the interfaces. Thus, the estimation of carbon stock and flow in SCEs is highly uncertain compared to that in other ecosystems. In this chapter, we discuss the potential for climate change mitigation by SCEs that have been strongly affected by human impacts for a long time.

11.2 CO$_2$ Uptake and Carbon Storage in SCEs

11.2.1 Relationship Between Carbon Storage and CO$_2$ Uptake

The essential functions required when considering mitigating climate change by utilizing blue carbon ecosystems are storing carbon (Miyajima and Hamaguchi 2018) and subsequently suppressing CO$_2$ emission to the atmosphere, net direct atmospheric CO$_2$ uptake (Tokoro et al. 2018), or both. However, SCEs are generally recognized to be net emitters of CO$_2$ to the atmosphere (Borges and Abril 2011), due to the fact that the water generally contains a large amount of CO$_2$ and organic green carbon inflowing from terrestrial sources (Laruelle et al. 2013; Regnier et al. 2013) (Fig. 11.2). Indeed, when summarized based on salinity, it is clear that those SCEs more influenced by fresh water and with lower salinity are greater sources of CO$_2$ (Fig. 11.3).

In any case, if we look at this carbon flow from the viewpoint of climate change mitigation, we note that SCEs have a positive function of storing organic carbon and a negative function of being a net source of CO$_2$ to the atmosphere. The dilemma of
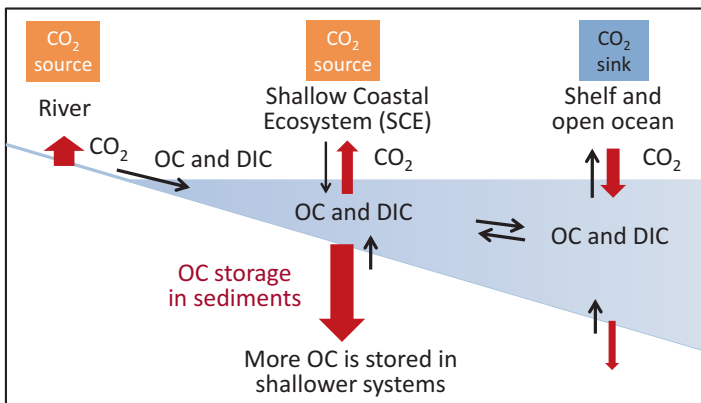

Fig. 11.2 Conventional findings on air–water CO$_2$ exchange and carbon storage in each marine geographic region. *OC* organic carbon, *DIC* dissolved inorganic carbon
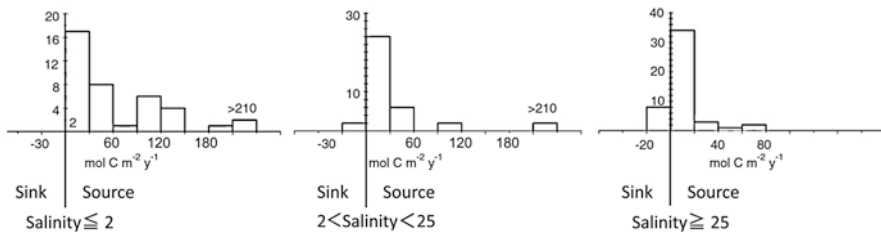

Fig. 11.3 Relationship between salinity and air–water CO$_2$ exchange in SCEs. Those SCEs with lower salinity emit more CO$_2$. (Modified from Chen et al. 2012)

"storing carbon but emitting CO$_2$" occurs because water intervenes between the sediment (the main pool of carbon) and the atmosphere. Similarly, this dilemma can also occur in inland waters such as lakes and rivers (Cole et al. 2007). In turn, in a forest or grassland ecosystem not interrupted by water, the same amount of carbon taken up from the atmosphere is stored in organisms and/or in the soil, assuming a closed system. Because of this, the dilemma has not been specifically discussed in terrestrial ecosystems. In reality, however, terrestrial ecosystems are also open systems, as large amounts of green carbon flow out of these ecosystems through rivers and into the sea (Fig. 11.1). Therefore, in forest and grassland ecosystems, the amount of net CO$_2$ uptake is larger than the amount of organic carbon stored.

11.2.2 Carbon Storage in SCEs

Among the various processes that influence carbon storage in SCEs, the major ones supporting the high accumulation of organic carbon in the sediment include (1) large supplies of autochthonous organic matter (i.e., blue carbon formed within SCEs) and/or allochthonous organic matter (green carbon flowing in from terrestrial sources and/or blue carbon flowing from outside the SCE); (2) a large supply of mineral particles, which are the main component of the sediment (Sholkovitz 1976); and (3) aggregation of the mineral particles and organic matter to promote sedimentation (Kennedy et al. 2010; Zonneveld et al. 2010).

The seabed of SCEs where carbon is deposited is also dynamic. Due to external forcing by waves and currents, the sediment surface layer is disturbed, its thickness varies, and the seabed topography changes. For example, erosion at the sea bottom implies outflow of sedimentary mineral particles and carbon from the sediment surface. In turn, when the waves and currents near the seabed are calm, the sediment and carbon accumulation rates increase. Furthermore, in such calm physical conditions, fine sediment particles are more easily deposited and organic matter adsorbs to the fine particles, often resulting in the formation of muddy sediments where much carbon is stored.

Decomposition of organic matter becomes slower after deposition on the sea bottom. This is related to the anoxic environment of the sediment except for its vast surface layer (e.g., about the top several millimeters in a muddy sediment). Because terrestrial soil is aerobically decomposed by exposure to oxygen from the air, its decomposition proceeds on a scale of decades, whereas in the anaerobic environment of the seabed, organic matter is decomposed and mineralized over thousands of years (Chambers et al. 2001). This suppression of the decomposition rate promotes accumulation of organic matter at the seabed (Miyajima and Hamaguchi 2018).

Vegetated SCEs such as mangroves, salt marshes, and seagrass meadows have among the fastest rates of carbon storage to their sediments, with average values ranging from 138 to 226 g C/m^2/year (range: 18–1713 g C/m^2/year); the rates are at least 1000 times greater than that in the open ocean (0.018 g C/m^2/year)

(Nellemann et al. 2009; McLeod et al. 2011). This difference cannot be explained solely by the difference in the production rate of blue carbon (SCE: 1044–2784 g C/m^2/year, open ocean: 120 g C/m^2/year; Gattuso et al. 1998). Rather, the existence of vegetation slows water currents and promotes the trapping and sedimentation of suspended particulate organic matter, causing an increase in the carbon accumulation rate (Hendriks et al. 2007; Kennedy et al. 2010).

Other factors also influence the carbon storage rate in SCEs, as explained in Chap. 2 (Miyajima and Hamaguchi 2018). These include chemical factors such as the quality (e.g., whether it is easy or difficult to decompose) of organic matter supplied and degradation enzyme activity; geophysical factors such as temperature, water depth, and the grain size and surface area of the sediment (Miyajima et al. 2017); and biological factors such as bioturbation (Zonneveld et al. 2010; Koho et al. 2013).

11.2.3 Requirements for a SCE Becoming a Net Sink of Atmospheric CO$_2$

As we explained, the carbon storage rate in aquatic ecosystems is not equal to the net atmospheric carbon uptake rate because these are open systems in which water intervenes between the sediment and atmosphere. In addition, the inorganic–organic conversion in the water column is complex. As a result, the amount of material exchanged at the air–water interface and that exchanged at the water–sediment interface generally do not balance.

Gas exchange between the atmosphere and the ocean occurs at the air–water interface. If the concentration of CO$_2$ in seawater is lower than that in air, then atmospheric CO$_2$ will be absorbed into the sea (Wanninkhof 1992). Currently, the atmospheric CO$_2$ concentration fluctuates from about 350 to 450 ppm; in turn, the CO$_2$ concentration in SCE surface waters ranges from about 20 ppm to more than 3000 ppm. Thus, the actual gas exchange rate and direction of the flux (i.e., whether the ecosystem is a sink or a source of CO$_2$) are dependent on the CO$_2$ concentration in the surface water.

The CO$_2$ concentration in the surface water becomes undersaturated and atmospheric CO$_2$ is taken up (1) if the CO$_2$ concentration in the influent water from outside the target area is lower than that of the atmosphere, or (2) if the concentration decreases below the atmospheric concentration due to the occurrence of processes lowering the CO$_2$ concentration in the surface water. Rivers are major CO$_2$ influents from outside SCEs, and their CO$_2$ concentrations are high. The partial pressure of CO$_2$ in more than 95% of global inland waters is higher than that in the air, with a median value of about 3100 μatm (Raymond et al. 2013). Thus, in order for the surface water of SCEs to be undersaturated, it is necessary to have a process that lowers the CO$_2$ concentration in surface water. As explained in Chap. 6, such processes include decreasing temperature, increasing total alkalinity (Ca^{2+} and NO$_3^-$
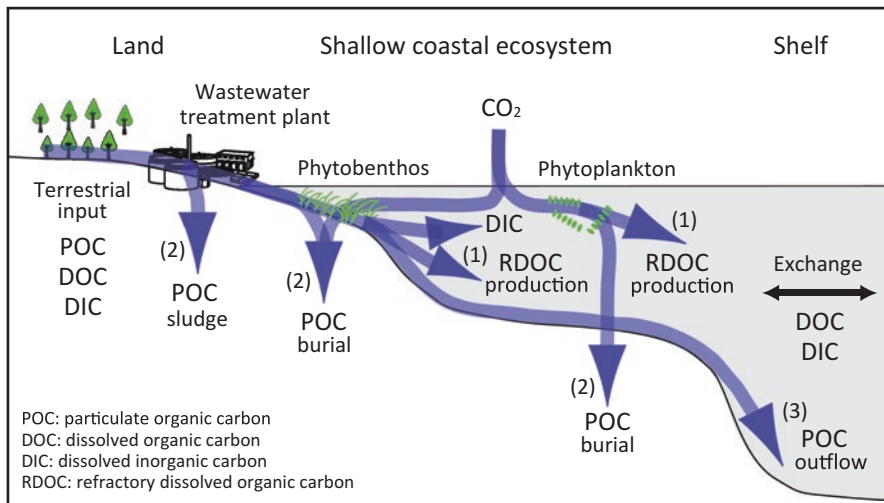
Fig. 11.4 Conceptualized diagram of carbon flow contributing to net uptake of atmospheric CO$_2$ in SCEs. We assume that net uptake of atmospheric CO$_2$ occurs only when there is a unidirectional carbon flow (pump) over a long period of time, resulting in the water CO$_2$ concentration being lower than the atmospheric CO$_2$ concentration. The net uptake of atmospheric CO$_2$ occurs when (1) CO$_2$ emission is suppressed by generation of refractory dissolved organic carbon (RDOC); (2) precipitation and burial of particulate organic carbon (POC); and (3) transportation of POC and DOC to the deep sea. Although the wastewater treatment plant that removes POC (sludge) indirectly contributes to lowering the CO$_2$ concentration in the SCE, the treatment plant functions as a CO$_2$ emitter because organic matter in the wastewater is decomposed and CO$_2$ is generated in the open aeration tank. (Modified from Kuwae et al. 2016)

concentrations are the main ions that determine total alkalinity), and net uptake of CO$_2$ by organisms (Tokoro et al. 2018).

The environmental conditions that result in the uptake of CO$_2$ are not continuous in the natural world. In reality, as environmental conditions such as light, temperature, and salinity change from moment to moment, cycles of uptake and emission occur frequently (Tokoro et al. 2014, 2018). In other words, it is critical to take a long-term view of the balance of uptake and emission as we discuss an ecosystem contributing to the mitigation of climate change. The requirements for SCEs serving as long-term net sinks are conceptualized in Fig. 11.4. Overall, the system can also be viewed as a process of transporting carbon like a pump; that is, the carbon transport is unidirectional from the viewpoint of the long-term balance. This type of pump is well-known in the field of marine science: "biological pump" in the open ocean (Longhurst and Harrison 1989) and "continental shelf pump" in shelves (Tsunogai et al. 1999).

Among the various unidirectional pumps, those particularly important for the net uptake of atmospheric CO$_2$ are (1) formation of refractory dissolved organic carbon (RDOC); (2) particulate organic carbon (POC) being conveyed to the sea bottom and stored in the sediment (Miyajima and Hamaguchi 2018); and (3) POC and

dissolved organic carbon (DOC) export (Sugimatsu et al. 2015; Abo et al. 2018). Although the components of RDOC and the reasons for the refractory properties are still not fully understood, Arrieta et al. (2015) proposed that RDOC has a molecular or physical structure (unspecified) that is difficult for bacteria to use, or its concentration is too low to be available for bacteria. Because these three pumps tend to not flow in reverse (i.e., the opposite process is weak), they function to suppress both the decomposition of organic matter and the emission of CO_2 to the atmosphere over a long period.

11.2.4 Carbon Storage in Water and Organisms

Of the three requirements for a net long-term CO_2 sink (Fig. 11.4), the storage of RDOC in water is the least understood (Jiao et al. 2014). The organic carbon pool is not limited to sediments and organisms but can be in the water column as well if only the DOC is refractory. DOC accounts for 28% (246 Tg C/year) of the total green carbon flowing from rivers to oceans on the global scale (Cai 2011). Thus, how much DOC decomposes in microbial and photochemical reactions (Moran et al. 2000), how much DOC remains as refractory dissolved green carbon (Kubo et al. 2015), and how much refractory dissolved blue carbon is newly formed at the site can be major factors determining the amount of CO_2 uptake and emission.

Among them, new formation of refractory dissolved blue carbon is particularly unclear. Phytoplankton, bacteria, macrophytes (seagrasses and seaweeds), and corals are organisms responsible for the formation of refractory dissolved blue carbon (Ogawa et al. 2001; Wada et al. 2008; Kragh and Søndergaard 2009; Lønborg et al. 2009; Tanaka et al. 2011a, b). From a technical perspective, however, it is extremely difficult to quantify refractory dissolved blue carbon separately from refractory dissolved green carbon because the concentration of DOC is low and salt in seawater acts as an inhibitor in the chemical analysis.

The sequence of (1) uptake of CO_2 by macrophytes and phytoplankton, (2) production of their body (POC) and mucus (DOC), and (3) transportation and sinking of POC and DOC in the deep ocean is also an important mechanism for carbon storage. Even if POC and DOC get decomposed in the deep ocean and become CO_2, the transport to the surface and return to the atmosphere occur over geological time scales. According to recent reports, the global estimate of POC and DOC derived from seagrasses transported from SCEs to the deep ocean is about 24 Tg C/year (Duarte and Krause-Jensen 2017) and that derived from kelps is around 36–279 Tg C/year (Krause-Jensen and Duarte 2016). However, the variability in these amounts and the factors controlling their transport are still unknown, leading to high uncertainty in the estimates.

11.3 Hypothesis that Human-Impacted SCEs Act As a Net CO$_2$ Sink

Strong human impacts can result in changes to the carbon cycle (McIntyre et al. 2000). In particular, nutrient load, wastewater treatment, and freshwater use will increase with increasing human and livestock populations and farmland area. As a result of human impacts, the cycling of green carbon and blue carbon related to climate change mitigation, such as CO$_2$ exchange between the atmosphere and water and carbon storage in SCEs, is affected (Table 11.1).

Kuwae et al. (2016) hypothesized that some characteristics of SCEs subject to human impacts actually strengthen the carbon cycling structure that supports the net uptake of atmospheric CO$_2$ (net CO$_2$ sink; Fig. 11.5). This idea is likely to be controversial, because urban coastal waters are seen as places where eutrophication progresses and a large amount of CO$_2$ is emitted by decomposition of organic matter. In this section, we explain why a human-impacted SCE functions as a sink of atmospheric CO$_2$ from a mechanistic perspective and provide empirical evidence from previous studies.

11.3.1 Wastewater Treatment

Urban and agricultural nutrient loading and wastewater treatment have a major influence on a SCE's biogeochemical cycling (Grimm et al. 2008; Kaushal and Belt 2012). The following two points are particularly relevant to air–seawater CO$_2$ gas exchanges and wastewater treatment. First, in the most common wastewater treatment method (i.e., the activated sludge method), carbon is removed more efficiently than nitrogen and phosphorus from wastewater (e.g., Sedlak 1991). Hence, the treated water has relatively less carbon than nitrogen and phosphorous. When such treated water flows into a SCE, primary production is promoted due to the abundant nutrients, while decomposition and mineralization are suppressed by less abundant organic carbon. This means that wastewater treatment suppresses the rise in CO$_2$ concentration in the water column of a SCE.

The second important point is that organic matter in the treated water is refractory (Kubo et al. 2015), because labile organic matter has already been decomposed and removed during wastewater treatment. Therefore, further decomposition and mineralization of the organic matter contained in the treated water is slow, resulting in suppression of the rise in CO$_2$ concentration.

Through these two mechanisms, CO$_2$ concentration in seawater is lowered and uptake of CO$_2$ from the atmosphere is promoted. That is, both nutrient loads derived

Table 11.1 Characteristics of human-impacted SCEs, drivers, key mechanisms, and the relevance to atmospheric CO_2 uptake and carbon storage

| Characteristics	Driver	Key mechanism	Relevance to atmospheric CO_2 uptake and carbon storage
Large amount of nutrient input	Human, livestock, and farmland	Enhancement of high primary production	Low CO_2 in surface water
Relatively small amount of labile carbon input	Wastewater treatment (removal and mineralization of labile organic carbon)	Low carbon/nutrient ratio water inflow	Low CO_2 in water
		Suppression of mineralization but less suppression of primary production	
Large amount of freshwater discharge	Freshwater demand due to population (importation of water, watershed alteration)	Enhancement of stratification	Low CO_2 in surface water
		Suppression of upwelling of bottom waters with high DIC concentration due to stratification	
		Low turbidity in surface water due to suppression of resuspension and upwelling of POC from bottom water, enhancing light availability and photosynthesis	
Presence of hypoxic water mass	Stratification	Anoxia/hypoxia in both bottom water and surface sediments	Enhancement of carbon storage
	High organic matter input		
	Freshwater input	Suppression of mineralization	
		Production of POC by anoxic/hypoxic polymerization	
Shallow water depth	Geological settings	Short degradation time during POC sinking in water column	Enhancement of carbon storage
High turbidity	Plankton blooming	Enhancement of primary production due to increase in phytoplankton biomass, lowering CO_2	Variability of CO_2 in surface water
	Mineral particle input from land		
		Suspended particles suppressing light availability and photosynthesis, raising CO_2	
Change in residence time	Freshwater input	Influenced by the quantity and quality (CO_2 and POC) of inflowing water	Variability of CO_2 in surface water and carbon storage
	Alteration of sea-bottom topography		

Modified from Kuwae et al. (2016)
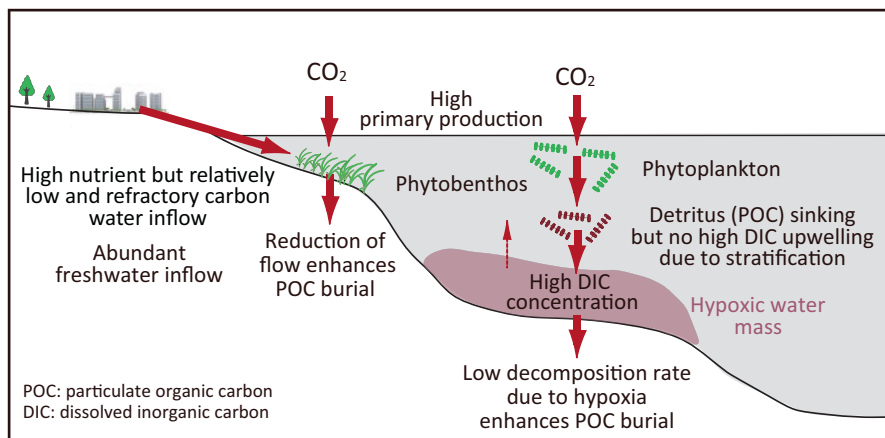
Fig. 11.5 Conceptual diagram illustrating how human-impacted SCEs become net sinks for atmospheric CO$_2$. (Modified from Kuwae et al. 2016)

from urban/agricultural land uses and wastewater treatment that reduces the labile organic carbon load are important factors in a human-impacted SCE becoming a net sink for atmospheric CO$_2$.

However, the inflow of treated water may accelerate decomposition of refractory organic matter in a SCE and may somewhat slow the decrease of CO$_2$ concentration in seawater. This is due to the "priming effect" of decomposing refractory organic matter, which is enhanced at high nutrient concentrations (Taylor and Townsend 2010; Jiao et al. 2014). This phenomenon occurs due to the presence of bacteria that decompose and mineralize refractory organic matter using nutrients in the natural environment. Therefore, how the interaction between refractory organic matter and nutrients affects carbon storage is complex.

11.3.2 Freshwater Inflow, Stratification, and Hypoxic Water Mass

The large inflow of fresh water, stratification (the state where water bodies with different properties, such as temperature or salinity, are layered without mixing), and oxygen-depleted (hypoxic) conditions of human-impacted SCEs are also deeply involved in CO$_2$ gas exchange. Urban centers often divert rivers to meet their demand for fresh water. An increase in the inflow of fresh water and heated effluents from urban areas strengthen the stratification structure and promote seawater exchange in SCEs. Changes in the physical oceanographic structure caused by such human impacts have an indirect but major influence on the SCE's biogeochemical cycling. When a SCE becomes stratified, upwelling of the high concentration of dissolved inorganic carbon (DIC) in the bottom layer and the subsequent rise in the

surface CO_2 concentration, which is exchanged with the atmosphere, are suppressed (Fig. 11.5). In turn, POC as a source for increasing the surface CO_2 concentration gradually precipitates due to its own weight. Thus, even if there is stratification, the SCE's sedimentation is not disturbed (Kone et al. 2009).

Because SCEs are shallow, POC sinks and reaches the sea bottom in a short time, leading to less mineralization during sinking in the water column. This also suppresses a rise in the CO_2 concentration in surface water. Furthermore, sediments are often resuspended due to the effects of wind-driven waves in SCEs, but the resuspension is suppressed when stratification develops. This suppression decreases the turbidity of the surface water and increases the light intensity available for photosynthesis, and the increased photosynthesis by phytoplankton lowers the CO_2 concentration in the surface water (Chen et al. 2008).

Stratification occurs seasonally: it develops in the summer when the surface water is heated with strong sunlight. This seasonality also plays an important role in CO_2 gas exchange. During the summer, upwelling of the bottom layer water containing a high DIC concentration is blocked due to stratification. Seawater is well mixed vertically in other seasons when stratification does not develop. As a result of this mixing, the surface CO_2 concentration rises. However, because the water temperature is lower and solubility of CO_2 is higher in seasons other than summer, less CO_2 is emitted into the atmosphere.

Although there is debate on the topic, the decomposition and mineralization rates of organic matter are generally considered to be faster when the oxygen concentration is higher (Canfield 1994; Hartnett et al. 1998; Miyajima and Hamaguchi 2018). In addition, the rate of decomposition of organic matter increases where conditions fluctuate between aerobic and anaerobic, thus promoting symbiosis between aerobic and anaerobic heterotrophic bacteria (Zonneveld et al. 2010). This suggests that the presence of diverse chemical and biological environments may promote the decomposition of more diverse organic matter. For example, if labile organic matter is first decomposed and mineralized under aerobic conditions in the bottom water and sedimentary surface layer and then undecomposed organic matter is transported to the deeper anaerobic environment and further mineralized, the mineralization rate per unit area may increase as a whole.

Nevertheless, when hypoxic conditions occur in the bottom water during stratification, the aerobic sediment surface layer becomes anaerobic throughout the sediment layers, and the decomposition and mineralization rates of organic matter decrease. Consequently, organic matter accumulates at the seabed at a faster rate. Also, because decomposition of organic matter by benthic animals is suppressed under hypoxic conditions, the presence of hypoxia facilitates the accumulation of organic matter in sediments (Koho et al. 2013).

Hypoxic water masses are usually seen as purely detrimental, as hypoxia causes mortality of benthic macrofauna such as fish and shellfish. From the viewpoint of carbon storage or climate change mitigation, however, hypoxic water masses have some positive effects, as we have explained. However, hypoxic water masses may promote the production of other greenhouse gases, such as N_2O and CH_4, and further research on the topic is warranted.

Increased turbidity may function to either increase or decrease the CO_2 concentration of surface water, depending on the cause. If the source of turbidity is phytoplankton, primary production is promoted and the surface CO_2 concentration is reduced. If the source of turbidity is inorganic mineral particles (sand and mud), photosynthesis is suppressed due to decreased light intensity in water and the concentration of CO_2 increases (Chen et al. 2012).

Furthermore, the residence time (exchange) of seawater is also an important factor determining CO_2 and organic matter concentrations (Gazeau et al. 2005). These depend on the concentrations in and amount of incoming river water and offshore seawater. Thus, changes in the residence time of seawater may function both in increasing and decreasing CO_2 and organic matter concentrations.

11.3.3   Evidence from Field Studies

The air–seawater CO_2 exchange in the world's SCEs was summarized by Borges and Abril (2011), who noted only one case serving as a net sink for atmospheric CO_2, and by Laruelle et al. (2013) and Regnier et al. (2013), who concluding that SCEs serve as a net emitter worldwide. In light of the growing literature after those summaries were published, however, we used the Google Scholar and Scopus databases to identify new reported cases of SCEs serving as net sinks for CO_2 (Table 11.2) to clarify the characteristics of these exceptional SCE cases.

First, a SCE serving as a net sink of atmospheric CO_2 is often located next to an urbanized area or agricultural lands. These findings support our hypothesis that human-impacted SCEs can act as a sink for atmospheric CO_2. Second, such SCEs are often affected by wastewater treatment, stratification, and hypoxia. These three characteristics are consistent with the Japanese cases of Tokyo Bay (Fig. 11.6) (Kubo et al. 2017) and Osaka Bay (Fig. 11.7) (Fujii et al. 2013). The effluent flowing into human-impacted SCEs has high nutrient and phytoplankton (chlorophyll *a*) concentrations and high primary production due to loads derived from urban and agricultural activities. In addition, previous studies revealed that net uptake of atmospheric CO_2 occurs when net ecosystem production increases (Maher and Eyre 2012; Tokoro et al. 2014, 2018).

As cases of vegetated ecosystems acting as net sinks of atmospheric CO_2, seagrass meadows and one kelp bed were extracted. The uptake rate in the seagrass meadows was 24.6 ± 44.1 mmol C/m²/day and that in the kelp bed was 59.4 mmol C/m²/day (Ikawa and Oechel 2015), all of which were faster than the uptake rate of SCEs without seagrass meadows (9.6 ± 6.7 mmol C/m²/day). There were also cases of coral reefs in which the CO_2 concentration in water was undersaturated and the system acted as a sink (Kayanne et al. 1995, 2005; Delille et al. 2009), although the uptake rate was not described.

The global average of the net CO_2 emission rate from SCEs is about 40–50 mmol C/m²/day (Laruelle et al. 2013). However, most of the data for these statistics were acquired intermittently at fragmented spatial scales; there are very few cases for

Table 11.2 Previous reports of SCEs affected by both seawater and fresh water (salinity range limited to 1–33) that act as net atmospheric CO_2 sinks

Location	Site condition			Hypoxic water mass	Chl-a (µg/L)	Flux and measurement condition			References
	Land use	Treated wastewater input	Stratification			CO_2 uptake rate (mmol C/ m²/day)	Measurement interval	Measurement season	
Estuarine systems									
Noordwijk	Urban/ farmland	Yes	Yes	–	–	<20.0	24 h continuous	September	Bakker et al. (1996)
York River estuary	Urban/ forest	Yes	Yes	–	–	2.1–5.6	Daytime snapshot	November to April	Raymond et al. (2000)
Randers Fjord	Farmland	Yes	Yes	No	2–6	10.0	24 h	April	Gazeau et al. (2005)
Tendo lagoon	Farmland	No	Yes	Yes	8–27	3.0–17.7	Snapshot	March to December	Kone et al. (2009), Kouame et al. (2009)
Aby lagoon	Farmland	No	Yes	Yes	–	7.4	Snapshot	Annual average	Kone et al. (2009), Kouame et al. (2009)
Changjiang estuary	Urban/ farmland	Yes	Yes	Yes	0–18	0.7	Snapshot	Annual average	Zhai and Dai (2009)
Bellamy River estuary	Urban/ farmland	No	–	–	3–7	12.0	–	April	Hunt et al. (2011)
Oyster River estuary	Urban/ farmland	Yes	–	–	4–5	17.2	–	April	Hunt et al. (2011)
Neuse River estuary	Urban/ farmland	Yes	Yes	–	7–20	0.5	Daytime continuous	Annual average	Crosswell et al. (2012)
Neuse River estuary	Urban/ farmland	Yes	Yes	–	–	0.1	Day/night	Annual average	Crosswell et al. (2017)
Godthabsfjord	Icecap	–	–	–	–	20.0	Snapshot	Annual average	Rysgaard et al. (2012)

Columbia River estuary	Urban/farmland	Yes	Yes	Yes	6	6.5–9.5	Daytime continuous	April	Evans et al. (2013)
Osaka Bay	Urban	Yes	Yes	Yes	10–50	8.3	Snapshot	Annual average	Fujii et al. (2013)
Tokyo Bay	Urban	Yes	Yes	Yes	0–300	8.8	Daytime snapshot	Annual average	Kubo et al. (2017)
Guanabara Bay	Urban	No	Yes	Yes	19–108	26.4–49.7	Day/night	Annual average	Cotovicz et al. (2015)
Matla estuary	Forest/farmland	Yes	No	No	3	7.9–8.6	24 h	Annual average	Akhand et al. (2016)
Simple mean and SD						10.8 ± 9.51			
Seagrass meadows, % cover									
Hasting River 10%	Farmland	Yes	–	–	–	1.0	Day/night	Annual average	Maher and Eyre (2012)
Camden haven 37%	Forest	Yes	–	–	–	5.0	Day/night	Annual average	Maher and Eyre (2012)
Wallis Lake 37%	Forest	Yes	–	–	–	5.0	Day/night	Annual average	Maher and Eyre (2012)
Albufera des Grau	Urban/farmland	Yes	Yes (slight)	Yes	0–200	8.1	Daytime snapshot	Annual average	Obrador and Pretus (2012)
Shiraho	Farmland	No	No	No	–	1.9	24 h	September	Watanabe et al. (2013)
Furen lagoon 80%	Farmland	Yes	Yes	No	1–7	6.0–10.4	24 h continuous	August	Tokoro et al. (2014)
Furen lagoon 80%	Farmland	Yes	Yes	No	–	1.5	Daytime snapshot	Annual average	Tokoro et al. (2014)
Kurihama Bay	Urban	Yes	No	No	1–4	2.5	Daytime snapshot	March and April	Tokoro et al. (2014)

(continued)

Table 11.2 (continued)

Location	Site condition					Flux and measurement condition				
	Land use	Treated wastewater input	Stratification	Hypoxic water mass	Chl-*a* (μg/L)	CO₂ uptake rate (mmol C/ m²/day)	Measurement interval	Measurement season	References
Fukido estuary	Forest	No	No	No	<2	86.4	24 h continuous	August	Tokoro et al. (2014)
Simple mean and SD						24.6 ± 44.1			
Kelp bed									
Southern California bight	Urban	–	–	–	0.5–8	59.4	24 h continuous	Annual average	Ikawa and Oechel (2015)

Most of the data summarized here were measured as snapshots (not 24-h continuous measurements) and did not include an annual cycle, so they may be biased and have high uncertainty. Modified from Kuwae et al. (2016)
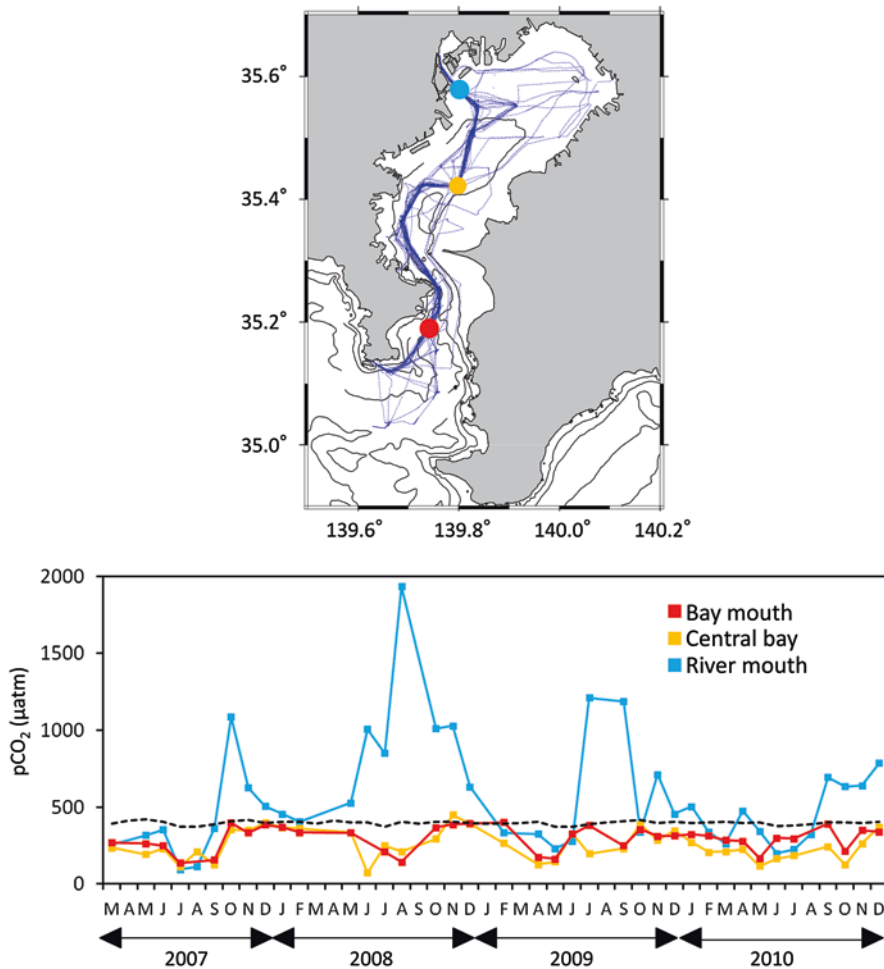
Fig. 11.6 The CO$_2$ concentration in seawater in Tokyo Bay. The dotted line shows the concentration of CO$_2$ in the atmosphere. When the concentration is below the dotted line, CO$_2$ in the atmosphere is taken up by the seawater. Except for the site near the incoming river, atmospheric CO$_2$ is taken up in the seawater throughout the year in Tokyo Bay. The bay becomes a sink even when considering the annual average of CO$_2$ gas exchange over its entire area (ca. 140 g CO$_2$/m^2/year). (Modified from Kubo et al. 2017)

which fluctuations in CO$_2$ concentration were measured continuously at various time scales, such as 24 h or throughout the year. Therefore, these statistics include large uncertainty and bias. In particular, in low-salinity waters, total alkalinity is generally low and the buffer effect of carbonate chemistry is weak, causing high temporal variability in CO$_2$ in water.
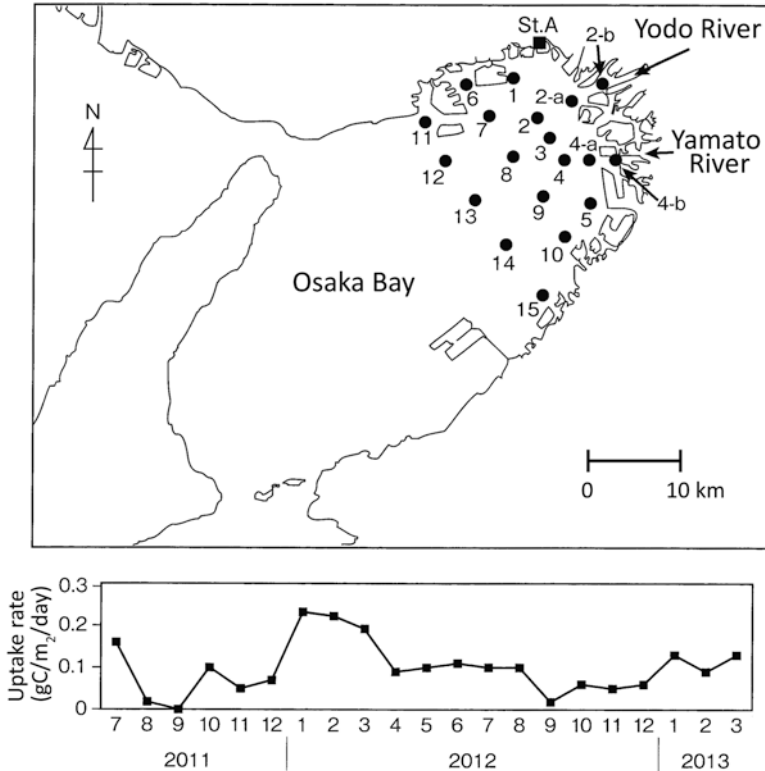
Fig. 11.7 Atmospheric CO_2 uptake rate in Osaka Bay. Atmospheric CO_2 is taken up throughout the year (ca. 133 g CO_2/m^2/year). The numbered dots indicate the sampling locations. (Modified from Fujii et al. 2013)

11.4 Future Studies

11.4.1 Enhancement of CO_2 Gas Exchange Data

Compared to terrestrial and open oceans, the data for CO_2 gas exchange in SCEs are limited (Laruelle et al. 2013), and there has been no description of SCE gas exchange even in the latest assessment report of the Intergovernmental Panel on Climate Change (IPCC 2013). In order to evaluate whether each SCE is a net sink or source, key data for carbon cycling such as CO_2 gas exchange, carbon chemistry in water, and the dynamics of organic carbon are indispensable (Maher and Eyre 2012; Obrador and Pretus 2012; Tokoro et al. 2014; Watanabe and Kuwae 2015). Furthermore, because the range and uncertainty of the gas exchange rate differ depending on the measurement period, long-term data are important for predicting future gas exchange rates and the extent of human impacts (Crosswell et al. 2017). Indeed, a numerical simulation predicted that the uptake rate of atmospheric CO_2 in

areas from estuaries to shelves will be accelerated in the future due to an increase in atmospheric CO$_2$ concentration and increased nutrient loads (Andersson and Mackenzie 2004).

11.4.2 Revaluation of Stored Carbon

Many studies on the importance of blue carbon ecosystems and their conservation are based on the premise that if the ecosystem degrades or disappears, all of the carbon stored will be mineralized and released into the atmosphere as CO$_2$ (e.g., McLeod et al. 2011). This assumption, however, is a worst case scenario and clearly overestimates emissions (Pendleton et al. 2012; Macreadie et al. 2014; Lovelock et al. 2017). Thus, further research is needed to examine the relationship between the degree of degradation or extinction of the ecosystem and indices such as the ecosystem area, vegetation biomass, net ecosystem production rate, and amount of carbon storage (Kuwae and Hori 2018).

As green carbon is stored in SCEs together with blue carbon, there is room for discussion as to whether the land-derived green carbon should also be included in the blue carbon storage function. It may be reasonable to include green carbon if the decision is based on the site where carbon is stored. Similarly, it may be reasonable to exclude green carbon if it is based on the site where CO$_2$ is first captured from the atmosphere. Indeed, some studies have estimated the contribution of blue carbon and green carbon separately (Middelburg et al. 1997; Kennedy et al. 2010; Dubois et al. 2012; Miyajima et al. 2015; Watanabe and Kuwae 2015; Kubo and Kanda 2017). Likewise, there needs to be discussion as to whether particulate blue carbon (POC) and macrophyte drifts that flow out of the SCE and are stored at the seabed of the shelf or the open ocean is also included as SCE blue carbon storage (Krause-Jensen and Duarte 2016; Duarte and Krause-Jensen 2017; Abo et al. 2018).

11.4.3 Mitigation of Climate Change Through Wastewater Treatment

In this chapter, we noted that CO$_2$ emission from human-impacted SCEs is suppressed because carbon flowing into the SCE has been largely removed by wastewater treatment. This means that CO$_2$ that would be emitted from the sea surface is instead emitted from the wastewater treatment plant. In other words, if we view the land and SCE as an integrated system, the amount of CO$_2$ taken up by the SCE may be canceled out by the emission from decomposition of organic matter in the open aeration tank of the wastewater treatment plant. However, by appropriate management of wastewater treatment, we are able to suppress CO$_2$ emission from the treatment plant or capture carbon (Fig. 11.8). For example, the generated sludge can be
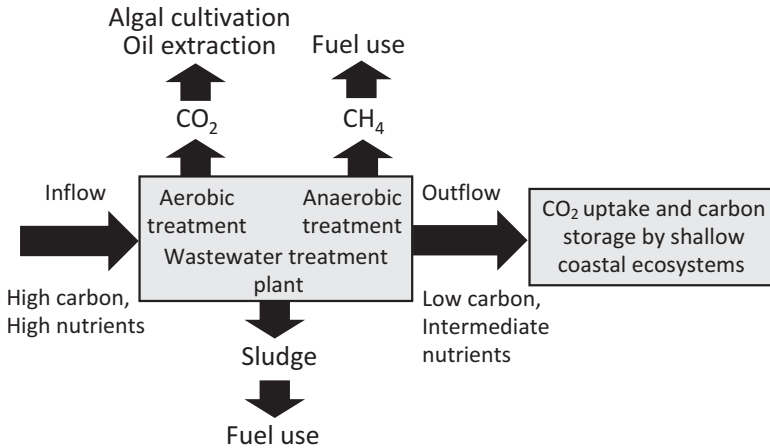
Fig. 11.8 Conceptual diagram for the effective reduction of greenhouse gas emissions using wastewater treatment and SCEs in an integrated terrestrial–marine system

used as fuel. In addition, by collecting CO_2 generated by wastewater treatment and introducing it into a culture tank of algae, CO_2 can be absorbed by algae. The oils extracted from the algal bodies can also be used as an alternative fuel and industrial material. Moreover, by using an anaerobic treatment method (e.g., methane fermentation), the generated gas can also be converted into fuel (Parkin and Owen 1986). Furthermore, it is also possible to adjust the quality of the treated water, such as the carbon and nutrient concentrations, by regulating the extent of the treatment as well as selecting the treatment method, including removal of phosphorus by the coagulating sedimentation method and removal of nitrogen by the anaerobic-anoxic-oxic (A2O) method.

The complexity of the relationship between wastewater treatment and CO_2 gas exchange in SCEs reflects the complex relationship between the social system and adjacent ecosystem. Therefore, biogeochemical models and numerical simulations are necessary to enact appropriate ecosystem-based mitigation measures.

11.5 Conclusions

In this chapter we discussed how human-impacted SCEs can be managed to help mitigate climate change. Through a detailed review of past findings and in situ case studies, we provided a mechanistic explanation of how SCEs can serve as net sinks for atmospheric CO_2. Furthermore, we showed that the environmental conditions necessary for a net sink match with those of SCEs affected by human impacts. That is, by coordinating the interrelationships between social systems and ecosystems, we can create new means of utilizing human-impacted SCEs to mitigate climate

change (as a carbon reservoir and as a sink of atmospheric CO$_2$). In particular, vegetated SCEs or blue carbon ecosystems (e.g., mangroves, salt marshes, and seagrass meadows) are important because of their strong capability for carbon accumulation and long-term storage.

In addition, technology to mitigate climate change through conservation and restoration of SCEs, that is, technology utilizing blue carbon ecosystems, is both feasible and more sustainable than other mitigation measures (e.g., marine iron fertilization and carbon capture and storage) in terms of technical difficulty, cost, ecological risk, social acceptance, operation, and ethics (Nellemann et al. 2009; Cusack et al. 2014). Furthermore, the conservation and restoration of SCEs can result in not only the mitigation of climate change but also other ecosystem services (co-benefits), including an improved food supply, water purification, tourism, recreation, and disaster prevention (Kuwae and Hori 2018). However, because ecosystem-based mitigation technologies use natural systems, there are large diurnal, seasonal, and annual fluctuations and high uncertainty. Therefore, as we develop systems for the utilization of SCEs to help mitigate climate change, it is necessary to gather field data enabling the evaluation of uncertainty as well as to improve coupled geophysical–biogeochemical modeling for future projections.

References

Abo K, Sugimatsu K, Hori M et al (2018) Quantifying the fate of captured carbon: from seagrass meadow to deep sea. In: Kuwae T, Hori M (eds) Blue carbon in shallow coastal ecosystems: carbon dynamics, policy, and implementation. Springer, Singapore, pp 251–271

Akhand A, Chanda A, Manna S et al (2016) A comparison of CO$_2$ dynamics and air-water fluxes in a river-dominated estuary and a mangrove-dominated marine estuary. Geophys Res Lett 43:11726–11735

Akhand A, Chanda A, Das S, Hazra S, Kuwae T (2018) CO$_2$ fluxes in mangrove ecosystems. In: Kuwae T, Hori M (eds) Blue carbon in shallow coastal ecosystems: carbon dynamics, policy, and implementation. Springer, Singapore, pp 185–221

Andersson AJ, Mackenzie FT (2004) Shallow-water oceans: a source or sink of atmospheric CO$_2$? Front Ecol Environ 2:348–353

Arrieta JM, Mayol E, Hansman RL, Herndl GJ, Dittmar T, Duarte CM (2015) Dilution limits dissolved organic carbon utilization in the deep ocean. Science 348:331–333

Bakker DC, de Baar HJ, de Wilde HP (1996) Dissolved carbon dioxide in Dutch coastal waters. Mar Chem 55:247–263

Bauer JE, Cai WJ, Raymond PA, Bianchi TS, Hopkinson CS, Regnier PA (2013) The changing carbon cycle of the coastal ocean. Nature 504:61–70

Borges A, Abril G (2011) Carbon dioxide and methane dynamics in estuaries. In: Wolanski E, McLusky D (eds) Treatise on estuarine and coastal science, volume 5: biogeochemistry. Academic, Waltham, pp 119–161

Borges AV, Delille B, Frankignoulle M (2005) Budgeting sinks and sources of CO$_2$ in the coastal ocean: diversity of ecosystem counts. Geophys Res Lett 32:L14601

Cai WJ (2011) Estuarine and coastal ocean carbon paradox: CO$_2$ sinks or sites of terrestrial carbon incineration? Annu Rev Mar Sci 3:123–145

Canfield DE (1994) Factors influencing organic carbon preservation in marine sediments. Chem Geol 114:315–329

Chambers JQ, Higuchi N, Tribuzy ES, Trumbore SR (2001) Carbon sinks for a century. Nature 410:429

Chen CTA, Zhai W, Dai M (2008) Riverine input and air–sea CO_2 exchanges near the Changjiang (Yangtze River) estuary: status quo and implication on possible future changes in metabolic status. Cont Shelf Res 28:1476–1482

Chen CTA, Huang TH, Fu YH, Bai Y, He X (2012) Strong sources of CO_2 in upper estuaries become sinks of CO_2 in large river plumes. Curr Opin Environ Sustain 4:179–185

Chen CTA, Huang TH, Chen YC, Bai Y, He X, Kang Y (2013) Air–sea exchange of CO_2 in world's coastal seas. Biogeosciences 10:6509–6544

Cole JJ, Prairie YT, Caraco NF et al (2007) Plumbing the global carbon cycle: integrating inland waters into the terrestrial carbon budget. Ecosystems 10:172–185

Cotovicz LC Jr, Knoppers BA, Brandini N, Santos SC, Abril G (2015) A strong CO_2 sink enhanced by eutrophication in a tropical coastal embayment (Guanabara Bay, Rio de Janeiro, Brazil). Biogeosciences 12:6125–6146

Crosswell JR, Wetz MS, Hales B, Paerl HW (2012) Air–water CO_2 fluxes in the microtidal Neuse River estuary, North Carolina. J Geophys Res 117:C8

Crosswell JR, Anderson IC, Stanhope JW et al (2017) Carbon budget of a shallow, lagoonal estuary: transformations and source-sink dynamics along the river-estuary-ocean continuum. Limnol Oceanogr 62:S29–S45

Cusack DF, Axsen J, Shwom R, Hartzell-Nichols L, White S, Mackey KRM (2014) An interdisciplinary assessment of climate engineering strategies. Front Ecol Environ 12:280–287

Delille B, Borges AV, Delille D (2009) Influence of giant kelp beds (*Macrocystis pyrifera*) on diel cycles of pCO_2 and DIC in the Sub-Antarctic coastal area. Estuar Coast Shelf Sci 81:114–122

Duarte CM, Krause-Jensen D (2017) Export from seagrass meadows contributes to marine carbon sequestration. Front Mar Sci 4:13

Duarte CM, Losada IJ, Hendriks IE, Mazarrasa I, Marbà N (2013) The role of coastal plant communities for climate change mitigation and adaptation. Nat Clim Chang 3:961–968

Dubois S, Savoye N, Grémare A et al (2012) Origin and composition of sediment organic matter in a coastal semi-enclosed ecosystem: an elemental and isotopic study at the ecosystem space scale. J Mar Syst 94:64–73

Endo T, Otani S (2018) Carbon storage in tidal flats. In: Kuwae T, Hori M (eds) Blue carbon in shallow coastal ecosystems: carbon dynamics, policy, and implementation. Springer, Singapore, pp 129–151

Evans W, Hales B, Strutton PG (2013) pCO_2 distributions and air–water CO_2 fluxes in the Columbia River estuary. Estuar Coast Shelf Sci 117:260–272

Fourqurean JW, Duarte CM, Kennedy H et al (2012) Seagrass ecosystems as a globally significant carbon stock. Nat Geosci 5:505–509

Fujii T, Fujiwara T, Nakayama K (2013) Fluxes of carbon dioxide in the eastern regions of Osaka Bay. JSCE Ann J Coast Eng 69:1111–1115 (in Japanese, English summary)

Gattuso JP, Frankignoulle M, Wollast R (1998) Carbon and carbonate metabolism in coastal aquatic ecosystems. Annu Rev Ecol Syst 29:405–434

Gazeau F, Borges AV, Barron C et al (2005) Net ecosystem metabolism in a micro-tidal estuary (Randers Fjord, Denmark): evaluation of methods. Mar Ecol Prog Ser 301:23–41

Grimm NB, Faeth SH, Golubiewski NE et al (2008) Global change and the ecology of cities. Science 319:756–760

Hartnett HE, Keil RG, Hedges JI, Devol AH (1998) Influence of oxygen exposure time on organic carbon preservation in continental margin sediments. Nature 391:572–574

Hendriks IE, Sintes T, Bouma T, Duarte CM (2007) Experimental assessment and modeling evaluation of the effects of seagrass (*P. oceanica*) on flow and particle trapping. Mar Ecol Prog Ser 356:163–173

Hunt CW, Salisbury JE, Vandemark D, McGillis W (2011) Contrasting carbon dioxide inputs and exchange in three adjacent New England estuaries. Estuar Coasts 34:68–77

Ikawa H, Oechel WC (2015) Temporal variations in air-sea CO$_2$ exchange near large kelp beds near San Diego, California. J Geophys Res Ocean 120:50–63

Inoue T (2018) Carbon sequestration in mangroves. In: Kuwae T, Hori M (eds) Blue carbon in shallow coastal ecosystems: carbon dynamics, policy, and implementation. Springer, Singapore, pp 73–99

IPCC (2013) Fifth assessment report of the intergovernmental panel on climate change. IPCC, Geneva

Jiao N, Robinson C, Azam F et al (2014) Mechanisms of microbial carbon sequestration in the ocean: future research directions. Biogeosciences 11:5285–5306

Kaushal SS, Belt KT (2012) The urban watershed continuum: evolving spatial and temporal dimensions. Urban Ecosyst 15:409–435

Kayanne H, Suzuki A, Saito H (1995) Diurnal changes in the partial pressure of carbon dioxide in coral reef water. Science 269:214–216

Kayanne H, Hata H, Kudo S et al (2005) Seasonal and bleaching-induced changes in coral reef metabolism and CO$_2$ flux. Glob Biogeochem Cycles 19:GB3015

Kennedy H, Beggins J, Duarte CM et al (2010) Seagrass sediments as a global carbon sink: isotopic constraints. Glob Biogeochem Cycles 24:GB4026

Koho KA, Nierop KGJ, Moodley L et al (2013) Microbial bioavailability regulates organic matter preservation in marine sediments. Biogeosciences 10:1131–1141

Kone YJM, Abril G, Kouadio KN, Delille B, Borges AV (2009) Seasonal variability of carbon dioxide in the rivers and lagoons of Ivory Coast (West Africa). Estuar Coasts 32:246–260

Kouame KV, Yapo OB, Mambo V, Seka A, Tidou AS, Houenou P (2009) Physicochemical characterization of the waters of the coastal rivers and the lagoonal system of Cote d'Ivoire. J Appl Sci 9:1517–1523

Kragh T, Søndergaard M (2009) Production and decomposition of new DOC by marine plankton communities: carbohydrates, refractory components and nutrient limitation. Biogeochemistry 96:177–187

Krause-Jensen D, Duarte CM (2016) Substantial role of macroalgae in marine carbon sequestration. Nat Geosci 9:737–742

Kubo A, Kanda J (2017) Seasonal variations and sources of sedimentary organic carbon in Tokyo Bay. Mar Pollut Bull 114:637–643

Kubo A, Kawai MY, Kanda J (2015) Seasonal variations in concentration and composition of dissolved organic carbon in Tokyo Bay. Biogeosciences 12:269–279

Kubo A, Maeda Y, Kanda J (2017) A significant net sink for CO$_2$ in Tokyo Bay. Sci Rep 7:44355

Kuwae T, Hori M (2018) The future of blue carbon: addressing global environmental issues. In: Kuwae T, Hori M (eds) Blue carbon in shallow coastal ecosystems: carbon dynamics, policy, and implementation. Springer, Singapore, pp 347–373

Kuwae T, Kanda J, Kubo A et al (2016) Blue carbon in human-dominated estuarine and shallow coastal systems. Ambio 45:290–301

Laruelle GG, Durr HH, Lauerwald R et al (2013) Global multi-scale segmentation of continental and coastal waters from the watersheds to the continental margins. Hydrol Earth Syst Sci 17:2029–2051

Lønborg C, Álvarez-Salgado XA, Davidson K, Miller AE (2009) Production of bioavailable and refractory dissolved organic matter by coastal heterotrophic microbial populations. Estuar Coast Shelf Sci 82:682–688

Longhurst AR, Harrison WG (1989) The biological pump: profiles of plankton production and consumption in the upper ocean. Prog Oceanogr 22:47–123

Lovelock CE, Atwood T, Baldock J et al (2017) Assessing the risk of carbon dioxide emissions from blue carbon ecosystems. Front Ecol Environ 15:257–265

Macreadie PI, Baird ME, Trevathan-Tackett SM, Larkum AWD, Ralph PJ (2014) Quantifying and modelling the carbon sequestration capacity of seagrass meadows: a critical assessment. Mar Pollut Bull 83:430–439

Maher DT, Eyre BD (2012) Carbon budgets for three autotrophic Australian estuaries: implications for global estimates of the coastal air-water CO_2 flux. Glob Biogeochem Cycles 26:GB1032

McIntyre NE, Knowles-Yánez K, Hope D (2000) Urban ecology as an interdisciplinary field: differences in the use of "urban" between the social and natural sciences. Urban Ecosyst 4:5–24

McLeod E, Chmura GL, Bouillon S et al (2011) A blueprint for blue carbon: toward an improved understanding of the role of vegetated coastal habitats in sequestering CO_2. Front Ecol Environ 9:552–560

Middelburg JJ, Nieuwenhuize J, Lubberts RK, van de Plassche O (1997) Organic carbon isotope systematics of coastal marshes. Estuar Coast Shelf Sci 45:681–687

Miyajima T, Hamaguchi M (2018) Carbon sequestration in sediment as an ecosystem function of seagrass meadows. In: Kuwae T, Hori M (eds) Blue carbon in shallow coastal ecosystems: carbon dynamics, policy, and implementation. Springer, Singapore, pp 33–71

Miyajima T, Hori M, Hamaguchi M et al (2015) Geographic variability in organic carbon stock and accumulation rate in sediments of East and Southeast Asian seagrass meadows. Glob Biogeochem Cycles 29:397–415

Miyajima T, Hori M, Hamaguchi M, Shimabukuro H, Yoshida G (2017) Geophysical constraints for organic carbon sequestration capacity of *Zostera marina* seagrass meadows and surrounding habitats. Limnol Oceanogr 62:954–972

Moran MA, Sheldon WM, Zepp RG (2000) Carbon loss and optical property changes during long-term photochemical and biological degradation of estuarine dissolved organic matter. Limnol Oceanogr 45:1254–1264

Nellemann C, Corcoran E, Duarte CM et al (2009) Blue carbon: a rapid response assessment. United Nations Environmental Programme, GRID-Arendal, Birkeland Trykkeri AS, Birkeland

Obrador B, Pretus JL (2012) Budgets of organic and inorganic carbon in a Mediterranean coastal lagoon dominated by submerged vegetation. Hydrobiology 699:35–54

Ogawa H, Amagai Y, Koike I, Kaiser K, Benner R (2001) Production of refractory dissolved organic matter by bacteria. Science 292:917–920

Otani S, Endo T (2018) CO_2 flux in tidal flats and salt marshes. In: Kuwae T, Hori M (eds) Blue carbon in shallow coastal ecosystems: carbon dynamics, policy, and implementation. Springer, Singapore, pp 223–250

Parkin GF, Owen WF (1986) Fundamentals of anaerobic digestion of wastewater sludges. J Environ Eng 112:867–920

Pendleton L, Donato DC, Murray BC et al (2012) Estimating global "blue carbon" emissions from conversion and degradation of vegetated coastal ecosystems. PLoS One 7:e43542

Le Quéré C, Moriarty R, Andrew RM et al (2018) Global Carbon Budget 2017. Earth Syst Sci Data 10:405–448

Raymond PA, Bauer JE, Cole JJ (2000) Atmospheric CO_2 evasion, dissolved inorganic carbon production, and net heterotrophy in the York River estuary. Limnol Oceanogr 45:1707–1717

Raymond PA, Hartmann J, Lauerwald R et al (2013) Global carbon dioxide emissions from inland waters. Nature 503:355–359

Regnier PAG, Friedlingstein P, Ciais P et al (2013) Anthropogenic perturbation of the carbon fluxes from land to ocean. Nat Geosci 6:597–607

Rysgaard S, Mortensen J, Juul-Pedersen T et al (2012) High air–sea CO_2 uptake rates in nearshore and shelf areas of southern Greenland: temporal and spatial variability. Mar Chem 128:26–33

Sedlak RI (1991) Phosphorus and nitrogen removal from municipal wastewater: principles and practice. CRC Press, Boca Raton

Sholkovitz ER (1976) Flocculation of dissolved organic and inorganic matter during the mixing of river water and seawater. Geochim Cosmochim Acta 40:831–845

Smith SV (1981) Marine macrophytes as a global carbon sink. Science 211:838–840

Sugimatsu K, Yagi H, Abo K et al (2015) A coupled particle tracking– carbon cycle modeling system for sedimentary organic carbon derived from drafting seagrass in Seto Inland Sea. JSCE Annu J Coast Eng 71:1387–1392 (in Japanese, English summary)

Tanaka Y, Ogawa H, Miyajima T (2011a) Bacterial decomposition of coral mucus as evaluated by long-term and quantitative observation. Coral Reefs 30:443–449

Tanaka Y, Ogawa H, Miyajima T (2011b) Production and bacterial decomposition of dissolved organic matter in a fringing coral reef. J Oceanogr 67:427–437

Taylor PG, Townsend AR (2010) Stoichiometric control of organic carbon–nitrate relationships from soils to the sea. Nature 464:1178–1181

Tokoro T, Hosokawa S, Miyoshi E et al (2014) Net uptake of atmospheric CO$_2$ by coastal submerged aquatic vegetation. Glob Chang Biol 20:1873–1884

Tokoro T, Watanabe K, Tada K, Kuwae T (2018) Air–water CO$_2$ flux in shallow coastal waters: theoretical background, measurement methods, and mechanisms. In: Kuwae T, Hori M (eds) Blue carbon in shallow coastal ecosystems: carbon dynamics, policy, and implementation. Springer, Singapore, pp 153–184

Tsunogai S, Watanabe S, Sato T (1999) Is there a continental shelf pump for the absorption of atmospheric CO$_2$? Tellus 51:701–712

Wada S, Aoki MN, Mikami A et al (2008) Bioavailability of macroalgal dissolved organic matter in seawater. Mar Ecol Prog Ser 370:33–44

Wanninkhof R (1992) Relationship between wind-speed and gas-exchange over the ocean. J Geophys Res 97:7373–7382

Watanabe K, Kuwae T (2015) How organic carbon derived from multiple sources contributes to carbon sequestration processes in a shallow coastal system. Glob Chang Biol 21:2612–2623

Watanabe A, Nakamura T (2018) Carbon dynamics in coral reefs. In: Kuwae T, Hori M (eds) Blue carbon in shallow coastal ecosystems: carbon dynamics, policy, and implementation. Springer, Singapore, pp 273–293

Watanabe A, Yamamoto T, Nadaoka K et al (2013) Spatiotemporal variations in CO$_2$ flux in a fringing reef simulated using a novel carbonate system dynamics model. Coral Reefs 32:239–254

Zhai W, Dai M (2009) On the seasonal variation of air–sea CO$_2$ fluxes in the outer Changjiang (Yangtze River) Estuary, East China Sea. Mar Chem 117:2–10

Zonneveld KAF, Versteegh GJM, Kasten S et al (2010) Selective preservation of organic matter in marine environments: processes and impact on the sedimentary record. Biogeosciences 7:483–511

Chapter 12
Carbon Offset Utilizing Coastal Waters: Yokohama Blue Carbon Project

Masato Nobutoki, Satoru Yoshihara, and Tomohiro Kuwae

Abstract Although the coastal port city of Yokohama has carried out a campaign to improve conditions for marine ecosystems, the nation of Japan has not yet utilized coastal waters as an option for global warming countermeasures. Based on the concept of blue carbon ecosystems advocated by the United Nations Environment Programme, since 2011 Yokohama City has been conducting a social experiment called the Yokohama Blue Carbon Project, which serves to counter climate change and includes a novel carbon offset campaign. Yokohama City, which was chosen by the Japanese government as an environmental Future City in countering global warming, is aiming to transition from being a port city to a marine environmental city. In this chapter, we describe the successes and challenges of the Yokohama Blue Carbon Project and we report on the project's involvement in the World Triathlon Series held in Yokohama as an example of a carbon offset credit framework utilizing coastal waters.

12.1 Introduction

To date, urban design and development in coastal communities have been a story of land development, with little thought given to the adjacent ocean. For urbanized coastal areas in Japan, the ocean has mainly provided logistical functions in urban design and, in that sense, contributed greatly to industrial development. Furthermore,

M. Nobutoki (✉)
Climate Change Policy Headquarters, City of Yokohama, Naka-ku, Yokohama, Japan

EX Research Institute, Toshima-ku, Tokyo, Japan

S. Yoshihara
Technical Development Department, Yachiyo Engineering Co., Ltd, Taito-ku, Tokyo, Japan

T. Kuwae
Coastal and Estuarine Environment Research Group, Port and Airport Research Institute, Yokosuka, Japan

in order to expand and develop cities, the coast and ocean have provided a place for landfill with waste and sand/mud.

Likewise, measures against global warming have primarily focused on land-based efforts. The municipal government and other institutions in Yokohama City have worked to improve environmental conditions along the coast and protect marine ecosystems. As a result, Yokohama now has water quality that is good enough to allow the World Triathlon Series to be held there. Despite these environmental efforts, however, little focus has been given to the relationship between global warming countermeasures and the sea.

Yokohama City was selected as an Environmental Model City in 2008 by the Cabinet Office, Government of Japan. This designation is awarded to advanced cities that aim to "realize urban design that results in a considerable reduction of CO_2 and fosters sustainable low-carbon lifestyles". In April 2010, Yokohama City was selected as a next-generation energy and social system demonstration area by the Japanese Ministry of Economy, Trade and Industry. Furthermore, it was selected as an environmental Future City in December 2011 by the Cabinet Office, Government of Japan. As such, Yokohama City will continue to focus on the three values of environment, society, and economy while solving common problems associated with environmental degradation and an aging society. The Future City initiatives resulted in the subsequent blue carbon initiative, the Yokohama Blue Carbon Project.

Using carbon offsets as a measure against global warming requires raising the awareness and changing the behavior of citizens. Furthermore, carbon offset needs to be integrated into urban design. In 2009, the United Nations Environment Programme published the Blue Carbon Report (Nelleman et al. 2009), which highlights the critical role of shallow coastal ecosystems in maintaining climate and aims to assist policymakers in incorporating an oceans agenda into national and international climate change initiatives. Although the region's blue carbon potential was high, at that time Yokohama City officials thought that it would not be possible to initiate blue carbon measures because it was difficult to effectively demonstrate the outcomes. However, officials also felt that the ocean could be worked into urban design and blue carbon could be coupled with land-based global warming countermeasures. The Future City initiatives inspired local government planners to manage all the new measures comprehensively from this new perspective, and the city decided to bet on blue carbon. Leaders were also motivated by the challenges of this project, as there were no practical examples in the world to follow.

In this chapter, we describe the progress of the Yokohama Blue Carbon Project started in 2011, which is to our best knowledge, the first carbon offset project in the world utilizing coastal waters, and the expected future development of this project.

12.2   City Development and Global Warming Countermeasures

Countermeasures against global warming are an urgent task for humanity. At COP 21 held in 2015, numerous countries entered into the groundbreaking Paris Agreement, which requires the implementation of various countermeasures in the future. To date, Japan's global warming countermeasures have given priority to the implementation of advanced environmental technologies. Central and local governments have been given subsidies to introduce advanced technologies at which Japan excels, such as electric vehicles and solar power generation, as countermeasures. In Yokohama City, officials used subsidies to introduce new technologies and environmental awareness projects.

   The mayor of Copenhagen gave a speech at an international conference held in Yokohama City, saying that "Our aim is not only to reduce carbon dioxide but also that people select this city and comfortably spend their lives here as citizens. The purpose is to make it viable." Yokohama City officials decided it was necessary to administer these projects from this viewpoint to evolve into one of the world's top cities. The Yokohama municipal government began to enact global warming countermeasures in all departments, aiming to be one of the most advanced cities from various livability perspectives in addition to reducing atmospheric carbon dioxide (CO_2) levels.

12.2.1   Launch of Climate Change Policy Headquarters

In 2007, Yokohama City set up the Climate Change Policy Headquarters, an agency run by the deputy mayor, established councils that represent government–citizen partnerships, and opened headquarters to promote global warming countermeasures in each of its 18 districts. In addition, the city created the Yokohama Eco School, which is a place for educating members of industry, government, and academia, for collaborating on policy proposals, and for developing future leaders in combating climate change. In this way, Yokohama City has developed a coherent system to promote global warming countermeasures that includes all municipal departments and citizens.

   Although some departments were resistant to such changes, the mayor and deputy mayor supported these efforts and recognized that the programs would be meaningless unless done in all departments. Consequently, the officials of Yokohama City insisted that it be an all-department project, created a subcommittee organization, promoted a comprehensive understanding by a large number of staff, and

offered a great deal of encouragement. In addition, the city government set concrete numerical targets, such as "reduce per capita greenhouse gas emissions by 30% or more by 2025 compared to 2004" and prepared comprehensive measures to combat global warming.

The headquarters developed a comprehensive approach to environmental management, including hard areas such as urban development, architecture, roads, and harbors and soft areas such as citizens, education, health and welfare, children, young adults, and so on. However, it was not easy to raise the awareness of global warming issues in departments that did not directly oversee environmental management. It took additional budget and extra work to accomplish that.

These initiatives required not only energy conservation in the city but also energy creation, energy storage, and technologies related to the construction and renovation of buildings and houses, as well as establishing economic adaptability, effective environmental education represented by Education for Sustainable Development, and citizen activities. The headquarters thus continued to communicate with department heads to understand what each required to advance these initiatives in a balanced manner. It was also necessary to fully use the power of citizens.

The natural conditions of Yokohama City also include lush green forests and agricultural fields. However, of the 140 km of coastline in Yokohama City, the natural and restored beaches that are accessible to citizens are only about 1 km, with the rest occupied by industrial and port facilities. Taking all of these facts into consideration, Yokohama City officials are making the best use of these resources while pursuing a new city structure that will help to mitigate global warming.

12.2.2 Yokohama Green Valley Initiative

Along with 12 other cities, Yokohama City was designated as an Environmental Model City in a program established by the Japanese government in 2008. The theme of Yokohama City's proposal was "achieving a zero carbon lifestyle in a mega city by demonstrating citizen power through sharing knowledge, expanding options, and promoting action."

The Yokohama Green Valley Initiative was established as one of the pillars of being selected as an Environmental Model City. Similar to Silicon Valley in the United States in the information and communication technology field, Yokohama Green Valley is nomenclature that implies a concentration of companies working in the environment and energy fields. The coastal area of Kanazawa Ward was selected as a model because it has about 1000 small and medium-sized companies and various public facilities and universities, and it is the only area with natural coastline in Yokohama City.

Yokohama Green Valley became the basis for implementing the Yokohama Blue Carbon Project. Three key items of the Green Valley concept are described below.

Developing Energy Measures for a Low-Carbon Society As an Environmental Model City, citizens are working toward saving energy and various renewable energy projects have been introduced, which have helped to reduce the utility expenses of citizens and business operators. Furthermore, by utilizing a region rich in natural resources such as clean air, rivers, and ocean, forming an ultimate low-carbon life practice area that anyone with a balance between environment and economy.

Fostering Environmental and Energy Industries Required Worldwide Having all business operators create their own energy supply and establishing a mechanism that enables business operators to flexibly deal with energy supply and demand allows business activities to be low-carbon. In addition, collaboration among businesses, government agencies, research institutes, universities, and colleges fosters the creation of products and services that are available to world markets. These new collaborative mechanisms and organizations in turn foster new entrepreneurs in the environmental and energy fields.

Creating a Leading Environmental Education Base in Japan The Yokohama Green Valley provides an opportunity for environmental education courses that allow students to experience and learn about innovative technologies and social institutions as well as the conservation of natural environments in urban areas. These educational experiences are available not only to Japanese citizens but also to visitors and tourists from all over the world.

Indeed, Yokohama City has entered an era of great change. Citizens and municipal officials aim for the port city of Yokohama to become an oceanic environmental city with an international perspective. The philosophy underlying the Green Valley concept is future community development based on reviewing and revitalizing regional industries, acknowledging the existence and potential of the ocean, and initiating global warming countermeasures.

12.3 Launch of the Yokohama Blue Carbon Project

12.3.1 Carbon Offset Project with Forests

In 2009, Yokohama City began carbon offset projects with forests, and the lessons learned in these projects were helpful in the subsequent Yokohama Blue Carbon Project. First, city officials established a joint research group on global warming countermeasures with three local governments, aiming to devise a mechanism to obtain carbon offset credit. The waterworks bureau, which is responsible for reforestation of water source forests (forests for protecting the source of a stream), is currently promoting the project, with 16 companies and organizations participating.

In conjunction with these 16 partners, Yokohama City owns more than 2800 ha of water source forest in Doshi village, Minamitsuru gun, Yamanashi prefecture. In short, Yokohama City provides funds for the management and recharging of water source forests, and the companies and organizations acquire the credits for CO_2 uptake by the forests. As a result, clean water is secured in the downstream area of Yokohama and carbon is sequestered as a global warming countermeasure. Yokohama City believes that such collaboration between cities and private companies will be a very effective measure in the future.

12.3.2 Initiation of the Blue Carbon Project

Japan's coastline spans about 35,000 km, the sixth largest in the world, making it a good candidate as a major blue carbon reservoir. Yokohama City officials anticipated the great potential of blue carbon and recognized this as a good future business opportunity for the local economy. In addition, the ability to offset carbon along the local coast should inspire citizens of other ocean cities, making Yokohama City a model of sustainable community development for the future. After much preliminary work and a delay caused by the Great East Japan Great Earthquake, the project was started in November 2011.

The first problem that needed to be solved was selecting the project sites. The seas around Japan are strictly regulated and managed, and it was anticipated that obstacles would arise in relation to port and fishery authorities. Even though the goal of the project was mitigation of global warming, we recognized that site selection would be difficult.

Yokohama City officials had an opportunity to discuss the project with Mr. Nobuyuki Furukawa, the president of Yokohama Hakkeijima Inc., located in Kanazawa Ward. Yokohama Hakkeijima Sea Paradise is an amusement park complex including one of the Japan's largest aquariums, a shopping mall, a hotel, a marina, and other attractions. In these discussions, the president recognized the importance of this work and soon gave permission for the Blue Carbon Project to be located within the sea owned by Yokohama Hakkeijima. The president said that while some overseas aquariums are based on marine research laboratories, those in Japan are solely for entertainment, and he relished the opportunity for the company to become involved in these experiments.

12.4 Implementation of the Yokohama Blue Carbon Project

12.4.1 Project Framework and Objectives

As detailed in the framework illustrated in Fig. 12.1, in addition to blue carbon, Yokohama City introduced the concept of blue resources, both of which are included in the Yokohama Blue Carbon Project in order to make the carbon credit more
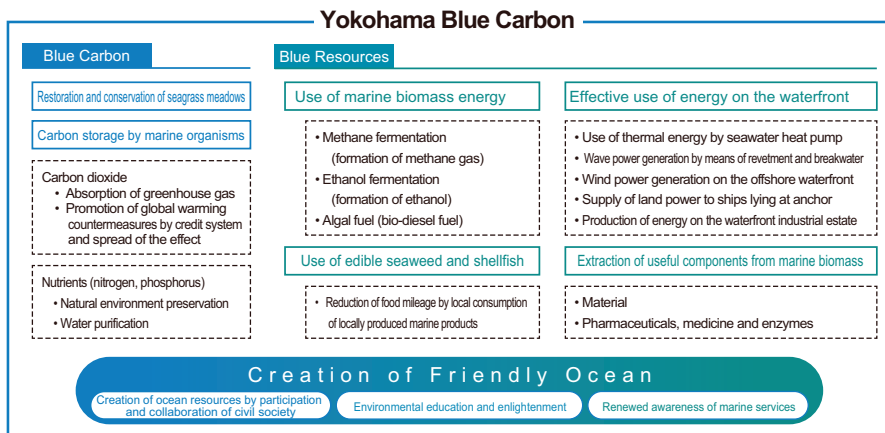
Fig. 12.1   Framework of Yokohama Blue Carbon Project

attractive for citizens and local companies. Blue resources are tailored to be comprehensive measures undertaken in the ocean and seaside area, with a view toward use of energy from the sea (biomass energy, seawater-source heat pump) and reducing the carbon footprint through the reduction of seafood mileage and use of alternative materials from marine sources.

In addition to blue carbon and blue resources, Yokohama City officials decided to pursue a "Friendly Ocean" (Fig. 12.1) because they recognized that building a good relationship between people and the ocean is also important for the success of the project. Thus, the objectives of the Yokohama Blue Carbon Project are not limited to measures against global warming, but also forging connections between the environment (terrestrial and marine), society (citizens, administration), economy (enterprise, regional industry, tourism), innovation, and improving the quality of civic life. Specifically, from the environmental point of view, this project aims at preventing global warming, water purification, and biodiversity conservation; from the societal point of view, enhancing social amenities and improving the Yokohama brand; and from the economic point of view, increasing resources, food supply, tourism, and various synergistic effects (co-benefits) centered around global warming prevention.

The social experiments started in 2014. The first experiment was a carbon offset project related to the Fifth Yokohama Seaside Triathlon (Table 12.1), a sports event held in Yokohama. This experiment had two objectives regarding the early operation of the Yokohama Blue Carbon Credit system: (1) grasp the issues involved in the actual operation of the credit system in collaboration with city officials and consider improvement measures, and (2) increase awareness of the Yokohama Blue Carbon Project among citizens and assess the effect of raising awareness.

This social experiment was to offset the CO_2 emissions associated with holding the Yokohama Seaside Triathlon through emission reduction by the Yokohama City Fishery Cooperative Association (reducing energy use of edible seaweed production and food mileage) and Yokohama Hakkeijima Inc. (use of seawater-source heat

Table 12.1 Summary of the fifth Yokohama Seaside Triathlon

Places	Yokohama Hakkeijima Sea Paradise
	Sea Park in Yokohama City around Kanazawa Industrial Park
Date	28 September 2014 (Sunday)
Number of competitors	1014 (from all over Japan and Yokohama)
Sponsor	Yokohama Seaside Triathlon Convention Executive Committee
Greenhouse gas emissions	5.7 tonnes CO_2 (including offset target of 4.4 tonnes CO_2)
Remarks	Places where credits were created and used were close
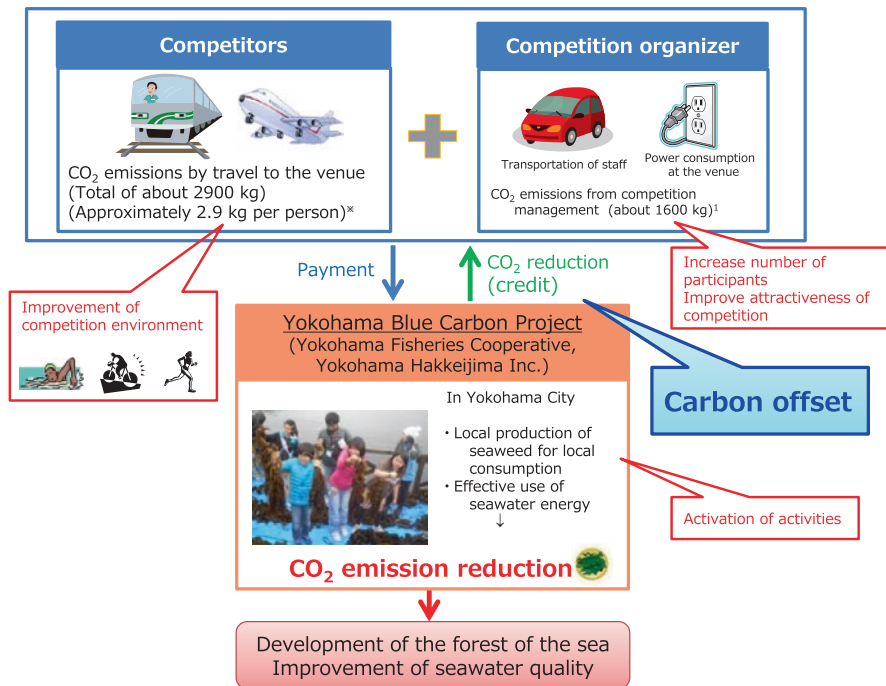
[1] Calculated using the results of the competition in 2013

Fig. 12.2 Overview of carbon offset in the Yokohama Blue Carbon Project

pump) (Fig. 12.2). Here, CO_2 emissions associated with holding the event were calculated with reference to Japanese Ministry of the Environment guidelines (Table 12.2), namely, emission from (1) transportation of operators and participants based on fuel or electricity consumption of airplanes, automobiles, trains, and other modes, and (2) electricity usage at the event venue, calculated based on the electricity usage associated with setting up the venue, operation, and withdrawing the venue. The Yokohama Seaside Triathlon Convention Executive Committee decided to offset the emitted carbon by purchasing and utilizing carbon offset credits generated by

Table 12.2 CO_2 emissions associated with the fifth Yokohama Seaside Triathlon

Emitter	Emissions activities	Calculation recommendation item[a]	CO_2 emissions (kg CO_2)[b]
Competition organizer	(1) Energy consumption for transportation	A	1456
	(2) Energy consumption for accommodation	B	143
Competitors	(3) Energy consumption for transportation	A	2819
	(4) Energy consumption for accommodation	B	749
Competition venue	(5) Power consumption at conferences and events	A	76
	(6) Waste	B	141
	(7) Paper	B	266
	(8) Water	B	1
Total amount (A + B)			5651
Total amount (A)			4351

[a]A: Items to be in the scope of calculation, B: items that should be in the scope of inclusion
[b]Based on data from the Japanese Ministry of the Environment (2011, 2013)

reducing energy use of seaweed production and food mileage and incorporating the use of a seawater-source heat pump.

12.4.2   Estimating CO_2 Emission Reduction

In the social experiment, Yokohama City calculated the amount of CO_2 emission reduction by the consumption of marine products (locally produced seaweed) and utilization of marine energy (seawater-source heat pump introduction). Both of these were credits based on blue resources (i.e., reduction of CO_2 emissions utilizing marine resources) and not blue carbon (i.e., carbon storage by marine organisms) because the method of calculating blue carbon credits was simply under investigation.

12.4.2.1   Local Seaweed Production

Two CO_2 reduction effects were expected by implementing a new wakame seaweed (brown kelp, *Undaria pinnatifida*) production area at the site, so the reduction amount was calculated using the life cycle assessment method (Japan Environmental Management Association for Industry 2010).

The first effect was reducing CO_2 emissions by shortening the transportation distance. Approximately 70% of the wakame seaweed consumed in Japan is
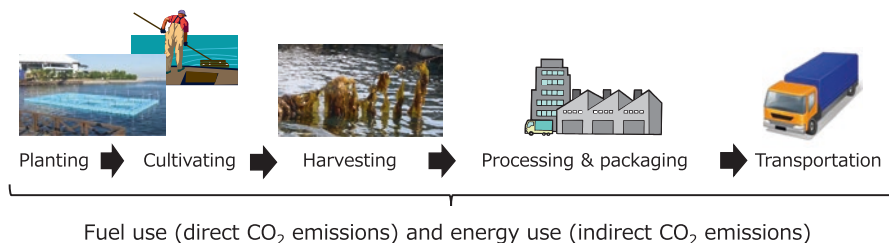
Planting ➡ Cultivating ➡ Harvesting ➡ Processing & packaging ➡ Transportation

Fuel use (direct CO_2 emissions) and energy use (indirect CO_2 emissions)

Fig. 12.3 Scope of the calculation of CO_2 emissions

Table 12.3 Seaweed products, production area, and boundary (scope of calculation)

Products[a]	Raw seaweed, salted seaweed, dried seaweed
Production area	Made in Yokohama
	Made elsewhere: domestic production (Tohoku and Shikoku regions), China, South Korea
Boundary	Planting, cultivating, harvesting, processing, packaging, transportation
	Scope 1 (direct emissions from fuel use), Scope 2 (indirect emissions derived from energy)

[a]Results of interviews with staff of the Kanazawa Fishing Port, Shiba Fishing Port, and Yokohama Hakkeijima Inc

imported from China and South Korea, with the rest produced domestically outside of Yokohama City. Thus, implementation of local seaweed production in Yokohama City will shorten the food transportation distance and reduce CO_2 emissions associated with fuel consumption of ships and autos.

Second, we expected a reduction of CO_2 emissions in aquaculture and manufacturing processes. Seaweed cultivation is being carried out by the Yokohama City Fishery Cooperative Association and Yokohama Hakkeijima. Because it is assumed that production involves a lot of manual work on a small scale compared to the cultivation method elsewhere, the amount of CO_2 emissions associated with it will be reduced.

Calculation Periods and Scope In the conventional calculation method, the amount of CO_2 reduction is calculated based on the difference in emission before and after the project implementation. We defined the before and after periods as that without local seaweed production (all seaweed is imported as usual) and that with local seaweed production (less seaweed is imported and some is obtained from local production), respectively.

The amount of CO_2 reduction accompanying local production of seaweed was based on planting, cultivating, harvesting, processing, packaging, and transportation (Fig. 12.3). The targeted product was seaweed produced in Yokohama City, and the production areas outside the city were in Tohoku and Shikoku, Japan, and overseas in China and South Korea (Table 12.3).

Calculation Method The CO_2 reduction amount was calculated as follows:

$$\begin{aligned}
CO_2 \text{reduction}\left(\text{kg}\,CO_2\right) &= BF - PF \\
&= BF - \left(BF - SF + YF\right) \\
&= SF - YF \\
&= \left(N \cdot x1 + E \cdot x2 + K \cdot x3\right) - \left(N' \cdot x1 + E' \cdot x2 + K' \cdot x3\right)
\end{aligned}$$

where

BF: baseline emissions (kg CO_2)
PF: project emissions (kg CO_2)
SF: CO_2 emissions (kg CO_2) associated with production outside Yokohama City after project implementation
YF: CO_2 emissions (kg CO_2) associated with production in Yokohama City after project implementation
N: amount of raw seaweed made outside the city (kg)
E: amount of salted seaweed made outside the city (kg)
K: amount of dried seaweed made outside the city (kg)
N': amount of raw seaweed made in Yokohama (kg)
E': amount of salted seaweed made in Yokohama (kg)
K': amount of dried seaweed made in Yokohama (kg)
$x1$: CO_2 emissions from raw seaweed (kg CO_2/kg)
$x2$: CO_2 emissions of salted seaweed (kg CO_2/kg)
$x3$: CO_2 emissions of dried seaweed (kg CO_2/kg)

To obtain information on CO_2 emissions by each seaweed product and production area, we conducted interviews regarding the aquaculture of Yokohama seaweed and consulted the Embodied Energy and Emission Intensity Data for Japan Using Input-Output Tables (2005), Multiple Interface Life Cycle Assessment (Japan Environmental Management Association for Industry 2010), and Carbon Footprint of Products Database (Japan Environmental Management Association for Industry 2012) for seaweed aquaculture outside the city. The conditions for carrying out the inventory analysis and the CO_2 emission coefficients used for calculation are listed in Table 12.4. The manufacturing process (planting to harvesting) accounted for more than 85% of the CO_2 emissions (Fig. 12.4). The manufacture of seaweed in Yokohama emitted less CO_2 compared to that outside the city, thus the total CO_2 emissions for the local seaweed were lower.

As shown in Fig. 12.5, the total seaweed consumption in Yokohama City was assumed to be constant, and the products and production area were assumed to have changed before and after the project implementation. In addition, the proportion of the production area outside the city was set based on the production amount in each production area and was assumed to be unchanged before and after the project. The increased amount of seaweed produced in Yokohama City by the project should replace the consumption of seaweed produced outside the city.

Table 12.4 Implementation conditions of the inventory analysis

	Seaweed made in Yokohama			Made outside the city			
	Shiba fishing port	Kanazawa fishing port	Yokohama Hakkeijima Inc.	Domestic production (Tohoku region)	Domestic production (Shikoku region)	Made in China	Made in South Korea
Products consumed in Yokohama	Raw seaweed[a] Salted seaweed[a]	Raw seaweed[a] Salted seaweed[a] Dried seaweed[a]	Raw seaweed[a]	Salted seaweed[b] Dried seaweed[b]	Salted seaweed[b] Dried seaweed[b]	Salted seaweed[b] Dried seaweed[b]	Salted seaweed[b] Dried seaweed[b]
Process							
Planting, cultivating, harvesting	Calculated using actual ship fuel use in planting, management and harvesting[a]	Calculated using actual ship fuel use in planting, management and harvesting[a]	No use of boat etc.[a]	Using the inventory data for fuel consumption of boats[c]	Using the inventory data for fuel consumption of boats[c]	Using the inventory data for fuel consumption of boats[c]	Using the inventory data for fuel consumption of boats[c]
Processing	Calculated using fuel consumption in each process of boiling, cooling/draining, salting, dewatering, and drying[c,d]	Calculated using fuel consumption in each process of boiling, cooling/draining, salting, dewatering, and drying[c,d]	Calculated using fuel consumption in each process of boiling, cooling/draining, salting, dewatering, and drying[c,d]	Calculated using fuel consumption in each process of boiling, cooling/draining, salting, dewatering, and drying[d,e,f]	Using the value excluding CO_2 emissions due to dewatering from the calculated value of domestic production (Tohoku)[b]	Using the value of domestic production (Tohoku)[b]	Using the value of domestic production (Tohoku)[b]
Packaging	Assuming that bag filling is done manually[h,i]	Assuming that bag filling is done manually[h,i]	Assuming that bag filling is done manually[h,i]	Assuming bagging using packaging machine[h,i]	Assuming bagging using packaging machine[h,i]	Assuming bagging using packaging machine[h,i]	Assuming bagging using packaging machine[h,i]

Transportation

	Method	Distance	Route course
	Domestic: Cargo truck (10-ton type)[g,h] Raw seaweed and salted seaweed: loading rate 100%, dried seaweed: loading rate 50%	14.5 km	Shiba fishing port→Yokohama City Hall
	Domestic: Cargo truck (10-ton type)[g,h] Raw seaweed and salted seaweed: loading rate 100%, dried seaweed: loading rate 50%	16.4 km	Kanazawa fishing port→Yokohama City Hall
	Domestic: Cargo truck (10-ton type)[g,h] Raw seaweed and salted seaweed: loading rate 100%, dried seaweed: loading rate 50%	14.8 km	Yokohama Hakkeijima Sea Paradise →Yokohama City Hall
	Domestic: Cargo truck (10-ton type)[g,h] Raw seaweed and salted seaweed: loading rate 100%, dried seaweed: loading rate 50%	623.9 km	Tohoku Fisheries Cooperative Association →Yokohama City Hall
	Domestic: Cargo truck (10-ton type)[g,h] Raw seaweed and salted seaweed: loading rate 100%, dried seaweed: loading rate 50%	553.1 km	Shikoku Fisheries Cooperative Association →Yokohama City Hall
	Overseas: Ship (container ship <4000 TEU)[g] Domestic: Cargo truck (10-ton type)[g,h] Raw seaweed and salted seaweed: loading rate 100%; dried seaweed: loading rate 50%	Overseas: 2111 km Domestic: 30.3 km	Shanghai →Tokyo Port Terminal Corporation →Yokohama City Hall
	Overseas: Ship (container ship <4000 TEU)[g] Domestic: Cargo truck (10-ton type)[g,h] Raw seaweed and salted seaweed: loading rate 100%; dried seaweed: loading rate 50%	Overseas: 1270 km Domestic: 30.3 km	Busan →Tokyo Port Terminal Corporation →Yokohama City Hall

[a]Interviews with staff of Kanazawa fishing port, Shiba fishing port, Yokohama Hakkeijima Inc.

[b]Interviews with staff of Japan Seaweed Association

[c]Based on Japan Environmental Management Association for Industry (2010)

[d]Based on Japan Construction Machinery and Construction Association (2013)

[e]Based on Hasegawa and Suzuki (2005)

[f]Based on Endo and Nakai (2012)

[g]Based on Kagoshima Prefectural Fisheries Technology and Development Center (2000)

[h]Based on Japan Food Machinery Manufacturers' Association (2012)

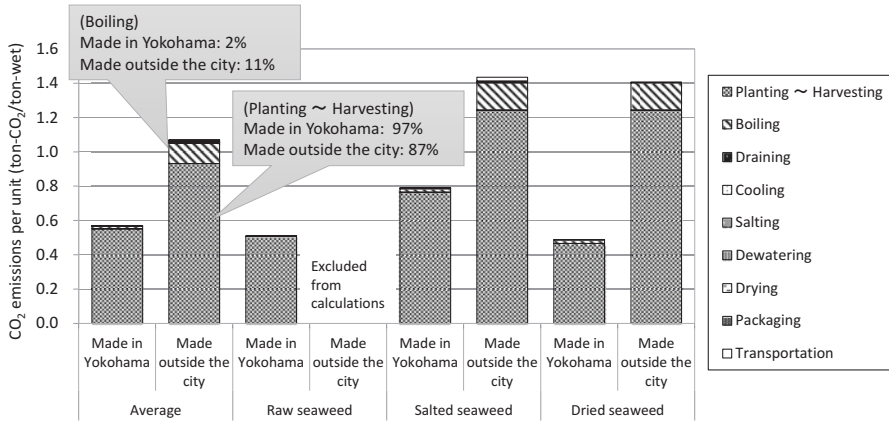[i]Based on Japan Environmental Management Association for Industry (2011)

Fig. 12.4 Estimated CO_2 emissions from edible seaweed production based on life cycle assessment
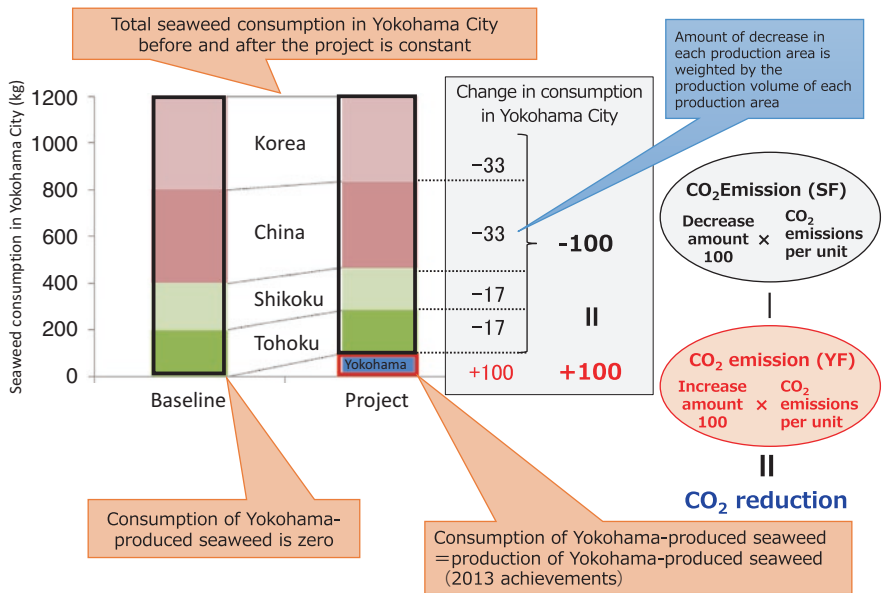

Fig. 12.5 Schematic diagram of change in the consumption of edible seaweed (brown kelp, *Undaria pinnatifida*) in Yokohama City before and after the Yokohama Blue Carbon Project

Calculation Results and Future Tasks As a result of the calculation, total baseline emission was 23,757 kg CO_2, project emission was 15,891 kg CO_2, and resulting CO_2 emission reduction was 7866 kg.

Those values for which there were no data were estimated based on similar cases. To improve accuracy in the future, it is desirable to replace the estimated values with directly measured data.

12.4.2.2 Seawater-Source Heat Pump

In an air-source heat pump generally used for air conditioning, outside air is used as a heat source. Thus, hot air is supplied during summer days and cold air during winter nights, resulting in a decline in energy consumption efficiency. In contrast, the heat source of a seawater-source heat pump is seawater, which shows small temperature changes throughout the day and year, thus it will use cold air even during the summer days and warm air even during winter nights by heat exchange between seawater and air, resulting in a consistently high energy consumption efficiency. Therefore, by updating the air-source heat pump with a seawater-source heat pump, energy consumption efficiency improves and power consumption for air conditioning decreases, so CO_2 emission reduction is expected.

An outline of the update was conducted by Yokohama Hakkeijima Inc., as shown in Table 12.5. The equipment was installed in 2013, and the values cover the CO_2 emission reductions with the operation for one year from a month after installation.

Calculation Assumptions Formulating the amount of CO_2 reduction required two conditions to be satisfied simultaneously: (1) the accuracy of the CO_2 reduction calculation is high to secure the reliability of carbon credits, and (2) the calculation is as simple as possible to reduce the burden on creditors. However, since these conditions are in a trade-off relationship, Yokohama City tried to maintain a balance between the two.

Calculation of Target Emission Activities Calculation of the targets of CO_2 reduction was based on the introduction of methodology EN-S-002 (ver. 1.0) of the J-Credit Scheme (Japanese Ministry of Economy, Trade and Industry, 2013). As shown in Table 12.6, use of electricity by the seawater-source heat pump, heat-source water pump, and air-source heat pump was extracted for the calculation of target activities.

Table 12.5 Heat pump project outline

Project	Update from an air-source heat pump to a seawater-source heat pump
Project implementer	Yokohama Hakkeijima Inc.
Calculation period of CO_2 emission reduction	1 April 2013–31 March 2014
Installation of seawater-source heat pump	Central monitoring room (24 h a day, 365 days a year) in the Aqua Museum at Yokohama Hakkeijima Sea Paradise in March 2013

Table 12.6 Target emission activities for CO_2 reduction due to upgrading to a seawater-source heat pump

	Emissions activities	Greenhouse gas	Calculation target of this project?
Project emissions	Power use by seawater-source heat pump	CO_2	Yes
			Power usage
	Power use by heat source water pump	CO_2	Yes
			Power usage
	Power use by lifting pump	CO_2	No
			Use seawater pumped for other purpose
	Leakage of refrigerant from seawater-source heat pump	CFC substitutes	No
			No leakage accident
	Disposal of air-source heat pump using refrigerant	CFC substitutes	No
			Cfc recovery at the time of disposal
Baseline emissions	Power use by air-source heat pump	CO_2	Yes
			Power usage
	Leakage of refrigerant from air-source heat pump	CFC substitutes	No
			No leakage accident

CFC chlorofluorocarbon

Calculation Method The CO_2 reduction amount was calculated as follows:

$$CO_2 \text{reduction} \left(\text{kg CO}_2 \right) = EM_{BL} - EM_{PJ}$$
$$= \left(ELC_{BL} \times CEF \right) - \left(ELC_{PJ} \times CEF \right)$$

where

$$ELC_{BL} = \Sigma \left(ELC_{PJ} \times COP_{SSHP} / COP_{ASHP} \right)$$
$$ELC_{PJ} = \Sigma \left[OT_{SSHP} \times \left(ELP_{SSHP} + ELP_{HSWP} \right) \right]$$

and

EM_{BL}: baseline CO_2 emissions (kg CO_2)
EM_{PJ}: project CO_2 emissions (kg CO_2)

ELC_{BL}: baseline power consumption (kWh)
ELC_{PJ}: project power consumption (kWh)
CEF: CO_2 emission coefficient of power (kg CO_2/kWh) in 2014
OT_{SSHP}: monthly operation time (h) of seawater-source heat pump
ELP_{SSHP}: monthly power consumption of seawater-source heat pump (kW)
ELP_{HSWP}: monthly power consumption of heat-source water pump (kW)
COP_{SSHP}: monthly COP (coefficient of performance) of seawater-source heat pump
COP_{ASHP}: monthly COP of air-source heat pump

The operating time and power consumption of the seawater-source heat pump were not monitored, so they were estimated from the air temperature and the seawater temperature, respectively. As noted above, the baseline power consumption (i.e., power consumption when running an existing air-source heat pump) was calculated as $EM_{BL} = \Sigma (ELC_{PJ} \times COP_{SSHP}/COP_{ASHP})$, so it was possible to ignore the difference in climatic conditions before and after the equipment update by obtaining the power consumption when the air-source heat pump was assumed to be in use in 2013.

Calculation Results As shown in Fig. 12.6, the CO_2 emissions were estimated to be 6085 kg CO_2 for baseline emissions and 5137 kg CO_2 for project emissions, and the resulting CO_2 emission reduction was estimated to be 948 kg CO_2. In terms of air conditioning, project emissions decreased for cooling compared to baseline emissions, whereas for heating they increased. This is because, although CO_2
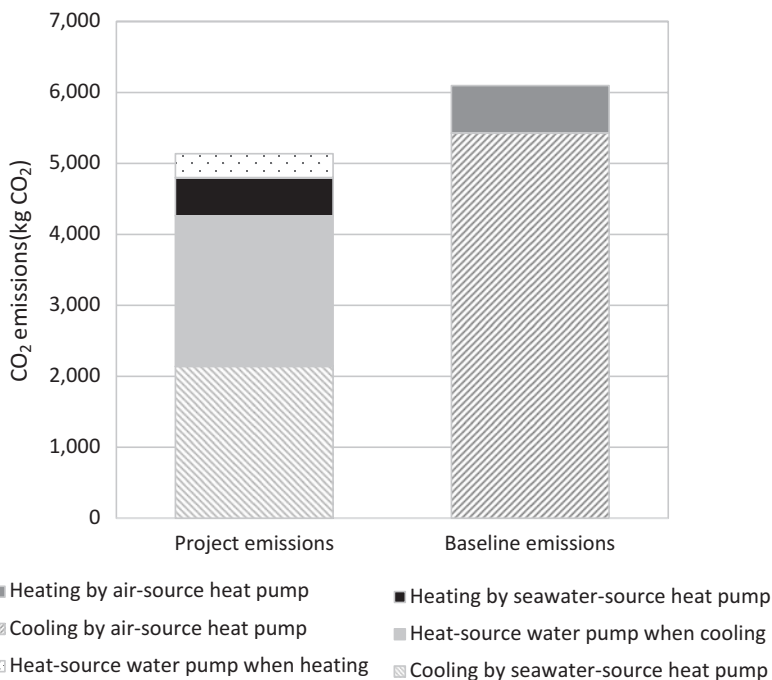

Fig. 12.6 Calculation of CO_2 emission reduction by updating from air-source heat pump to seawater-source heat pump

emissions from seawater-source heat pumps in heating mode are less than those from air-source heat pumps, the difference was small, while project emissions were larger than the difference due to CO_2 emissions from the installed heat-source water pump.

Future Tasks Facility personnel manually controlled and recorded the operation time for the power consumption of the heat pump. This was done because an emphasis was placed on simplicity, and we adopted a method allowing calculation within the range of monitoring currently being carried out. However, to improve the calculation accuracy of the CO_2 emission reduction amount, it is desirable to monitor the power automatically with a watt meter.

12.4.3   Implementation of the Social Experiment

In an agreement with the triathlon committee, the CO_2 emitted when a participant traveled from home to the convention site was offset (64.9% of the participants agreed to pay to offset). The organizer agreed to pay to offset the CO_2 (about 1.6 tonnes) emitted by the use of electricity at the venue. Trading of carbon credit were made directly between the credit creator (Yokohama City Fishery Cooperative Association and Yokohama Hakkeijima Inc.) and the credit user (Yokohama Seaside Triathlon), and Yokohama City conducted certification and issuance of certificates for the credit (Fig. 12.2). Carbon offset in this social experiment was implemented by buying and selling only Yokohama Blue Carbon Credit, and the unit price of trading was set at 10,000 yen/tonne CO_2 (excluding tax).

12.4.4   Issues and Future Tasks for the Social Experiment

To assess the outcomes of and problems with the social experiment, Yokohama City conducted a questionnaire survey of visitors to exhibition booths and triathlon participants on the day of the event. Of the visitors surveyed, 30.1% recognized Yokohama Blue Carbon (Fig. 12.7). Of the race participants, 40.5% said they agreed to pay to offset because "I want to contribute to the prevention of global warming" and 32.4% responded "I want to improve the environment of the city" (Fig. 12.8). Although the awareness of blue carbon was still low, the visitors and participants showed interest in environmental issues.

To improve recognition of the Yokohama Blue Carbon Project, Yokohama City ran a seaweed tasting booth on the day of the event. Also, the Carbon Offset Certificate award ceremony was held at the Third International Blue Carbon Symposium in Yokohama in January 2015. Here, the mayor of Yokohama gave a Carbon Offset Certificate to the Yokohama Seaside Triathlon Convention Executive Committee, which purchased carbon offset credits, and a letter of appreciation was given to the credit creators, Yokohama City Fishery Cooperative and Yokohama Hakkeijima Inc.

Fig. 12.7 Recognition of Yokohama Blue Carbon among local visitors to the Yokohama Seaside Triathlon (n = 198)

- 10.4% — I knew both the words and the contents
- 19.7% — I knew the words, but I did not know the contents
- 69.9% — I did not know

- 40.5% — I would like to contribute to the prevention of global warming
- 16.2% — I would like to support the "seaweed activity" of the donation destination
- 32.4% — I want to improve the environment of the sea and Yokohama City
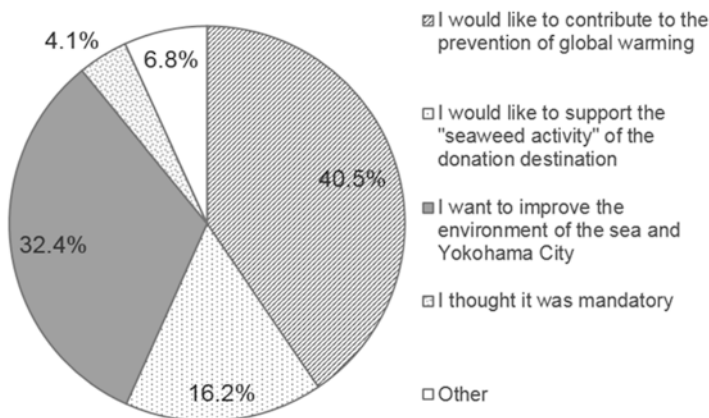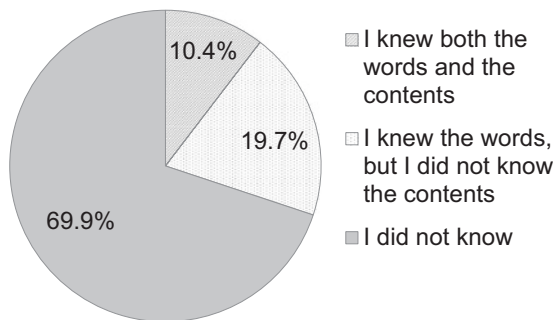- 4.1% — I thought it was mandatory
- 6.8% — Other

Fig. 12.8 Reasons why the participants of the Yokohama Seaside Triathlon chose to make the environmental donation (n = 74)

Numerous future tasks have been identified (Table 12.7). For example, in the creation of credits, the accuracy of calculation should be improved and monitoring should be implemented; in the credit transactions, the application format should be simplified and a donation system should be designed; and in the promotion of the project, the dissemination of information should be strengthened and a co-benefit evaluation method should be constructed. The tasks were identified by examining the successes and failures of the first trial of the social experiment, which is an important step for improving the project in the future.

12.4.5 Development of Calculation Methods for Blue Carbon Storage Rate

The high potential capacity for blue carbon production by the seagrass *Zostera marina* is clear from Chaps. 1 and 2 (Hori et al. 2018; Miyajima and Hamaguchi 2018). In 2014, however, Yokohama City issued offset credits targeting only blue

Table 12.7 Issues and future tasks identified in the 2014 social experiment of carbon offset

	Issues	Future tasks
Credit creation	(1) Calculation accuracy and improvement of carbon emission reduction by seaweed fishery	(1) Monitoring the implementation of fishery boat usage
	(2) Confirming measurement of seawater temperature data on seawater-source heat pump	(2) Data provision from the implementer
	(3) Too little credit creation	(3) Expansion of implementing entities and scope using the current methodology
Credit utilization	(1) Participant approval rate was not high enough (64.9%)	(1) Study how to improve the approval ratio
	(2) Identifying reduction efforts by the credit buyers	(2) Interviewing the credit buyers
Credit transaction	(1) Application form has many input items and is complicated	(1) Simplification of the application form
	(2) There is no system for donations	(2) Construction of a system for donations
	(3) Certification entity is in Yokohama City	(3) Transfer to third party organization
Effect of social experiment	(1) Approximately 40% awareness of Yokohama blue carbon project	(1) Efforts aimed at raising awareness
Project promotion	(1) Difficult for citizens to understand the Yokohama blue carbon project	(1) Preparation and implementation of environmental education programs for elementary and junior high school students, coordination with related parties
		(1) Strengthening of information dissemination (enhancement of portal site)
		(1) Development of marketing and branding strategy
		(1) Information dissemination domestically and abroad through the triathlon world competition
	(2) Evaluation method of co-benefits	(2) Improve co-benefit evaluation method and addition to credit

resources, namely CO_2 emission reduction by reducing energy use for edible seaweed production and introduction of a seawater-source heat pump. In the second year of the project, Yokohama City officials developed a methodology for blue carbon, namely devising a means of blue carbon storage by shallow coastal systems, which is the core of the Yokohama Blue Carbon Project.

City officials attempted to formulate the blue carbon storage rate in seagrass meadows and developed field survey methods for seagrass biomass, which can be implemented sustainably by citizen groups. A seagrass distribution area survey and measurement of seagrass biomass per unit area were conducted at the Sea Park Yokohama (Table 12.8). This survey was conducted within the managed area of the Sea Park in consultation with relevant stakeholders.

Table 12.8 Overview of the field survey at Sea Park Yokohama

	Aerial survey	Field survey	Wet mass of seagrass
Date	May 2015	June 2015	July 2015
Conductor	Yokohama city	Yokohama city	Yokohama city
		Yokohama Hakkeijima Inc.	
		Citizens[a]	
Method	Taking photos by unmanned aerial vehicle	Shallow area: Taking photos of the edge of the eelgrass bed with smartphones to capture GPS data	Setting 11 cultivation sites (every 15 m from shoreline) in the eelgrass bed and cultivating them[b,c]
		Deeper area: Record the location data of eelgrass bed edge with GPS unit by a scuba diver	

[a]Including the participation of students of Yokohama City University and local wind surfers (17 participants in total)
[b]Measuring aboveground biomass
[c]The retrieval area is 50 cm × 50 cm

Table 12.9 Estimated blue carbon storage rate in the seagrass meadows of Sea Park Yokohama[a]

Items	Whole area	High-density area
Area (m^2)	67,205	51,289
Biomass (kg wet/m^2)	1.175	1.440
Biomass in the area (kg wet)	78,966	73,856
Water content (%) of seagrass body[b]	84.2	84.2
Carbon content (kg C/kg dry) of seagrass body[c]	0.323	0.323
Carbon storage rate/biomass ratio (/year)[d]	0.115	0.115
Carbon storage rate (tonne C/year)	0.5	0.4
Carbon storage rate (tonne CO$_2$/year)	1.7	1.6

[a] Only aboveground biomass was considered
[b] Based on Kawabata et al. (1993)
[c] Based on Terawaki et al. (2002)
[d] See Table 12.10

12.4.5.1   Calculation Method for Blue Carbon Storage Rate

Part of the organic carbon originates from seagrass deposits on the seabed, but it is difficult to monitor the amount of the deposits within and outside the meadows. Therefore, based on biomass (wet mass basis) measured in the project area and values reported in the literature (Kawabata et al., 1993; Terawaki et al., 2002), the following formula for calculating the blue carbon storage rate was developed (see also Table 12.9):

$$\text{annual carbon storage rate} \left(\text{kg C / year} \right) = B \times \left(1 - WC \right) \times CC \times SR$$

Table 12.10 Calculation of the carbon storage rate/biomass ratio

	Mathematical variables	Value
Seagrass biomass[a]	A	531.8 g dry/m^2
Net production rate[a]	B	5.83 g dry/m^2/day
Litter production/net production ratio[a]	C	0.09
Litter production rate	$D = B \times C$	0.52 g dry/m^2/day
Drifting seagrass production rate[a]	E	2.28 g dry/m^2/day
Litter and drifting seagrass production rate	$F = D + E$	2.80 g dry/m^2/day
Percentage of refractory organic carbon in seagrass[a]	G	6%
Refractory organic carbon production rate in litter and drifting seagrass	$H = F \times G$	0.17 g dry/m^2/day
	$I = H \times 365$	61.3 g dry/m^2/year
Carbon storage rate/biomass ratio	$I = H/A$	0.115/year

[a]Based on data from the Japanese Fisheries Research Agency (2012)

where

B: seagrass biomass (kg wet/m^2)
WC: water content of seagrass body (%)
CC: carbon content of seagrass body (kg C/kg dry)
SR: carbon storage rate/biomass ratio (/year)

Calculation of the carbon storage rate/biomass ratio was developed as shown in Table 12.10, assuming that all refractory carbon in the litter and drifting parts of seagrass is stored (Abo et al. 2018). At Sea Park Yokohama, the blue carbon storage rate was calculated in the seagrass meadows for two target cases in the seagrass distribution: the whole area (including both high and low seagrass density areas) and the high-density area (Table 12.9). The whole area covered 67,205 m^2 and had a carbon storage rate of 1.7 tonne CO_2/year, whereas the high-density area covered 51,289 m^2 and had a carbon storage rate of 1.6 tonne CO_2/year.

12.4.5.2 Future Tasks

Advantages and disadvantages of the two target areas in the estimation of the seagrass distribution are summarized in Table 12.11. It is necessary to consider investigation methods that citizens can continuously implement. In addition, the literature values used for calculation of the blue carbon storage rate were survey data from elsewhere and had no clear definition of the aboveground and underground biomass, leading to uncertainty in the estimation. To prevent overestimation of the blue

Table 12.11 Advantages and disadvantages of including the whole area or only the high-density area in the estimation seagrass distribution area

	Whole area	High-density area
Advantages	It is possible to quantify the actual distribution area	It is relatively easy for citizen scientists to judge the edge of the seagrass meadows
Disadvantages	It is necessary to periodically take aerial photos to quantify percent cover	Possibility of underestimating the area
	Judging the edge of the seagrass meadows is somewhat difficult for citizen scientists, leading to possible overestimation	
	Large variance (uncertainty) is possible depending on observers	

carbon storage rate, this trial considered only aboveground biomass, but quantification including the underground biomass would be more desirable.

More importantly, the blue carbon storage rate reported here is the baseline rate before implementation of the global warming mitigation project. Therefore, in order for this project to become a carbon offset credit scheme, it is also necessary to increase the amount of blue carbon storage by increasing storage rates by means of human intervention (Kuwae and Hori 2018).

12.5   Future Prospects

Although blue carbon initiatives require further development before it can be used as an offset, Yokohama City is committed to the concept of being a Living Lab, using the urban landscape and its citizens to test countermeasures against global warming and other sustainability options. By fostering cooperation with businesses and universities and building industry–academia partnerships in the urban area, Yokohama City officials are trying to encourage the spread of new technologies and creation of new businesses and to increase the visibility of Yokohama among the cities of the world. In that sense, the initial blue carbon trial helped to cement an attitude that Yokohama will become a leader in that field, while developing a new sustainability sector in Japan.

Because city officials needed to make the Yokohama Blue Carbon Project to publicize for citizens, they implemented the carbon offset project at the Yokohama Seaside Triathlon in 2014 and the World Triathlon Series Yokohama in 2015. Working with Yokohama City, the events' organizers asked participants to pay a carbon offset in addition to the participation fee, and as a result they gained the involvement of 100% of foreign participants in the World Triathlon Series Yokohama in 2015 and up to 70% of Japanese participants in the Yokohama Seaside Triathlon in 2014. Citizens' understanding of the Yokohama Blue Carbon Project advanced because of this public collaboration. In addition, officials were pleasantly surprised

that one organization that participated in the event donated all the day's profits to cleaning the ocean and helping to reduce atmospheric CO_2.

Despite these early successes, however, there is more work to do in the future, such as advancing the research initiated by the Yokohama Blue Carbon Project. In addition, credits are currently given exclusively for the reduction of CO_2 emissions through local seaweed production. We are working to create new methodologies aimed at energy-saving measures in coastal zones through cooperation with the port sector and to expand the project and number of credit creators. To date, creating carbon credits by eating seaweed is not possible from the viewpoint of natural carbon cycling. However, Yokohama City also hopes to foster research to develop a credit mechanism for seaweed consumption.

Yokohama City officials are pleased that the Yokohama Seaside Triathlon is gaining a reputation as an environmentally friendly event. At present, however, the contribution of participants is the major funding source of the projects, with that of citizens being minor. Therefore, city officials need to publicize the importance of local support for the triathlon by building a more open, easy-to-understand structure for citizen participation in the Yokohama Blue Carbon Project. Likewise, it is necessary to simplify procedures while ensuring reliability of the guidelines and forms used to implement the credit system to reduce the burden on registrants and build a truly sustainable scheme.

Finally, with the aim of building a sustainable city that interweaves the environment, society, and the economy, methodology for promotion and expansion of the value of costal zones and citizens' interest in the sea must be investigated. This will require effective public relations and environmental awareness activities, while highlighting the ocean's potential and co-benefits, such as climate change mitigation, food supply, disaster prevention, and sightseeing, all with the cooperation of private industry, academia, and government agencies.

12.6   Conclusions

In the context of the United Nations Framework Convention on Climate Change, ratification of the Paris Agreement, and a recognition that the world must move toward zero CO_2 emissions during this century, awareness of environmental issues related to the world's oceans will undoubtedly improve. In the future, Yokohama City should pursue efforts to invest municipal and corporate funds not only in forests, where the carbon offset scheme has already been constructed, but also in the ocean to fully utilize its benefits.

The use of carbon offsets is a global warming countermeasure, but Yokohama City officials also recognize it as an initiative that can be used to encourage citizen enlightenment and environmental action. Furthermore, Yokohama City is working to reaffirm the characteristics of the place where we live and is encouraging further developments in sustainable urban design. Yokohama City officials also believe that the model of the Yokohama Blue Carbon Project is applicable to other coastal cities

around the world. Success in this realm will require making comprehensive plans including new perspectives (e.g., energy, resources, food, global warming counter-measures) and further effective use of the ocean, as well as the incorporation of both terrestrial and marine environments in city master plans.

Recently, the traditional Japanese managed landscapes of *satoyama* (terrestrial–aquatic ecosystems including secondary forests, plantations, grasslands, agricultural fields, pasture, and irrigation ponds and canals) and *satoumi* (marine–coastal ecosystems including seashore, rocky shore, tidal flats, and seaweed and eelgrass beds) have gained recognition (Japanese Ministry of the Environment 2018). These concepts highlight the importance of reviewing location and effectively utilizing the local resources for future regional planning and management. These reviews should assess the region's existing capital (nature, companies, universities, citizens) and identify new values to edit and make the best use of the capital. For marine coastal cities, implementation of blue carbon initiatives will become an important element of *satoumi* and a fundamentally unavoidable basis for management.

References

Abo K, Sugimatsu K, Hori M et al (2018) Quantifying the fate of captured carbon: from seagrass meadow to deep sea. In: Kuwae T, Hori M (eds) Blue carbon in shallow coastal ecosystems: carbon dynamics, policy, and implementation. Springer, Singapore, pp 251–271

Embodied Energy and Emission Intensity Data for Japan Using Input-Output Tables (2005) http://www.cger.nies.go.jp/publications/report/d031/eng/index_e.htm. Accessed 17 June 2018

Endo H, Nakai K (2012) Empirical study of the efficiency of the system of large-scale renovation cultivation of seaweed. Iwate Prefectural Fisheries Technology and Development Center Annual Report. http://agriknowledge.affrc.go.jp/RN/3030185488. Accessed 17 June 2018

Hasegawa K, Suzuki S (2005) Work analysis of harvesting and salt-preserved wakame seaweed (*Undaria pinnatifida*) processing. Technical report of National Research Institute of Fisheries Engineering, vol 27, pp 61–80

Hori M, Bayne CJ, Kuwae T, Hori M (2018) Blue carbon: characteristics of the ocean's sequestration and storage ability of carbon dioxide. In: Kuwae T, Hori M (eds) Blue carbon in shallow coastal ecosystems: carbon dynamics, policy, and implementation. Springer, Singapore, pp 1–31

Japan Construction Machinery and Construction Association (2013) Calculation table of loss on construction machinery. http://jcmanet.or.jp/tosho/2013/1305101.pdf. Accessed 17 June 2018

Japan Environmental Management Association for Industry (2010) http://www.jemai.or.jp/english/. Accessed 17 June 2018

Japan Environmental Management Association for Industry (2012) https://www.cfp-japan.jp/english/. Accessed 17 June 2018

Japan Food Machinery Manufacturers' Association (2012) General catalogues for food machinery of Japan, 174 p

Japanese Fisheries Research Agency (2012) Report for the project of enhancement of counter-measures against global warming: evaluation of carbon sink and development of enhancement technology for CO_2 in seagrass meadows, macroalgal beds, and tidal flats. http://www.maff.go.jp/j/budget/yosan_kansi/sikkou/tokutei_keihi/seika_h24/suisan_ippan/pdf/60100434_00.pdf. Accessed 17 June 2018

Japanese Ministry of Economy, Trade and Industry (2013) J-Credit scheme. https://japancredit.go.jp/english/. Accessed 17 June 2018

Japanese Ministry of the Environment (2011) Guideline for calculation method of greenhouse gas emissions resulting from target activity of carbon offset, Ver. 2.0. https://www.env.go.jp/press/files/jp/17125.pdf. Accessed 17 June 2018

Japanese Ministry of the Environment (2013) Carbon offset third party certification criteria, Ver. 2.0. https://www.env.go.jp/earth/ondanka/mechanism/carbon_offset/guideline/cc-tpc.pdf. Accessed 17 June 2018

Japanese Ministry of the Environment (2018) https://www.env.go.jp/water/heisa/satoumi/en/index_e.html. Accessed 17 June 2018

Kagoshima Prefectural Fisheries Technology and Development Center (2000) http://kagoshima.suigi.jp/ayumi/. Accessed 17 June 2018

Kawabata T, Kayata K, Inui M, Hirayama K (1993) An estimation of net production rate of eelgrass *Zostera marina* at Yanai Bay during spring and summer. Nippon Suisan Gakkaishi 59(3):455–459

Kuwae T, Hori M (2018) The future of blue carbon: addressing global environmental issues. In: Kuwae T, Hori M (eds) Blue carbon in shallow coastal ecosystems: carbon dynamics, policy, and implementation. Springer, Singapore, pp 347–373

Miyajima T, Hamagichi M (2018) Carbon sequestration in sediment as an ecosystem function of seagrass meadows. In: Kuwae T, Hori M (eds) Blue carbon in shallow coastal ecosystems: carbon dynamics, policy, and implementation. Springer, Singapore, pp 33–71

Nelleman C, Corcoran E, Duarte CM, et al (2009) Blue Carbon: a rapid response assessment. United Nations Environmental Programme, GRID-Arendal, Birkeland Trykkeri AS, Birkeland

Terawaki T, Tamaki H, Nishimura S, Yoshikawa K, Yoshida G (2002) Total amount of carbon and nitrogen in *Zostera marina* in Hiroshima Bay, western Seto Inland Sea. Jpn Bull Fish Res Agency 4:25–32

Chapter 13
The Future of Blue Carbon: Addressing Global Environmental Issues

Tomohiro Kuwae and Masakazu Hori

Abstract In this chapter, we first summarize the quantitative data for carbon flows and stocks in various shallow coastal ecosystems, which were reviewed in the previous chapters. The capability of net uptake of atmospheric CO_2 and soil organic carbon accumulation in global shallow coastal ecosystems are estimated to be about 1070 Tg C year^{-1} and about 140 Tg C year^{-1}, respectively, with considerably large variabilities and uncertainties. Next, we discuss future needs for scientific and technological progress to constrain these large variabilities and uncertainties. We then review how blue carbon is being discussed at international conferences and within frameworks on climate change. Finally, we discuss how conserving, restoring, and utilizing blue carbon ecosystems can meet social needs in the future. In particular, the management of blue carbon ecosystems can serve not only as a mitigation measure against climate change but also as an adaptation measure.

13.1 Introduction

In this book, the authors have reviewed the progress of research on the functioning of CO_2 uptake and carbon storage in shallow coastal ecosystems (SCEs), which include blue carbon ecosystems, as well as the social efforts involved in their management. The science and technology surrounding blue carbon are still in the development stage. In particular, some types of data, such as the organic carbon concentration in sediments, have been frequently measured and reported for the

T. Kuwae (✉)
Coastal and Estuarine Environment Research Group, Port and Airport Research Institute, Yokosuka, Japan
e-mail: kuwae@p.mpat.go.jp

M. Hori
National Research Institute of Fisheries and Environment of Inland Sea, Japan Fisheries Research and Education Agency, Hatsukaichi, Hiroshima, Japan

functional evaluation of blue carbon ecosystems (Howard et al. 2017a), whereas other types, such as the concentration of refractory dissolved organic carbon, are mostly lacking.

Like green carbon in terrestrial ecosystems, the functioning of blue carbon has attracted attention as a countermeasure to global warming. Thus, researchers need to improve the level of scientific and technological knowledge of blue carbon so that these findings can be implemented by societies around the world. However, a large gap remains between scientific research on environmental issues and policy implementation. For instance, policy-makers often have to make decisions based on too little scientific evidence. To solve this problem, several global platforms that connect science and policy, such as the Intergovernmental Panel on Climate Change (IPCC) and Intergovernmental Science-Policy Platform on Biodiversity and Ecosystem Services (IPBES), have been formed, and interdisciplinary research and discussions have begun within these platforms.

In conjunction with such international movements, the importance of blue carbon and efforts toward social implementation has begun to be recognized in local communities. Some private companies, regional administrative organizations, and managers and engineers have a strong interest in future socioeconomic development that incorporates the conservation, restoration, and utilization of blue carbon ecosystems. For example, as in the case of Yokohama City introduced in Chap. 12 (Nobutoki et al. 2018), climate change countermeasures utilizing SCEs may be implemented worldwide in the future. In addition, such ecosystem-based climate change countermeasures may create new business opportunities (Thomas 2014).

In this chapter, we first estimate global annual CO_2 exchange and soil organic carbon accumulation rates in SCEs using the data reported in previous chapters and elsewhere. Next, we propose future needs for field observations and analyses and discuss the scientific and technological issues to be solved. At present, basic research on blue carbon is insufficient, and additional observations and measurements at various locations and occasions are needed to strengthen our knowledge of the subject. We then review how blue carbon is being discussed at international conferences on climate change and within other international frameworks. Finally, we describe the social needs that can be met in the future by conserving, restoring, and utilizing SCEs and blue carbon.

13.2 Carbon Cycling in SCEs Worldwide

We estimated the global annual CO_2 exchange and soil organic carbon accumulation rates in SCEs using the data reported in previous chapters and the literature (Table 13.1). Both estimates show considerably high variability, stemming from both the large variability of the rates per unit area and the uncertainty in the global area for each ecosystem (Lavery et al. 2013). Future research should significantly reduce data variability and uncertainty. Keeping in mind these large uncertainties, below we discuss the estimated values.

Table 13.1 Global annual CO_2 exchange (negative values indicate net uptake of atmospheric CO_2) and soil organic carbon accumulation rates in different shallow coastal ecosystems

Ecosystem	Exchange interface	CO_2 exchange[a]						References	Chapter	Soil carbon accumulation rate						References	Chapter	Global area			References	Chapter
		mol C m^{-2} year^{-1}			Tg C year^{-1}					mol C m^{-2} year^{-1}			Tg C year^{-1}					million km^2				
		mean	min	max	mean	min	max			mean	min	max	mean	min	max			median	min	max		
Mangroves	Air-ecosystem	−193	−619	−21	−336	−1263	−35	Akhand et al. (2018)	7	13.0	9.6	18.8	23	16	38	Inoue (2018)	3	0.15	0.14	0.17	McLeod et al. (2011) and Pendleton et al. (2012)	1
	Air-soil	57	39	100	99	66	204	Akhand et al. (2018)	7													
	Air-water	5	0	12	9	0	24	Akhand et al. (2018)	7													
Seagrass meadows	Air-water	−9	−17	−1	−32	−122	−1	Tokoro et al. (2014) and Tokoro and Kuwae (unpublished)	6	2.5	0.2	7.1	9	0	51	Miyajima and Hamaguchi (2018)	2	0.30	0.18	0.60	McLeod et al. (2011) and Pendleton et al. (2012)	1
Macroalgal beds	Air-water	−22	−48	2	−913	−4202	202	Ikawa and Oechel (2015)	7	0.1	0.0	0.1	6	0	11	Krause-Jensen and Duarte (2016)	7	3.51	0.52	7.31	Krause-Jensen and Duarte (2016)	

(continued)

Table 13.1 (continued)

Ecosystem	Exchange interface	CO₂ exchange[a] mol C m⁻² year⁻¹ mean	min	max	Tg C year⁻¹ mean	min	max	References	Chapter	Soil carbon accumulation rate mol C m⁻² year⁻¹ mean	min	max	Tg C year⁻¹ mean	min	max	References	Chapter	Global area million km² median	min	max	References	Chapter
Tidal marshes	Air-ecosystem	−108	−379	29	−66	−1817	139	Otani and Endo (2018)	8	12.6	1.5	144.2	8	0	692	Nellemann et al. (2009)		0.05	0.02	0.40	McLeod et al. (2011) and Pendleton et al. (2012)	1
	Air-soil	40	−13	84	244	−77	502	Otani and Endo (2018)	8													
Tidal flats	Air-soil	−9	−13	−2	−8	−12	−2	Otani and Endo (2018)	8	7.1	4.8	9.4	6	4	8	Endo and Otani (2018)	5	0.08[b]			Smardon (2004)	
Coral reefs	Air-water	1	−4	66	3	−173	3108	Watanabe and Nakamura (2018)	10	0.9			3	1	43	Watanabe and Nakamura (2018)	10	0.26	0.11	3.90	Spalding and Grenfell (1997)	
Estuaries	Air-water	13	−18	132	281	−395	2858	Laruelle et al. (2013) and Cotovicz et al. (2015)	11	3.8			81			Nellemann et al. (2009)	1	1.80			Nellemann et al. (2009)	1
Total[c]					−1071	−7984	6268						136	22	844							

[a]References showing annual gas fluxes are extracted

[b]Wadden Sea only

[c]CO₂ exchange: air-ecosystem values are used for mangroves and salt marshes, air-soil values for tidal flats, and air-water for other ecosystems
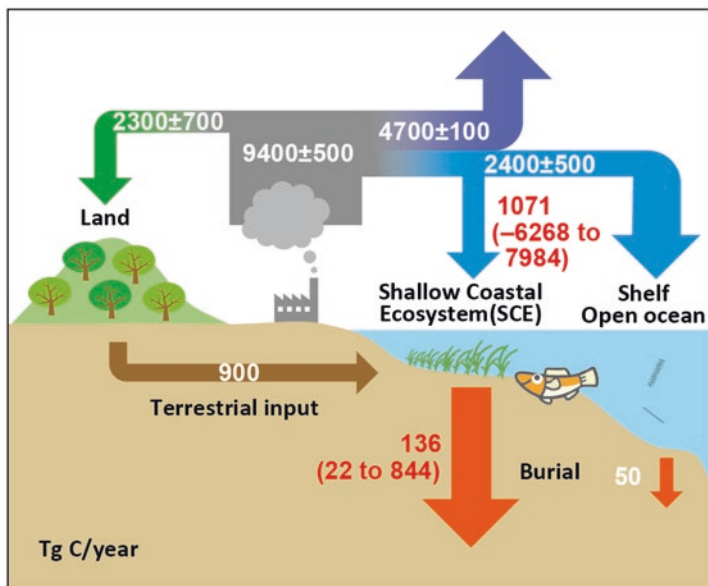
Fig. 13.1 Global carbon cycling amended (red numbers) based on the values in Table 13.1. See Le Quéré et al. (2018) for atmospheric data (mean ± SD for 2007–2016) and IPCC (2013) for terrestrial input

The global estimate of the soil organic carbon accumulation rate in SCEs ranged from 22 to 844 Tg C year^{-1}, with a mean value of 136 Tg C year^{-1}, which is comparable to previous reports (Nellemann et al. 2009; Pendleton et al. 2012). Estuaries (mean, 81 Tg C year^{-1}) were major contributors to the total accumulation rate in SCEs, as reported previously (Nellemann et al. 2009).

To the best of our knowledge, this work provides the first global estimate of CO_2 exchange rates in SCEs. The estimated rates ranged from −7984 to 6268 Tg C year^{-1}, with a mean of −1071 Tg C year^{-1} (negative value: net uptake of atmospheric CO_2). This mean rate is surprisingly higher than expected, given that the estimate of CO_2 flux in the world's oceans is −2400 ± 500 Tg C year^{-1} (Quéré et al. 2018) (Fig. 13.1), and about 8 times higher than the soil organic carbon accumulation rate.

One explanation supporting this high rate might be the outflow of CO_2 taken up to outside as is or converted into another form of carbon (particulate or dissolved and organic or inorganic), as explained in Chap. 11 (Kuwae et al. 2018; see also Krause-Jensen and Duarte 2016; Duarte and Krause-Jensen 2017). Another explanation might be that the estimate of major contributors to the high exchange rate, namely, mangroves (mean, −336 Tg C year^{-1}) and tidal marshes (mean, −66 Tg C year^{-1}), have already been implicitly included in the global estimate of the terrestrial CO_2 exchange rate (−2300 ± 700 Tg C year^{-1}). This is because the terrestrial rate

was indirectly calculated as the residual value of the global carbon budget and the mangrove and tidal marsh contributions were excluded from the oceans' uptake rate (Le Quéré et al. 2018).

However, even when we subtract these two estimates from the total SCE uptake rate, the CO_2 exchange rate (-669 Tg C year^{-1}) is still higher than the soil carbon accumulation rate. The estimate for macroalgal beds ranged from -4202 to 202 Tg C year^{-1}, with a mean of -913 Tg C year^{-1}, contributing to the high net uptake rate. We should note that only one study investigated macroalgal beds (Ikawa and Oechel 2015) and thus this ecosystem type has a considerable spatial uncertainty as a global estimate, although the study included 3 years of observational data gathered using the state-of-the-art eddy covariance technique.

Studies dealing with a suite of key processes for air–water CO_2 fluxes, such as carbonate chemistry and organic carbon dynamics, are still scarce in SCEs (but see Maher and Eyre 2012; Tokoro et al. 2014; Watanabe and Kuwae 2015), although recent studies have begun to address the abundance and burial rates for both organic and inorganic carbon in sediments and soils (e.g., Mazarrasa et al. 2015; Fodrie et al. 2017; Macreadie et al. 2017; Howard et al. 2018). In particular, even though SCEs are significant organic carbon reservoirs, they can also be net emitters of CO_2 to the atmosphere through air–sea gas exchange, depending on the organic and inorganic carbon dynamics (Regnier et al. 2013), as autochthonous calcification increases the CO_2 concentration in water (Ware et al. 1992; Watanabe and Nakamura 2018).

Nevertheless, our results should help to encourage discussions regarding the uncertainty in the current estimates of global carbon cycling for both terrestrial and marine ecosystems. In addition, our findings also reveal the necessity for more research on carbon dynamics to improve our understanding of the potential functioning of SCEs for climate change mitigation.

13.3 Toward Strengthening Science and Technology

13.3.1 Current Status

Ecosystem management can be effective for maintaining multiple ecosystem services in a sustainable manner (Hori et al. 2018). However, problems often arise when decision-makers (e.g., governmental and administrative agencies) have to make policy decisions without scientific and technological knowledge (Russell-Smith et al. 2015). Thus, it is important that policy-making organizations are closely connected with the science and engineering researchers assessing changes in ecosystem status.

Blue carbon initiatives are moving from the advocating stage with reports from the United Nations Environmental Programme (UNEP) (Nellemann et al. 2009) and the International Union for Conservation of Nature (Laffoley and Grimsditch 2009)

to the social penetration, policy-making, and implementation stages. Thus, it is important for the science, technology, policy, and implementation of blue carbon systems to keep pace with one another. The primary objective of the UNEP report was to advocate for the importance of blue carbon, despite the insufficient knowledge and data, so it may have fully fulfilled its purpose. However, Nellemann et al. (2009) also noted that the report contained many uncertainties and biases, as it compiled data on specific species or geographic regions. Indeed, some knowledge and ideas introduced in this book were not included in the UNEP report, and some results and views presented here differ from those of Nellemann et al. (2009).

### 13.3.2 Proposed Future Research Topics

As discussed throughout this book, the accumulation and analysis of scientific and technological evidence corresponding to social needs is still very important for connecting blue carbon initiatives to policy-making and implementation. It is necessary to first build key datasets in each location to strengthen scientific and technological evidence. There have been many achievements in blue carbon research, such as the measurement of seagrass and mangrove biomass, as described in Chaps. 3 and 4 (Inoue 2018; Yoshida et al. 2018). In most parts of the world, however, the interrelationships between inorganic and organic carbon at the air–water and water–sediment interfaces, as described in Chaps. 6 and 8 (Otani and Endo 2018; Tokoro et al. 2018), and the carbon flow, such as the sedimentary carbon accumulation rate introduced in Chaps. 2 and 5 (Endo and Otani 2018; Miyajima and Hamaguchi 2018), have not been measured.

In particular, high-precision measurement using state-of-the-art technologies are needed in addition to monitoring changes in the blue carbon stock (mainly sedimentary organic carbon and vegetation biomass). Such advances include the stable isotopic signature and DNA analyses of sediment cores to measure carbon sources, as introduced in Chap. 2 (Miyajima and Hamaguchi 2018), use of the eddy covariance method to measure the air–water CO_2 exchange, as discussed in Chap. 6 (Tokoro et al. 2018), and development of a coupled ecosystem–ocean physics model to measure carbon transport, as described in Chap. 9 (Abo et al. 2018).

Ideally, standardized field observations of blue carbon storage and CO_2 uptake should be performed at SCEs worldwide to fill the gaps at unmeasured sites and to reduce the uncertainty at measured sites. Here we describe three areas of blue carbon research that require further global field observations:

1. Gathering key data for carbon stocks and flows (primarily CO_2 uptake and blue carbon storage) using conventional methods for various SCEs (Kuwae et al. 2016; Crosswell et al. 2017). It is particularly important to enhance long-term, continuous, large-scale in situ observation data and to collect monitoring data using remote sensing technology to measure changes in the biomass distribution area of target ecosystems.

Fig. 13.2 Relationships between the key processes contributing to climate change mitigation (vertical axis) and the ecosystem variables (horizontal axis) that vary with management (restoration and conservation) of shallow coastal ecosystems. The response function of each key process may be approximated with either a Type I or Type II curve depending on the particular location and occasion
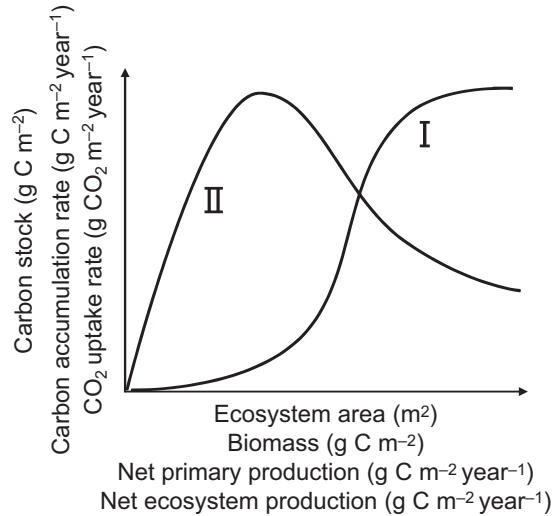
2. Establishing new measurement techniques for the carbon stocks and flows that researchers have not been able to quantify via conventional methods, especially for seasonal fluctuation of macrophyte biomass and the amount that drifts, as well as the formation of refractory dissolved organic matter in SCEs (Wada et al. 2008; Orr 2014; Hill et al. 2015; Krause-Jensen and Duarte 2016; Duarte and Krause-Jensen 2017; Abo et al. 2018; Jiao et al. 2018). It is also necessary to elucidate the underlying processes and mechanisms using the new measurement techniques.

3. Estimating spatiotemporal variability of measured carbon stocks and flows, particularly in response to disturbances such as climate change (Arias-Ortiz et al. 2018), human activities (e.g., Macreadie et al. 2015; Serrano et al. 2016; Atwood et al. 2017; Kauffman et al. 2017; Lovelock et al. 2017), altered food web structure (Atwood et al. 2015), and non-steady-state conditions such as storm and tsunami events (Cahoon et al. 2003).

We must also use these data to respond to social needs. For example, researchers and engineers must be prepared to answer questions from policy-makers and practitioners, such as how much carbon stock can be changed if the area of seagrass meadows and kelp beds are increased, or how much atmospheric CO_2 can be absorbed by increasing the biomass of primary producers. Figure 13.2 illustrates two types of functional relationships between the key processes contributing to climate change mitigation (carbon stock, carbon accumulation rate, and CO_2 uptake rate) and ecosystem variables (ecosystem area, biomass, net primary production, and net ecosystem production). Researchers and engineers must assess whether these relationships show a logistic curve (Type I) or a curve with a local maximum (Type II) in response to management, including restoration and conservation, of SCEs.

In addition, the temporal and spatial scales on the axes for these functional relationships need to be clearly defined because the shape of the response curve changes according to the scales set. For example, by considering only the left side of the Type I logistic curve, we would approximate an exponential increase, whereas the middle portion of the Type I curve indicates a linear increase and the right side a saturated (leveled-off) curve. The importance of the temporal scale definition appears to be supported by several reports showing that it takes 10–20 years in seagrass meadows (Duarte et al. 2013a; Greiner et al. 2013; Marbà et al. 2015), at least 25–100 years in tidal marshes (Craft et al. 2003; Burden et al. 2013), and 20–25 years in mangroves (Osland et al. 2012; Salmo et al. 2013) for restored sites to achieve the soil organic carbon pool or accumulation rate of natural sites.

Furthermore, a debate exists about whether such a clear relationship is found in reality. For instance, some research has shown no significant correlation between the standing stock of biomass and the amount of organic carbon in soils and sediments (Kennedy et al. 2010; Howard et al. 2018), as reported in Chap. 2 (Miyajima and Hamaguchi 2018), whereas at least one other study has shown a linear relationship between them (Tanaya et al. 2018). The reason for this contradictory result may be the use of more sophisticated methods and strategies for sample collections, that is, utilization of a new device for extracting intact core samples and selection of well-controlled sampling sites for variables other than biomass (Tanaya et al. 2018).

Finally, converting the vertical axis of the response relationships of Fig. 13.2 into the amount of benefits and human well-being and the horizontal axis into the costs (time and money) of implementation would be needed to make use the results of science and technology for social implementation.

13.3.3 Cooperation Within International Frameworks

To overcome global climate change issues, it is also necessary to develop observation technologies that can be commonly used to acquire standardized datasets worldwide, targeting long-term, continuous, large-scale data that can be measured simply and at low cost. Various international research networks and governmental/intergovernmental scientific research organizations have been established. These include the International Long Term Ecological Research Network and Future Earth (described in detail below) for international promotion of large-scale climate change research using interdisciplinary approaches, in addition to ecosystem monitoring networks such as the Global Coral Reef Monitoring Network, the International Society for Mangrove Ecosystems, the Global Seagrass Monitoring Network, the Zostera Experimental Network for eelgrasses, and the Kelp Ecosystem Ecology Network.

In blue carbon studies, it is also important to utilize these existing networks and/or establish a new global research network in the future. In the field of marine science in the open ocean and high seas, some research organizations have been led by governments with common interests at the regional scale, such as the North Pacific

Marine Science Organization and the International Council for the Exploration of the Sea, whereas global research networks led by intergovernmental bodies are rare (cf. the Argo project). Some frameworks are being formed to strengthen the connection between scientific researchers and policy-makers. This movement is explained in detail in the next section.

13.4 International Frameworks for Blue Carbon

13.4.1 The United Nations Framework Convention on Climate Change and IPCC

Because the term "blue carbon" is used in the context of climate change, the most relevant international initiative is, of course, the United Nations Framework Convention on Climate Change (UNFCCC) (Fig. 13.3). Parties ratifying the UNFCCC have a legally binding responsibility to report to the Treaty Secretariat on the inventory of its greenhouse gas emissions and removals. The method of preparing these greenhouse gas inventories conforms to the guidelines developed by the IPCC. Inventories prepared by each country undergo rigorous checks from the UNFCCC expert review team.

When preparing an inventory, it is necessary to calculate the amount of greenhouse gas absorbed and released throughout the country; thus, the calculation is actually categorized into various sectors such as energy and agriculture. Land Use and Land Use Change and Forestry (LULUCF) are related sectors of an ecosystem. In the LULUCF sector, an inventory is created for each land use; forests are the primary sink for atmospheric CO_2, whereas cropland is the main source for
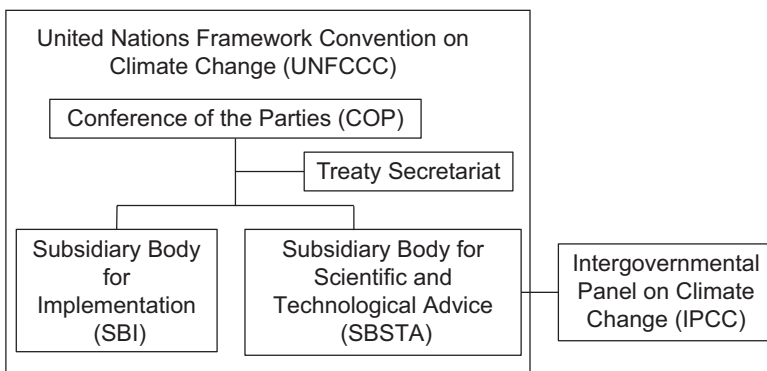

Fig. 13.3 Interrelationship between the United Nations Framework Convention on Climate Change, the Conference of the Parties, the Intergovernmental Panel on Climate Change (IPCC), the Subsidiary Body for Implementation, and the Subsidiary Body for Scientific and Technological Advice (SBSTA). The IPCC is responsible for advising the SBSTA on science and technology

atmospheric CO_2. The 2013 Supplement to the 2006 IPCC Guidelines for National Greenhouse Gas Inventories: Wetlands (Wetlands Supplement) (IPCC 2014) includes a methodology that was not fully covered under the 2006 IPCC Guidelines (IPCC 2006) and covers mangroves, tidal marshes, and seagrass meadows among SCEs, but macroalgal beds and tidal flats are currently not included.

In Subsidiary Body for Scientific and Technological Advice (SBSTA) 37 of the annual meeting of UNFCCC held in December 2012, the Coalition of Rainforest Nations noted the importance of blue carbon, and the UNFCCC Workshop on Technical and Scientific Aspects of Ecosystems with High-Carbon Reservoirs Not Covered by Other Agenda Items under the Convention was held in October 2013. At this workshop, proposals were made to report the absorption of CO_2 and mitigation of climate change by SCEs in the agenda of SBSTA 39 in 2013. In the international negotiations at UNFCCC-SBSTA 39, there was discussion as to whether calculation using the 2013 IPCC Wetland Supplement would be obligatory for Annex I Parties.
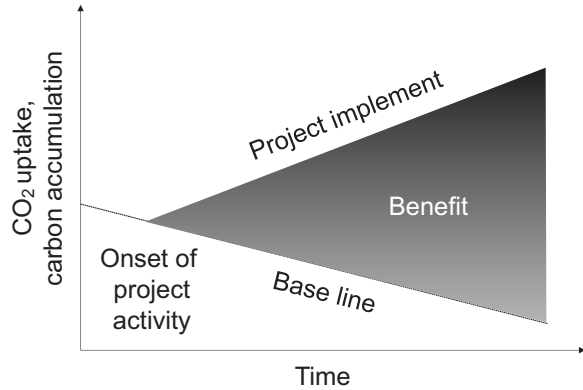
As of 2018, SCEs (blue carbon ecosystems) are classified as "arbitrary" in calculating the greenhouse gas inventory of the LULUCF sector because each Party does not have enough experience in the calculation of the inventory for SCEs. This classification is scheduled to be reconsidered at the UNFCCC-SBSTA in the near future. If the calculation of carbon stocks and flows for SCEs is obligated in the future, the reduction of carbon stocks and CO_2 emission by development projects (e.g., human activities such as dredging, excavation, and aquaculture) in SCEs will also have to be measured and reported in addition to the natural restoration and conservation projects that contribute to the absorption and emission reduction of atmospheric CO_2.

There has been no major progress on blue carbon in the international negotiations of UNFCCC since 2014, but discussions have been taking place in side events during the COP holding period. Also, through the SBSTA, discussions on whether to include SCEs in the inventory are repeatedly requested by high-interest island countries and tropical countries. Based on this international situation, Australia has officially decided to measure and report changes in the carbon stocks of the country's blue carbon ecosystems and included these in its national greenhouse gas accounts for 2017, ahead of other countries (Kelleway et al. 2017).

In the new legally binding framework after 2020 (Paris Agreement) adopted at COP 21 in 2015, each country has adopted a Nationally Determined Contribution (NDC) toward the reduction of greenhouse gas emissions. The mitigation measures are undertaken in unique ways by each country, and a mutual verification mechanism (pledge and review approach) is the basic policy. Moreover, because each country is required to review prospective and ambitious NDCs every 5 years, the NDC can respond flexibly to scientific and technological progress and social changes. At the same time, the NDC is structured so that each country's efforts cannot step backward.

The Paris Agreement includes the following adoptions related to conservation, restoration, and utilization of blue carbon:

(1) Conserve and enhance, as appropriate, sinks and reservoirs of greenhouse gases (Article 5.1);
(2) Implement and support, including through results-based payments, the existing framework as set out in related guidance and decisions already agreed under the Convention for policy approaches and positive incentives for activities relating to Reducing Emissions from Deforestation and forest Degradation (REDD), the role of conservation, sustainable management of forests, and enhancement of forest carbon stocks in developing countries (REDD+), and alternative policy approaches, such as joint mitigation (Article 5.2);
(3) Reaffirm the importance of incentivizing, as appropriate, non-carbon benefits (Article 5.2);
(4) Recognize the fundamental priority of safeguarding food security (Preamble);
(5) Note the importance of ensuring the integrity of all ecosystems, including oceans, and the protection of biodiversity (Preamble);
(6) Uphold and promote regional and international cooperation to mobilize stronger and more ambitious climate action by all Parties and non-Party stakeholders, including civil society, the private sector, financial institutions, cities and other subnational authorities, local communities, and indigenous peoples (Preamble of COP 21).

With regard to item (1), restoring and conserving SCEs that are major atmospheric CO_2 sinks and carbon reservoirs promote conservation and strengthen CO_2 absorption and carbon storage, which reconcile very well with the contents of the Paris Agreement. Next, utilizing the mechanism and concept of REDD+ noted in item (2), making agreements with the Coalition of Rainforest Nations that stores large amounts of blue carbon in mangroves, seagrass meadows, and coastal peatlands, and promoting the restoration and conservation of blue carbon resources are all activities in line with the contents of the Paris Agreement. Carbon credits (benefits) by REDD+ may be obtained based on the difference in the amount of absorption/emission or carbon stocks between the case where no restoration/conservation project is carried out (baseline) and the case where the activities are performed (Fig. 13.4).
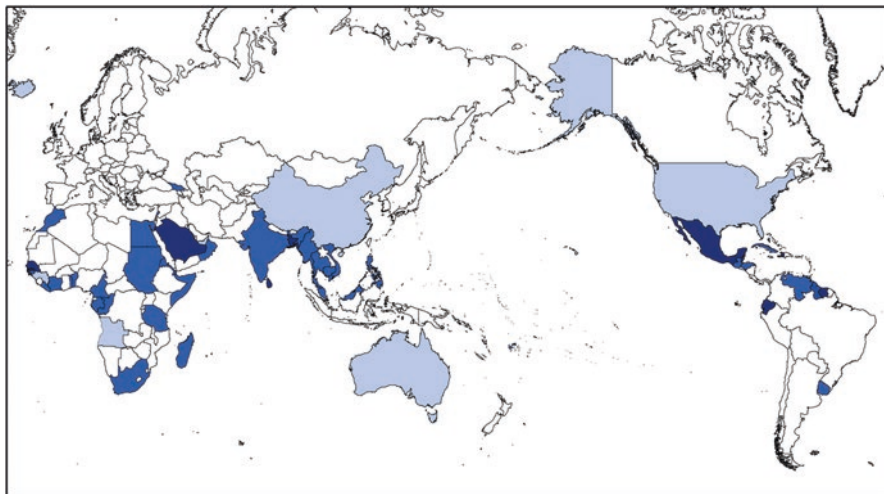
Fig. 13.5 Countries that refer to the utilization of shallow coastal ecosystems or blue carbon in their Nationally Determined Contribution of the Paris Agreement (as of 2016). Those that mention only the mitigation effect are shown in light blue, only the adaption effect are shown in medium blue, and both effects are shown in dark blue (Based on Herr and Landis 2016)

Furthermore, conservation, restoration, and utilization of blue carbon are simply those of SCEs while focusing on the carbon cycling, which is the basis of a variety of ecosystem services. In other words, by conserving, restoring, and utilizing SCEs, it is possible to combine food provision and other ecosystem services (co-benefits) and contribute to food security, ecosystem integrity, and biodiversity, as noted in items (3) to (5). In this way, blue carbon resources are actually closely linked to marine ecosystems and biodiversity. Therefore, in the following sections we will outline contents related to blue carbon within the international framework on biodiversity.

Finally, climate action by non-Party stakeholders (i.e., taking a bottom-up approach) noted in (6) is consistent with the contents of measures against global warming led by cities and municipalities explained in Chap. 12 (Nobutoki et al. 2018). The limitations of conventional international frameworks in the UNFCCC and IPCC (i.e., use of the top-down approach) on climate change measures are expected to be overcome by using this new approach.

Although utilization of blue carbon is becoming an international trend, how many countries actually mention the use of blue carbon or SCEs in their NDCs? To answer this, a survey was conducted in 2016 (Herr and Landis 2016; Martin et al. 2016) (Fig. 13.5). Of the 151 countries that ratified the Paris Agreement, 28 (19%) refer to the use of blue carbon or SCEs for climate change mitigation and 59 countries (39%) refer to their use for climate change adaptation.

13.4.2   International Framework for Coastal Management

Changes in the global environment including water, atmosphere, and climate have led to a serious decline of biodiversity. This, in turn, has led to the deterioration of various ecosystem services, which has increased concern about significant changes in local traditions and regional cultures as well as economic activity. Therefore, in 2012 the IPBES was founded to realize a sustainable world coexisting with nature, to adequately reflect the results of natural science research in society and policy, and to tackle various issues related to biodiversity and ecosystem services. The IPBES Secretariat is set up in Bonn, Germany, and the first General Assembly was held in 2013 with 105 countries from around the world.

The IPBES aims to strengthen the linkage between science and policy on biodiversity and ecosystem services and to properly reflect scientific evidence in policies. In other words, IPBES is expected to function as a biodiversity version of the IPCC. Specifically, it has four key functions: generating knowledge, providing regular and timely assessments, supporting policy foundation and implementation, and capacity building.

Establishing the IPBES was contemplated at the 10th Conference of the Parties to the Convention on Biological Diversity (CBD-COP 10, hereafter COP 10) held in Aichi, Japan, in 2010. CBD is a framework corresponding to a biodiversity version of UNFCCC. In 2006, there was a lively discussion about the following five topics at CBD-COP 8, especially in reference to COP 8 Decision VIII/20 (Biological diversity of inland water ecosystems: reporting processes, improving the review of implementation and addressing threats), Decision VIII/21 (Marine and coastal biological diversity: conservation and sustainable use of deep seabed genetic resources beyond the limits of national jurisdiction), Decision VIII/22 (Marine and coastal biodiversity: enhancing the implementation of integrated marine and coastal area management), and Decision VIII/24 (Protected areas):

1. Compiling scientific criteria for identifying Ecologically or Biologically Significant Marine Areas to promote the protection of marine and coastal biodiversity;
2. Promoting efforts to construct a network of marine protected areas by 2012;
3. Providing scientific support to promote biodiversity conservation in the high seas, including open ocean waters and deep sea habitats;
4. Cooperating with relevant organizations to estimate the impact of non-sustainable fisheries;
5. Considering the impact of ocean acidification related to climate change.

These decisions were mostly included in the Aichi Targets at COP 10, which is an action plan to prevent further loss of biodiversity and is also included in some Sustainable Development Goals described later.

Among the Aichi Targets, direct goals regarding marine and coastal biodiversity are as follows:

Target 4: By 2020, at the latest, Governments, business, and stakeholders at all levels have taken steps to achieve or have implemented plans for sustainable production and consumption and have kept the impacts of use of natural resources well within safe ecological limits.

Target 6: By 2020, all fish and invertebrate stocks and aquatic plants are managed and harvested sustainably, legally and applying ecosystem-based approaches, so that overfishing is avoided, recovery plans and measures are in place for all depleted species, fisheries have no significant adverse impacts on threatened species and vulnerable ecosystems, and the impacts of fisheries on stocks, species and ecosystems are within safe ecological limits.

Target 8: By 2020, pollution, including from excess nutrients, has been brought to levels that are not detrimental to ecosystem function and biodiversity.

Target 10: By 2015, the multiple anthropogenic pressures on coral reefs and other vulnerable ecosystems impacted by climate change or ocean acidification are minimized, so as to maintain their integrity and functioning.

Target 11: By 2020, at least 17% of terrestrial and inland water and 10% of coastal and marine areas, especially areas of particular importance for biodiversity and ecosystem services, are conserved through effectively and equitably managed, ecologically representative, and well-connected systems of protected areas and other effective area-based conservation measures and integrated into the wider landscapes and seascapes.

Target 15: By 2020, ecosystem resilience and the contribution of biodiversity to carbon stocks has been enhanced, through conservation and restoration, including restoration of at least 15% of degraded ecosystems, thereby contributing to climate change mitigation and adaptation and to combating desertification.

Issues directly related to blue carbon (e.g., climate change, acidification, and carbon storage) and those covered by comprehensive management of blue carbon are included in the targets. They also include maintaining the ecosystem functions and services of coastal ecosystems closely related to blue carbon, such as securing marine reserves at 10%, managing fishery resources, and managing water pollution.

In order to achieve these targets, it is essential to scientifically evaluate biodiversity and ecosystem functions and to adequately reflect the results in policy. Since the IPBES 1st General Assembly held in 2013, collaboration with policy- and decision-making bodies on climate change such as the UNFCCC and IPCC, as well as Future Earth, a policy-oriented international global environmental research program, has been promoted, and IPBES is indeed strengthening the connection between global scientific research and decision-making.

Future Earth is a comprehensive global environmental research program undertaken via alliances among many international organizations (Fig. 13.6). Although it is primarily a scientific research program, various policy stakeholders, administrative agencies, and stakeholders in social and economic circles participate as well, which promotes both global environmental conservation and sustainability through transdisciplinary approaches.
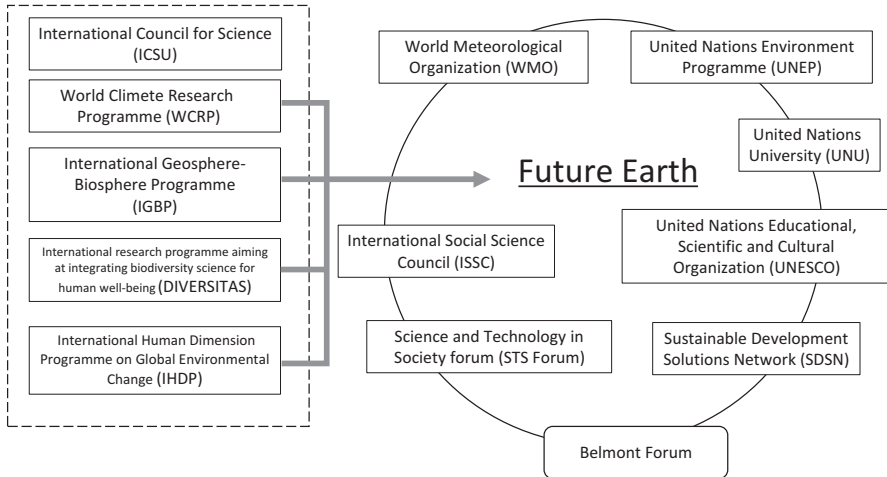
Fig. 13.6 Framework of Future Earth, which was organized for the purpose of integrating four interdisciplinary fields (WCRP, IGBP, DIVERSITAS and IHDP) related to global environmental change promoted by the International Council for Science and aims to foster transdisciplinary research. Other international organizations also participate and support Future Earth. The Belmont forum is typical in terms of a multilateral joint research funding agency for research on global environmental change

Until now, the evaluation of ecosystem services has been conducted mostly by natural science researchers, but Future Earth aims to emphasize the knowledge of social scientists to better communicate the research results to communities, which matches the aim of the IPBES, namely, strengthening the linkage between science and policy. Through this transdisciplinary research, Future Earth will help to co-design/co-create the entire process of research from problem discovery to practical solutions with the stakeholders of each society.

Among the international frameworks that are related to blue carbon, the most integrative framework is the outcome document of the United Nations Sustainable Development Summit, held in September 2015, "Transforming Our World: The 2030 Agenda for Sustainable Development." This agenda, which includes 17 Sustainable Development Goals and 169 targets, is positioned as the successor to the Millennium Development Goals (adopted in September 2000), with the goals to be achieved by 2030 for people, the planet, and prosperity. The 17 Sustainable Development Goals include issues such as poverty, hunger, energy, health, and welfare (Fig. 13.7); the urgent action to combat climate change and the conservation and sustainable use of the ocean are listed as independent goals.

Climate change is Goal 13: taking urgent action to combat climate change and its impacts. Three targets are included:

13.1 Strengthen resilience and adaptive capacity to climate-related hazards and natural disasters in all countries;

Fig. 13.7 The 17 Sustainable Development Goals adopted by the United Nations that are to be achieved by 2030 for people, the planet, and prosperity

13.2 Integrate climate change measures into national policies, strategies, and planning;

13.3 Improve education, awareness raising, and human and institutional capacity on climate change mitigation, adaptation, impact reduction, and early warning.

The goal for the ocean is Goal 14: conserve and sustainably use oceans, seas, and marine resources for sustainable development. The targets include multiple specific measures for climate change, pollution prevention, and sustainable improvement of food production. As suggested by the Aichi Targets, the necessity of coastal ecosystem management also has been documented. To support the implementation of Goal 14, the first United Nations Ocean Conference took place in 2017 and aimed to reverse the decline in the health of our ocean for people, the planet, and prosperity (United Nations Ocean Conference 2017). As a means of securing implementation, the conference established a mechanism for every entity (e.g., governments, United Nations, international organizations, non-governmental organizations, civil society, academic institutions, and the private sector) to register a Voluntary Commitment and publish it on the conference website. The Voluntary Commitment is also a means of realizing the measures written in the Call for Action to voluntarily implement initiatives for Goal 14.

13.4.3 From International Frameworks to Local Activities

Some consider the various international frameworks as simply policy slogans, with the organizations unlikely to become involved in actual situations. However, these frameworks are actually closely related to local environmental conservation

activities. The conservation and utilization of blue carbon have led to comprehensive ecosystem management including other ecosystem services. As explained in detail in Chap. 1 (Sect. 1.3), the ecosystem functioning of SCEs is generated by their foundation species, which support the base of the ecosystem and establish the biological and physicochemical characteristics of the ecosystem. In many cases, the foundation species and whole ecosystem that drives their functioning are regarded as a target of conservation and management. Having awareness of how the initiatives will be positioned in the international community and how they can connect to local policies and implementations should be the first step to integrating local initiatives with the global restoration, conservation, and utilization of blue carbon.

Other relevant policy frameworks and case studies are available elsewhere (e.g., Laffoley and Grimsditch 2009; Crooks et al. 2011; Lutz et al. 2014; Wylie et al. 2016; EX-ACT 2017; Howard et al. 2017b; International Partnership for Blue Carbon 2017; Villa and Bernal 2018; Wyndham-Meyers et al. 2018).

13.5 Remaining Issues and Future Efforts

13.5.1 Comparison of Mitigation Technologies

There are two types of technologies for the development of carbon sinks. Engineering-based technologies include carbon capture and storage (i.e., chemical industrial recovery of CO_2 emitted from plants, transported to a storage site, and enclosed) and ocean iron fertilization, whereas ecosystem-based technologies include forest management and soil management. All the sciences and technologies related to blue carbon and SCEs introduced in this book are ecosystem-based.

The costs and benefits of engineering- and ecosystem-based mitigation technologies differ. First, ecosystem-based technologies have advantages such as sustainability and small barriers to implementation. Engineering-based technologies such as carbon capture and storage, algae biofuel plants, and ocean iron fertilization have disadvantages such as high cost, CO_2 emission during the manufacturing and transportation process, and adverse environmental effects and thus have issues to be solved before sustainable implementation can be achieved (Cusack et al. 2014). Second, unlike engineering-based technologies, ecosystem-based technologies not only help to mitigate climate change but also provide co-benefits from other ecosystem services, such as food provision, water purification, recreation, and disaster prevention. Finally, because ecosystem-based technologies use natural processes, there are disadvantages such as higher uncertainty and lower efficiency (e.g., slower CO_2 uptake from the atmosphere) than engineering-based technologies.

Therefore, when introducing carbon sink technology utilizing blue carbon, it is necessary to keep in mind that there are few barriers to implementation and co-benefits are obtained, but CO_2 absorption occurs with relatively low efficiency.

13.5.2 Promoting New Values of SCEs

In many countries, numerous conservation and restoration projects for SCEs have been performed as public works. However, given that public financing has become tight in many places, the initiation of nature restoration projects may decline if their cost-effectiveness is viewed only in terms of the conventional value of SCEs, such as food provision, recreation, and environmental purification. Therefore, the exploration and promotion of new values of SCEs will become increasingly important in the future.

The socioeconomic benefits of blue carbon initiatives include improving the capital value and economic benefits of SCEs, the cost effectiveness as public works, and promotion of local businesses (Thomas 2014). The benefits referred to here are all economic incentives, such as carbon offset credit (market transaction), payment for ecosystem services, and income from funds (Murray et al. 2011; Herr et al. 2015). Also, by appealing to the private sector with monetary incentives, it is expected that private-led nature restoration projects will be developed. Thus, efforts for mitigation measures in the future are expected to be not only top-down but also bottom-up approaches as we comply with the basic policy of the Paris Agreement that climate change countermeasures will be promoted by both global and local measures.

13.5.3 Carbon Offset Credit

Carbon offset credit has been a top-down approach in which international markets are first established and then credit markets are created at the national and local government levels. However, if a bottom-up approach is to be formed in the future, a market must be newly established at the local government level, such as the case of Yokohama City described in Chap. 12 (Nobutoki et al. 2018), with national and international organizations supporting and verifying the market.

In order to develop the social implementation of local blue carbon credit schemes, independent methods for the measurement, reporting, and verification (MRV) of the credits would be needed, namely, measuring blue carbon accurately, objectively, and quantitatively based on scientific and technological knowledge, transparent reporting, and verification. The submission of greenhouse gas inventories to the UNFCCC Convention Secretariat is based on the principle of MRV.

Three approaches can be used to store atmospheric CO_2 in the sea via natural restoration projects and to help mitigate climate change: (1) creation of target ecosystems (i.e., carbon reservoirs and atmospheric CO_2 sinks); (2) reduction of the decline of target ecosystems by restoration and conservation; and (3) improvement of the management of target environments and ecosystems (i.e., improvement of carbon storage rate and CO_2 uptake rate per unit area).

If blue carbon credit schemes are to be applied to the concept as shown in Fig. 13.4, baseline measurements, time series data for target areas, and time series data for carbon storage capacity and/or CO_2 uptake per area are essential. The baseline refers to the amount of carbon stock and/or CO_2 uptake at the control site or period in which conservation and restoration activities are not carried out. It is necessary to estimate how much the carbon stock and/or CO_2 uptake increases by conserving and restoring the target area. In fact, baseline is usually obtained based on the spatiotemporal trends before the onset of the projects. However, objectively setting the trends and/or control sites for the baseline is scientifically and technically challenging.

13.5.4   Guidelines for Measurement Methods

Various guidelines for measuring carbon storage and CO_2 uptake by blue carbon ecosystems have been developed. Australia has included blue carbon ecosystems in its national greenhouse gas accounts, and the guidelines of the Australian Government's Emissions Reduction Fund are comprehensive (Kelleway et al. 2017). Other guidelines include those of the IPCC (2014); Conservation International; the United Nations Educational, Scientific and Cultural Organization; the International Union for Conservation of Nature (Howard et al. 2014); UNEP and the Center for International Forestry Research (Crooks et al. 2014); and the Verified Carbon Standard (2015), which is an independent carbon trading certification body in the United States. In Japan, guidance for measurement methods in seagrass meadows, tidal flats, embayments, and port facilities have been prepared (Tokoro et al. 2015). Thus, the movement toward the creation of credits for blue carbon is beginning to take place.

13.6   Blue Carbon As a Climate Change Adaptation

13.6.1   Coastal Defense Using Green Infrastructure

Coastal facilities made of concrete during the global economic growth period are becoming degraded and require renewal. If climate change accelerates aging and damage of these facilities, the need for renewal may be advanced. In addition, if we anticipate the stagnation of economic growth and tightening of public financing in the future, it is unlikely that the renewal and maintenance of coastal facilities will be covered by public financial resources as before.

To maintain coastal facilities and consequent socioeconomic sustainability, attention has been paid to coastal defense using not only artificial capital, so-called gray infrastructure, but also natural capital, or green infrastructure (Temmerman et al. 2013). Disaster prevention using green infrastructure is also called Eco-DRR
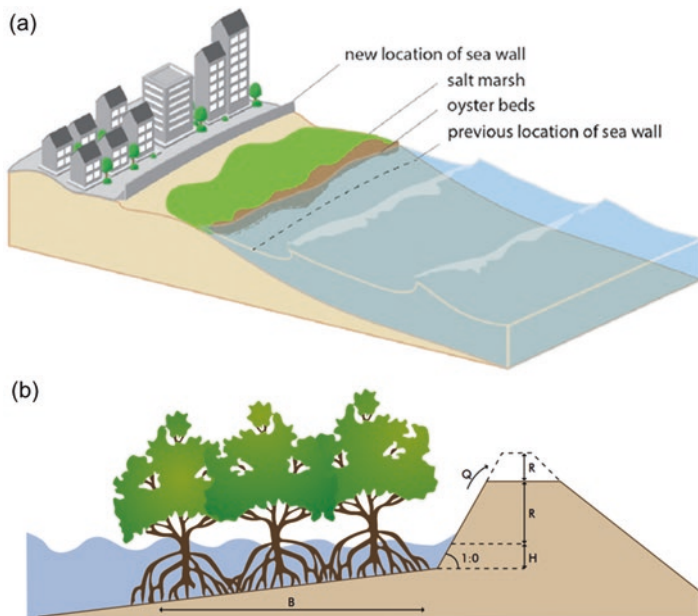
Fig. 13.8 (**a**) Representative arrangement and (**b**) representative structure of hybrid green–gray infrastructure. The wave attenuation effect by the mangrove makes it possible to lower the height of the levee and increase cost effectiveness while satisfying the safety performance requirement. ((**a**) From Sutton-Grier et al. (2015) and (**b**) from World Bank (2017))

(ecosystem-based disaster risk reduction). Although green infrastructure may be inferior to gray infrastructure in terms of disaster prevention from inundation and erosion, depending on the type of ecosystem, various other ecosystem services including climate change mitigation can be expected by utilizing green infrastructure.

Furthermore, by appropriately maintaining and managing green infrastructure, we can not only prevent its deterioration, but also expect enhanced functioning via the growth of ecosystem components. As a result, maintenance and management costs can be reduced compared to those of gray infrastructure due to green infrastructure's self-recovery ability even after disaster events. One new idea for the utilization of both green and gray infrastructure includes a hybrid arrangement (Fig. 13.8).

13.6.2 Adaptation to Climate Change Using Blue Carbon

Blue carbon ecosystems can also be used as adaptation measures for climate change (Koch et al. 2009; Duarte et al. 2013b; Spalding et al. 2014). Because vegetation generates drag force in the water column and attenuates wind-driven waves, coastal

erosion can be suppressed by blue carbon ecosystems in places where the degree and frequency of wind-driven waves will increase in the future due to climate change. Furthermore, current velocity also decreases due to the presence of vegetation, and suspended matter is trapped and settles in the blue carbon ecosystems. This process raises the elevation of the ecosystems due to sediment deposition, such that they can keep up with projected sea level rise due to climate change. Overall, utilization of vegetated coastal ecosystems can be an effective climate change measure in terms of both mitigation and adaptation.

Moreover, coral reef ecosystems have great wave attenuation effects due to their reef topography. Coral reefs formed in the tropics and subtropics have a width of several hundred meters to several kilometers, and rising ridges are often formed off the reef. This coral reef topography functions as a natural breakwater because the waves from the open ocean break around the reef ridge, and large waves generated by storms are prevented from reaching the coast. Furthermore, because corals and foraminifera grow up to near the low water level and form land foundations by calcification, coral reef ecosystems can be utilized as an autonomous adaptation measure to sea level rise due to climate change.

13.7 Concluding Remarks

We compiled the carbon flows and stocks related to climate change mitigation, based on data reported in previous chapters and the literature. Although the functioning of both blue carbon storage and CO_2 gas exchange should be focused on when SCEs are utilized to mitigate climate change, an information gap regarding these two key processes has hindered our integrated understanding of blue carbon science. Thus, in this book we aimed to quantitatively explain the mechanisms and extent of the key processes, using a global review of the literature and many Japanese case studies.

We also extended the definition of classical blue carbon ecosystems (mangroves, seagrass meadows, and tidal marshes) to include macroalgal beds, tidal flats, coral reefs, and urbanized shallow waters to show the potential of these additional ecosystems to serve as carbon sinks. Such an extension allowed us to focus on carbon storage in sediments as well as that in the water column as refractory organic carbon and at offshore sites such as the deep sea.

We also discussed the scientific and technological knowledge regarding blue carbon as it relates to the international governance of societies and communities as well as possible future developments. We described the international policies and frameworks related to blue carbon and introduced a case study of the application and implementation of carbon offset credit in Japan. We anticipate that it will be important to explore ways to introduce new funds and market economy mechanisms to assist in policy planning, community design, and the conservation, restoration, and management of SCEs.

Although this book focused on the specific ecosystem service of climate regulation, SCEs represent natural capital and provide various ecosystem services. Thus, it is important to manage this natural capital to take advantage of co-benefits such as health, employment creation, and food safety. However, we hope that by highlighting climate change countermeasures, in which society is becoming increasingly interested and concerned, this would help to initiate and/or accelerate the conservation and restoration of SCEs. We also recognize that the climate regulation service and other ecosystem services are hinged on the biodiversity within SCEs.

We hope that the knowledge presented here can help to build bridges between science and technology and socioeconomics. Like the milestone UNEP report that created the new world of blue carbon, we close by proposing several goals to foster the conservation, restoration, and utilization of blue carbon ecosystems:

1. To acquire standardized datasets on blue carbon ecosystems worldwide, targeting long-term, continuous, large-scale data gathered by simple means at low cost;
2. To develop technologies that make it possible to measure currently unmeasurable natural phenomena to elucidate the unknown mechanisms of SCEs;
3. To enable the quantitative prediction of the effects of disturbing factors such as climate change and human activities and the effects of non-steady-state conditions such as storms on SCEs;
4. To connect scientific and technological knowledge of SCEs to economic evaluations such as cost-effectiveness analysis to strengthen the coupling with socioeconomics;
5. To encourage communication between science and engineering researchers and local stakeholders, such as municipalities, cities, companies, and citizens, in addition to conventional international and national entities. As a means to do so, priority is given to direct dialogue between the researchers and the stakeholders and dissemination of information to the general public.

References

Abo K, Sugimatsu K, Hori M, Yoshida G, Shimabukuro H, Yagi H, Nakayama A, Tarutani K (2018) Quantifying the fate of captured carbon: from seagrass meadow to deep sea. In: Kuwae T, Hori M (eds) Blue carbon in shallow coastal ecosystems: carbon dynamics, policy, and implementation. Springer, Singapore, pp 251–271

Akhand A, Chanda A, Das S, Hazra S, Kuwae T (2018) CO_2 fluxes in mangrove ecosystems. In: Kuwae T, Hori M (eds) Blue carbon in shallow coastal ecosystems: carbon dynamics, policy, and implementation. Springer, Singapore, pp 185–221

Arias-Ortiz A, Serrano O, Masqué P et al (2018) A marine heatwave drives massive losses from the world's largest seagrass carbon stocks. Nat Clim Chang 8:338–344

Atwood TB, Connolly RM, Ritchie EG et al (2015) Predators help protect carbon stocks in blue carbon ecosystems. Nat Clim Chang 5:1038–1045

Atwood TB, Connolly RM, Almahasheer H et al (2017) Global patterns in mangrove soil carbon stocks and losses. Nat Clim Chang 7:523–528

Burden A, Garbutt RA, Evans CD et al (2013) Carbon sequestration and biogeochemical cycling in a saltmarsh subject to coastal managed realignment. Estuar Coast Shelf Sci 120:12–20

Cahoon DR, Hensel P, Rybczyk J et al (2003) Mass tree mortality leads to mangrove peat collapse at Bay Islands, Honduras, after Hurricane Mitch. J Ecol 91:1093–1105

Cotovicz LC Jr, Knoppers BA, Brandini N, Santos SC, Abril G (2015) A strong CO_2 sink enhanced by eutrophication in a tropical coastal embayment (Guanabara Bay, Rio de Janeiro, Brazil). Biogeosciences 12:6125–6146

Craft C, Megonigal P, Broome S et al (2003) The pace of ecosystem development of constructed *Spartina alterniflora* marshes. Ecol Appl 13:1417–1432

Crooks S, Herr D, Tamelander J, Laffoley D, Vandever J (2011) Mitigating climate change through restoration and management of coastal wetlands and near-shore marine ecosystems: challenges and opportunities. https://www.uncclearn.org/sites/default/files/inventory/wb87.pdf

Crooks S, Emmer I, Murdiyarso D, Brown B (2014) Guiding principles for delivering coastal wetland carbon projects. Report to the United Nations Environment Program and the Center for International Forestry Research. http://www.cifor.org/publications/pdf_files/Books/BMurdiyarso1402.pdf

Crosswell JR, Anderson IC, Stanhope JW et al (2017) Carbon budget of a shallow, lagoonal estuary: transformations and source-sink dynamics along the river-estuary-ocean continuum. Limnol Oceanogr 62(S1):S29–S45

Cusack DF, Axsen J, Shwom R, Hartzell-Nichols L, White S, Mackey KRM (2014) An interdisciplinary assessment of climate engineering strategies. Front Ecol Environ 12:280–287

Duarte CM, Krause-Jensen D (2017) Export from seagrass meadows contributes to marine carbon sequestration. Front Mar Sci 4:13

Duarte CM, Sintes T, Marbà N (2013a) Assessing the CO_2 capture potential of seagrass restoration projects. J Appl Ecol 50:1341–1349

Duarte CM, Losada IJ, Hendriks IE, Mazarrasa I, Marbà N (2013b) The role of coastal plant communities for climate change mitigation and adaptation. Nat Clim Chang 3:961–968

Endo T, Otani S (2018) Carbon storage in tidal flats. In: Kuwae T, Hori M (eds) Blue carbon in shallow coastal ecosystems: carbon dynamics, policy, and implementation. Springer, Singapore, pp 129–151

EX-ACT (2017) EX-ante carbon balance tool, blue carbon and fisheries. Food and Agriculture Organization. http://www.fao.org/3/a-i8342e.pdf

Fodrie FJ, Rodriguez AB, Gittman RK et al (2017) Oyster reefs as carbon sources and sinks. Proc R Soc B 284:2017089

Greiner JT, McGlathery KJ, Gunnell J, McKee BA (2013) Seagrass restoration enhances "blue carbon" sequestration in coastal waters. PLoS One 8:e72469

Herr D, Landis E (2016) Coastal blue carbon ecosystems. Opportunities for nationally determined contributions: policy brief. IUCN/The Nature Conservancy, Washington, DC/Gland

Herr DT, Agardy D, Benzaken F, et al (2015) Coastal "blue" carbon: a revised guide to supporting coastal wetland programs and projects using climate finance and other financial mechanisms. IUCN, Gland. https://doi.org/10.2305/IUCN.CH.2015.10.en

Hill R, Bellgrove A, Macreadie PI et al (2015) Can macroalgae contribute to blue carbon? An Australian perspective. Limnol Oceanogr 60:1689–1706

Hori M, Bayne CJ, Kuwae T (2018) Blue carbon: characteristics of the ocean's sequestration and storage ability of carbon dioxide. In: Kuwae T, Hori M (eds) Blue carbon in shallow coastal ecosystems: carbon dynamics, policy, and implementation. Springer, Singapore, pp 1–31

Howard J, Hoyt S, Isensee K, Pidgeon E, Telszewski M (2014) Coastal blue carbon: methods for assessing carbon stocks and emissions factors in mangroves, tidal salt marshes, and seagrass meadows. Conservation International, Intergovernmental Oceanographic Commission of UNESCO, International Union for Conservation of Nature, Arlington, Virginia

Howard J, Sutton-Grier A, Herr D et al (2017a) Clarifying the role of coastal and marine systems in climate mitigation. Front Ecol Environ 15:42–50

Howard J, McLeod E, Thomas S et al (2017b) The potential to integrate blue carbon into MPA design and management. Aquat Conserv Mar Freshwat Ecosyst 27(S1):100–115

Howard JL, Creed JC, Aguiar MVP, Fouqurean JW (2018) CO_2 released by carbonate sediment production in some coastal areas may offset the benefits of seagrass "blue carbon" storage. Limnol Oceanogr 63:160–172

Ikawa H, Oechel WC (2015) Temporal variations in air-sea CO_2 exchange near large kelp beds near San Diego, California. J Geophys Res Ocean 120:50–63

Inoue T (2018) Carbon sequestration in mangroves. In: Kuwae T, Hori M (eds) Blue carbon in shallow coastal ecosystems: carbon dynamics, policy, and implementation. Springer, Singapore, pp 73–99

International Partnership for Blue Carbon (2017) Coastal blue carbon: an introduction for policy makers. https://bluecarbonpartnership.org/wp-content/uploads/2017/11/Introduction-for-policy-makers_FINAL_web.pdf

IPCC (2006) IPCC guidelines for national greenhouse gas inventories. http://www.ipcc-nggip.iges.or.jp/public/2006gl/

IPCC (2013) Fifth assessment report of the Intergovernmental Panel on Climate Change. IPCC, Geneva

IPCC (2014) 2013 Supplement to the 2006 IPCC guidelines for national greenhouse gas inventories: wetlands. Hiraishi T, Krug T, Tanabe K et al (eds) IPCC, Geneva

Jiao N, Wang H, Xu G, Aricò S (2018) Blue carbon on the rise: challenges and opportunities. Natl Sci Rev. https://doi.org/10.1093/nsr/nwy030/4862478

Kauffman BJ, Arifanti VB, Trejo HH et al (2017) The jumbo carbon footprint of a shrimp: carbon losses from mangrove deforestation. Front Ecol Environ 15:183–188

Kelleway J, Serrano O, Cannard T, et al (2017) Technical review of opportunities for including blue carbon in the Australian Government's Emissions Reduction Fund. CSIRO, Canberra

Kennedy H, Beggins J, Duarte CM et al (2010) Seagrass sediments as a global carbon sink: isotopic constraints. Global Biogeochem Cycles 24:GB4026

Koch EW, Barbier EB, Silliman BR et al (2009) Non-linearity in ecosystem services: temporal and spatial variability in coastal protection. Front Ecol Environ 7:29–37

Krause-Jensen D, Duarte CM (2016) Substantial role of macroalgae in marine carbon sequestration. Nat Geosci 9:737–742

Kuwae T, Kanda J, Kubo A et al (2016) Blue carbon in human-dominated estuarine and shallow coastal systems. Ambio 45:290–301

Kuwae T, Kanda J, Kubo A, Nakajima F, Ogawa H, Sohma A, Suzumura M (2018) CO_2 uptake in the shallow coastal ecosystems affected by anthropogenic impacts. In: Kuwae T, Hori M (eds) Blue carbon in shallow coastal ecosystems: carbon dynamics, policy, and implementation. Springer, Singapore, pp 295–319

Laffoley DA, Grimsditch G (2009) The management of natural coastal carbon sinks. IUCN, Gland, 53 pp. https://portals.iucn.org/library/sites/library/files/documents/2009-038.pdf

Laruelle GG, Durr HH, Lauerwald R et al (2013) Global multi-scale segmentation of continental and coastal waters from the watersheds to the continental margins. Hydrol Earth Syst Sci 17:2029–2051

Lavery PS, Mateo MÁ, Serrano O, Rozaimi M (2013) Variability in the carbon storage of seagrass habitats and its implications for global estimates of blue carbon ecosystem service. PLoS One 8:e73748

Le Quéré C, Moriarty R, Andrew RM et al (2018) Global carbon budget 2017. Earth Syst Sci Data 10:405–448

Lovelock CE, Atwood T, Baldock J et al (2017) Assessing the risk of carbon dioxide emissions from blue carbon ecosystems. Front Ecol Environ 15:257–265

Lutz SJ, Neumann C, Bredbenner A (2014) Building blue carbon projects: an introductory guide. https://gridarendal-website-live.s3.amazonaws.com/production/documents/:s_document/317/original/building_blue_carbon_projectsLowRes.pdf?1489067674

Macreadie PI, Trevathan-Tackett SM, Skilbeck CG et al (2015) Losses and recovery of organic carbon from a seagrass ecosystem following disturbance. P Roy Soc B Biol Sci 282:1–6

Macreadie PI, Serrano O, Maher DT, Duarte CM, Beardall J (2017) Addressing calcium carbonate cycling in blue carbon accounting. Limnol Oceanogr Lett 2:195. https://doi.org/10.1002/lol2.10052

Maher DT, Eyre BD (2012) Carbon budgets for three autotrophic Australian estuaries: implications for global estimates of the coastal air-water CO_2 flux. Glob Biogeochem Cy 26:GB1032

Marbà N, Arias-Ortiz A, Masqué P, Kendrick GA, Mazarrasa I, Bastyan GR, Garcia-Orellana J, Duarte CM (2015) Impact of seagrass loss and subsequent revegetation on carbon sequestration and stocks. J Ecol 103:296–302

Martin A, Landis E, Bryson C, Lynaugh S, Mongeau A, Lutz S (2016) Blue carbon: nationally determined contributions inventory. Appendix to: coastal blue carbon ecosystems: opportunities for nationally determined contributions. GRID, Arendal

Mazarrasa I, Marbà N, Lovelock CE et al (2015) Seagrass meadows as a globally significant carbonate reservoir. Biogeosciences 12:4993–5003

McLeod E, Chmura GL, Bouillon S et al (2011) A blueprint for blue carbon: toward an improved understanding of the role of vegetated coastal habitats in sequestering CO_2. Front Ecol Environ 9:552–560

Miyajima T, Hamagichi M (2018) Carbon sequestration in sediment as an ecosystem function of seagrass meadows. In: Kuwae T, Hori M (eds) Blue carbon in shallow coastal ecosystems: carbon dynamics, policy, and implementation. Springer, Singapore, pp 33–71

Murray BC, Pendleton L, Jenkins WA, Sifleet S (2011) Green payments for blue carbon: economic incentives for protecting threatened coastal habitats. Nicholas Institute for Environmental Policy Solutions, Report NI, 11(04). https://nicholasinstitute.duke.edu/sites/default/files/publications/blue-carbon-report-paper.pdf

Nellemann C, Corcoran E, Duarte CM, et al (2009) Blue Carbon: a rapid response assessment. United Nations Environmental Programme, GRID-Arendal, Birkeland Trykkeri AS, Birkeland

Nobutoki M, Yoshihara T, Kuwae T (2018) Carbon offset utilizing coastal waters: Yokohama blue carbon project. In: Kuwae T, Hori M (eds) Blue carbon in shallow coastal ecosystems: carbon dynamics, policy, and implementation. Springer, Singapore, pp 321–346

Orr KK (2014) Floating seaweed (Sargassum). In: Laffoley D, Baxter JM, Thevenon F, Oliver J (eds) The significance and management of natural carbon stores in the open ocean. Full report. IUCN, Gland, pp 55–67

Osland MJ, Spivak AC, Nestlerode J et al (2012) Ecosystem development after mangrove wetland creation: plant–soil change across a 20-year chronosequence. Ecosystems 15:848–866

Otani S, Endo T (2018) CO_2 flux in tidal flats and salt marshes. In: Kuwae T, Hori M (eds) Blue carbon in shallow coastal ecosystems: carbon dynamics, policy, and implementation. Springer, Singapore, pp 223–250

Pendleton L, Donato DC, Murray BC et al (2012) Estimating global "blue carbon" emissions from conversion and degradation of vegetated coastal ecosystems. PLoS One 7:e43542

Regnier PAG, Friedlingstein P, Ciais P et al (2013) Anthropogenic perturbation of the carbon fluxes from land to ocean. Nat Geosci 6:597–607

Russell-Smith J, Lindenmayer D, Kubiszewski I, Green P, Costanza R, Campbell A (2015) Moving beyond evidence-free environmental policy. Front Ecol Environ 13:441–448

Salmo SG, Lovelock CE, Duke NC (2013) Vegetation and soil characteristics as indicators of restoration trajectories in restored mangroves. Hydrobiology 720:1–18

Serrano O, Ruhon R, Lavery PS et al (2016) Impact of mooring activities on carbon stocks in seagrass meadows. Sci Rep 6:23193

Smardon R (2004) Sustaining the world's wetlands. Springer, Heidelberg

Spalding M, Grenfell A (1997) New estimates of global and regional coral reef areas. Coral Reefs 16:225–230

Spalding M, McIvor A, Tonneijck FH, Tol S, van Eijk P (2014) Mangroves for coastal defence: guidelines for coastal managers and policy makers. Wetlands International and The Nature

Conservancy, 42 p. https://www.nature.org/media/oceansandcoasts/mangroves-for-coastal-defence.pdf

Sutton-Grier AE, Wowk K, Bamford H (2015) Future of our coasts: the potential for natural and hybrid infrastructure to enhance the resilience of our coastal communities, economies and ecosystems. Environ Sci Pol 51:137–148

Tanaya T, Watanabe K, Yamamoto S, Hongo C, Kayanne H, Kuwae T (2018) Contributions of the direct supply of belowground seagrass detritus and trapping of suspended organic matter to the sedimentary organic carbon stock in seagrass meadows. Biogeosciences 15:4033–4045

Temmerman S, Meire P, Bouma TJ, Herman PM, Ysebaert T, De Vriend HJ (2013) Ecosystem-based coastal defence in the face of global change. Nature 504:79–83

Thomas S (2014) Blue carbon: knowledge gaps, critical issues, and novel approaches. Ecol Econ 107:22–38

Tokoro T, Hosokawa S, Miyoshi E et al (2014) Net uptake of atmospheric CO_2 by coastal submerged aquatic vegetation. Glob Chang Biol 20:1873–1884

Tokoro T, Watanabe K, Tada K, Kuwae T (2015) Guideline of blue carbon (CO_2 absorption and carbon sequestration) measurement methodology in port areas. Technical note of the port and airport research institute no 1309 (in Japanese)

Tokoro T, Watanabe K, Tada K, Kuwae T (2018) Air–water CO_2 flux in shallow coastal waters: theoretical background, measurement methods, and mechanisms. In: Kuwae T, Hori M (eds) Blue carbon in shallow coastal ecosystems: carbon dynamics, policy, and implementation. Springer, Singapore, pp 153–184

United Nations Ocean Conference (2017) https://oceanconference.un.org/

Verified Carbon Standard (2015) Methodology for tidal wetland and seagrass restoration. http://www.v-c-s.org/methodologies/methodology-tidal-wetland-and-seagrass-restoration-v10

Villa JA, Bernal B (2018) Carbon sequestration in wetlands, from science to practice: an overview of the biogeochemical process, measurement methods, and policy framework. Ecol Eng 114:115–128

Wada S, Aoki MN, Mikami A et al (2008) Bioavailability of macroalgal dissolved organic matter in seawater. Mar Ecol Prog Ser 370:33–44

Ware JR, Smith SV, Reaka-Kudla ML (1992) Coral reefs: sources or sinks of atmospheric CO_2? Coral Reefs 11:127–130

Watanabe K, Kuwae T (2015) How organic carbon derived from multiple sources contributes to carbon sequestration processes in a shallow coastal system. Glob Chang Biol 21:2612–2623

Watanabe A, Nakamura T (2018) Carbon dynamics in coral reefs. In: Kuwae T, Hori M (eds) Blue carbon in shallow coastal ecosystems: carbon dynamics, policy, and implementation. Springer, Singapore, pp 273–293

World Bank (2017) Implementing nature based flood protection: principles and implementation guidance. http://documents.worldbank.org/curated/en/739421509427698706/Implementing-nature-based-flood-protection-principles-and-implementation-guidance

Wylie L, Sutton-Grier AE, Moore A (2016) Keys to successful blue carbon projects: lessons learned from global case studies. Mar Policy 65:76–84

Wyndham-Meyers L, Crooks S, Troxler T (2018) A blue carbon primer: the state of coastal wetland carbon science, practice and policy. CRC Taylor and Francis, Boca Raton, 352 p

Yoshida G, Hori M, Shimabukuro H, Hamaoka H, Onitsuka T, Hasegawa N, Muraoka D, Yatsuya K, Watanabe K, Nakaoka M (2018) Carbon sequestration by seagrass and macroalgae in Japan: estimates and future needs. In: Kuwae T, Hori M (eds) Blue carbon in shallow coastal ecosystems: carbon dynamics, policy, and implementation. Springer, Singapore, pp 101–127

Correction to: The Future of Blue Carbon: Addressing Global Environmental Issues

Tomohiro Kuwae and Masakazu Hori

Correction to:
Chapter 13 in: T. Kuwae, M. Hori (eds.),
Blue Carbon in Shallow Coastal Ecosystems,
https://doi.org/10.1007/978-981-13-1295-3_13

This chapter was inadvertently published with errors. The following corrections have been made after original publication.

Page 347 Abstract lines 3–6:

"The capability of net uptake of atmospheric CO_2 and soil organic carbon accumulation in global shallow coastal ecosystems are estimated to be about 1670 Tg C year^{-1} and about 200 Tg C year^{-1}, respectively, with considerably large variabilities and uncertainties."

has been revised to

"The capability of net uptake of atmospheric CO_2 and soil organic carbon accumulation in global shallow coastal ecosystems are estimated to be about 1070 Tg C year^{-1} and about 140 Tg C year^{-1}, respectively, with considerably large variabilities and uncertainties."

© Springer Nature Singapore Pte Ltd. 2019
T. Kuwae, M. Hori (eds.), *Blue Carbon in Shallow Coastal Ecosystems*,
https://doi.org/10.1007/978-981-13-1295-3_14

P350 Table 13.1

Tidal marshes: CO_2 exchange, mean –661 Tg C year^{-1}, min –2271 Tg C year^{-1}, max 174 Tg C year^{-1}; Soil carbon accumulation rate, mean 77 Tg C year^{-1}, max 865 Tg C year^{-1}; Global area, median 0.51 million km^2, max 0.50 million km^2

Total: CO_2 exchange, mean –1666 Tg C year^{-1}, min –8438 Tg C year^{-1}, max 6302 Tg C year^{-1}; Soil carbon accumulation rate, mean 205 Tg C year^{-1}, max 1017 Tg C year^{-1}

has been revised to

Tidal marshes: CO_2 exchange, mean –66 Tg C year^{-1}, min –1817 Tg C year^{-1}, max 139 Tg C year^{-1}; Soil carbon accumulation rate, mean 8 Tg C year^{-1}, max 692 Tg C year^{-1}; Global area, median 0.05 million km^2, max 0.40 million km^2

Total: CO_2 exchange, mean –1071 Tg C year^{-1}, min –7984 Tg C year^{-1}, max 6268 Tg C year^{-1}; Soil carbon accumulation rate, mean 136 Tg C year^{-1}, max 844 Tg C year^{-1}

P351 lines 1 to 10:

The global estimate of the soil organic carbon accumulation rate in SCEs ranged from 20 to 1,017 Tg C year^{-1}, with a mean value of 205 Tg C year^{-1}, which is comparable to previous reports (Nellemann et al. 2009; Pendleton et al. 2012). Estuaries (mean, 81 Tg C year^{-1}) were major contributors to the total accumulation rate in SCEs, as reported previously (Nellemann et al. 2009).

To the best of our knowledge, this work provides the first global estimate of CO_2 exchange rates in SCEs. The estimated rates ranged from –8438 to 6302 Tg C year^{-1}, with a mean of –1666 Tg C year^{-1} (negative value: net uptake of atmospheric CO_2).

has been revised to

The global estimate of the soil organic carbon accumulation rate in SCEs ranged from 20 to 844 Tg C year^{-1}, with a mean value of 136 Tg C year^{-1}, which is comparable to previous reports (Nellemann et al. 2009; Pendleton et al. 2012). Estuaries (mean, 81 Tg C year^{-1}) were major contributors to the total accumulation rate in SCEs, as reported previously (Nellemann et al. 2009).

To the best of our knowledge, this work provides the first global estimate of CO_2 exchange rates in SCEs. The estimated rates ranged from –7984 to 6268 Tg C year^{-1}, with a mean of –1071 Tg C year^{-1} (negative value: net uptake of atmospheric CO_2).

P351 lines 17–21:

Another explanation is that the estimate of major contributors to the large exchange rate, namely, mangroves (mean, -336 Tg C year^{-1}) and tidal marshes (mean, -661Tg C year^{-1}), have already been implicitly included in the global estimate of the terrestrial CO_2 exchange rate ($-2,300 \pm 700$ Tg C year^{-1}).

has been revised to

Another explanation is that the estimate of major contributors to the large exchange rate, namely, mangroves (mean, -336 Tg C year^{-1}) and tidal marshes (mean, -66 Tg C year^{-1}), have already been implicitly included in the global estimate of the terrestrial CO_2 exchange rate ($-2,300 \pm 700$ Tg C year^{-1}).

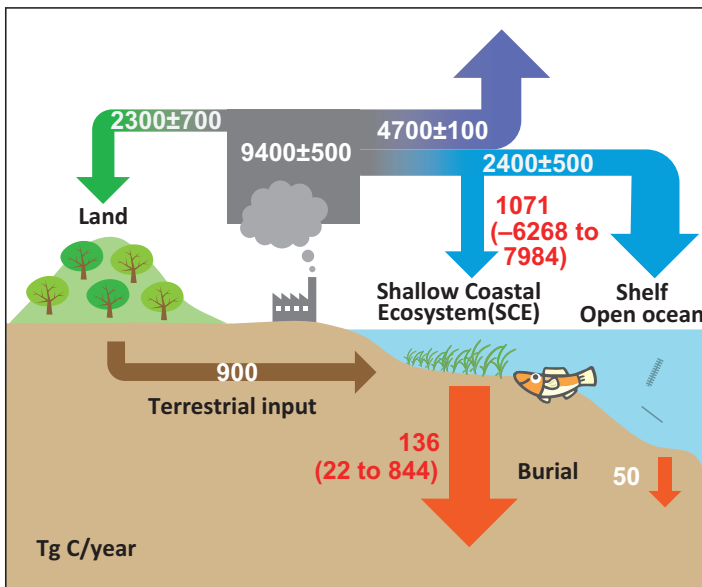**Fig. 13.1 has been revised as below**

Fig. 13.1 Global carbon cycling amended (red numbers) based on the values in Table 13.1. See Le Quéré et al. (2018) for atmospheric data (mean ± SD for 2007–2016) and IPCC (2013) for terrestrial input